INFLUENCE OF GEOMETRY ON CREEP AND MOISTURE MOVEMENT OF CLAY, CALCIUM SILICATE AND CONCRETE MASONRY

by

Che Sobry Abdullah

Thesis Submitted in Accordance with the Requirement
of the Degree of Doctor of Philosophy

Department of Civil Engineering
The University of Leeds

September, 1989

Dedicated
to

My wife
Rohani

and sons
Azzam
Ammar
Hanzolah
Suheil

ABSTRACT

This investigation involved creep and moisture movement measurements for about six months on 13-course clay (Engineering class B) and calcium silicate brickwork, and 5-course concrete blockwork, consecutively. Four different geometries of masonry were built, namely: single-leaf wall, cavity wall, hollow pier and solid pier, respectively having volume/surface area (V/S) ratios of 44, 51, 78 and 112 mm. Deformations were also measured on one-brick wide 5 or 6-stack high model brickwalls which were partly sealed to simulate the V/S ratios of the corresponding 13-course brickwork. At the same time, deformations were also measured on individual mortar prisms and brick or block units in order to verify composite model expressions for predicting masonry movements. Simulation of moisture diffusion of the corresponding mortar joints and embedded bricks or block were made in terms of V/S ratio by partial sealing of the individual mortar prisms and brick or block units.

The tests reveal that the modulus of elasticity to be independent of masonry geometry. However, there is a clear influence of geometry on the vertical ultimate creep and moisture movement of all the masonry types, i.e. creep and shrinkage increase with a decrease of V/S ratio. A similar trend occurs for horizontal shrinkage except for the clay brickwork which undergoes moisture expansion. Deformations of the model walls show reasonable agreement with the 13-course brickwork.

When results of individual mortar and brick/block specimens are inserted in composite models, the predicted strains show good agreement with the measured strains, particularly in the vertical direction.

There is no consistent pattern in the distribution of load and moisture strains for the different masonry geometries, and the measurements reveal that actual strains can be up to 100% higher than the average strains.

ACKNOWLEDGEMENTS

The author wishes to express his sincere gratitude to his supervisor, Dr. J.J. Brooks for his ungrudging and remarkably insightful guidance, help and support throughout the duration of this research. Without his dedication and encouragement this research might not have come to light.

The author is grateful to Professor A.R. Cusens, head of the Department of Civil Engineering, for providing the research facilities.

A special appreciation is given to all the technical staff in the department for their friendly assistance during the period of research and in particular to V.W. Lawton, G. Kemp and G. Broadhead.

The author would also like to thank his sponsors, the University of Technology Malaysia and the Public Service Department of Malaysia for having offered the opportunity to undertake the research programme.

Thanks are extended to friends and colleagues whose names are too many to be mentioned here for their help and support during the course of this research.

I am highly indebted to my mother, whom after the death of my father (so suddenly, in the first year of my research) has to shoulder the burden of the family and with great patient. The sacrifices of my mother and my late father in the upbringing of their children are invaluable and may God reward them generously for what they have done.

Finally, no words are adequate enough to express my deep sense of gratitude to my wife, Rohani, for her contribution in preparing this manuscript and for taking most of the task of upbringing my children, Azzam, Ammar, Hanzolah and Suheil while I was busy with this research. Their presence have undoubtedly relieved the tension of work. May God shower His blessings upon us all.

CONTENTS

CHAPTER 5 - MATERIALS AND EXPERIMENTAL DETAILS

CHAPTER 6 - RESULTS OF STRAIN MEASUREMENTS

CHAPTER 8 - DISTRIBUTION OF STRAIN

CHAPTER 9 - CONCLUSIONS AND RECOMMENDATIONS FOR FURTHER RESEARCH

LIST OF FIGURES

LIST OF PLATES

LIST OF TABLES

NOTATIONS

E_w, E_b, E_m	Moduli of elasticity of masonry, brick or block and mortar joints, respectively
$A_w, A_b, A_m (A_j)$	Cross-sectional area (plan) of masonry, brick or block and mortar vertical joints, respectively
f_w, f_b, f_m	Compressive strength of masonry, brick or block and mortar, respectively.
H	Height of masonry
H_b or b_y or h	depth of brick or block units
H_m or m_y or j	Thickness of mortar bed joint
A_{bm}, A_{bj}	Area of elements (see Fig. 4.11(d))
F	Force
E'	Effective modulus of elasticity
σ	Stress
ε	Strain
Δ	Elemental change
C_{wy}, C_{wx}	Vertical and horizontal creep of masonry, respectively
S_{wy}, S_{wx}	Vertical and horizontal shrinkage of masonry, respectively
$\chi(t, t_0)$	Aging coefficient at time at time t for load applied at time t_0
$\phi(t, t_0), \phi_\infty$	Creep coefficient at time at time t for load applied at time t_0, ultimate creep coefficient
c, C	Creep, specific creep
S	Shrinkage
$E_R(t, t_0)$	Relaxation function at time at time t for load applied at time t_0
β or γ	Strain magnification factor as defined by Ameny et al[38]
α	Ratio of prism to cylinder strength

$(t-t_0)$ or t	Time after the application of load
$\varepsilon_{wy}, \varepsilon_{bmy}, \varepsilon_{hmy}$	Strains in masonry, brick/mortar components and horizontal mortar joint, respectively
$\sigma_{by}, \sigma_{vmy}$	Stresses in brick or block and vertical mortar joint, respectively
$\varepsilon_{bmx}, \varepsilon_{hmx}$	Brick/mortar components and horizontal mortar joint, respectively
$\sigma_{bx}, \sigma_{hmy}$	Stresses in brick or block and horizontal mortar joint, respectively
$C, C+1$	number of brick or block and mortar courses, respectively
W_x, W_z	Width of masonry in x and z axis, respectively
m_x, m_z	Thickness of mortar in x and z axis, respectively of assumed cross-section of masonry model layout
b_x, b_z	Width of brick or block in x and z axis, respectively of assumed cross-section of masonry model layout
n	number of steps (increment)
f_k	Characteristic compressive strength
S_R	Strain ratio
t	Thickness
a, b	Coefficients of hyperbolic-time expressions
T_e or h_0	Theoretical thickness
T_a	Average thickness
T_d	Equivalent thickness
V/S	Volume to exposed surface area ratio
μ	Poisson's ratio

Subscripts

$_w$	masonry
$_b$	brick or block
$_m$	mortar
$_x$ or $_h$	Horizontal
$_y$ or $_v$	Vertical
$_c$ or $_s$	for creep and shrinkage
$_1$ or $_2$	for element 1 and 2
$_e$	Elastic
$_{sh}$	Shrinkage
$_u$ or $_\infty$	ultimate
$_i$	initial
$_{x,y,z}$	in x, y, and z axis

CHAPTER 1

INTRODUCTION

1.1 Background

Masonry is a composite material comprised of brick or block or stone as the building unit and mortar as the jointing material. The thickness of the mortar joint both horizontal and vertical is generally standardised at 10 mm. The brick unit has a standard size of about 216 x 102.5 x 65 mm, whereby the block unit has various combinations of standard sizes. The masonry units are laid in several artistic patterns called bond patterns, the most common are the stretcher, English and Flemish bonds.

Masonry like many other structural and building materials deform when subjected to loading. When subjected to a sustained applied load it undergoes an instantaneous or elastic deformation followed by a time-dependent deformation. The time-dependent deformation : creep and shrinkage (or expansion), have a bearing in the design for movement in masonry structures. Modern masonry exhibit larger movements compared with traditional masonry due to combined effects of elasticity, creep, moisture expansion, shrinkage and thermal strain. Those larger movements arise from the uses of slender sections, higher working stresses, thicker mortar joints and new bricks and blocks which are more sensitive to stress and environment. Failure to allow for creep and moisture movements in the design and construction of masonry members may cause serviceability problems through spalling and buckling, or cracking in case of restraint. Also, creep induces greater deflections in reinforced brickwork beams and loss of prestress in post-tensioned brickwork.

Unfortunately, compared with concrete there are very few data available on the time-dependent properties masonry such as creep, and although a significant contribution on the study of creep in masonry has been made by a number of researchers[1-26], such results are still sparse and represent only a small aspect of masonry; there are many other aspects that have not been studied in detail. It seems

that this situation has restricted the development of universal design procedure. At present, existing design information relies the 'ultimate' values for creep and shrinkage for a limited range of brick and block masonry, which have been extrapolated from results of tests carried out under particular laboratory conditions. The influence of many factors, such as curing conditions, temperature, humidity, age at loading or exposure, type of mortar, geometry of masonry, presence of damp proof course, mortar bed reinforcement and anisotropic behaviour are not recognized. Consequently, it is desirable to investigate these aspects in detail so that adequate data is available and relevant influencing factors can be allowed for in estimating long-term deformations, as in the case of concrete[27-29].

One of the objectives of the present research is to investigate the influence of geometry on creep of masonry. For concrete, the influence of size and shape of member on creep and shrinkage are well known. All prediction methods for estimating the time-dependent deformation do allow for size and shape effect by coefficients related to effective thickness, average thickness and volume-to-exposed surface area (V/S) ratio[27-29]. Both creep and shrinkage of concrete depend on the rate of moisture diffusion which is governed by the average drying path. Essentially, under conditions of drying, creep and shrinkage are less for larger size members. In masonry, the average drying path length of the mortar bed joints in a solid pier is greater than that of a single-leaf wall of similar cross-section, and consequently the moisture loss is slower in the pier so that both creep and shrinkage should be less. In the long term, shrinkage and creep of the wall and pier might be expected to be similar, but this is not found to be the case for concrete members, probably because of structural changes in the cement paste (e.g. carbonation) which restrict moisture diffusion, especially in smaller members. By analogy to concrete, the influence of geometry on creep of masonry is anticipated to have a similar effect to that on shrinkage. There has been

no previous comprehensive study on the influence of geometry on creep of masonry except that carried out by Lenczner[13], who found that creep in piers was less than in walls.

Brooks and Bingel[32] have proposed that shrinkage is a function of size as expressed in terms of the volume-to-exposed surface area ratio (V/S) by an empirical function representing an approximation of the average drying path length of masonry of similar shape. The present investigation looks into this aspect further and extends it to creep so that a more accurate computation and prediction on the long-term movement can be made, for any geometry of masonry.

The elastic moduli of both mortar and units also vary within wide limits as do their strengths. In general, the mortar has a lower modulus of elasticity and higher creep than the brick or block units. The mortar will undergo shrinkage while the brick unit may undergo shrinkage or expansion. The presence of bond between the unit and the mortar joint ensures that masonry behaves as a composite continuum. The values of modulus of elasticity ,creep and shrinkage of the composite will therefore lie in between those individual values. Obtaining these strain related properties of any masonry experimentally is expensive due to lengthy tests, using bulky specimens and high capacity testing machines. On the other hand, separate measurement of the properties on mortar and brick or block are much simpler and cheaper. The data can then combined by a composite mathematical model to predict the behaviour of the larger masonry. Prediction of elasticity and time-dependent deformation of masonry by composite models has been proposed by several investigators[33-42], but there has been very little experimental verification of such models.

The main problem normally encountered when using composite model is the input of a representative data. For example, Ameny et al[38] had to adjust, empirically, the creep of individual block and mortar specimens in order to predict their composite effect in masonry. The data must be obtained from specimens which are representative

intrinsically and extrinsically to those in the masonry. Among the factors that have not been taken into account by previous researcher in their composite model is the drying effect of masonry. In the case of shrinkage and creep, it is necessary to determine the brick and mortar properties on specimens having similar pattern of moisture diffusion, which can be quantified as the V/S ratio, to that in the masonry mortar joints and embedded bricks to ensure correct modelling. For example, the foregoing could explain the observation of Ameny et al[38] that the bed joint creep in a blockwork prism was significantly less than that in a cylindrical specimen subjected to the same stress. Compared with the bed joints, the cylinder had a smaller V/S ratio and thus a greater creep. The V/S ratio effect on mortar and brick has been used in the verification of composite models for creep of clay and calcium silicate brickwork single-leaf walls[39] and for shrinkage of calcium silicate brickwork and concrete blockwork[41]. For the creep in masonry, since no data is available, the adjustment for the effect of size are made using factors from concrete technology[27-29]. It is therefore desirable to extend this work to cover other types of masonry so as to enable a more accurate modelling.

Another alternative solution to cut the high cost of full scale testing to assess the performance of masonry is by testing a scaled down model wall. In other engineering fields, normally a 'dimensionless analysis' is used to simulate the physical properties of the model to the prototype. It is difficult to apply this method in masonry although the technique has been used to predict some mechanical properties of masonry[43]. There has been one attempt to apply this approach to creep by Lenczner[4] who measured a much greater creep on model walls constructed from half-size bricks than the corresponding creep on brickwork built from standard size bricks. The reason the discrepancy is attributed to a lack of simulation between the smaller brickwork and the full-scale brickwork. It is therefore necessary to improve the methodology of model test by proper simulation of the moisture diffusion of the model wall to the prototype.

1.2 Brick and block units

For centuries clay bricks have been used in building construction which were normally hand made. However, the present-day production is highly mechanised, although in many parts of the world bricks are still made by hand. Units can also be made from other materials such as lime-sand mix and concrete, the latter being called a block because of its size being larger than the bricks. Nearly every building has some form of masonry work in the form of clay or calcium silicate bricks or concrete blocks or a combination of them.

1.2.1 Clay brick

Clay bricks are made by shaping suitable clays and shales to units of standard size, which are then fired to a temperature ranging from 900 to 1200°C. The fired product is a porous ceramic composed mainly of silica, SiO_2 (55-65% by weight), and alumina, Al_2O_3 (10-25%). The quality and properties of clay brick depend on the clay composition and firing process. Extruded bricks are generally perforated and pressed bricks commonly have frogs in one or both of the bed faces; both features reduce brick weight.

In practice bricks are classified into 3 categories[119], namely: common brick, for general building purposes; facing brick, manufactured for its appearance; and engineering brick, for use where high strength and durability are required. Other than the functional requirements, bricks are also classified according to their strength and water absorption in case of engineering bricks[119].

1.2.2 Calcium silicate brick

Calcium silicate bricks are suitable for use in both external and protected internal walling. They are available as facing bricks or as commons. The raw materials used in the manufacture are a very fine siliceous aggregate, a high calcium lime and water. Inert and stable pigments are normally added to give the required colour. The

materials are first mixed in the required proportions and are mechanically pressed under considerable pressure into moulds. They are then cured in high pressure steam autoclaves for several hours which results in the combination of the lime with part of the siliceous aggregate to produce a hydrous calcium silicate (tobermorite) which forms the binding medium in the finished brick.

As for clay bricks, the bricks are available in a solid or a frogged unit and are made to a standard size of 216 x 102.5 x 65 mm. The method of manufacture together with inherent properties of the mixed raw materials produce a brick with fine dimensional tolerances and good clean arrises.

1.2.3 Concrete block

The use of concrete blocks in building industry has increased in popularity over the last 30 years. Probably, the main advantage over clay bricks is the higher productivity because it is normally six times larger than bricks and the manufacturing is easier and cheaper. Blocks are made from autoclaved aerated concrete, lightweight-aggregate concrete and dense-aggregate concrete, the first being invariably solid while the others can be described as solid, hollow or cellular. The manufacturing process involves compaction of the newly mixed constituent materials in a mould followed immediately by extrusion of the pressed block so that the mould can be used repeatedly. Admixtures and cement replacement materials are used as in other concrete work but the mix proportions contain a higher fine aggregate content and less cement.

1.3 Purpose and scope of research.

The main aim of this research was to investigate the influence of geometry on creep in masonry, as quantified by the volume/exposed surface area ratio (V/S). The tests involved three commonly used masonry materials namely: clay brick (Engineering Class B), calcium silicate brick and concrete block.

The other objectives of the research were as follows:

(a) the experimental verification of the composite models developed by Brooks[41-42] to cover a wide range of types and geometries of masonry.

(b) the comparison of the creep of model walls and full size walls/piers of equal volume/exposed surface area ratio (V/S).

In addition, the moisture movement corresponding to the above areas of investigation was included.

The investigation on the geometry influence on moisture movement and creep of masonry involved axial and lateral strain measurements for about six months on 13-course brickwork and 5-course blockwork in the form of walls and piers having a range of V/S ratio. For the composite modelling, mortar and brick/block units were required to be sealed so as to have the same V/S ratio as the corresponding brickwork/blockwork: single leaf walls, cavity walls, hollow piers and solid piers. The moisture movement and creep of the brick/block and mortar phases could then combined in the composite models, so that the predicted values could be compared with the experimental values measured from the brickwork/blockwork.

The tests required for objective (b) were on one brick-wide 5 or 6-stack high model walls. The model walls were also sealed to simulate the V/S ratio that of the larger brickwork.

1.4 Definition of terms

Creep is defined as the increase in strain under a sustained constant stress taking into account the other time-dependent deformations not associated with stress, viz. shrinkage, swelling and thermal deformations. Creep increases quite rapidly at early age of load application then slows down if the level of applied stress is well below failure.

Moisture movement in masonry may either be referred to shrinkage or moisture expansion. Shrinkage of masonry is caused by loss of moisture by evaporation or by hydration of cement in the mortar, and also by carbonation. It is a volumetric strain but in practice it is measured as a linear strain. If there is continuous supply of moisture to the masonry, expansion may occur due to absorption of water by mortar and brick units, or expansion may occur due to the use of certain types of clay brick (irreversible moisture expansion).

The definition of terms used in this investigation are illustrated in Figure 1.1.

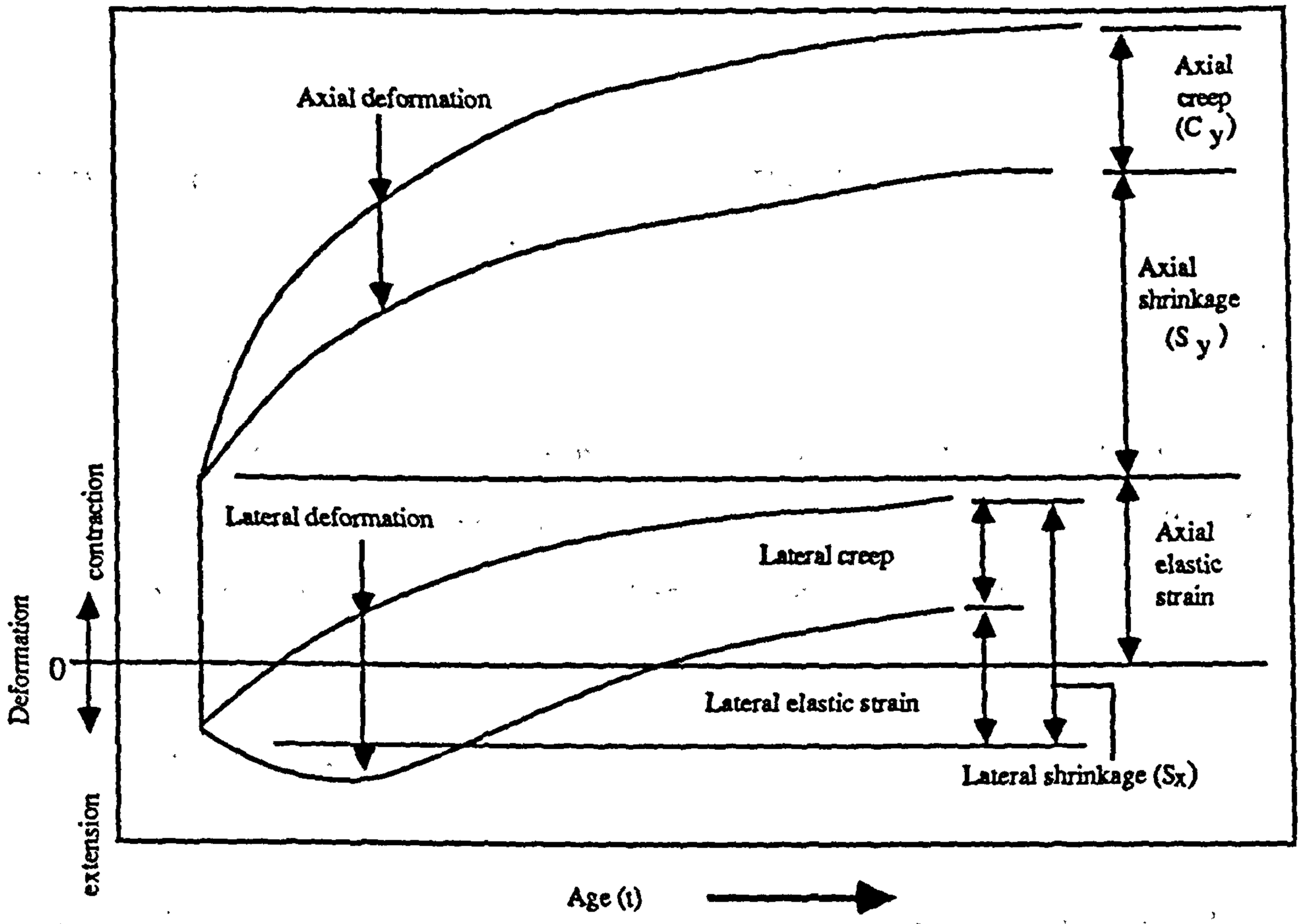

(a) Elastic, creep and shrinkage

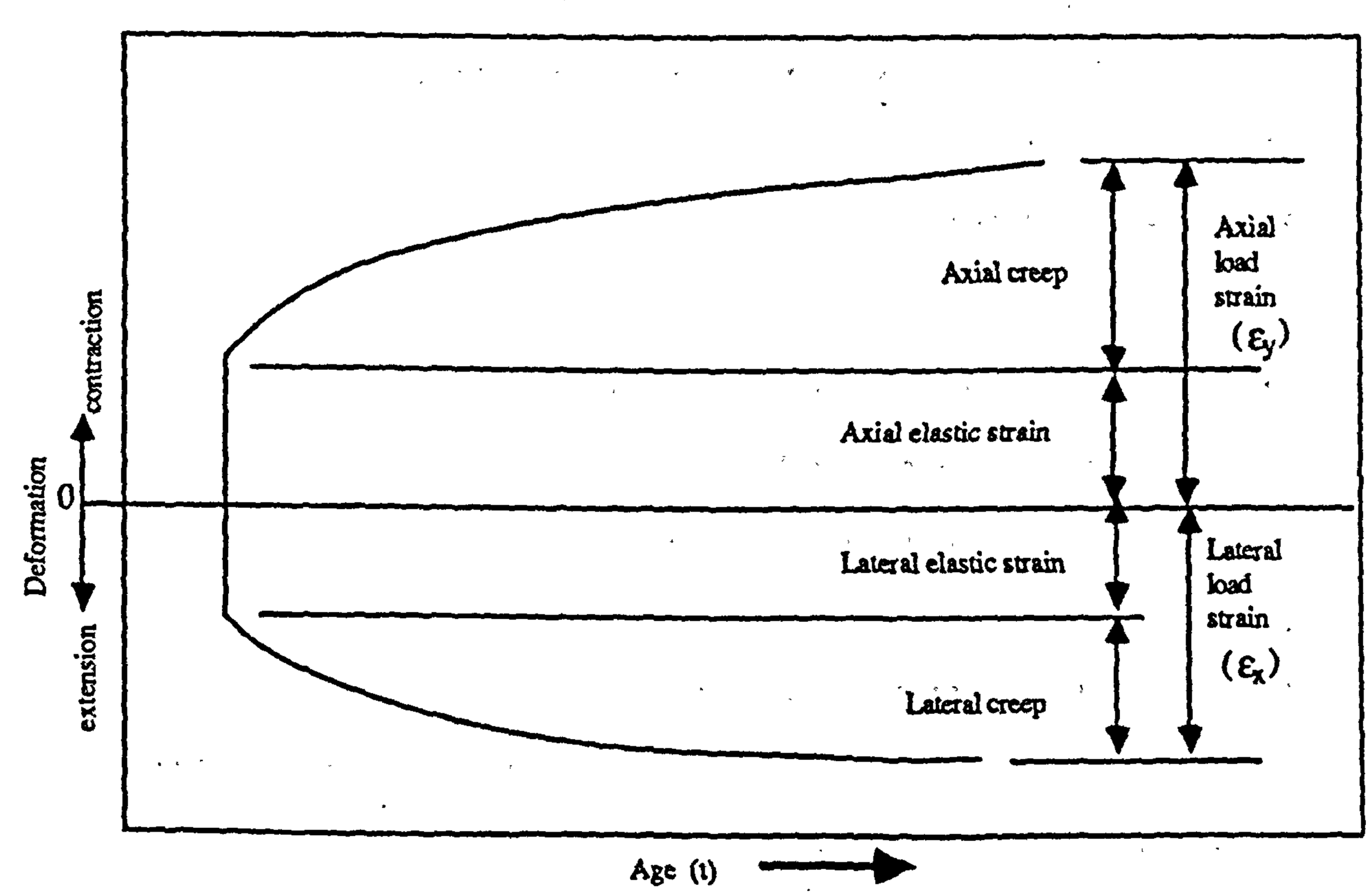

(b) Load strain after allowing for shrinkage

Fig. 1.1 - Definition of Terms

CHAPTER 2

REVIEW OF ELASTIC AND TIME-DEPENDENT DEFORMATION OF MASONRY

2.1 Introduction

In this chapter a literature review on the modulus of elasticity, moisture movement and creep of masonry are presented. In some cases the review includes the properties of the component material i.e. mortar and brick or block units. Finally, some general conclusions based on this review are presented.

2.2 Elastic behaviour

Under short-term load the stress-strain relationship of masonry, as that for concrete, is classified as non-elastic and non-linear. The strain behaviour is dependent on the corresponding characteristics of its component units and mortar joints. It is well known that the mechanical properties of bricks are influenced by the clay quality, the firing temperature and the porosity etc. All these parameters together with the properties of mortars and workmanship influence the behaviour of masonry under vertical and horizontal loads.

The modulus of elasticity in compression is a basic factor in computing displacement and subsequent prestress loss due to creep. Since instantaneous deformation at the application of load and subsequent creep are not easily separated from one another, it is important to define the starting point of creep. The problem is amplified by the non-linearity of the stress-strain relation of masonry which sometimes gives a negative curvature at low levels of stress so that it is difficult to choose a modulus of elasticity. A proper and accurate assessment of the modulus of elasticity is therefore important. In the following sub-sections, the elastic behaviour of mortar, brick and block units, and masonry are reviewed.

2.2.1 Mortar

The prime function of the mortar is to bond masonry units into a monolithic mass ensuring a watertight wall and providing required structural integrity. The thickness of the mortar joint is standardised to about 10 mm. Increasing joint thickness will reduce the strength of masonry[44]. Whereas weak mortars with a low modulus of elasticity are desirable to allow for brick or block movement without any conspicuous cracking, strong mortars provide higher bond strength and consequently stronger walls when subjected to transverse load[45].

The types of mortar generally used in masonry work are the cement:lime:sand, masonry cement:sand, and cement:sand with plasticizer or other additives. The standard mix proportions and other functional requirements for masonry mortar as given in BS 5628[46] are shown in Table 2.1.

Masonry mortars, as other concrete products, show a non-linear stress-strain relationship and hence are defined in similar manner to that of concrete, namely, initial tangent modulus, tangent modulus and secant modulus. According to Sahlin[47] the tests results of Hilsdorf[48] give the range of initial tangent modulus as 0.6 GPa for 1:3 (lime:sand) mortar to 24.8 GPa for 1:3 (cement:sand) mortar. He stresses that the choice of mortar should be made carefully when the modulus of elasticity is important. Using data from various investigators he indicates that the tangent modulus of elasticity for mortar, E_m (MPa) and the compressive strength, f_m (MPa) can approximately be related by

$$E_m = 1000 f_m \text{ for all strengths,} \tag{2.1}$$

and by

$$E_m = 0.043 \rho^{1.5} f_m^{0.5} \text{ for high strength mortars,} \tag{2.2}$$

where ρ is the density of mortar in kg/m^3.

Equation (2.2) is in fact recommended by ACI[49] for estimating modulus of elasticity of concrete. The above relationships were obtained empirically from tests on concrete of strength ranging from 14.7 to 44.1 MPa which explains why there are discrepancies for low strength mortar.

Lenczner's results[50] showed that the secant modulus (at 50% ultimate stress) increases with an increase in strength. Base and Baker[8] obtained distinctly non-linear stress-strain relationships and found Poisson's ratio, (μ) to be 0.15 from the age of 28 days using 70 x 70 x 140 mm mortar prisms. The strains measured in the mortar joints in the masonry were higher than those measured in the individual mortar prisms, as shown in Fig. 2.1 . Jessop et al[31] obtained the modulus of elasticity of mortar in-situ (bedded) which ranged from 7.2 to 8.24 GPa, and a very low average Poisson's ratio of 0.074 which was due to lateral constraint on the mortar. The secant modulus of 51 mm mortar cubes was generally lower than the in-situ modulus, which is a contradicting result to that by Base and Baker[51]. Various forms of modulus were computed and the results showed that the tangent modulus > secant modulus at 3 MPa > secant modulus at 5 MPa. Ameny et al[35] also showed the stress-strain relationship of mortar to be significantly non-linear.

Brooks[141] obtained a Poisson's ratio of 0.07 for mortar of strength 12.7±0.1 MPa. The secant modulus of elasticity measured from mortar creep specimen gave a value of 17.6 GPa. Later, Brooks and Amjad[54] obtained the secant modulus of elasticity of 6.5±2.2 GPa for a 8.9±4.3 MPa strength mortar. Lenczner[4] found that the differences of modulus of elasticity for 1:$\frac{1}{4}$:3 and 1:1:6 cement-lime mortar mixes to be insignificant even though the strength of first was twice as high as the latter mix. Binda et al[52] tested 40 x 40 x 120 mm mortar prisms made from three different types of mix. The high strength mortar showed a linear elastic brittle behaviour while the lower strength mortar showed a non-linear curve. The Poisson's ratio of the mortar ranged from 0.057 to 0.115.

2.2.2 Brick and block units

The elastic behaviour of clay bricks is not the same as for concrete. Sahlin[47] using results from the test referred to earlier showed that the initial tangent modulus of extruded bricks can be related to the strength:

$$E_b = 300 f_b \tag{2.3}$$

but the moduli for pressed bricks are higher. Hilsdorf[48] showed that bricks exhibit a substantial linear stress-strain relationship, the modulus being close to the value given by Equation (2.5) . The Poisson's ratio was about 0.2 at lower levels of stress but increased to 0.35 near to failure stress. To reduce the effect of platen restraint the tests were performed on 60 x 30 x 30mm specimens cut from different portions of bricks. He also measured strains on embedded bricks in a 5-stack and a 9-stack high brickwork prism. The modulus of brick was 15.7 GPa with a compressive strength of 36.6 MPa.

Francis et al[44] obtained the value of Poisson's ratio of 0.25 for both solid and perforated clay bricks. The strain measurements were made with a 5-stack high brickwork prism. Base and Baker[51] tested specially made extruded individual clay bricks of 229mm and 306 high bricks. Strains were also measured in the centrally embedded bricks from 5-stack bonded prisms of 312mm high bricks, and 3-stack bonded of 152mm high bricks. The modulus of elasticity of centrally embedded bricks was found to be higher than the average value of the single bricks, although they expected the reverse to occur, since in the central bricks, for a given axial stress the vertical strain is increased by the lateral expansion of the mortar joint. The results showed that the effect of mortar joint on the modulus of embedded bricks appears to be insignificant. The average stress-strain relationship was found to be practically linear up to the point of cracking. The Poisson's ratio for the embedded brick was 0.19 .

Page[53] applied uniaxial compression to the header faces of half scale clay bricks (114 x 54 x 32mm) cut from full sized dry-pressed bricks. The stress-strain curve was

linear except at high stress levels. He also loaded a 5-stack unbonded brickwork prism. Bonding was prevented by inserting a plastic sheet between the brick and the dental plastic joints. The stress-strain relationship of the centrally embedded brick was substantially linear. The ratio of modulus of elasticity loaded normal to bed joint to that loaded normal to header faces was 1.35 while the strength ratio was 13.7. The coefficient of variation of modulus of elasticity was about 30%. Nonetheless, the result clearly indicated the brick had anisotropic properties. The value of Poisson's ratio was 0.167 with a 25% coefficient of variation.

Jessop et al[31] computed the secant modulus of elasticity of a concrete brick embedded in a 5-stack bonded prism. The secant modulus obtained ranged from 7.2 to 8.42 GPa with a Poisson's ratio of 0.17. In 1983, Brooks[23] reported the anisotropic effect on the modulus of elasticity of calcium silicate and frogged Fletton clay bricks. The ratios of the modulus loaded between bed faces to the modulus loaded between header faces was 1.15 and 0.31 for calcium silicate and Fletton bricks, respectively, the later case reflecting the influence of the frog.

Ameny et al[35] tested 35 x 35 x 90 mm beige and brown concrete brick units. The units exhibited approximately elastic stress-strain behaviour. The moduli of elasticity were 5.11 GPa for the 19.0 MPa strength beige unit, and 5.32 to 8.64 GPa for the 25.9 MPa strength brown unit. Binda et al[52] showed a linear stress-strain relationship of a solid softmud brick (250 x 120 x 5.5 mm). The modulus at a stress level of 30% of the ultimate stress was 4.68 GPa for the brick strength of 26.9 MPa. The Poisson's ratio for the brick was found to be 0.094.

Recently, Brooks and Amjad[54] tested for the modulus of elasticity of perforated clay bricks by loading in a number of ways: (a) single brick between bed faces, (b) three-stack unbonded brick between bed faces, (c) five stack unbonded brick between bed faces, (d) single bricks between headers and (e) 50 x 25 mm diameter brick cored between all the three faces. Tests on cored samples showed anisotropy. Strength and

modulus decreased in order of testing between bed faces, header faces and stretcher faces. The presence of perforations greatly affected the anisotropy of the full size brick unit. The modulus measured by the 'standard' strength test for bricks unit was found to be similar to the 'unrestrained' modulus as given by the cored samples.

There are two main types of concrete masonry units or blocks: aggregate (normal or artificial) concrete and aerated concrete blocks, and their respective methods of manufacture are distinctly different. The blocks are moulded in three basic forms, i.e. solid, cellular and hollow blocks having various sizes.

The stress-strain relationship of the block as that for other concrete products is non-linear. Various works have suggested that the modulus of elasticity of the block can be related to the value of compressive strength. Using results obtained by Richart et al[55] who tested concrete blocks made from cinder, gravel, limestone or other aggregates, Sahlin[47] concluded that the modulus of elasticity (E_b) of the block may be related to the block strength (f_b) by;

$$E_b(\text{MPa}) = k f_b(\text{MPa}) \qquad (2.4)$$

The factor k ranges from 500 to 1500, with a mean of about 1000. Read and Clements[56] loaded, uniaxially, stretcher bonded blockwork panels and concluded that the initial tangent modulus of the block was dependent on the density of concrete and the compressive strength of the block. He suggested the equation as given in BS 8110[146] for the concrete block:

$$E_b = 0.85\rho^2 f_b^{0.5} \qquad (2.5)$$

where ρ is the density of the block in kg/m^3 and f_b is in MPa and E_b in GPa. Ameny[36] reported from his earlier tests on lightweight concrete block in 5 stack high prisms a value of Poisson's ratio of 0.16 for the unit at stress levels up to 22.5 % of the ultimate strength of the prism, and indicated that the value of Poisson's ratio increases at higher stress levels.

2.2.3 Masonry - the composite

Generally, the stress-strain relationships for brickwork and blockwork are non-linear. Very few investigators have[58-60] reported that the relationship showed either a very small linear portion or nearly linear. These observations were generally at low stress levels or for high strength masonry.

As in concrete, attempts have been made to establish the relationship between the modulus of elasticity of masonry and its compressive strength. These attempts suffer a disadvantage in that there is no standard method for testing for modulus of elasticity and the compressive strength which hampers the comparison of results. In concrete technology for example, the compressive strength is determined by testing 100 mm cubes or 200 diameter cylinders, and the modulus of elasticity is determined from a standard static modulus test or a dynamic modulus test, or computed from stress-strain curves on a standard size and shape of specimen which is specified for the United Kingdom in BS 1881[57]. A similar guide-line is not available in masonry, as yet.

The general form of the relationship between the modulus of elasticity (E_w) and the compressive strength (f_w) of masonry given by various investigators and design guides is in the form of;

$$E_w = k.f_w \tag{2.6}$$

where k is the multiplier, and E_w and f_w are both in MPa.

Sahlin[47] analysed test results of other investigators and deduced a value of k ranging from 400 to 1000. The average value of 700 was recommended but it is not applicable to very low strength mortar or to unusual ratios of mortar to brick strength. For masonry with high strength mortar and low to medium strength brick, the modulus of masonry tends to that of the brick. However, BS 5628[46] gives a value for k as 900, but the 'characteristic strength' (f_k) has been suggested instead of f_w which is applicable

for clay, calcium silicate and concrete masonry. The use of 'characteristic strength' offers an advantage since it allows for the variability of brick and, thus, brickwork strength.

For blockwork, Richart et al[55] suggested for a rough estimate of the initial tangent modulus of elasticity, the value of k as 1000. Hegemier[62], who tested blockwork prisms and blockwork panels, also suggested a value of 1000 for k. Hamid et al[63], on the other hand, used the secant modulus at 50% of the ultimate stress and found that the multiplier k was much less that 1000. This can be explained since generally for a parabolic stress-strain curves the secant modulus is much less than the initial tangent modulus. However, Hatzinikolas[64], who measured the initial modulus on a 5-stack high blockwork prism found the multiplier k to be 750, and also, Ameny[36] reported the value to be as low as 630 when testing lightweight concrete masonry.

Plowman[65], using data from previous research, suggested two relationships for modulus of elasticity of masonry, E_w (GPa). Based on the compressive strength of masonry, f_w (MPa):

$$E_w = f_w - 0.69 \tag{2.7}$$

and based on the compressive strength of brick, f_b (MPa):

$$E_w = \frac{1}{5}(f_b + 4.1) \tag{2.8}$$

The data were obtained from different sizes of brickwork specimens, and there was a large scatter about the lines represented by these equations.

Sinha and Hendry[66] gave the relationship between E_w (GPa) and stress, σ (MPa) as:

$$E_w = 5.269 \pm (0.0966 - 0.007\sigma) \tag{2.9}$$

Grimm[67] deduced from the analysis of past experimental data that the elastic modulus of elasticity of masonry, E_w (GPa) was also affected by height/thickness ratio (h/t) of the specimen. The relation given was as:

$$E_w = 0.00625 f_w \left(80 + \frac{h}{t}\right) \tag{2.10}$$

for h/t less than 45.

The Poisson's ratio (μ) of the masonry was found to range from 0.11 to 0.20. From his work on masonry walls and piers, Lenczner[16] reported that there was no direct relationship between the modulus of elasticity of masonry and the strength of masonry or mortar. Instead, he showed that the modulus can be related to the strength of brick or block units. These equations are:

(i) For the unit compressive strength of 20 MPa or less the elastic modulus (in MPa) is given by:

$$E_w = 5000 \tag{2.11}$$

(ii) For units with compressive strength between 20-70 MPa, the modulus is given by:

$$E_w = 300 f_b - 2000 \tag{2.12}$$

(iii) For units with compressive strength of 70 MPa and above the modulus is given by:

$$E_w = 12750 + 100 f_b \tag{2.13}$$

He stated that the geometry of the member did not appear to have any consistent effect on the modulus of elasticity. Equations (2.11) to (2.13) are shown in Fig.2.2.

Warren and Lenczner[22] derived an empirical relationship between modulus of elasticity of masonry and square root of brick strength on storey-high single leaf masonry walls made from different bricks with $1:\frac{1}{4}:3$ mortar mix. The equation is:

$$E_w = 5.171\sqrt{f_b} - 19.158 \tag{2.14}$$

The correlation coefficient (R) is 0.975 and E_w is in GPa.

Brooks[23] found that when using the above equation, there was good agreement between the measured modulus and the predicted modulus of a Fletton wall, while the predicted modulus of a calcium silicate brickwall was underestimated by 30%. The Poisson's ratio at loading and after creep for about 300 days was found to be 0.13 and 0.04, respectively, for calcium silicate brickwork, but a constant value of 0.05 was obtained for Fletton brickwork. Subsequent tests performed by Brooks and Amjad[54,68] showed that the strength and the modulus of elasticity were independent of concrete platen restraint, as measured by a height to least lateral dimension ratio of between 1 and 9.5 for clay and calcium silicate brickwork, and between 2 and 11 for concrete blockwork. Warren and Lenczner[22] reported the values of Poisson's ratio at 400 days after loading to be 0.087 and 0.197 for Kirton bricks and brickwork, respectively.

2.3 Moisture movement

Moisture movement has been accepted as a contributory factor in studies of the movement and cracking of brickwork. Thorough reviews on moisture movement in masonry have been given by various researchers[69-84]. This section is mostly based on those reviews, giving only the general conclusions.

2.3.1 Clay brick

Clay bricks show a reversible and irreversible expansion which is associated to moisture movement in the units. It expands or contracts when it gains or losses

moisture, respectively. The irreversible or permanent moisture expansion in clay brick begins during cooling process in the kiln. The rate of expansion is high at first and then continues at greatly reduced rate for many years.

The moisture movement in clay brickwork is therefore a composite effect resulting from the permanent moisture expansion of the bricks, the change of relative humidity of the environment and the drying shrinkage of the mortar joints. The net effect of these movements is generally a gradual expansion in most type of brickwork. When restrained, this may result such things as vertical cracks close to the corners of long walls, and, when unrestrained, the distortion of built-in frames. In general, reversible expansions of brickwork are small (usually < 0.02%) and barely significant in comparison with size changes produced by other causes, whereas irreversible expansions are much larger (up to 0.2%). Typical values of irreversible expansions as given in CP 121[85] are presented in Table 2.2.

2.3.1.1 Mechanism of expansion

The exact cause of irreversible expansion is uncertain. It has been explained that the physical adsorption of water in the brick was mainly responsible for the expansion. Intermolecular attraction applies compressive stresses to the interior of a solid which are reduced if water is adsorbed, resulting in an elastic expansion of the material. However, this physical phenomenon cannot be the main cause of expansion since adsorbed water can be removed by heating to 100°C, but moisture expansion of brick can only be removed by heating to temperatures of the order of 600°C and more. Irreversible expansion can also be due to the chemical reactions between water and certain constituents of ceramic bodies. Specifically, the chemical reactions are the hydration of amorphous silicates, silica, glasses and alumina constituents of the fired clay; in addition, free lime and some salts are capable of hydration and, therefore, of contributing to expansion. It has also been stated that the glass phase of a ceramic body is the major cause of expansion in the presence of moisture.

2.3.1.2 Factors affecting moisture expansion

The permanent moisture expansion of brickwork is affected by a number of factors. The magnitude of expansion has been shown to increase with time of exposure, the rate being highest at the beginning followed by a slower rate of growth which reduces with time. The age of the bricks is a factor, because the amount of expansion in a wall decreases with the length of time the bricks are stored before they are laid. Measurements by BRS[86] have shown that a typical brick would be expected to expand by about 0.08% in the first 8 years, of which about half occurs in the first week. Thus it is recommended that fired clay bricks should not be laid for at least one week after manufacture so as to avoid distress in the structure. It has also been reported that increasing the temperature causes an increased rate of permanent moisture expansion. It follows that brick walls exposed to sunshine will expand irreversibly more than shaded walls. Increasing the relative humidity to which the bricks are exposed also causes an increase in the rate of moisture expansion.

The brick firing temperature in the kiln has a marked effect on the subsequent moisture expansion. Low expansion occurs for bricks fired at low temperature while the expansion is a maximum for bricks fired between 900°C and 1050°C, after which it decreases for higher firing temperatures. The cyclic wetting of bricks at 21°C and drying at 100°C results in far greater expansions than if the bricks are continuously soaked at 21°C. Mortar joints are reported to restrain movement in the brick with the result that in brickwork walls the vertical expansion is more than the horizontal expansion. Extensive observations have indicated that the ratio of horizontal expansion of brickwork to the unrestrained expansion of individual bricks is less than the ratio of vertical expansion to the expansion of individual bricks. The method of manufacturing and clay composition have also been indicated to affect the moisture expansion. Bricks made by a dry process showed only about 50% the expansion of those made by an extrusion process. Since moisture expansion is due largely to chemical reactions, the

chemical composition of the clay from which the brick is made is an influencing factor.

2.3.1.3 Clay brickwork

Typical moisture expansions for clay brickwork, as given by CP 121[85], are shown in Table 2.3. Moisture expansion in brickwork has been a great concern by many investigators but most of the works have been concerned with moisture expansion of brickwork in the horizontal direction rather than in the vertical direction. This was probably due to the importance of induced cracking caused by horizontal restraint. Only in the 1960'S that the need to accommodate vertical moisture movement had been recognised. Problems of differential movement between downward shrinking and creeping of reinforced concrete frames and upward expansion of cladding brickwork supported by the frames has been reported[83]. In fact, the moisture movement in the vertical direction was found to be higher in the horizontal direction. This was because of reduced restraint in the former direction. However, Brooks and Bingel[32] stated that the difference between the vertical and lateral strain is mainly connected with the anisotropy of clay bricks which is associated with the manufacturing process , since, Brooks[39] measured a much greater expansion between bed faces than between header faces.

Lenczner and Salahuddin[12] obtained measurements for moisture movement at 28 days after building, and found for Fletton brickwork laid dry, the vertical expansion was nearly twice the horizontal expansion. For a Staffordshire brickwall, the strain of an embedded brick showed a gradual shrinkage at first followed by a gradual expansion. A similar trend was measured on Fletton walls by Brooks and Bingel[32]. Schubert's[26] work showed that the expansion of clay brickwork ranges from 0 to 200 x 10^{-6}. However, some design standards[46,117] suggest that expansion in clay brickwork is negligible.

2.3.2 Calcium silicate brick and brickwork

Calcium silicate brick shrinks on drying out in a similar manner to concrete. The magnitude of the drying shrinkage normally ranges from 0.01 to 0.04 per cent. Consequently the brickwork will undergo shrinkage.

There has been very little research into the study of moisture movement in calcium silicate brickwork. The possible reason for this is that calcium silicate is not as widely used as clay bricks and concrete blocks. Brooks[23] measured shrinkage in single-leaf calcium silicate brickwall up to 300 days. From the shrinkage-time relationship, when expressed as a hyperbolic function of time, the ultimate shrinkage was 232 x 10^{-6}. BS 5628:Part 2[46] recommends a value of 500 x 10^{-6} to be used in the design of load-bearing brickwork. The lateral shrinkage of the brickwork measured by Brooks and Bingel[32] was generally lower than the axial shrinkage which was mainly attributed to the anisotropy of shrinkage of the calcium silicate bricks viz. a lower shrinkage between header faces than between bed faces. Table 2.4 gives the design range[85] for calcium silicate bricks.

2.3.3 Concrete block and blockwork

Volume changes of concrete products depend mainly on the moisture content. A concrete block shrinks when it losses moisture and expands when moisture is gained, the shrinkage being reversible. Another minor cause of shrinkage is due to carbonation, the effect being permanent which is caused by the chemical reaction of carbon dioxide from the environment with calcium hydroxide in the concrete. Carbonation shrinkage is normally small but the effect may be apparent in a very small specimen. Measurement of drying shrinkage usually includes carbonation shrinkage. Typical design ranges for shrinkage of blocks are given in Table 2.4.

2.3.3.1 Mechanism of shrinkage

Although the understanding of the nature of shrinkage in concrete is far from complete, drying shrinkage has often been considered to be due to surface tension of water in the capillaries. When the material is saturated, surface tension forces are very small, but as moisture dries from the faces, the water surface regresses into the capillaries creating surface tension forces at the menisci. These forces put both the cement gel and aggregate in a state of compression and, hence, produce a reduction in volume. However, this cannot be the sole mechanism of drying shrinkage because, according to this theory, the concrete units would expand to its original dimension if surface tension forces were removed by complete drying, or by re-wetting. In reality, complete drying causes further shrinkage. As both mortar and block are concrete products, the shrinkage behaviour of the concrete blockwork behaves in similar manner as other concrete products. Since mortar is much weaker, the resultant shrinkage of the blockwork would be expected to be higher than the blocks alone.

2.3.3.2 Factors affecting shrinkage

The factors that affect shrinkage of concrete in general would, thus, affect the shrinkage of blockwork. The major factors affecting shrinkage of blockwork are method of curing, time of exposure, age at laying, moisture content, humidity, type of aggregate/mix and mortar.

Curing methods adopted in the manufacture of blocks may be classified into four categories, namely: moist air curing, low temperature steam curing at atmospheric pressure, high temperature steam curing at atmospheric pressure and high pressure steam curing (autoclaving). It has been shown that nearly the same final shrinkage of block units was obtained when cured at atmospheric pressure regardless whether in moist air, low temperature steam or high temperature steam. However, high pressure steam curing has been shown to reduce shrinkage to about half the shrinkage attained by other

methods. It has been pointed out that the main reason for autoclaving concrete products having a reduced shrinkage is due, largely, to the formation of a crystalline form of tobermorite in the process.

Numerous results have been reported showing an initial rapid shrinkage which then gradually diminishes to stability at 1 to 3 months. The longer the blocks are allowed to be exposed in air before laying, the smaller the shrinkage that subsequently occurs in the masonry. In general, it has been found that not much advantage is gained by storing units in air for more than 28 days.

For autoclaved products, the amount of shrinkage is approximately inversely proportional to the humidity level, i.e. the lower the humidity the higher the shrinkage. For air cured products, maximum shrinkage occurs when exposed to 40-50% relative humidity.

Another factor that influences shrinkage in blockwork is the type and amount of aggregate used in the manufacture of the blocks. The different shrinkage associated with different aggregates is attributed to the stiffness of the aggregates, since stiffer aggregates provide greater restraint to shrinkage of the cement paste. It follows that the elasticity of the masonry units will affect its shrinkage, as a low modulus will offer less restraint to the shrinkage of mortar.

It has also been reported[27] that the initial shrinkage, which takes place in a concrete block before being built into a wall, does not affect the subsequent behaviour of the wall. On the other hand, shrinkage of walls built with fresh mortar joints are influenced by plastic as well as the drying shrinkage of the mortar. In a wall, the mortar is restrained by the surrounding blocks or, in turn, the blocks may be restrained by the mortar. The restraints are effective in reducing the amount of shrinkage. Different mortars have only a minor effect on shrinkage of unrestrained walls, and no significant

effect on the restrained walls, while blocks built in restrained walls have a slightly smaller shrinkage than free blocks, a finding which has been attributed to the restraint offered by the mortar.

Very few reports are available on shrinkage of blockwork in connection with creep. Lenczner[7] reported shrinkage at 320 days of 410 x 10^{-6} for concrete blocks with a compressive strength of 5.63 MPa, and shrinkage of 525 x 10^{-6} for the subsequent blockwork which accounted for 31%-42% of the maximum overall total strain for the range of stress levels used in the tests. Brooks and Bingel[32], who were looking at the effect of size on shrinkage of lightweight concrete masonry, showed that the ultimate shrinkage in the lateral and vertical directions to be similar for single leaf wall, but the lateral shrinkage was greater for solid pier, and they attributed this to the anisotropy of shrinkage of the block units. The ultimate shrinkage was found to range from 217 x 10^{-6} to 522 x 10^{-6} in the vertical direction and 460 x 10^{-6} to 474 x 10^{-6} in the horizontal direction, the lower values being for the larger masonry units.

2.4 Creep

The study of creep in masonry has been made by a number of researchers[1-26], but however, such results are still sparse and cover only a small aspect of masonry. Most of the researches have been made on clay brickwork and concrete blockwork, the former being in the United Kingdom, while, the latter in Canada. However, very few reports are available on calcium silicate masonry and, also, on mortar and the individual units.

2.4.1 Brick and brickwork

2.4.1.1 Mechanism of creep

To date, it is still not possible to explain with any degree of certainty the basic cause of creep in clay bricks, thus clay brickwork. However, it can be expected to show some similarity to that of concrete. Lenczner[19] suggested that creep in brickwork was

due to the internal seepage of absorbed layers of water in mortar and, to a much lesser extent, a crystalline rearrangement of the ceramic matrix under pressure of the externally applied load.

Johnson[25] stated that the process of creep in bricks is identical to mortar (concrete) but with two limitations. Firstly, the overall porosity of bricks is less than that of mortar and thus the ultimate creep will be relatively less, because there is less creep capacity, and secondly, creep in bricks will start to diminish sooner than creep in mortar because the increased ratio of large to small voids allows seepage to occur at an increased rate and with greater ease. It is probable that the viscous component of creep in bricks will constitute a larger proportion of the overall creep than in mortar. This is because seepage component is relatively small and also, the glass matrix of the bricks is known to be highly viscous at normal working temperature.

2.4.1.2 Past research on creep in brickwork

An early report on creep in masonry was that by Nylander and Ericson[1], who tested piers constructed from clay, lightweight concrete and concrete bricks under sustained compressive stresses of 0.8, 0.3 and 0.6 MPa, respectively, for 400 days. The creep strains were very low, but the specific creep being in the order of 25, 80 and 80 x 10^{-6} per MPa, respectively, and that the strain ratios (the ratio of maximum total load strain to instantaneous strain) were generally less than 1.4. The lime-rich mortars tended to produce considerably larger creep than the cement-rich mortar, but after 400 days the difference in total creep was small. Sahlin[47] reported two tests on clay masonry in which the loads were increased by increments to a maximum of 1 MPa. The load strain of the wall built in lime mortar was six time greater than for lime-cement mortar.

Poljakov[2] tested a series of brickwork prisms using a lever-type loading system. He subjected the brickwork specimens to sustained loads of 0.4 to 0.6 stress/strength ratio and found that the ultimate creep to be between 85 to 135% of the elastic strain. Specimens loaded at the age of 4 days developed 50% more creep than that loaded at

10 days, thus showing a significant effect of age of loading. He also obtained an approximately logarithmic relationship between creep and stress/strength ratio, and for stress/strength ratio of less than 0.6, the relationship could be replaced by a linear one. A more general exponential-type equation was also developed to express masonry creep as a function of age at loading, duration of load, stress/strength ratio and the type of brickwork. Some specimens were also tested under eccentric compressive load with an eccentricity ratio (eccentricity/depth) of 0.15 to 0.35, and it was found that there was no significant effect of eccentricity on creep of brickwork.

A substantial contribution on the work on creep in masonry had been by Lenczner[3-20], who had reported the influence of many factors on creep of masonry. His early work[4] was carried out on brickwork built using specially manufactured half-size model bricks (100 x 52.4 x 33.3 mm) and 1:1:6 (cement:lime:sand) mortar, with the purpose of cutting down on the size and capacity of testing machines. Hollow piers were 12 courses high and 4 bricks wide with 4.8 mm mortar joints, and single-leaf panels were approximately 1.27 m high and 0.71 m wide. The model bricks were laid, saturated-surface-dry, and tested in a controlled environment for about 70 days and in some cases up to 6 months. Creep strains were high: at 70 days creep varied from 730 x 10^{-6} at a stress/strength ratio of 0.06 to 4677 x 10^{-6} at a stress/strength ratio of 0.8. The creep of the single-leaf panels was about 20% lower then the piers. However, subsequent research showed that the model brickwork did not correctly represent the creep behaviour of full-size brickwork.

Lenczner's[5] later investigation was on hollow piers 1 m high built from full size bricks of 99 MPa compressive strength, and 1:$\frac{1}{4}$:3 and 1:1:6 lime mortar mixes of strength 16 and 7.8 MPa, respectively. Tests were conducted in an uncontrolled environment. The level of creep was found to be only 25% of that measured in the earlier model brickworks, hence, indicating the importance of size of units. A 'secondary creep' was observed at approximately 80 days after the application of load for brickwork

containing the 1:1:6 mortar. The brickwork containing the 1:1:6 mortar showed a higher maximum load strain/instantaneous strain ratio than brickwork containing the 1:$\frac{1}{4}$:3 mortar, and also, the creep of brickwork with the former mix started to diminish after a longer period than the latter mix, thus showing the influence of mortar type.

In 1971, Lenczner[6] showed that creep increased with applied stress and also, piers built from stronger bricks exhibited less creep than piers built from weaker bricks. When a damp proof course (d.p.c) was introduced at the bottom course, the creep strains measured above the level of d.p.c were found to be considerably greater than corresponding values without the d.p.c and he attributed this to the smaller lateral restraint above the d.p.c. When a strict control on temperature and humidity was imposed, there were increases in both the load and creep strains, and in the ratio of maximum load strain to instantaneous ratio, for the same stress/strength ratio. However, the 'secondary creep' was observed in brickwork tested in both controlled and uncontrolled environment.

Further tests were carried out by Lenczner et al[8] to look at the effect of stress level on creep of brickwork piers using Fletton bricks and a 1:$\frac{1}{4}$:3 lime mortar. For the stress/strength ratio in the range of 0.38 to 0.55, creep increased with stress with an exponential relationship.

The effects of age at loading and eccentricity of load were also examined by Lenczner and Salahuddin[11] who loaded single-leaf walls from Fletton and Staffordshire blue bricks with a 1:$\frac{1}{4}$:3 lime mortar. The walls were loaded at 14 and 28 days and they concluded that the age at application of load, provided it was greater than 14 days, did not significantly affect the creep behaviour. However, ages less than 14 days were not examined. Small eccentricities were also found not to affect the creep behaviour. Measurements were also made on bricks embedded within the wall and isolated individual bricks. An erroneous result was obtained on the embedded bricks, and the

isolated individual bricks effectively ceased after 30 days while creep in the brickwall continued for a long period, which indicated the major portion of creep in brickwork occurred in the mortar joints, accounting for 80% of the brickwork creep.

Lenczner[10] loaded a 2.215 m high and 0.897 m wide single-leaf wall constructed from London bricks with a 1:$\frac{1}{4}$:3 lime mortar. The maximum load strain of the single-leaf wall was 4.5 times greater than in hollow piers of previous reported tests of similar composition. He showed that the ratio of maximum load strain to instantaneous strain for hollow piers was 2 but it ranged from 3 to 4 for the walls. He attributed the subsequent decrease in the load strain to the difference of moisture strains between the loaded and control piers. However, this is not convincing, as this phenomena was mainly due to the difference of moisture diffusion rate. This aspect is dealt in detail in Chapter 3. He also reported that the bottom embedded brick showed the highest load strain, whilst the top brick the lowest. The highest lateral extensional load strain was also observed in the lower brick but the lowest strain occurred in the centrally embedded brick and not at the top brick.

Lenczner[14] also tested separate brickwork walls and blockwork walls to look into the composite effect of a cavity wall built from both brick and block units. When the elastic and creep parameters of the separate brickwork and blockwork walls were combined in a modified Kelvin model, there was a reasonably accurate prediction of the composite brick/block cavity wall.

Results of the analysis on the available but limited data on creep of masonry have been presented by various investigators. Wyatt and Morgan[21] tried to fit data from other investigators into a mathematical model. They showed that creep in masonry can be represented satisfactorily by a logarithmic relationship as:

$$\varepsilon = \frac{1}{E_w} + F(K)\ln(t+1) \qquad (2.15)$$

where ε = total strain per unit stress;

E_w = modulus of elasticity;

$F(K)$ = creep rate;

and t = time after loading in days.

Warren and Lenczner[22] used Ross's equation[30] as proposed for concrete in the hyperbolic form :

$$c = \frac{t}{(a + bt)} \tag{2.16}$$

By rearranging the equation in a form,

$$\frac{t}{c} = a + bt \tag{2.17}$$

Where c = creep; t = time ; a and b are constants.

Coefficients a and b can thus be obtained using a linear regression. For Equation (2.16)

1, as $t \rightarrow \infty$, $c \rightarrow 1/b = c_{max}$ or c_u.

They defined a parameter, strain ratio, S_R as,

$$S_R = \frac{\text{(Maximum Load Strain)}}{\text{(Instantaneous Strain)}} = \frac{\varepsilon_{max}}{\varepsilon_i} = \frac{(\varepsilon_i + c_u)}{\varepsilon_i} \tag{2.18}$$

Two equations were given;

For single-leaf wall for bricks laid dry,

$$S_R = 8.346 - 0.6153\sqrt{f_b} \tag{2.19}$$

and for bricks laid wet,

$$S_R = 4.2537 - 0.3058\sqrt{f_b} \tag{2.20}$$

Based on the results of his investigations, Lenczner[16] later gave two general equations which relates strain ratio (S_R) with brick strength;

For single-leaf brickwork walls,

$$S_{R1} = 5.46 - 0.33\sqrt{f_b} \tag{2.21}$$

and for brickwork piers,

$$S_{R2} = 2.73 - 0.14\sqrt{f_b} \tag{2.22}$$

Although earlier he had suggested an empirical equation to relate the strain ratio with the brickwork strength[13], the above equations were in fact more applicable because there was no a widely accepted method for testing brickwork strength. Although the bricks contributed little creep, they do restrain the lateral strain in mortar by virtue of the bond between them and this, in turn, affects the vertical strain. It follows that the stronger the brick, the more rigid it is and therefore the greater the restraint that it imposes on the mortar, resulting in lower creep. Figure 2.3 shows the variation of strain ratio for brickwork walls and piers with the square root of brick strength as derived by Lenczner.

Brooks[23] showed that Eq.(2.21) predicted the strain ratio of Fletton single-leaf wall to within 30% but overestimated the strain ratio of calcium silicate single leaf wall by 117%, and implied that the above may be applicable to clay brickwork only. Under a sustained load of 3MPa, and laboratory condition of 19±2°C and 67±5% relative humidity, he obtained the ultimate creep coefficients of Fletton and calcium silicate single-leaf walls to be 1.17 and 1.45, respectively. Testing single leaf walls at 20°C and 65% relative humidity, Schubert[26] reported creep coefficients ranging from 0.4 to 1.3 for clay bricks and ranging from 1.1 to 1.9 for calcium silicate bricks.

By analysing his own creep data, Lenczner[19] gave an empirical relationship between coefficients a and b from Eq.(2.16) for brickwork walls as,

$$a\sigma = 3.81 \ln(b\sigma) + 18.21 \tag{2.23}$$

where σ = stress.

No similar relationship was given for brickwork piers.

Recently, Lenczner[20] showed that Eq.(2.21 and (2.22) only apply to brickwork loaded at design stress or lower in case of single leaf walls because they overestimated the amount of creep for walls loaded higher than the design stress. He also showed that specific creep decreases with an increase in stress level. However, he concluded that more tests are necessary to confirm his findings because the results were based on a limited number of tests and because of the inherent variability of brickwork. It is interesting to note that in these later tests, the 'secondary creep' was not observed.

The creep strain distribution in an axially loaded brickwork wall has also been studied by Lenczner and Warren[15]. They reported that bricks were in compression in the vertical direction, the magnitude of compression decreasing from top to bottom of the wall. In addition, bricks toward the centre of the wall were more highly compressed than those towards the edge of the wall in the horizontal direction. The bricks near the wall base were under horizontal compression. While the mortar near the top of the wall was under tension at 600 days, the mortar in the mid-height and lower down was under compression. All vertical mortar joints were in lateral tension with the minimum being recorded at the mid-height.

2.4.2 Block and blockwork

2.4.2.1 Mechanism of creep

The mechanism of creep in blockwork is similar to concrete. In concrete, the mechanism of creep has been the subject of study for many years and many theories has been presented. An extensive review on this subject has been given by Neville et al[103]. However, it is generally agreed that the main mechanisms which describe creep are: (a) viscous flow of cement paste caused by sliding or shear of the gel particle lubricated by layers of absorbed water, (b) consolidation due to seepage in the form of adsorbed water or the decomposition of inter-layer hydrate water, (c) delayed elastic strain due to the cement paste acting as a restraint on the elastic deformation of the

skeleton formed by the aggregate and gel crystals, and (d) permanent deformation caused by local fracture (microcracking and crystal failure) as well as recrystallization and formation of new physical bonds.

2.4.2.2 Past research on creep in concrete blockwork

Tatsa et al[112] tested prisms from concrete hollow blocks and aerated concrete blocks with and without mortar joints, and also single-leaf walls. The reason for using jointless prisms was intended to eliminate the mortar joint effects. The prisms and panels were loaded at 0.45 of the ultimate strength of the blocks using prestressing strands under two environmental conditions: firstly, by storing the specimens for at least a week before prestressing and secondly, by prestressing after 24 hours curing under water; subsequent storage of the loaded specimens was at 20°C and 50% relative humidity. The 210-day creep of the in-situ hollow blocks were 10.6×10^{-6} and 13.4×10^{-6} for the former and the latter exposed conditions, respectively, and corresponding creep for aerated blocks were 10.6 x and 15.7×10^{-6}. The shrinkage was high with values of 135 x 10^{-6} and 220 x 10^{-6} for hollow blocks, and 150 x 10^{-6} and 330 x 10^{-6} for the aerated blocks for the respective storage conditions. The ratio of mortar creep to block creep was found to be 4.4 for non-presoaked hollow block masonry, but increased substantially to 16.8 for the pre-soaked masonry. For the aerated concrete masonry the corresponding values were 2.3 and 8.9.

Lenczner[7] tested 4-course high hollow piers from 457 x 229 x 102 mm concrete blocks with crushed limestone as aggregate and a 1:1:6 lime mortar mix. The blockwork was loaded at 4 stress levels ranging from 0.78-1.89 MPa (0.184-0.447 stress/strength ratio) under a controlled laboratory condition of 20°C and 50±3% relative humidity. Creep at 300 days reached 638 x 10^{-6} and 903 x 10^{-6} for the lower and upper range of load, respectively, which was considerably higher than creep of brickwork of his

previous tests at similar stress level. The strain ratio (S_R) decreased with increasing stress/strength ratio, being 7.64 and 4.27 for stress/strength ratios of 0.184 and 0.447, respectively.

Ameny[36] reported creep tests on 5-stack bonded prisms built from lightweight concrete blocks and a 1:1:6 lime mortar mix. The prisms were loaded at stress levels corresponding to stress/strength ratios ranging from 0.17 and 0.4 at the age of 7 days and it was found that within the stress range creep was proportional to stress/strength ratio. The 110-day creep ranged between 132 - 191 x 10^{-6} and the extrapolated the ultimate creep coefficient ranged from 1.09 - 1.64. The mortar mix and eccentricity of loading were reported not to affect creep. The overall creep of blockwork was found to be 18 - 43% higher than creep in the embedded blocks and it was concluded that creep in lightweight concrete blocks was of the same order of magnitude as creep in concrete made from similar materials.

Schubert[26] has reported values of creep coefficient of 0.8 to 2.3 and 1.0 to 4.0, respectively for lightweight and aerated concrete single-leaf blockwork.

2.4.3 Factors affecting creep in masonry

A considerable review on the factors that affect creep in concrete has been given by Neville et al[103]. It can be implied that factors which affect creep in concrete would also affect creep in masonry. However, the degree and extent can be different, due to the composite effect of the units and mortar joints. Various factors have been reported to have affected the behaviour of creep in masonry, such as: type of unit, type of mortar, relative humidity, age at loading, stress/strength ratio, slenderness ratio, eccentricity and geometry of masonry.

Masonry from concrete blocks has been found to creep more than brick masonry when tested using a similar mortar type and loading conditions[16]. The creep of calcium silicate brickwall was found to be less than that of Fletton brickwall[23] under

the same stress. Experimental evidence has also shown that masonry made from lightweight concrete block did not creep any more than normal weight concrete[2,36]. Also, brickwork made from low strength Fletton fired bricks showed more creep than that made from high strength Butterly bricks[6].

The above factors can be associated with the strength and absorption properties of the units which affected creep in different ways[19]. Stronger units are generally more rigid and allow less spread of mortar under a vertical load. This, in turn, reduces the vertical strain in the mortar where most of the creep occurs. The effect of absorption of the brick is more complex. On the one hand, bricks absorb water from the mortar and thus increase its strength, leading to a lower creep. Too much absorption, however, leaves insufficient water in the mortar for complete hydration, leading to a lower strength and thus, higher creep. There appears to be an optimum value of water content within the units and mortar for minimum creep.

Most of creep in masonry occurs in the mortar bed joints. However, there is a difference of opinion as to whether creep in masonry is affected by the mortar type or otherwise. Poljakov[2] showed that lime mortars creep more than Portland cement mortar, but Lenczner[4] showed that creep in brickwork piers using a 1:1:6 lime mortar did not significantly differ from brickwork with a $1:\frac{1}{4}:3$ lime mortar. Ameny[36] stated that in his earlier tests, that there was no significant difference of creep between a 1:1:6 lime mortar and a 1:3 (masonry cement:sand) mortar. It is well known that in concrete technology, creep is affected by strength and material composition[103]. It can thus be inferred that the higher the strength of mortar, the stiffer it is (the higher the elastic modulus) and hence the lower the amount of creep. However, for bedded mortar, with its relatively thin layer and the complexity of mortar-brick interaction, this aspect requires further investigation.

As for shrinkage, creep in brickwork has also been reported to decrease with an increase in the ambient relative humidity[6]. The moisture movement depends on the

water content of mortar mix and its consequent degree of freedom to move to its surrounding[25]. In exception, oven dried prisms exhibited increased creep with increasing humidity, due to absorption of moisture from atmosphere and its subsequent seepage within, or from, the specimen[24]. Temperature is an external parameter whose influence on creep and masonry depends on the magnitude of temperature range[10]. Temperature affects the properties of masonry components and the rate of moisture movement within the masonry member and hence creep. However, in the range 15 to 25°C the effect of temperature was negligible[24].

The degree of saturation of clay bricks at loading had a significant effect on creep of clay brickwork depending on the relative humidity during the test[24]. At low humidities creep increased with increasing saturation but at a decreasing rate. At higher humidities, creep increased to a maximum at a value of saturation, and as saturation increased this maximum value of creep decreased. Whereby, the value of critical saturation decreased with increasing humidity.

As stated earlier, no significant influence of age at loading has been detected for period longer than 14 days. However, specimens loaded at 4 days developed 50% more creep than specimens loaded at 10 days[2]. It would be expected that the effect will be more significant for mortars and concrete blocks than for fired bricks because of the gradual hardening of the cement paste.

Creep in masonry increases with stress and the relationship between creep and the stress/strength ratio has been found to be approximately linear within the expected design stress levels. At stress/strength above 0.5 creep increases exponentially with applied stress. The maximum strain ratio, S_R, does not quite depend on the stress, although in the case of Fletton brickwork the ratio appears to increase significantly with the stress/strength ratio. In the case of blockwork piers, Lenczner[7] found that the strain ratio decreased with an increase in stress/strength ratio.

It has also been reported that a small eccentricity does not influence creep in masonry. The geometry of masonry has also been recognised to be affecting creep in brickwork. Creep in single-leaf walls have been found to be 3-4 times the value for piers of the same bricks[16]. The presence of damp-proof course in the bed joint in brickwork piers increases the creep by a factor of two or more[6], which is attributed mainly to the reduction of lateral strain which, in turn, increases the axial strain of the member.

The history of previous loading has been noted to have an effect insofar as it increases the elastic modulus in brickwork piers and walls when stress is subsequently increased, although the effect of creep reduced the effective modulus[14]. The increased elastic modulus was thought to be due to precompression or hardening or a combination of both. In such a case creep is expected to be less compared to that of a member with no previous loading history.

2.5 Method of predicting elastic, and creep and moisture strains

The prediction of elastic strain and creep generally involves 3 methods: (i) from empirical expressions which was derived by fitting data collected for more than two decades, (ii) from a suitable creep-time expressions which enable creep to be predicted and long-term values can be extrapolated from data taken from a reasonably shorter duration, and (iii) from composite models where the data from the individual component materials are combined to estimate the performance of the composite masonry. The third method is presented in Chapter 4.

Lenczner[19] has illustrated the procedure in which some of the empirical equations given in the review can be used to predict the elastic strain and creep in brickwork:

(a) Modulus of elasticity

Equations already exist that relate the elastic modulus of brickwork with brickwork strength. BS 5628: Part 2; 1985[46] recommends the equation:

$$E_w = 900 f_k \tag{2.24}$$

where f_k is the characteristic compressive strength of masonry. The typical relationship between f_k and strength of unit for different mortar mixes, as given in BS 5628, is shown in Fig. 2.4.

Lenczner[19] recommends the use of an update version of Eq.(2.13) as follows:

$$E_w = 3750\sqrt{f_b} - 1000 \tag{2.25}$$

where E_w is the elastic modulus of brickwork (in MPa) and f_b is the strength of the brick units (in MPa).

Eq.(2.25) applies mainly to brickwork with mortar designation (i) but gives reasonably good results when mortar designation (ii) is used. For f_k greater than 6.5 MPa, Eq.(2.25) gives a higher modulus than Eq.(2.24).

(b) Creep

The parameter, 'creep coefficient', ϕ_∞, as used in concrete technology, is more convenient for predicting creep than the strain ratio, S_R. It is defined as the ratio of ultimate creep to instantaneous strain, or,

$$\phi_\infty = \frac{\varepsilon_u}{\varepsilon_i} \tag{2.26}$$

For practical purposes it may be assumed that the instantaneous strain equals the elastic strain, ε_e. For a given brick and mortar designation (i) or (ii), ϕ_∞ remains sensibly constant for stress levels in the region of the brickwork working stress, and this makes it convenient for design purposes. Thus, Eq.(2.21) and Eq.(2.22) can conveniently be rewritten as follows:

for single-leaf walls,

$$\phi_{\infty} = 4.46 - 0.33\sqrt{f_b} \tag{2.27}$$

and for piers (hollow),

$$\phi_{\infty} = 1.73 - 0.14\sqrt{f_b} \tag{2.28}$$

For the walls with bricks laid dry, for example an internal wall, an Eq.(2.19) has been recommended.

Figure 2.5 show the value of ϕ_{∞} for brickwork walls and piers with mortar designations (i) and (ii) for different values of f_k, which can be used for design purposes as an alternative to Fig. 2.3. It should be noted that Eq.(2.28) is based on tests on hollow piers and not solid piers or columns.

Knowing the creep coefficient for a particular brickwork from either Eq.(2.27) or Eq.(2.28), the ultimate creep can be computed from Eq.(2.26).

The different Standard Codes[46,113-114], at the moment only give a single 'ultimate' value for the different types of material. These values, as given in Table 2.5, have been obtained by extrapolation by the Ross equation (Eq. (2.16)).

(c) Moisture movement

Typical design ranges for shrinkage, as given by design guides[46,85,113] are given in Tables 2.6-2.7. The values in Table 2.7 were obtained by the use of method (ii) i.e. by using the Ross equation as for creep,

$$\varepsilon_{sh} = \frac{t}{(a + bt)} \tag{2.29}$$

The reciprocal of coefficient b yields the ultimate value for shrinkage of masonry.

2.6 Conclusions

The study of elastic and moisture movements in masonry has been enormous but the study of creep is still limited. Creep coefficients vary from 0.3 to 5.0 depending on the materials and geometry of masonry. A substantial amount of creep has been measured on existing buildings over the years[18] and also prestress losses in post-tensioned masonry can range between 20-30%. Consequently, creep cannot be ignored in the structural design of masonry.

Most of the investigations into the influencing factors on creep are in general terms only and do not deal with them with sufficient depth. The available data are not always explicit and in some cases not consistent. For example, it is generally agreed that most of the creep in masonry occurs in the mortar bed joints, however, contradictory results exist on the effect of mortar type on creep.

Equations (2.27) and (2.28) are based on clay brickwork using mortar mixes of strength of about 16 MPa, and it is not known if these equations apply to other brickwork of different types of bricks and mortar mixes. The equations are restricted to single leaf walls and solid piers, and estimates of creep coefficient can have errors of up to 30%-117%. In addition, no similar equations exist for blockwork.

It is well known that moisture content affects shrinkage and creep in concrete in many ways. In masonry, the importance of water content has not received sufficient attention. Nearly all the reports do not state the water content used in the mortar mix, probably because workability is more important and water content is highly variable. In most cases the amount of water used is left to the judgement of the mason, although initially a dropping ball test is carried out. In terms of elastic strain, the influence of moisture content in mortar may not be as important because most of the findings relate modulus to the brick strength, but for shrinkage and therefore creep, the effect could be more significant. Another problem which arises is the time to start taking shrinkage measurements in masonry. In the case of concrete, this is normally done after the curing

period. The amount of predrying before starting taking measurements affects significantly the magnitude of 'ultimate' shrinkage, and also affects creep because of a strong creep-shrinkage interaction. Also, the knowledge of irreversible moisture expansion of clay brickwork is lacking. In particular, the interaction of clay brick with mortar and the interaction of moisture expansion with creep.

As stated earlier, although the deformation properties of masonry have long been studied, there is still no recognised standard test procedure for measuring those properties. This hampers the comparison of results and the universal agreement on influencing factors. There is an urgency for standard procedures to be laid down in order to achieve consistency of method of measurement so that data may be compared and collated with confidence.

Table 2.1 - Requirements of Mortar, According to BS 5628[46]

Feature	Mortar Designation	Type of mortar (proportion by volume)			Mean compressive strength at 28 days	
		Cement: lime:sand	Masonry cement:sand	Cement:sand with plasticizer	Preliminary (laboratory) tests	Site tests
					MPa	MPa
Increasing strength ↑ / increasing ability to accomodate movement, e.g.due to settlement, temperature and moisture changes ↓	(i)	1:0 to $\frac{1}{4}$:3	-	-	16.0	11.0
	(ii)	1$\frac{1}{2}$:4 to 4$\frac{1}{2}$	1:2$\frac{1}{2}$ to 3$\frac{1}{2}$	1:3 to 4	6.5	4.5
	(iii)	1:1:5 to 6	1:4 to 5	1:5 to 6	3.6	2.5
	(iv)	1:2:8 to 9	1:5$\frac{1}{2}$ to 6$\frac{1}{2}$	1:7 to 8	1.5	1.0
Direction of change in properties is shown by the arrow		Increasing resistance to frost attack during construction → Improvement in bond and consequent resistance to rain penetration ←				

Table 2.2 - Expansion of Fired Clay Bricks Resulting from Changes in Moisture Content[85]

Clay from which units are made	Irreversible expansion (% calculated on original dry length) for bricks fired to average works temperature		Wetting movement (%)
	from kiln hot to 2 days	from 3 days to 128 days	
Lower Oxford	0.03	0.03	Generally less than 0.02 unless under fired
London Stock	0.05	0.02	
London clay	0.02	0.02	
Keuper marl	0.03	0.02	
Weald clay	0.08	0.04	
Carboniferous shale	0.04	0.07	
Devonian shale	0.03	0.05	
Gault	0.02	0.01	

Table 2.3 - Moisture Expansion of Fired Clay Brickwork[85]

Walls built of bricks made from:	Expansion at constant temperature (%)			
	Total after 15 days	Rate per 10 days after 15 days*	Total after 300 days	Rate per 10 days after 300 days*
Glacial clay	0.015	0.0026	0.039	0.0004
Coal measure shale	0.014	0.0027	0.050	0.0008

* *Covering the 5 day period either side of the 15 and 300 day period*

Table 2.4 - Drying Shrin kage of Concrete and Calcium Silicate Units (the upper limits are those set by the relevant British Standards)[85]

Material	Shrinkage (%)
Concrete bricks or Type A concrete blocks	0.02 - 0.06
Lightweight concrete blocks	0.04 - 0.09
Calcium silicate (including sandlime)	0.01 - 0.035

Table 2.5 - Creep Coefficient (ϕ_∞) of Masonry as Given by the Various Standard Codes.

Types of masonry	BS 5628[46]	DIN[113] 2-6#	DIN[113] 12-60#	ISO[114]
Fired clay	1.5	0.75	0.75	0.7
Calcium silicate	1.5	0.75	1.5	1.5
Autoclaved aerated concrete	-	2.0	1.5	1.5
Concrete	3.0	2.0	1.5	1.5
Lightweight concrete	-	2.0	1.5	2.0

\# *Strength range in MPa*

Table 2.6 - Typical Moisture Movement of Masonry[85]

Material	Reversible moisture movement (%)	Irreversible moisture movement (+) expansion (-) shrinkage (%)
Clay or shale brickwork	0.02	0.02 - 0.07 (+)
Calcium silicate brickwork	0.01 - 0.05	0.01 - 0.04 (-)
Dense aggregate blockwork	0.02 - 0.04	0.02 - 0.06 (-)
Lightweight aggregate blockwork	0.03 - 0.06	0.02 - 0.06 (-)
Aerated (autoclaved) blockwork	0.02 - 0.03	0.05 - 0.09 (-)
Mortar	0.02 - 0.06	0.04 - 0.10 (-)

Table 2.7 - Typical Shrinkage of Masonry as Given by the Various Standard Codes.

Types of masonry	BS 5628[46]	DIN[113]
Fired clay	0	0*
Calcium silicate	500	200
Autoclaved aerated concrete	500	200
Concrete	500	200
Lightweight concrete	500	400#

* *shrinkage and swelling ranging from -100 to 200 x 10-6, respectively.*

\# *when using natural pumice.*

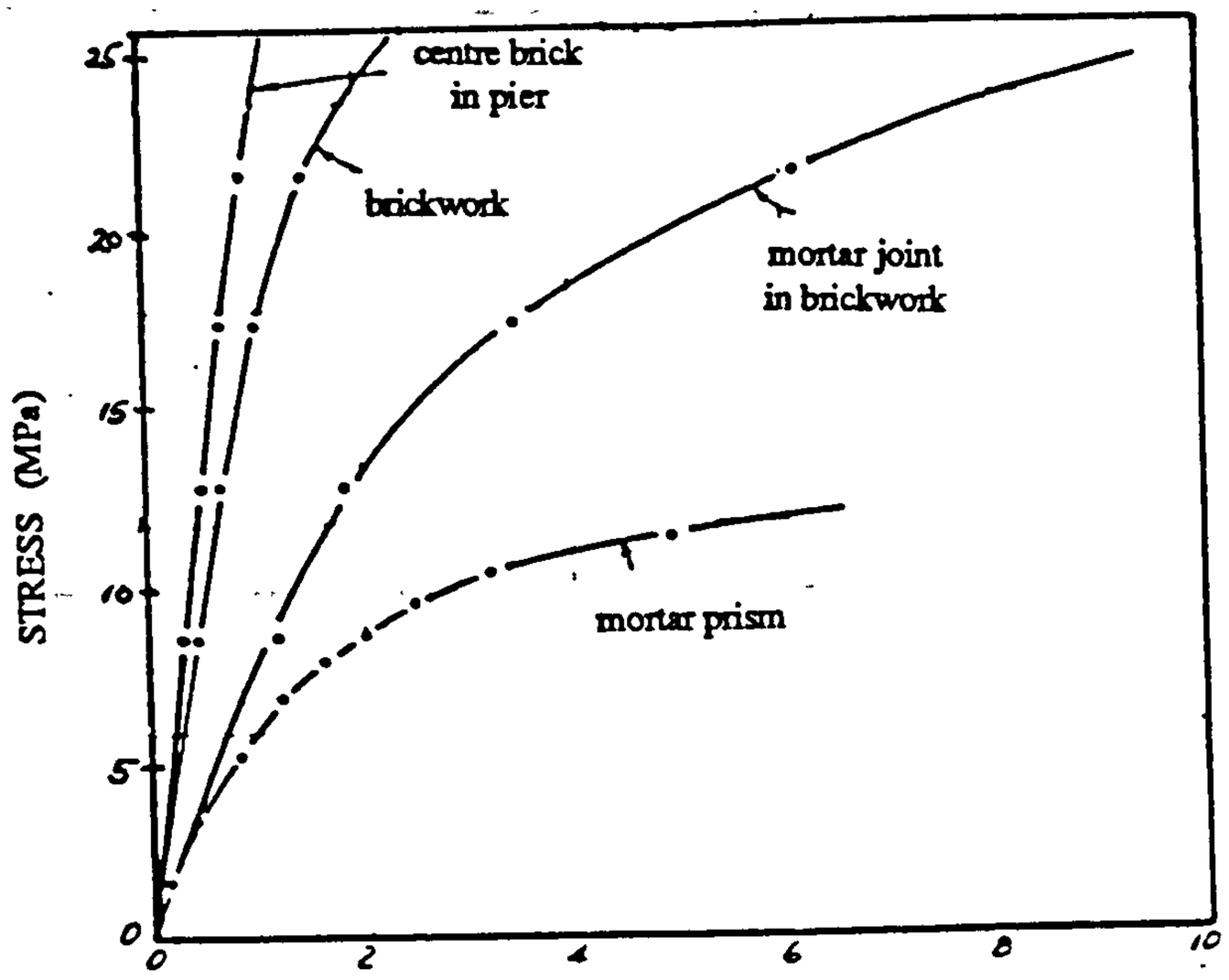

Fig. 2.1 - Stress-strain Curves of Masonry Prism as Measured at Different Positions[51]

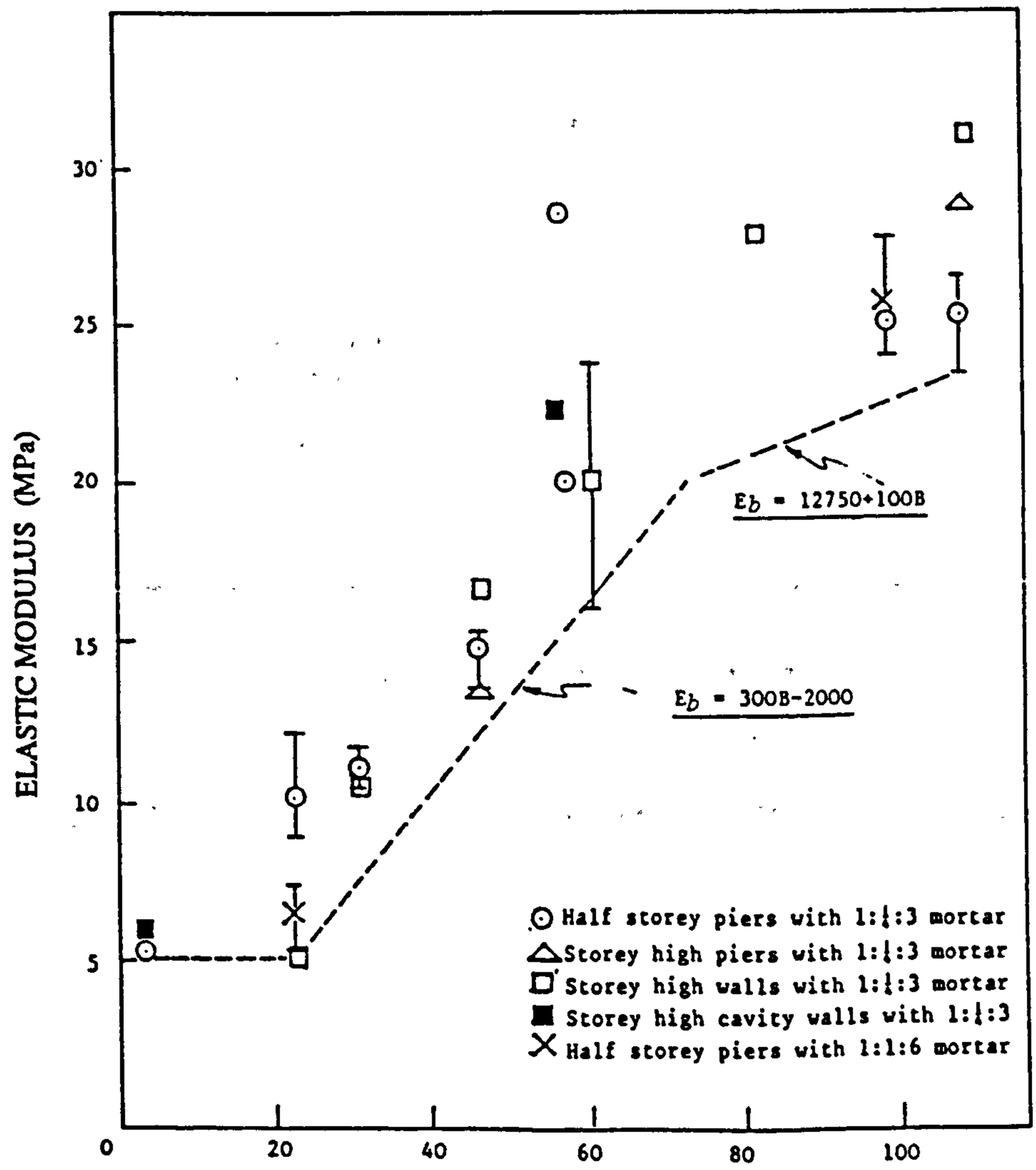

Fig. 2.2 - Variation of the Elastic Modulus of Brickwork with Strength of Bricks[16]

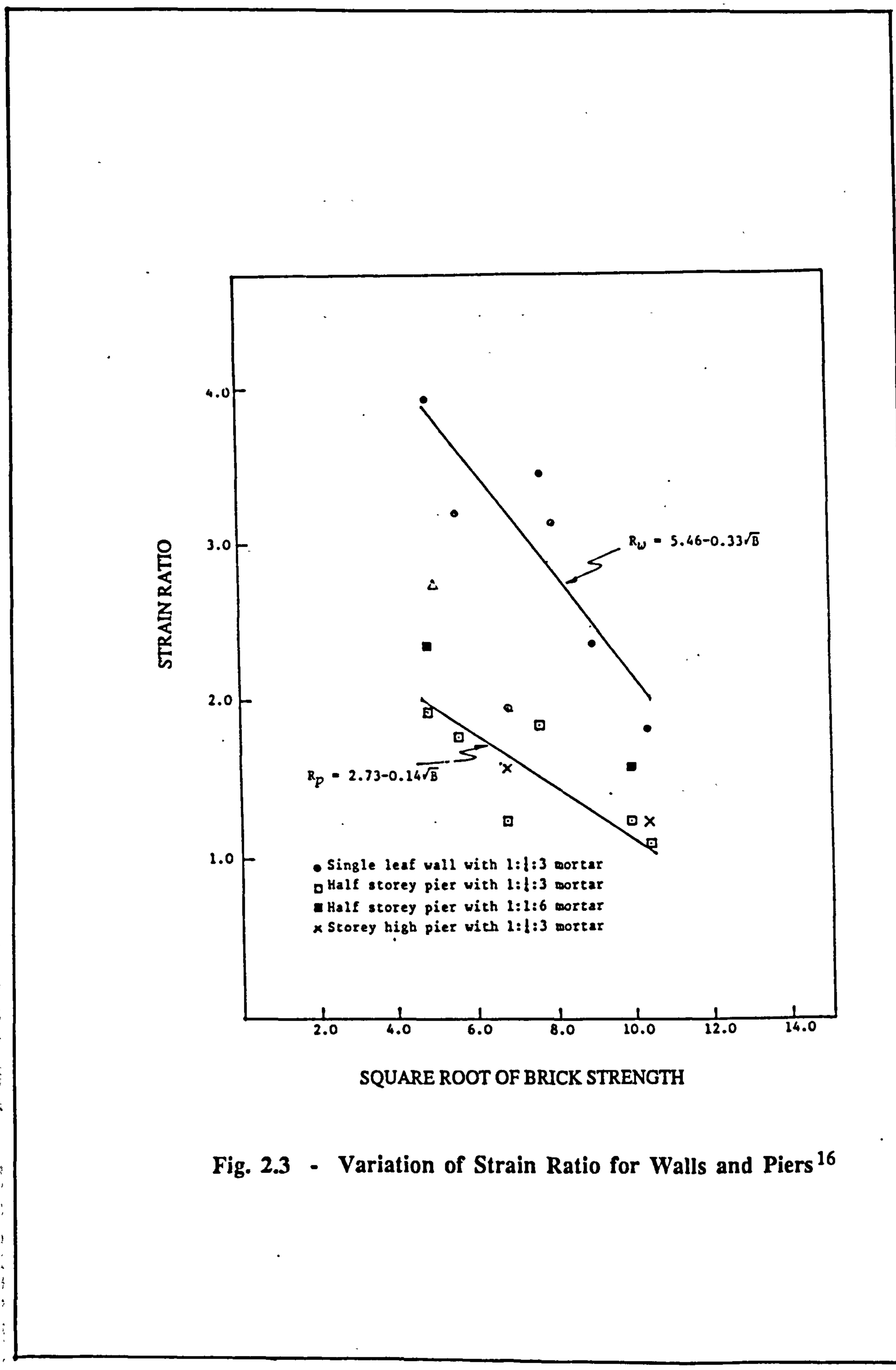

Fig. 2.3 - Variation of Strain Ratio for Walls and Piers[16]

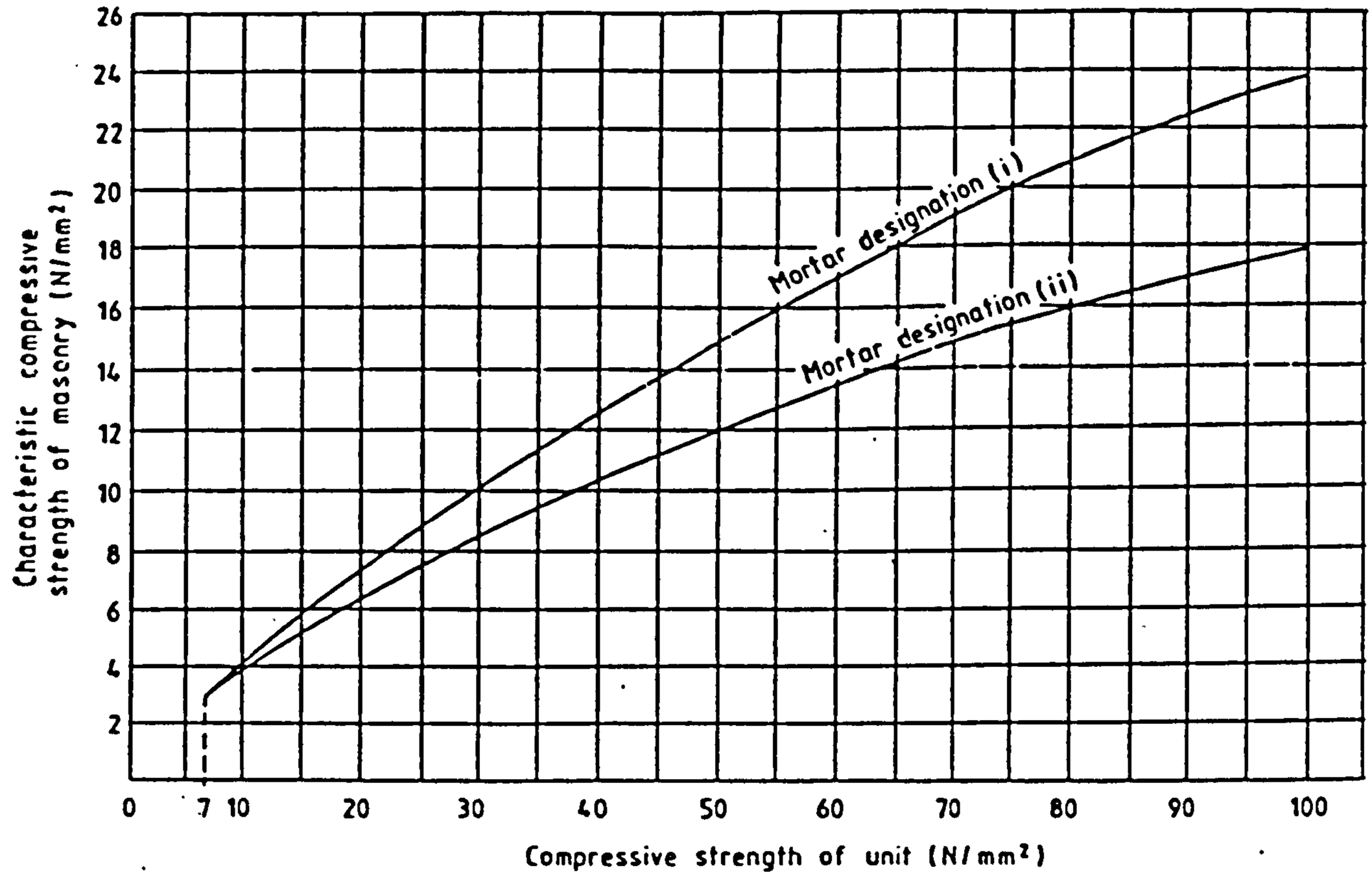

Masonry constructed with bricks or other units having a ratio of height to least horizontal dimension of 0.6

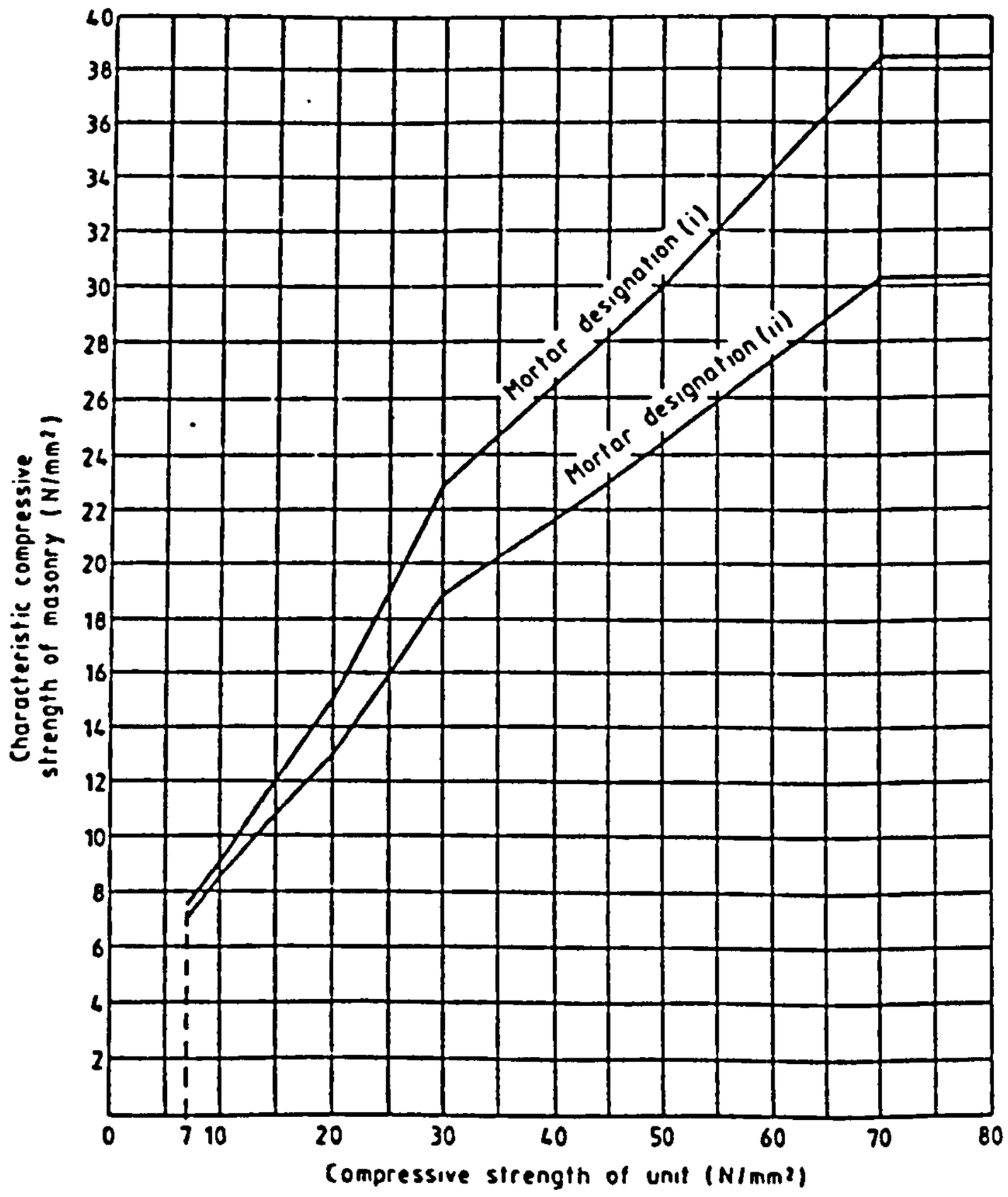

Block masonry constructed with solid blocks having a ratio of height to least horizontal dimension of between 2.0 and 4.0 (see table 3(C))

Fig. 2.4 - Typical Curves for Determining The Characteristic Compressive Strength of Masonry as given in BS 5628[46]

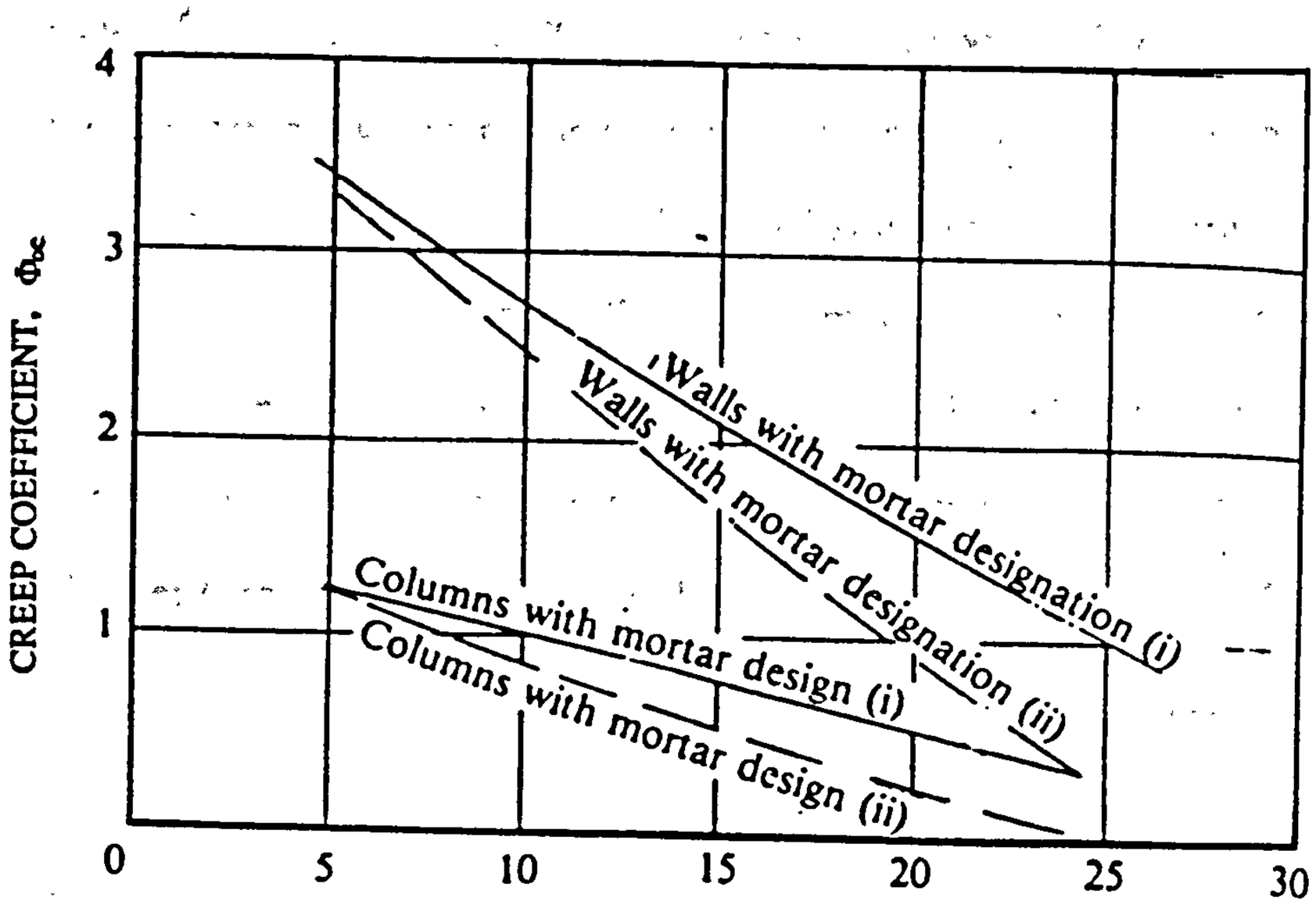

Fig. 2.5 - Variation of Creep Coefficient (Φ_{∞}) with Characteristic Strength of Brickwork (f_k) [19]

CHAPTER 3

EFFECT OF GEOMETRY ON TIME-DEPENDENT DEFORMATION OF CONCRETE

3.1 Introduction

Knowledge of the geometry effect on concrete is important because creep and shrinkage data are generally determined from laboratory cylindrical or prismatic specimens which are normally small in size. In actual situations concrete members are designed in a variety of sizes and shapes. Thus, it is important to relate the laboratory determined values to realistic values in actual structures. For example, it has been reported that the creep and shrinkage deflections of some concrete bridges are considerably higher than predicted by design based on laboratory specimens[94].

The influence of size and shape of members on creep and shrinkage of concrete is well known. Although the similar effect on time-dependent deformation of masonry has also been recognised, it appears that it has not been investigated in detail so that a review of the work for concrete is appropriate.

3.2 Effect of size and shape on shrinkage

Many investigators have looked into the effect of geometry of members on shrinkage of concrete. The approach to this problem has been both theoretical and empirical.

3.2.1 Theoretical approach

The 'linear diffusion theory', which was first introduced by Carlson[88], has been used extensively to predicted the behaviour drying shrinkage of concrete with the belief that moisture movement within the concrete obeys the diffusion theory and that shrinkage should be proportional to the moisture loss of the concrete. A theoretical background on this theory is given by Becker and Macinnis[89]. However, the theory has

been known to give a very poor fit of experimental data over long periods of time because drying in concrete is a highly non-linear problem[90]. Notably, as drying progresses the remaining moisture is lost with ever increasing difficulty and drying becomes much slower than an extrapolation of the initial drying curve which a linear diffusion theory would predict[91]. It has been known the diffusivity decreases with water content. Thus, with the availability of computers, the approach has been extended to a more complex 'non-linear diffusion theory'. From these theories mathematical solutions have been obtained for shrinkage for different geometries of concrete members. These theoretical approaches, however, will not be discussed here since their application would be more complex because of the composite nature of masonry and hence would require a separate investigation.

3.2.2 Empirical approach

After experiencing difficulty in using the diffusion theory in handling irregular shaped members, Ross[92] introduced a surface/volume ratio (S/V) as an indicator of size and shape of concrete members. The concept is that members having the same surface/volume ratio shrink in the same fashion. However, the most commonly used parameters to indicate the size and shape effect are the volume/surface area ratio (V/S), effective or theoretical thickness (T_e or h_o), average thickness (T_a) and equivalent thickness (T_d). All these parameters are to indicate the 'average drying path' (i.e. the average distance moisture has to travel to the drying surface) of a member. The various parameters are defined as follows:

$$\frac{V}{S}=\frac{\text{Total volume of the member}}{\text{Total drying surface area of the member}} \tag{3.1}$$

$$T_e=2\frac{A_c}{u}=2\left(\frac{V}{S}\right) \tag{3.2}$$

$$T_a=2T_e \tag{3.3}$$

$$T_d = 4\overline{d}_p \tag{3.4}$$

$$\text{where} \overline{d}_p = \frac{\Sigma V_i d_p}{V_t} \tag{3.5}$$

A_c = cross-sectional area of the member;

u = perimeter exposed to drying;

T_d = equivalent slab thickness;

d_p = distance between the centroid and

drying surface of volume V_i;

V_t = total volume of member.

The factor 2 in Eq.(3.2) is to achieve that, for an infinite extending slab, T_e would equal to the thickness of the slab. It can thus be seen that there are only two distinct parameters; firstly based on V/S concept and the other on the equivalent thickness concept. Table 3.1 show examples of these parameters for some typical member shapes.

3.2.2.1 Previous investigations on concrete and masonry

Ross[92] conducted tests of small prisms with various sizes and shapes (i.e. rectangular, square and triangular prisms, cylinders and circular tubes). As stated earlier, he introduced the surface/volume ratio (S/V) as a practical means of comparing the results. He concluded that shrinkage varies enormously with the size and shape of specimens and that the variation was largely a function of the surface/volume ratio. A more comprehensive study was carried out by Keeton[93] who tested specimen shape such as cylinders, square prisms, and I and T-sections. For the same V/S ratio, he obtained higher and faster shrinkage for cylinders than square prisms, with shrinkage of I and T-section in between. However, the ultimate values were inconclusive because of an insufficient observation period. As similar trend was also obtained by Kesler et al[94] for square prisms and cylinders.

L'Hermite and Mamillan[95] tested prisms of various sizes, two of which had similar V/S ratios. With all sides being exposed to drying, the different specimens showed different levels of shrinkage. The specimens with the same V/S ratio also showed a different shrinkage but they commented that the larger specimens were greatly influenced by thermal strains from heat of hydration. The results of their tests suggested that the ultimate shrinkage of all sizes was approximately the same. Figure 3.1 shows the results of their tests. Hansen and Mattock[96] tested cylinders of diameter ranging from 102 mm to 610 mm as well as I-sections. They concluded that both the rate of shrinkage and its ultimate value were influenced by size of specimen. However, the I-sections showed approximately 14% lower shrinkage than the cylinders and that the V/S ratio did not account perfectly for the variation of both size and shape of specimens. Hansen and Mattock's result are shown in Fig. 3.2.

Hobbs[97] conducted shrinkage tests on small slabs and prisms. The prisms were partly-sealed to simulate the slabs by painting with a bituminous material and sealed with a double layer of polythene. It was found that the rate of shrinkage depends upon the specimen size, but became approximately the same after two or three years of drying. According to him the theoretical shrinkage is independent of size but in practise this does not occur because of the effect of carbonation which causesmore shrinkage in smaller specimen. In a related study on moisture profiles in drying concrete, Parrott[98] showed that the weight loss of an unsealed cube specimen to be considerably higher than the part-sealed ones. Also, Terill et al[99] showed a pronounced bi-linear relationship between shrinkage and moisture loss.

Bazant and Panula[100] commented that the use of V/S ratio and effective thickness concepts are insufficient as indicators of the geometry of members. Knowing from previous results, that for the same V/S ratio, that cylinders and spheres shrank more and faster than prisms and cubes, respectively, they suggested a shape factor (k_s) to correct this discrepancy.

Bryant and Vadhanavikkit[87] used of the concept of equivalent thickness (T_d), as that defined in Eq.(3.4) and Eq.(3.5), as an indicator for both size and shape effect. The empirical parameter, T_d, is based on the non-linear diffusion theory. By expressing the coefficient f as a function of size and shape, they suggested an improved equation of that given by ACI-82[27] for shrinkage as:

$$(\varepsilon_{sh})_t = \frac{\left(\frac{t}{T_d^2}\right)^{\alpha}}{\bar{f} + \left(\frac{t}{T_d^2}\right)^{\alpha}} (\varepsilon_{sh})_u \tag{3.6}$$

$$\text{where} \bar{f} = \frac{f}{T_d^{2\alpha}} \tag{3.7}$$

t = time of shrinkage; $(\varepsilon_{sh})_u$ = ultimate shrinkage;

α = time ratio constant for a given member size and shape.

They showed that the modified equation gave a better prediction of the geometry effect on shrinkage of concrete members.

The only published work on the effect of geometry on moisture movement of masonry was by Brooks and Bingel[32], who tested Fletton clay, calcium silicate and lightweight concrete masonry. They concluded that, within the sizes tested, the axial shrinkage of calcium silicate brickwork and lightweight concrete blockwork depended on size, and was linearly related to V/S ratio. Generally, axial shrinkage decreased with increase in V/S ratio, so that piers undergo less shrinkage than walls. However, the lateral shrinkage was independent of size. For Fletton clay brickwork, no definite trend was established because of contradictory results between smaller brickwork and the larger brickwork. However, they commented there was an indication that axial moisture expansion was dependent on size. The linear expression given for axial shrinkage (S_{wy}) of calcium silicate brickwork as a function of V/S ratio was:

$$S_{wy} = x - y\left(\frac{V}{S}\right) \tag{3.8}$$

where coefficients x and y are expressed as hyperbolic function of time t (days):

$$x = \frac{100t}{81 + 0.18t} \tag{3.9}$$

$$y = \frac{t}{9.5 + 0.51t} \tag{3.10}$$

For lightweight concrete blockwork, two expressions were obtained.

For axial shrinkage:

$$S_{wy} = x' - y'\left(\frac{V}{S}\right) \tag{3.11}$$

where

$$x' = \frac{100t}{8 + 0.15t} \tag{3.12}$$

$$y' = \frac{t}{9.3 + 0.30t}, \tag{3.13}$$

and for lateral shrinkage:

$$S_{wx} = x'' - y''\left(\frac{V}{S}\right) \tag{3.14}$$

where

$$x'' = \frac{100t}{5 + 0.21t} \tag{3.15}$$

$$\frac{x''}{y''} = 149 + 0.29t \tag{3.16}$$

Results of their tests are given in Fig. 3.3.

3.2.2.2 Design guides approaches

Standard codes and prediction guides for shrinkage give factors to allow for the size and shape effects and these are discussed in turn.

(a) ACI-82

ACI-82[27] gives a coefficient, k_3', to allow for the size effect in terms of V/S ratio. For values of V/S<37.5 mm, k_3' is given in Table 3.2. When V/S is between 37.5 and 95 mm the coefficients are :

for time of drying ≤ 1 year

$$k_3' = 1.23 - 0.006\left(\frac{V}{S}\right) \tag{3.17}$$

for time of drying > 1 year

$$k_3' = 1.17 - 0.152\left(\frac{V}{S}\right) \tag{3.18}$$

and when V/S ≥ 95 mm,

$$k_3' = 1.2e^{-0.00473(V/S)} \tag{3.19}$$

(b) CEB-FIP (1970)

CEB-FIP(1970)[28] uses the theoretical thickness, h_o' as defined in Eq.(3.2) to obtain the coefficient of theoretical thickness, k_4. The relationship between k_4 and h_o' is given in Fig. 3.4.

(c) CEB-FIP (1978)

The CEB-FIP (1978)[29] is a new version of CEB-FIP (1970) which gives allowance for the variation of size effects with the relative humidity. The higher the relative humidity the smaller is the size effect, and shrinkage rates are slower at higher relative humidities. The coefficient for ambient humidity (λ) is multiplied by the theoretical thickness to obtain a modified size called 'notional thickness' (h_o),

$$h_o = \lambda 2 \frac{A_c}{u} \tag{3.20}$$

The value of λ is given in Table 3.3 and the shrinkage coefficient (ε_{sh2}) versus notional thickness (h_o) is shown in Fig. 3.5.

(d) Bazant and Panula (1978)

While the methods above assume that the size effect is independent of time, Bazant and Panula[100] allow for the effect of time. The term shrinkage 'square half-time' in the shrinkage equation given by them is a functions of both the size and shape of member and is given as:

$$t_{(1/2)sh} = 4\left(k_s \frac{V}{S}\right)^2 \frac{1}{D(t_{sh,0})} \tag{3.21}$$

where k_s = shape factor = 1.0 for a slab

= 1.15 for a cylinder

= 1.25 for a square prism

= 1.30 for a sphere

= 1.55 for a cube

3.3 Effect of size and shape on creep

The role of moisture diffusion which affects shrinkage also affects creep of concrete. As for shrinkage, several investigations have indicated that creep decreased with an increase in size of specimens.

Weil[101] tested cylinders of diameters ranging from 100-600 mm and found that the effect of size on creep increased during the first 60 days after the application of load, but the differences in creep between the different specimen sizes were approximately constant thereafter. Results of his experiments are shown in Fig. 3.6. Keeton's[93] experiments on cylinders showed a similar result. The work of L'Hermite and Mamillan[95] on square prisms having V/S ratio ranging from 17.5 to 50 mm showed that

the effect of size was greatest during the initial period after the application of load and that the rate of creep was the same for all the sizes between 100 and 1000 days after loading. Ulitskii[102] found that both creep and shrinkage showed a similar influence with size of specimen, and hence the relative creep and shrinkage of different size specimens can be calculated using factors given in Table 3.4.

According to Neville et al[103] the original explanation of the size effect in terms of the loss of water to the ambient medium (which would be greater in a small specimen where the surface/volume ratio is larger) can apply only if drying creep takes place, because in basic creep no loss of water to outside is involved. In many practical cases, however, creep and shrinkage operate simultaneously. Thus in a small specimen a greater part of the concrete is subjected to creep while drying takes place, and a larger creep is therefore recorded. The converse is true in a larger specimen, and even if, with time, the drying effect reaches the core, the concrete there will changed substantially from the state which existed when load was first applied. A greater degree of hydration will have been achieved and a higher strength will have been developed in the core so that the creep response to the 'creep while drying' condition will be small. This explanation is predicated on the assumption that it is only the drying creep that is subjected to the size effect. However, they stated the tests by Troxell et al indicated that a small size effect is present even with storage in a relative humidity of 100%.

Hansen and Mattock[96] loaded identical specimens as that used for shrinkage test and indicated that both creep and shrinkage are functions of the V/S ratio. It also appeared that after about 100 days under load the creep rate for all sizes was approximately equal to the basic creep rate and when the specimen was fully sealed, creep was unaffected by the size of member. The relation between the creep coefficient and volume/surface ratio given by them is shown in Fig. 3.7. Also, the decrease in creep with increase in size was smaller than in the case of shrinkage. But the rates of change

of creep and shrinkage were the same, indicating the both phenomena were the same function of V/S ratio. These results were obtained for concrete exposed to 50% relative humidity.

As for the effect of shape (for equal V/S ratio), it can be seen from Fig. 3.7 that, its influence on creep is of less importance than in the case of shrinkage. The shape of specimen affects the moisture distribution within it. Neville et al[103] quoted that in a prism the variation in relative humidity along a diagonal was different than along a normal surface. Bryant and Vadhanavikkit[87] showed that the equivalent thickness, T_d, was a better indicator than V/S ratio of size and shape of specimen for both shrinkage and creep as illustrated in Fig.3.8. The concept of 'average' drying path (d_p) is different from that defined by the other parameters, because it also depends on the shape of specimens. On the whole, however, the shape factor is of very much lesser importance than size factor and, for most practical purposes, can be neglected[103].

3.3.1 Design Guides Approaches

(a) ACI (1982)

ACI-82[27] gives the coefficient k_3 for member size in terms of V/S ratio. For members having values of V/S ratio less than 37.5 mm, k_3 is given in Table 3.2. When V/S is between 37.5 and 95 mm, k_3 is given by:

for time after loading ≤ 1 year

$$k_3 = 1.14 - 0.00364\frac{V}{S} \tag{3.22}$$

for time after loading > 1 year

$$k_3 = 1.10 - 0.00268\frac{V}{S} \tag{3.23}$$

and when V/S ≥ 95 mm,

$$k_3 = \frac{2}{3}(1 + 1.12e^{-0.0212(V/S)}) \tag{3.24}$$

(b) CEB-FIP (1970)

As for shrinkage, CEB-FIP (1970)[28] uses the coefficient of theoretical thickness, k_4, obtained from the curve shown in Fig. 3.9. The theoretical thickness, $h_0^{'}$, as that defined before in Eq.(3.2).

(c) CEB-FIP (1978)

CEB-FIP (1978)[29] gives an allowance for the variation of size effect with the relative humidity in a similar manner to that used for shrinkage. The coefficient of ambient humidity (λ) is as given for shrinkage in Table 3.3 and the notional thickness (h_0) is obtained as before in Eq.(3.20). The graph of creep coefficient versus notional thickness is given in Fig. 3.10. As with other methods, creep is less affected by specimen geometry than is shrinkage.

(d) Bazant and Panula (1978)

Allowance for size and shape effect of concrete member is similar to that for shrinkage[100], the drying creep coefficient being partially a function of shape factor (k_s) and shrinkage 'square half-time' ($t_{(1/2)sh}$).

3.4 General Remarks

The size and shape of specimens significantly affect the rate of shrinkage and creep development of concrete. Similar trends have been observed on shrinkage of masonry. Generally, the influence of size on creep is less than for shrinkage. At earlier periods the effect is pronounced, but at later periods and thus, for ultimate values, the effect less certain. However, the Standard Codes seem to recognised the size is effect on the ultimate values. The use of V/S ratio has been adopted by the Codes probably because it is the best and the simplest method available. Only recently has the concept

of average thickness been introduced which offers an advantage over the V/S ratio because it also takes into account the shape of a member. From the experimental evidence it was claimed to give better predictions of the geometry effect of both creep and shrinkage. However, the use of V/S ratio is much simpler and for similar shape of specimens it is linearly related to the average thickness as illustrated in Fig.5.5.

Table 3.1 : Examples of V/S Ratio, Effective Thickness (T_e) and Equivalent Thickness (T_d) of Some Member Shapes

Member Shape	$\frac{V}{S}$	$T_e = 2\frac{V}{S}$	$T_d = 4\overline{d}_p$
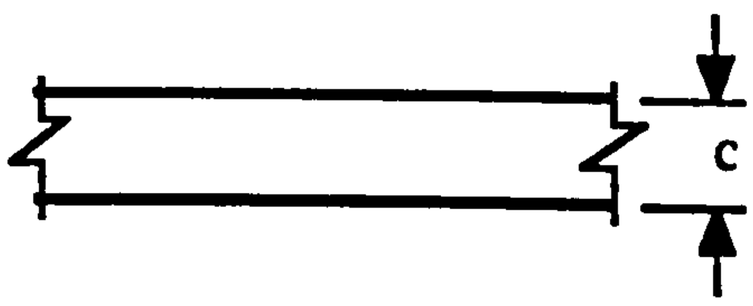 slab	$\frac{c}{2}$	c	c
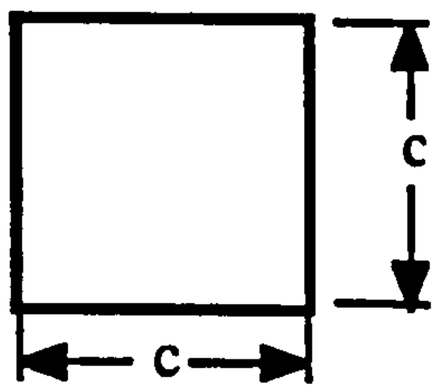 square prism	$\frac{c}{4}$	$\frac{c}{2}$	$\frac{2}{3}c$
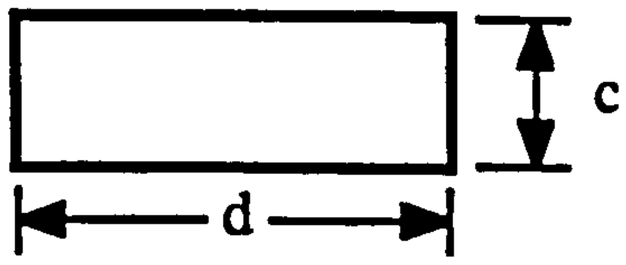 rectangular prism	$\frac{cd}{2(c+d)}$	$\frac{cd}{(c+d)}$	$c - \frac{c^2}{3d}$
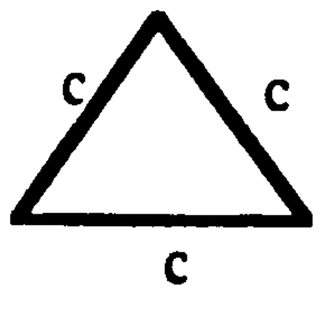 triangular prism	$\frac{\sqrt{3}}{12}c$	$\frac{\sqrt{3}}{6}c$	$\frac{2\sqrt{3}}{9}c$

Table 3.2 : Values of Coefficients to Allow for Member Size in Predicting Creep and Shrinkage as Given by ACI (1982)[27]

V/S ratio (mm)	Coefficient k_3' for shrinkage	Coefficient k_3 for creep
12.5	1.35	1.30
19	1.25	1.17
25	1.17	1.11
31	1.08	1.04
37.5	1.00	1.00

Table 3.3 : CEB-FIP (1978)[29] Coefficient of Ambient Relative Humidity

Ambient Environment	Relative Humidity (%)	Coefficient λ
Water	-	30
Very damp atmosphere	90	5
Outside in general	70	1.5
Very dry atmosphere	40	1

Table 3.4 : Size Factors for Creep and Shrinkage of Concrete Specimen[102] (from Ref. 103)

Minimum Thickness (mm)	Correction factor
<50	1.6
50	1.5
70	1.3
100	1.15
150	1.05
200	1.00
250	0.95
300	0.9
400	0.8
500	0.75
600	0.7
800	0.55
1000	0.5
>1000 and sealed concrete	0.4

NB: if one of the surfaces is sealed, the actual thickness is doubled.

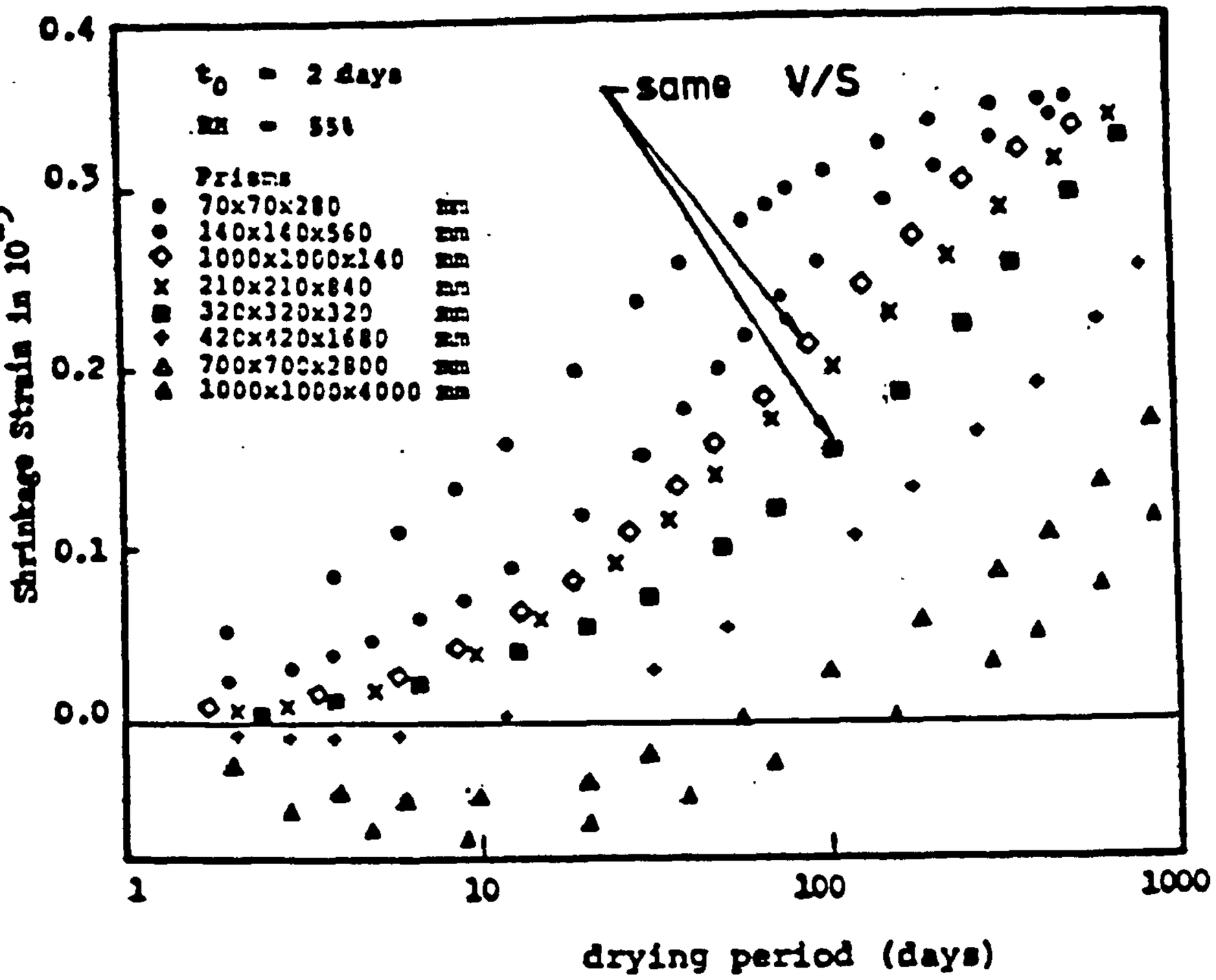

Fig. 3.1 - Results of L'Hermite and Mamillan's Tests on the Effect of Size on Shrinkage of Concrete[95]

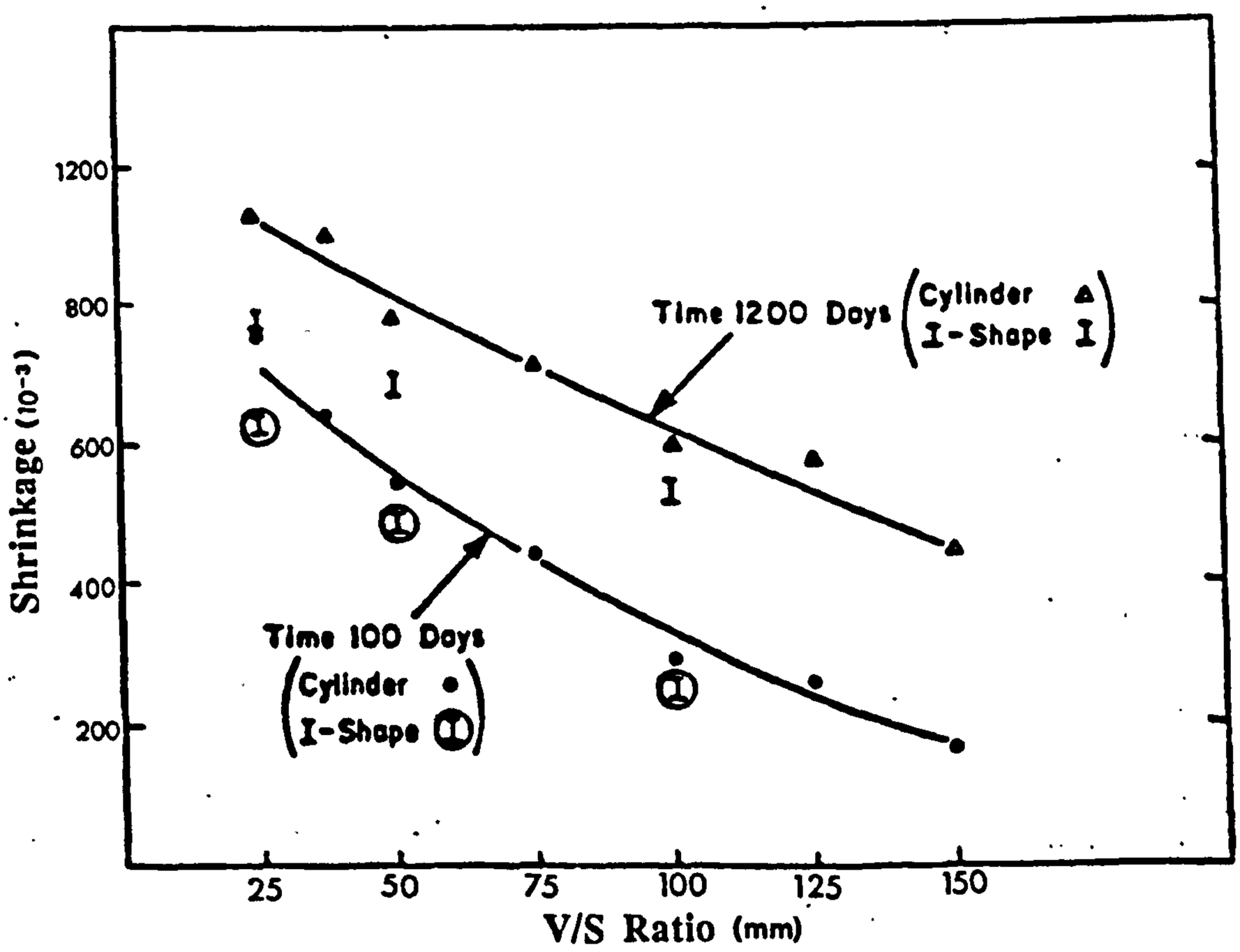

Fig. 3.2 - Influence of V/S Ratio on Shrinkage of Concrete[96]

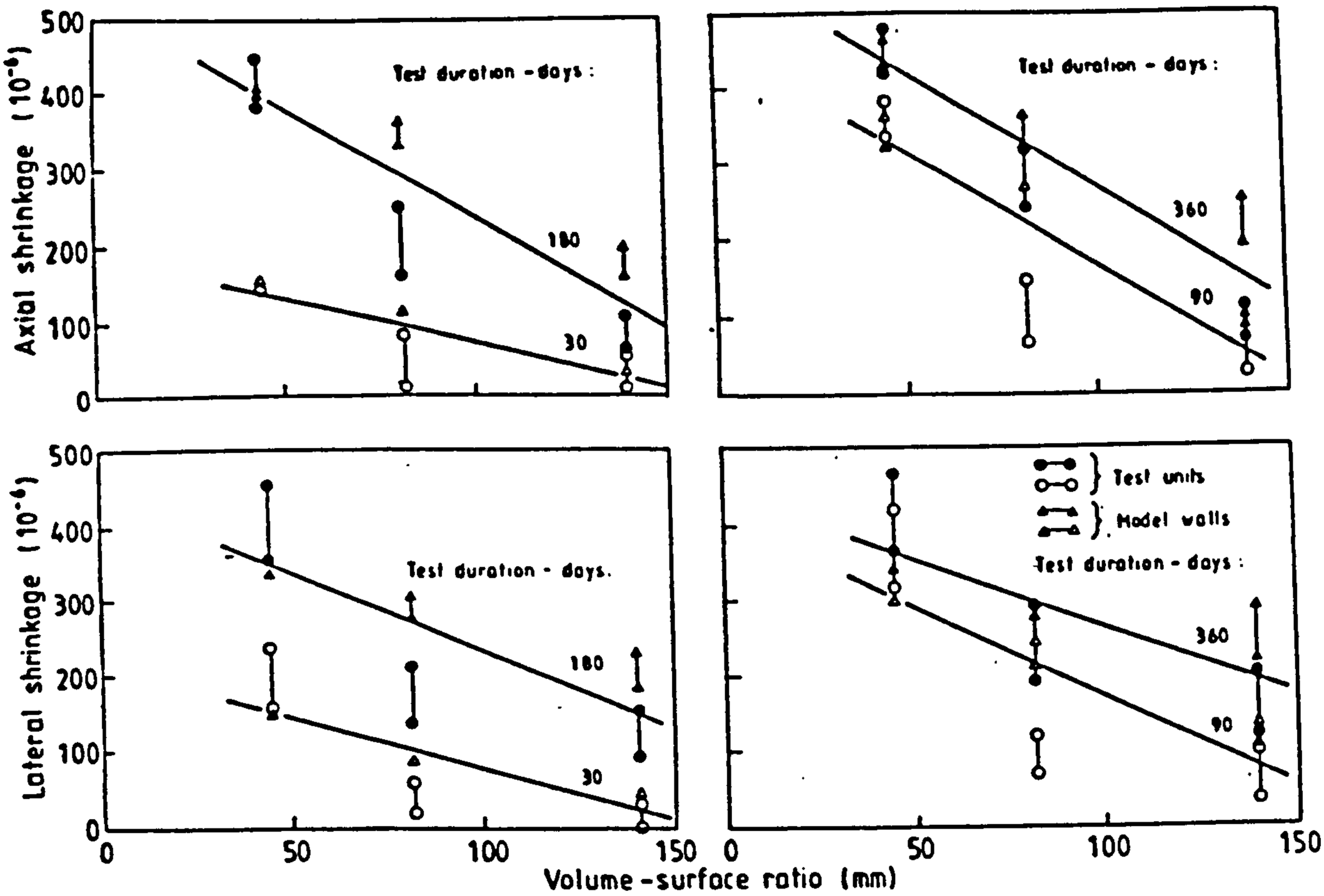

(a) Lightweight Concrete Blockwork

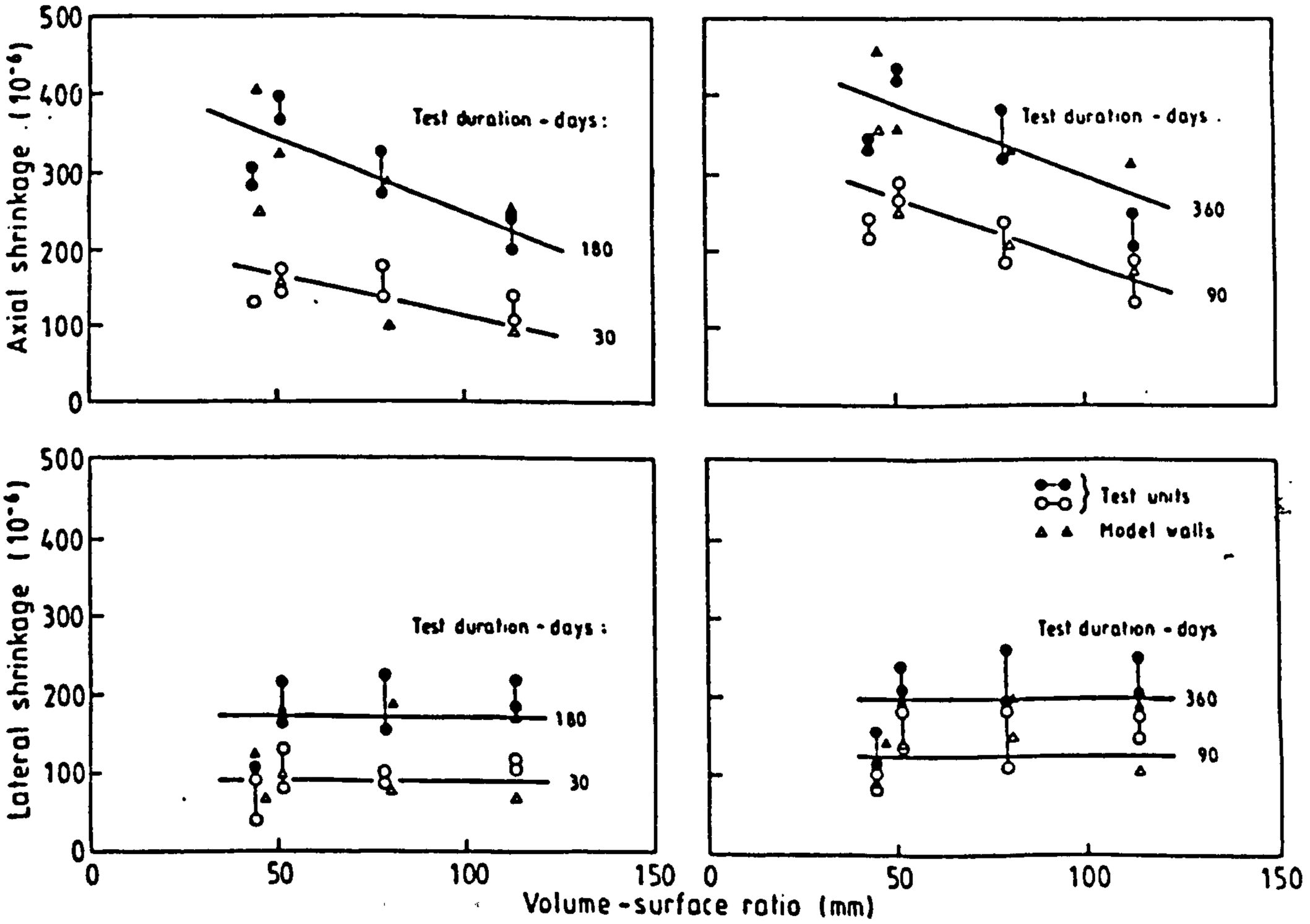

(b) Calcium Silicate Brickwork

Fig. 3.3 - Influence of V/S Ratio on Shrinkage of Masonry[32]

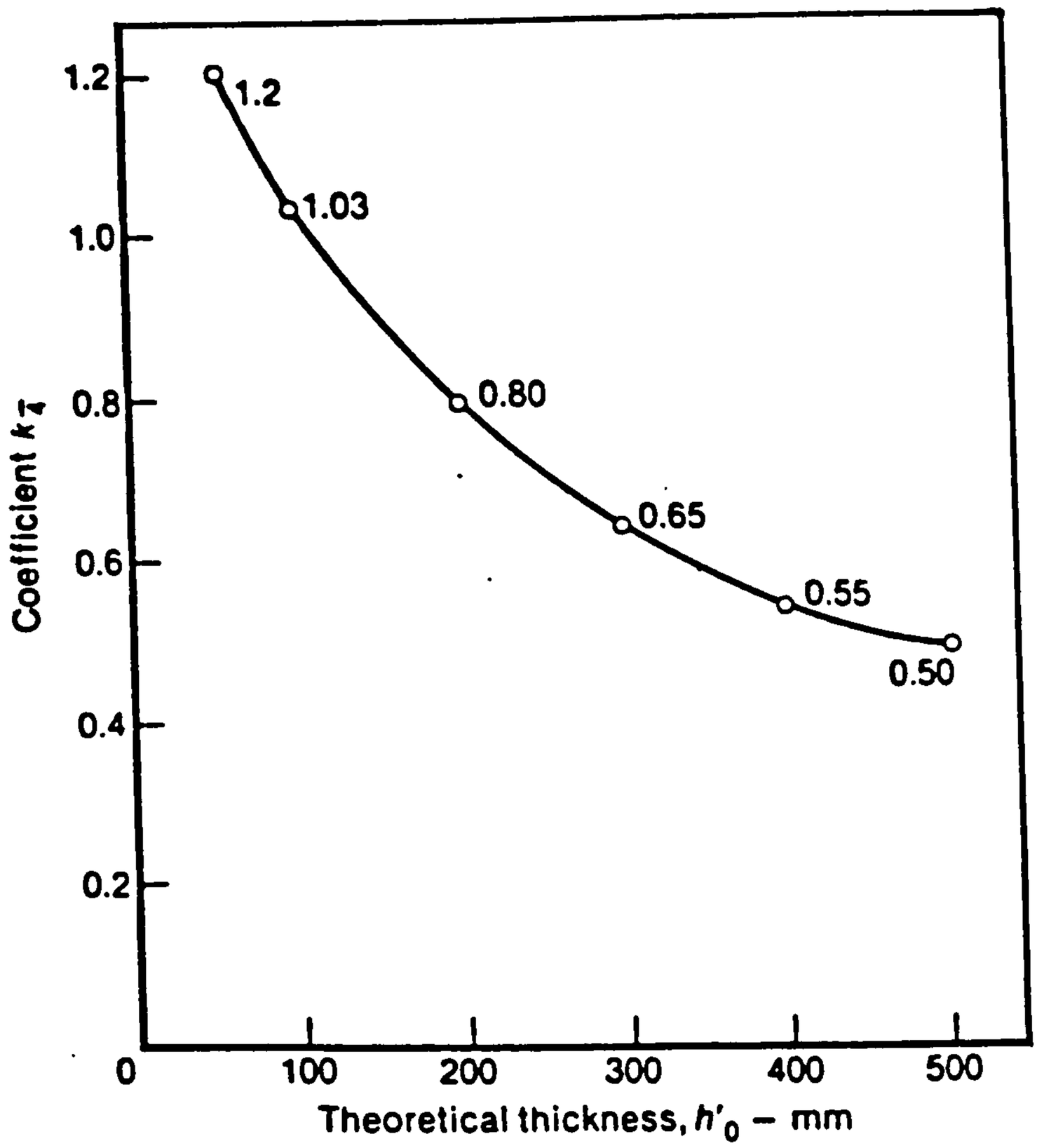

Fig. 3.4 - Coefficient for Theoretical Thickness, k $\bar{4}$, for Shrinkage Prediction (CEB-FIP,1970)[28]

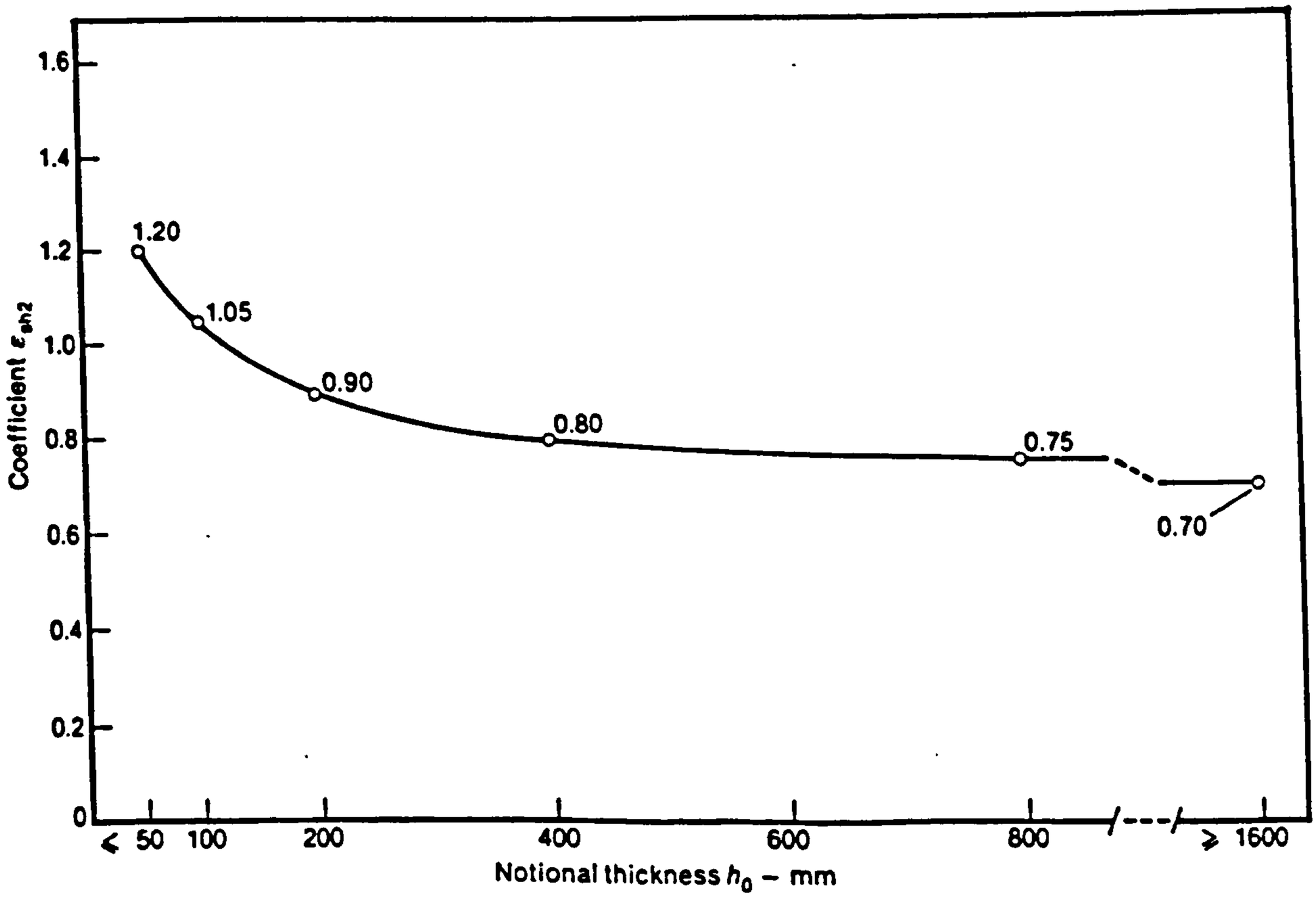

Fig. 3.5 - Influence of Notional Thickness (h_o) on Shrinkage of Concrete (CEB-FIP,1978)[29]

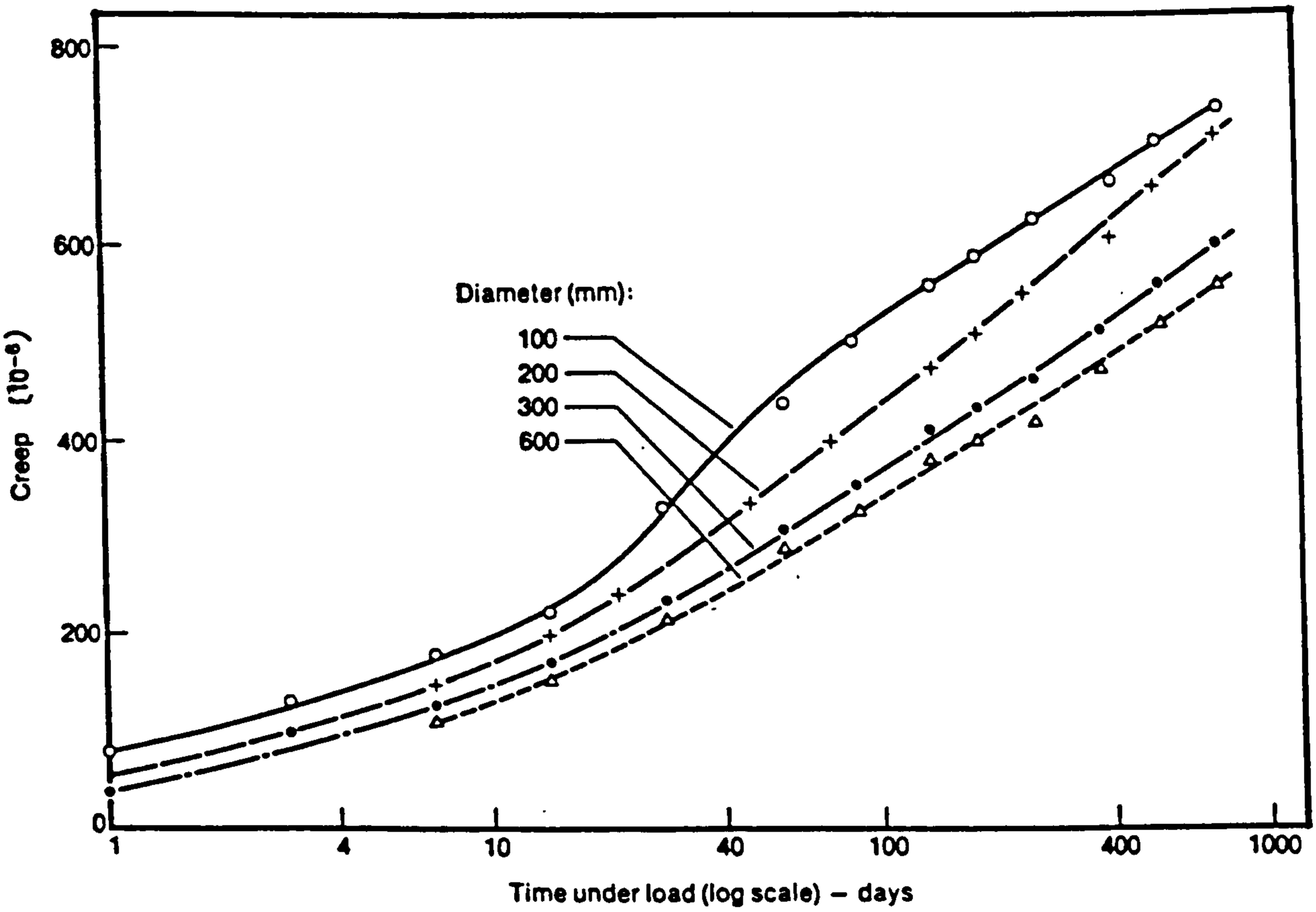

Fig. 3.6 - Creep of Concrete Specimens of Different Sizes[97]

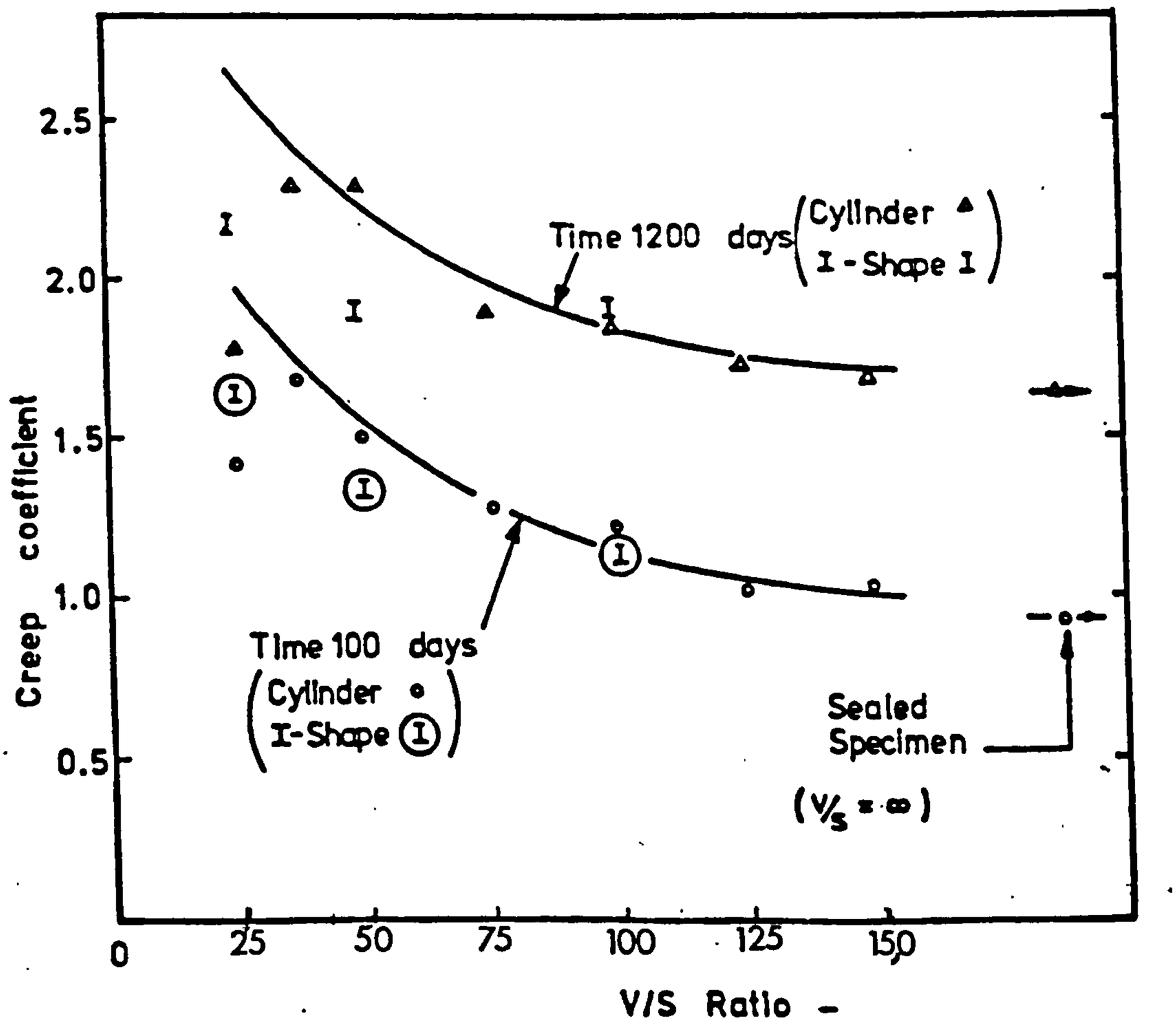

Fig. 3.7 - Influence of V/S Ratio on Creep of Concrete[96]

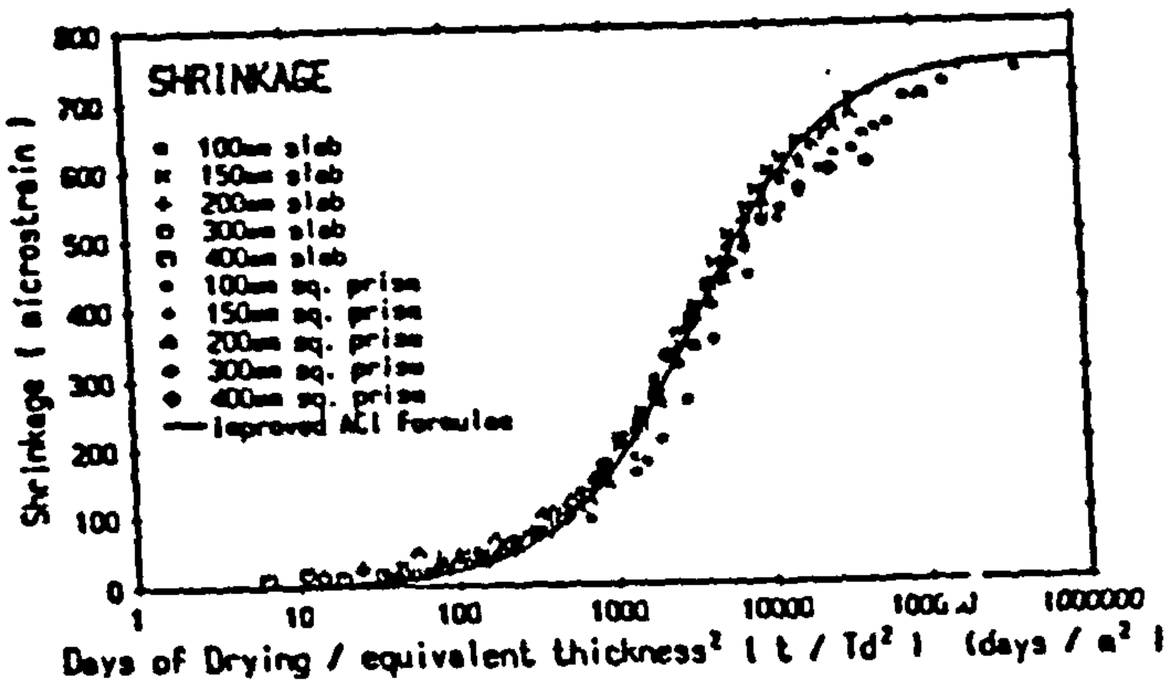

(a) Shrinkage

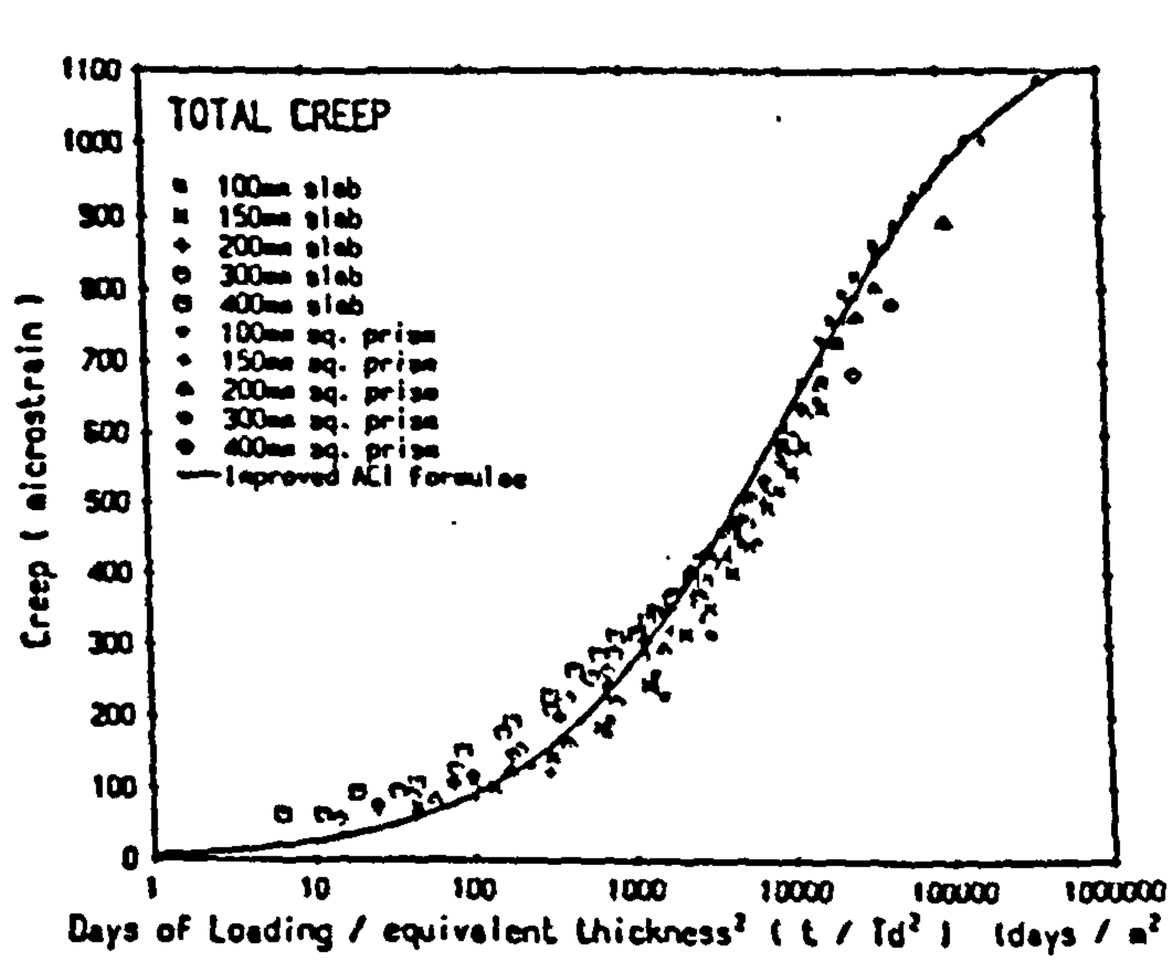

(b) Creep

Fig. 3.8 - Prediction Curves of Shrinkage and Creep of Concrete using Average Thickness (T_d) [87]

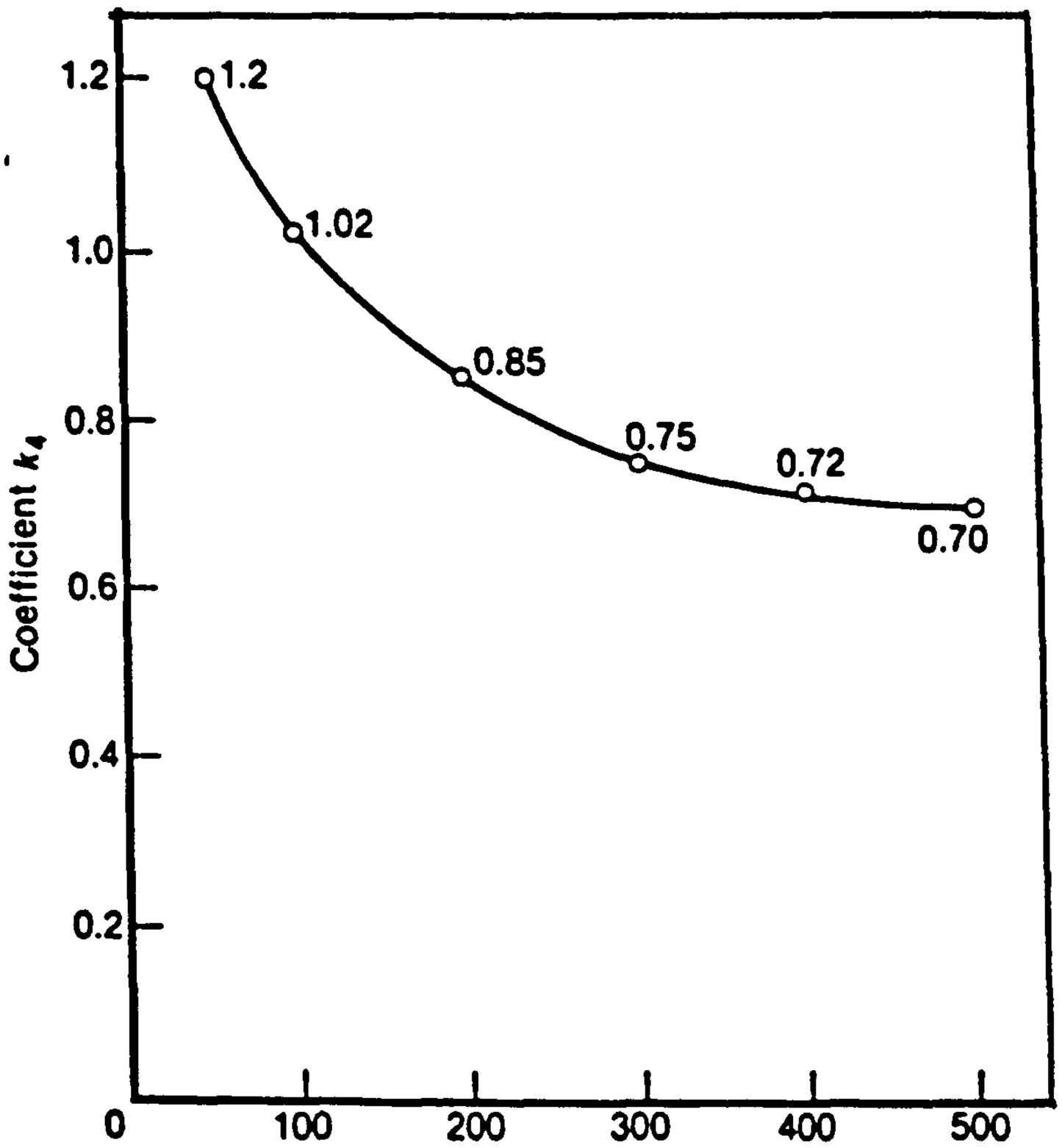

Fig. 3.9 - Coefficient of Theoretical Thickness, k_4 , for Creep Prediction of Concrete (CEB-FIP,1970)[28]

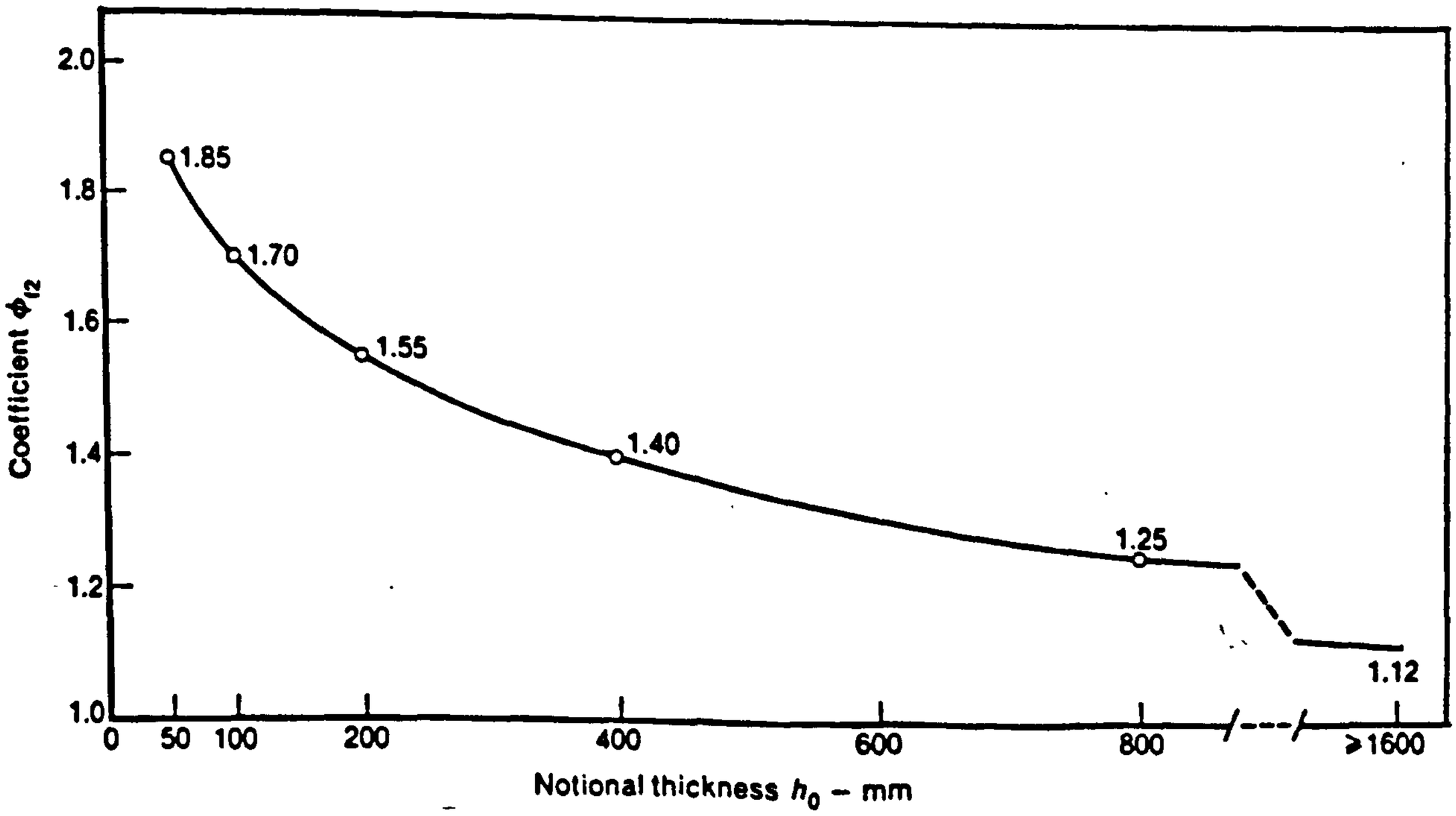

Fig. 3.10 - Influence of Notional Thickness (h_0) on Creep of Concrete (CEB-FIP,1978)[29]

CHAPTER 4

COMPOSITE MODELS

4.1 Introduction

As in the case of concrete, composite models have been proposed for creep and shrinkage of masonry. But unlike concrete which are generally unsuitable for practical application because of difficulties in measuring the properties of aggregate and cement paste as they exist in concrete, composite modelling of masonry is a real practical possibility since representative specimens of brick, block and mortar can be prepared readily. In addition, the brick or block units and mortar in masonry can easily be quantified dimensionally when compared to the irregular shape of aggregate which is bounded by the cement matrix in the case for concrete.

4.2 Previous models

4.2.1 Modulus of elasticity

The first model for modulus of elasticity of masonry appears to have been by Sahlin[47] who proposed the use of the model by Hansen[122] and Paul[123] for concrete. Neglecting the effect of lateral stresses, the model for a column of stack-bonded solid unit was given as,:

$$E_w = \frac{1}{\frac{1-g}{E_m} + \frac{g}{E_b}} \tag{4.1}$$

where $g = b_y/(b_y + m_y)$

He reported reasonable agreement between predicted values and the limited measured data available. Base and Baker[51] showed that Eq.(4.1) was approximately 1% less than the measured value when 76mm high bricks were used. When using 152 mm high bricks,

the predicted modulus was on average of 14% higher than the measured values. The cause of prediction error was attributed to the variability of brick properties and the unrepresentativeness of E_m measured on mortar prisms to the in-situ values.

Jessop at al[31] developed a model by considering a wall in running bond (stretcher bond) consisting of a repetition of representative elements. Two kinds of representative elements were considered, i.e. small and large elements as shown in Fig. 4.1(a). The small element is divided into sub-elements (for units and mortar) acting in two different ways i.e. parallel and series (Fig 4.1(b&c)) while the large element is divided into series sub-elements acting parallel with each other (Fig. 4.1(d)). Using conditions of equilibrium and compatibility they obtained 3 sets of equations. These equations were then generalised by Shrive et al[33] by using the cross-sectional areas of mortar and units instead of the edge dimensions used originally. The equations given are as follows:

For small elements in series (Fig. 4.1(b)),

$$E_w = \frac{A_j E_m (H_b + H_m)(A_b E_b + A_m E_m)}{A_w [A_j E_m H_b + (A_b E_b + A_m E_m) H_m]} \qquad (4.2a)$$

where

$$A_w = \frac{A_j (A_b + A_m)(H_b + H_m)}{A_j H_b + (A_b + A_m) H_m} \qquad (4.2b)$$

For small elements in parallel (Fig. 4.1(c)),

$$E_w = \frac{(H_b + H_m)}{A_w} \left[\frac{A_b A_j E_b E_m}{A_b E_b H_m + A_j E_m H_b} + \frac{A_m E_m}{H_b + H_m} \right] \qquad (4.3a)$$

where

$$A_w = (H_b + H_m) \left[\frac{A_b A_j}{A_b H_m + A_j H_b} + \frac{A_m}{H_b + H_m} \right] \qquad (4.3b)$$

For large elements (Fig. 4.1(d)),

$$E_w = E_m E_b \frac{(H_b + H_m)}{A_w}\left[\frac{4A_m A_{bm}(A_{bj}E_b H_b + A_j E_m H_b) + A_j A_{bj}[A_{bm}E_b(H_b + 2H_m) + A_m E_m H_b]}{(A_{bj}E_b H_m + A_j E_m H_b)(A_{bm}E_b(H_b + 2H_m) + A_m E_m H_b)}\right] \tag{4.4a}$$

where

$$A_w = \frac{(H_b + H_m)[4A_m A_{bm}(A_{bj}H_m + A_j H_b) + A_j A_{bj}[A_{bm}(H_b + 2H_m) + A_m H_b]]}{(A_{bj}H_m + A_j H_b)(A_{bm}(H_b + 2h_m) + A_m H_b)} \tag{4.4b}$$

The values of the individual units were obtained from that embedded in the masonry prisms. The predicted elastic modulus was found to be within 8 to 18 % of the measured value, the larger difference being for a brickwall using lime mortar. The authors[31] have illustrated that all the equations above gave similar predictions as shown in Fig. 4.2, which means that the use of Eq.(4.2), being simpler, is thus preferable. However, the models have been tested on single-leaf walls only and although it was claimed they would be applicable to more general mortaring schemes, the application of the models to other masonry geometries has not been demonstrated.

In 1980, Ameny et al[35] simplified the equation given by Jessop et al[31] for a masonry prism without any vertical mortar joints. The equation given was in fact identical to Eq.(4.1). For a hollow blockwork prism, the predicted modulus was found to fall within 19% of the measured values. Ameny at al[35] later published new models for the short-term deformation of masonry. The arrangement of repetitive elements for stack bonded prisms made from hollow units was slightly different from that of Jessop et al[31] is as shown in Fig. 4.3(a). In addition to masonry made with solid units, different expressions were developed for the different ways the mortar is laid on the bed face when hollow units are used, as shown in Figs. 4.3(b) and (c). For the example of a vertical stacked prism with full-bedded solid units, the stiffness was given as

$$(EA)_w = \frac{(h+j)A_bA_mE_bE_m}{hA_mE_m + jA_bE_b} \tag{4.5}$$

They also demonstrated that when lateral stresses were taken into account, the predicted modulus was only about 2% higher compared with modulus when the stresses were neglected. When mortar is only laid on the outer web of face-shell of hollow units, they illustrated that the predicted stiffness of masonry was 24% lower than the case of full-bedded mortar.

Following the approach of Jessop et al[31], and Shrive and England[37], in considering the large element (Fig. 4.1(d)), Ameny[36] gave a model for a single-leaf wall arranged in running bond for fully-bedded solid units. Lateral and shear stresses were neglected. The stiffness of masonry was given as

$$(EA)_w = \frac{2(1+\alpha')(h+j)A_{b1}A_{m1}E_bE_m}{A_{m1}E_mh + A_{b1}E_b(h+2j)} \tag{4.6a}$$

where

$$\alpha' = \left(\frac{h}{A_{b1}E_b} + \frac{(h+2j)}{A_{m2}E_m}\right) / \left(\frac{2h}{A_{b2}E_b} + \frac{2j}{A_{m2}E_m}\right) \tag{4.6b}$$

A_w may be taken as the net cross-sectional area of the element.

4.2.2 Creep

In proposing a model for creep, the representative element (Fig. 4.1(d)), as that use for modulus of elasticity, was again considered by Jessop et al[31]. They used the concept of stress and temperature normalised creep, as developed by England[104], and performed a step-by-step analysis. The model was analysed for elasticity and then re-analysed for creep response. Several assumptions were made: (i) creep only occurs in mortar and not in the units; (ii) shrinkage of mortar is taken as a multiple of creep; (iii) creep and shrinkage of grout are multiples of the corresponding mortar; and (iv) lateral stresses are neglected. Assumption (i) seems reasonable if clay bricks are used

but will contribute to serious error when concrete blocks are used because it is known that concrete products creep considerably under normal working load. Also assumption (ii) is not true since the relationship between creep and shrinkage is not simple because it depends upon a number of factors, such as, the extent of predrying before loading, the stress level etc. However, no experimental verification of such model was given and the authors did not demonstrate clearly how the model could be used.

Shrive and England[37] also took the large representative element of masonry wall in 'running bond' (Fig. 4.1(d)) and considered the parallel sub-elements as in Fig. 4.4. It was assumed that lines A-A and B-B remain straight when vertical load is applied and consequently a vertical step-displacement occurred over the areas a-a. Also, it was assumed that the two elements were horizontally independent. The overall displacement of A-A is

$$\Delta = \frac{F_1 h}{A_{b1}E_b} + \frac{F_1(h+2j)}{A_{m1}E_m} + C_{m1} + C_{b1} + S_{m1} + S_{b1}$$

$$= \frac{F_2 2h}{A_{b2}E_b} + \frac{F_2 2j}{A_{m2}E_m} + C_{m2} + C_{b2} + S_{m2} + S_{b2} \qquad (4.7a)$$

and for equilibrium, the total force

$$F = F_1 + F_2 \qquad (4.7b)$$

The model are analysed using a 'step-by-step' approach and an effective modulus method. The method was demonstrated by assuming creep to occur in mortar only. When using the effective modulus method they defined a non-aging 'shrinkage-adjusted' modulus as

$$E' = \frac{\sigma}{\varepsilon_e + \varepsilon_c + \varepsilon_s} \qquad (4.8)$$

The 'step-by-step' approach seems not a simple method to use although it has an advantage over the effective modulus method because it takes into account the stress history. However, it was found that the differences between the two methods was

generally less than 1.5%, thus suggesting that the use of the effective modulus method as an acceptable solution for the time-dependent behaviour of masonry, although the use of 'step-by-step' method was not fully described. Again, because of lack of experimental data the accuracy of the model could not be tested.

Ameny et al[38] extended the models for modulus of elasticity to cover creep and shrinkage. Several models have been derived which represent several combinations of unit-type, bond patterns and bedding arrangements. In using the models, the use of effective modulus method, rate of creep method and age adjusted method were described. The proposed model for solid units laid in running bond is only given here. When using the effective modulus method, the expressions for the long term stiffness masonry with solid units in running bond[36] are given as

$$(EA)'_w = \frac{2(h+j)(K'_1+K'_2)}{K'_1.K'_2} \qquad (4.9a)$$

where

$$K'_1 = \frac{h}{A_{b1}E'_b} + \frac{h+2j}{A_{m1}E'_m} \qquad \text{and,}$$

$$K'_2 = 2\left(\frac{h}{A_{b2}E'_b} + \frac{j}{A_{m2}E'_m}\right) \qquad (4.9b)$$

The used the effective modulus as defined by Shrive and England[37], viz.,

$$E'_b = \frac{1}{1/E_b + C_b + S_b/\sigma_b} \qquad \text{and,}$$

$$E'_m = \frac{1}{1/E_m + C_m + S_m/\sigma_m} \qquad (4.10)$$

For the rate of creep method, the final expression given was as

$$\Delta F_{1,n}=\frac{1}{K_1+K_2}\{\Delta F_n K_2-F_{1,n-1}\left[\frac{h}{A_{b1}}\Delta C_{b,n}+\frac{(h+2j)}{A_{m1}}\Delta C_{m,n}\right]+$$

$$(F_{n-1}-F_{1,n-1})\left(\frac{2h}{A_{b2}}\Delta C_{b,n}+\frac{2j}{A_{m2}}\Delta C_{m,n}\right)+h(\Delta S_{b,n}-\Delta S_{m,n})\} \quad (4.11)$$

For the age-adjusted method, the authors described a modification of the 'relaxation' method of Trost[105]. The age adjusted effective modulus E'' was given as

$$E''=\frac{E(t_0)}{1+\chi(t,t_0)\phi(t,t_0)} \quad (4.12)$$

and, the aging coefficient

$$\chi(t,t_0)=\left[1-\frac{E_R(t,t_0)}{E(t_0)}\right]^{-1}-\frac{1}{\phi(t,t_0)} \quad (4.13)$$

However, due to the lack of necessary data, experimental verification was only demonstrated for stack bonded masonry prisms using the effective modulus method, for which the predicted results were found to be acceptably close to the experimental values.

4.2.3 Relationships between creep of mortar and unit test specimens, and creep of the corresponding insitu mortar joints and units

As stated earlier, investigators have faced difficulties in incorporating representative data in their models. In the case of concrete several models have been proposed[105-111], but they are unsuitable for application because of difficulties in assessing the properties of aggregate and cement as they exist in concrete. Although in the case of masonry, the properties of the component materials can individually be prepared and tested, the results of these tests do not not truly represent the as-built materials. For mortar, the tests specimens are geometrically different from the insitu mortar, which, consequently, will affects the pattern of moisture diffusion which, in turn, affects the

creep and moisture movement. For example, Ameny et al[36] tested mortar cylinders while the bedded mortar had a thin layer sandwi ched between the more stiffer units, so that the strain behaviour was influenced by the restraining effect from the units. Although the geometry of brick or block units are the same for bedded and unbedded tests, restraint due to bonding with mortar joints will influence the insitu strain behaviour of the units. Bonding between mortar and units are affected by a number of factors and, consequently, the degree of bonding will influence the stress distribution over the masonry. The relationship between the tests specimens and the corresponding as built materials is thus complex, and as such various assumptions have to be made in the derivation of the models.

Experimental verification has been claimed but Ameny et al[35] have to adjust, empirically, the creep of unbonded block and mortar specimens in order to predict their composite effect in masonry. The creep of mortar cylinders (C_m) was related to the mortar joints (C'_m) by,

$$C_m = \frac{\beta_c}{\alpha} C'_m \quad . \tag{4.14}$$

The average value of $\beta_c = 0.5$. The specific creep of insitu block unit (C'_b) and 35 x 35 x 90 mm specimen (C_b) was related by

$$C_b = \gamma C'_b \tag{4.15}$$

γ was found to vary with brick and mortar types. For the combination of WF bricks and N or M mortar, γ was taken as 1.0, and for BF bricks and N mortar

$$\gamma = 9.02 - 0.034(t - t_0) \tag{4.16a}$$

For the combination of BF bricks and M mortar

$$\gamma = 10.3 - 0.023(t - t_0) \tag{4.16b}$$

It can thus be seen that, the relationship between the individual test specimens and the insitu units is not simple. The authors stated that the above relationship would also be affected by the confinement of mortar joint by the brick, the suction rate of the bricks and, therefore, the effective water/cement ratio of the mortar joint, and effect of lateral stresses. As such, for different combinations of unit and mortar different relationships would be required. It should be pointed out that corresponding relationships for shrinkage have not been considered.

4.3 Models of this investigation

The composite models considered in this investigation have been developed by Brooks[41-42], and are based on Counto's approach for concrete[111]. The models differ from those models developed in Canada[33-38] in three respects: the whole masonry is considered, the influence of moisture diffusion is taken into account when determining creep and shrinkage of the component materials, and models for shrinkage are developed separately from that of the load strain. Models were first developed only for single-leaf walls[39] and since have been extended to a more general application to cover any size and shape of masonry[41-42]. The model expressions are described in the following sections.

4.3.1 Modulus of elasticity

In arriving at the model expressions, the assumptions made are as follows:

(i) effects of bond between brick and mortar are neglected;

(ii) Poisson's effect is neglected;

(iii) strain is proportional to stress;

(iv) there is no external restraint;

(v) elasticity of mortar is isotropic but elasticity of brick is anisotropic.

The derivation of the model[41] is given below.

The layout of masonry subjected to axial or vertical loading is shown in Fig. 4.5. The overall change in height of the masonry unit subjected to an axial compressive stress σ_{wy} is equal to the sum of the changes in height of the brick/mortar composite and the horizontal joint. Thus,

$$H.\varepsilon_{wy} = b_y.C.\varepsilon_{bmy} + m_y.(C+1).\varepsilon_{hmy} \tag{4.17}$$

From the stress-strain relations:

$$\varepsilon_{wy} = \frac{\sigma_{wy}}{E_{wy}}, \varepsilon_{bmy} = \frac{\sigma_{wy}}{E_{bmy}}, \text{and} \varepsilon_{hmy} = \frac{\sigma_{wy}}{E_m} \tag{4.18}$$

Substitution of Eq.(4.18) in Eq.(4.17) yields

$$\frac{1}{E_{wy}} = \frac{b_y.C}{H}.\frac{1}{E_{bmy}} + \frac{m_y.(C+1)}{H}.\frac{1}{E_m} \tag{4.19}$$

To find the brick/mortar modulus, E_{bmy}, in terms of the moduli and mortar, consider the compatibility of strain in the brick/mortar composite, i.e. $\varepsilon_{bmy} = \varepsilon_{by} = \varepsilon_{vmy}$, so that

$$\frac{\sigma_{wy}}{E_{bmy}} = \frac{\sigma_{by}}{E_{by}} = \frac{\sigma_{vmy}}{E_m} \rightarrow \sigma_{vmy} = \sigma_{by}.\frac{E_m}{E_{by}} \tag{4.20}$$

Equating the force on the unit to the sum of forces acting on the composite, yields

$$A_w\sigma_{wy} = A_b\sigma_{by} + A_m\sigma_{vmy} \tag{4.21}$$

From Eq.(4.20), Eq.(4.21) gives

$$\sigma_{by} = \frac{A_w\sigma_{wy}}{A_b + \frac{A_m.E_m}{E_{by}}} \tag{4.22}$$

Substituting σ_{by} in Eq.(4.20) yields:

$$\frac{1}{E_{bmy}} = \frac{A_w}{E_{by}.A_b + E_m.A_m} \tag{4.23}$$

Hence by substituting $1/E_{bmy}$ in Eq.(4.19) gives the modulus of masonry in terms of the moduli of brick and mortar:

$$\frac{1}{E_{wy}} = \frac{b_y.C}{H} \cdot \frac{1}{E_{by}} \left[\frac{A_w}{A_b + \frac{E_m}{E_{by}} A_m} \right] + \frac{m_y.(C+1)}{H} \cdot \frac{1}{E_m} \tag{4.24}$$

Similarly, considering masonry subjected to lateral or horizontal loading as in Fig. 4.6. For compatibility of lateral strain, the strains in the masonry unit, horizontal mortar joint and brick/mortar composite are equal (Fig.4.6(b) and (c)), i.e.

$$\varepsilon_{wx} = \varepsilon_{bmx} = \varepsilon_{hmx} \tag{4.25}$$

From the relations between stress and strain:

$$\frac{\sigma_{wx}}{E_{wx}} = \frac{\sigma_{bmx}}{E_{bmx}} = \frac{\sigma_{hmx}}{E_m} \tag{4.26}$$

where the stresses (σ) are defined in Fig.4.6.

For the change in length of the brick/mortar composite:

$$W_x \cdot \frac{\sigma_{bmx}}{E_{bmx}} = 2m_x \cdot \frac{\sigma_{bmx}}{E_m} + \frac{b_x \cdot \sigma_{bx}}{E_{bx}} \tag{4.27}$$

To solve Eq.(4.27), σ_{bx} is required as a function of σ_{bmx}, and the solution is obtained by considering the inner brick/mortar composite as shown in Fig.4.6(d). For compatibility of strain:

$$\sigma'_{hmx} = \frac{E_m}{E_{bx}} \cdot \sigma_{bx} \tag{4.28}$$

and for equilibrium of forces:

$$2\sigma'_{hmx} \cdot m_z \cdot b_y + \sigma_{bx} \cdot b_z \cdot b_y = \sigma_{bmx} \cdot W_z \cdot b_y \tag{4.29}$$

The dimensions m_z and b_z (Fig.4.6(c)) are arranged in proportion to their total thicknesses over the cross-section of the masonry.

Substitution of Eq.(4.28) in Eq.(4.29) gives:

$$\sigma_{bx} = \frac{\sigma_{bmx} \cdot W_z}{\left[2 \cdot \frac{E_m}{E_{bx}} \cdot m_z + b_z\right]} \tag{4.30}$$

Hence, substitution of Eq.(4.30) in Eq.(4.27) gives

$$\frac{1}{E_{bmx}} = \frac{2m_x}{E_x} \cdot \frac{1}{E_m} + \frac{b_x}{W_x} \cdot \frac{W_z}{(2E_m \cdot m_z + E_{bx} \cdot b_z)} \tag{4.31}$$

Before solving Eq.(4.26) to obtain the modulus of masonry (E_{wx}), the relation between σ_{bmx} and σ_{wx} is required. Since the lateral force on the masonry unit is equal to the sum of forces acting on the brick/mortar composite and the horizontal mortar joint:

$$\sigma_{wx} \cdot H \cdot W_z = m_y \cdot (C+1)\sigma_{hmx} \cdot W_z + C \cdot \sigma_{bmx} \cdot b_y \cdot W_z \tag{4.32}$$

Hence,

$$\sigma_{bmx} = \frac{\sigma_{wx} \cdot H - m_y \cdot (C+1)\sigma_{hmx}}{C \cdot b_y} \tag{4.33}$$

From Eq.(4.26)

$$\sigma_{hmx} = \frac{E_m}{E_{bmx}} \cdot \sigma_{bmx} \tag{4.34}$$

and substitution in Eq.(4.33) gives

$$\sigma_{bmx} = \frac{\sigma_{wx} \cdot H}{C \cdot b_y + m_y \cdot (C+1) \cdot \frac{E_m}{E_{bmx}}} \tag{4.35}$$

and therefore from Eq.(4.26)

$$E_{wx}=\frac{C\cdot b_y}{H}\cdot E_{bmx}+\frac{m_y\cdot(C+1)}{H}\cdot E_m \tag{4.36}$$

Finally, substitution for E_{bmx} (from Eq.(4.31)) in Eq.(4.36) gives the modulus of elasticity for masonry subjected to lateral or horizontal loading as:

$$E_{wx}=\frac{C.b_y}{H}\left[\frac{W_x.E_m(2E_m.m_z+b_z.E_{bx})}{2m_x(2E_m.m_z+b_z.E_{bx})+E_m.b_x.W_z}\right]+\frac{m_y.(C+1)}{H}.E_m \tag{4.37}$$

4.3.2 Creep

Equations (4.24) and (4.37) also represent the time-dependent load strain (elastic plus creep) per unit stress, with the elastic moduli being replaced by the effective moduli E'. Thus, specific vertical creep of masonry (C_{wy}) is:

$$C_{wy}=\frac{1}{E'_{wy}}-\frac{1}{E_{wy}} \tag{4.38a}$$

and specific horizontal creep of masonry (C_{wx}) is:

$$C_{wx}=\frac{1}{E'_{wx}}-\frac{1}{E_{wx}} \tag{4.38b}$$

For mortar, specific creep (C_m) is given by:

$$C_{m_y}=C_{mx}=C_m=\frac{1}{E'_m}-\frac{1}{E_m} \tag{4.39}$$

while corresponding expressions for specific vertical creep of unit (C_{by}) and specific horizontal creep of unit (C_{bx}) are, respectively:

$$C_{by}=\frac{1}{E'_{by}}-\frac{1}{E_{by}} \tag{4.40a}$$

and,

$$C_{bx} = \frac{1}{E'_{bx}} - \frac{1}{E_{bx}} \tag{4.40b}$$

4.3.3 Moisture movement

The derivation of expressions for moisture movement in masonry as published previously[42] is as follows.

Taking the two-phase system as shown in Fig. 4.7, each phases is assumed to be subjected to nominal stresses: σ_{by} in the brick and σ_{vmy} in the vertical mortar joints. The overall axial shrinkage of masonry (S_{wy}) is obtained by assuming the changes in length of the brick/mortar composite and the horizontal mortar joint, hence

$$H.S_{wy} = b_y.C.\varepsilon_{bmy} + m_y.(C+1)S_m,$$

which gives

$$S_{wy} = \frac{b_y.C}{H}.\varepsilon_{bmy} + \frac{m_y.(C+1)}{H}.S_m \tag{4.41}$$

For compatibility of strain in the brick/mortar composite

$$\varepsilon_{bmy} = \varepsilon_{by} = \varepsilon_{vmy} \tag{4.42}$$

where

$$\varepsilon_{by} = S_{by} + \frac{\sigma_{by}}{E_{by}}, \tag{4.43}$$

and

$$\varepsilon_{vmy} = S_m + \frac{\sigma_{vmy}}{E_m} \tag{4.44}$$

Since there is no net vertical force on the masonry:

$$A_b.\sigma_{by} + A_m.\sigma_{vmy} = 0 \tag{4.45}$$

Hence, from Eq.(4.43), (4.44) and (4.45)

$$\sigma_{by} = \frac{E_m.(S_m - S_{by})}{\left[\frac{A_b}{A_m} + \frac{E_m}{E_{by}}\right]} \tag{4.46}$$

Substitution of Eq.(4.43) in Eq.(4.43) and (4.42) yields

$$\sigma_{bmy} = S_{by} + \frac{(S_m - S_{by})}{\left[1 + \frac{A_b}{A_m} \cdot \frac{E_{by}}{E_m}\right]} \tag{4.47}$$

and by substituting Eq.(4.47) in Eq.(4.41) and replacing the elastic modulus (E) with the time-dependent modulus (E'), gives the vertical shrinkage of masonry:

$$S_{wy} = \frac{b_y.C}{H}.S_{by} + \frac{m_y.(C+1)}{H}.S_m + \frac{b_y.C}{H} \cdot \frac{(S_m - S_{by})}{\left[1 + \frac{A_b}{A_m} \cdot \frac{E'_{by}}{E'_m}\right]} \tag{4.48}$$

The arrangement of the composite model for any size of masonry undergoing lateral or horizontal shrinkage is shown in Fig. 4.8. The brick or block/mortar composite is subjected to a nominal stress σ_{bmx} , while the horizontal mortar joint is subjected to a nominal stress σ_{hmx} (Fig. 4.8(b)), because of differential shrinkage between the two phases. For compatibility of lateral strain, shrinkage of the masonry (S_{wx}) is equal to the strain in the brick/mortar composite (ε_{bmx}) which is equal to the strain in the horizontal mortar joint (ε_{hmx}), i.e.

$$S_{mx} = \varepsilon_{bmx} = \varepsilon_{hmx} \tag{4.49}$$

$$\text{where} \varepsilon_{bmx} = S_{bmx} + \frac{\sigma_{bmx}}{E_{bmx}} \tag{4.50}$$

$$\text{and} \varepsilon_{hmx} = S_m + \frac{\sigma_{hmx}}{E_m} \tag{4.51}$$

Considering the change in length of brick/mortar composite (Fig. 4.8(c) and (d):

$$W_x\left[S_{bmx} + \frac{\sigma_{bmx}}{E_{bmx}}\right] = 2m_x\left[S_m + \frac{\sigma_{bmx}}{E_m}\right] + b_x\left[S_{bx} + \frac{\sigma_{bx}}{E_{bx}}\right] \tag{4.52}$$

The stress on the brick σ_{bx} can be expressed as a function of σ_{bmx} from consideration of the inner brick/mortar composite of Fig. 4.8(d).

The compatibility of strain:

$$S_{bx}+\frac{\sigma_{bx}}{E_{bx}}=S_m+\frac{\sigma'_{hmx}}{E_m} \tag{4.53}$$

and for the equilibrium of force:

$$2\sigma'_{hmx}.m_z.b_y+\sigma_{bx}.b_z.b_y=\sigma_{bmx}.W_z.b_y \tag{4.54}$$

The dimensions of m_z and b_z are chosen in proportion to their actual thickness over the cross-section of the masonry.

Substitution of Eq.(4.53) in Eq.(4.54) gives

$$\sigma_{bx}=\frac{\sigma_{bmx}.W_z-2(S_{bx}-S_m)E_m m_z}{\left[2\frac{E_m}{E_{bx}}.m_z+b_z\right]} \tag{4.55}$$

Substituting Eq.(4.55) in Eq.(4.52) gives

$$S_{bmx}+\frac{\sigma_{bmx}}{E_{bmx}}=\frac{\sigma_{bmx}}{W_x}\left[2\frac{m_x}{E_m}+\frac{b_x}{(2E_m.m_z+b_z.E_{bx})}\right]+2\frac{m_z}{W_x}.S_m$$

$$+\frac{b_x}{W_x}.S_b-\frac{2(S_{bx}-S_m).E_m.m_z.b_x}{W_x(2E_m.m_z+b_z.E_{bx})} \tag{4.56}$$

Since the sum of forces acting on the brick/mortar composite and the horizontal mortar joint is zero (Fig. 4.8 (b)):

$$\sigma_{bmx}=-\frac{m_y(C+1)}{b_y.C}\sigma_{hmx} \tag{4.57}$$

From Eq.(4.49) and (4.51):

$$\sigma_{bmx}=(S_{wx}-S_m)E_m \tag{4.58}$$

so that substitution in Eq.(4.57) gives:

$$\sigma_{hmx} = -\frac{m_y(C+1)}{b_y.C}.[S_{wx} - S_m]E_m \tag{4.59}$$

Also, from Eq.(4.49) and (4.50)

$$S_{wx} = S_{bmx} + \frac{\sigma_{bmx}}{E_{bmx}} \tag{4.60}$$

Finally equating Eq.(4.56) and (4.60), and substituting for σ_{bmx} from Eq.(4.58), and also replacing the elastic modulus (E) with the time dependent elastic modulus (E'), the expression for horizontal shrinkage is given:

$$S_{wx} = \frac{K_{bx}.S_{bx} + K_m.S_m}{K_{wx}} \tag{4.61}$$

where

$$K_{wx} = 1 + \frac{m_y(C+1)}{b_y.C.W_x}2m_x + \frac{m_y(C+1)}{b_y.C.W_x}.\frac{E'_m.W_z.b_x}{2E'_m.m_z + b_z.E'_{bx}} \tag{4.62}$$

$$K_{bx} = \frac{b_x}{W_x} - \frac{2E'_m.m_z.b_x}{W_x(2E'_m.m_z + b_z.E'_{bx})} \tag{4.63}$$

$$K_m = \frac{2m_x}{W_x} + \frac{m_y(C+1)}{b_y.C.W_x}.2m_x + \frac{m_y(C+1)}{b_y.C.W_x}.\frac{E'_m.W_z.b_x}{2E'_m.m_z + b_zE'_{bx}} + \frac{2E'_m.m_z.b_x}{W_x(2E'_m.m_z + b_z.E'_{bx})} \tag{4.64}$$

4.3.4 Application of model expressions

In many practical applications, some of the foregoing expressions can be simplified. For example, for the vertical elastic modulus (E_{wy}), the coefficient in square brackets of Eq.(4.24) is usually equals to unity, and for vertical moisture movement (S_{wy}), the third term of Eq.(4.48) is usually negligible. An interesting feature is that both vertical and horizontal moisture movement expressions (Eq.(4.48) and Eq.(4.64)) are

functions of the effective modulus ratio, E'_b/E'_m, which is affected mainly by creep of mortar. Although the influence of that ratio is usually negligible in case of vertical movement, it can have an appreciable affect in horizontal movement. Consequently, the magnitudes of creep of unit and mortar should be considered before making general approximations for model expressions.

The expressions can be further simplified since mortar joint thickness is generally standardised and bricks units normally have standard dimensions. The new approach in simulating the strains of individual test specimens and the corresponding insitu values and other relevant details on the applications of these models are described in Chapter 7.

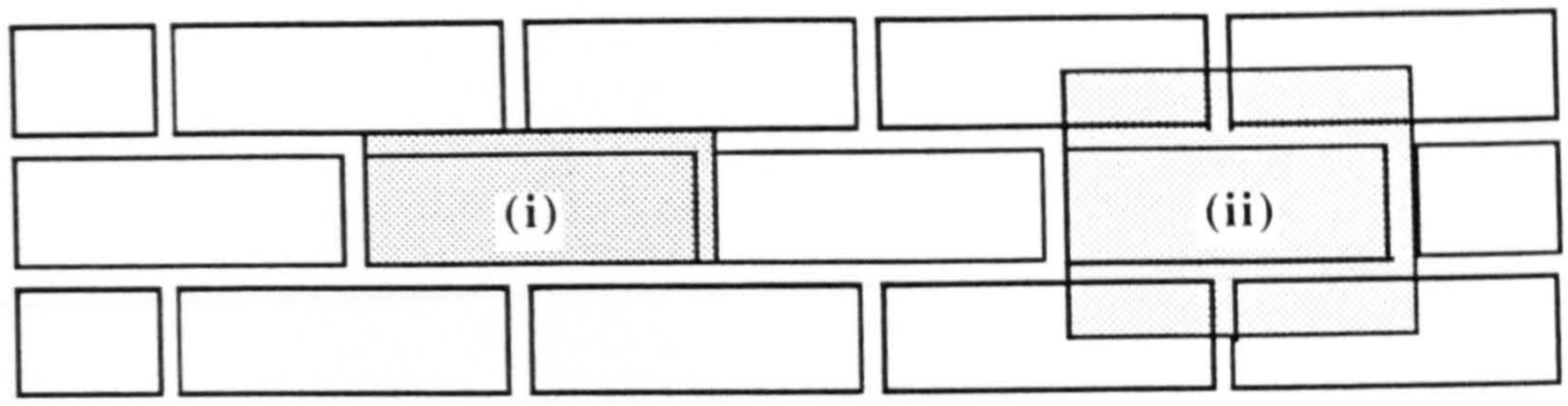

(a)

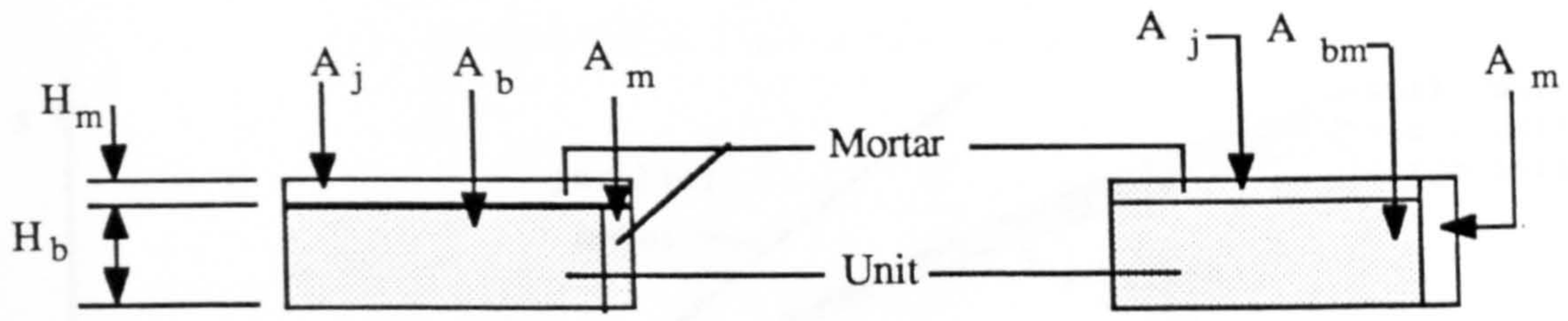

(b)

(c)

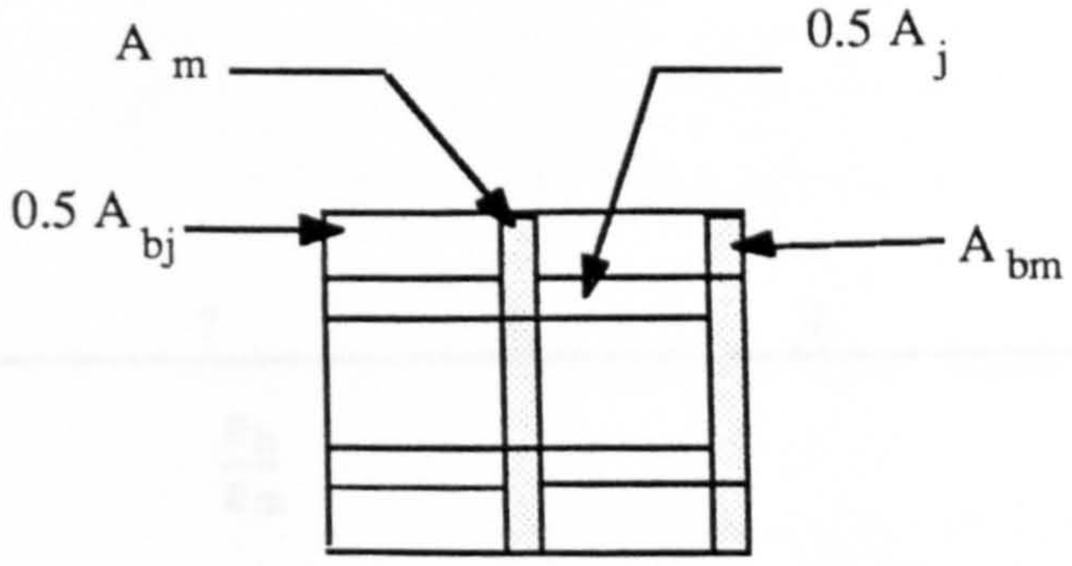

(d)

Fig. 4.1 - Repeating Units and Models for a Single Wythe Wall[31]

(a) Repeating units in a single wythe wall
(i) small unit (ii) large unit

(b) Brick/block in parallel with vertical mortar joint, this in series with horizontal mortar bed [from (i)]

(c) Brick and part of horizontal bed in series, with this parallel with vertical mortar joint [from (i)]

(d) Two series combinations in parallel with each other [from (ii)]

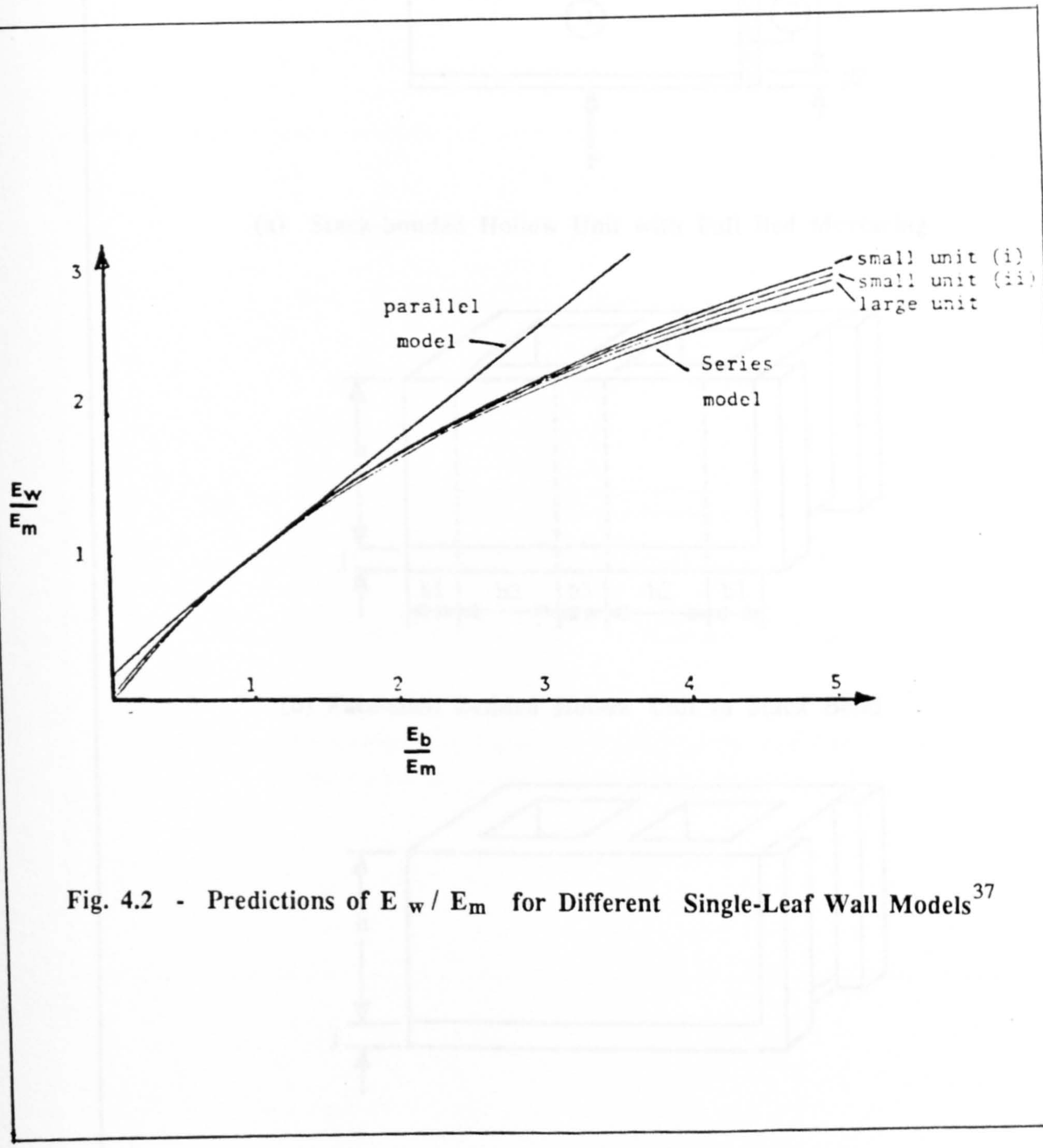

Fig. 4.2 - Predictions of E_w / E_m for Different Single-Leaf Wall Models[37]

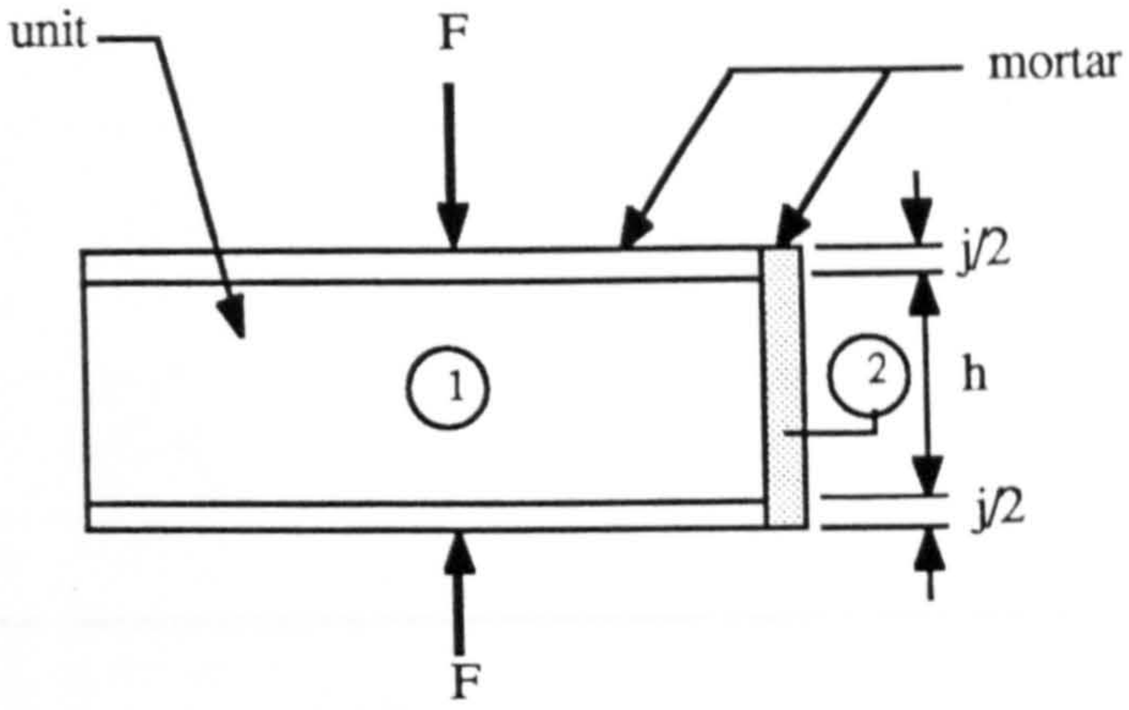

(a) Stack-bonded Hollow Unit with Full Bed Mortaring

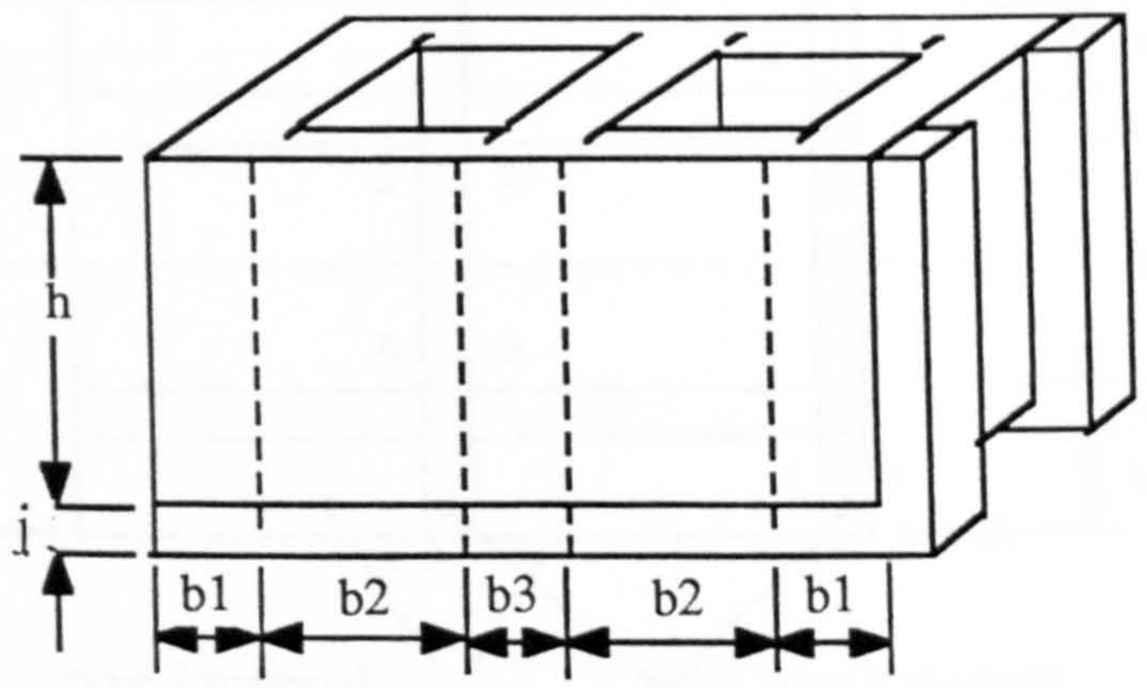

(b) Face-shell Bedded Hollow Unit in Stack Bond

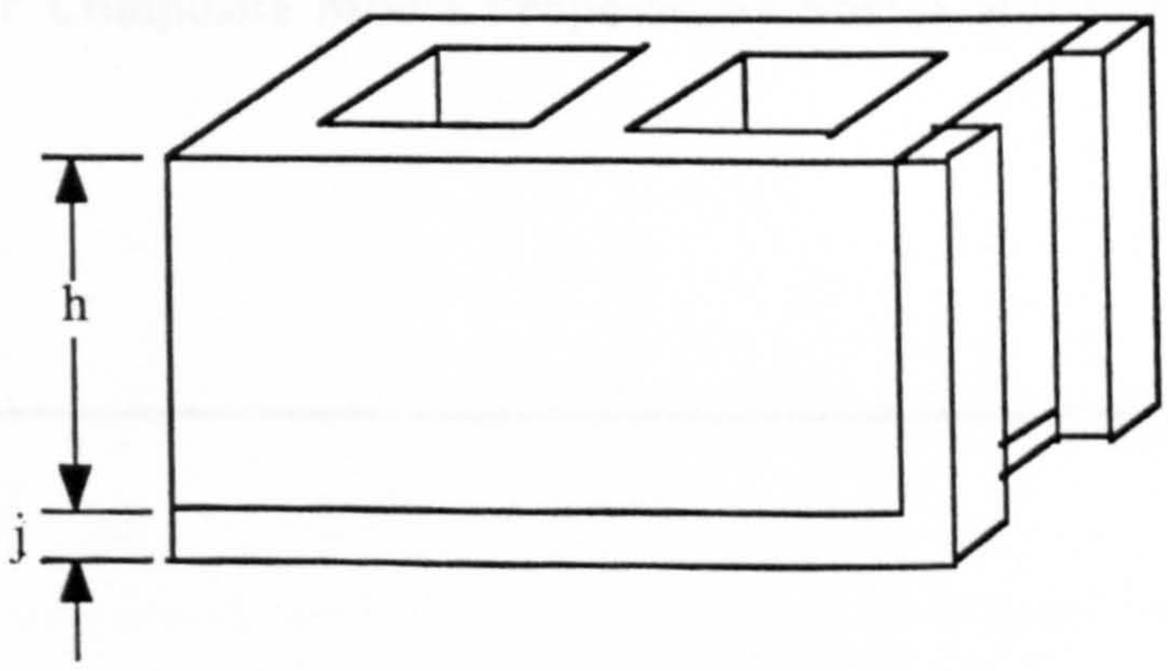

(c) Face-shell Bedded Hollow Unit

Fig.4.3 - Repetitive Elements for Composite Model (Ameny et al)[36]

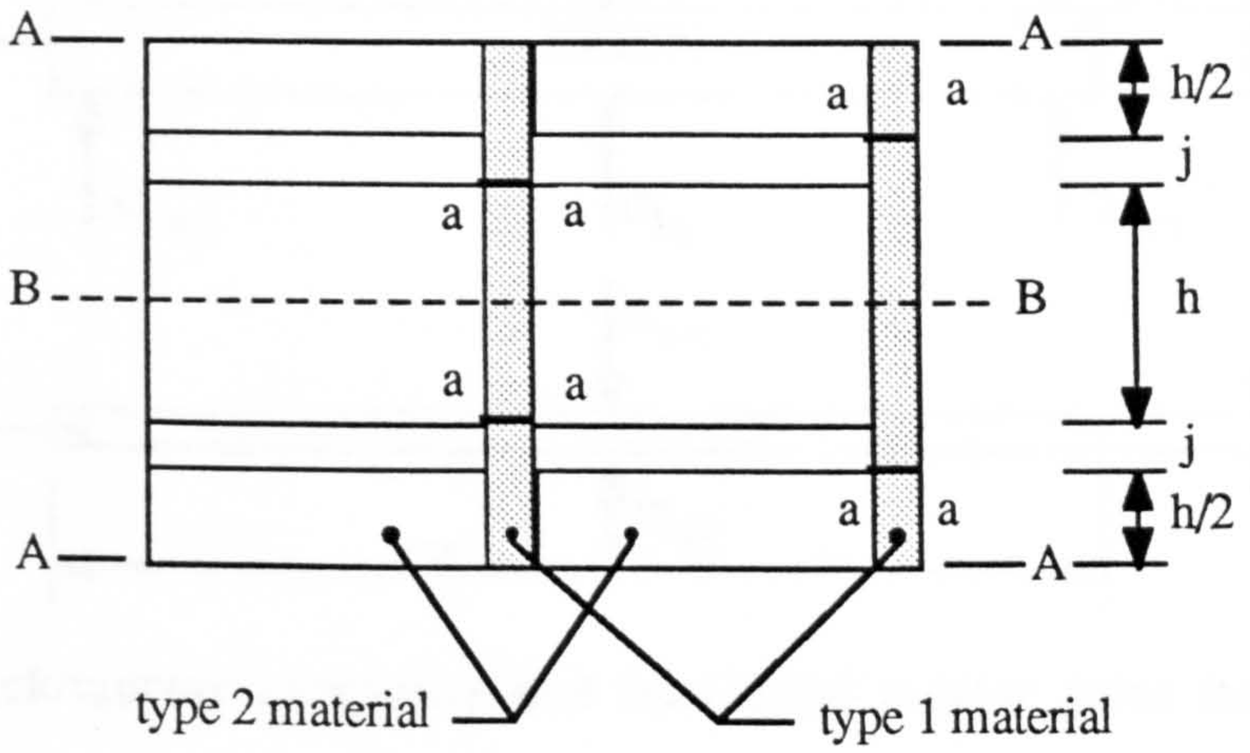

Fig. 4.4 - Break-down of Large Repeating Units into Discrete Element for Composite Model Proposed by Shrive and England[37]

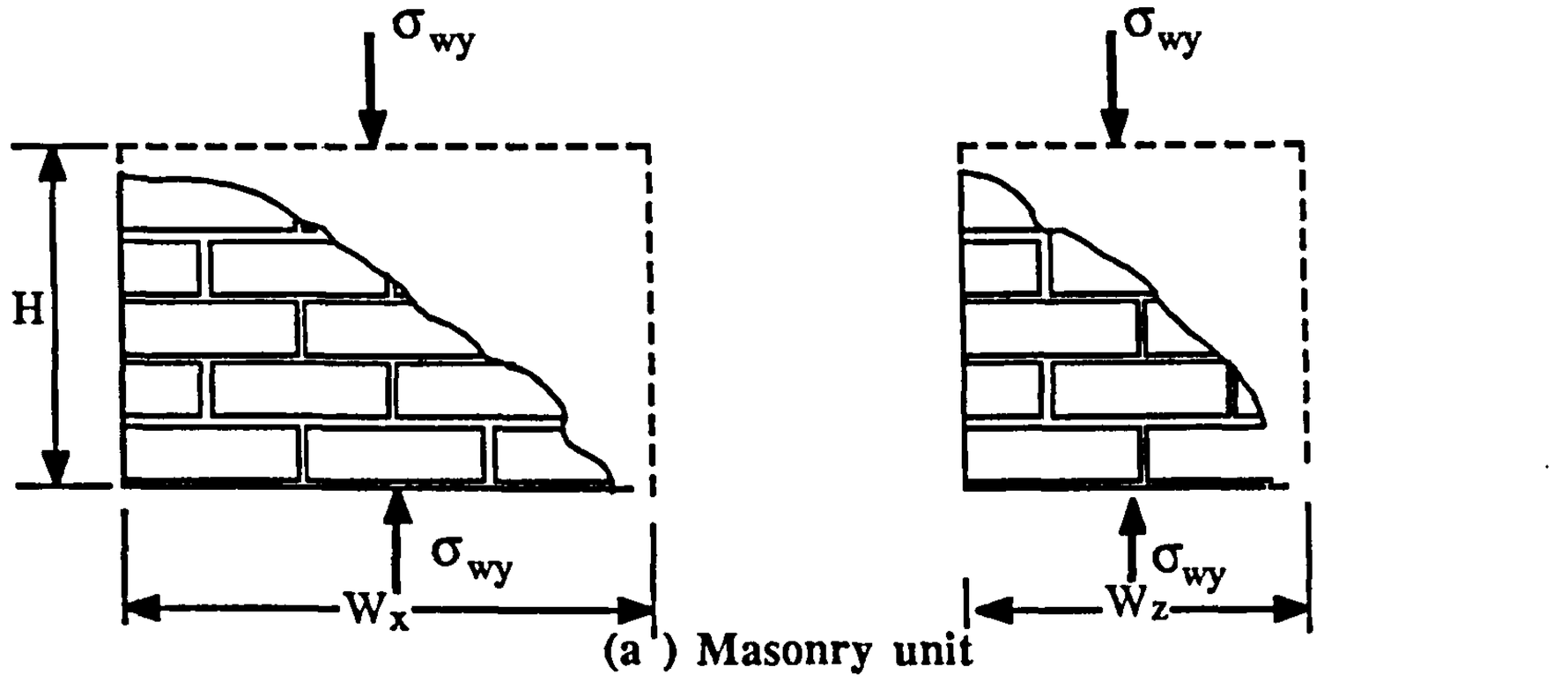

Fig. 4.5 - Composite Model Layout for Vertical Modulus of Elasticity of Masonry, E_{wy} [Eq.(4.24)] [41]

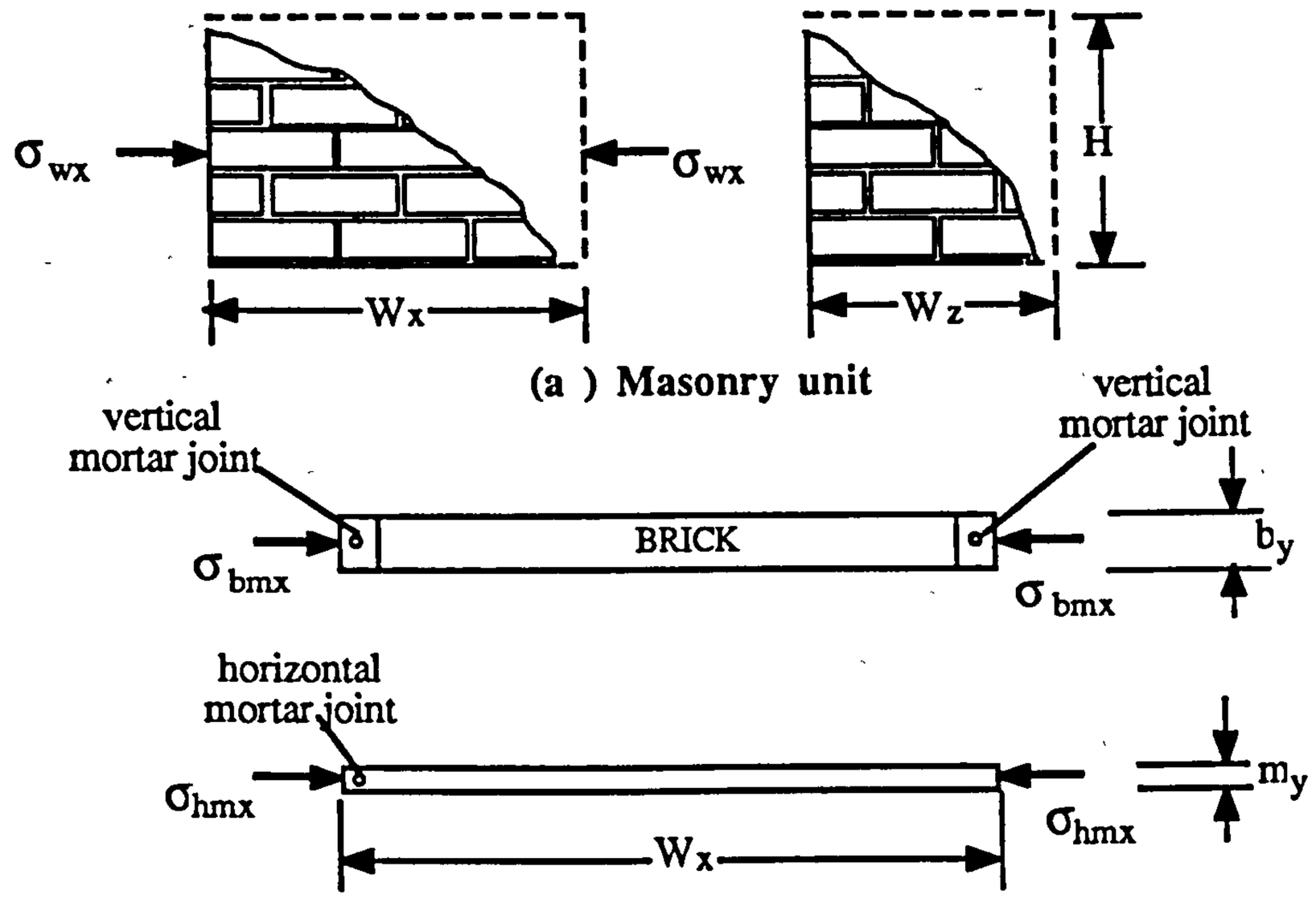

Fig. 4.6 - Composite Model Layout for Lateral Modulus of Elasticity of Masonry, E_{wx}[Eq.(4.37)][41]

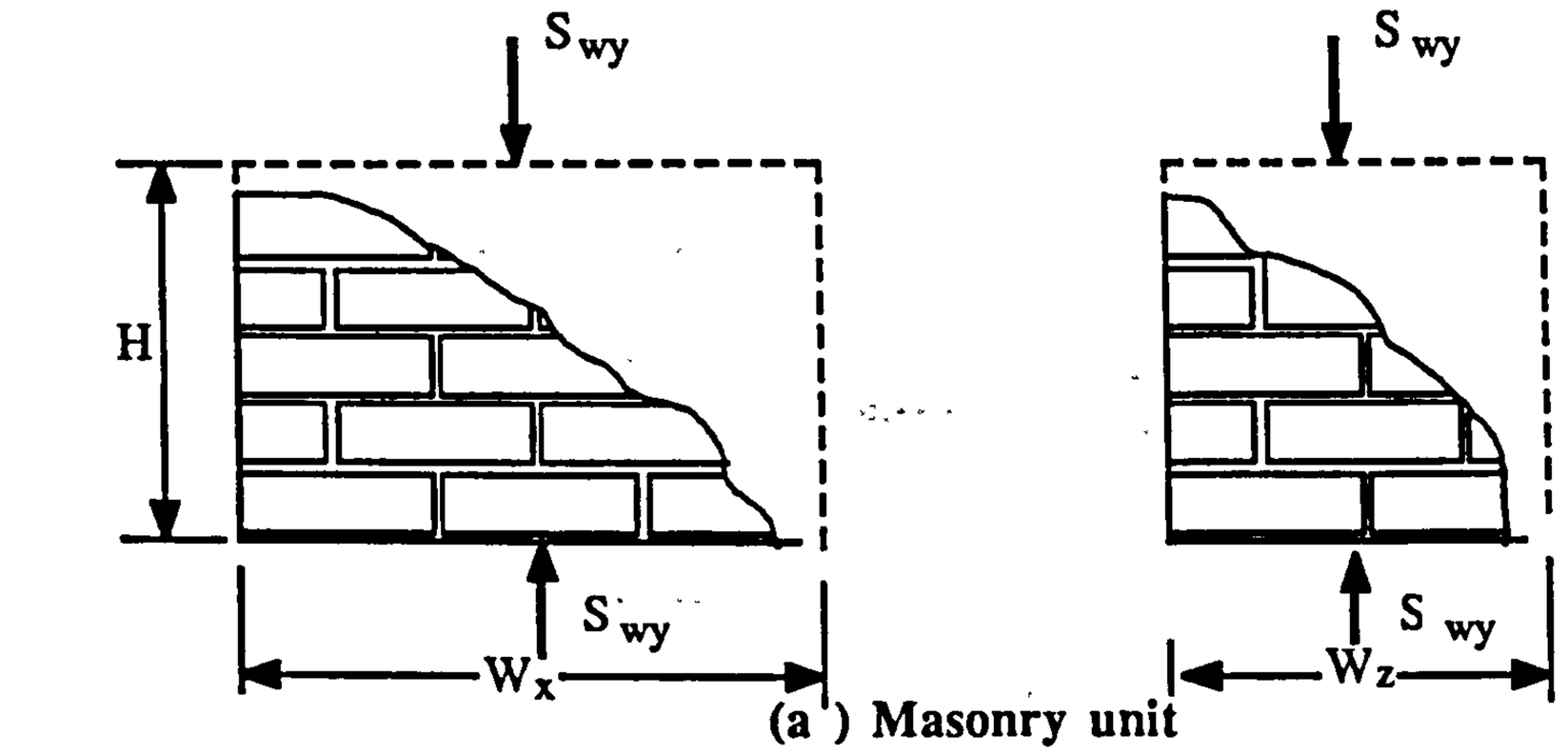

(a) Masonry unit

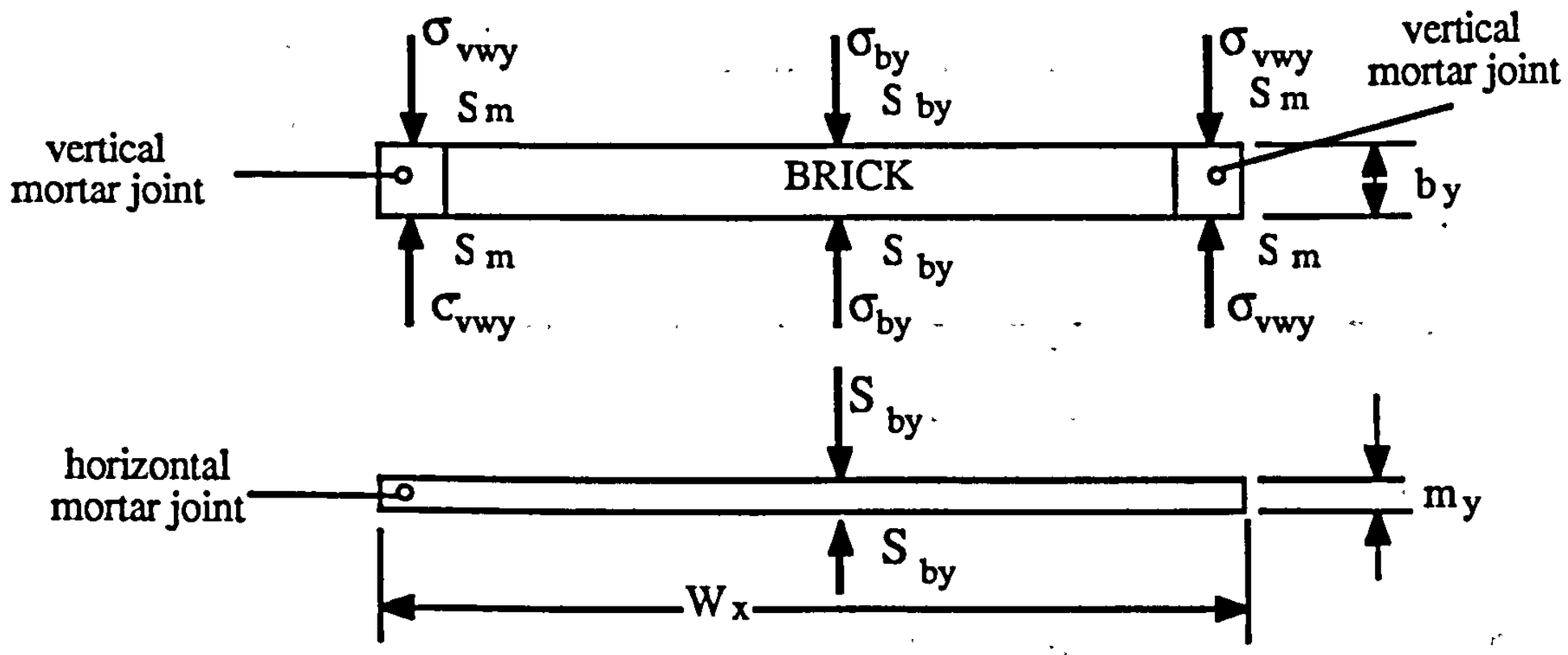

(b) Brick/mortar composite and horizontal mortar joint (section)

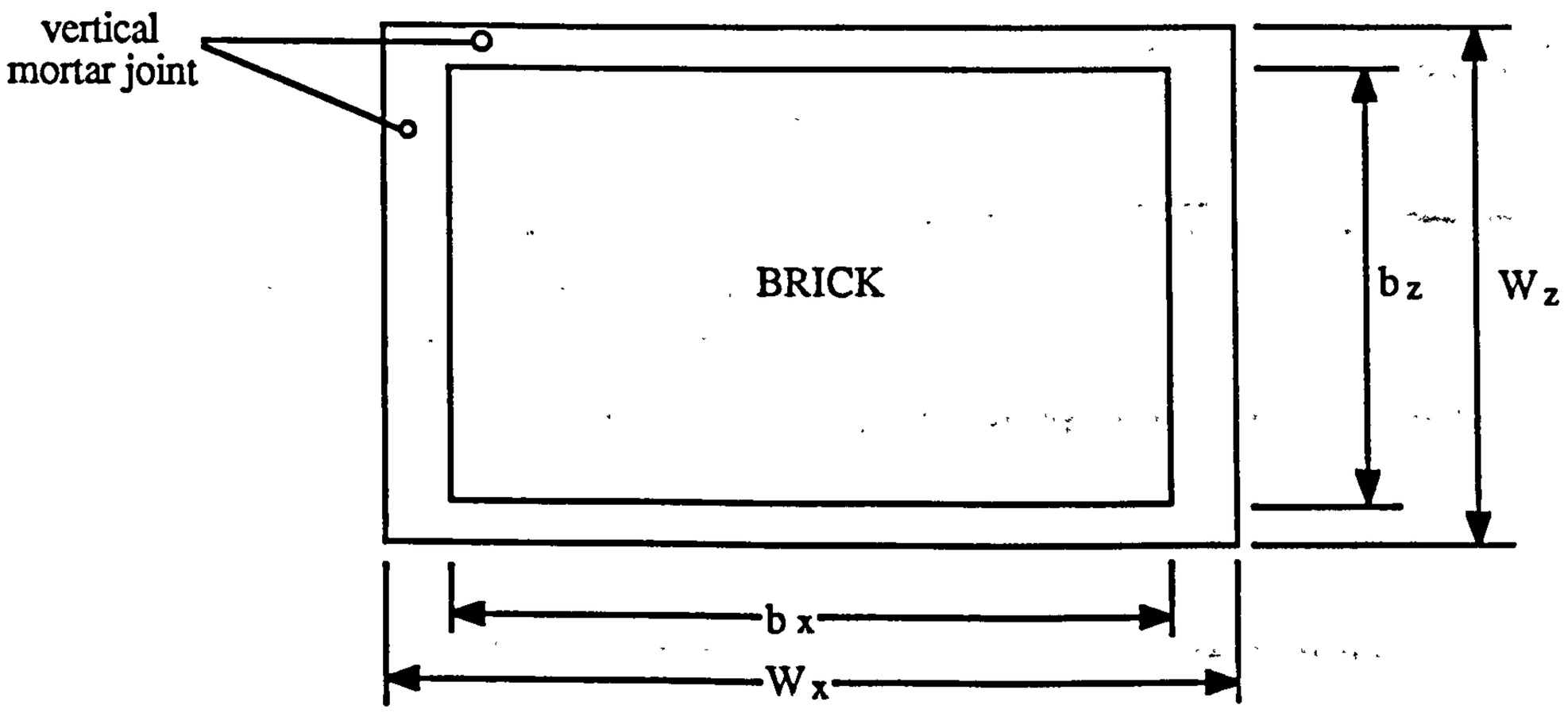

(c) Brick/mortar composite (plan)

Fig. 4.7 - Composite Model Layout for Vertical Shrinkage of Masonry, S_{wy} [Eq.(4.48)][42]

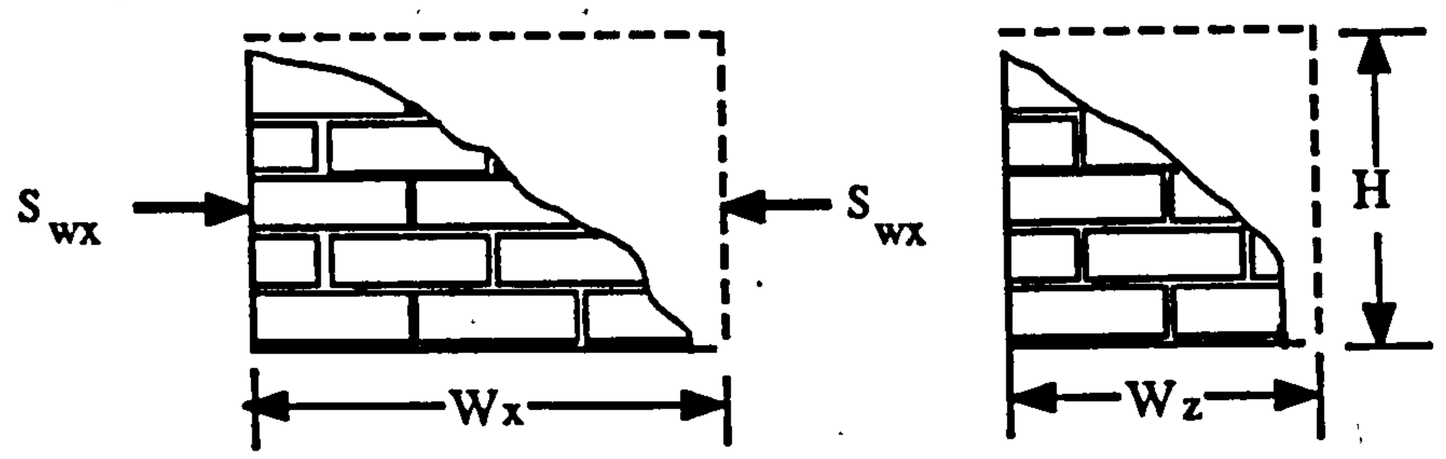

(a) Masonry unit

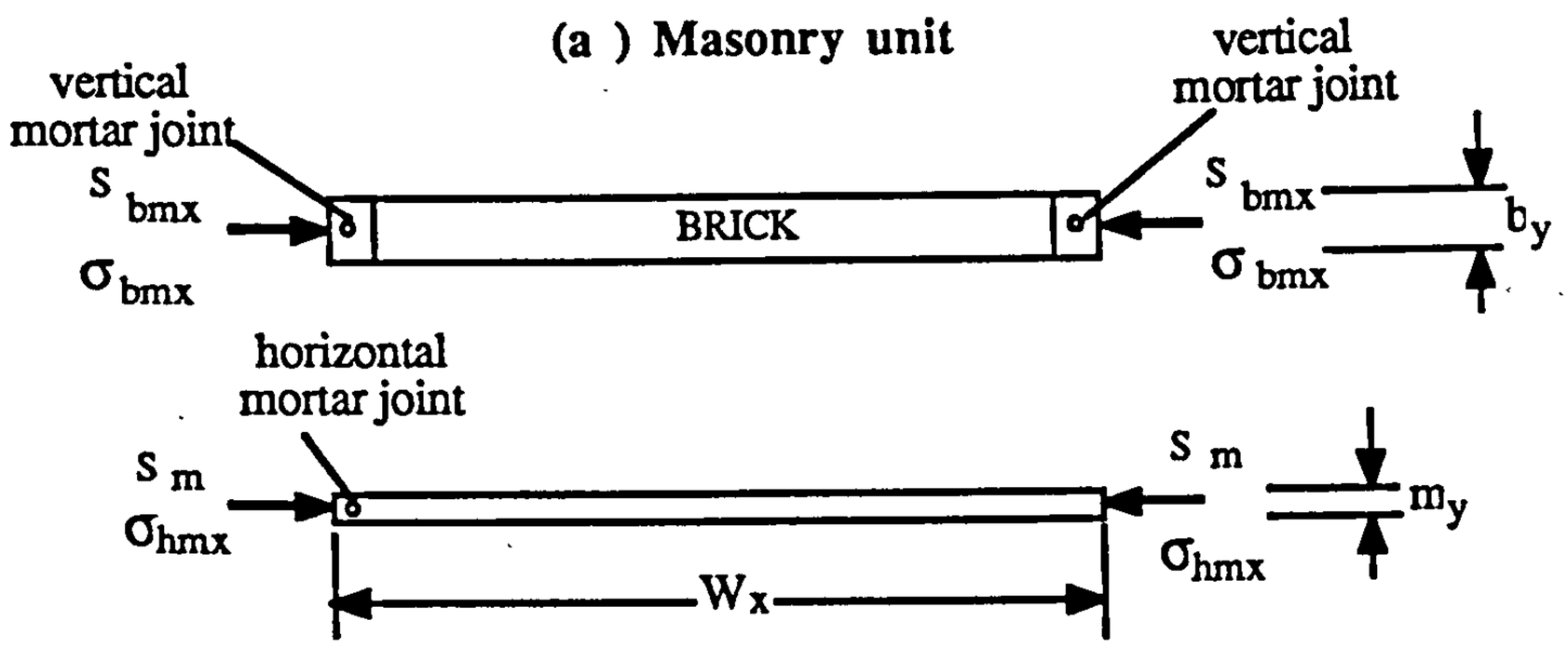

(b) Brick/mortar composite and horizontal morta2 joint (section)

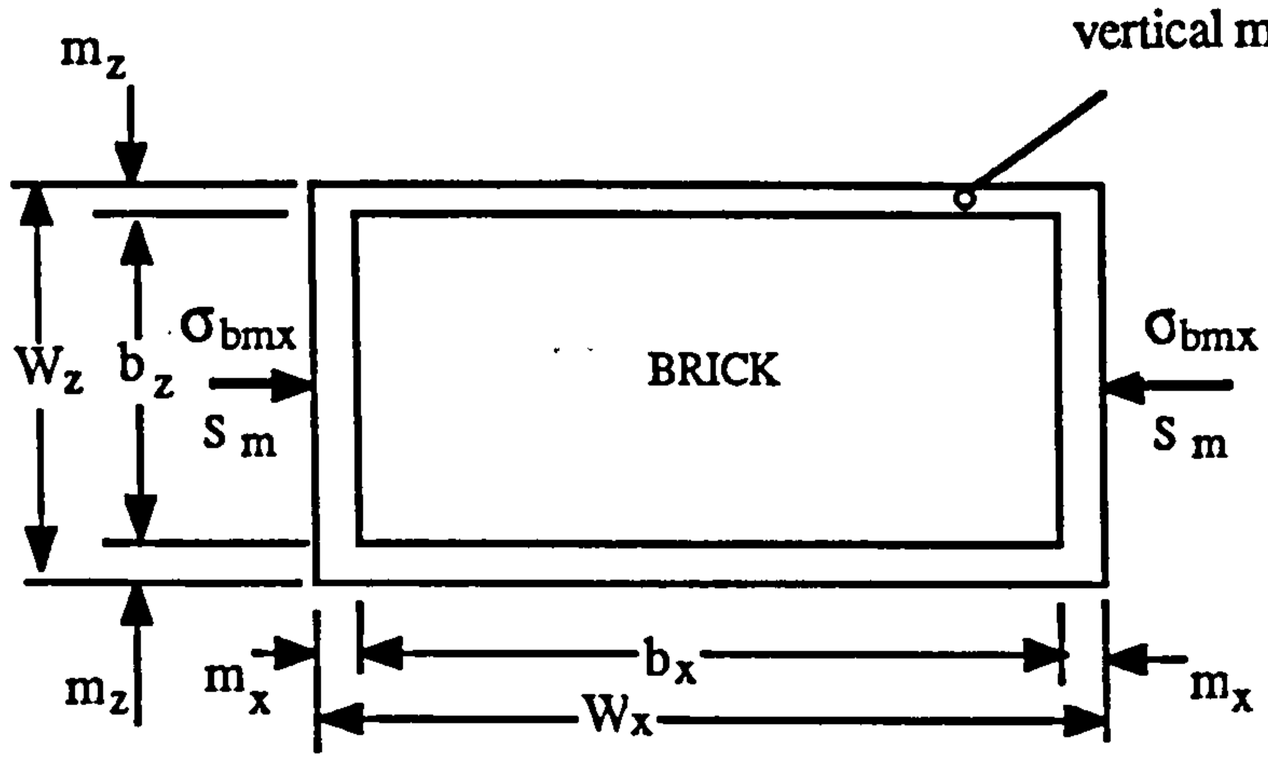

(c) Brick/mortar composite (plan)

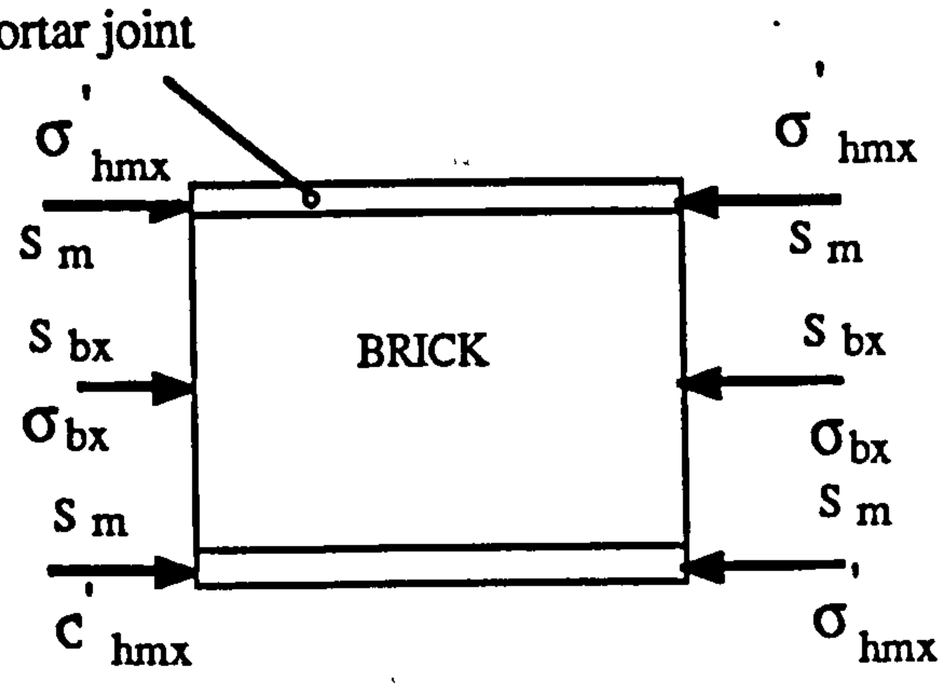

(d) Inner brick/mortar composite (plan)

Fig. 4.8 - Composite Model Layout for Horizontal Moisture Movement of Masonry, S_{wx} [Eq.(4.64)][42]

CHAPTER 5

MATERIALS AND EXPERIMENTAL DETAILS

5.1 Introduction

The experimental work consisted of measuring of strains due to load and moisture movement in a number of masonry walls and piers, and of measuring corresponding strains in unembedded mortar and brick or block units. Three completely different types of masonry units were chosen for the test programme so as to be representative of masonry in practise. Each type of masonry formed the phases of the test programme, namely:

Phase 1 - clay brick (Engineering class B)

Phase 2 - calcium silicate brick

Phase 3 - concrete block

The materials and experimental details are fully described in this chapter.

5.2 Materials

5.2.1 Brick or block units

The three types of masonry units used are described follows:

(a) Clay brick - Engineering class B, having 3 perforations of diameter ranging from 25-30 mm. At the time of laying the bricks were approximately 2 months old. Manufactured and supplied by George Armitage and Sons PLC, Wakefield, West Yorkshire.

(b) Calcium silicate brick - With one side frogged. The average depth of the frog was approximately 8 mm. Supplied by Esk Manufacturing Co. Ltd.

(c) Concrete block - 440 x 215 x 100 mm normal weight solid block supplied by Tilcon Special Products Division.

The brick and block units are shown in Plate 1.

5.2.2 Mortar

Mortar designation (ii) i.e. a $1:\frac{1}{2}:4\frac{1}{2}$ (cement:lime:sand) mix by volume as specified in BS 4551[118] was used throughout the test programme. However, for practical reasons the mortar was batched by mass in the percentage ratio of 15.6:3.1:81.3, it being assumed that the bulk densities of cement, hydrated lime and sand were, respectively, 1450, 575 and 1675 kg/m^3. Sufficient quantities of hydrated lime and sand were ordered for the complete test programme and those materials were stored in air-tight containers until used. The cement used was that readily available in the laboratory. Details of the materials are given below:

(a) Cement

The Blue Circle OPC used was supplied by Caolite Building Supplies in Leeds.

(b) Hydrated lime

White hydrated building lime was used throughout the test programme. The lime was also supplied by Caolite Building Supplies.

(c) Building sand

The building sand was obtained from Caolite Building Supplies. Sieve analysis was carried out in accordance to BS 1200[132]. The results of the tests carried out on the 3 different phases are shown in Fig. 5.1. It can be seen that sand contained a high percentage of fines.

(d) Water/cement ratio

The water/cement ratio was initially determined using the dropping ball tests as described in BS 4551[118]. The w/c ratio for a 10 mm ball penetration was found to range from 1.9 to 2.2. However, the w/c of 2.2 was used throughout the test programme for ease of laying as required by the brick layer.

For the clay and calcium silicate brickwork construction, 3 similar batches of mortar were necessary because of the amount and time of work involved, whereas, only 2 batches was required for the blockwork construction. For each batch, the required number of mortar cubes and prisms were also prepared. A typical batch mix was as follows:

OPC	- 16.9 kg.
Hydrated lime	- 3.4 kg.
Sand	- 88.1 kg.
water	- 3.7 kg.

5.3 Tests for material properties

The relevant tests were carried out on brick/block units and mortar specimens to obtain their properties. The summary of the tests carried out and number of specimens are given in Table 5.1.

5.3.1 Water absorption

Ten clay bricks were tested for water absorption as required by BS 3921[115]. A similar test was also carriied out for calcium silicate bricks but not for the concrete block. A large boiling water tank, already available in the laboratory was used for this purpose. The results of this test are given in Appendix A.

5.3.2 Compressive strength

The compressive strength test of masonry units was carried out 1 day before the creep specimens were loaded in a Dartec Tonni-Pact 3000 KN capacity testing machine, as follows:

(a) Clay brick

Ten specimens were tested between 3 mm plywood sheets as described in BS 3921[115]. A constant loading rate of 5.6 kN/sec (15 MPa/min) was applied until the brick failed. The bricks was also loaded between header faces where the 3 mm plywood sheets were used. Compressive strength were also determined between bed and header faces using 50 x 25 mm diameter cores.

(b) Calcium silicate brick

The compressive strength was determined in accordance with BS 3921[115] as specified in BS 187[116]. Two test procedures were used: Firstly, as for clay bricks but with frog down and secondly, with the frog filled with mortar (1:11/2, cement-sand mix) as required by BS 3921. Compressive strength was also determined between header faces and from core specimens as in the case of clay bricks.

(c) Concrete block

The compressive strength of six of whole concrete blocks was determined in accordance with BS 6073[117]. Perspex sheets were used to level

the high alumina cement mortar bedding (1:1 mix). Compressive strength was also determined from 100 x 100 x 200 prisms cut normal to both the bed and header faces of the whole block.

(d) Mortar

The compressive strength of mortar was carried out on 75 mm cubes. Three cubes were moulded from every batch of mortar mixes, cured in the fog-room and tested at 28 days.

5.3.3 Modulus of elasticity

No standard test method was available to determine the modulus of elasticity for bricks. As such several techniques were carried out to determine this property. Generally, the purposes of these tests were to eliminate the platen effect and to look at the anisotropic property of brick or block modulus, the latter being required when using the composite models. For all tests a loading rate of 15 MPa/min was applied throughout. Before strain readings were taken the specimens loaded and unloaded in two cycles to eliminate any component of creep and to stabilise any unevenness that may exist. The details of the test for each units are described below:

(a) Clay brick

Five different tests were adopted to determine the modulus of elasticity of brick: (i) single brick between bed faces as that for compressive strength; (ii) 3-stack unbonded brick between bed faces; (iii) 5-stack unbonded between bed faces; (iv) single brick between header faces; (v) 50 x 25 mm diameter cores between bed and header faces. In addition, lateral strains were also measured for tests (i), (ii) and (iii). Six specimens were tested for each case. The tests had to be carried out in a dry state in order to attach electrical resistance strain (ERS) gauges. For tests (ii) and (iii) the same bricks as for test (i) were used.

Grinding was first carried out in the brick bed faces for tests (ii) and (iii), and in the header faces for test (iv). ERS gauges were attached to the stretcher faces of the brick: PL-60 were gauges attached parallel to bed faces and PL-30 attached parallel to the header faces. The details for tests (i)-(iv) are shown in Fig. 5.2. The test was carried out between 3 mm plywood platens. Strain readings were taken in the middle brick and were recorded on a data logger. However, the 5-stacked bricks did not show a consistent result, probably due to unevenness of the bed faces, and was therefore discarded from the test programme.

The cored specimens were prepared in the Mining Department of Leeds University. Two specimens were cored from six bricks, one from the header face and the other from the bed face. The ends of the core were ground level and later smoothed using a file, before attaching two PL-10 ERS gauges. The specimens were loaded using the Instron testing machine and strain readings were recorded on a data logger. Typical test samples are shown in Plate 3.

(b) Calcium silicate brick

Similar tests as that for clay bricks were carried out on calcium silicate bricks, but for tests (i) and (iii) the frogs were filled with mortar (1:1 ratio of high alumina cement:sand mix) and were then ground. The bricks was tested with frog down.

(c) Concrete block

Only two sets of tests were carried out on the concrete blocks. For both cases, the modulus was determined from the same specimens for compressive strength test. For the whole bricks loaded between bed faces, PL-60 ERS gauges were attached in the direction of the load on the stretcher faces. Instead of cores, 100 x 100 x 200 mm prisms were cut between the bed and header

faces. For each face six specimens were cut from three blocks and then were instrumented with PL-60 gauges. The load-strain curves were recorded on an x-y plotter.

(d) Mortar

The tests for modulus of elasticity were carried out on 75 x 75 x 200 mm mortar prisms. The specimens were moulded and stored beside the brickwork/blockwork in a control environment room. For each phase of testing, 6 specimens were tested (2 and 3 specimens form every batch for brickwork and blockwork, respectively). Prior to testing the top of the prism was levelled by grinding. The strain measurements were then made using 150 mm Demec gauge.

5.4 Creep tests

Similar sizes and shapes of masonry were built for clay and calcium silicate brickwork. Due to the larger size of the concrete blocks a different set of masonry was built. The masonry was constructed in stretcher bond. Individual bricks or block units and mortar were also prepared for creep tests.

5.4.1 Clay and calcium silicate brickwork

Brickwork specimens were built in pairs from clay and calcium silicate bricks. One of each pair was loaded in the creep frame and the other was the control units where moisture strains were measured.

Four pairs of approximately 1 m high brickwork of different geometries were built as follows:

(1) Single-leaf wall - 450 mm x 103 mm, 13 courses high.

(2) Cavity wall - 450 mm x 330 mm, 13 courses high.

(3) Hollow pier - 450 mm x 450 mm, 13 courses high.

(4) Solid pier - 450 mm x 450 mm, 13 courses high.

Figure 5.3 shows the plan-view of the brickwork.

5.4.2 Concrete blockwork

Four pairs of blockwork were built as follows:

(1) Single-leaf wall - 890 mm x 100 mm, 5 courses high.

(2) Cavity wall - 550 mm x 330 mm, 5 courses high.

(3) Hollow pier - 550 mm x 550 mm, 5 courses high.

(4) Solid pier - 440 mm x 440 mm, 5 courses high.

The sectional view of the concrete blockwork is shown in Fig. 5.4.

5.4.2.1 Volume to surface area ratio

The volume to surface area ratio (V/S) for the clay and calcium silicate brickwork, their model walls and their corresponding component materials are given in Table 5.2. The values of V/S ratio for concrete blockwork are given in Table 5.3.

As was pointed out in the literature review (Chapter 3), the average thickness (T_d) has been shown to be a better indicator of size and shape for concrete[87] compared to the V/S ratio. However, in this investigation the V/S ratio, being simpler to calculate, is adopted because the parameter is more commonly used in concrete. Furthermore, for similar shape of specimens, but for different sizes, the relationship between V/S ratio and T_d is linear and it was thought that only when different shapes of specimens are involved the use of T_d would be an advantage. However, for the size and shape of masonry of this investigation, the relationship between V/S ratio and T_d was found to be a linear as shown in Fig. 5.5. Hence, the use of V/S ratio as an indicator of size and shape of masonry is reasonable, since, in most cases, masonry members come in shapes of rectangular form.

5.4.3 Model walls

Four pairs of one-brick wide model walls were built from clay and calcium silicate bricks. The clay model walls were 6-course high, whereas the calcium silicate model walls were only 5-course high. The 6-course model walls were built in order to simulate the height width ratio of the single-leaf wall, but later this was thought unnecessary and the 5-course calcium silicate model walls were built instead, as this had the advantage of symmetry with an odd number of courses.

No model walls were built from concrete blocks. In order to simulate the moisture diffusion in the larger masonry the model walls were partly sealed so as to give the required V/S ratio; details are shown in Fig. 5.6 and Table 5.4.

5.4.4 Brick and block units

For the tests on unembedded units, four clay and four calcium silicate bricks were partially sealed for each of the four required V/S ratios in Table 5.2. Two were used as creep specimens while the other two were the control specimens. In addition, six bricks of each type were layered with mortar on both sides of the bed face to investigate the effect of mortar joints on moisture movement of bricks.

For the concrete block tests, 215 x 100 x 65 mm bricks were cut normal to bed-faces from the whole units, partly sealed and tested in the same manner as clay and calcium silicate bricks. In addition, pairs of the whole concrete block units were partly sealed to give the same V/S ratio of the corresponding embedded blocks, one was loaded between headers in the creep rig while the other was a control unit. The sealing details are given in Fig. 5.6 and Table 5.4.

5.4.5 Mortar prisms

For each phase of the testing programme, 24 - 75 x 75 x 200 mm prisms were moulded in purpose made moulds. Sixteen prisms were partly sealed to give the required

V/S ratio, four for each V/S ratio. The remaining prisms were unsealed and were used for the determination of modulus of elasticity as described in Section 5.3.2. The sealing details are given in Fig. 5.6 and Table 5.4.

5.4.6 Laying

The construction of the masonry test units was carried out by a laboratory technician. The bricks and blocks were all laid dry. As a substantial number of bricks were involved (about 1274 units) and only one technician was available, the brick-laying work was completed over $1\frac{1}{2}$ days. However for the blockwork, the laying was completed within a day. In order to reduce the variability between the masonry units, the laying was done in steps of 3 courses, i.e. 3 courses were laid for all units first before proceeding to the next 3 courses. The last 4 courses were laid the following morning. For the model walls, the laying was done in steps of 2 courses. As stated earlier, 3 batches of mortar were mixed for the brickwork (2 batches on the first day and the other the following morning), and 2 batches for the blockwork.

5.4.7 Sealing

In order to get the same range of V/S ratios as the corresponding embedded mortar and brick/block units, the individual brick/block and mortar prisms for the creep tests were partly sealed. The model walls were also partly sealed to give the same V/S ratio as the corresponding masonry units. The sealing was carried out by painting with two layers of bituminous paint and covering with two layers of a waterproof polythene 'all-weather' cellotape after the paint had dried. The use of the cellotape sheet offered an advantage than the conventional polythene sheet in that it had adhesive and could be stuck on the painted surface of the specimens. However, as an extra precaution, the sides of the tape were brushed with 'Evostik' general adhesive to prevent peeling. The sealings was carried out within 7 days after brick-laying.

Before this technique was adopted, preliminary tests were carried out to investigate the effectiveness of sealing: Nine matured (after more than six months of curing in the fog room) and fully saturated mortar specimens used, three of each were: fully sealed, partly sealed and unsealed, respectively. Essentially, the specimens were weighed before and after sealing. Over a period of six months, the weight loss of the sealed specimen was found to be insignificant, while the weight loss of the partly sealed specimens was in between the fully sealed and the unsealed specimens. The results are given in Table A2, Appendix A. The matured mortar specimens were chosen to minimise the effect of weight loss due to the hydration of the cement.

5.5 Environmental conditions

The masonry tests units were built and tested in a controlled environmental room with a relative humidity of 65±5 % and a temperature of 21±1°C. After construction the masonry units were covered with polythene sheets. It was intended to keep the units covered until loading commenced, i.e. up to 28 days, but unfortunately, during the commencement of the phase 1 tests, the clay brickwork was found to be left uncovered after 10 days of laying, and for reasons of consistency for other phases of testing, the units were covered for the first 10 days only, before exposure to drying. The bricks or blocks and mortar prisms were placed beside the corresponding masonry units and were kept covered under the same polythene sheetings for the initial 10 days.

5.6 Creep frames

Two different systems of creep frames were used in this investigation. The first for the masonry units and the other for the individual specimens.

5.6.1 Full size and model masonry Units

The financial and space constraints were the major factors that influenced the design of the creep rig. As such, those rigs which had been used by Brooks[41] and Lenczner[3] could not be adopted in the present investigation. A simple and cheap frame

layout was designed for the different masonry geometries and was used throughout all the 3 phases of testing programme with the exception of a slight modification which was necessary for the concrete masonry. Details of the frames for each type of masonry can be found as follows:

(a) Single-leaf wall

The details are shown in Fig. 5.7. The rig was modified for concrete block-wall, as shown in Fig. 5.7(b).

(b) Cavity wall

The details are shown in Fig. 5.8.

(c) Hollow pier

The details are shown in Fig. 5.9.

(d) Solid pier

The details are as for hollow pier (Fig. 5.9).

(e) Model walls

The details are shown in Fig. 5.10. A total of four frames were made.

Essentially, each creep frame rig consisted of a base and a header plate, and steel tie-rods (two for single-leaf brickwall and model walls, and four for the other masonry) which were threaded at the ends. The base plates were designed such that the thickness could take the amount of load without any appreciable bending when a stress of 1.5 MPa was to be applied on the masonry unit. Similarly, the tie rods were designed to withstand the load such that the induced stress would not produce any significant creep in the rod itself.

Holes were made at each corner of the plates for the tie rods to go through. In addition, for the cavity wall, four 36 mm diameter holes were drilled at the centre of the plates to allow drying of the cavity. Bolt threads were designed and cut at each ends of the tie-rod so as to withstand the tensile force applied.

The use of RHP thrust ball bearings between the steel header plate and the tie-rod BSW nut facilitated manual tightening of the nut, otherwise manual tensioning of the rod to the required load would have been impossible.

5.6.1.1 Tie-rod calibration

The tie-rods also acted as load cells. The surface at the mid-point of the tie-rod was first smoothed and cleaned, after which a pair of 2-axial ERS foil gauges (FCA-6 type) were attached using a creep-free performance adhesive. The adhesive was prepared by mixing a curing agent (AE-10) in a bottle of epoxy based resin (GA-2). Setting of the mix was prolonged by occasional stirring and by placing the bottle in a specially made brass container. The strain gauges were then attached after a thin layer had been applied to both the surface of the steel rod and the gauge. A pad of silicone gum and a back-up plate were then placed on top of the strain gauges. Using a spring clamp, pressure was applied to the back-up plates and maintained for 48 hours for the adhesive to be fully set. The strain gauges were then wired in full-bridge arrangement and then painted with a protective coating. The wiring arrangement is shown in Fig. 5.11.

All of the tie-rods were calibrated using an Avery-Denison machine and a strain measuring unit (Peekel) which was then used throughout the test programme for monitoring the tie-bar stress. During the calibration, before the appropriate strain readings were taken, the rods were loaded and unloaded in 3 or 4 cycles so as to stabilise the adhesive and to minimise hysteresis. The short term zero shift was found to be very small (less than 0.1%) and the long term (after 2 months) the shift was less than 0.5%. For every phase of testing programme the tie-rods were recalibrated. Holes for Demec gauges were also drilled in the tie-rods as a precaution in case of ERS gauge failure.

5.6.1.2 Loading procedure

The application of the axial compressive load on the masonry test units was performed by tensioning the calibrated tie-rods. This was achieved by tightening manually the top nuts in the tie-rods with a large spanner. For the initial application of load, alternate nuts were tensioned in small load increments until equal loads (given by the tie-rod calibration) for all tie-rods were obtained. The nuts were retightened occasionally to compensate the loss of load due to creep and shrinkage of the masonry units. As there was a total of 22 tie-rods in one phase of the programme (24 in case of blockwork), a distribution box was used to connect the strain gauges to the strain measuring units. The arrangement is shown in Fig. 5.12 and the equipment used is shown in Plate 2.

5.6.2 Individual brick/block and mortar specimens

Similar creep frames to those used extensively in the department for cylindrical concrete specimens[103] were modified for this investigation. The modifications were made at the end and intermediate plates to suit the size and shape of the bricks and mortar specimens. Also, the overall length of the frames had to be shortened. Essentially, two specimens were held in series with a calibrated steel-tube dynamometer by four tie-rods, the loss of load due to creep and shrinkage being compensated manually by re-tensioning the tie-rods. The layout of the creep frames for brick and mortar specimens is shown in Fig. 5.13. Four pairs of each type were made and were arranged horizontally on timber shelves after the specimens were subjected to the initial load. For the individual block tests those frames designed for the model brickwall were used.

5.7 Creep test procedure

About two weeks after laying, a layer of mortar was laid on top of masonry units. For the walls and piers, and model walls, taking precautions against exerting any load on the masonry, the header plates were lowered and levelled on the mortar while

it was still plastic. In order to avoid the mortar from being bonded to the header plate, polythene sheets were used. The header plates were lifted after 24 hours and the polythene sheets were removed prior to loading. For the control units, the mortar layer was painted and sealed with the same materials used for partial sealing of bricks and mortar prisms, while for the hollow pier the cavity was fully sealed with polythene sheet and a piece of hardboard placed on the top.

The headers of the individual bricks and mortar creep specimens were ground prior to sealing and later brushed with silicon grease.

The initial application of load for single-leaf and cavity walls was carried out at 28 days after laying, while, for hollow and solid piers the load was applied a day later.

The creep specimens were loaded with a sustained stress of 1.5 MPa which was the working stress for Class 4 bricks with mortar designation (ii). This calculation based on BS 5628[46], is given in Appendix A. The loads were adjusted (by re-tightening of the nuts) hourly after the application of load for the first day, then daily for the first week and less frequent afterwards. The individual bricks and blocks were loaded between header faces. The model walls and individual specimens (bricks and mortar prisms) were loaded and monitored at the same interval as the corresponding masonry units. The tests were terminated after about 6 months under load. Plates 4, 5 and 6 show clay, calcium silicate and concrete masonry under test. Typical bricks and mortar specimens under test are as shown in Plate 7.

5.7.1 Strain measurement

Prior to load application, both the creep and control specimens were fitted with Demec points. The five different sizes of Demec gauges and their readings per division were as follows :

(a) 750 mm gauge - 2.1×10^{-6} per division

(b) 400 mm gauge - 4.0×10^{-6} per division

(c) 200 mm gauge - 8.0×10^{-6} per division

(d) 150 mm gauge - 10.8×10^{-6} per division

(e) 50 mm gauge - 19.9×10^{-6} per division

Plate 8 shows the different Demec gauges used for the strain measurements. The readings using 750 and 400 mm Demec gauges were taken to the nearest division, while for 200, 150 and 50 mm gauges the reading were taken to the nearest 1/2 division. The 50 mm gauge was used to measure strain in a centrally embedded brick but this proved to be difficient on clay brickwork. Subsequently, 16-51 mm acoustic vibrating wire gauges (VWG) were used on the calcium silicate brickwork. The VWG was capable of measuring a change of strain of 1 microstrain which is given as:

$$\Delta\varepsilon = 4 \times 10^{-10}\left(\frac{1}{T_1^2} - \frac{1}{T_2^2}\right) \qquad (5.1)$$

where T_1 and T_2 are periods of frequency.

The period frequency signals were read from a unit as shown in Plate 3.

Measurements were started just prior to application of load and immediately after loading to obtain the elastic strain. Measurements were then made at 1,3,7,14 days, and then weekly and less frequently at later periods after loading for both the creep and control units. As far as possible, the measurements of strain of the model walls and the individual units were made at the same time as the corresponding masonry units. Details of the strain measurements for the test specimens were as follows:

(a) Masonry walls and piers

Figure 5.14 shows details of Demec positions for both the creep and control clay and calcium silicate brickwork and Fig. 5.15 shows the of Demec positions for concrete blockwork. The vertical Demec positions for brickwork

and blockwork are also shown in Figs. 5.3 and 5.4, respectively. For the brickwork, vertical strains were measured with 750 and 150 mm Demec gauges, and horizontal strains were measured using the 400 mm gauge. On the other hand, for the blockwork, 400 and 200 mm gauges were used for measuring vertical strains, and the 400 mm gauge was also used to measure the horizontal strains, except for the single-leaf blockwork where the 750 mm gauge was used instead.

For vertical strains using the 750 mm gauge (400 in the case of blockwork), measurements on the major faces (see Fig. 5.14) were made at 3 positions , whereas for the minor faces measurements were made at 1 position only. In the case of horizontal strain, measurements were made on the major faces only.

Strain measurements for the centrally embedded clay bricks were made by 50 mm and 150 mm Demec gauges in the vertical and horizontal direction, respectively. For calcium silicate embedded units, 51 mm VWG and 150 mm Demec gauge were used for the corresponding positions. However, for the embedded blocks, being larger in size, the 150 mm Demec gauge was used in both the vertical and horizontal directions.

(b) Model walls

The positions of Demec points are shown in Fig. 5.16. For clay model walls, 200 mm and 150 mm Demec gauges were used to measure the vertical and horizontal strains, respectively. While for calcium silicate model walls, the 150 mm Demec gauge was used for both directions.

(c) Individual units

For both brick and mortar specimens the 150 mm Demec gauge was used to measured the strains. Demec points for the 50 mm gauge were intended

to be used for lateral strain but no measurements were made because the space between tie-rods was to small for the gauge. In the case of the whole blocks, 200 and 150 mm gauges were used in the vertical and horizontal direction, respectively.

Table 5.1 - Number of Specimens for Strength and Elasticity Tests

	Strength			Modulus of Elasticity				
	bed face	header face	core	Single unit		unbonded stack		core
			bed & header faces	bed face	header face	3 stack	5 stack	bed & header faces
Clay brick	10	10	6	6	6	6	6	6
Calcium silicate brick	10	10	6	6	6	6	-	6
Concrete block	6	-	6*	6	-	-	-	6*

** 75 x 75 x 200 mm prisms cut from the whole block*

Table 5.2 - Volume-Surface Area of Clay and Calcium Silicate Brickwork*

Type of brickwork	Volume (V) (10^{-6} mm^3)			Surface Area (S) (10^{-6} mm^3)			V/S (mm)		
	Brickwork	Bricks	Mortar	Brickwork	Bricks	Mortar	Brickwork	Bricks	Mortar
Single-leaf wall	45.362	37.417	7.945	1.043	0.870	0.181	44	43	44
Cavity wall	116.324	93.452	22.782	2.270	1.825	0.445	51	51	51
Hollow pier	137.213	112.250	24.963	1.748	1.442	0.307	78	78	81
Solid pier	196.053	149.666	46.386	1.758	1.442	0.317	112	104	146
Model wall									
1	8.413	7.062	1.351	0.191	0.164	0.030	44	43	45
2	8.413	7.062	1.351	0.165	0.139	0.026	51	51	51
3	8.413	7.062	1.351	0.108	0.090	0.018	78	78	78
4	8.413	7.062	1.351	0.075	0.061	0.014	112	112	112

** The values are approximately similar for clay and calcium silicate 13-course and model brickwork*

Table 5.3 - Volume-Surface Area of Concrete Blockwork

Type of blockwork	Volume (V) (10^{-6} mm^3)			Surface Area (S) (10^{-6} mm^2)			V/S (mm)		
	Brickwork	Bricks	Mortar	Brickwork	Bricks	Mortar	Brickwork	Bricks	Mortar
Single-leaf wall	101.015	94.600	6.415	2.247	2.107	0.140	44	44	44
Cavity wall	154.360	142.560	11.800	3.065	2.838	0.226	51	51	51
Hollow pier	204.300	189.200	15.100	2.497	2.332	0.175	82	81	86
Solid pier	219.736	189.200	30.536	1.998	1.849	0.149	110	102	205

Table 5.4 -Sealing of Specimens - Values of x in Fig. 5.6

(a) Model walls and individual whole block

V/S Ratio (mm)	Value of x	
	5-leaf	6-leaf
44	-24	-24
51	-1	-1
78	37	38
112	59	58

(b) Individual bricks

V/S Ratio (mm)	Value of x
44	-8
51	0
78	11
104	18

(c) Mortar prism

V/S Ratio (mm)	Value of x
44	5
51	10
81	20
146	28

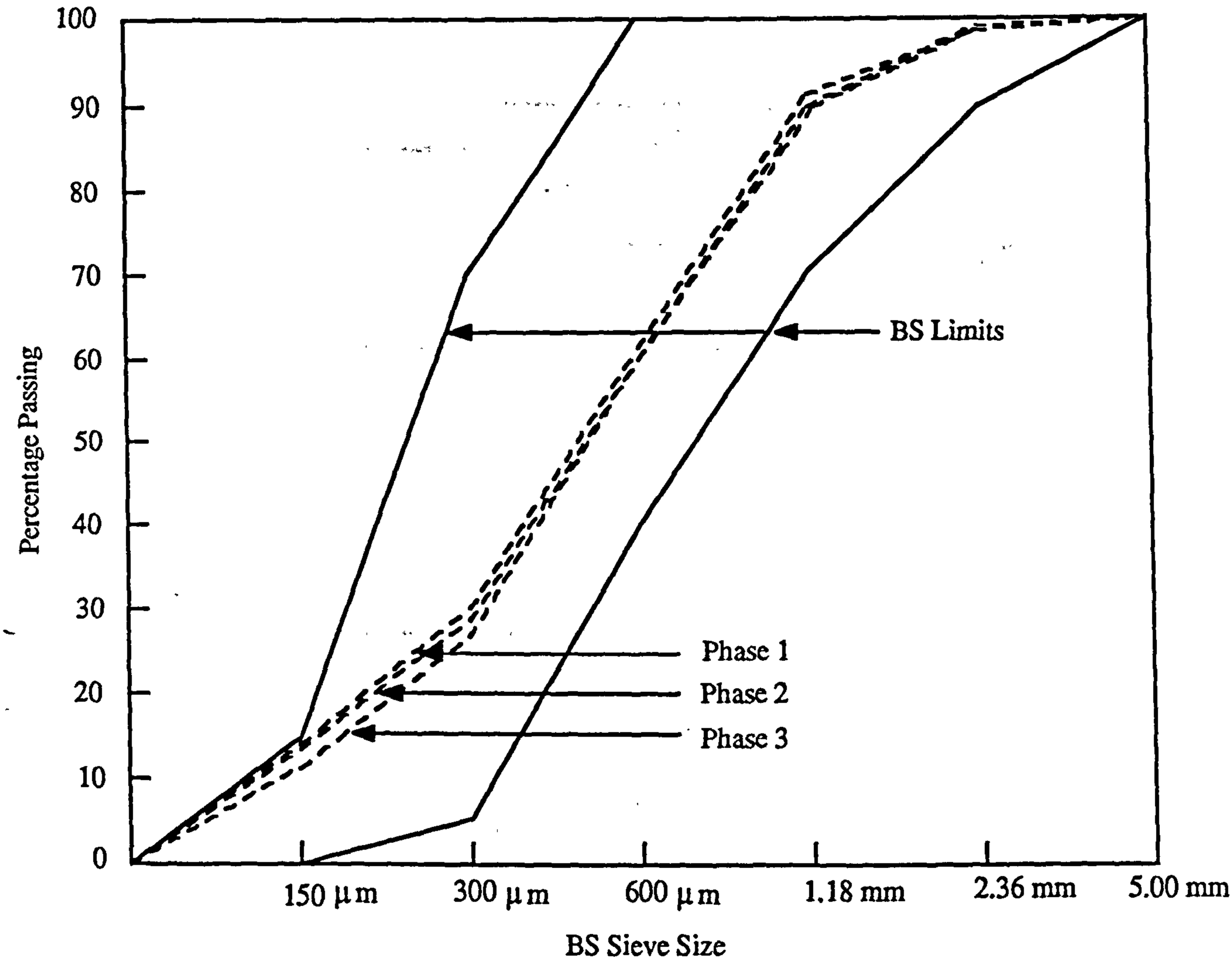

Fig. 5.1 - Results of the Sieve Analysis for Sand Complying to BS 1200 [135]

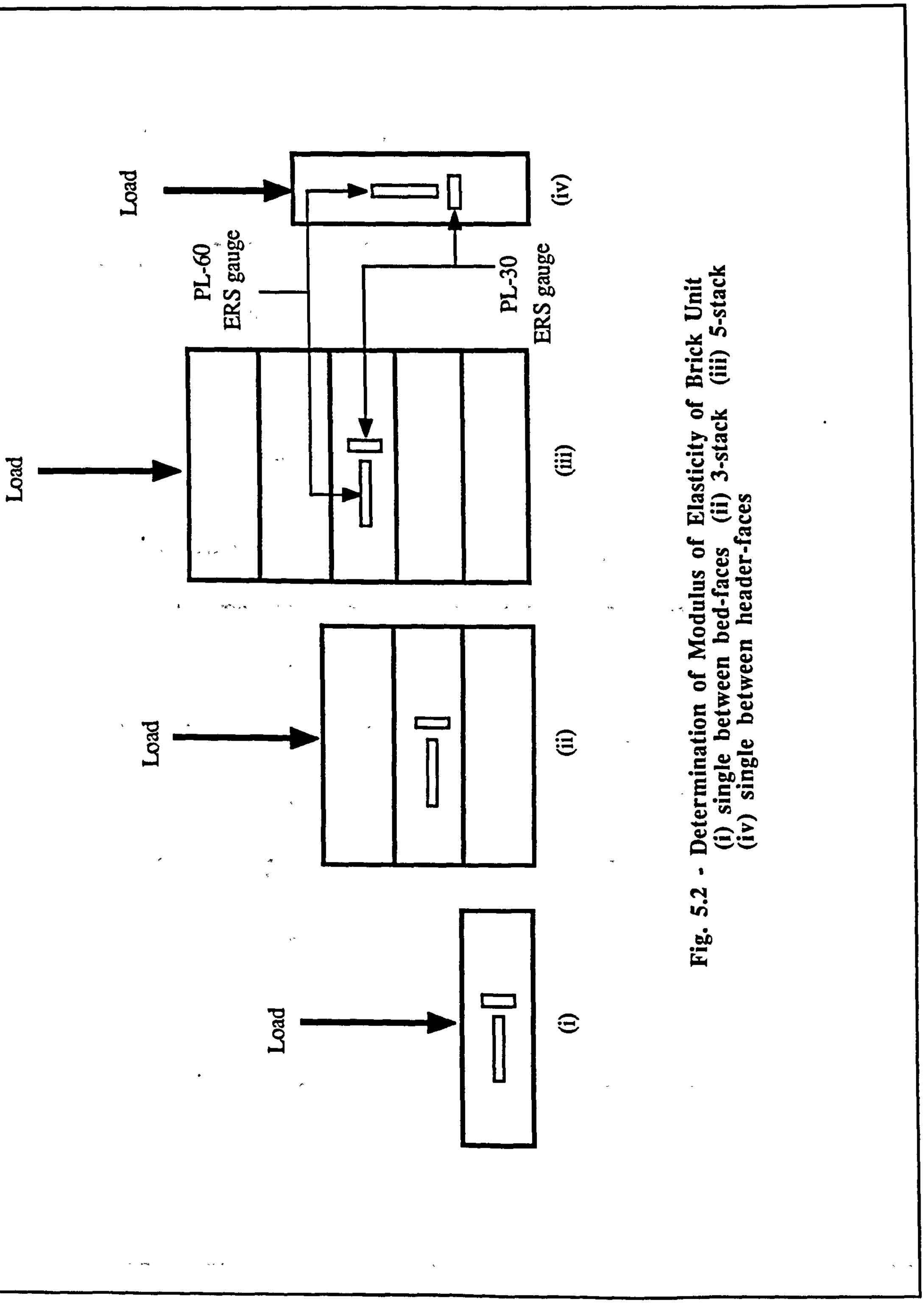

Fig. 5.2 - Determination of Modulus of Elasticity of Brick Unit
(i) single between bed-faces (ii) 3-stack (iii) 5-stack
(iv) single between header-faces

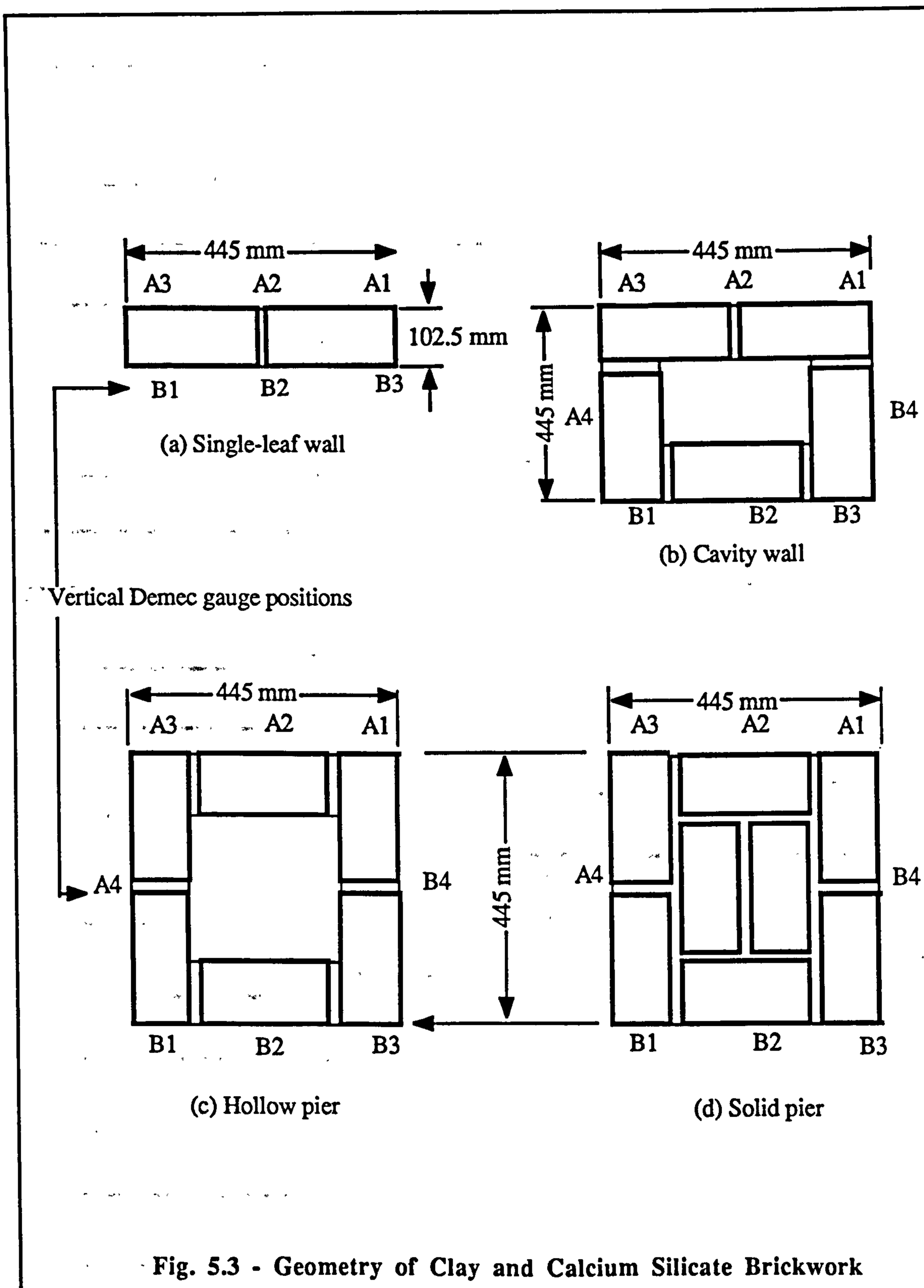

(a) Single-leaf wall

(b) Cavity wall

(c) Hollow pier

(d) Solid pier

Fig. 5.3 - Geometry of Clay and Calcium Silicate Brickwork

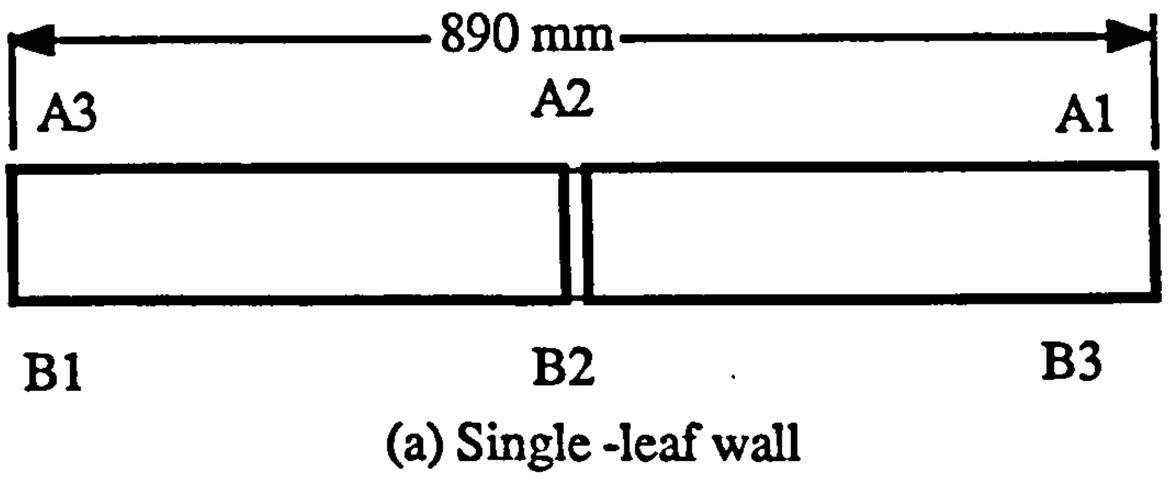

(a) Single -leaf wall

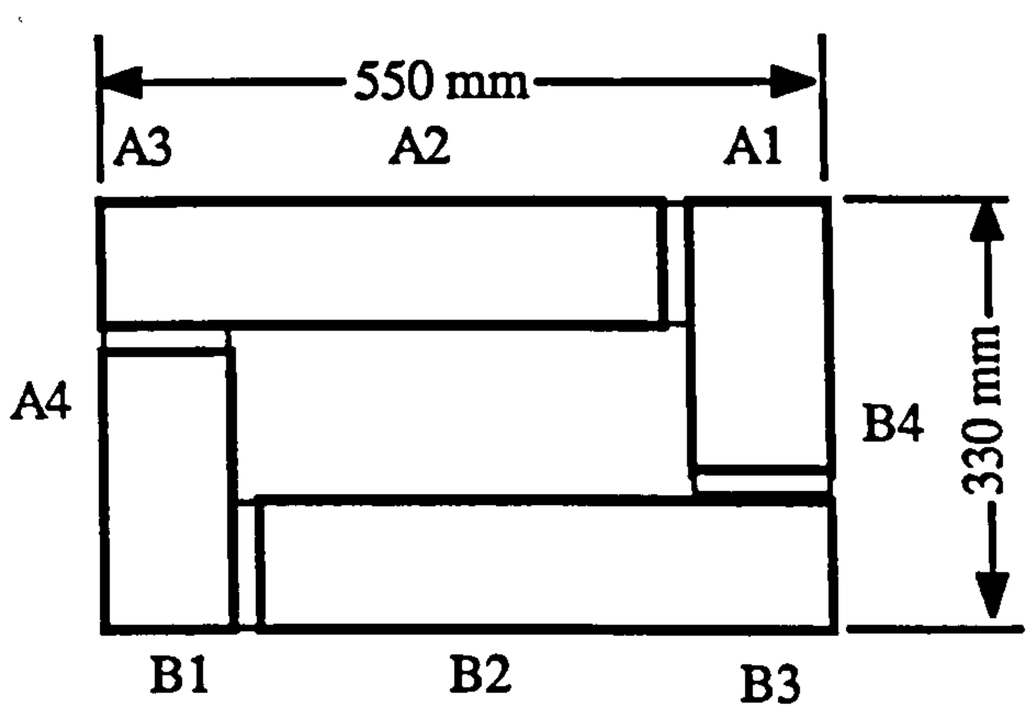

(b) Cavity wall

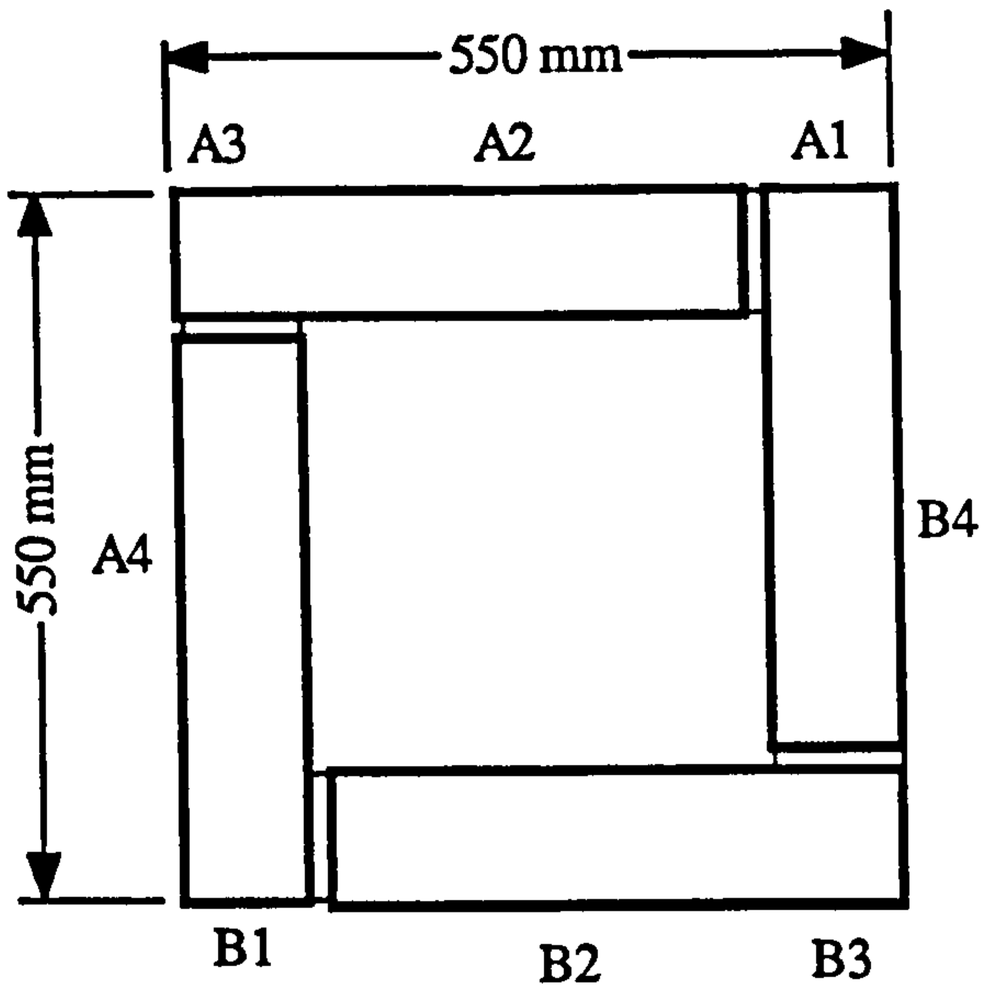

(c) Hollow pier

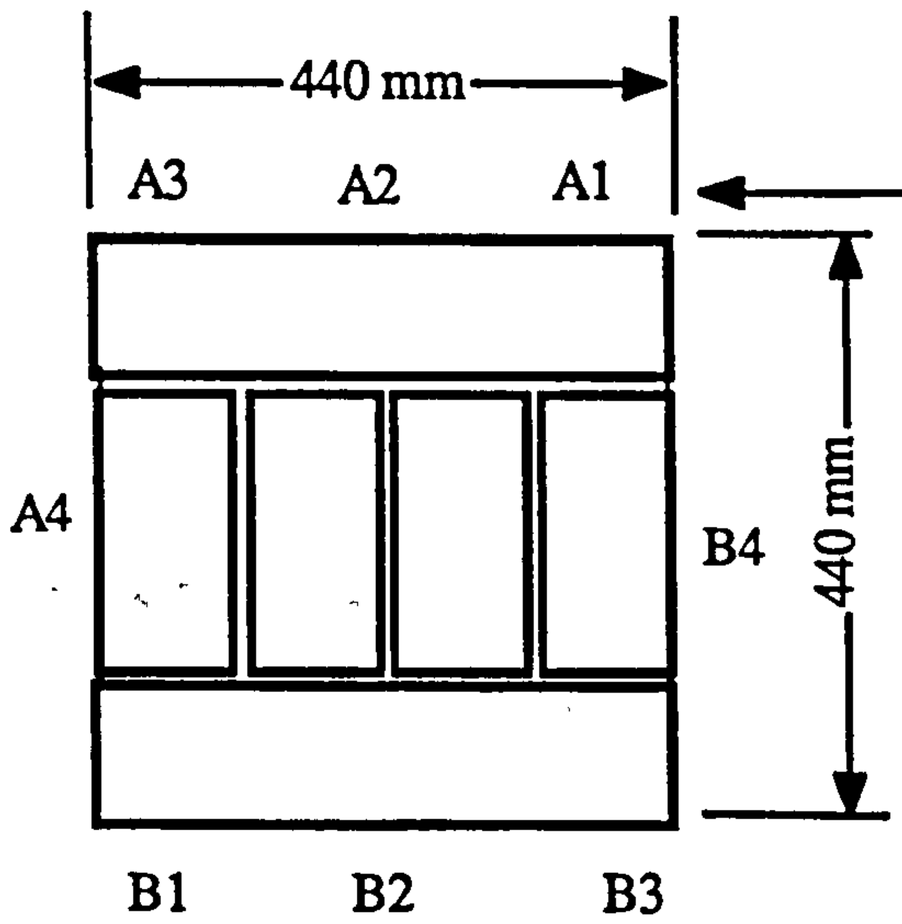

(d) Solid pier

Vertical Demec point positions

Fig. 5.4 - Geometry of Concrete Blockwork

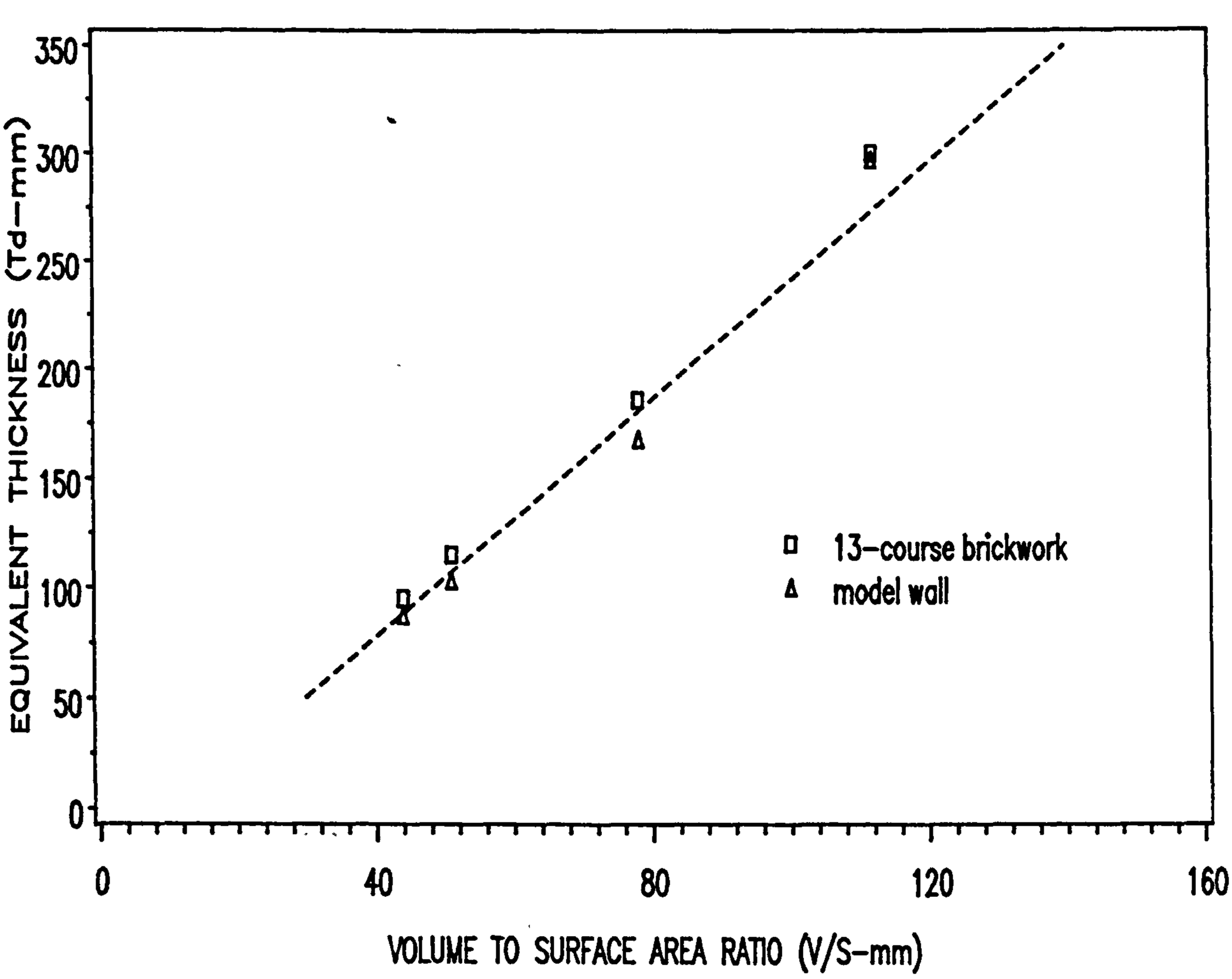

Fig. 5.5 – Comparison between Equivalent Thickness (Td) and Volume to Surface Area Ratio (V/S) for Brickwork

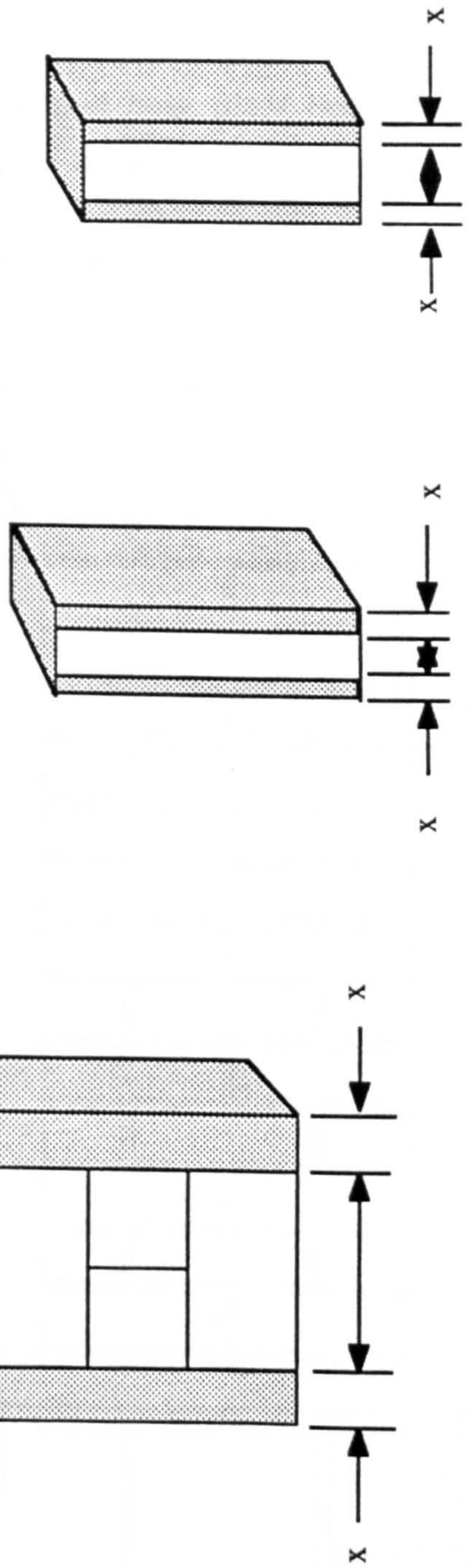

(a) Model wall and concrete block

(b) Brick

(c) Mortar prism

x - Dimension x varies , see Table 5.4)

Fig. 5. 6 - Partial Sealing of Specimens (D

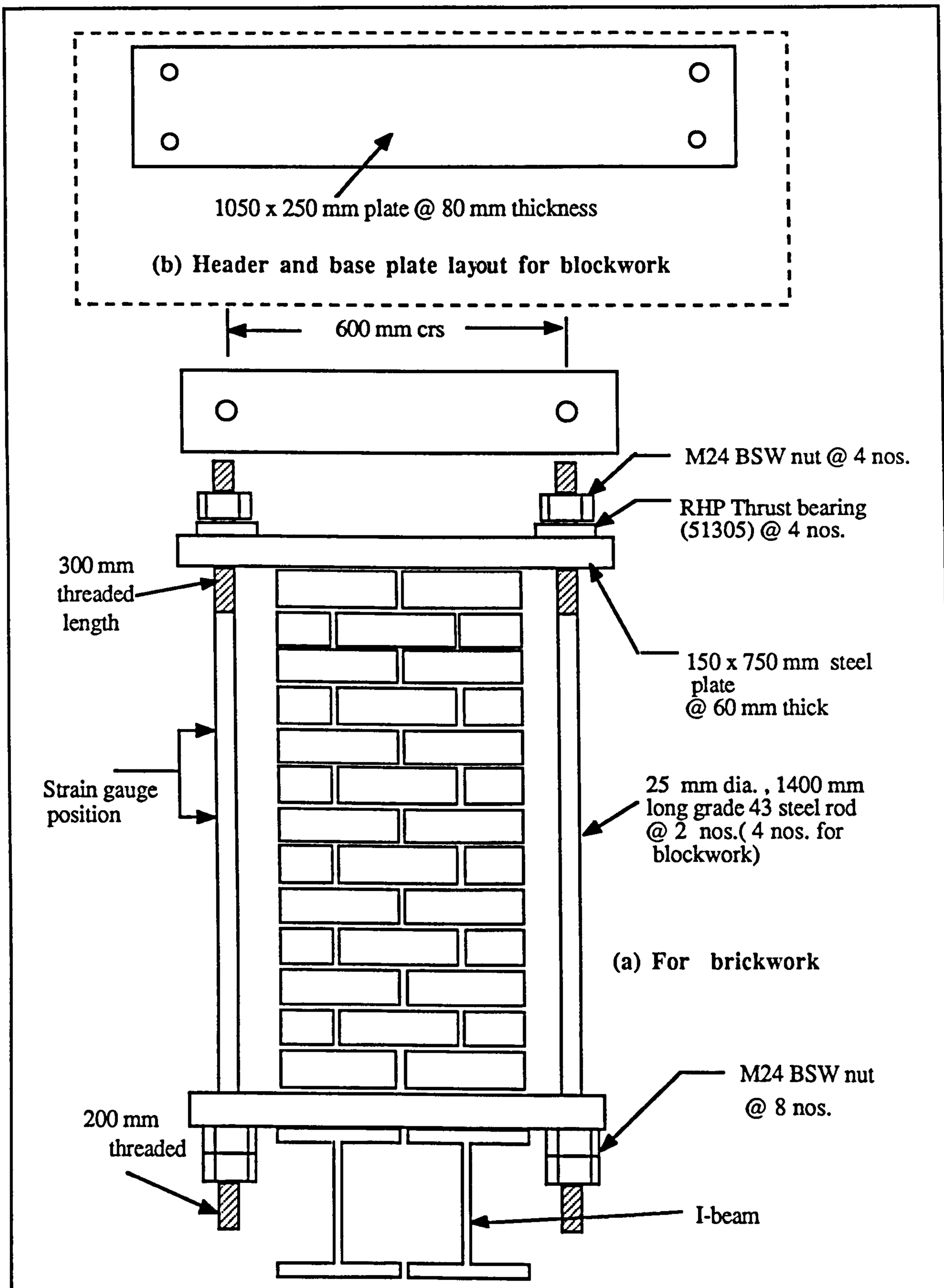

Fig. 5.7 - Creep Frame for Single-leaf Wall

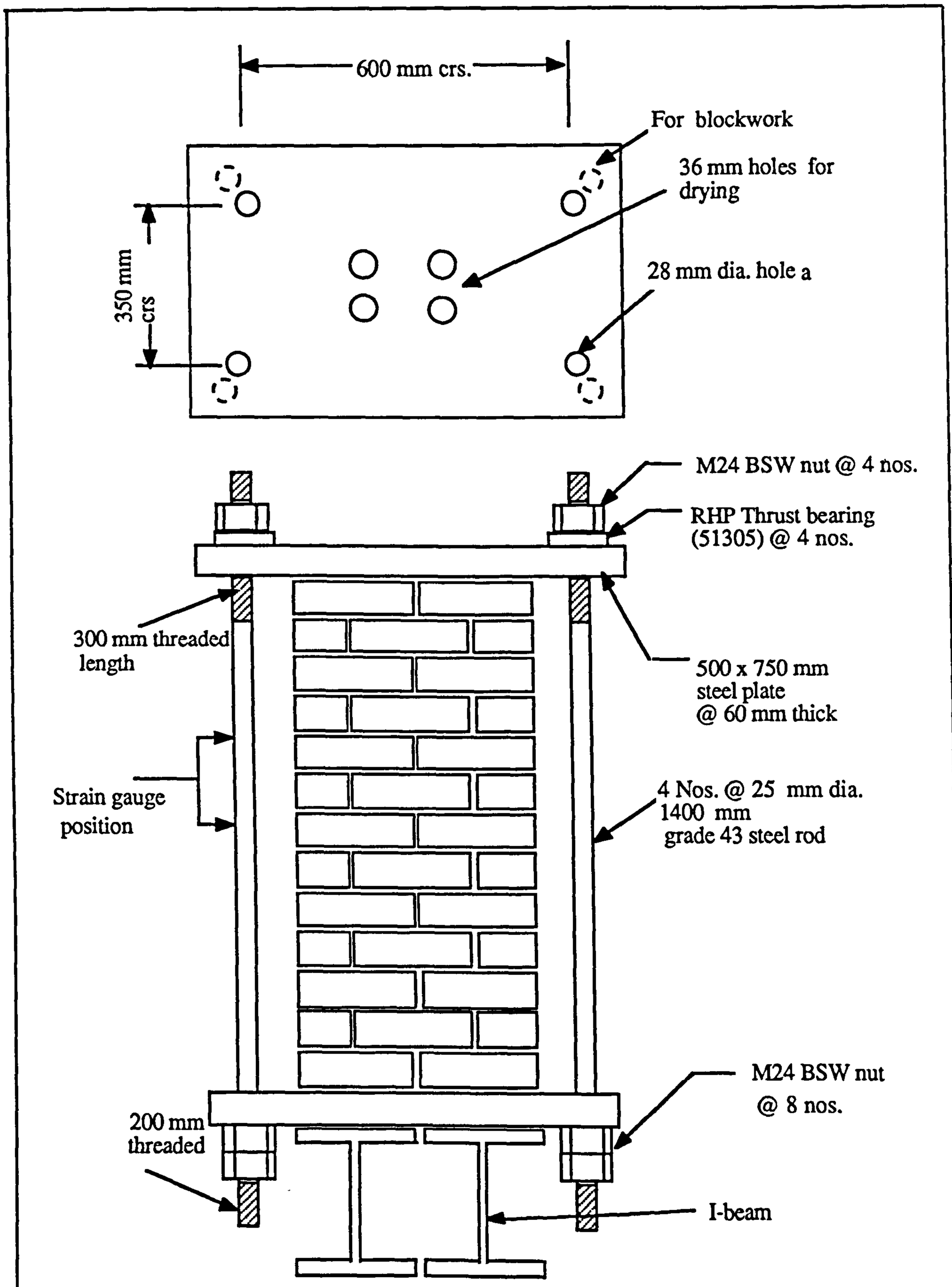

Fig. 5.8 - Creep Frame for Cavity Wall

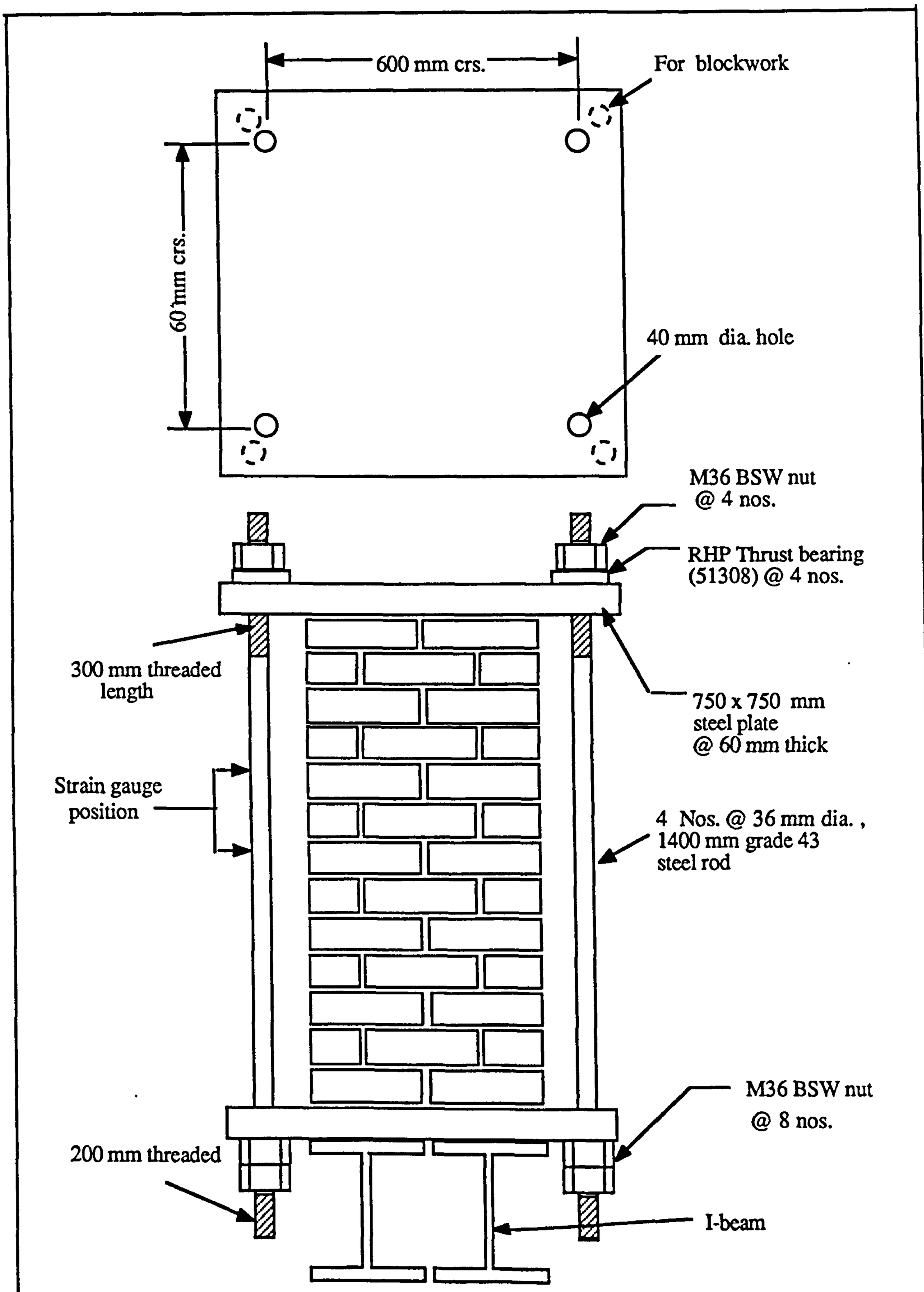

Fig. 5.9 - Creep Frame for Hollow and Solid Piers

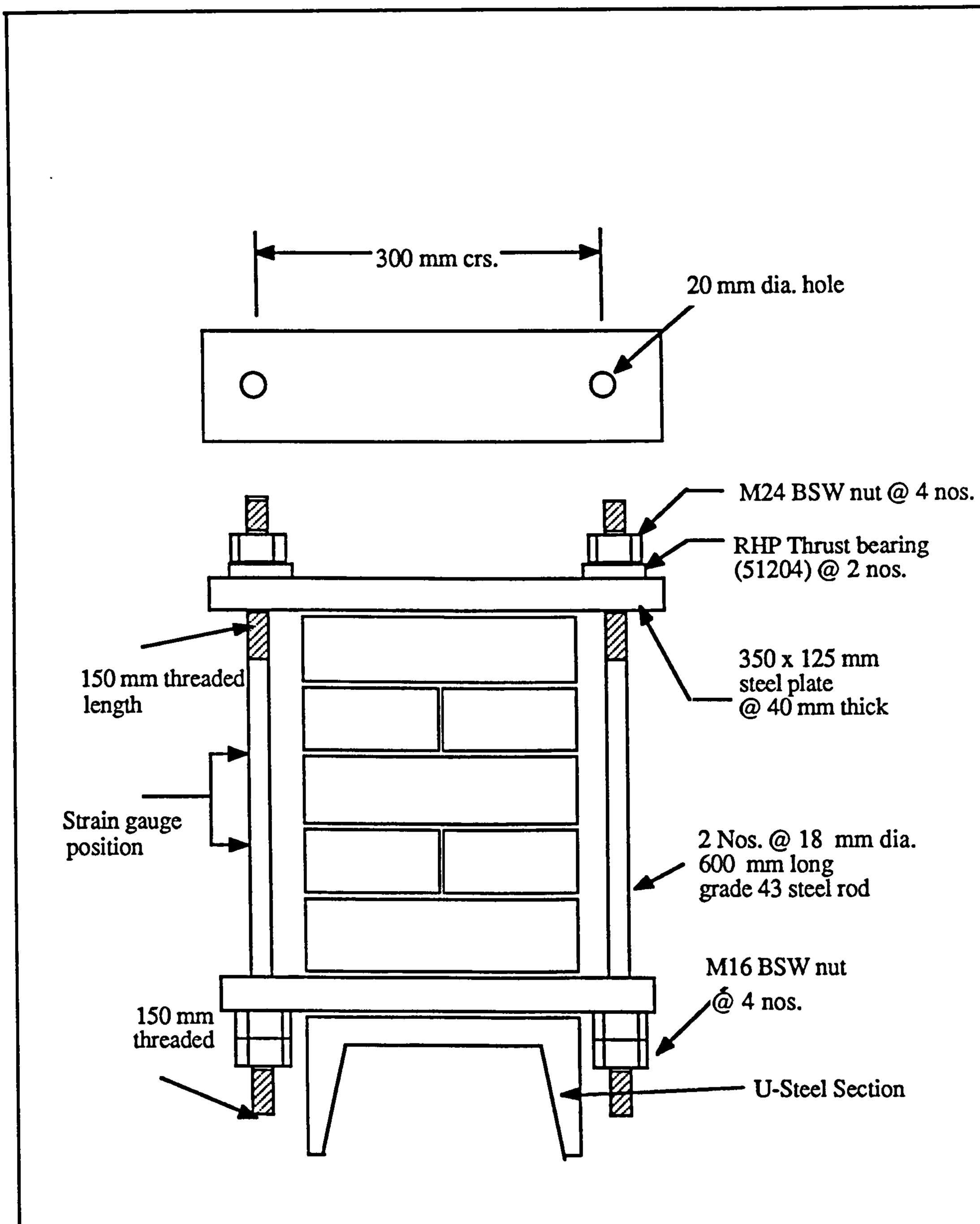

Fig. 5.10 - Creep Frame for Model Wall

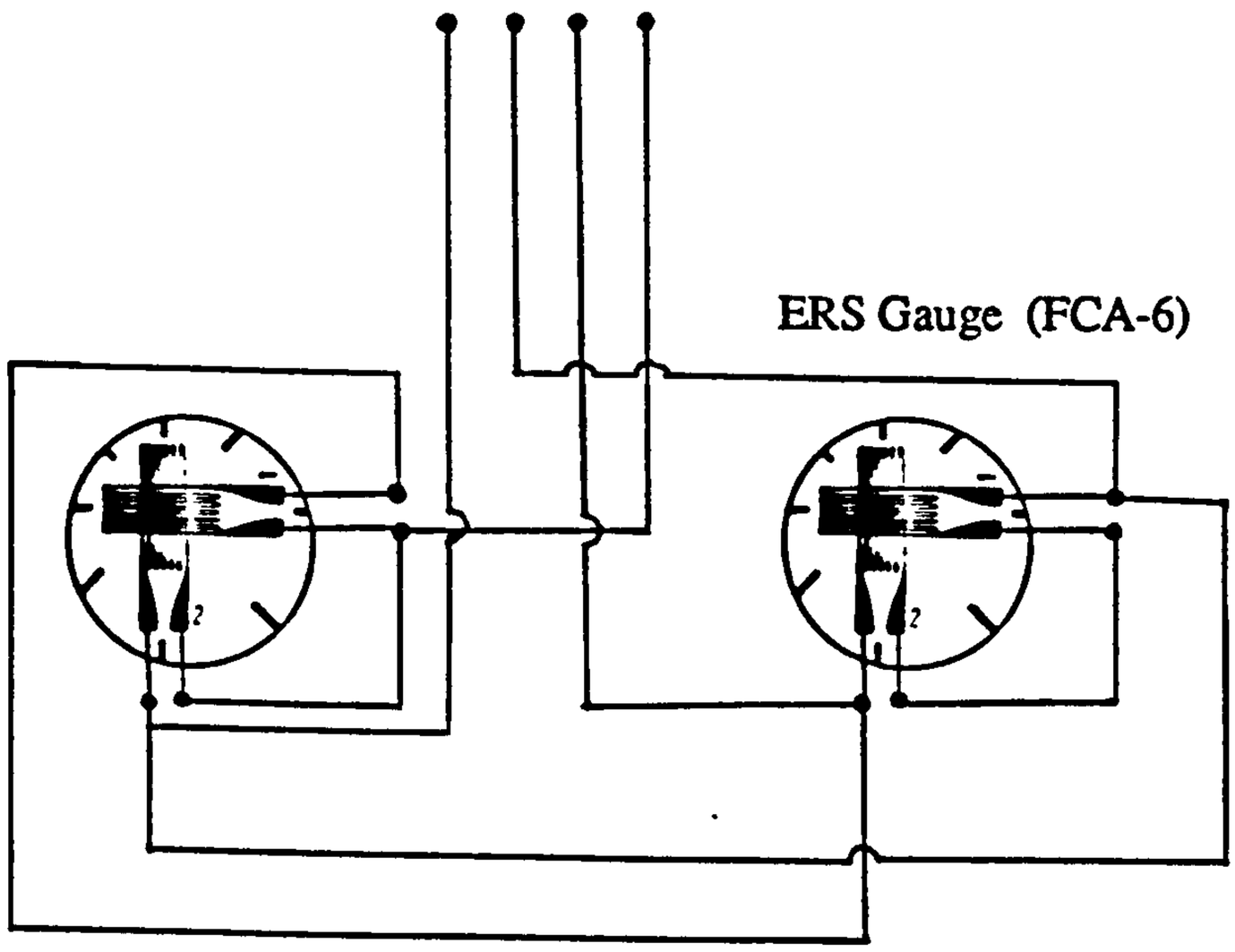

Fig. 5.11 - Tie-rod Strain Gauge Connection for Load Measurement

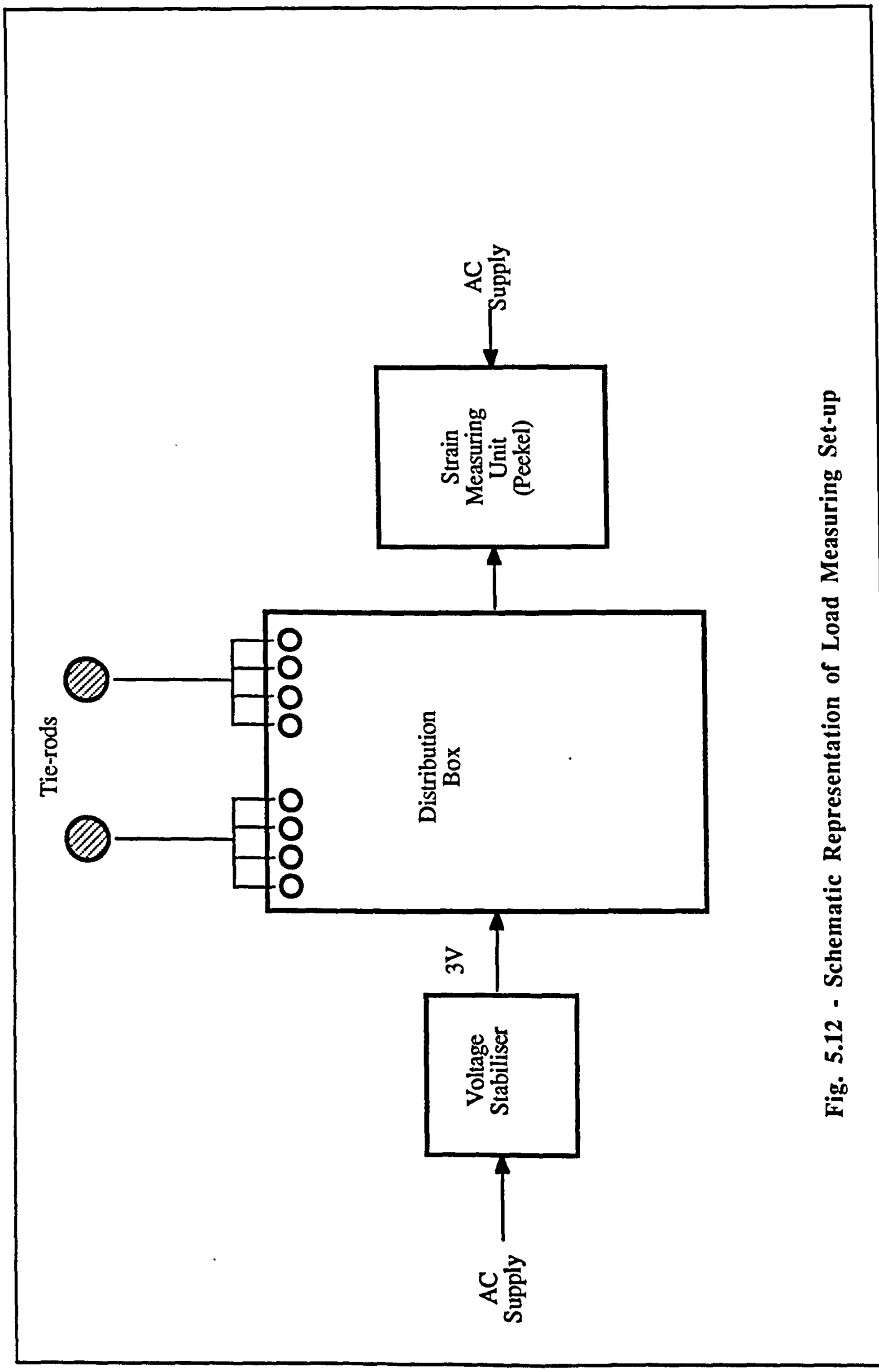

Fig. 5.12 - Schematic Representation of Load Measuring Set-up

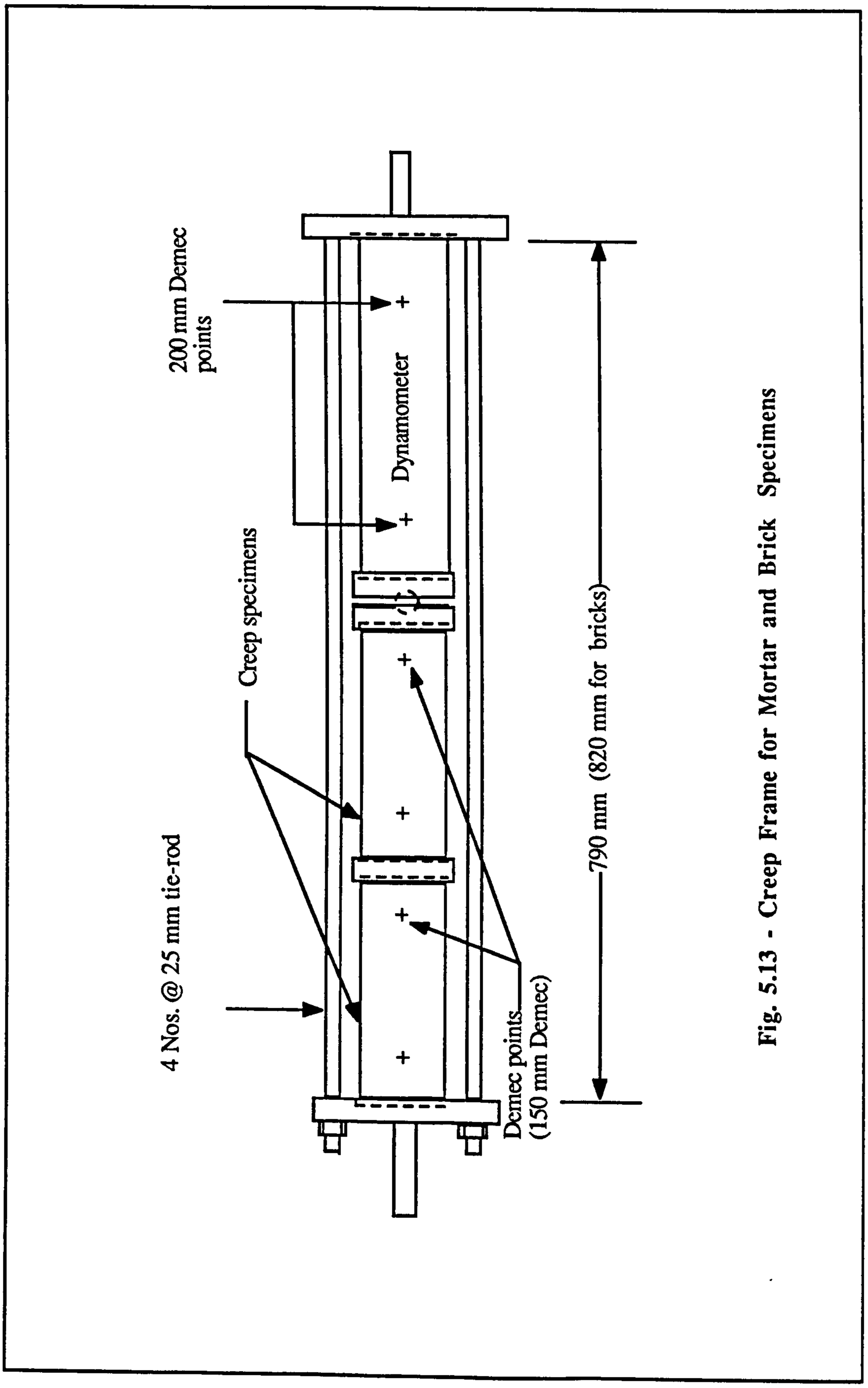

Fig. 5.13 - Creep Frame for Mortar and Brick Specimens

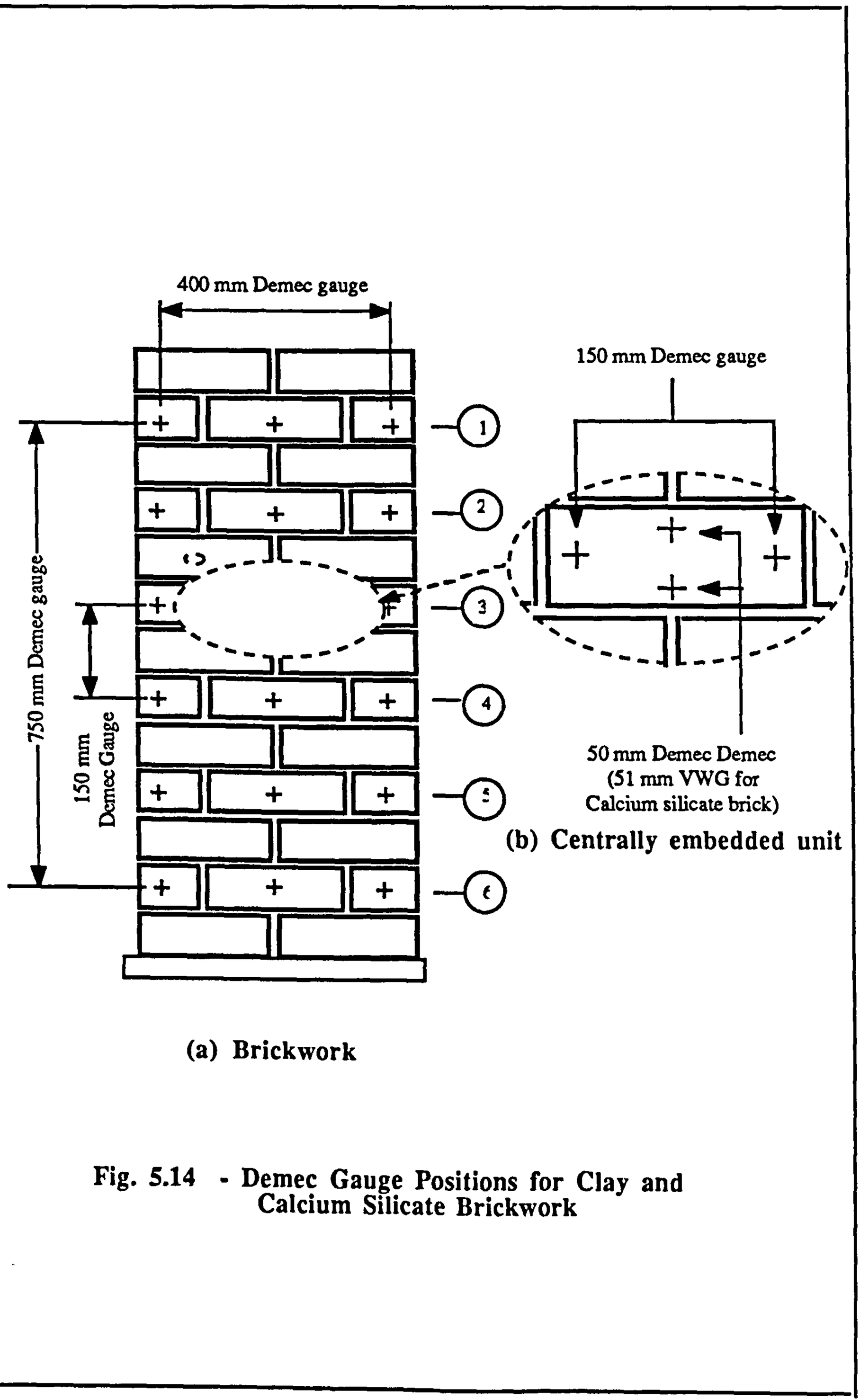

Fig. 5.14 - Demec Gauge Positions for Clay and Calcium Silicate Brickwork

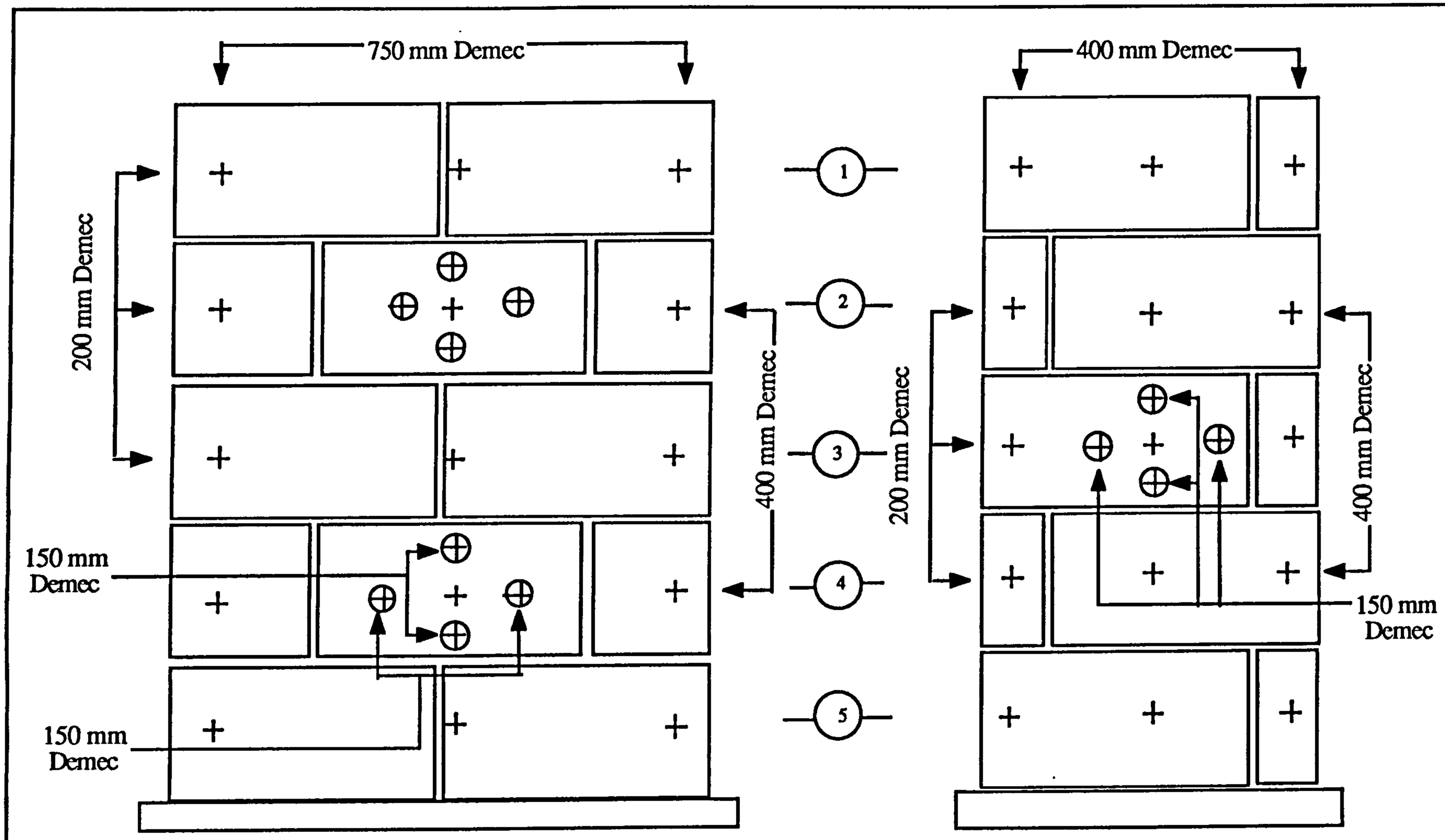

(a) Single-leaf wall

(b) Cavity wall and hollow pier

Fig. 5.15(i) - Demec Gauge Positions for Concrete Blockwork

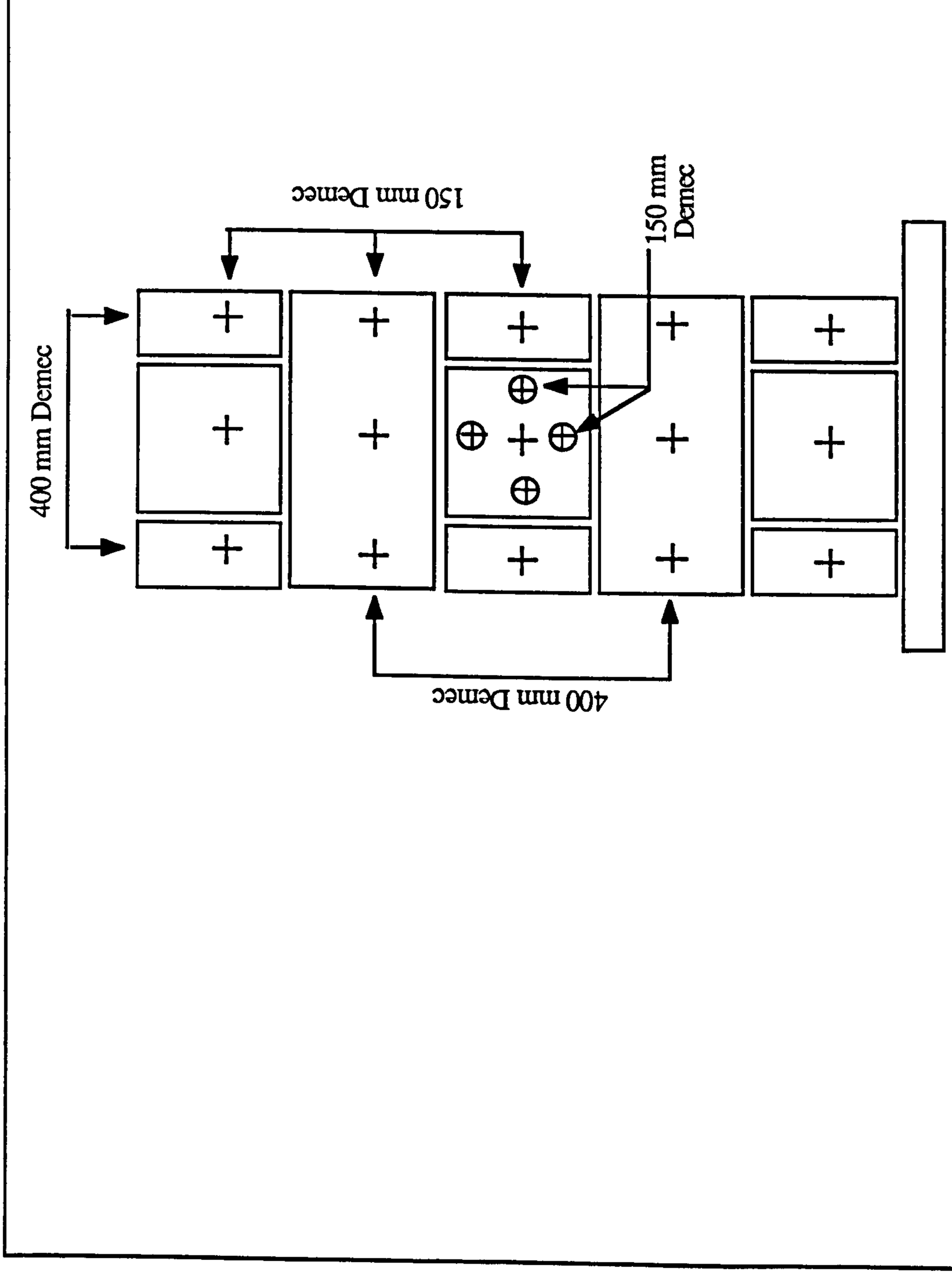

(c) Solid pier

Fig. 5.15(ii) - Demec Gauge Positions for Concrete Blockwork

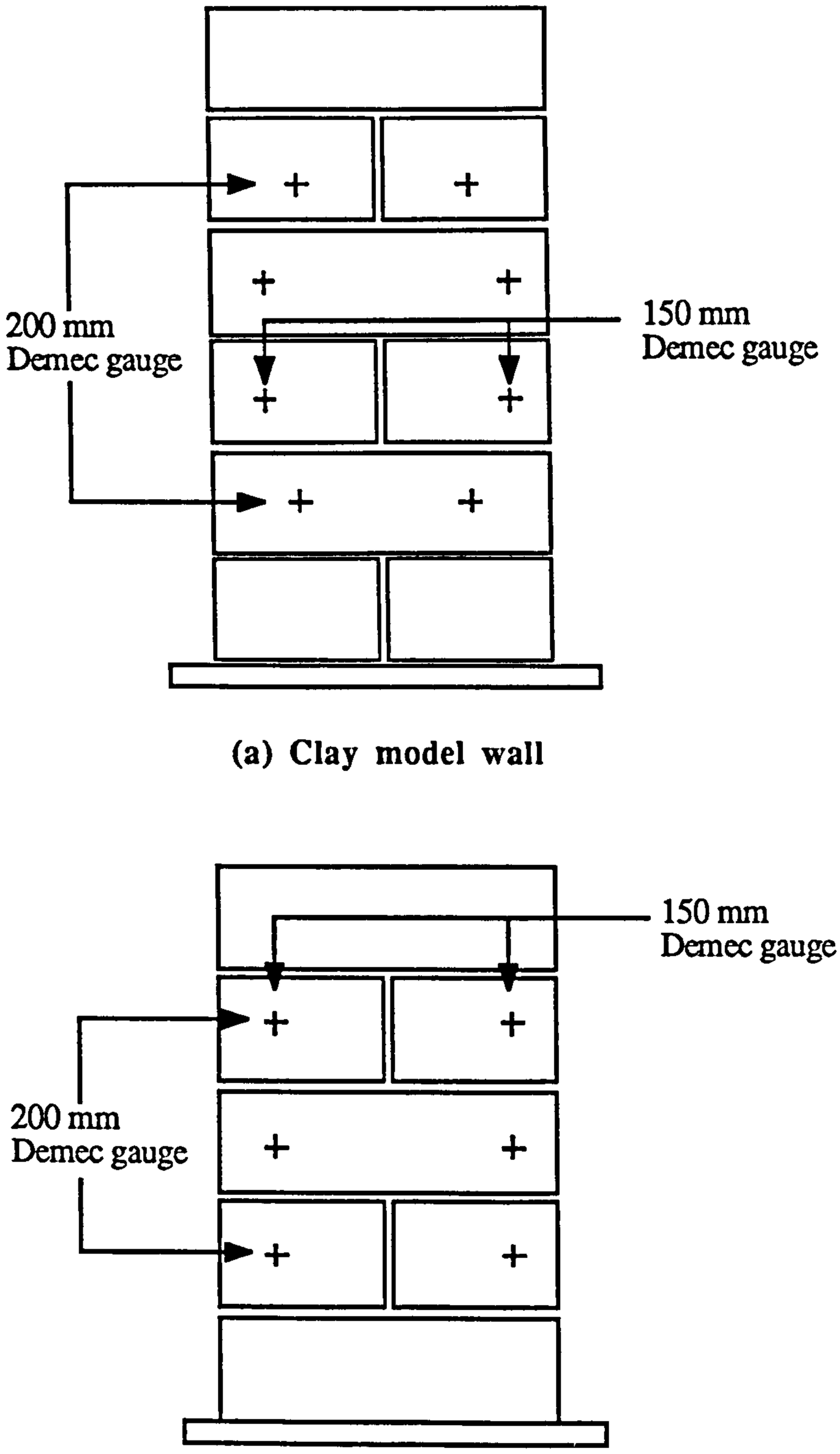

(a) Clay model wall

(b) Calcium silicate model wall

Fig. 5.16 - Demec Gauge Positions for Model Walls

PLATE 1

Brick and Block Units Used in the Present Investigation

PLATE 2

Strain Measuring Equipment (for Load Monitoring of Tie-rods and Strain Measurement of the Acoustic V.W.G (marked x))

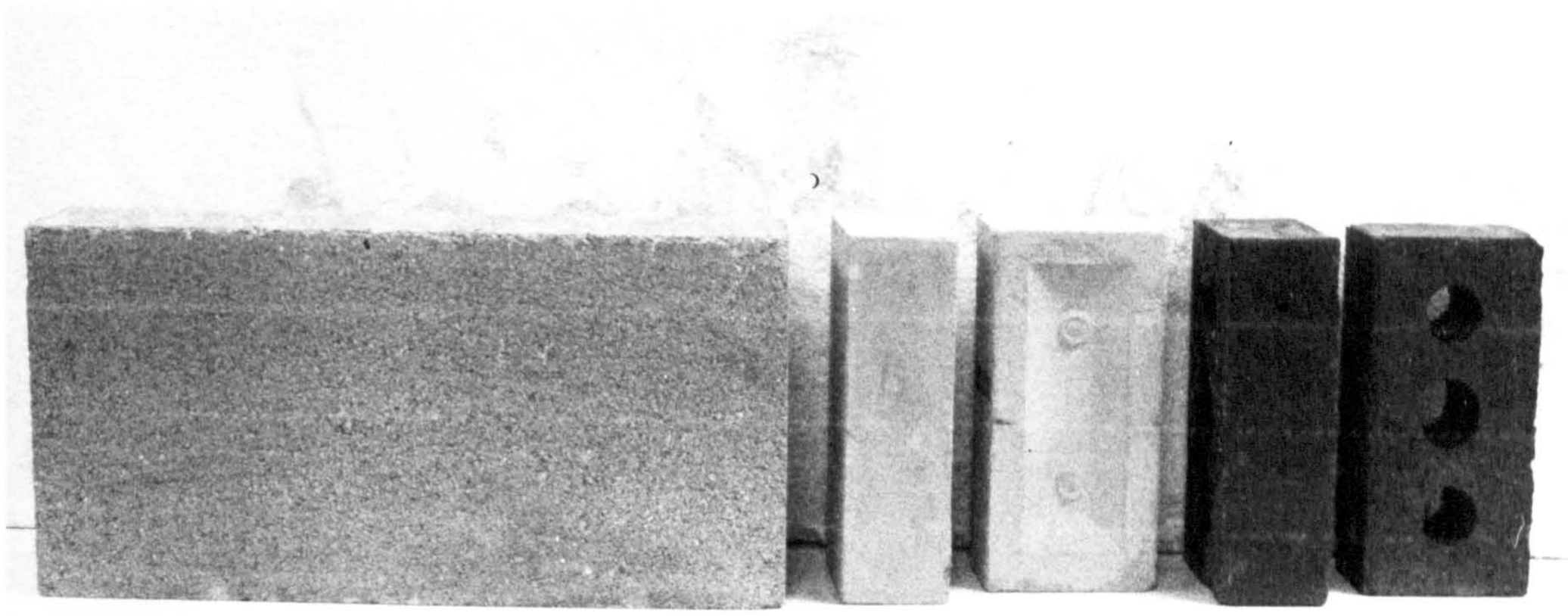

PLATE 1

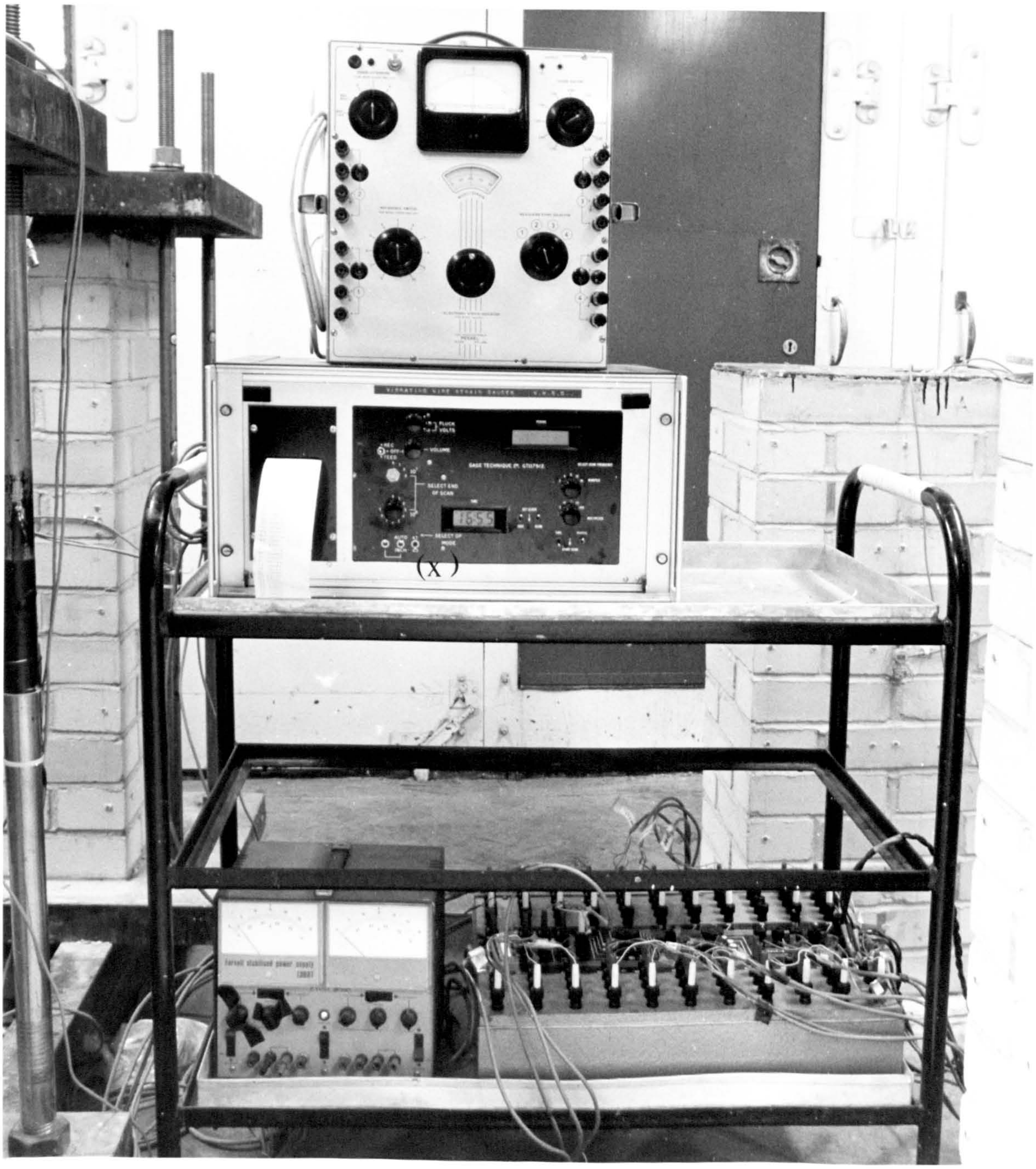

PLATE 2

PLATE 3

Cored and Cut Specimens for Modulus of Elasticity Tests

PLATE 3

PLATE 4

Clay Brickwork under Test

PLATE 5

Calcium Silicate Brickwork under Test

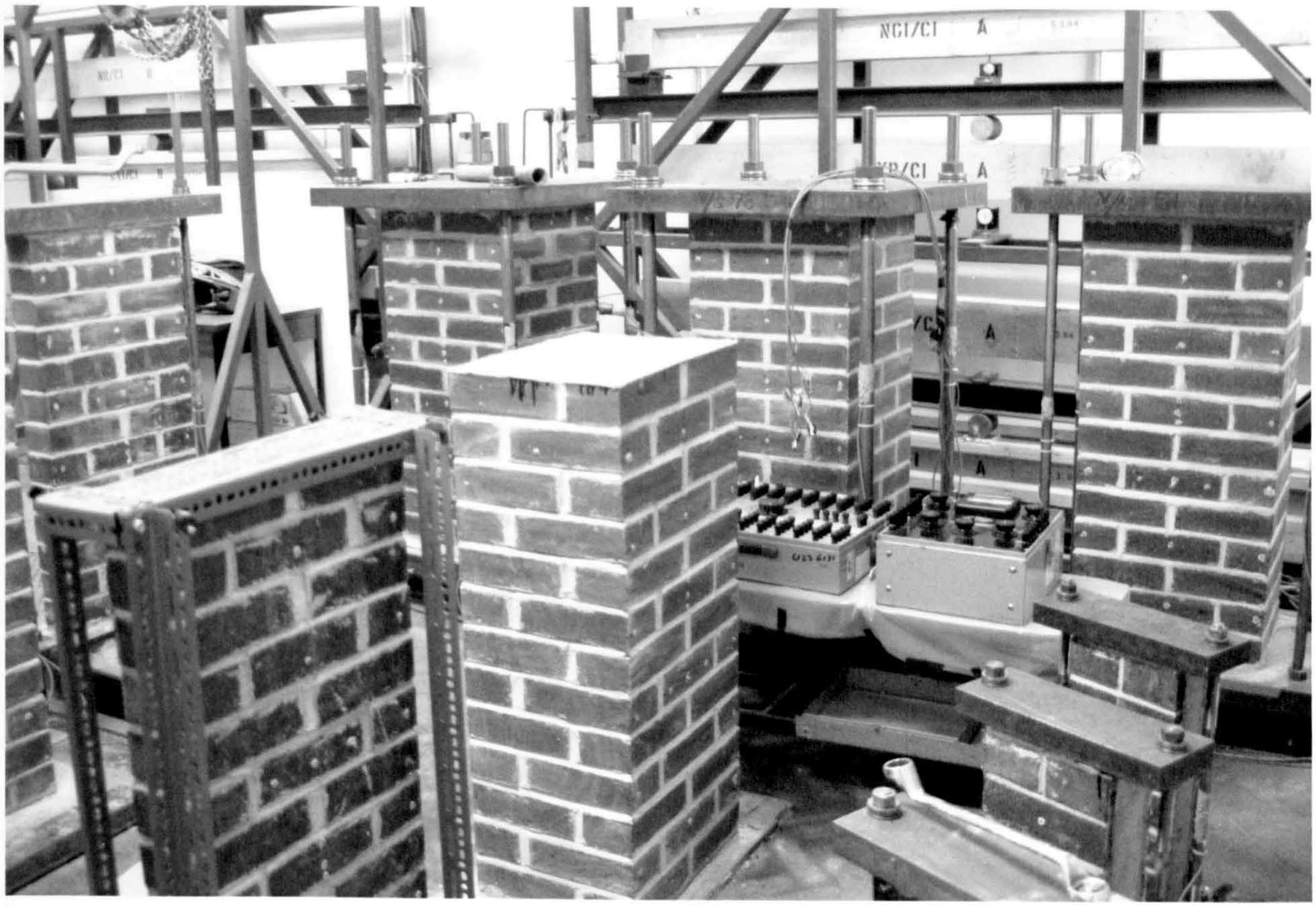

PLATE 4

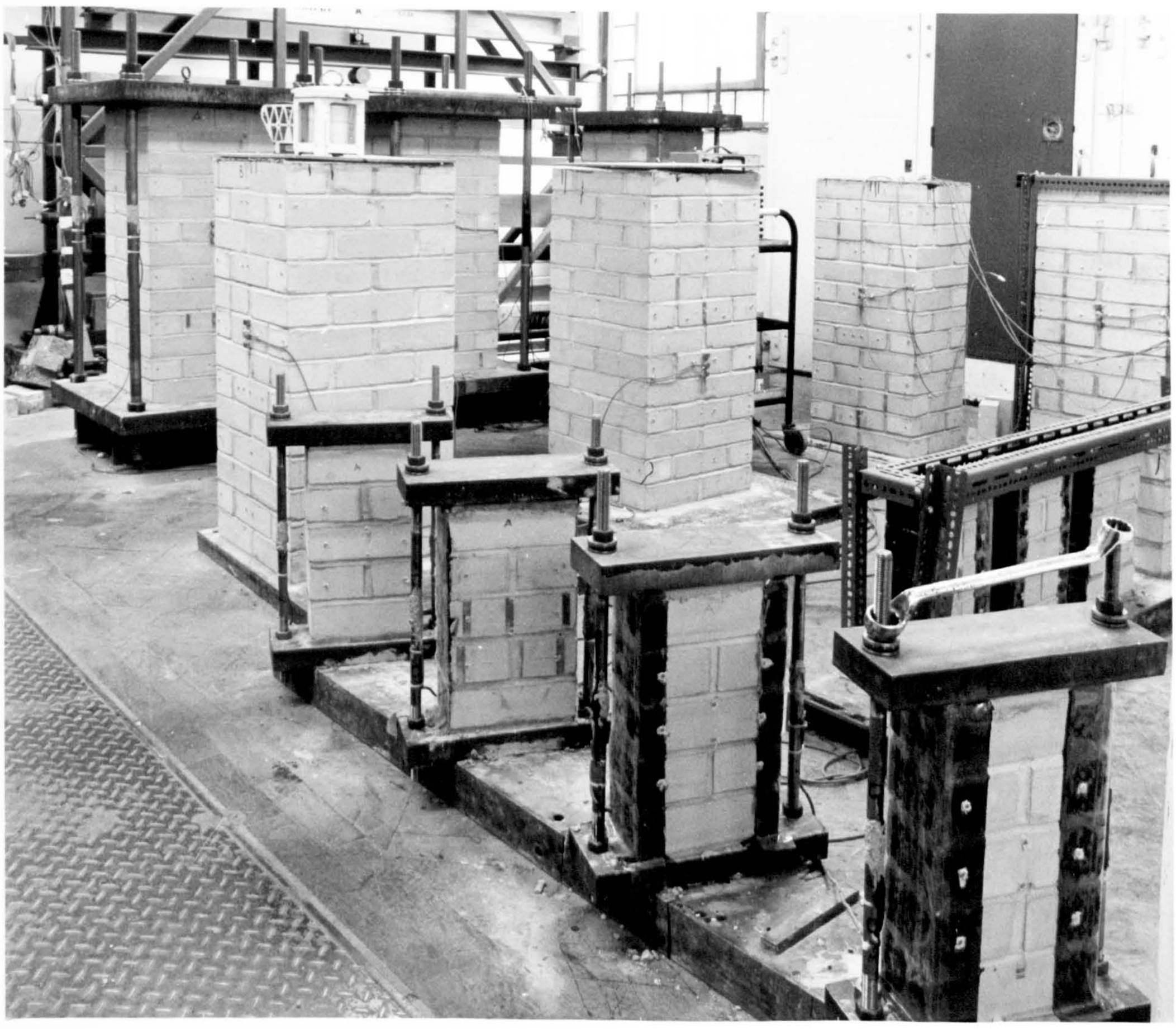

PLATE 5

PLATE 6

Concrete Blockwork under Test

PLATE 7

Brick and Mortar Specimens under Test

PLATE 6

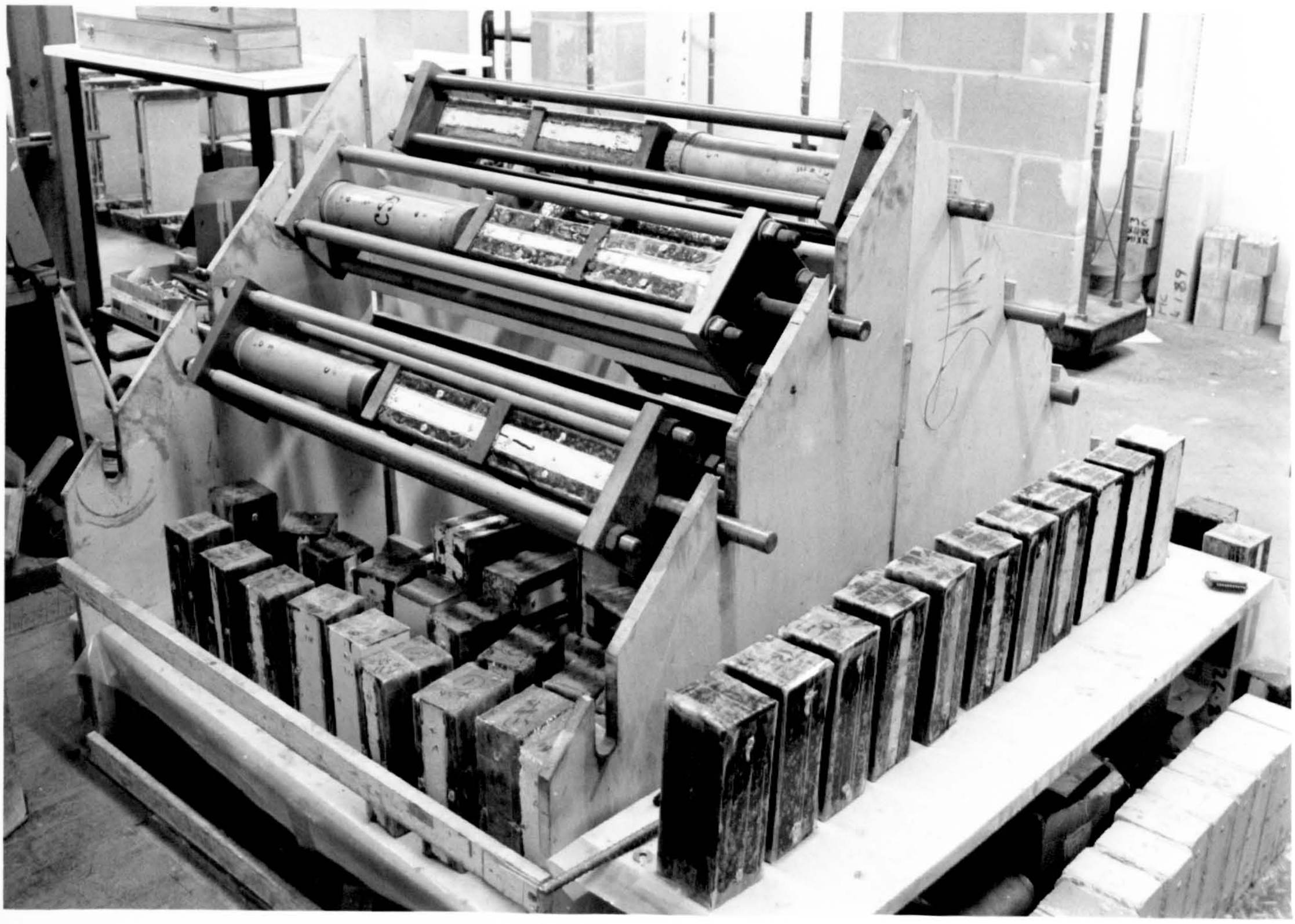

PLATE 7

PLATE 8

Demec Gauges
(from left to right - 750, 400, 200, 150 and 50 mm Gauges)

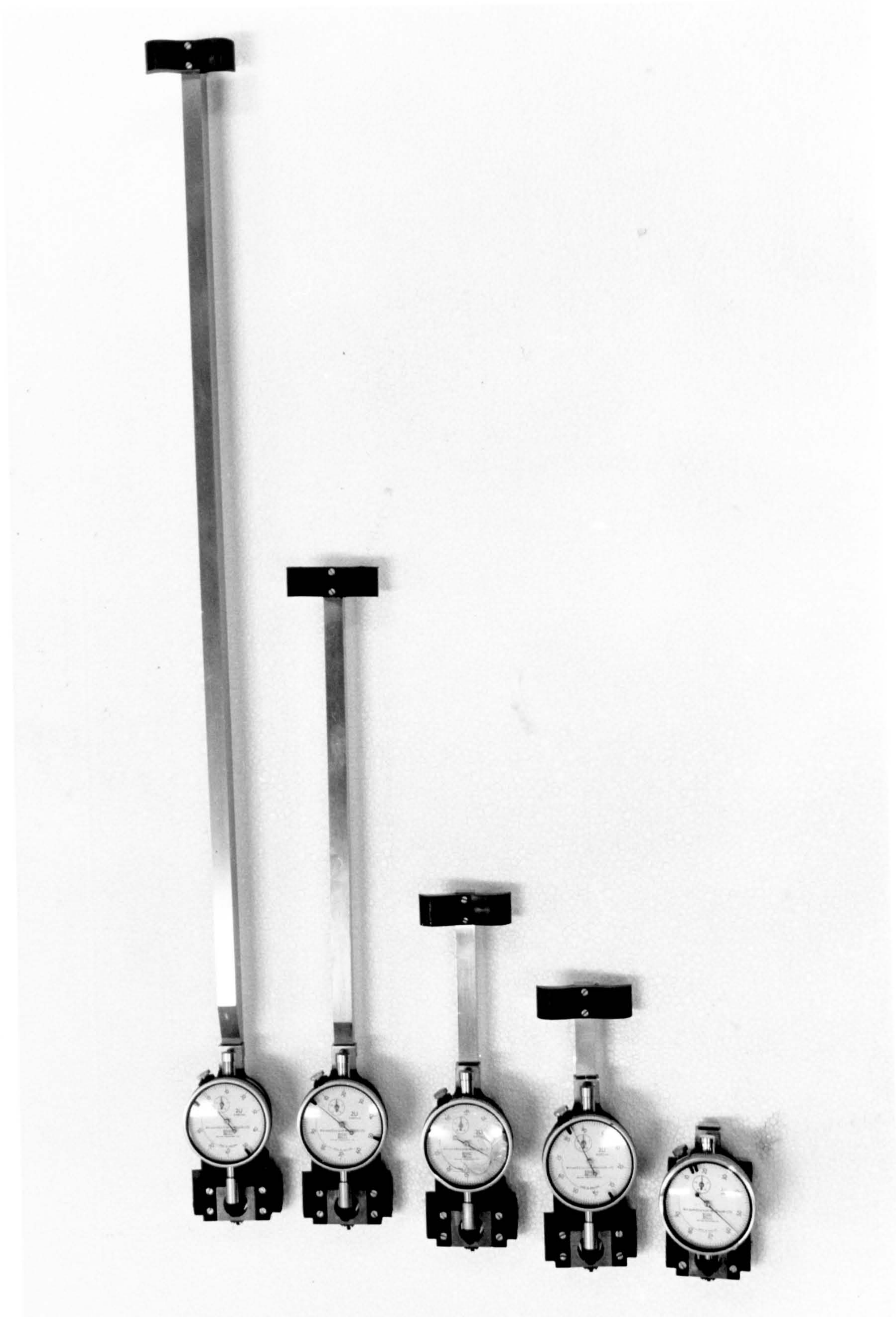

PLATE 8

CHAPTER 6

RESULTS OF STRAIN MEASUREMENTS

6.1 Introduction

In this chapter the results of strain measurements of the 13-course brickwork, 5-course blockwork and model walls are presented and discussed. Particular emphasis is given to the influence of geometry on the instantaneous and time-dependent properties of masonry. Test results on the individual component materials, i.e. mortar, bricks and blocks are presented in Chapter 7.

6.2 Full size masonry units

6.2.1 Vertical strain

For each geometry and type of masonry, typical strains as measured at different positions of the walls or piers for both the loaded and control specimens are given in Appendix B. The creep strains were obtained by subtracting from the average measurements on the loaded masonry units the average elastic strains plus the average moisture strain (shrinkage) recorded on the corresponding control walls.

6.2.1.1 Modulus of elasticity

The modulus of elasticity, as determined from the initial strain after loading the creep test units is given in Table 6.1 . For various cross-sections, there was no consistent influence of V/S ratio on the modulus of clay, calcium silicate and concrete masonry, although the modulus of the clay single leaf wall was appreciably less than the moduli of other clay brickwork. The independence of modulus of elasticity on geometry of brickwork agrees with the findings of Lenczner[16].

The lower modulus for single-leaf clay brickwall was thought to be due to eccentricity induced during loading which is more likely to occur in the single-leaf wall with higher height/width ratio of 9.7 as compared to 2.9 and 2.2 for cavity wall

and the piers, respectively. This is evident since the difference in elastic strain between face A and face B of the wall was 122 microstrain as can be seen in Appendix B. However, the effect was not evident for the calcium silicate single-leaf wall although the modulus was slightly lower then the moduli of brickwork of other geometry.

For the similar type of mortar used, the modulus of elasticity decreases in the order: clay brickwork > concrete blockwork > calcium silicate brickwork. Athough the modulus of calcium silicate brick was higher than the concrete block, the height of unit to mortar bed thickness (h/m_y) of the blockwork was higher than the calcium silicate brickwork so that the brickwork had relatively more mortar bed joints than the blockwork; hence a lower modulus occurred in the brickwork. In general, the modulus of the masonry was slightly lower than that measured by Brooks and Amjad[15] since the time taken to load and to take strain measurement using Demec gauges were longer than in their method. However, the differences were not significant.

The measured moduli given in Table 6.1 can be compared to the predicted values based on brick/block strength or stress given in Table 6.2. It can be seen that for clay brickwork, prediction equations by the British Standard[46] gives good cover of the range of the measured moduli. While equations by Plowman[65], Sinha and Hendry[66] and Lenczner[16] (from his earlier work) were within 10% of the 'frog-down' calcium silicate brickwork. Their brick strength was generally similar to the strength of calcium silicate brick of this investigation.It should be noted that Brooks and Amjad[68] reported that better predictions were obtained for 'frog-up' calcium silicate when using the equation of BS 5628[46], the modulus of 'frog-up' construction being higher than the 'frog-down' construction. Although according to Plate 9, it appears evident that the frogs are fully filled, any air entrapped between the frog face of brick and mortar during construction would form a cavity when mortar sets. When the brickwork is first loaded the cavity would tend to close up and in turn result in a higher initial strain.

Furthermore, as pointed out by Sinha and Hendry[66] the measurement for modulus is affected by the shrinkage cracks between the mortar and the units and at lower stresses, the value of secant modulus of elasticity is irregular. BS 5628[46] gives very good predictions for modulus of elasticity of all brickwork and blockwork and, as expected, the other equations give poor predictions, since, they were empirically derived only from tests on clay brickwork.

In general, the prediction equation by BS 5628[46], gives good estimate of elastic modulus of masonry. The use of the 'characteristic strength' concept is a practical solution when dealing with the high variability of brick properties. On the other hand, the later equation by Lenczner[16] (Eq.(2.25)) which has been recommended to be use in conjunction with creep of masonry gives poor estimate of modulus of brickwork in this investigation.

6.2.1.2 Creep

The creep-time characteristics of clay, calcium silicate and concrete masonry are shown in Figs. 6.1, 6.3 and 6.5, respectively. In all cases there was a clear influence of geometry or V/S ratio on creep. The influence of V/S on creep is twofold. Firstly, the rate of creep increases with a decreasing V/S ratio, and secondly, a higher creep occurs with a lower V/S ratio. The trend of higher creep in brickwork having lower V/S ratio confirms the significance of the role of moisture diffusion rate, as stated in Chapter 3, and thus explains the general observation of Lenczner[5], who reported less creep in clay brick piers than in single-leaf walls.

It is interesting to note that the 'two-stage' creep as that reported by Lenczner[16] and Ameny et al[38] has not been observed in the present test. This is a confirmation of Ameny's explanation that the change in creep rate was caused by a large and steady change in relative humidity, since in the present case the relative humidity was constant throughout the entire testing period.

Figure 6.7 shows a stronger influence of V/S ratio on calcium silicate brickwork at later ages than on clay and concrete masonry. The influence of a greater height of unit to mortar bed thickness in the concrete blockwork than in calcium silicate was to produce a lower creep in the blockwork compared with the calcium silicate brickwork.

6.2.1.2.1 Ultimate creep

The ultimate creep was computed using reciprocal of constant b from the hyperbolic creep-time expression as suggested by Ross[30] as given by Eq.(2.16). The regression analysis was carried out using the 'smoothed' creep-time curves of Figs. 6.1, 6.3 and 6.5 from a time of 10 days since loading. As described by Warren and Lenczner[22],and Brooks[41], the above equation underestimates the creep of masonry at earlier ages (up to 40 days) but for long-term data there is usually good agreement. In using the above expression for concrete, there is a suggestion to use data at equal logarithmic time intervals which means that, for example, over a time after loading from 0 to 100 days there will be more data considered than for 100 to 200 days. For masonry, it has also been suggested to use data for times after loading in a sequence, such as 1,3,7,28 days, in the hyperbolic expression. For the present data, this approach underestimated, creep at earlier ages.

Various combinations were tried with the present data and it was found that the best correlations were obtained by taking data at equal intervals such as 20, 40, 60 days, with a c/t versus t plot. When using the irregular time interval as described above, in some cases the extrapolated ultimate values did not show any trend with V/S ratio, whereas for up to about 200 days the measured values still showed the effect of V/S ratio. This problem was further amplified if data at earlier ages were only considered, where the lower creep rate for the higher V/S ratio seemed to show that the effect of V/S ratio was to delay creep and to have a similar or higher ultimate

value. Hence, in order to obtain a reasonable estimate of creep-time behaviour and the ultimate value, it is suggested to use data for a minimum of 150 days or twice the time period where the creep rate starts to significantly reduce.

The ultimate creep extrapolated from the hyperbolic-time expression, which gives a high correlation coefficient, is shown in Table 6.3. The results of this investigation are compared with previous data on the basis of ultimate creep relative to that of single-leaf wall, as illustrated in Fig. 6.8. Although there is a reasonable agreement with the average value for concrete[27-29], the relative ultimate creep of piers is much greater than that found by Lenczner[16]. Also when compared in terms of strain ratio (S_R), as given in Table 6.1, the present values are higher than that of Lenczner's[16]. The differences cannot be readily explained although the reason may be due to the low strength mortar, ranging from 6.1 to 7.3 MPa, as compared with 17.5 to 23.2 MPa strength mortar used by Lenczner[3-14]. Although Lenczner[4] stated that creep of masonry was not affected by type of mortar there has been little evidence to confirm this. It should also be noted that Lenczner's data apply to brickwork stored at a lower relative humidity of 50% before loading which would have the effect of reducing creep. Consequently, the degree of drying may be a factor on creep-V/S ratio relation as well as the general level of creep.

The results of this investigation are higher than values given by Standard Codes[46,113-114] (Table 2.5) for clay and calcium silicate brickwork, ranging from 1.5 to 2.1 times and from 1.1 to 1.7 times, respectively. On the other hand, for concrete blockwork, the result falls within the range given by the Codes.

6.2.1.3 Moisture strain

All the brickwork exhibited shrinkage in the vertical direction as shown in Figs. 6.2, 6.4 and 6.6. There was a similar influence of V/S ratio to that on creep at early periods. The slight decrease of moisture strain at later duration (after 80 days) for the clay single leaf wall suggested that there was an effect of brick moisture

expansion, although for the other geometries of clay brickwork there was no similar indication. Shrinkage for the single-leaf wall was rapid at the early period, for example at 80 days shrinkage was approximately 90% of the maximum shrinkage. At early periods shrinkage in the mortar is very much higher than the expansion in the brick units (see Figs. 7.1(a) and 7.5) but later the contribution of the brick expansion is more influential and as such the shrinkage of the brickwork reduces. For the other geometries of clay brickwork the shrinkage of the mortar develops more slowly due to a longer drying path length and there is no evidence of a contribution of opposing brick expansion. In this investigation, the moisture expansion effect is much less than that reported previously[32] with Fletton clay brickwork which exhibited vertical moisture expansion from approximately 70 days.

For calcium silicate brickwork and concrete blockwork shrinkage was still progressing quite rapidly even after 200 days. The shrinkage of the single-leaf walls do not show similar behaviour to that for clay single-leaf wall. Shrinkage of the clay brickwork was considerably less than that of calcium silicate brickwork because of a greater elastic modulus and the effect of moisture expansion of the clay brick. The general level of shrinkage of the blockwork was slightly higher than that of the calcium silicate brickwork since shrinkage of the block units was higher than shrinkage of the calcium silicate bricks.

The shrinkage of the calcium silicate brickwork was greater than that measured by Brooks[23] using solid bricks. The differences were generally influenced by the difference in shrinkage of the bricks used. In addition to that, the effective mortar thickness in this investigation was higher than that by Brooks due to the frog as described in Section 7.5.2.1. Also, the influence of V/S ratio (Fig. 6.9(c)) is less pronounced than that obtained by Bingel[120], particularly at later ages. In the case of concrete blockwork, the levels of shrinkage were higher than those of Bingel's, and his data show a greater influence of V/S ratio.

6.2.1.3.1 Ultimate shrinkage

The ultimate vertical shrinkage of masonry,computed in the same manner as for creep using a hyperbolic shrinkage-time expression, is given in Table 6.4. In contrast to creep, the predicted ultimate shrinkage is affected less by V/S ratio as illustrated in Fig. 6.9. The ultimate shrinkage of this investigation is compared with the limited published data in Fig. 6.10. Generally, both calcium silicate brickwork and concrete blockwork show a similar trend of vertical shrinkage to concrete[27-29] although at different level, but the clay brickwork of this investigation exhibited a small opposite trend with V/S ratio but this influence is not thought to be significant.

6.2.2 Horizontal strain

The horizontal strains were measured using the 400 mm Demec gauge except for single-leaf concrete blockwork where the 750 mm Demec gauge was used. Measurements were made at various positions over the height of the masonry (see Figs. 5.14-5.15) in two opposite faces. These measurements will be discussed in detail in Chapter 8. However, the measurements over the central part of the masonry are discussed in this section and are assumed to be independent of the platen effect. The average strains were computed from positions 3 and 4, and positions 2, 3 and 4 for brickwork and blockwork, respectively.

6.2.2.1 Creep

Lateral creep was assessed in the same manner as creep, i.e. the time-dependent load strain after allowing for horizontal shrinkage or expansion as measured on the control specimens. Figs. 6.11,6.13 and 6.15 show that lateral creep of all masonry is very small compared with vertical creep and there is no appreciable influence of V/S ratio. While the calcium silicate brickwork and the concrete blockwork gradually expands with time, most of the clay brickwork contracts, the exception being the solid pier.

6.2.2.2 Poisson's ratio

The Poisson's ratio (μ) of the masonry as determined at various times after loading is given in Table 6.1. The values of μ for the various ages were computed from the smoothed creep-time curves of Figs. 6.11, 6.13 and 6.15 plus the elastic strains. As the elastic modulus, the Poisson's ratio is not affected by the masonry geometry. Over the time period, μ was more uniform for the brickwork than for the concrete blockwork. It should be noted that for the brickwork, the time-dependent μ slightly differs from that reported previously[140] although the same data have been used. This is because the previous values were calculated from the individual measured values of axial and lateral creep.

From the present results and those obtained by Brooks[23,42] earlier, the time-dependent Poisson's ratio can be assumed to be equal to the elastic value of 0.10 for clay and calcium silicate brickwork, and 0.20 for concrete blockwork.

The relation between the vertical and horizontal load strain over time after loading days for the masonry are described in terms of 170 days Poisson's ratio are also given in Table 6.1. The results show that creep does not significantly change the Poisson's ratio of clay and calcium silicate brickwork but the effect of creep on the concrete blockwork was to reduce the Poisson's ratio to about $\frac{1}{4}$ of the elastic Poisson's ratio.

6.2.2.3 Moisture strain

The development of horizontal moisture strain with time for clay, calcium silicate and concrete masonry are illustrated in Figs. 6.12, 6.14 and 6.16, respectively. Unlike calcium silicate and concrete masonry, clay brickwork exhibited moisture expansion. Whereas the small moisture expansion of the clay brickwork was not apparently influenced by V/S ratio, the horizontal shrinkage of calcium silicate and concrete masonry are influenced by geometry in a similar manner to vertical shrinkage.

It can also be seen that the influence of the moisture expansion of clay bricks in the horizontal direction was more apparent than in the vertical direction as that observed by Beard et al[81] and Brooks[23]. As explained by Brooks[23] this can be attributed to the anisotropic property of the bricks. The observation as described Section 6.2.1.3, i.e. a more pronounced influence of moisture expansion of clay brick on shrinkage-time curves for single-leaf wall then the other geometry brickwork, can also be due to less vertical restraint to upward movement for single-leaf wall compared to the others. This was because the single-leaf wall had less vertical mortar joints, while the other brickwork also have vertical mortar joints on the stretcher faces.

For calcium silicate brickwork the amount of lateral shrinkage was generally higher than vertical shrinkage. A similar trend was observed by Brooks[23] for solid bricks which was attributed to the anisotropic character of the calcium silicate bricks. The difference decreases as V/S ratio increases. On the other hand, the lateral shrinkage of concrete blockwork was lower than the vertical shrinkage for the single-leaf and cavity walls, but the level was generally the same for the hollow and solid piers; the shrinkage of the blocks was found to be nearly isotropic.

6.2.2.3.1 Ultimate shrinkage

The ultimate horizontal shrinkage was determined in the same manner as that for vertical creep and shrinkage. Since the clay brickwork exhibited moisture expansion in the horizontal direction with no uniform trend it was difficult to obtain a reasonable prediction of the ultimate expansion. The results suggested that the upper limit of moisture expansion in clay brickwork to be about 100 microstrain. A previous report[70] stated that the amount of moisture expansion of clay brickwork was in the range of 50 - 100% of the expansion of the individual unrestrained brick. However in this investigation, the expansion in individual bricks was found to be very small (Fig. 6.12). The experimental results also suggested that the embedded bricks have absorbed

moisture from the mortar during laying thus undergo more expansion than the individual bricks. Alternatively, there could have been an interactive effect due to the transport of C_3A thus causing sulphate expansion.

The ultimate horizontal shrinkage for calcium silicate and concrete masonry is tabulated in Table 6.4. The values are compared with the limited previous data in Fig. 6.18. In general, both the calcium silicate and concrete masonry show the same trend of horizontal shrinkage to concrete[27-29] although at a different level.

When compared with the design range given in Tables 2.6 and 2.7, in both vertical and horizontal directions, the estimated shrinkage falls within the range given by CP 121[85] and BS 5628[46], whereas the shrinkage levels are higher than that given by the German standard[113].

The ratio of horizontal to vertical ultimate shrinkage of the present results, as given in Table 6.5, show a general trend in which the ratio reduces as V/S ratio increase for calcium silicate brickwork. This is in contrast to the results by Brooks and Bingel[23] which show an opposite trend for both calcium silicate and concrete masonry. This phenomenon cannot be readily explained although different types of brick and block were used. Further research is required into this behaviour.

6.3 Model wall tests

This section discusses the results of tests on one-brick wide model test units; i.e. 6-course high for clay brickwork and 5-course high for calcium silicate brickwork whose surfaces were partly-sealed so as to give the same V/S ratio as the corresponding 13-course brickwork. No model test units were constructed from concrete blocks. The model wall tests result are compared with the corresponding larger brickwork.

6.3.1 Vertical strain

6.3.1.1 Modulus of elasticity

The modulus of elasticity of the model walls is given in Table 6.6, the modulus being determined from the initial elastic strain. The geometry as quantified in terms of the V/S ratio does not show any influence on the modulus of the model walls. For the clay brick, the average modulus of model walls was 13.9±1.3 GPa compared to 14.5±1.5 GPa for the full size units as given in Table 6.1. For the calcium silicate brick laid 'frog down', the modulus was 5.0±0.2 GPa for the 5-course model wall compared to 5.2±0.2 GPa for the 13-course brickwork. In general, model walls showed a lower modulus than the larger brickwork but the differences were insignificant. This finding is in agreement with that of Brooks and Amjad[54,68] who reported that the modulus of brickwork tested between steel platens is independent of brickwork geometry of height/least lateral dimension ratios between 1 and 9.5.

6.3.1.2 Creep

The vertical strain-time curves of model walls as compared to the full size brickwork are given in Figs. 6.19 and 6.20 for clay and calcium silicate bricks, respectively.

For clay brickwork the difference of creep between the 6-course and the 13-course brickwork was small, the highest difference being for model wall with V/S of 44mm which was about 19% lower than the single-leaf wall. Very good agreements were obtained between calcium silicate model walls and the larger units, the difference being less than 8% at any time after loading. Consequently, the model walls indicated the influence of V/S ratio on the level of creep over the time period.

The ultimate creep for the part-sealed model walls were computed in the same manner as described earlier and are given in Table 6.6. The ultimate creep for clay model walls was within 19% of that of the bigger units (Table 6.3) and do not

seem to show any dependency of geometry, i.e. similar to that of larger brickwork. On the other hand, the ultimate creep of calcium silicate model walls does show a trend with V/S ratio, although the level of ultimate creep is generally higher than the larger units by approximately 8%.

The above observation is encouraging, since model walls can be used with reasonable accuracy to predict the performance of creep of the larger units so long as the behaviour of moisture diffusion of the component materials in the model wall is simulated. This may explain the observations by Lenczner[4], who measured a higher creep for model brickwork (about 5 times higher) compared to the full scale brickwork. His model walls and model piers had V/S ratios of 13 mm and 36 mm, respectively, compared to 78mm (or 112mm) of the hollow brickwork piers which he tested separately[21]. In addition, the half-size brick units that he used in the model brickwork had a V/S ratio of only 8.6mm compared to 16.8mm of the full-size brick units. Although other factors such as stress/strength ratio, temperature and humidity may have contributed to the higher creep in the model brickwork, the difference in of moisture diffusion is thought to be the prime factor for the large difference in creep.

6.3.1.3 Shrinkage

Shrinkage of clay model walls was generally higher than shrinkage of the larger clay brickwork (Figs. 6.19(a)-(d)). Also, as for the larger brickwork, shrinkage of the model walls is affected by the V/S ratio, although the effect does not necessarily exist for the predicted ultimate values (Table 6.6). A better representation of the larger brickwork is obtained with the calcium silicate model walls for which the shape of shrinkage curves were almost similar to that of the larger units and there was a similar trend with V/S ratio (Figs. 6.20(a)-(d)). The predicted ultimate shrinkage of the calcium silicate model walls (Table 6.6) was exceptionally close to that of the larger brickwork (Table 6.4).

It should be pointed out that, although the strain-time curves for the model walls and the full size brickwork are nearly similar, the predicted ultimate value using the hyperbolic strain-time expression may not necessarily give a similar values because of the reasons stated in Section 6.2.1.2.1.

6.3.2 Horizontal strain

The horizontal strains of model wall were measured at positions as illustrated in Fig. 5.16. Measurements over the stretcher face of a whole single unit were not considered. A comparison of horizontal strain-time curves of the 5 or 6-course model walls with the 13-course brickwork is shown in Figs. 6.21 - 6.22.

6.3.2.1 Creep

In contrast to vertical creep, lateral creep of clay model walls showed little agreement with that of larger brickwork, however, good correlations were obtained between the small and the larger calcium silicate brickwork. The best correlations were obtained for single-leaf walls and model walls with V/S of 44mm. As a whole, the levels of creep were small and may be considered not significant.

6.3.2.2 Poisson's ratio

Given in Table 6.6 are the Poisson's ratios of the model walls and these can be compared to the values of the full size brickwork in Table 6.1. For both clay and calcium silicate brickwork, there was no significant difference of the instantaneous Poisson's ratio between the model and the larger brickwork, however, the variation of Poisson's ratio of the model walls was greater.

The time-dependent Poisson's ratio (at 170 days) are also given in Table 6.6, and when compared with the corresponding larger units in Table 6.1 showed good agreement for calcium silicate brickwork but poor correlation for clay brickwork. The

values were considerably influenced by shrinkage or swelling and therefore not very accurate. Any anisotropic nature of swelling would consequently aggravate this influence and explain the poor correlation for clay brickwork.

6.3.2.3 Horizontal moisture strain

As for the larger brickwork, the clay model walls exhibited moisture expansion though the level was not quite the same. The model wall with V/S of 44mm showed better correlation with single-leaf wall. This was also true for calcium silicate model wall with V/S of 44mm, notwithstanding that other V/S ratios model walls do show good agreement with the corresponding brickwork particularly at later periods. The extrapolated ultimate lateral shrinkage of the calcium silicate model walls were also acceptably close to that of the larger brickwork, and as the larger units the smaller brickwalls showed a generally higher ultimate lateral shrinkage than in the vertical direction.

6.3.2.4 General

Generally, better correlation between model walls and the larger brickwork was obtained for vertical strains than for horizontal strains. However, it should be noted that, with model walls, the variation in brick and mortar properties will not be represented as in larger units since there were only 5 or 6 bricks in the model wall compared to 26 and 104 bricks for single-leaf wall and solid pier, respectively. This is more evident for clay brickwork. In addition, for lateral strains, the degree of restraint of the single wythe model wall are not the same as the larger brickwork, particularly with the cavity, hollow and solid brickwork.

Table 6.1 - Modulus of Elasticity and Poisson's ratio of Masonry

Type of Brick/block	Size of Masonry	Volume to Surface (mm)	Modulus of Elasticity (GPa)	Poisson's ratio (μ)	
				at loading	at 170 days
Engineering Clay	Single-leaf wall	44	11.8	0.08	0.11
	Cavity Wall	51	15.9	0.11	0.10
	Hollow Pier	78	14.8	0.10	0.14
	Solid Pier	112	14.5	0.10	0.14
Calcium Silicate	Single-leaf wall	44	5.0	0.04	0.08
	Cavity wall	51	5.1	0.09	0.07
	Hollow pier	78	5.5	0.08	0.09
	Solid pier	112	5.0	0.08	0.12
Concrete	Single-leaf Wall	44	9.9	0.20	0.06
	Cavity wall	51	9.2	0.19	0.05
	Hollow pier	78	9.7	0.21	0.04
	Solid pier	112	9.6	0.16	0.06

Table 6.2 - Prediction of Modulus of Elasticity from Brick Strength or Stress Level

Types of Masonry	BS 5628[46] Eq.(2.24)	Plowman[65] Eq.(2.8)	Sinha and Hendry[66] Eq.(2.9)	Lenczner[16] Eqs.(2.11) - (2.13)	Lenczner[16] Eq.(2.25)
Engineering clay	15,75	19.56	5.36	22.12	26.30
Calcium silicate	7.02	5.96	5.36	5.68	9.01
Concrete	9.00	3.42	5.36	5.00	3.52

Table 6.3 - Ultimate Creep and Strain Ratio of Masonry

Type of Brick/block	Size of Masonry	Volume to Surface (mm)	Elastic Strain (10^{-6})	Ultimate Creep (10^{-6})	Strain Ratio (S_R)
Engineering Clay	Single-leaf wall	44	127	406 (0.998)	4.20 [3.20]
	Cavity Wall	51	94	368 (0.997)	4.91 [3.91]
	Hollow Pier	78	101	352 (0.998)	4.48 [3.48]
	Solid Pier	112	100	321 (0.996)	4.21 [3.21]
Calcium Silicate	Single-leaf wall	44	301	756 (0.998)	3.51 [2.51]
	Cavity wall	51	297	658 (0.995)	3.22 [2.22]
	Hollow pier	78	275	539 (0.998)	2.96 [1.96]
	Solid pier	112	298	505 (0.995)	2.69 [1.69]
Concrete	Single-leaf Wall	44	151	435 (0.999)	3.88 [2.88]
	Cavity wall	51	164	377 (0.999)	3.29 [2.29]
	Hollow pier	78	155	317 (0.999)	3.05 [2.05]
	Solid pier	112	156	305 (1.0)	2.96 [1.96]

( ) - *correlation coefficient*
[ ] - *creep coefficient*

Table 6.4 - Ultimate Vertical and Horizontal Shrinkage of Masonry

Type of Brick/block	Size of Masonry	Volume to Surface (mm)	Ultimate Vertical Shrinkage (10^{-6})	Ultimate Horizontal Shrinkage (10^{-6})
Engineering Clay	Single-leaf wall	44	149 (0.995)	
	Cavity Wall	51	151 (0.992)	
	Hollow Pier	78	156 (0.981)	-
	Solid Pier	112	158 (0.978)	
Calcium Silicate	Single-leaf wall	44	341 (0.999)	431 (0.999)
	Cavity wall	51	330 (0.999)	378 (0.989)
	Hollow pier	78	306 (0.997)	352 (0.982)
	Solid pier	112	293 (0.993)	291 (0.975)
Concrete	Single-leaf Wall	44	409 (0.998)	367 (0.996)
	Cavity wall	51	394 (0.999)	328 (0.998)
	Hollow pier	78	377 (0.994)	341 (0.998)
	Solid pier	112	350 (0.991)	346 (0.998)

Table 6.5 - Ratio of Horizontal to Vertical Ultimate Shrinkage of Masonry

Type of Brick/block	Size of Masonry	Volume to Surface Ratio (mm)	Ratio of Horizontal/Vertical Ultimate Shrinkage	
			Present data	Brooks and Bingel[23]
Calcium Silicate	Single-leaf wall	44	1.26	0.48
	Cavity wall	51	1.14	0.50
	Hollow pier	78	1.15	0.56
	Solid pier	112	0.99	0.68
Concrete	Single-leaf Wall	44	0.90	0.91
	Cavity wall	51	0.83	-
	Hollow pier	78	0.90	1.17
	Solid pier	112	0.99	2.1 (V/S 140)

Table 6.6 - Modulus of Elasticity and Poisson's ratio of Model Walls.

Type of Brick/block	Size of Masonry	Volume to Surface (mm)	Modulus of Elasticity (GPa)	Poisson's Ratio (μ)	
				at loading	at 170 days
Clay	Model wall 1	44	13.1	0.19	-0.01*
	Model wall 2	51	12.6	0.01	-0.03
	Model wall 3	78	15.9	0.11	0.01
	Model wall 4	112	13.9	0.10	-0.08
Calcium Silicate	Model wall 1	44	5.22	0.03	0.06
	Model wall 2	51	4.86	0.04	0.05
	Model wall 3	78	5.18	0.07	0.07
	Model wall 4	112	4.69	0.18	0.11

** negative Poisson's ratio for axial contraction and lateral contraction.*

Table 6.7 - Ultimate Creep and Shrinkage of Model Walls.

Type of Brick/block	Size of Masonry	Volume to Surface (mm)	Ultimate Creep (10^{-6})	Ultimate Shrinkage (10^{-6})	Ultimate Lateral Shrinkage (10^{-6})
Clay	Model wall 1	44	332	149	-
	Model wall 2	51	304	145	
	Model wall 3	78	327	153	
	Model wall 4	112	348	147	
Calcium Silicate	Model wall 1	44	810	348	407
	Model wall 2	51	745	311	337
	Model wall 3	78	548	312	214
	Model wall 4	112	537	299	263

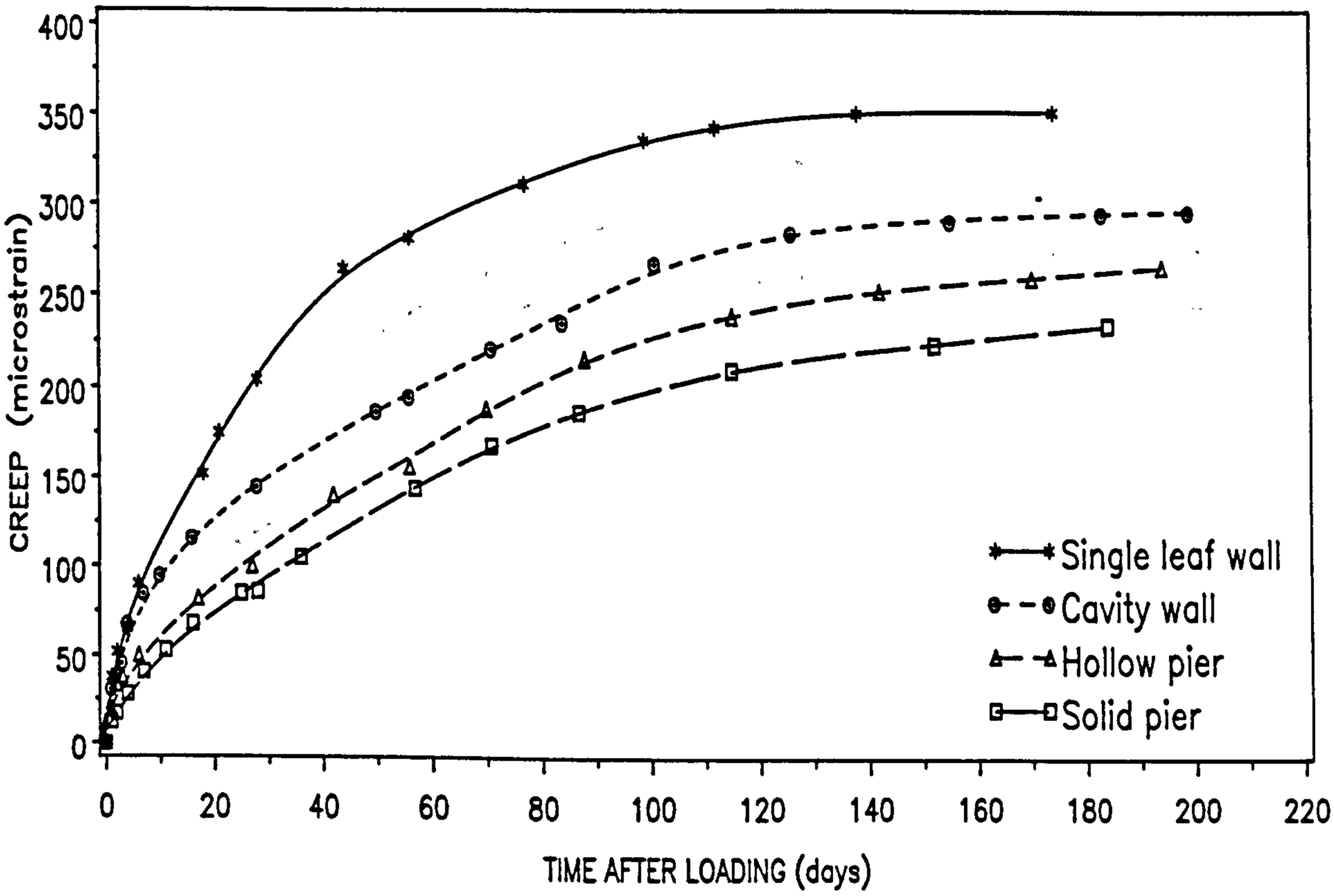

Fig. 6.1 – Axial Creep–time Curves for Engineering Clay Brickwork

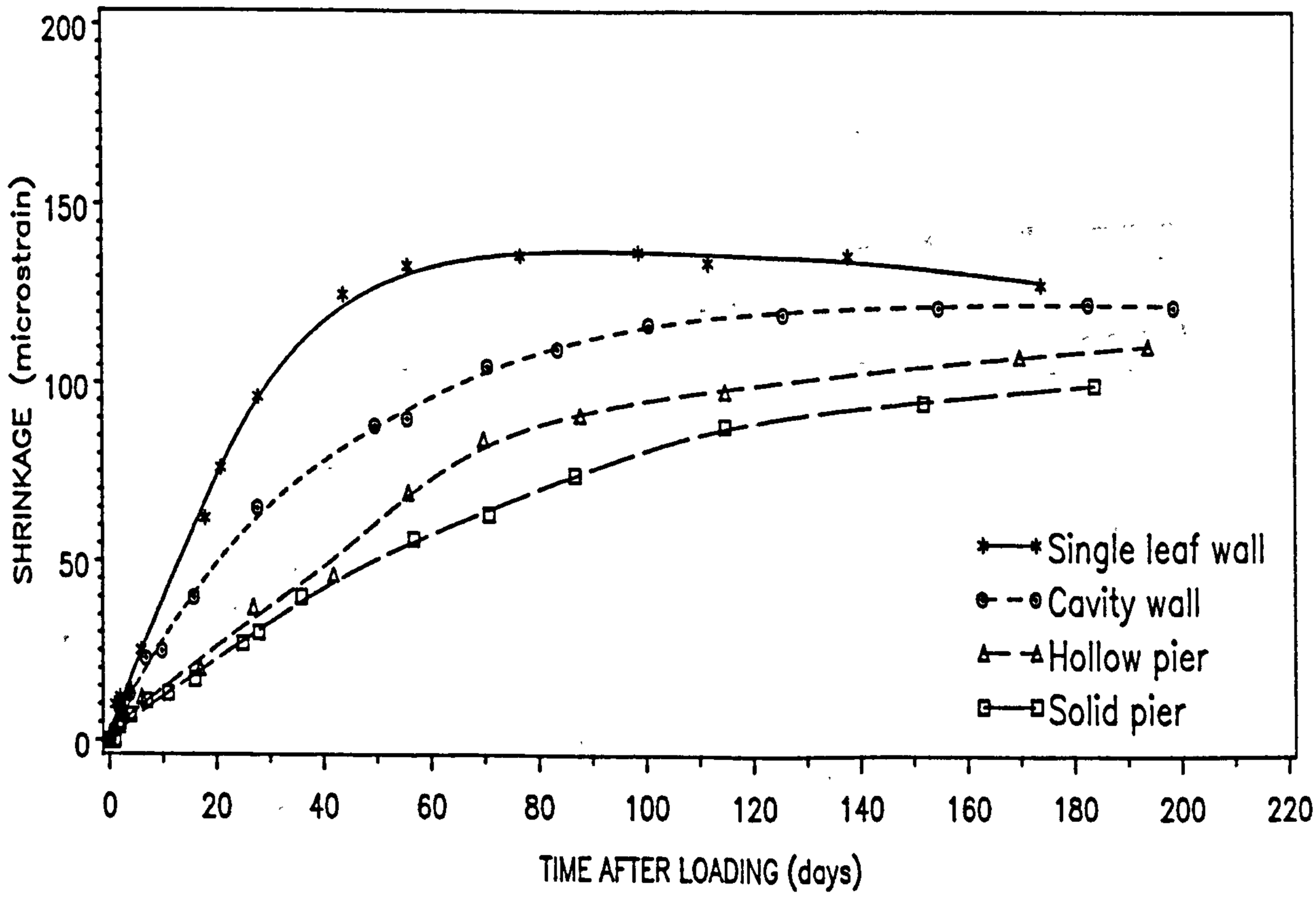

Fig. 6.2 – Axial Shrinkage–time Curves for Engineering Clay Brickwork

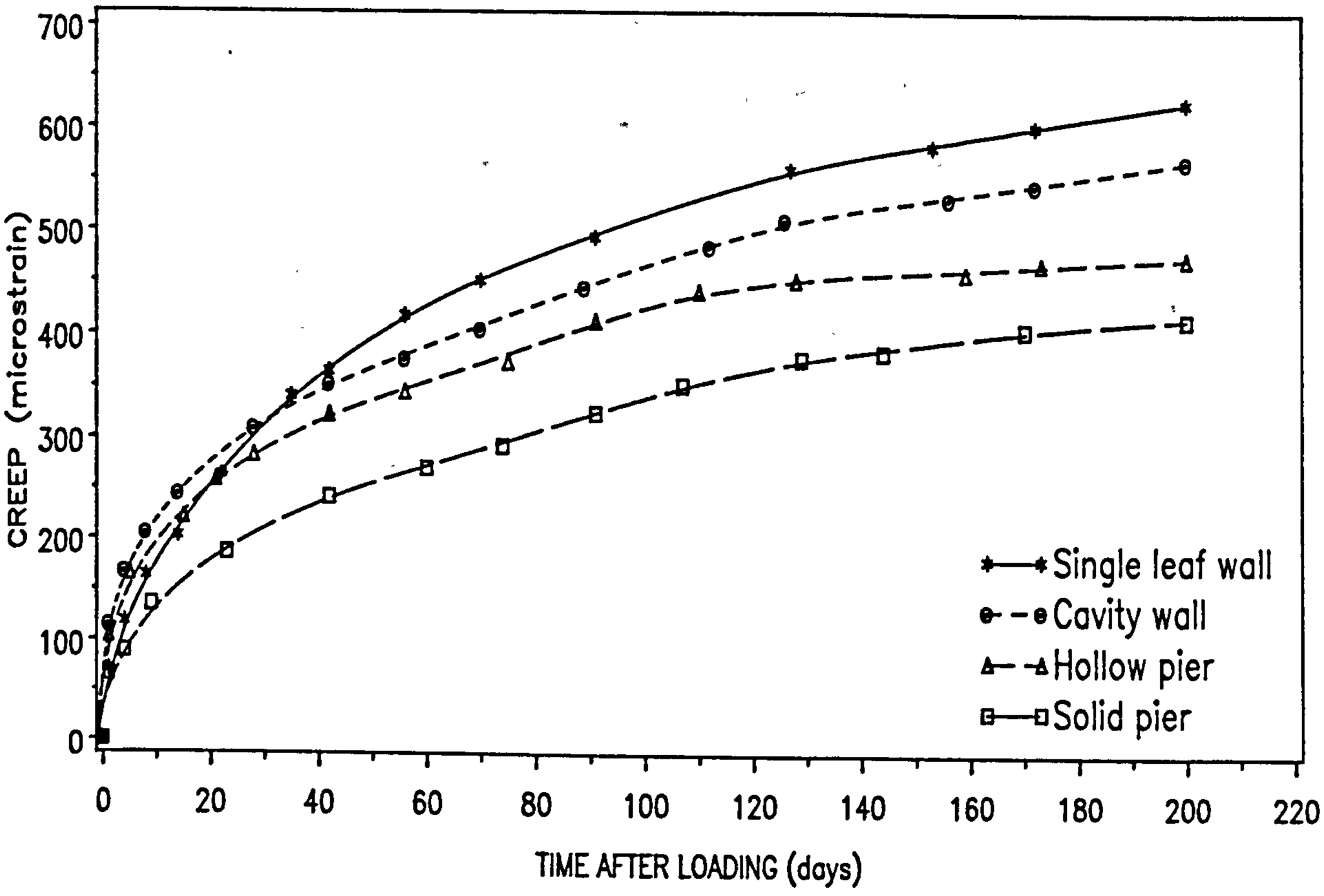

Fig. 6.3 – Axial Creep–time Curves for Calcium Silicate Brickwork

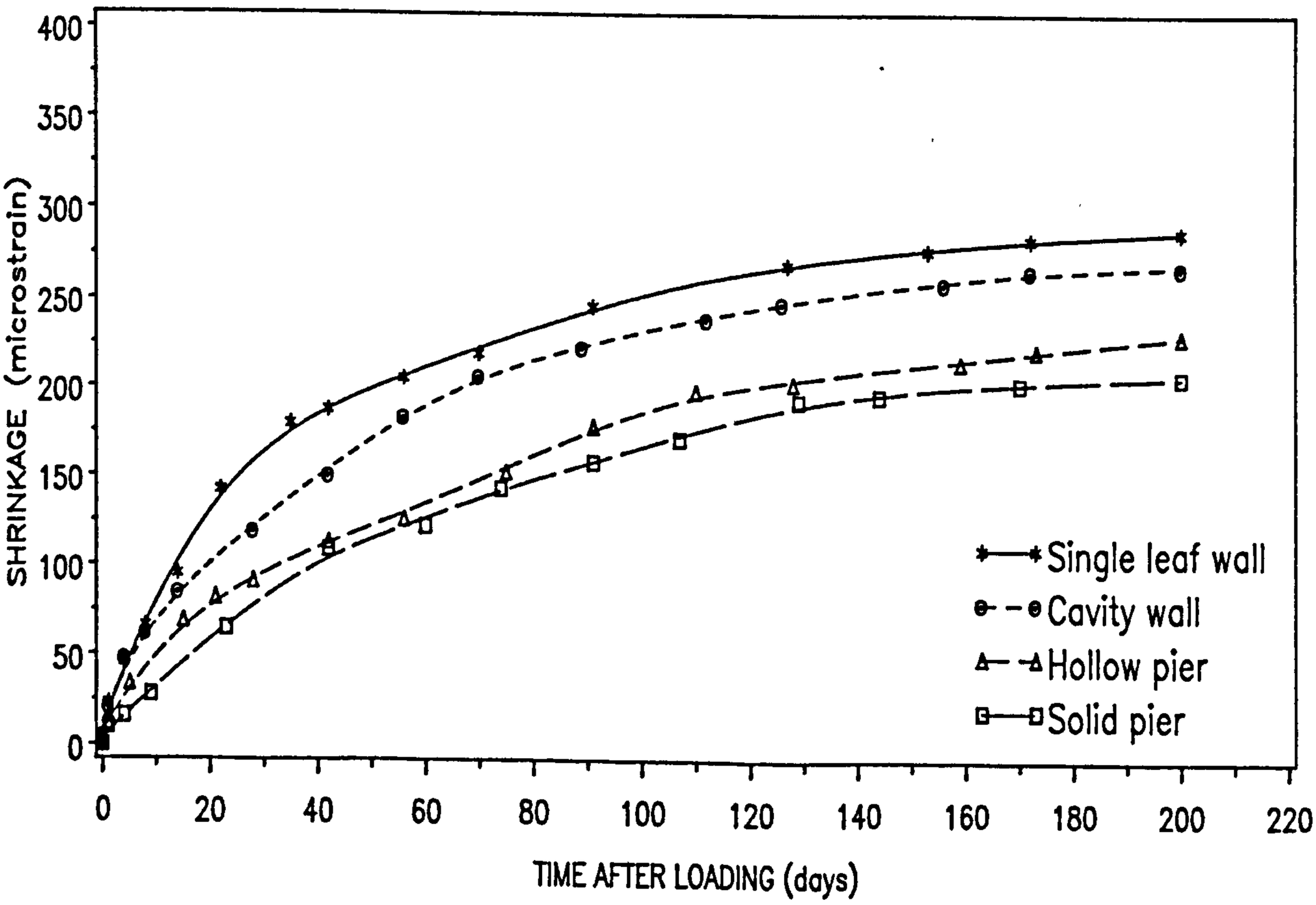

Fig. 6.4 – Axial Shrinkage–time Curves for Calcium Silicate Brickwork

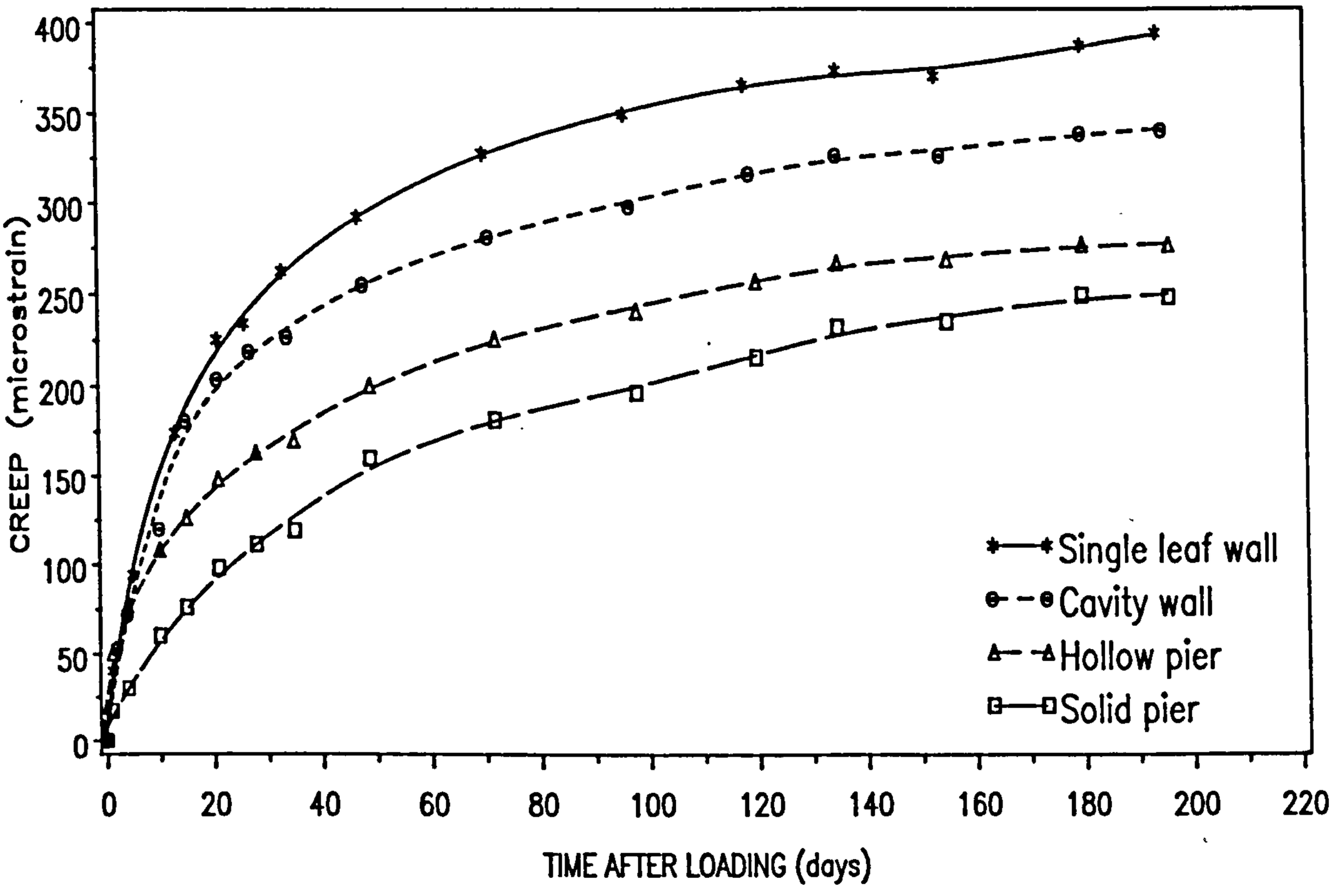

Fig. 6.5 – Axial Creep–time Curves for Concrete Blockwork

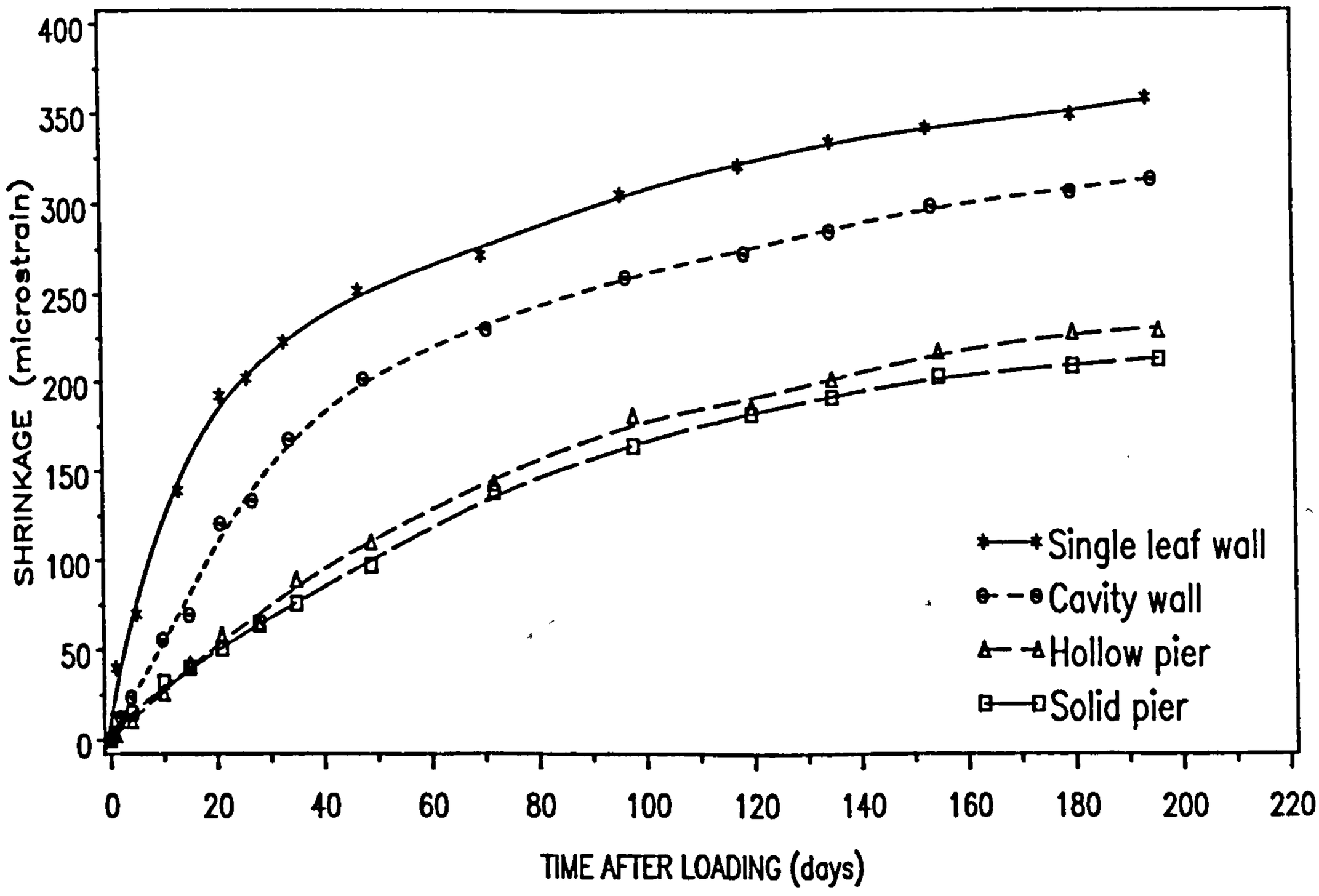

Fig. 6.6 – Axial Shrinkage–time Curves for Concrete Blockwork

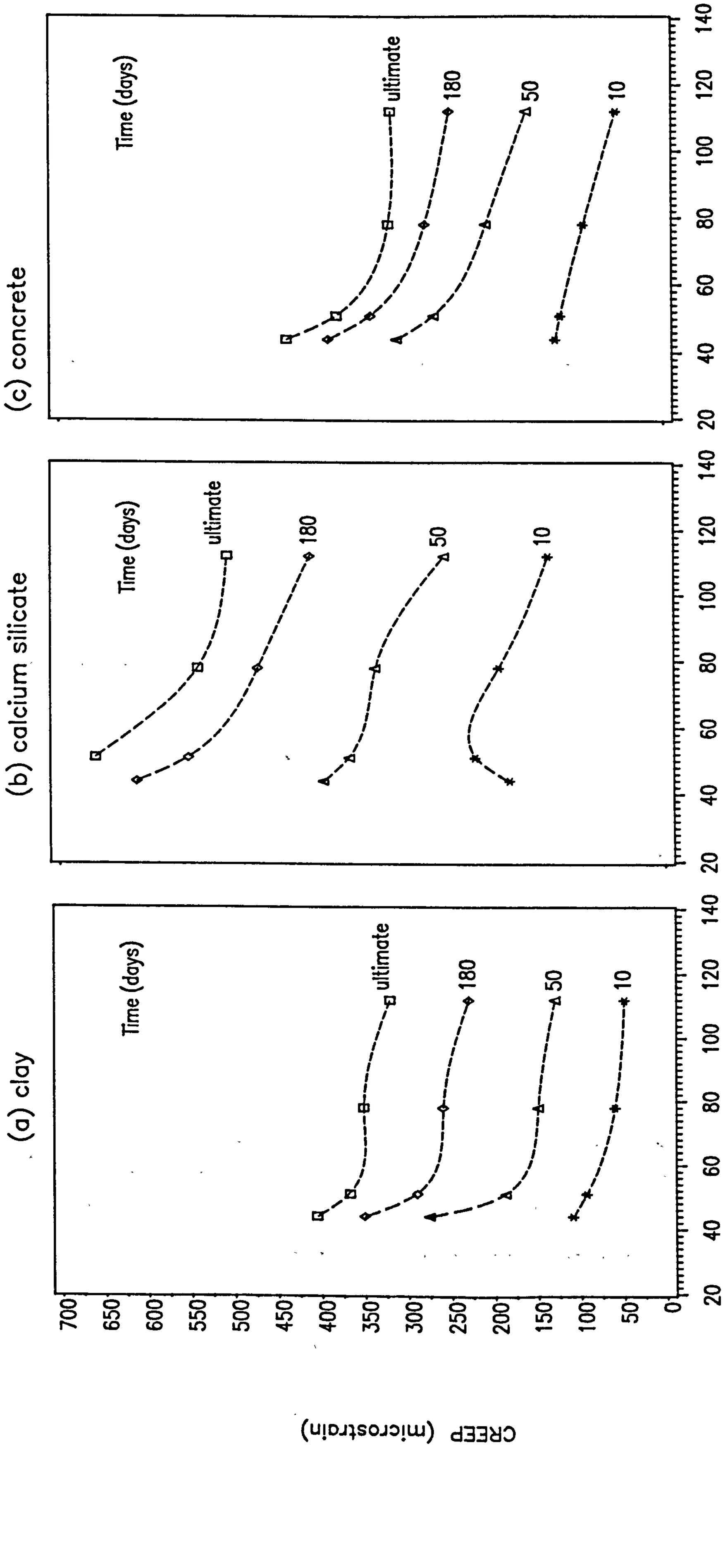

Fig. 6.7 – Influence of V/S Ratio on Creep of Masonry

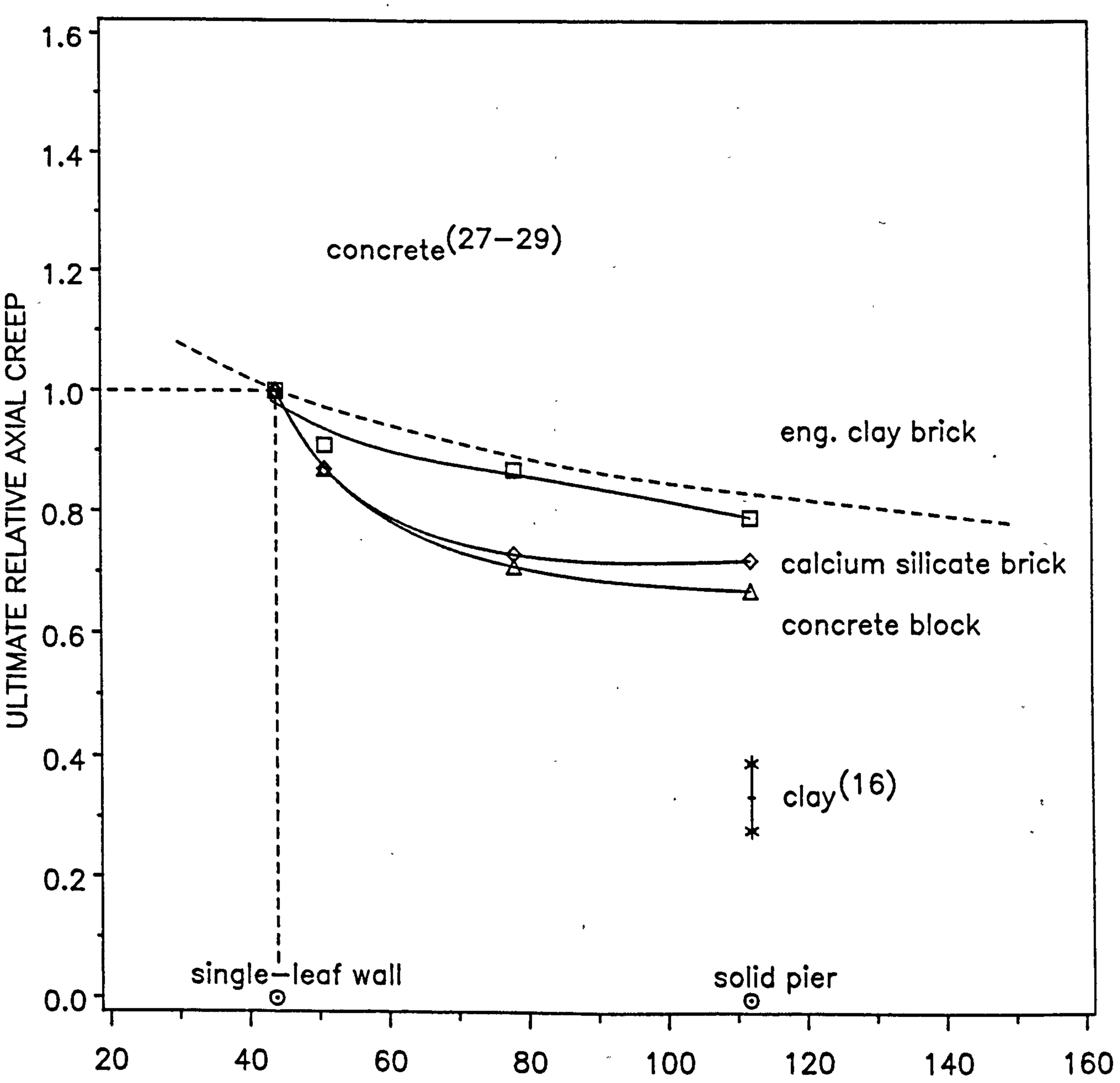

Fig. 6.8 – Ultimate Creep Relative to that of a Single Leaf Wall as a Function of V/S Ratio for Present Investigation and Previous Data

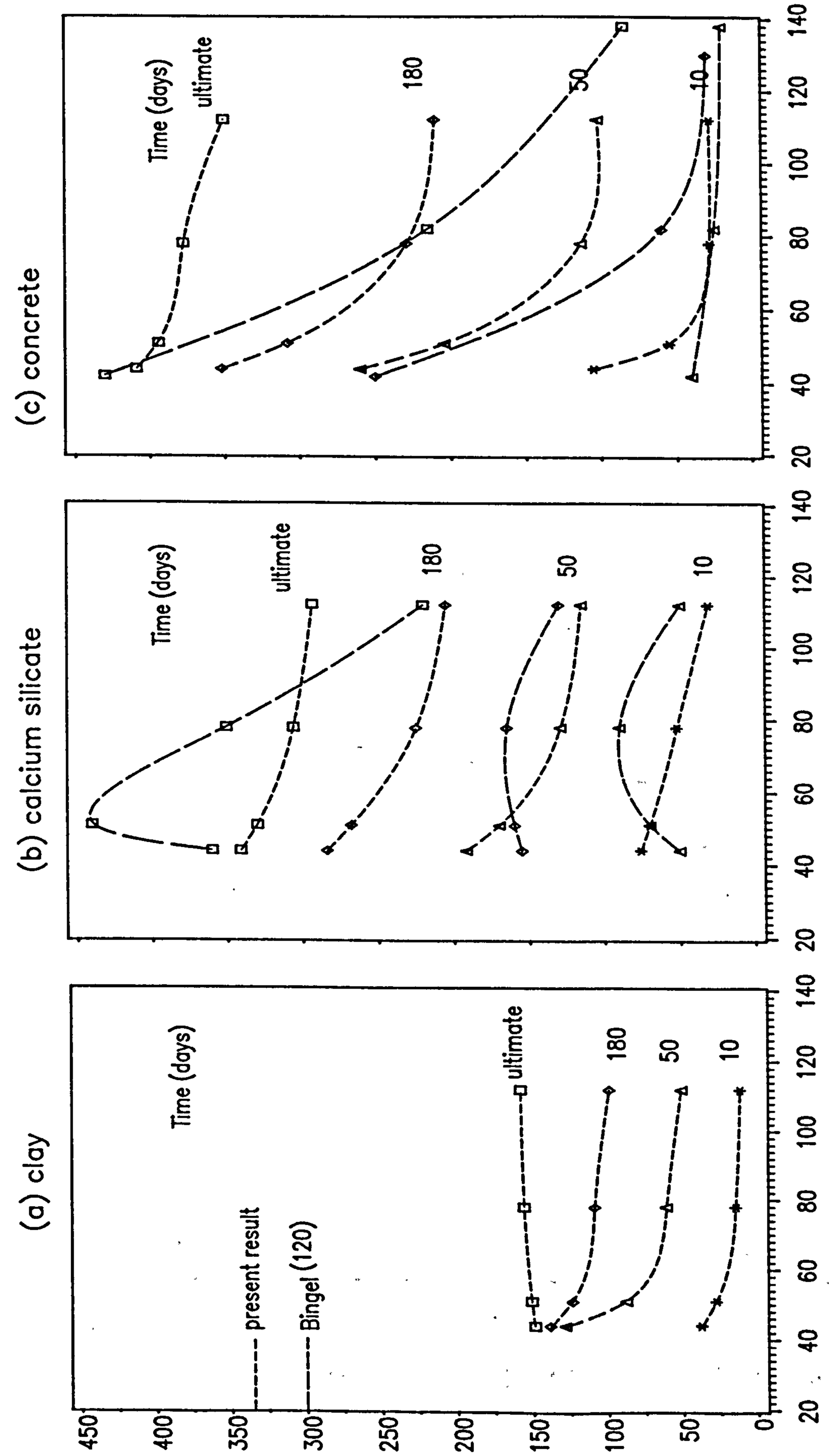

Fig. 6.9 – Influence of V/S Ratio on Shrinkage of Masonry

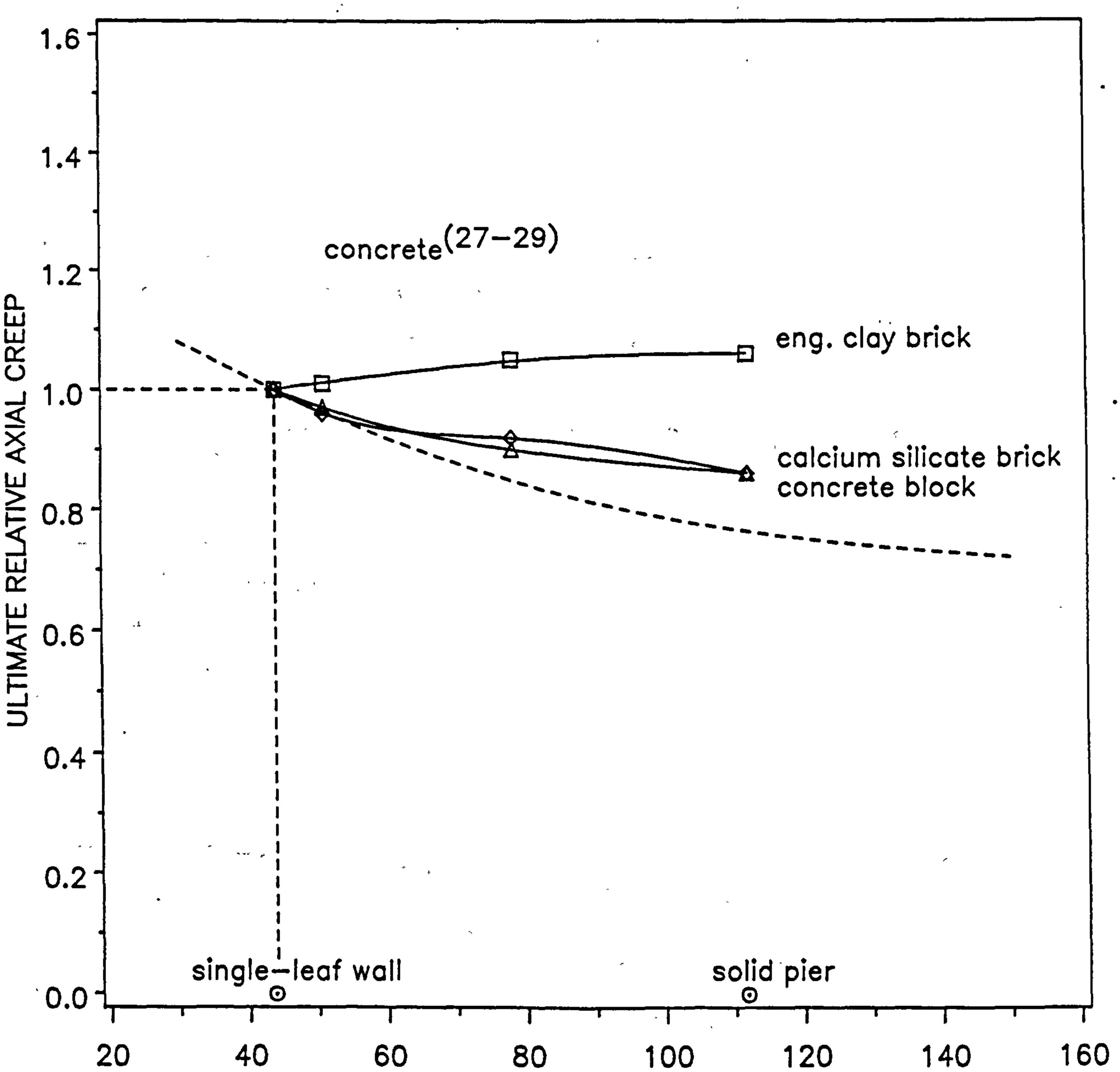

Fig. 6.10 – Ultimate Shrinkage Relative to that of a Single Leaf Wall as a Function of V/S Ratio for Present Investigation and Previous Data

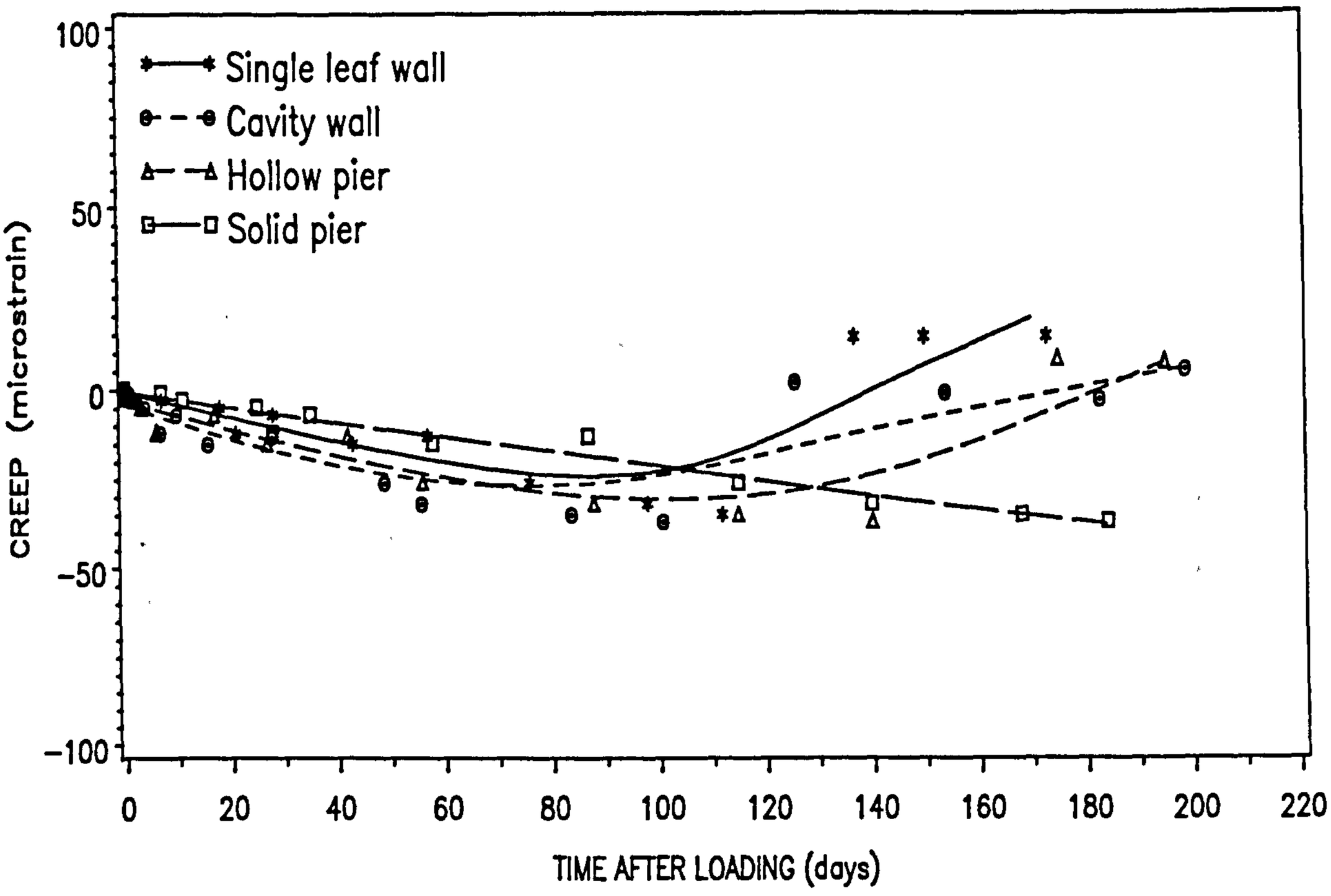

Fig. 6.11 – Lateral Creep–time Curves for Engineering Clay Brickwork

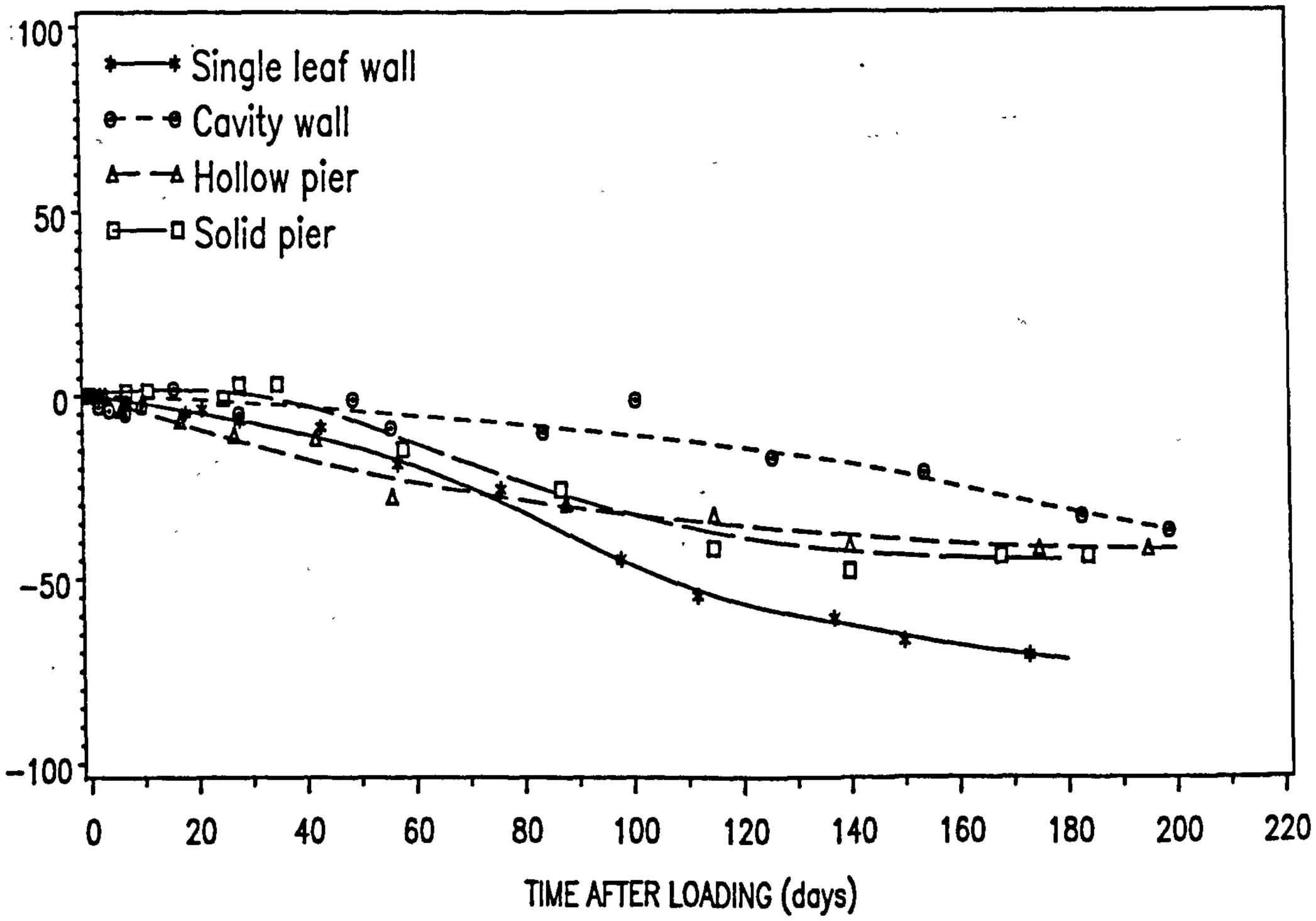

Fig. 6.12 – Lateral Shrinkage–time Curves for Engineering Clay Brickwork

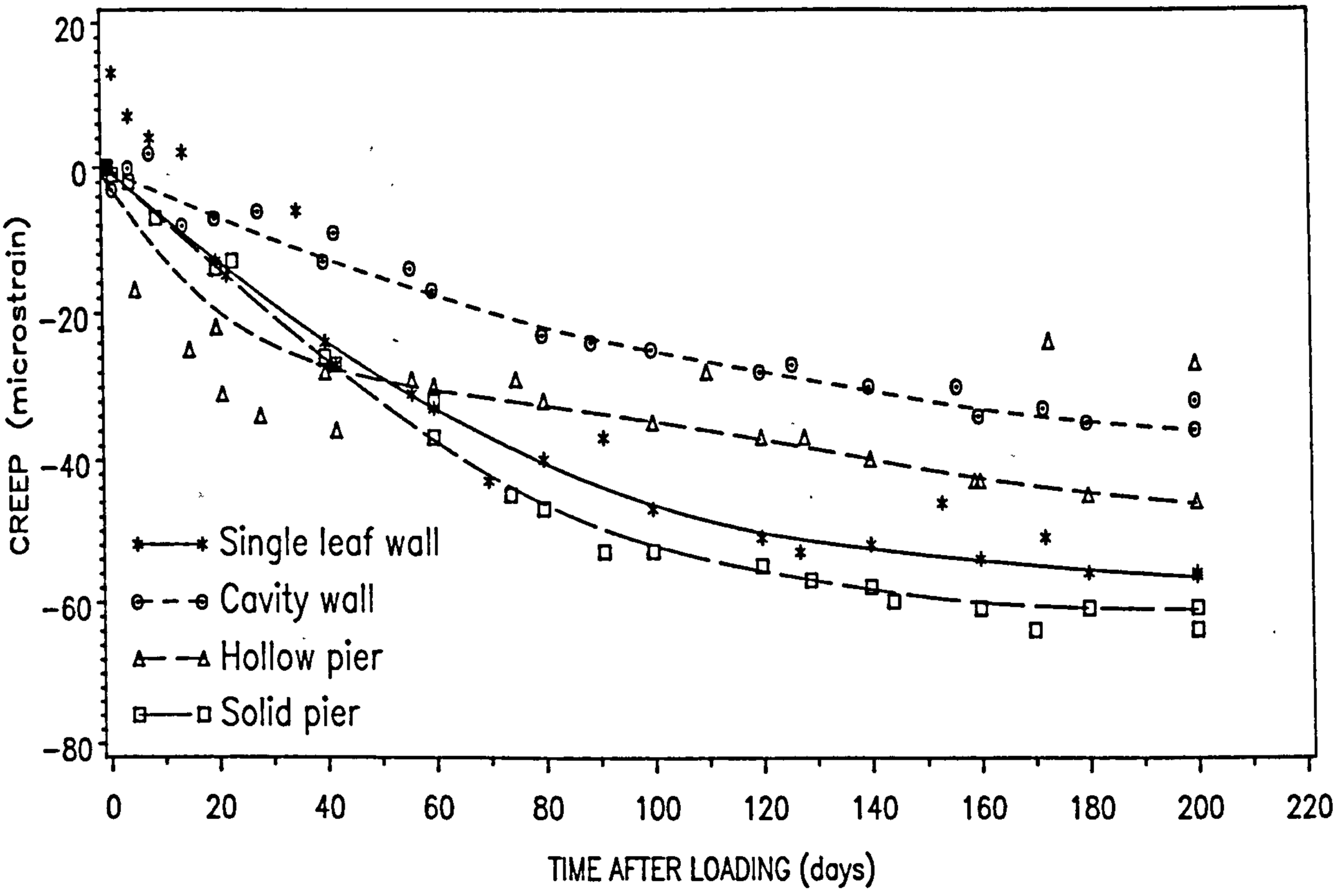

Fig. 6.13 – Lateral Creep–time Curves for Calcium Silicate Brickwork

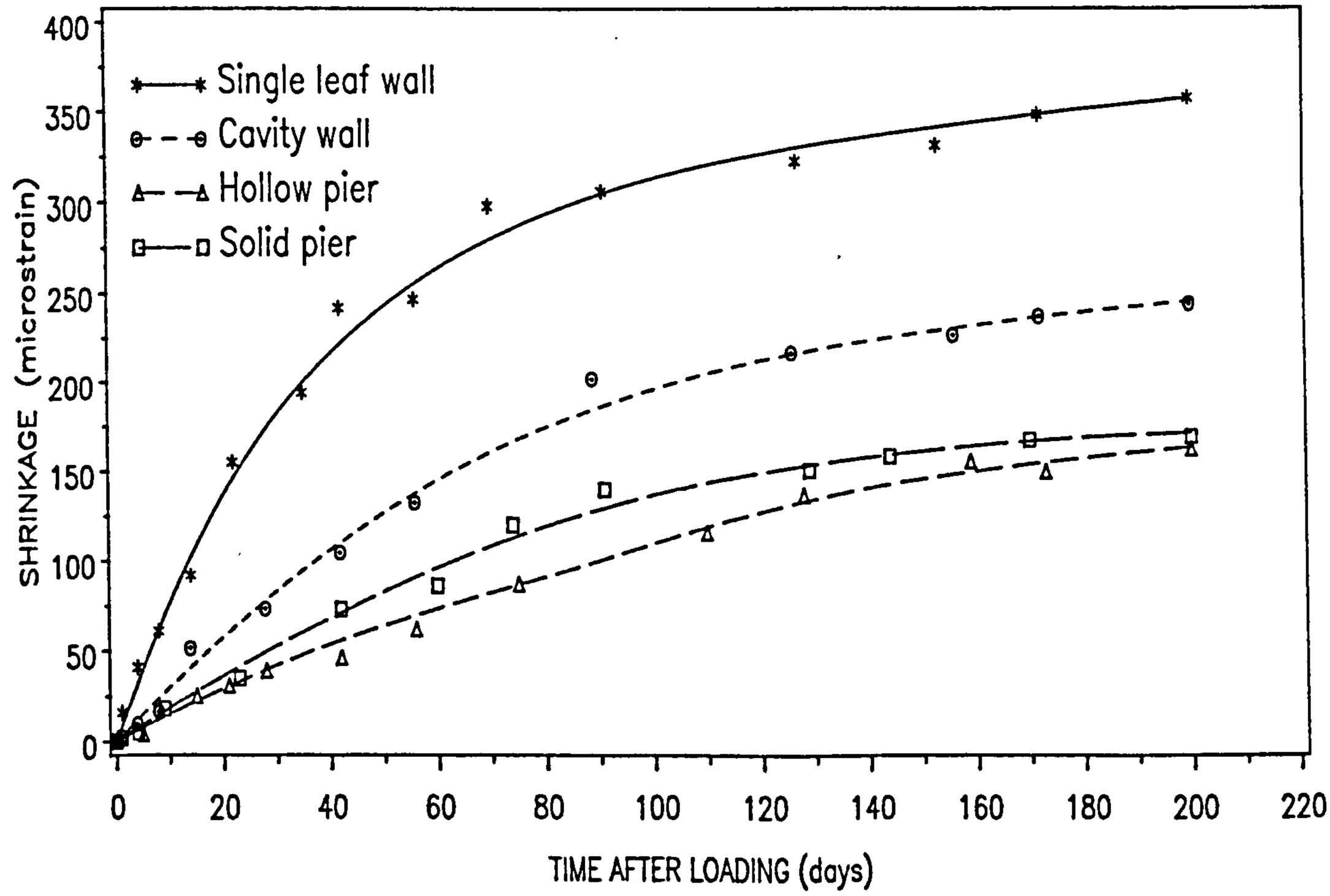

Fig. 6.14 Lateral Shrinkage–time Curves for Silicate Brickwork

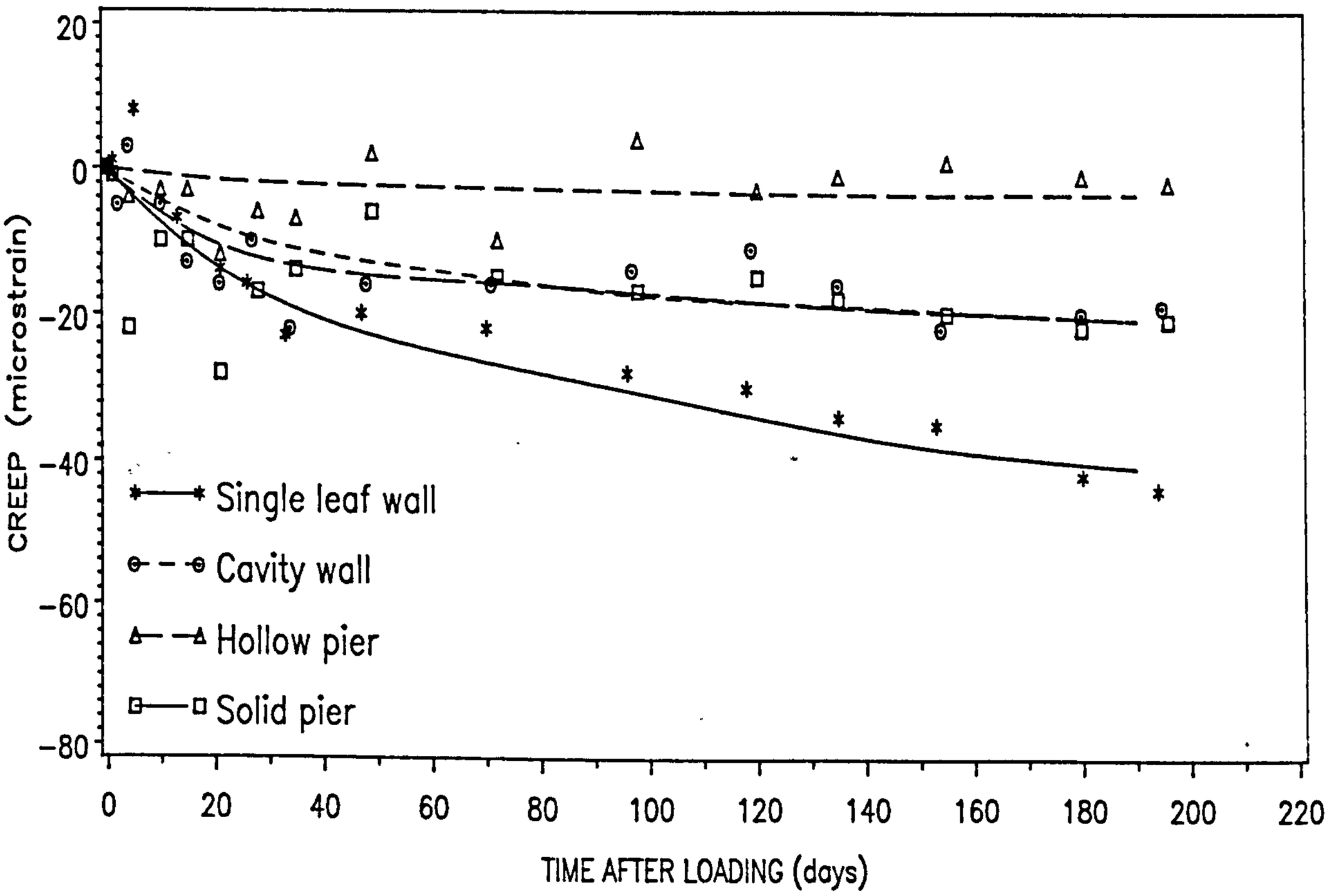

Fig. 6.15 – Lateral Creep–time Curves for Concrete Blockwork

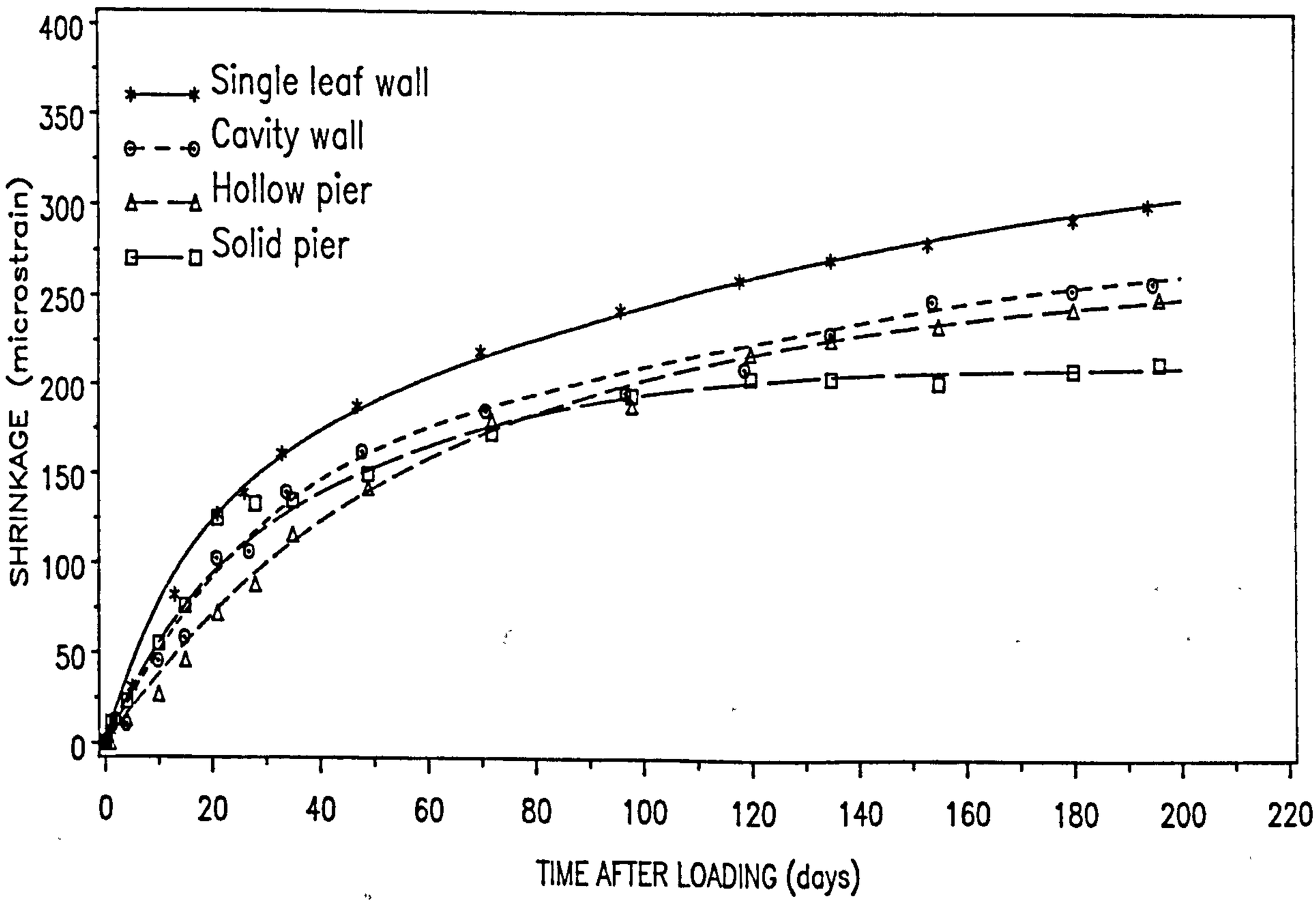

Fig. 6.16 Lateral Shrinkage–time Curves for Concrete Blockwork

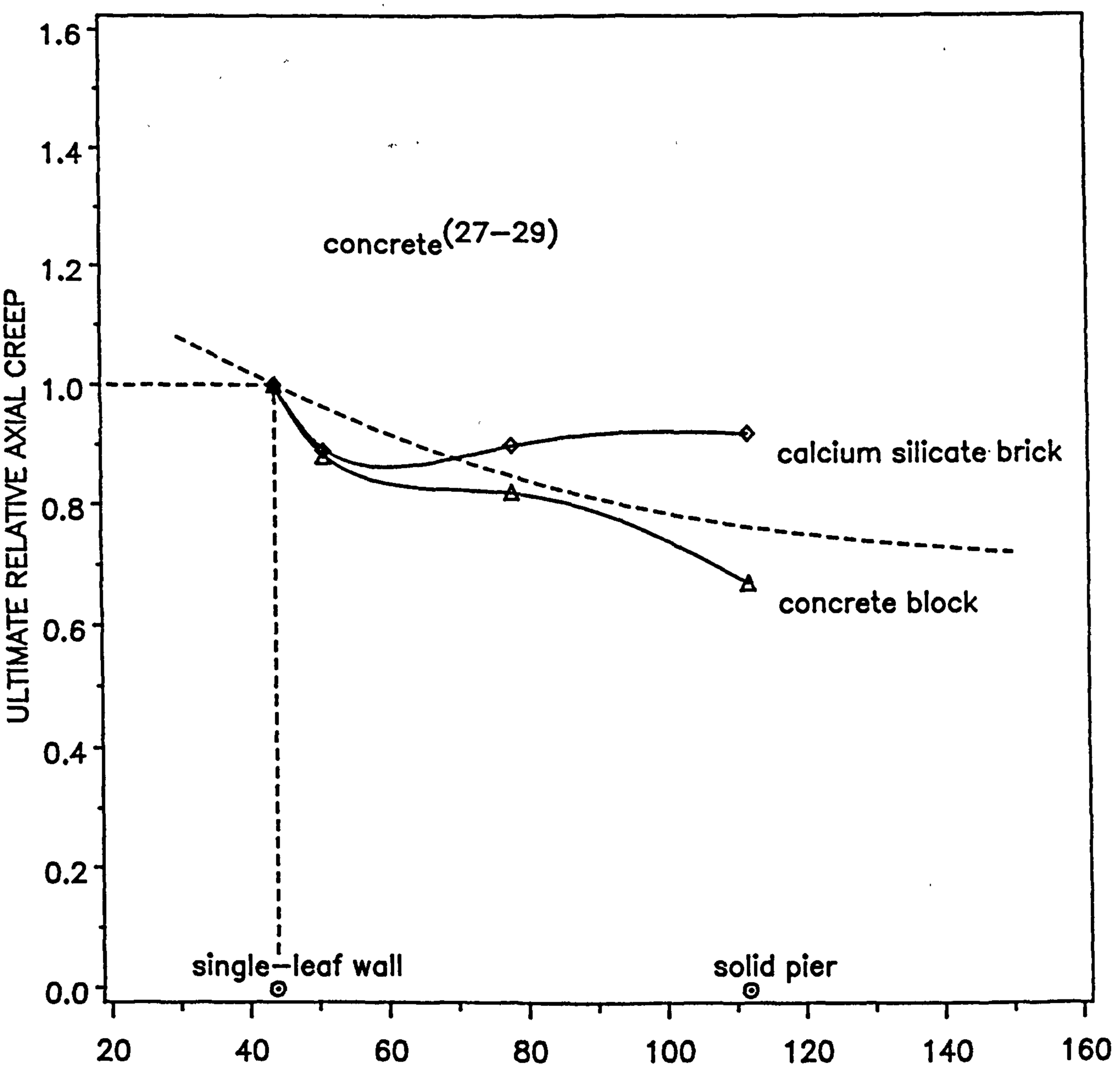

Fig. 6.17 – Ultimate Lateral Shrinkage Relative to that of a Single Leaf Wall as a Function of V/S Ratio for Present Investigation and Previous Data

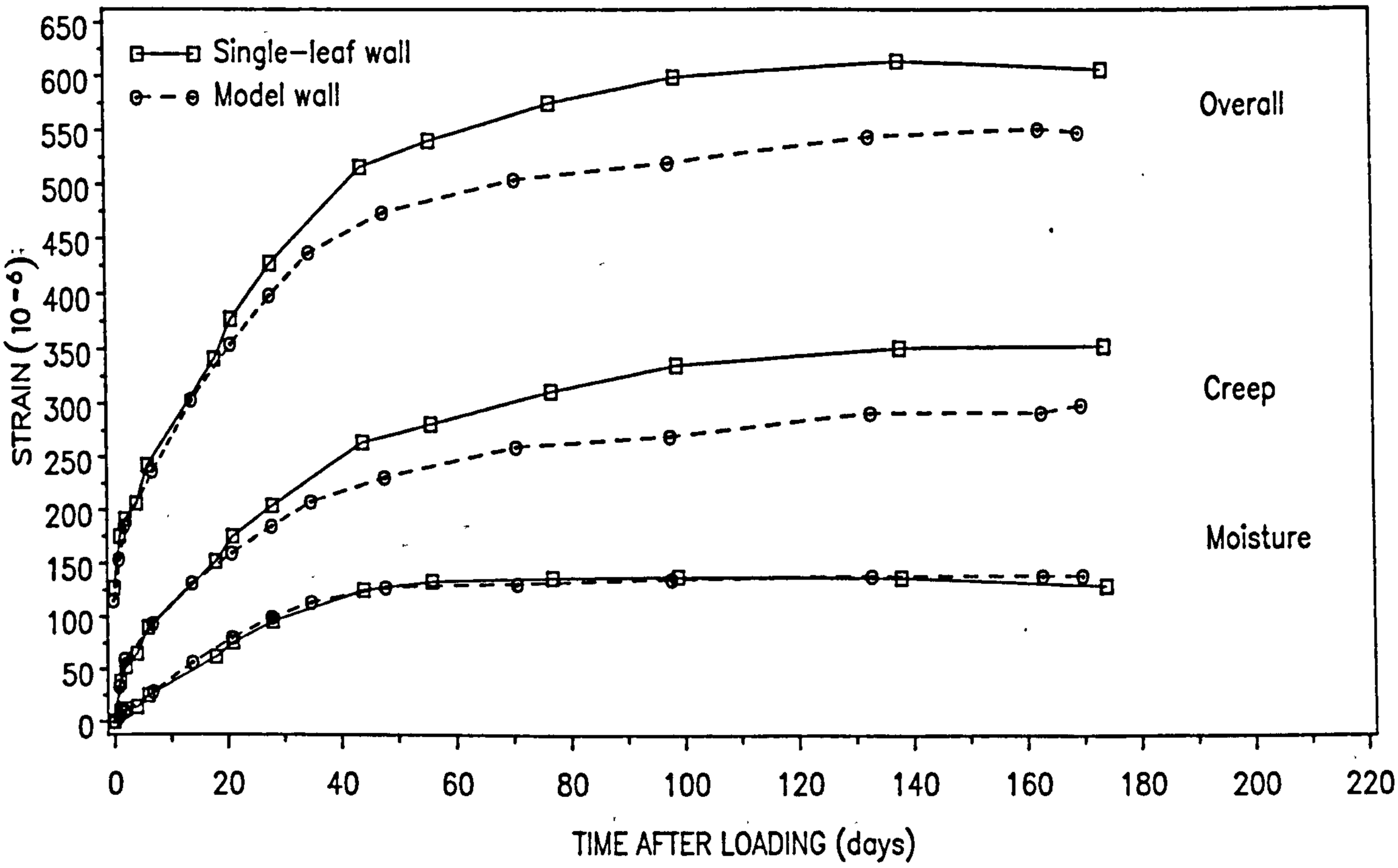

Fig. 6.18(a) – Comparison of the Strain–time Curves of the Model and Full Size Clay Brickwork with V/S = 44

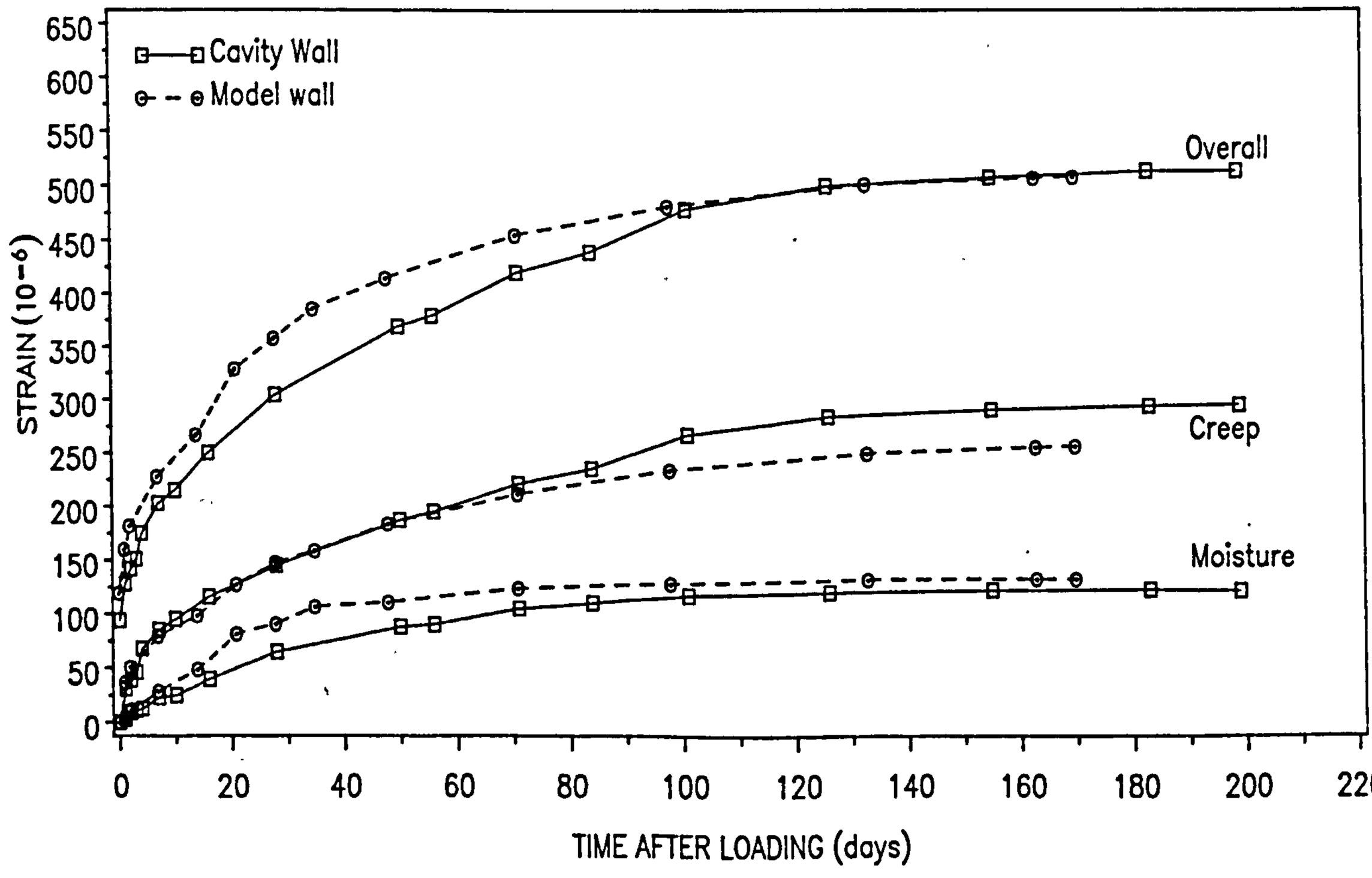

Fig. 6.18(b) – Comparison of the Strain–time Curves of the Model and Full Size Clay Brickwork with V/S = 51

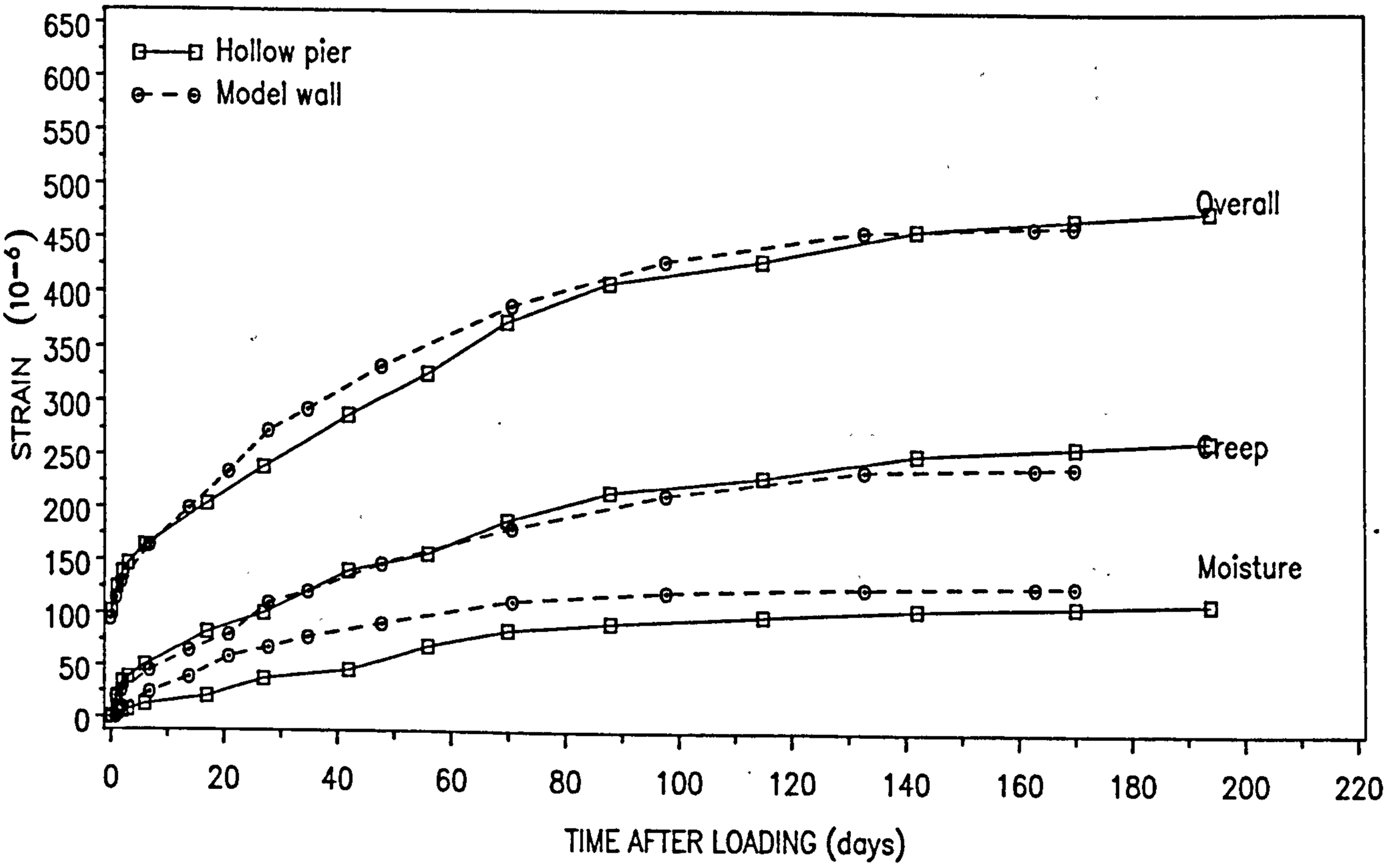

Fig. 6.18(c) – Comparison of the Strain–time Curves of the Model and Full Size Clay Brickwork with V/S = 78

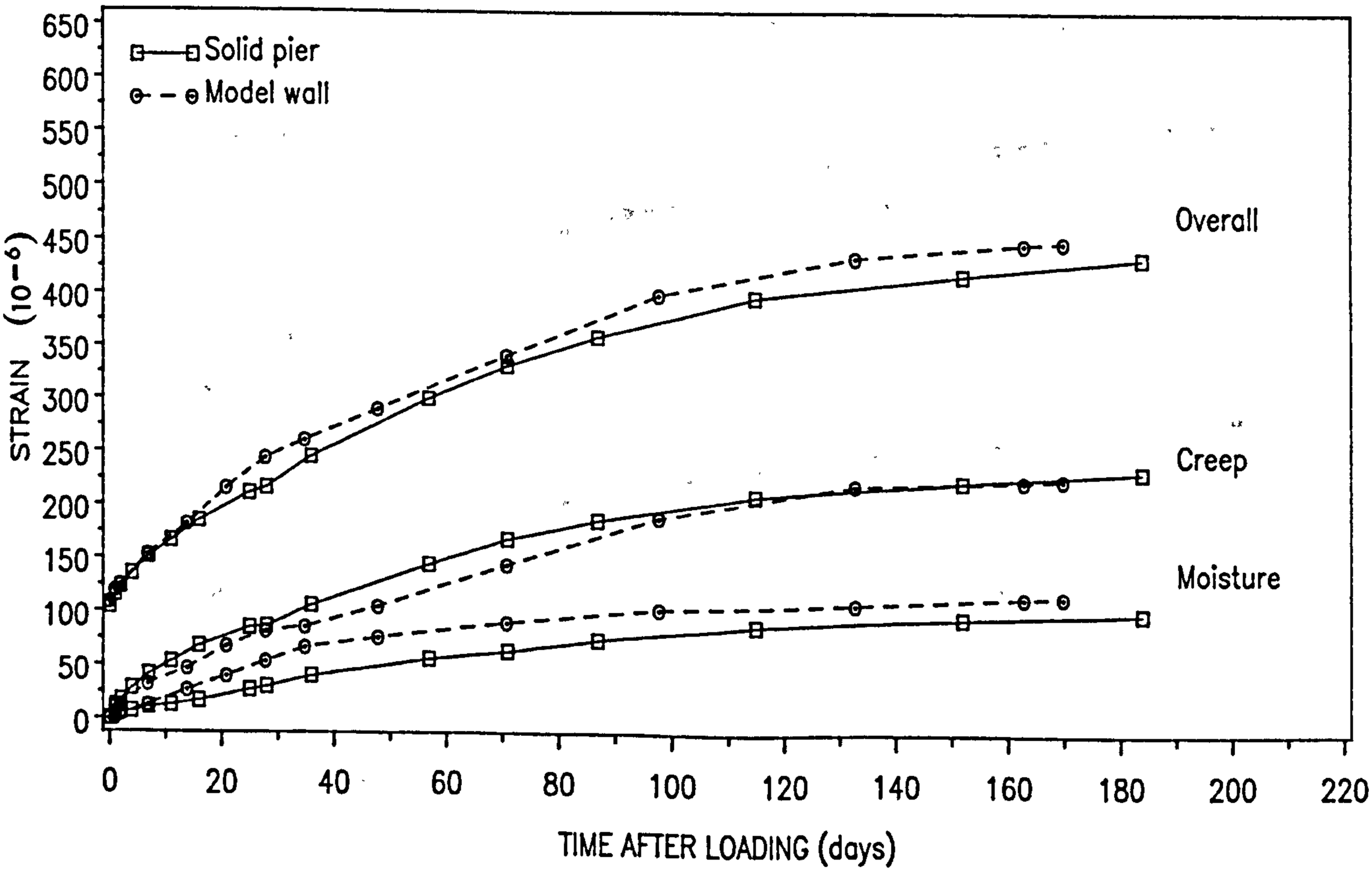

Fig. 6.18(d) – Comparison of the Strain–time Curves of the Model and Full Size Clay Brickwork with V/S = 112

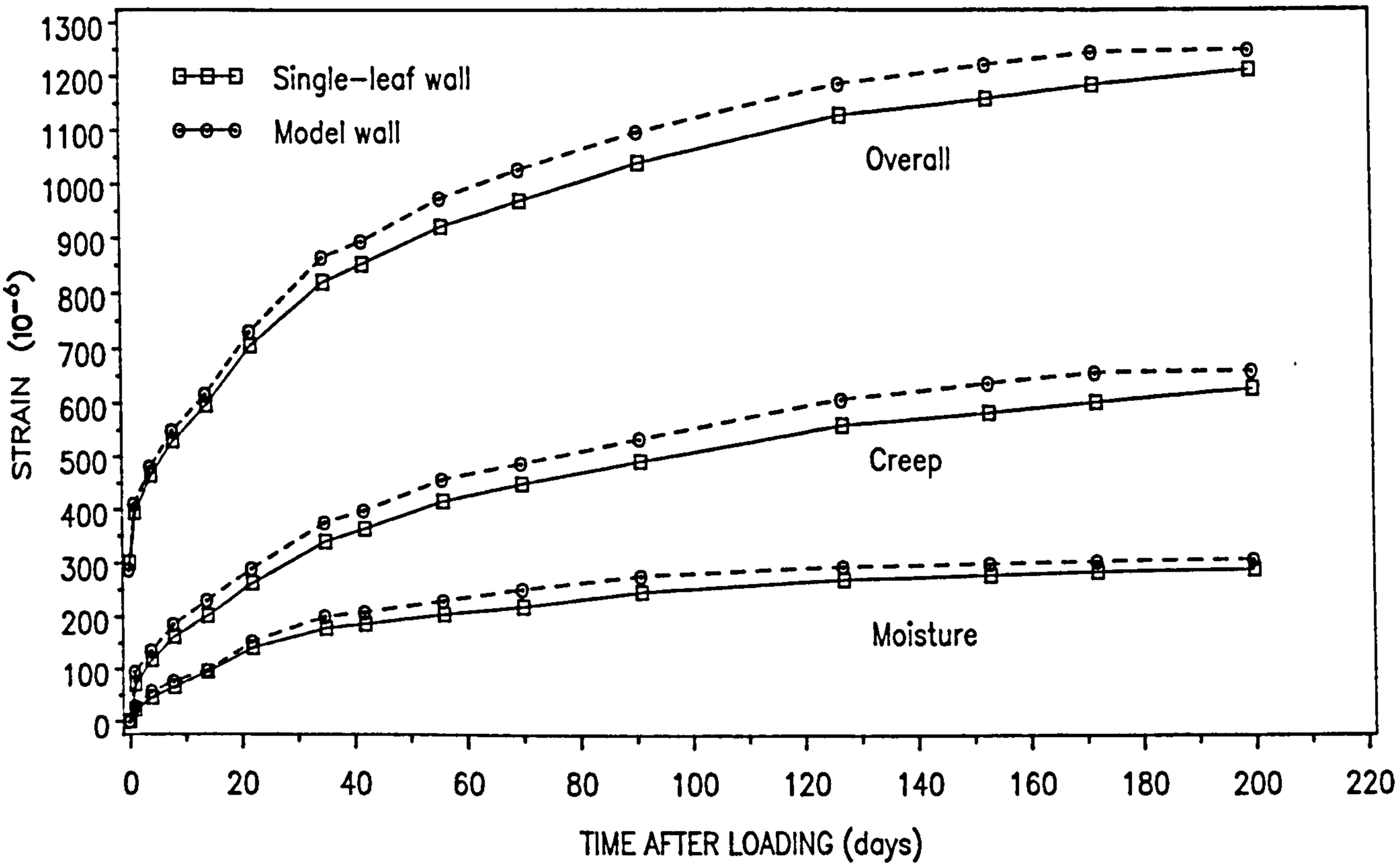

Fig. 6.19(a) – Comparison of the Strain–time Curves of the Model and Full Size Calcium Silicate Brickwork with V/S = 44

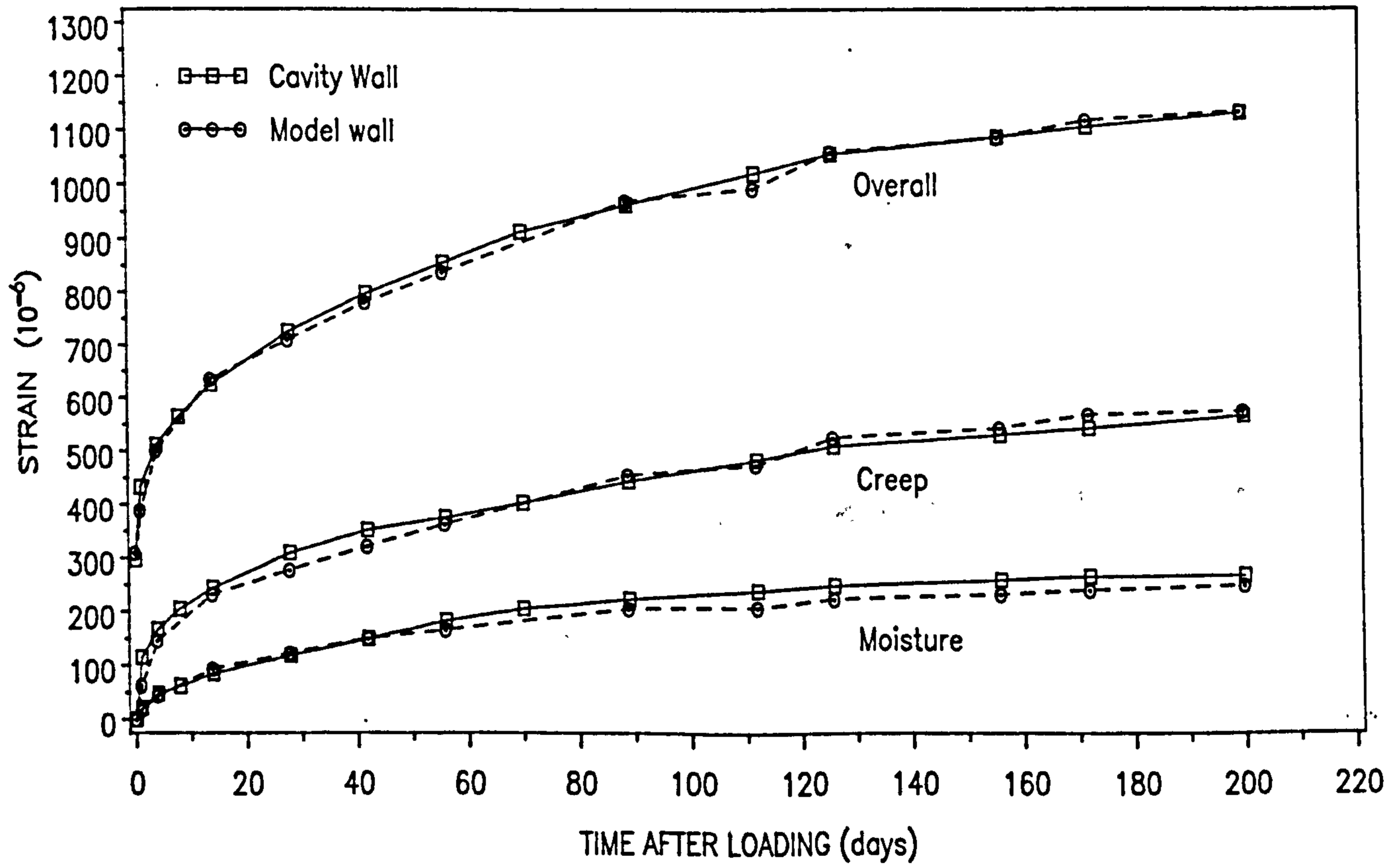

Fig. 6.19(b) – Comparison of the Strain–time Curves of the Model and Full Size Calcium Silicate Brickwork with V/S = 51

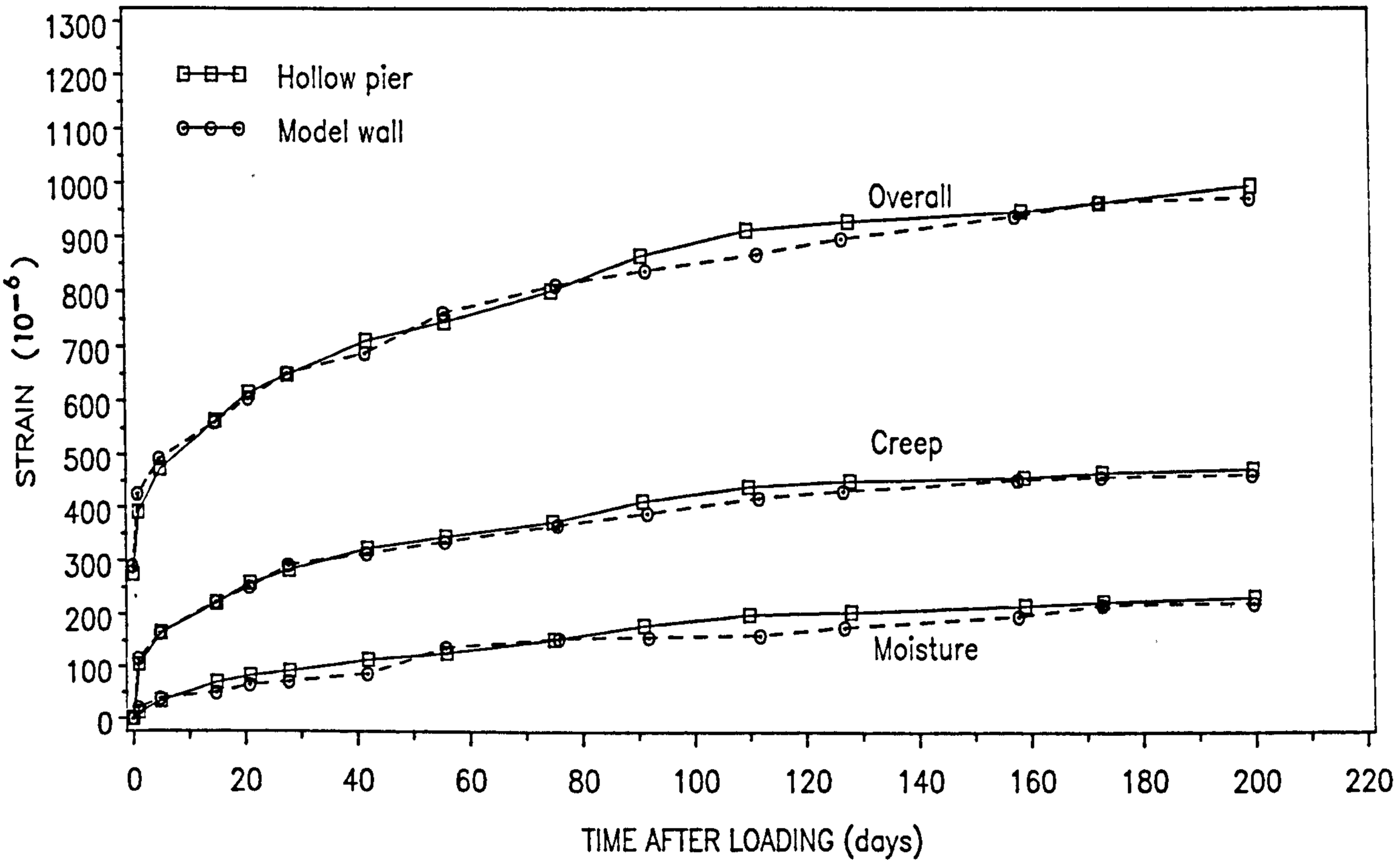

Fig. 6.19(c) – Comparison of the Strain–time Curves of the Model and Full Size Calcium Silicate Brickwork with V/S = 78

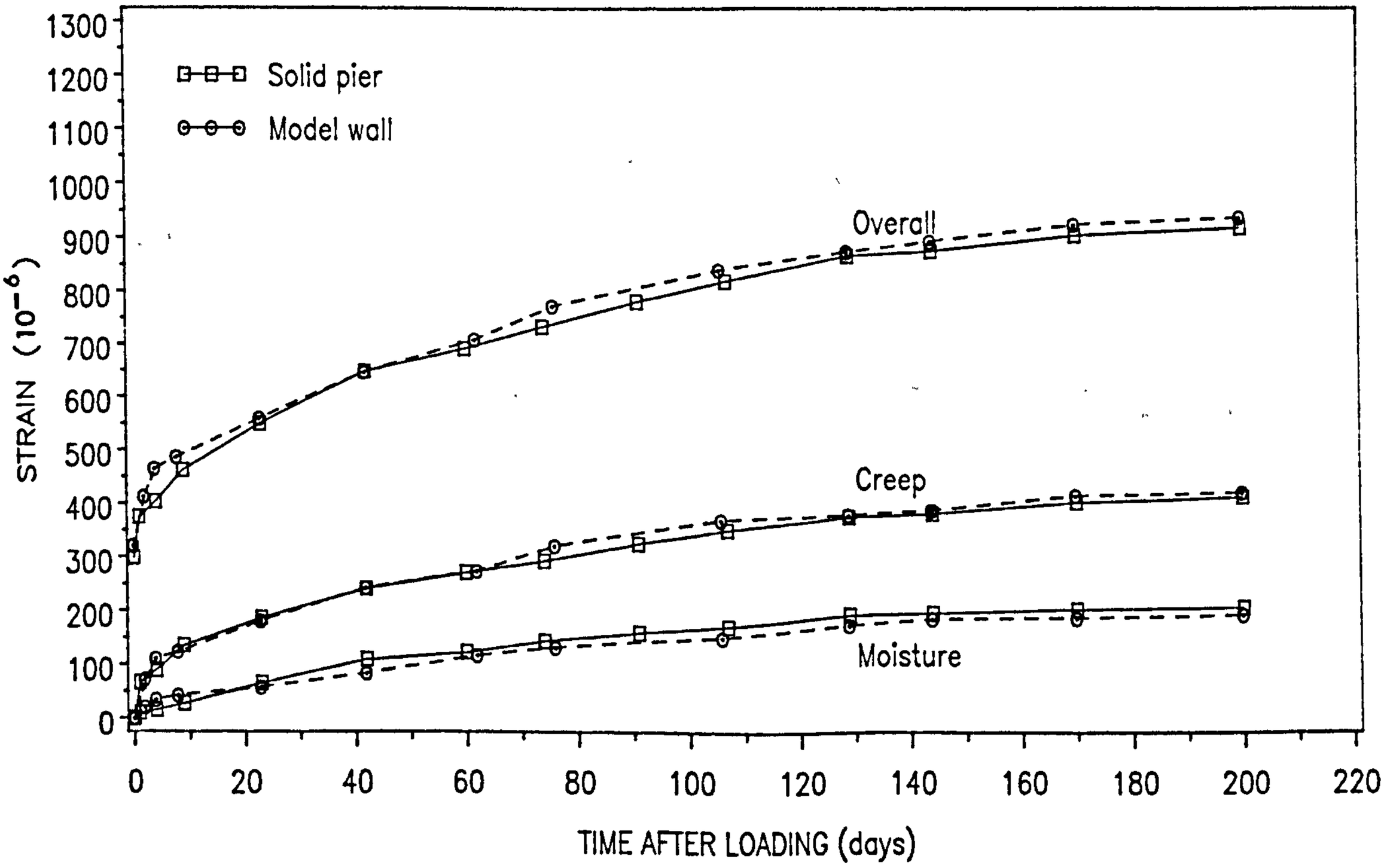

Fig. 6.19(d) – Comparison of the Strain–time Curves of the Model and Full Size Calcium Silicate Brickwork with V/S = 112

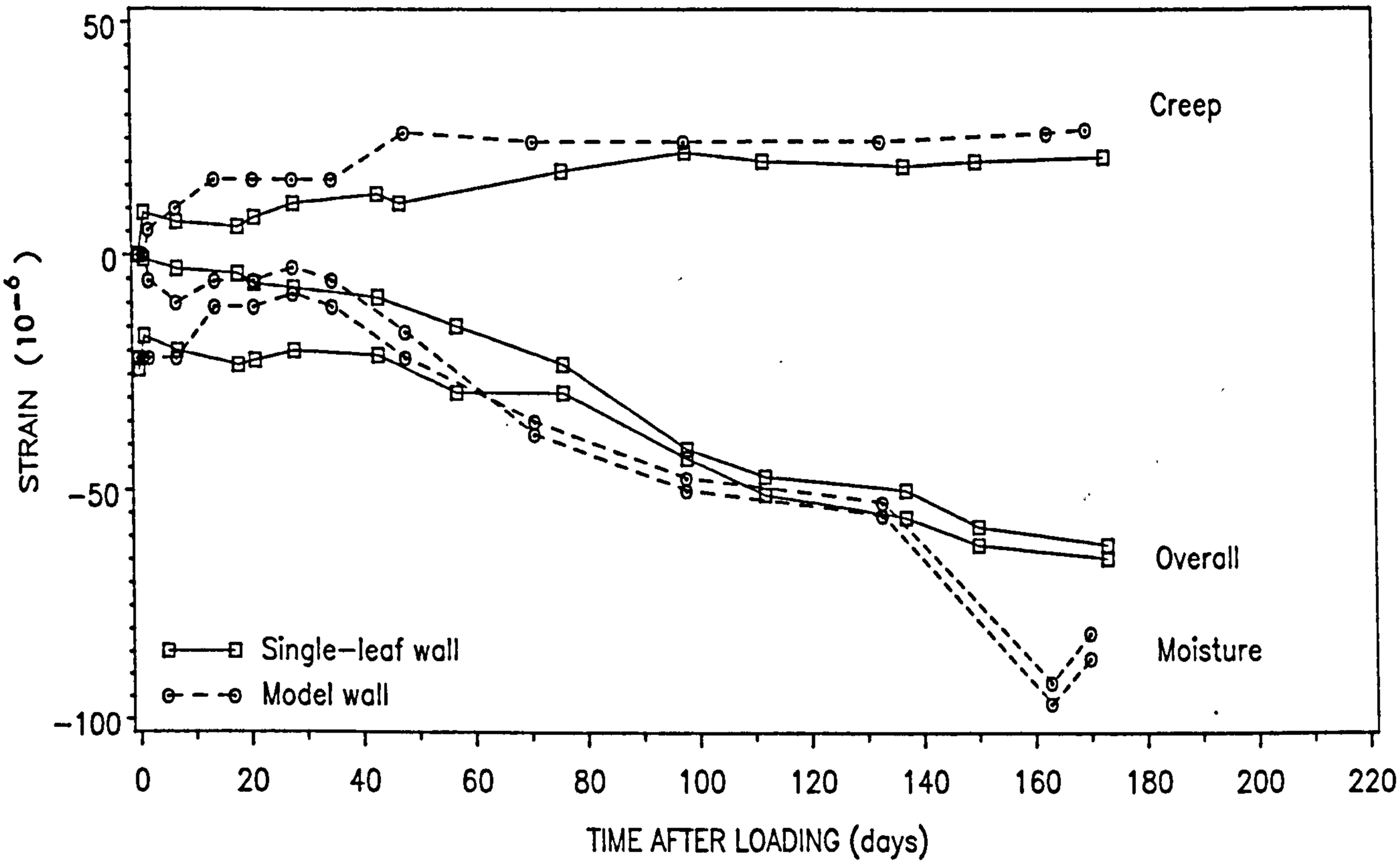

Fig. 6.20(a) – Comparison of the Lateral Strain–time Curves of the Model and Full Size Clay Brickwork with V/S = 44

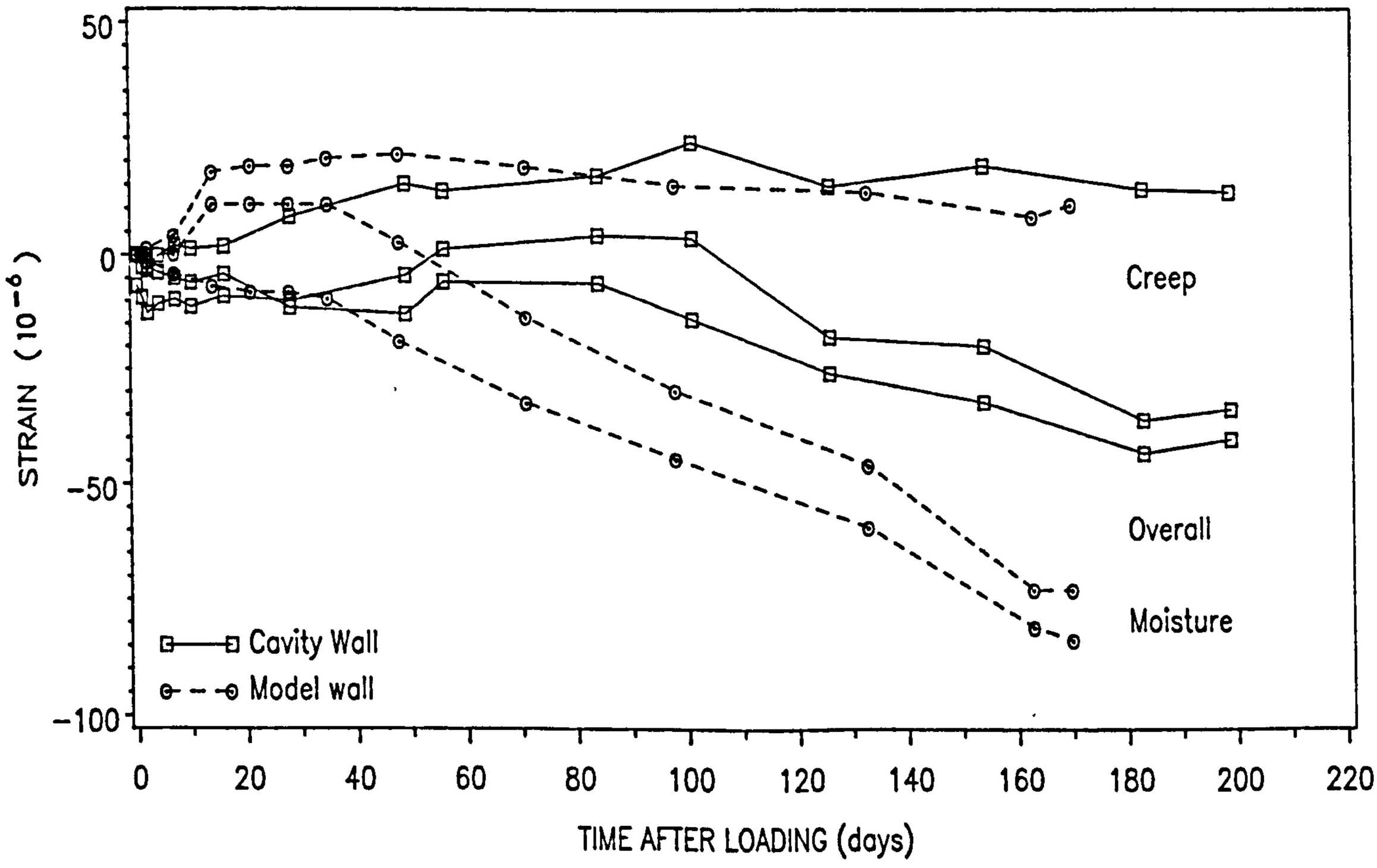

Fig. 6.20(b) – Comparison of the Lateral Strain–time Curves of the Model and Full Size Clay Brickwork with V/S = 51

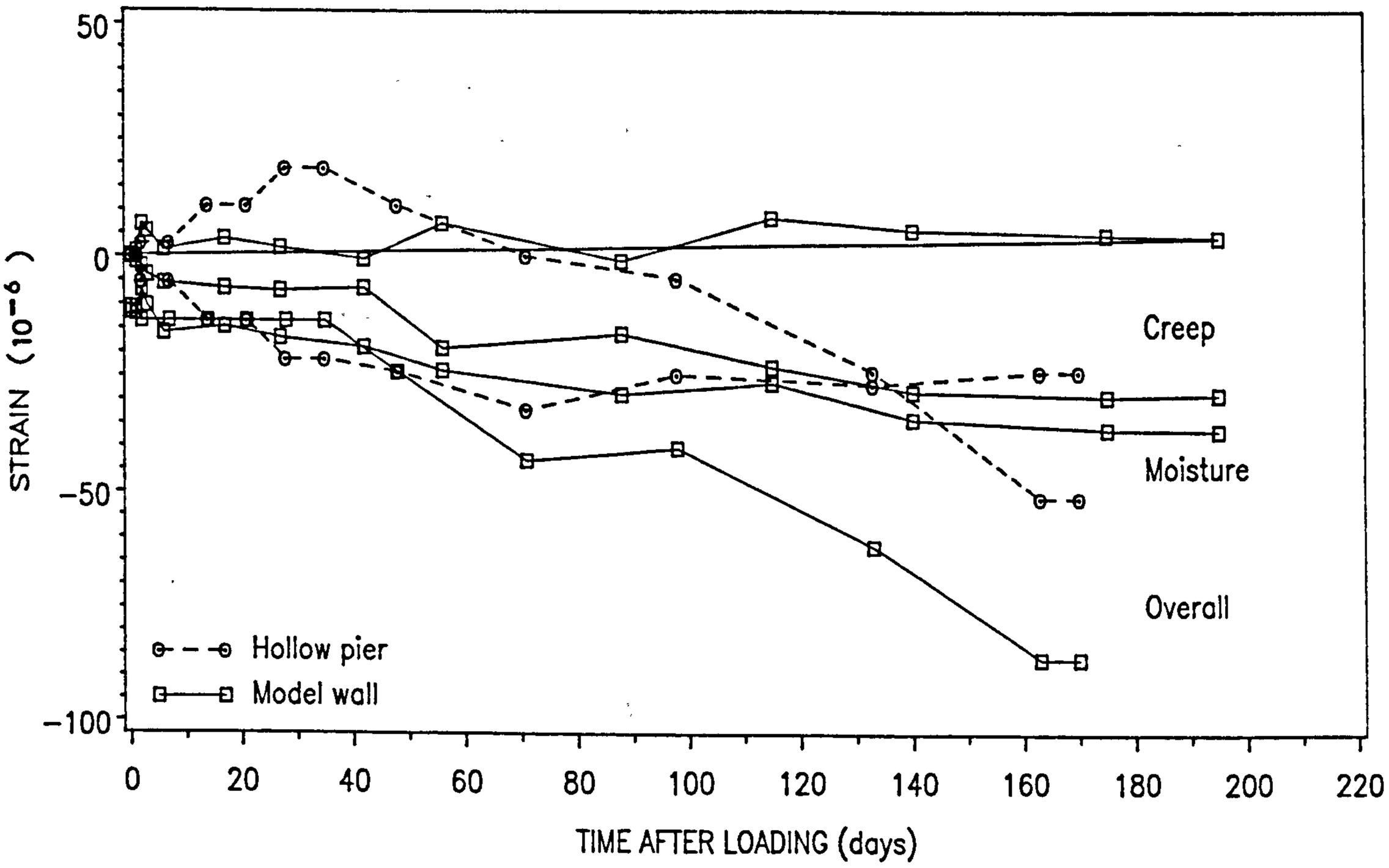

Fig. 6.20(c) – Comparison of the Lateral Strain–time Curves of the Model and Full Size Clay Brickwork with V/S = 78

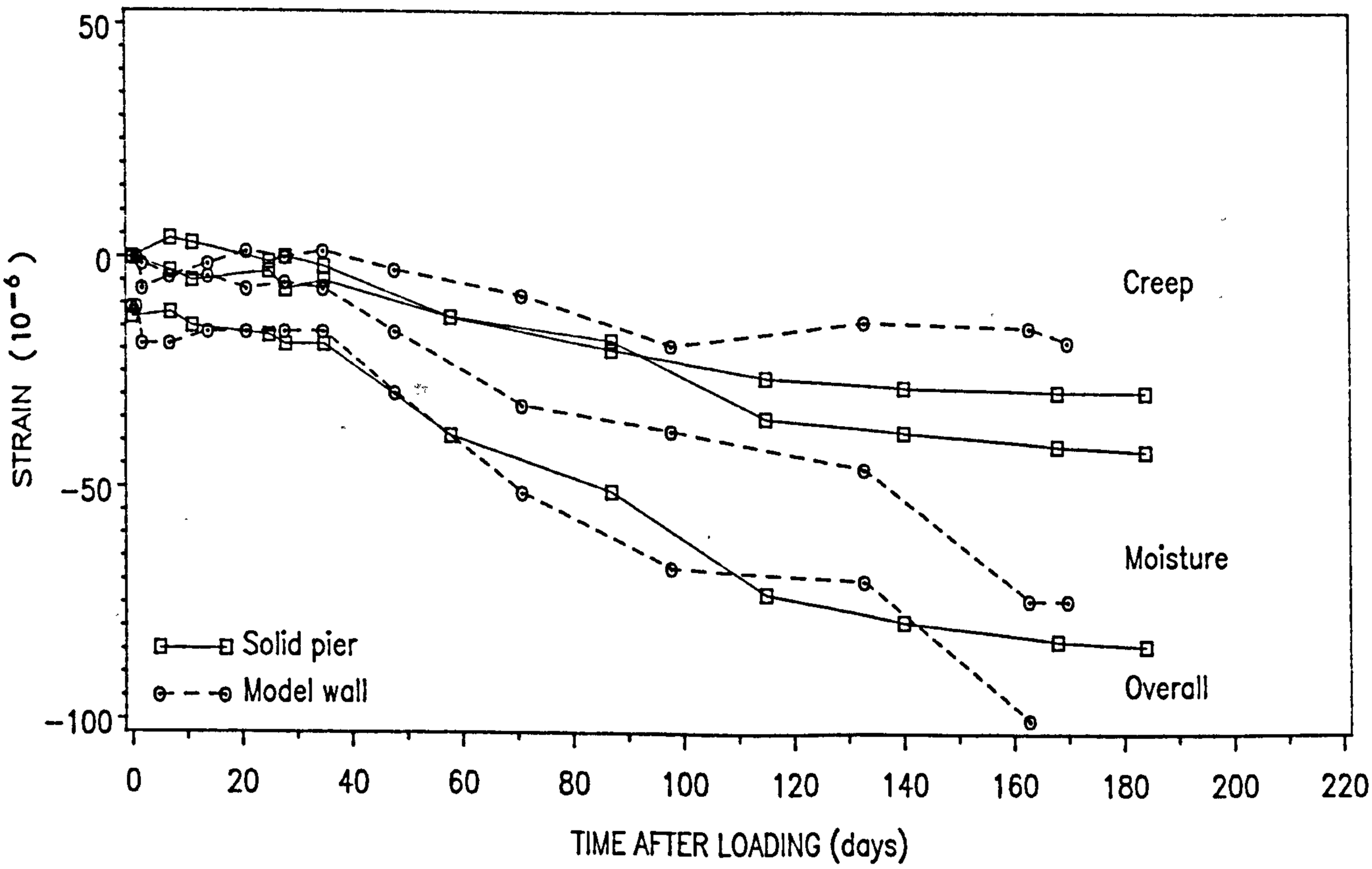

Fig. 6.20(d) – Comparison of the Lateral Strain–time Curves of the Model and Full Size Clay Brickwork with V/S = 112

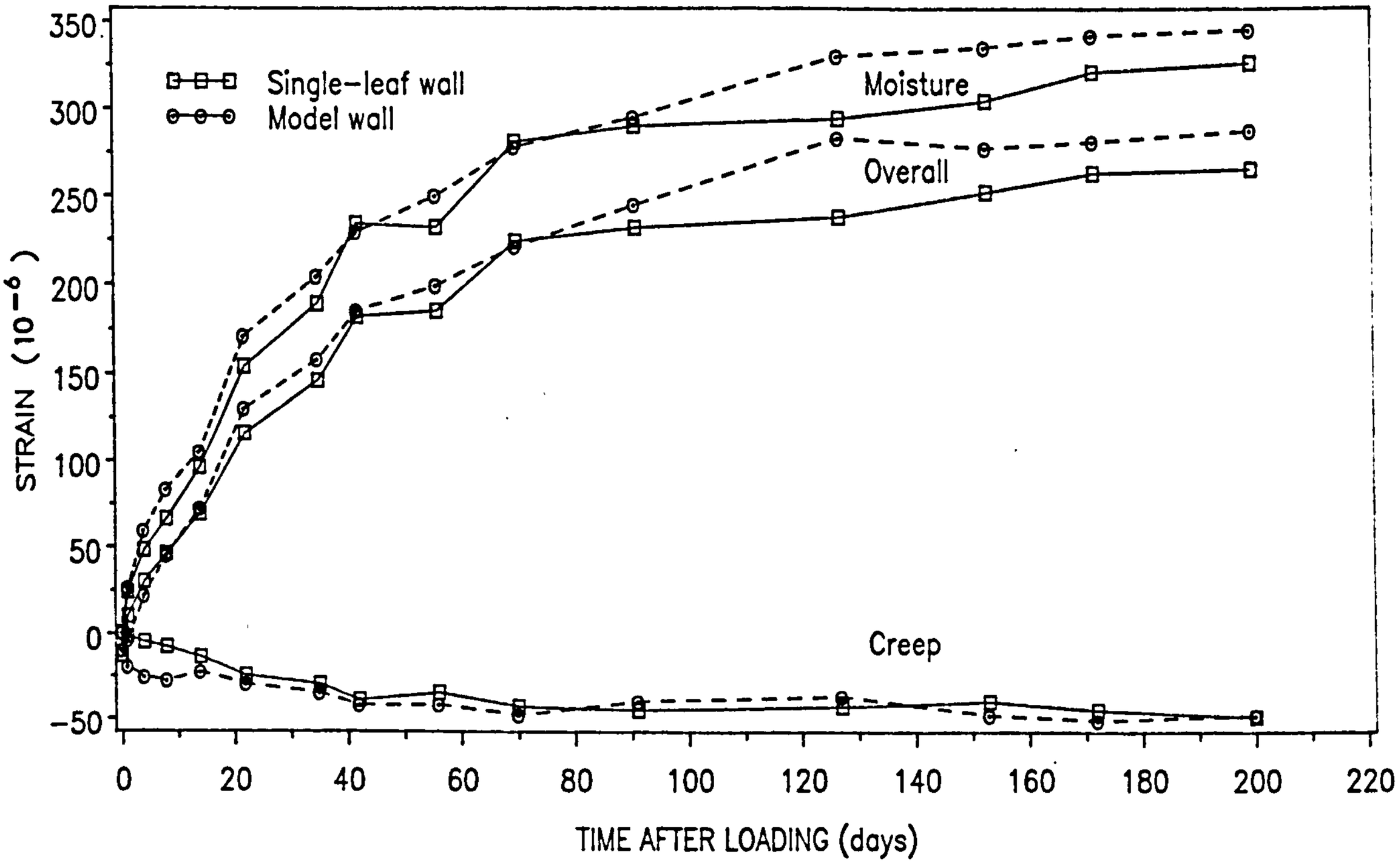

Fig. 6.21(a) – Comparison of the Lateral Strain–time Curves of the Model and Full Size Calcium Silicate Brickwork with V/S = 44

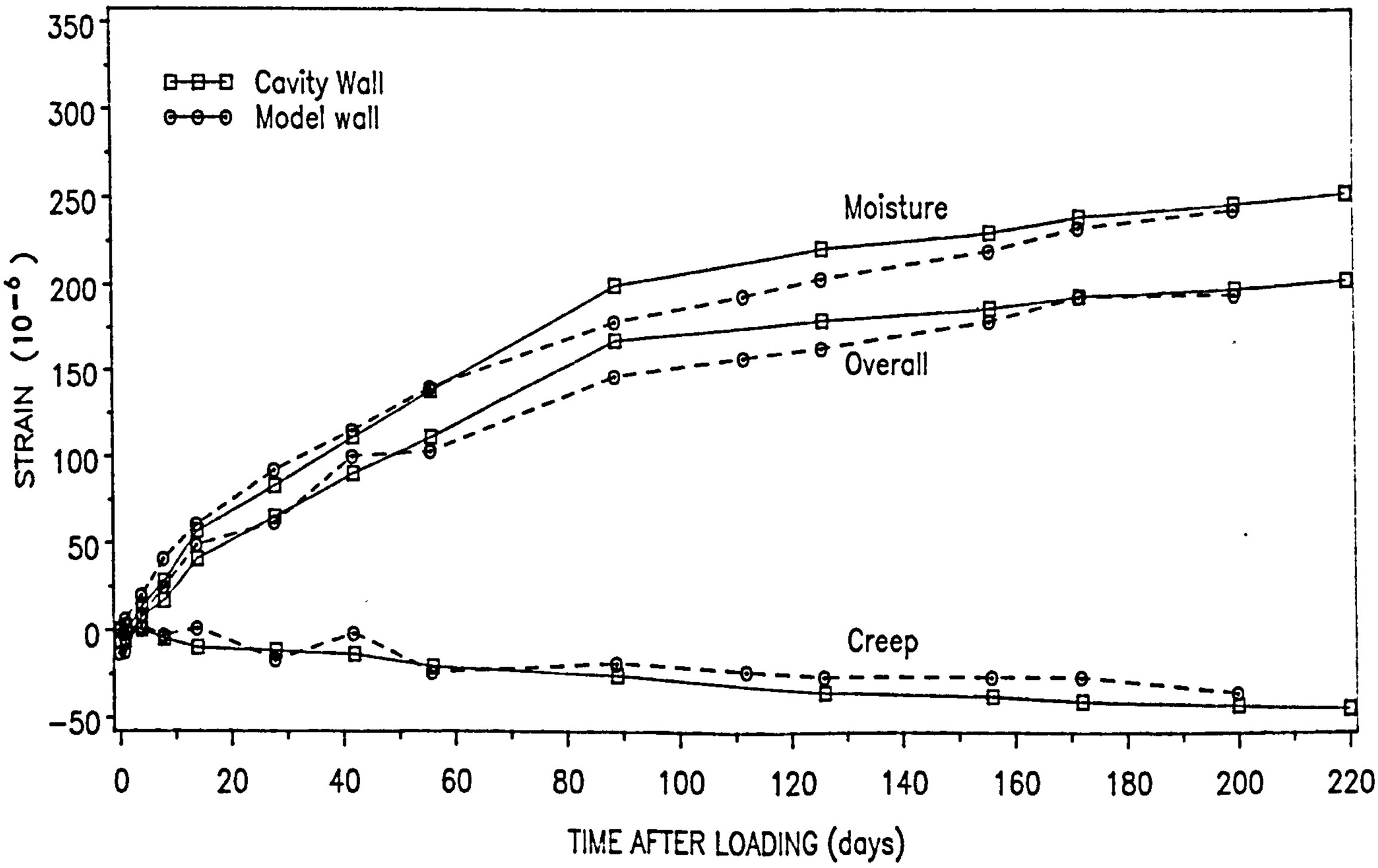

Fig. 6.21(b) – Comparison of the Lateral Strain–time Curves of the Model and Full Size Calcium Silicate Brickwork with V/S = 51

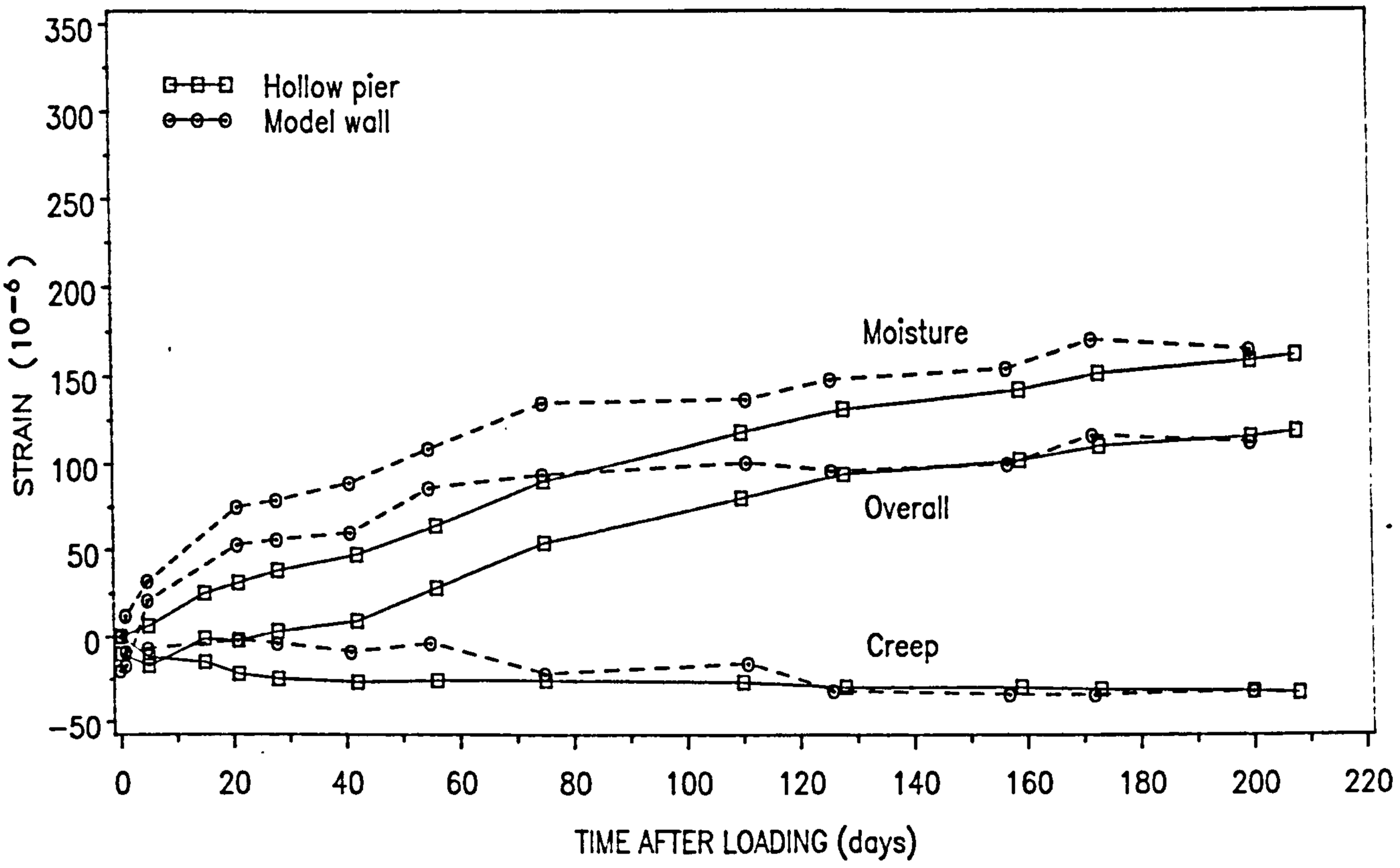

Fig. 6.21(c) – Comparison of the Lateral Strain–time Curves of the Model and Full Size Calcium Silicate Brickwork with V/S = 78

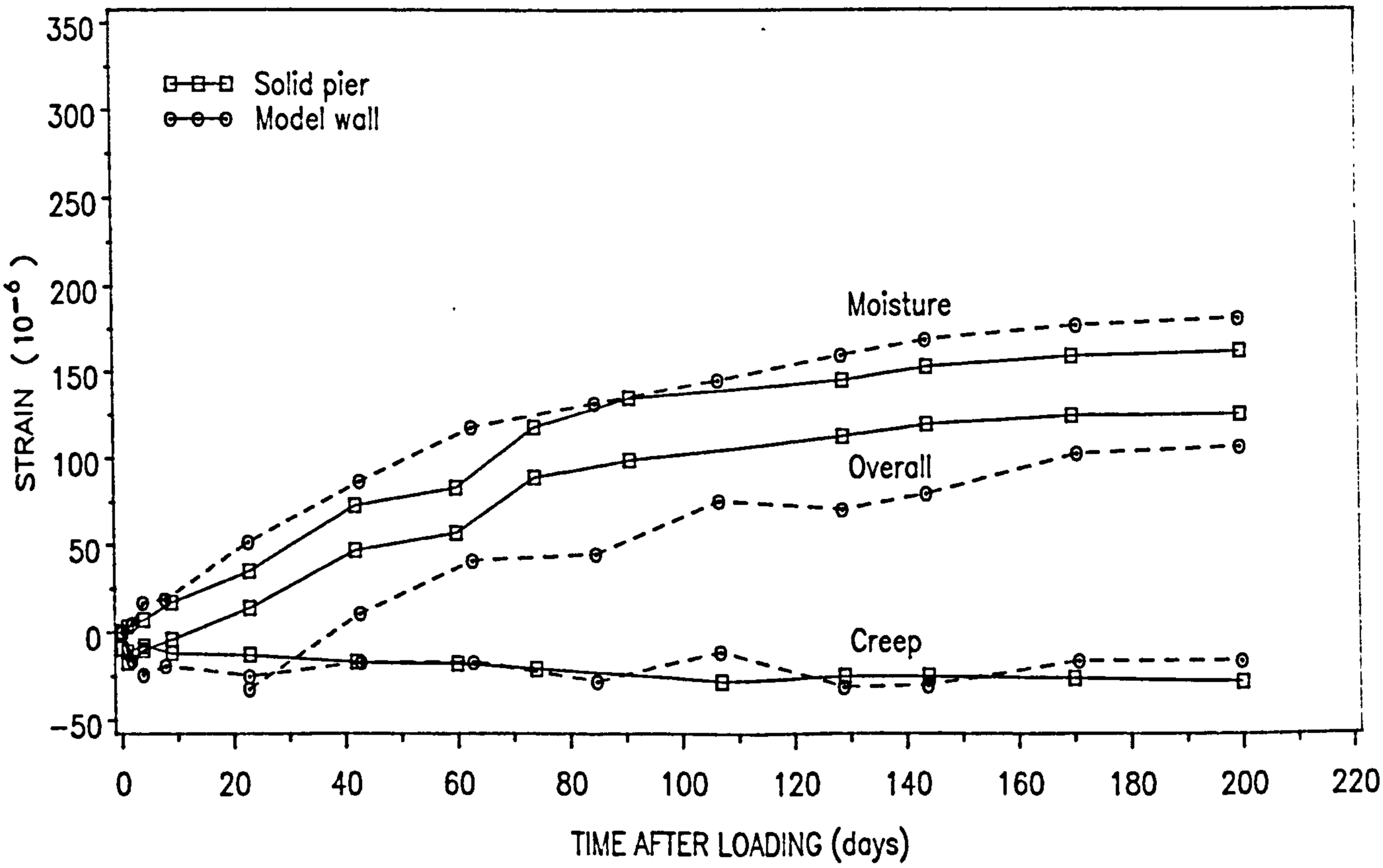

Fig. 6.21(d) – Comparison of the Lateral Strain–time Curves of the Model and Full Size Calcium Silicate Brickwork with V/S = 112

PLATE 9

Comparison of Frog-up (left) and Frog-down (right) Construction Showing the Mortar Bed Joints

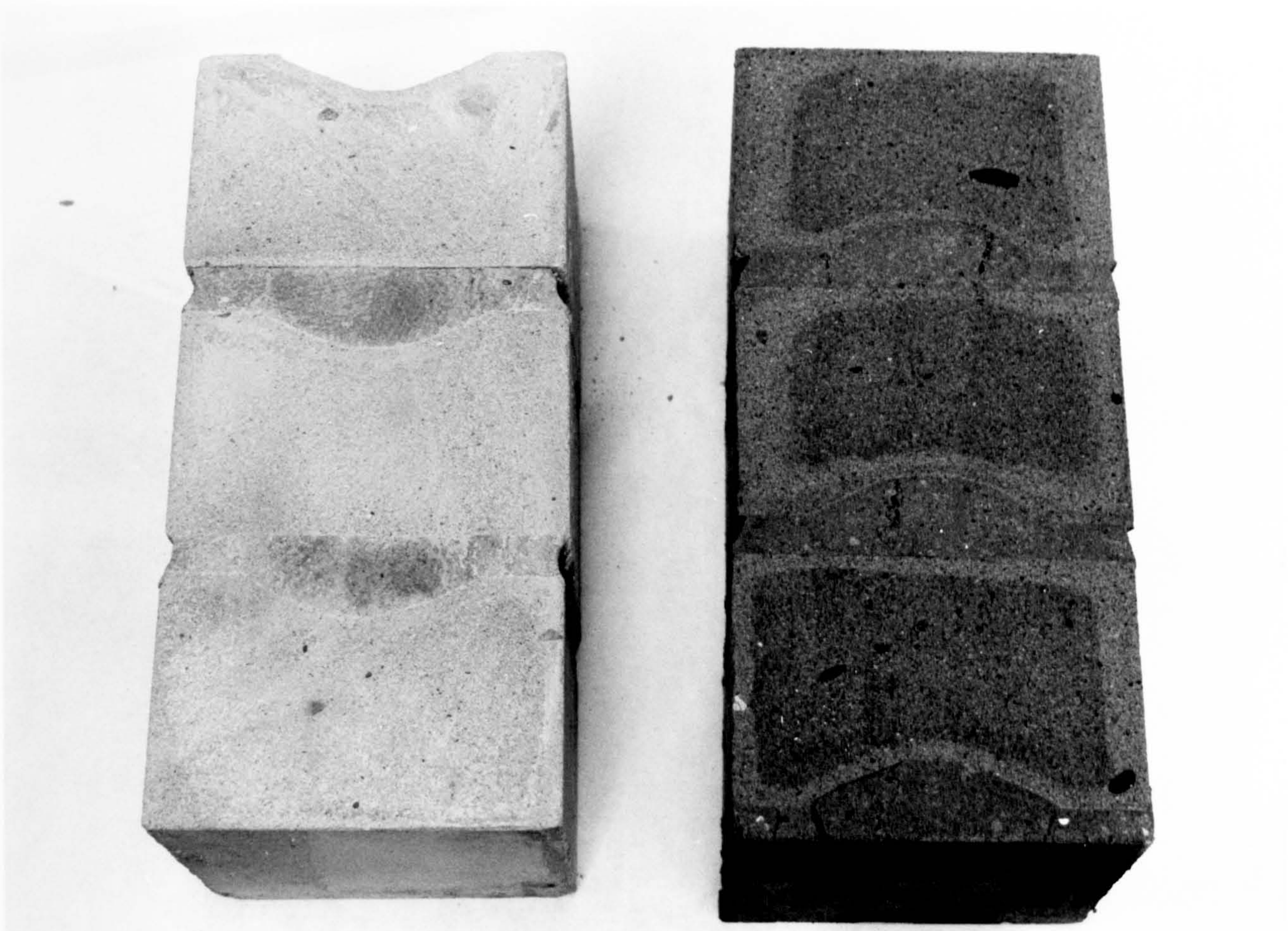

PLATE 9

CHAPTER 7

PREDICTION OF DEFORMATIONS USING COMPOSITE MODELS

7.1 Introduction

Before incorporating the relevant parameters into the composite models, the test results on mortar and units are first presented and discussed. The predicted masonry strains are then compared with the experimentally determined results presented in Chapter 6.

7.2 Mortar

7.2.1 Compressive strength

The results of 75mm mortar cube compressive strength tests are given in Table 7.1. The 28-day strength was 6.5±0.71, 7.3±0.50 and 6.1±0.33 MPa for mortar mixes used in clay, calcium silicate and concrete masonry, respectively. The results were within the limit of mortar designation (ii) as given in BS 5628[46].

7.2.2 Modulus of elasticity

The modulus of elasticity of 75 x 75 x 200 mm mortar prisms measured from the creep specimens (average of two specimen per V/S ratio) and from the static modulus tests (average of 6 specimens) are given in Table 7.2 . Evidently, the sealing of specimens have no influence on the modulus of elasticity of mortar.

Except for calcium silicate brickwork mortar, the static moduli were generally higher than the secant moduli obtained from the creep specimens, mainly due to elimination of creep and faster time taken by the former method. When using Eq.(2.1), the predicted tangent moduli were 6.5, 7.3 and 6.1 GPa for clay brickwork, calcium silicate brickwork and concrete blockwork mortars, respectively. The levels of elastic modulus in the present investigation were lower, possibly because of the finer grade sand used as illustrated in Fig. 5.1.

7.2.3 Creep

Creep measurements on the 75 x 75 x 200 mm mortar prisms were made using 150mm Demec gauges. Figure 7.1(a)-(d) show the creep-time curves of the different batches of mortar used in the three different types of masonry; for each V/S ratio the results were the average of two specimens. It can be seen that sealing, and thus the V/S ratio, had a substantial influence on both the level and rate of creep of mortar. The depletion of rate of creep started at earlier periods but at higher level of creep for mortar with a lower V/S ratio, and as the V/S ratio increased the change of creep rate became more gradual.

The creep curves for each masonry mortar were more or less similar in shape except for the mortar with V/S ratios of 44mm and 51mm used in the clay brickwork. The level of mortar creep reduced in the order: concrete, clay brick and calcium silicate masonry, particularly at early periods. The differences can be related to the strength of the mortar, where lower strength mortar resulted in higher creep.

The values of ultimate creep were determined as for masonry and high correlation coefficients were obtained. The results were then compared with the average V/S ratio applicable to concrete[27-29] on the basis of ultimate creep to that having a V/S ratio of 44 mm, as given in Fig. 7.2, which shows a reasonable agreement although generally creep of mortar shows a greater influence of V/S ratio. When presented in terms of strain ratio (S_R), the mortar yields average values of 6.8, 6.9, 5.5 and 5.2 for V/S ratios of 44, 51, 78 and 112, respectively. A similarly high value of 7.3 has been reported by Ameny[36] for N mortars for 1 year creep. He attributed this as a high 'strain collapse' which was not caused by failure but due to possibly a significant structural disruption. The mechanism of mortar creep is expected to be the same as for concrete.

7.2.4 Shrinkage

Shrinkage was measured on the unloaded specimens with 150 mm Demec gauge at the same positions as the creep specimens. No measurements were made across the narrow faces (between bed faces) since, for the creep specimens, the similar measurement was not possible using the 50 mm Demec gauge in the creep rig as the gap between the legs of the creep rig was too small for the gauge to be positioned. However, it has been shown by Brooks[41] that the difference of shrinkage between the two directions was very small. The shrinkage-time curves for masonry mortars are also shown in Figs. 7.1(a)-(d). The shrinkage strains were substantially lower than the creep strain which was mainly due to pre-drying of the specimens before measurements were made at 28 days. It was originally intended to start taking shrinkage measurements as early as one day after laying for all tests units, but due to the enormous amount of work for other preparations, for example, sealing of specimens, measurements had to be started only 28 days after laying i.e. at the age of loading.

As for creep, sealing showed a similar influence on shrinkage of mortar. There was similarity in the shape of curves for the different masonry mortars having the same V/S ratio, except for a small variation for the clay brickwork mortar with V/S ratios of 44 mm and 51 mm. These observations suggest a reasonable consistency between the different batches of mortar used.

The trend of ultimate shrinkage, extrapolated from the hyperbolic shrinkage-time relationship, with the average V/S ratio concrete[27-29] showed reasonable agreement as illustrated in Fig. 7.3. It follows that partial sealing of specimens can confidently be used to simulate the shrinkage of mortar in terms of the V/S ratio, in a similar manner to concrete.

7.3 Brick and block units

7.3.1 Strength

a) Clay brick

The results of the compressive strength tests for the clay bricks are given in Table 7.3. The strength tested between bed faces according to BS 3921[115] was 93.7 MPa and the compressive strength tested between header faces was 14.3 MPa. The average ratio of bed to header face strength was 6.5 which reflects the influence of the perforations and the height/width ratio. The tests between bed faces showed failure by crushing, whilst between header faces the failure was due to a single crack occurring in the direction of the load and across the perforations. The degree of anisotropy obtained from core specimens was significant; a behaviour commonly found in clay bricks by virtue of the extrusion process[137,142].

b) Calcium silicate brick

The compressive strength as tested according to BS 187:1978[116] was 25.7 MPa and 25.4 MPa for frog-filled and unfilled (using net area), respectively. The strength when tested between header faces was 20.1 MPa which reflects the presence of the frog and the influence of height/width ratio. From the results of the core specimens, calcium silicate bricks strength showed an almost isotropic character. The test results are also given in Table 7.3.

c) Concrete block

The compressive strength tests results on 100 x 100 x 200 prisms cut from the blocks and from standard tests as described in BS 6073[117] are given in Table 7.3. The strength ratio of prisms cut through header face to that through bed face was found to be 0.95, indicating that the strength of the concrete blocks was almost isotropic. There was no significant difference between the level of strength

as measured from the cut units and that from the standard test. The finding is encouraging since prism strength can be related to the standard tests which means a reduction in the cost of testing bulky specimens in a massive testing machine.

7.3.2 Modulus of elasticity

a) Clay Brick

Data on modulus of elasticity of clay bricks are given in Table 7.4. Between bed faces, the static modulus of a full brick was similar for the arrangements: single brick and three-stack, the average value of 34.2 GPa being that for single brick tests. The average ratio of header face to bed face static modulus (E_{bx}/E_{by}) for the full brick units was 0.52. The results of the core tests indicated an anisotropy of modulus without the perforations; the ratio of header to bed face being 0.88. Table 7.5 shows the secant modulus of the units measured from the creep specimens, i.e. corresponding to the initial elastic strain after the application of load; the average value being 20.0±1.7. It can be seen that there was no influence of V/S ratio on the secant modulus of clay brick.

b) Calcium silicate brick

The modulus of elasticity of the calcium silicate brick as obtained by the various techniques are given in Table 7.4. The ratio of header face modulus to bed face modulus (E_{bx}/E_{by}) was 0.89 and 0.93, as measured on single units and on brick cores, respectively, and thus the ratios indicated that calcium silicate bricks are more isotropic than perforated wire-cut clay bricks. The secant modulus of elasticity of units between header faces as shown in Table 7.6 was not influenced by the V/S ratio, the average value being 12.3 ± 1.4 GPa.

c) Concrete block

The results of modulus tests on 100 x 100 x 200 mm prisms cut from concrete blocks are given in Table 7.4. For the concrete block, prisms were cut instead of 25 diameter cores because of the rougher texture (due to coarser aggregate) than in the case of the clay and calcium silicate bricks.

The ratio of header face modulus to bed face modulus was 0.96 indicating the isotropic characteristic of concrete block. Approximately the same ratio was observed by Brooks and Amjad[68]. The secant modulus obtained from the creep specimens loaded between header faces is given in Table 7.5; the average value was 11.1±1.5 GPa. As for mortar, clay and calcium silicate bricks, the V/S ratio had no influence on the modulus of elasticity of the concrete block.

Generally, there was a larger variability of modulus of the clay brick than of calcium silicate brick, which in turn were more variable than concrete block.

7.3.3 Poisson's ratio

The values Poisson's ratio (μ) as obtained from tests method (i) and (ii) [see Section 5.3.3 (a)] are shown in Table 7.6. The values were calculated at a stress of 1.5 MPa. Although the variability is large it can be assumed that the Poisson's ratio of clay and calcium silicate bricks as 0.10 and 0.15, respectively. For the concrete block, an average of 0.12 was obtained, which was slightly lower than that normally found for other concrete product (of about 0.15 to 0.20) probably because of the platen effect.

7.3.4 Creep

For the clay and calcium silicate bricks, creep was based on the average of two units for each V/S ratio, while for the concrete block creep was from one unit only. The tests for the concrete block were conducted on the creep-rigs that were used

for the brickwork model wall tests. Initially, pairs of concrete bricks (100 x 65 x 215 mm bricks cut from the block units) were tested in similar manner as for the clay and calcium silicate bricks, but the results were misleading since during the cutting process water was used. Even though the creep was quite similar to that obtained on the whole unit, shrinkage was much higher and hence, such results were not representative.

a) Clay brick

The creep-time curves for clay bricks with different V/S ratios are shown in Fig. 7.4. The level of creep are very small, the six-month values being between 30 and 40 x 10^{-6}, and there was no obvious trend on the effect of V/S ratio on creep. The reason was that the applied stress of 1.5 MPa was equivalent to a very low stress/strength ratio (1.6%).

b) Calcium silicate Brick

The creep-time curves for part-sealed calcium silicate units are presented in Fig. 7.6. Generally, creep is less for a higher V/S ratio, the magnitude of creep being significantly greater than creep in clay bricks. The ultimate specific creep in the order of ascending V/S ratio was 123, 105, 104 and 93 x 10^{-6} per MPa, respectively; these values was generally similar to that measured by Brooks[23] (122 x 10^{-6} per MPa) for a solid and unsealed unit.

c) Concrete block

The creep results for part-sealed concrete blocks loaded between headers are shown in Fig. 7.8 which indicates a similar influence of V/S ratio on creep as for the calcium silicate brick. The level of creep was generally higher than that for calcium silicate bricks.

The relative ultimate creep as given by the hyperbolic-time expression is compared with the average data from concrete technology[27-29] in Fig. 7.10, which shows a greater influence on creep of bricks and block units by the V/S ratio.

7.3.5 Moisture strain

a) Clay Brick

Figure 7.5 shows that the clay bricks exhibited a small moisture expansion between header faces but there was no clear influence of the V/S ratio on the moisture expansion; the 200-day values were between 10 and 30 x 10^{-6}.

b) Calcium silicate brick

Calcium silicate bricks exhibited shrinkage and its development, as measured between the header faces of the part-sealed units over a period of about 200 days, is shown in Fig. 7.7. Generally, shrinkage was less for a higher V/S ratio though the difference was not significant. Initially, measurements were also made between bed faces to investigate the anisotropic character of the brick, but the attempt was terminated after few measurement, because either the Demec points fell off or the Demec readings were inconsistent. This problem was caused by attaching the Demec points to the specimens after painting and sealing. Also, the 50mm Demec gauge was too insensitive (1 div. = 19.9 x 10^{-6}) to monitor small changes in shrinkage.

c) Concrete block

The shrinkage data for concrete blocks, as measured between header faces and bed faces, are shown in Fig. 7.9; both directions show an influence of V/S ratio. There was no significant difference in shrinkage between both faces. The level of shrinkage was generally higher than for calcium silicate bricks and it would seem that the blocks were newly manufactured when laid.

When compared with concrete[27-29] (Fig. 7.11), as for creep, the present data for shrinkage showed a greater influence with the V/S ratio for lower values but a smaller influence for higher values.

7.4 Application of the composite models

To obtain the necessary parameters the following were taken into account:

7.4.1 Anisotropy of brick

For creep, adjustments were required to allow for the anisotropy of the bricks, since they were tested between headers whereas the models required creep between bed faces. The adjustment assumed that creep is proportional to the initial elastic strain. Results from the cored specimens gave the anisotropy of the brick without taking into account of the shape and the presence of perforations and frog. Hence, it was more appropriate use the results from a single unit, which yielded factors of 0.52 and 0.89, i.e. the ratio of header to bed face modulus (E_{bx}/E_{by}), for clay and calcium silicate bricks, respectively. The values of brick creep (c_{bx}) could then be multiplied by the appropriate factor to obtain the values of c_{by}. A similar adjustment was not required for the concrete block since tests indicated that it was isotropic.

For the brick units, the moisture movement between header faces was assumed to be equal to that between bed faces. For the clay brick this assumption would seem to be reasonable because of the small expansion, but for the calcium silicate brick, Brooks[41] reported that the difference in shrinkage between bed faces was about 15% lower than between header faces for unsealed units. This assumption was made since no data were obtained for the reason given in Section 7.2.4. In the case of the concrete block, this problem did not arise since measurements were also made between bed faces.

No adjustments were made for creep and shrinkage of mortar so that it was assumed that the time-dependent deformations were similar between both directions. This was thought to be a reasonable assumption since there are both vertical (stretcher face and header face joints) and horizontal (bed) joints in the masonry and even if the mortar was anisotropic, the assumption of isotropy would approximate to the practical situation.

7.4.2 Volume to surface area ratio

It may be recalled that Brooks[39] adjusted his time-dependent deformations to allow for the effect of the V/S ratio. Ameny et al[38] also found an empirical adjustment necessary in order for their model to predict creep. However, in this investigation, no adjustment was necessary since, both mortar and units were partly-sealed to have a similar V/S ratio to the respective mortar joints and units in the corresponding walls or piers.

7.5 Prediction of deformation

The results of the individual units and the corresponding mortar prisms were incorporated in the relevant equations derived from the composite model theory to yield predictions of modulus of elasticity, creep and shrinkage of masonry. The parameters for each geometry and type of masonry with the corresponding calculations are detailed in Appendix C. As no experiment subjecting masonry to lateral loading was carried out, experimental verification for composite model of Fig. 4.6 (Eq.(4.37)) is not given. The predictions using the various composite models are discussed below:

7.5.1 Modulus of elasticity (E_{wy})

As the modulus of mortar and brick/block units were found to be independent of the V/S ratio, the average value for each masonry type are considered

rather than the individually measured results. The predicted modulus of elasticity of masonry (E_{wy}) using Eq. (4.24) are compared with the measured value are given in Table 7.7.

The predicted and the measured moduli of clay brickwork are in general agreement, with the average predicted modulus being about 9% lower than the average measured modulus. However, in the case of calcium silicate bricks laid 'frog-down', the predicted modulus is overestimated by about 70% probably because of entrapped air voids in the frog cavity; when the load was applied, the air voids would be compressed and thus causing an additional strain and yielding a lower elastic modulus. Brooks and Amjad[68], who tested similar bricks, reported that the prediction was good up to a stress of 2 MPa, but at higher stresses the 'frog-down' stress strain curve became non-linear due to excessive strain. The slower rate of load application at the beginning of the present test could have caused the voids and cracks in the frog mortar to close at a lower stress of 1.5 MPa. Brooks and Amjad[68] have shown reasonable accuracy of prediction on calcium silicate bricks laid 'frog-up' and also, earlier, Brooks[39] showed that the composite model works reasonably well to predict the elastic strain of single-leaf wall constructed from 'frog-up' Fletton bricks.

There was no significant difference between the predicted and the measured moduli of concrete blockwork. Due to a lower number of mortar joints the modulus of blockwork tended to the value of modulus of the block units. It seems that the composite models give a more accurate prediction for masonry built from solid units than those from perforated and frogged units. The variation of modulus of the individual units would also influence the accuracy of the prediction.

7.5.2 Vertical creep (c_{wy})

The predicted creep-time characteristics using Eqs. (4.24), (4.38a), (4.39) and (4.40a) are compared with the experimentally determined data in Figs. 7.12, 7.14 and 7.16. Since creep of the clay bricks is very small, a single curve, shown in Fig.

7.4, was used to predict the creep of all the four different geometries of clay brickwork. Overall, the accuracy of creep prediction for clay brickwork was within 10% of the measured value; for the single-leaf and cavity walls, particularly at later periods, there were slight over-estimations, and for the hollow and solid piers there were slight under-estimations. The creep the mortar significantly dominates the creep behaviour of the clay brickwork.

For all types of calcium silicate brickwork the prediction was within 15% of the measured creep, the highest variation being for the single-leaf wall. Hence the model seems appropriate for bricks laid 'frog-down'. The problem arising from the frog-down construction with prediction of modulus does not appear to have a similar effect in the measurement of creep. The reason was thought to be due to the closure of the air voids and cavities after the initial application of load which then resulted in proper contact between mortar and unit, thus spreading the load through the brickwork. Plate 9 shows a typical section cut from the brickwork which illustrates that the frog was fully filled with mortar and cracks on 'air voids' are hardly visible. In this connection, the finding of Brooks and Amjad[68] is relevant. They showed that the compressive strength of calcium silicate brickwork for bricks laid 'frog-down' was not significant different from that laid 'frog-up', so that there was no apparent weakness due to the presence of trapped voids or cracks. It should also be noted that in the computation of the composite model the thickness of mortar (m_y) was taken as 15 mm to allow for the additional thickness of mortar in the frog of 4 mm average.

Better creep predictions were obtained for concrete blockwork, being within than 8% of the measured values. The creep-time behaviour follows a similar shape to the individual block units due to the units having relatively higher creep as compared to the bricks, and also due to the influence of the block height to mortar bed thickness ratio (b_y/m_y).

It can also be seen that, for all cases, partial sealing of individual units and mortar, quantified in terms of the V/S ratio, successfully simulates the geometry effect on creep of masonry. Generally, the level of accuracy of prediction using the composite model are better for the straight forward solid units than for the more complex perforated and frogged units.

7.5.3 Vertical moisture movement ($S_{w,y}$)

The comparisons of measured vertical moisture movement of various geometries with that predicted by the composite model using Eq.(4.48) for clay, calcium silicate and concrete masonry are shown in Figs. 7.13, 7.15 and 7.17, respectively.

The accuracy of prediction for shrinkage of clay brickwork was within 20%, most of the predictions being higher than the measured shrinkage. There are three possible explanations for a lower measured shrinkage. Firstly, the embedded units could have undergone a higher expansion than the part-sealed individual units because of a brick/mortar interaction, but this was not proved since the moisture expansion measured on separate units which was covered with mortar on the bed faces (Appendix A) was similar to that of the part-sealed units. Secondly, there could have been moisture expansion anisotropy of the brick units, but measurements on the centrally embedded unit did not reveal any evidence of anisotropy. Thirdly, there was the variability of moisture expansion of the embedded units, as illustrated in Fig. 7.5, which was only representative of eight bricks, whereas in the brickwork there were more units and the scatter of moisture expansion could have been much bigger.

The prediction of vertical shrinkage of calcium silicate brickwork gave a general over-estimation of 19% after 200 days, although the trend of shrinkage with geometry of masonry was correct. In this case, however, the unit shrinkage between bed faces was assumed to be equal to shrinkage between headers which may not be

the case, since, as stated earlier, a previous investigation[23] using solid units revealed a lower shrinkage of about 15% between bed faces. Hence, a similar allowance for shrinkage of the brick in the present investigation would yield a better prediction.

As for creep, the composite model gives a very satisfactory prediction of vertical shrinkage of concrete blockwork, viz. within 10%, except for the cavity wall being underestimated by about 15%. Again, this shows that the performance of masonry built from solid unit are predicted better than when built from the perforated and frogged units.

7.5.4 Horizontal moisture movement (S_{wx})

The predicted horizontal moisture strains using Eq.(4.61) for clay, calcium silicate and concrete masonry are shown in Figs. 7.18, 7.19 and 7.20, respectively. Due to the very low level and the insignificant influence of V/S ratio on moisture expansion of brick, a single curve, as shown in Fig. 7.5, was incorporated in the composite model.

The combination of mortar shrinkage and clay brick expansion in the composite model yielded brickwork shrinkage whereas, actually, the clay brickwork expanded. However, the level of predicted shrinkage was small as was the measured expansion.

On the other hand, the prediction of horizontal shrinkage of calcium silicate brickwork indicated a smaller influence of geometry than in the case of vertical shrinkage, but the observed horizontal shrinkage of the single leaf wall was underestimated by about 30% at 200 days (Fig. 7.19).

Good agreement was obtained between the predicted and measured horizontal shrinkage of concrete blockwork, the difference being less than 10% at 200 days and the trend of horizontal shrinkage with geometry of blockwork was also correct (Fig. 7.20).

As stated earlier, better predictions were obtained for solid units than for perforated and frogged units, in which case, the perforations and the frog might have provided an extra restraint to the horizontal movement. In general it should be noted that prediction of moisture movement, whether horizontally or vertically is more complex and is affected by the confinement of the joint by the unit and also the moisture suction of the bricks and therefore the effective moisture content of the mortar joints and the embedded units. It should be remembered that the composite model applies to an unrestrained condition which is difficult to simulate in practice.

7.6 Comparison with other models

The result of this investigation have been used to compare predictions by other relevant models. The comparison is discussed below:

7.6.1 Modulus of elasticity

The values predicted using the composite models of Jessop et al[31] (Eq.(4.2)) and Ameny[36] (Eq.(4.6)) are compared with the measured values of single-leaf walls in Table 7.7. Only these models are relevant here because they were based on running bond arrangement (stretcher bond) while the others were based on stack-bond arrangement. All the composite models give close estimates and, as reported by Brooks and Amjad[68], there was a general improvement in prediction using the composite model (Eq.(4.24)) in this investigation.

7.6.2 Creep

Most of the models as described in the literature review cannot be tested with the present data. The only model that is applicable is that by Ameny[36] (Eq.(4.9)). The models developed much earlier by Shrive and England[37] could not be considered because the publication lacks information on its application. In fact, Ameny's model

could only be applied to the single-leaf wall since the model only deals with stack or running bonded masonry, although there is possibility that the model can be expanded to cover a larger variation of masonry layout.

When the present data (from part-sealed specimens) were incorporated in Ameny's model, there was a slightly higher estimate than the present model for both creep and shrinkage of clay single leaf walls, as shown in Figs. 7.21 and 7.22, respectively. For calcium silicate Ameny's model gave a marginally lower value then the value from the present model, as illustrated in Figs. 7.23 and 7.24. As shown in Figs. 7.25 and 7.26, the present model provides better predictions than Ameny's model for the single-leaf concrete blockwork. In general, the use of Ameny's model with the V/S ratio influence of moisture diffusion yield similar predictions to the present models. This confirms that proper simulation of moisture diffusion of individual mortar and units with the respective mortar joints and embedded units are necessary to give a reasonably accurate prediction of the long-term deformation of masonry.

In order to relate the creep of mortar cylinder and individual blocks to the mortar joints and embedded blocks in the masonry, Ameny et al[38] used strain 'magnification factors' and in addition for mortar, he also used a prism to cylinder strength factor. For the mortar of his investigation, the product of the magnification factor and cylinder to strength factor yielded an average value of approximately 0.65. For blocks, their magnification factors were 1 and 2.2 for the combination of WF blocks with N mortar and BF blocks with N mortar, respectively at 200 days. Expressed in terms of V/S ratio, the mortar cylinder has a value of 18 mm compared to 44 mm for the mortar joint which from Fig. 7.2 gives a creep ratio (mortar joint creep/cylinder creep) of approximately 0.71 which is reasonably close to a factor of 0.65 used by Ameny. In contrast, for blocks (V/S = 36 mm for embedded and V/S = 9 mm for individual specimens), extrapolating from Fig. 7.10, yields a factor of approximately 0.5. It would be expected that the creep in block specimen would be higher than creep

in the embedded block. It should be pointed out that the level of creep measured by Ameny[36] on block specimens was very small (specific creep less than 25 x 10^{-6} per MPa for WF block and less than 10 x 10^{-6} per MPa for BF block) and that the results for WF blocks varied considerably. With similar level of creep for clay bricks in this investigation, it can be recalled that no correction was made. Thus, the correction factor of one for WF block obtained by Ameny et al[38] seems reasonable.

However, similar correction factors for shrinkage of mortar and block units were not given by Ameny[36] since the amount of shrinkage of masonry in his investigation was found to be insignificant, although he stated that there were indications that shrinkage in mortar joints to be 33-50% of those in the cylinder.

Using the models of this investigation and consideration of the rate of moisture diffusion of the insitu mortar and units in terms of V/S ratio (extrapolated from Fig. 7.2 and 7.10, respectively), with the test data of Ameny et al[38] have been analysed. The predicted elastic moduli and creep (only masonry with BF blocks are given for creep) are compared to their respective measured values in Table 7.8 and Fig. 7.27. It can be seen that there is a satisfactory prediction for both the short-term and long-term deformations. The 'secondary creep' due to variation of the relative humidity of the environment was also predicted by the composite model as long as the individual specimens and masonry are tested under similar environment. Brooks[141] had also demonstrated a satisfactory predictions using this model on the full data of Ameny et al[38] but using V/S factors from concrete technology[28-29].

7.7 Closing remarks

As a whole, the theoretical 'composite models developed by Brooks[41-42] yield expressions for both short-term and long-term deformations in any direction, and for any configuration of brickwork or blockwork. Satisfactory predictions have been obtained for vertical and horizontal movements of masonry constructed from clay bricks exhibiting moisture expansion, calcium silicate bricks and concrete blocks

exhibiting shrinkage. A representative sample of mortar and brick or block units should be tested to assess the range of properties and to assess the degree of anisotropy. The use of the parameter V/S ratio is more flexible to adjust creep and shrinkage for any type of bricks and can be used reasonably well with the existing composite models. The use of 'magnification factors' has not been found to be applicable to a much wider range of brick or block type. The verification of the present model using tests data of Ameny et al[38] has indicated that when deformation phases are adjusted according to V/S ratio, there is no need for empirical factors as proposed by the authors[38].

Table 7.1 - Compressive Strength of 75mm Mortar Cubes at 28 Days (MPa)

Mix No.	Clay Brickwork	Calcium Silicate Brickwork	Concrete Blockwork
1	6.4 6.9 7.5	7.2 7.7 7.6	6.0 5.5 6.6
2	7.8 5.8 6.0	7.6 7.9 7.3	5.9 6.3 6.2
3	6.3 5.7 6.0	6.6 7.1 6.3	-
Mean	6.5	7.3	6.1
Std. Dev.	0.71	0.50	0.33

Table 7.2 - Modulus of Elasticity of Mortar for Different Masonry

Masonry Type	Secant Modulus of Elasticity (GPa) for V/S Ratio:					Static Modulus (GPa)
	44 mm	51 mm	78 mm	112 mm	Mean	
Clay Brickwork	3.16	3.50	3.10	3.06	3.15	3.00
Calcium Silicate Brickwork	4.54	4.82	4.52	4.79	4.67	5.24
Concrete Blockwork	2.99	3.39	3.33	2.97	3.17	3.22

Table 7.3 - Strength (MPa) of Brick/Block Units

Units	Header Face		Bed Face		
	1-unit	core	1-unit		core
			full unit	frog filled	
Clay Brick	14.3 (1.6)	110.3 (13.1)	93.7 (6.8)	-	122.0 (15.3)
Calcium Silicate Brick	20.1 (1.4)	20.9 (2.1)	25.4* (2.5)	25.7 (1.8)	21.2 (1.6)
Concrete Block	-	13.1# (2.0)	13.0 (0.9)	-	13.8# (2.2)

* *based on net area*
\# *100 x 100 x 200 mm cut prisms*
( ) *standard deviation*

Table 7.4 - Modulus of Elasticity (GPa) of Clay Brick, Calcium Silicate Brick and Concrete Block

Units	Header Face			Bed Face		
	1-unit	3-stack	core	1-unit	3-stack	core
Clay Brick	17.8 (1.7)	-	27.7 (2.2)	34.2 (4.5)	28.6 (2.8)	31.4 (3.1)
Calcium Silicate Brick	10.4 (1.0)	-	11.1 (1.9)	11.7 (1.1)	12.5 (1.0)	11.9 (1.6)
Concrete Block	-	-	12.1* (0.4)	12.00 (0.8)	-	12.6* (1.2)

* *100 x 100 x 200 mm cut prisms*
( ) *standard deviation*

Table 7.5 - Secant Modulus of Elasticity (GPa) of Units as Obtained from Creep Specimens on Header Face.

Units	V/S Ratio: (mm)				
	44	51	78	112	Mean
Clay Brick	19.8	22.2	17.4	20.6	20.0
Calcium Silicate Brick	12.1	14.3	11.1	11.8	12.3
Concrete Block	10.3	10.0	10.3	13.7	11.1

Table 7.6 - Poisson's Ratio (μ) of Brick/Block Units

Units	1-unit between Bed-faces	3-Stack
Clay Brick	0.07 (0.04)	0.10 (0.07)
Calcium Silicate Brick	0.11 (0.03)	0.14 (0.03)
Concrete Block	0.13 (0.04)	-

Table 7.7 - Comparison of Measured and Predicted Modulus of Elasticity of Masonry using Composite Models

Type of Brick/block	Size of Masonry	Modulus of Elasticity (GPa)			
		Measured	Predicted		
			Eq.(4.24)	Jessop et al[31]	Ameny[36]
Clay	Single-leaf wall	11.8	13.1	13.84	12.94
	Cavity Wall	15.9	13.1	-	-
	Hollow Pier	14.8	13.0	-	-
	Solid Pier	14.5	12.7	-	-
Calcium Silicate	Single-leaf wall	5.0	8.8	9.03	8.7
	Cavity wall	5.1	8.7	-	-
	Hollow pier	5.5	8.7	-	-
	Solid pier	5.0	8.7	-	-
Concrete	Single-leaf Wall	9.9	10.2	10.54	10.33
	Cavity wall	9.2	9.9	-	-
	Hollow pier	9.7	9.6	-	-
	Solid pier	9.6	9.7	-	-

Table 7.8 - Comparison of Measured and Predicted Moduli of Elasticity Using Composite Model of this Investigation (Eq.(4.24)) on Data of Ameny et al[38].

Masonry Type (Mortar/Block)	Secant Modulus of Elasticity	
	Measured	Predicted (Eq.(4.24))
N/WF	4.8	5.0
M/WF	4.8	5.4
N/BF	5.1	5.2-7.8
M/BF	8.0	5.6-8.9

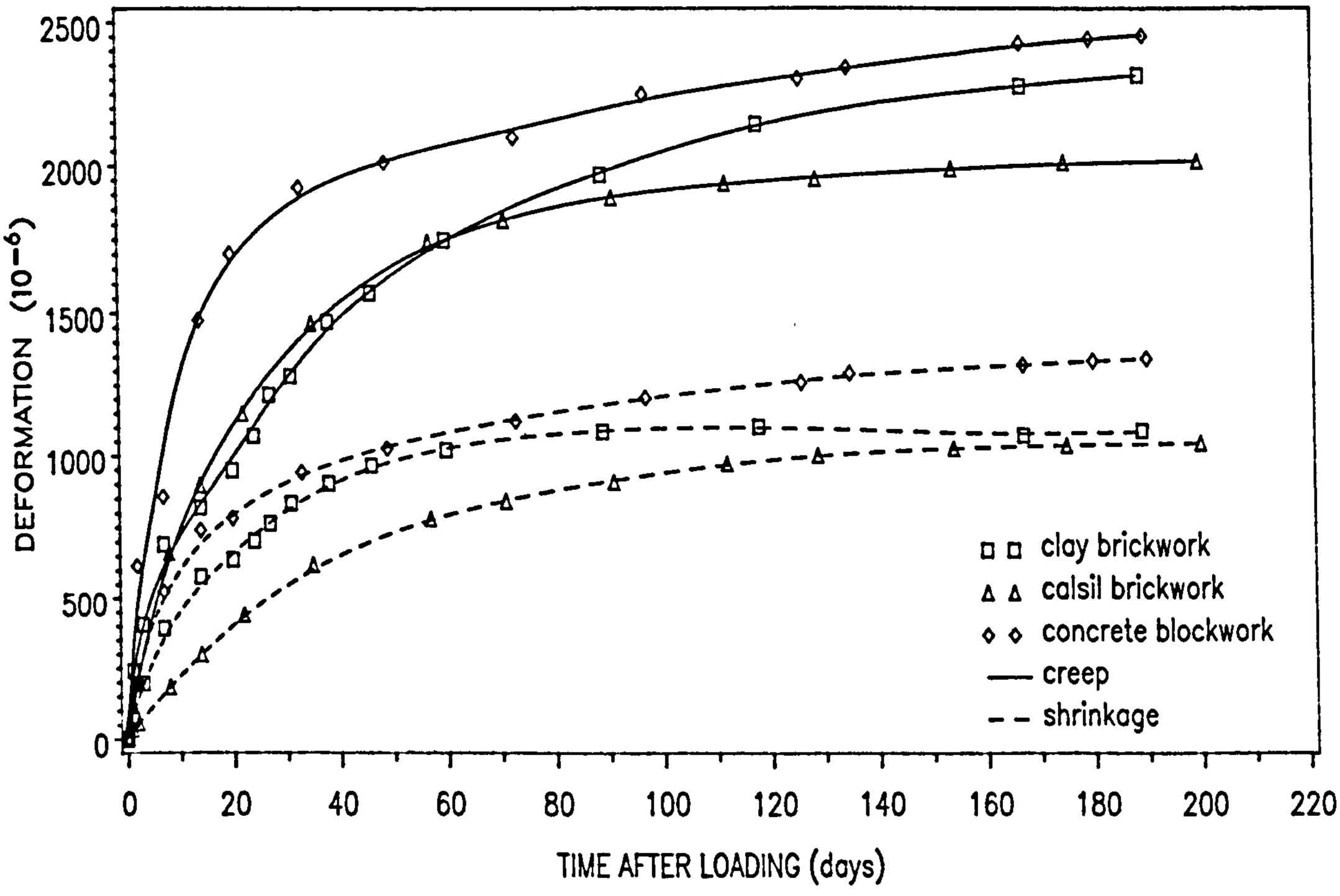

Fig. 7.1(a) – Creep and Shrinkage of Mortar for Different Types of Masonry with V/S = 44

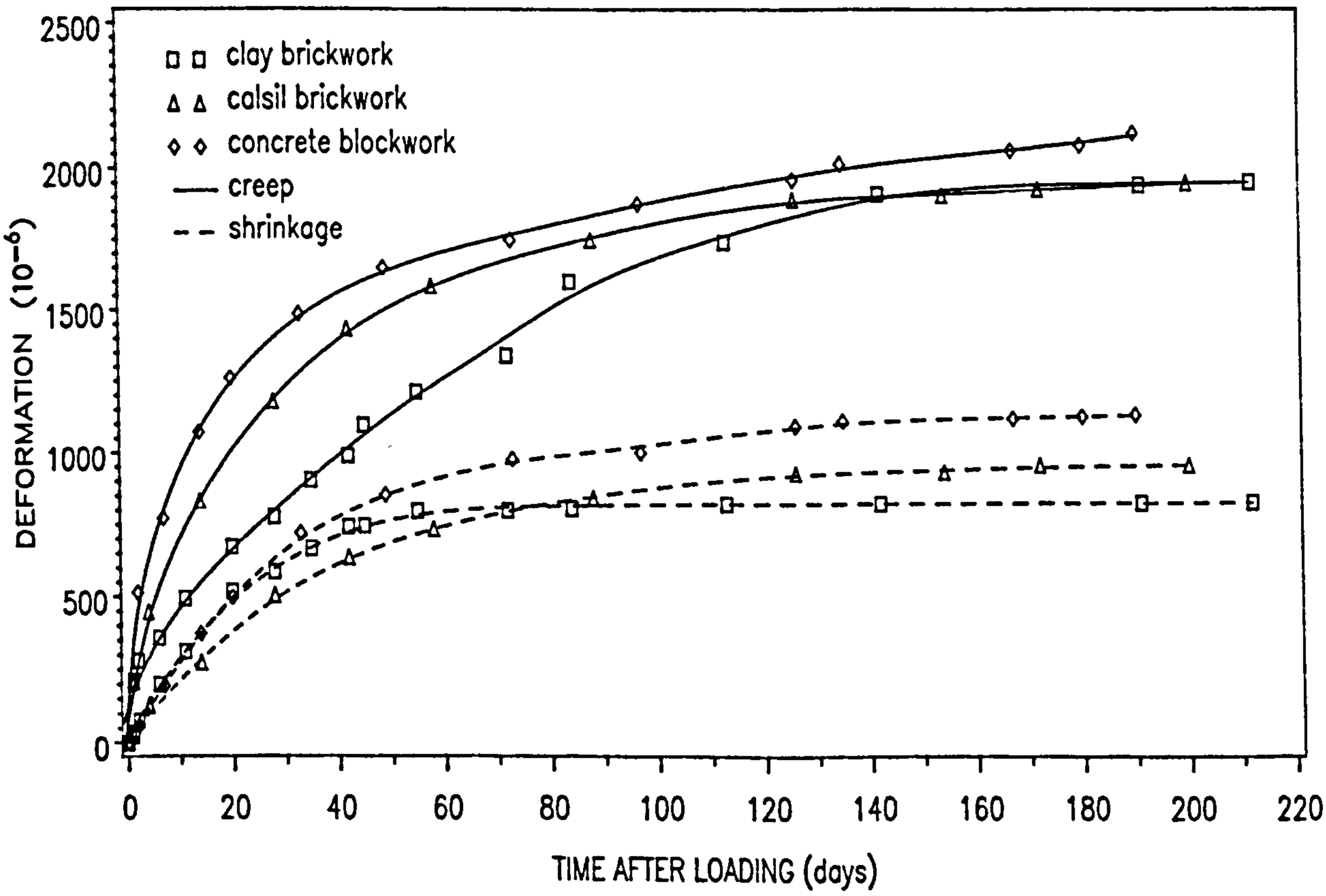

Fig. 7.1(b) – Creep and Shrinkage of Mortar for Different Types of Masonry with V/S =51

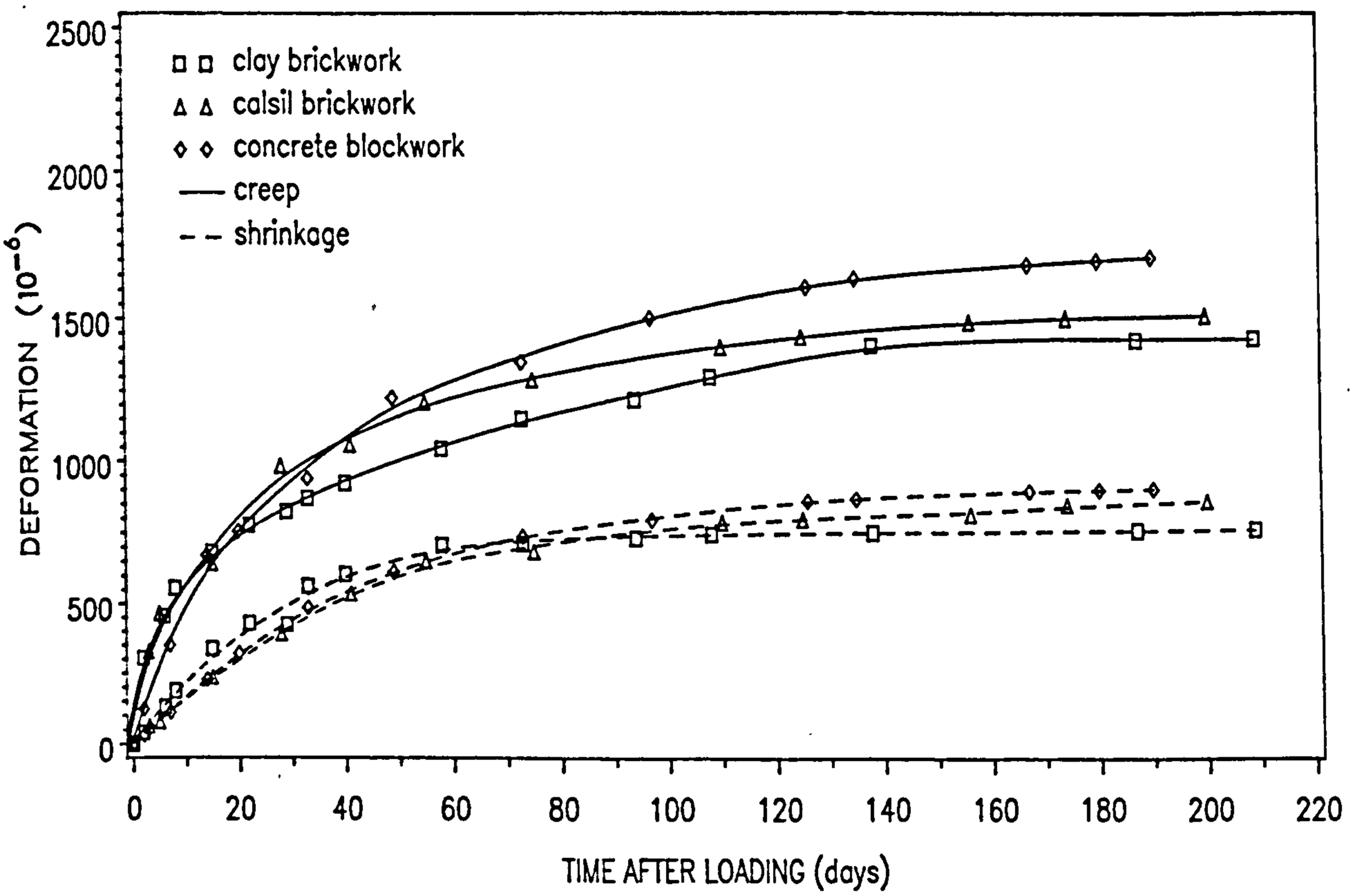

FIG. 7.1(c) – Creep and Shrinkage of Mortar for Different Types of Masonry with V/S = 78

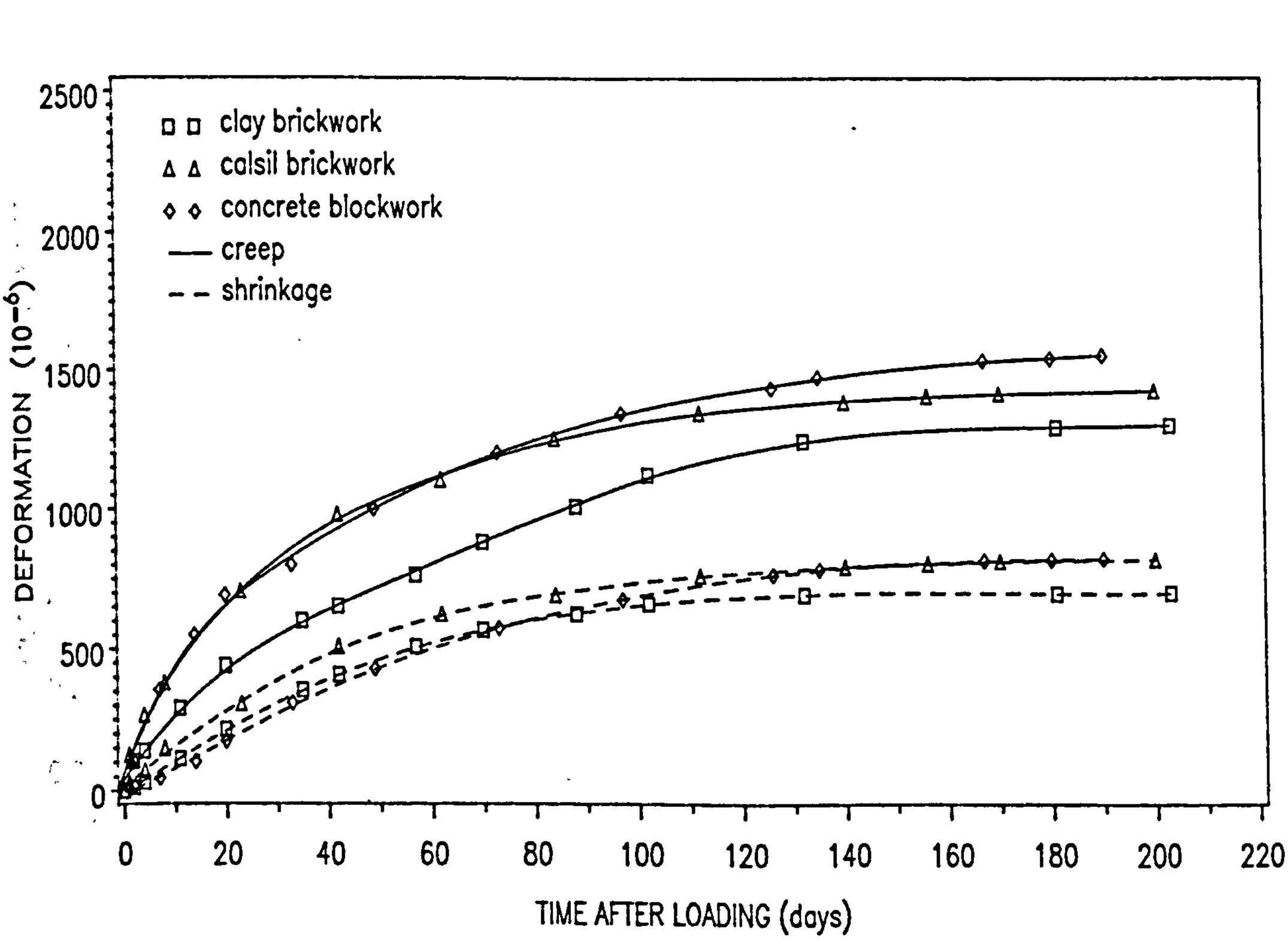

Fig. 7.1(d) – Creep and Shrinkage of Mortar for Different Types of Masonry with V/S =112

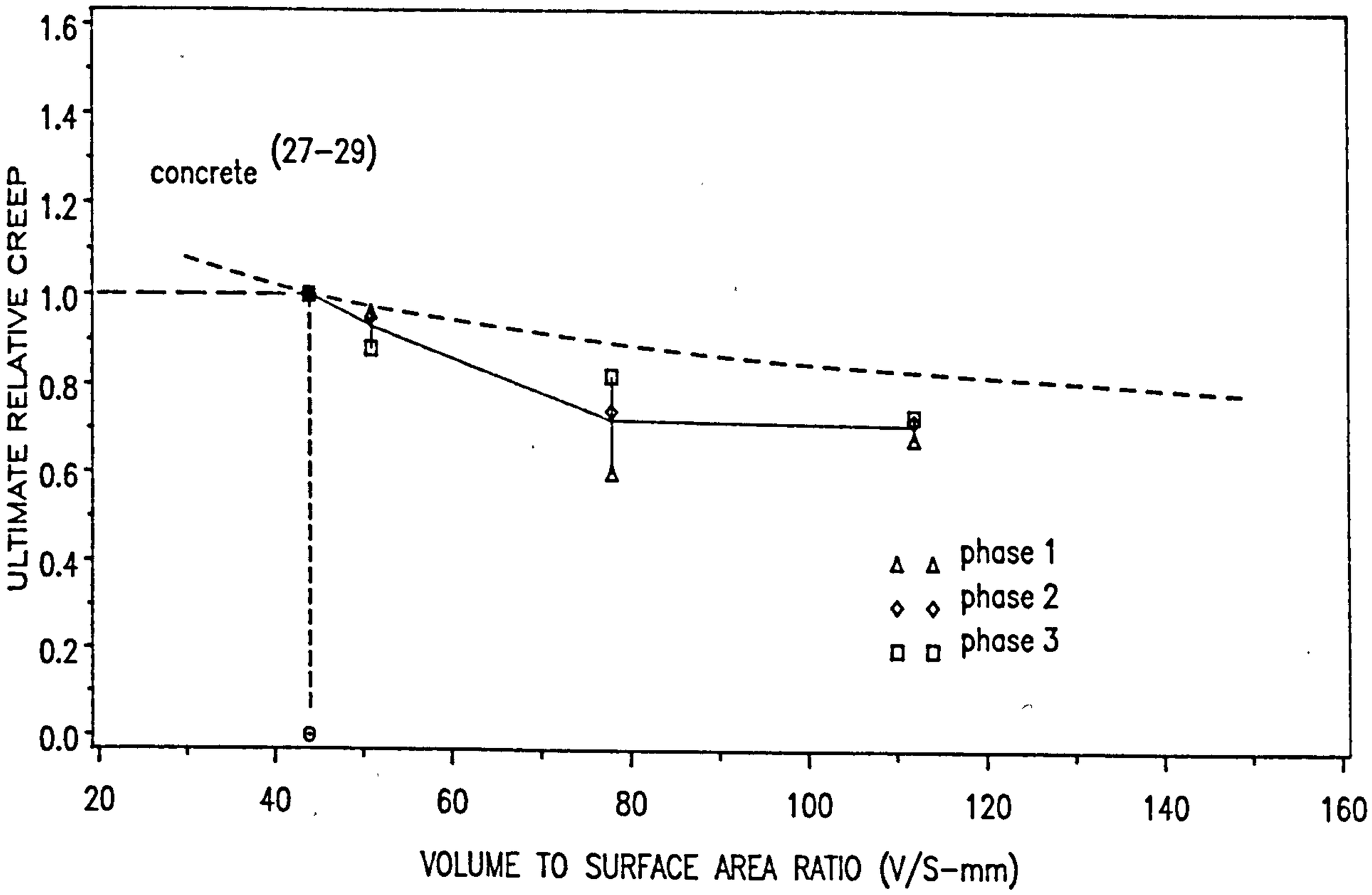

Fig. 7.2 – Ultimate Creep of Mortar Relative to That Having a V/S Ratio of 44 mm for Present Investigation and Previous Data

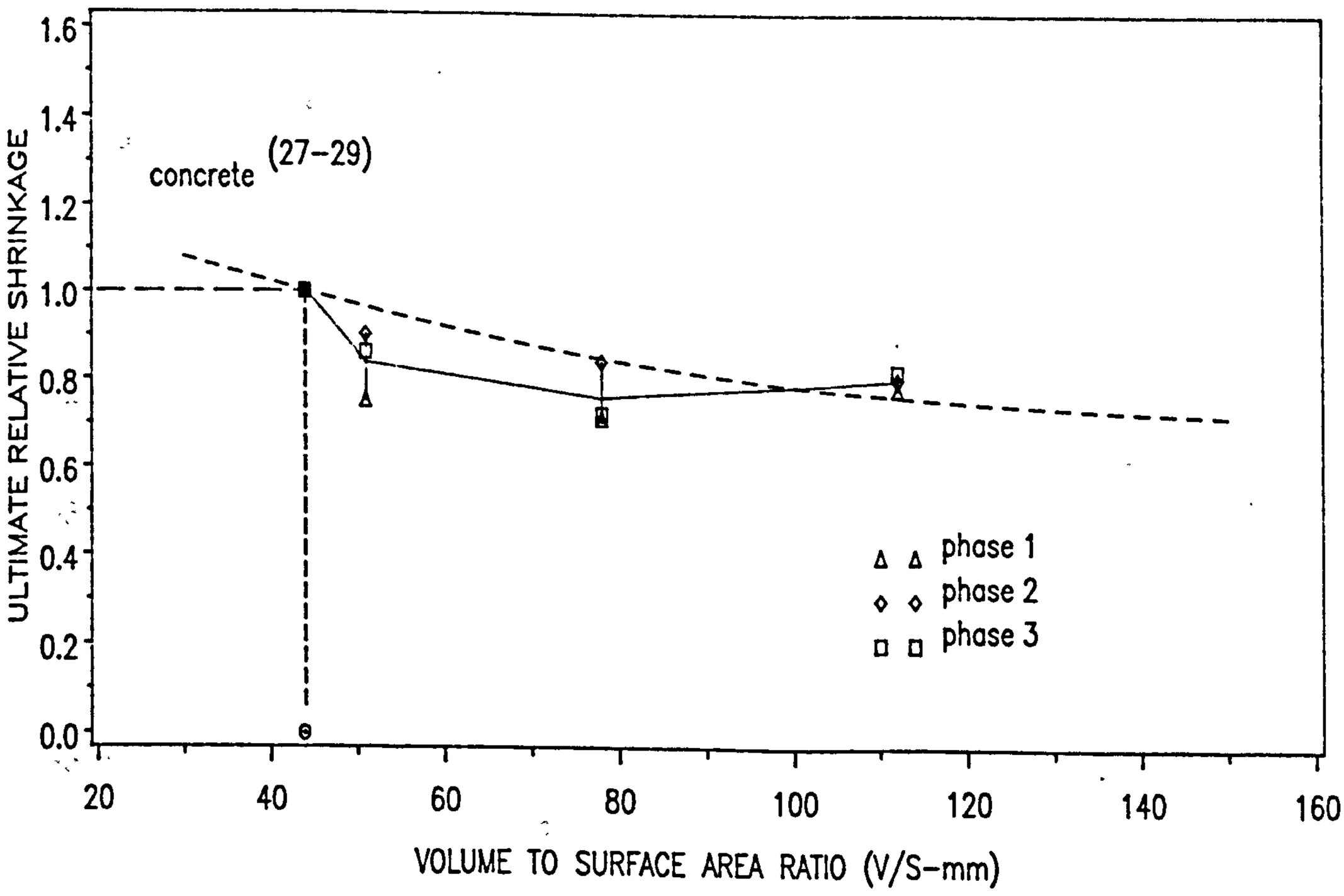

Fig. 7.3 – Ultimate Shrinkage of Mortar Relative to That Having a V/S Ratio of 44 mm for Present Investigation and Previous Data

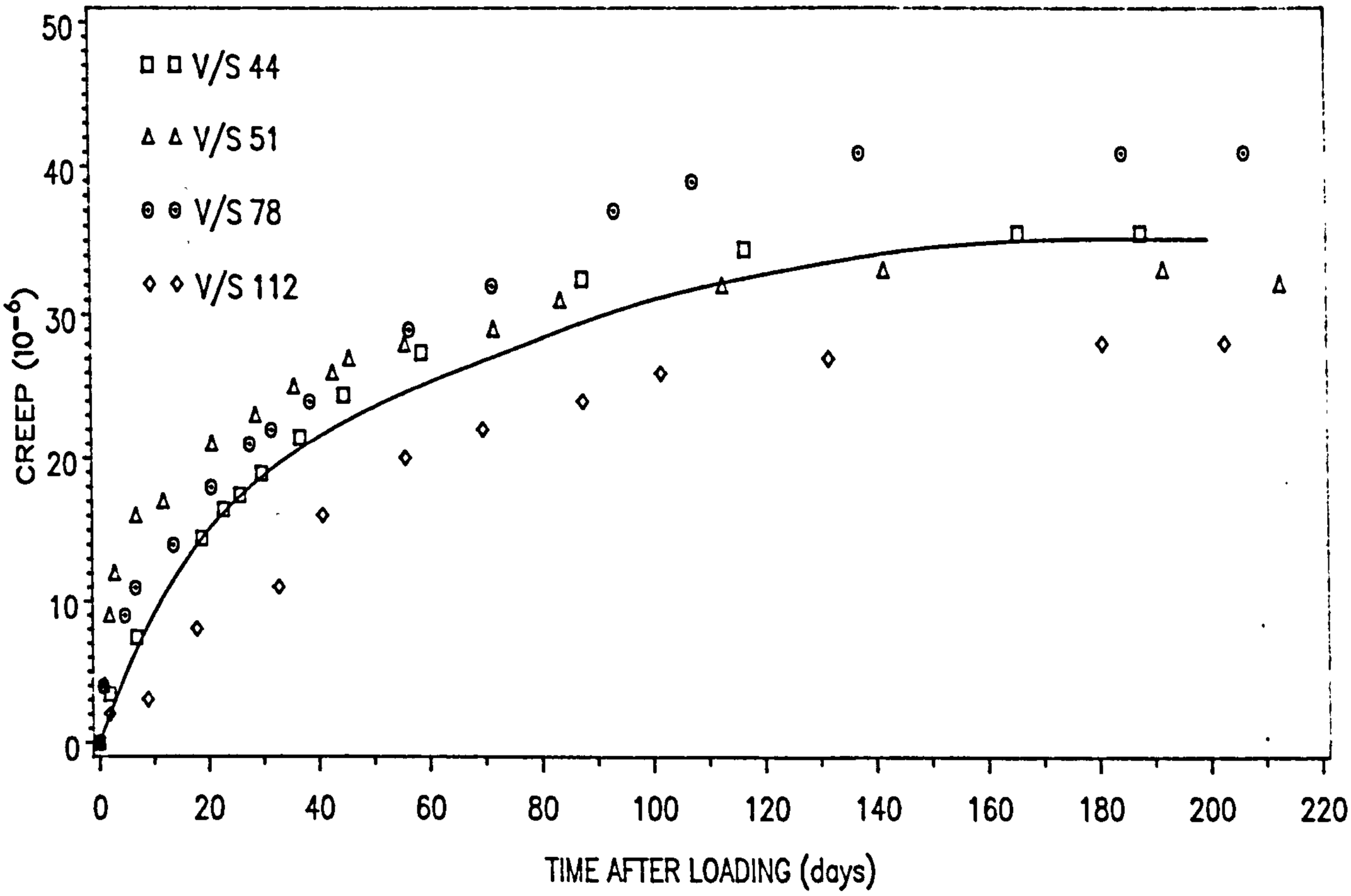

Fig. 7.4 – Creep–time Curves for Clay Brick of Different Volume–Surface Area Ratios

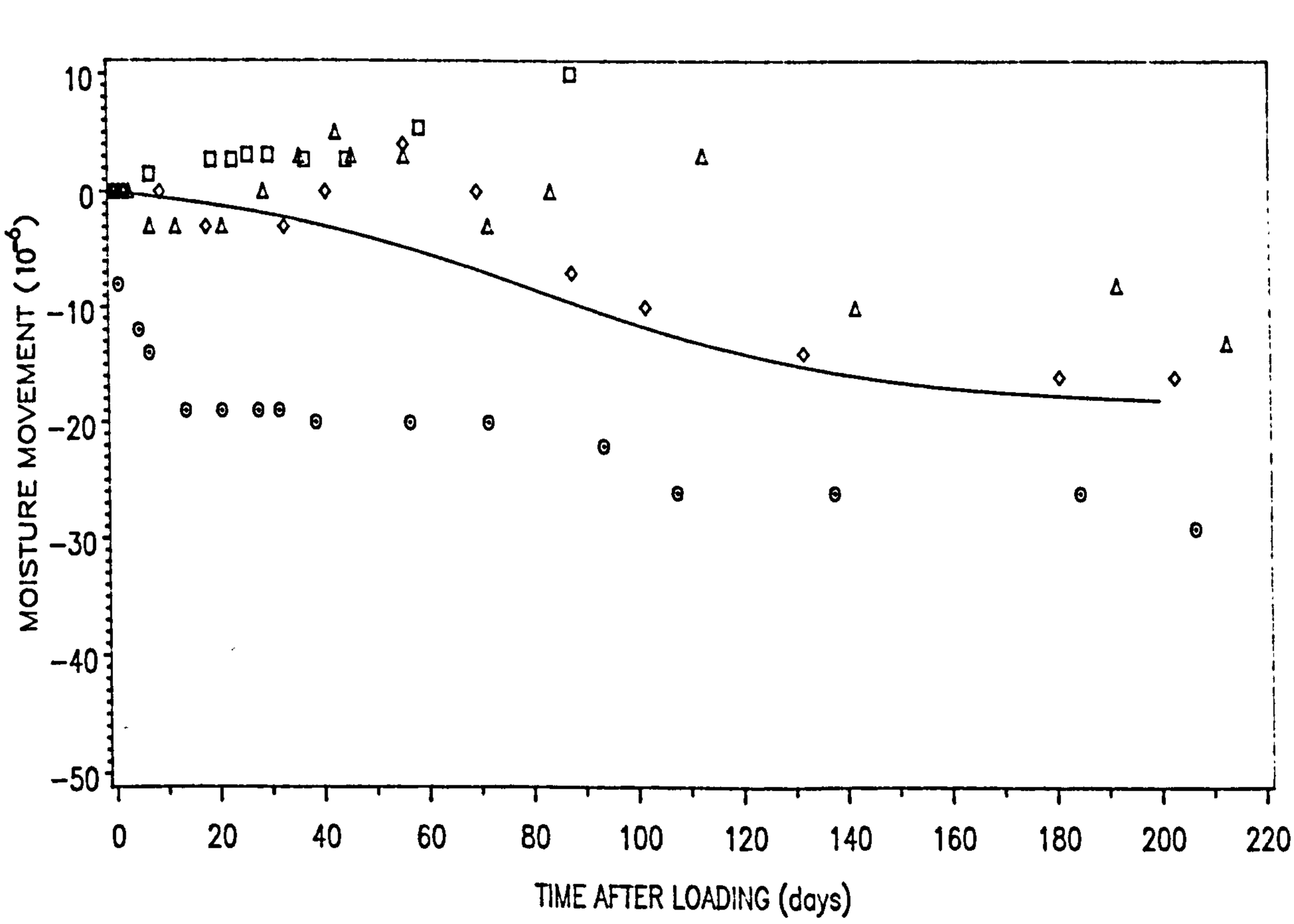

Fig. 7.5 – Moisture Strain–time Curves for Clay Bricks of Different Volume–Surface Area ratios

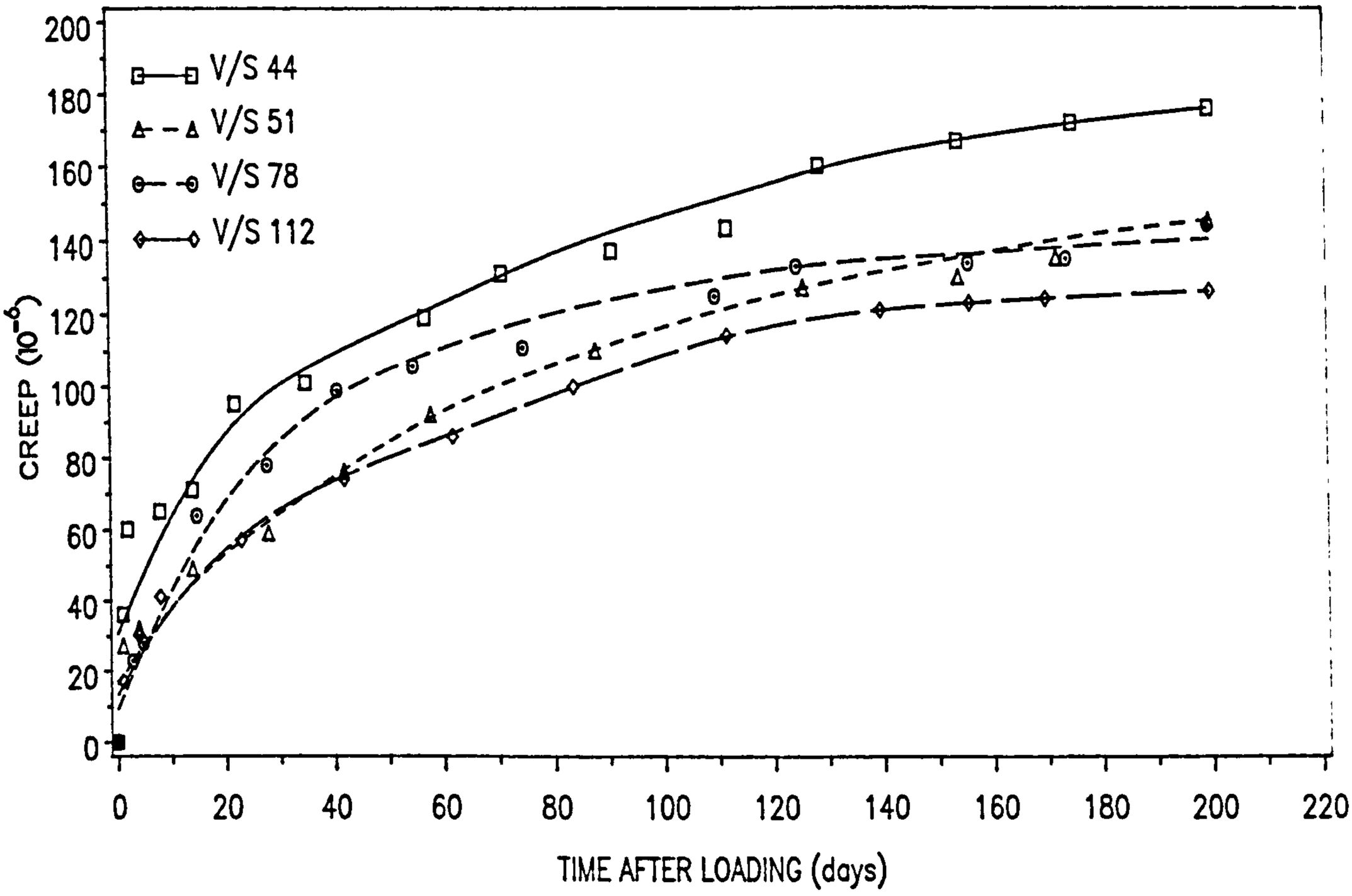

Fig. 7.6 – Creep–time Curves for Calcium Silicate Bricks of Different Volume–Surface Area Ratios

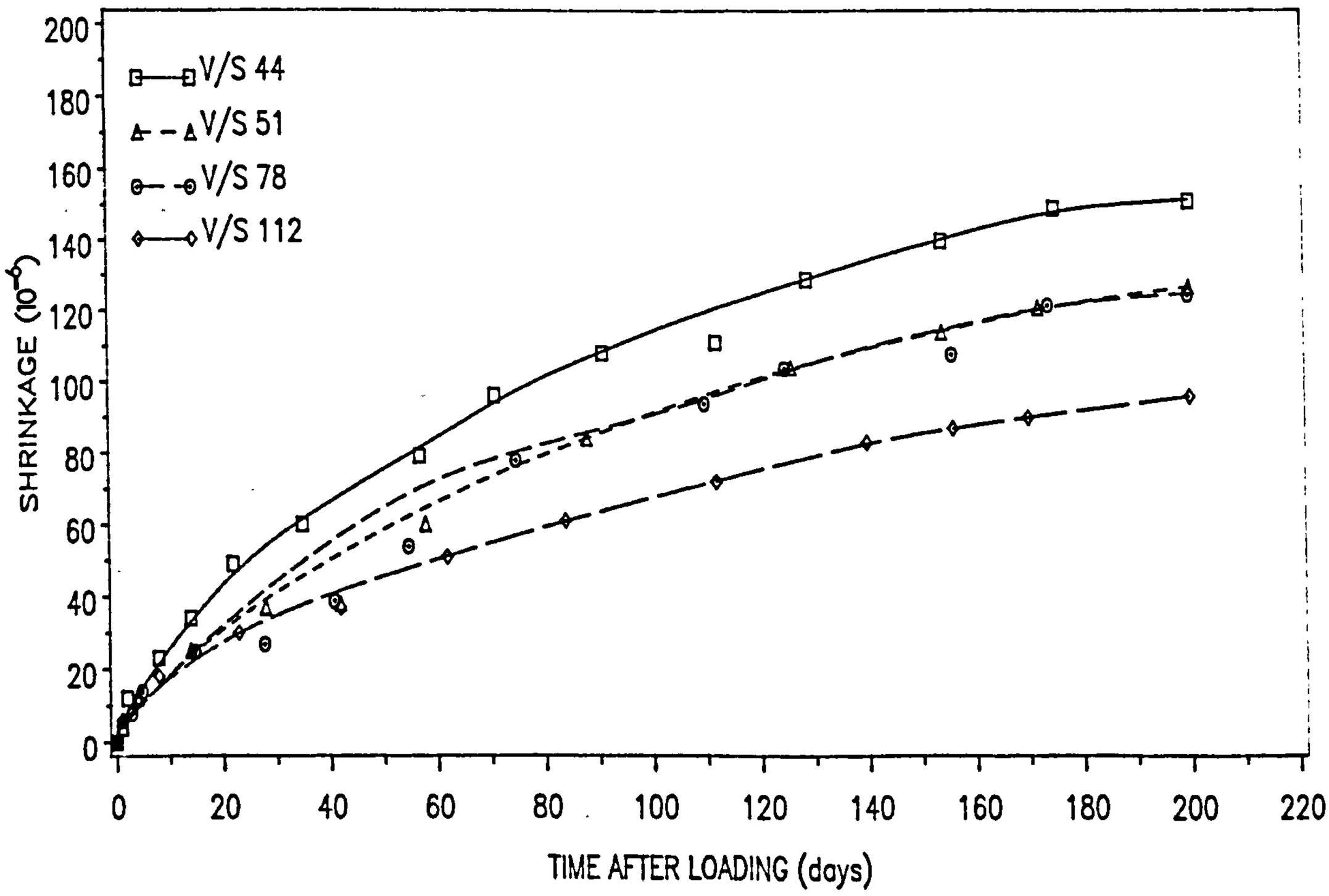

Fig. 7.7 – Shrinkage–time Curves for Calcium Silicate Bricks of Different Volume–Surface Area Ratios

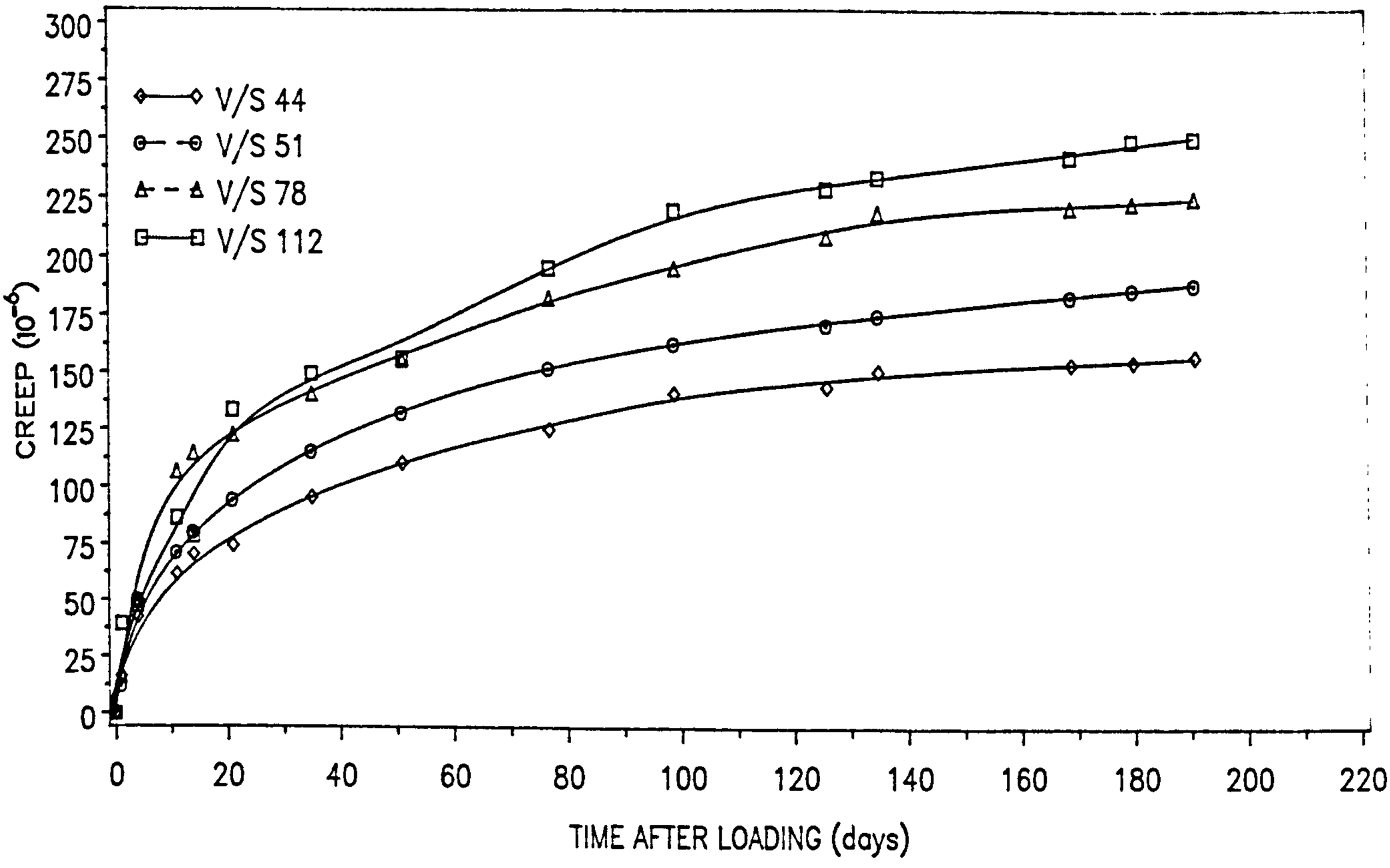

Fig. 7.8 – Creep–time Curves for Concrete Blocks with Different Volume–Surface Area Ratios

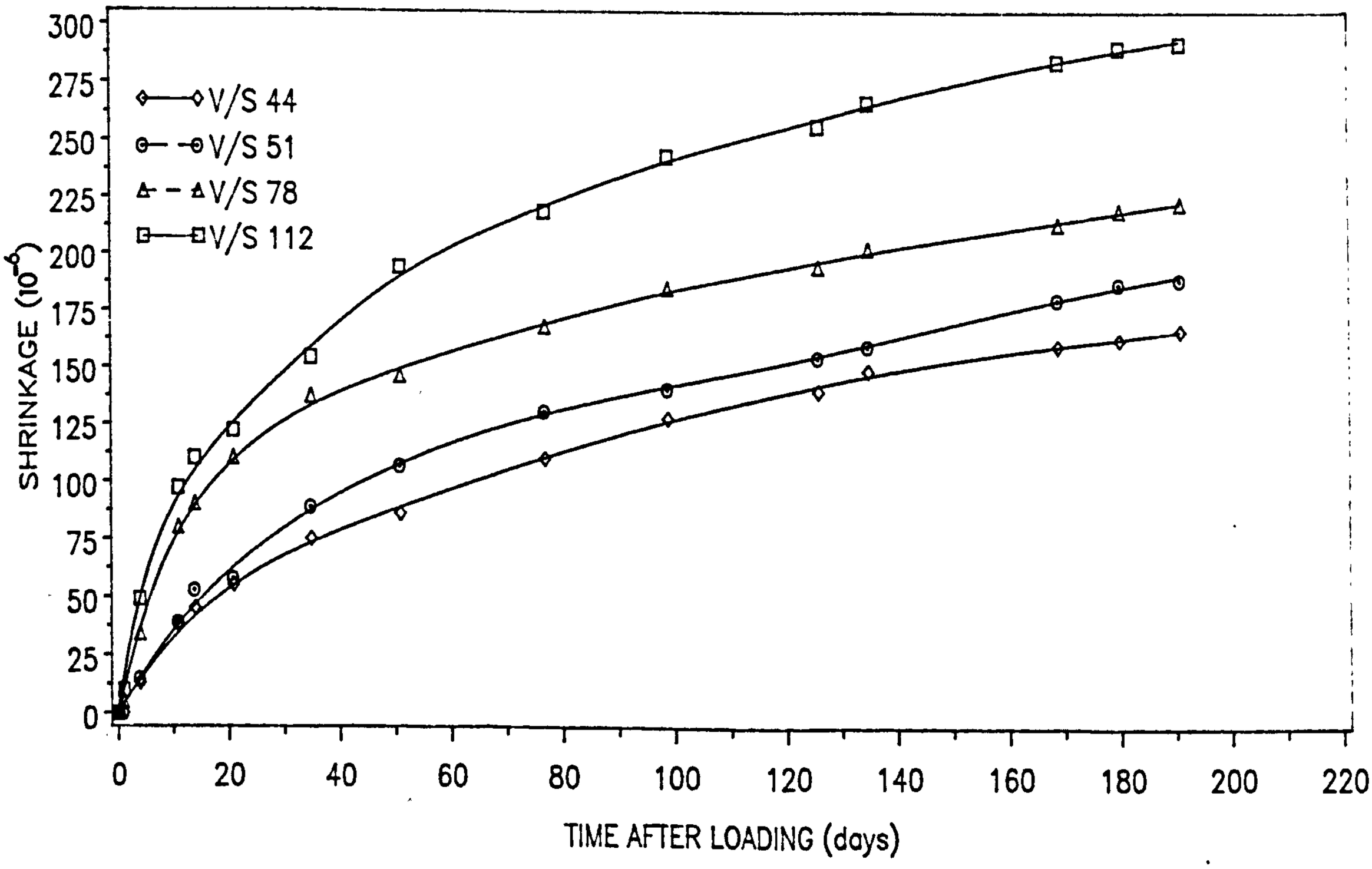

Fig. 7.9 – Shrinkage–time Curves for Concrete Blocks with Different Volume–Surface Area Ratios

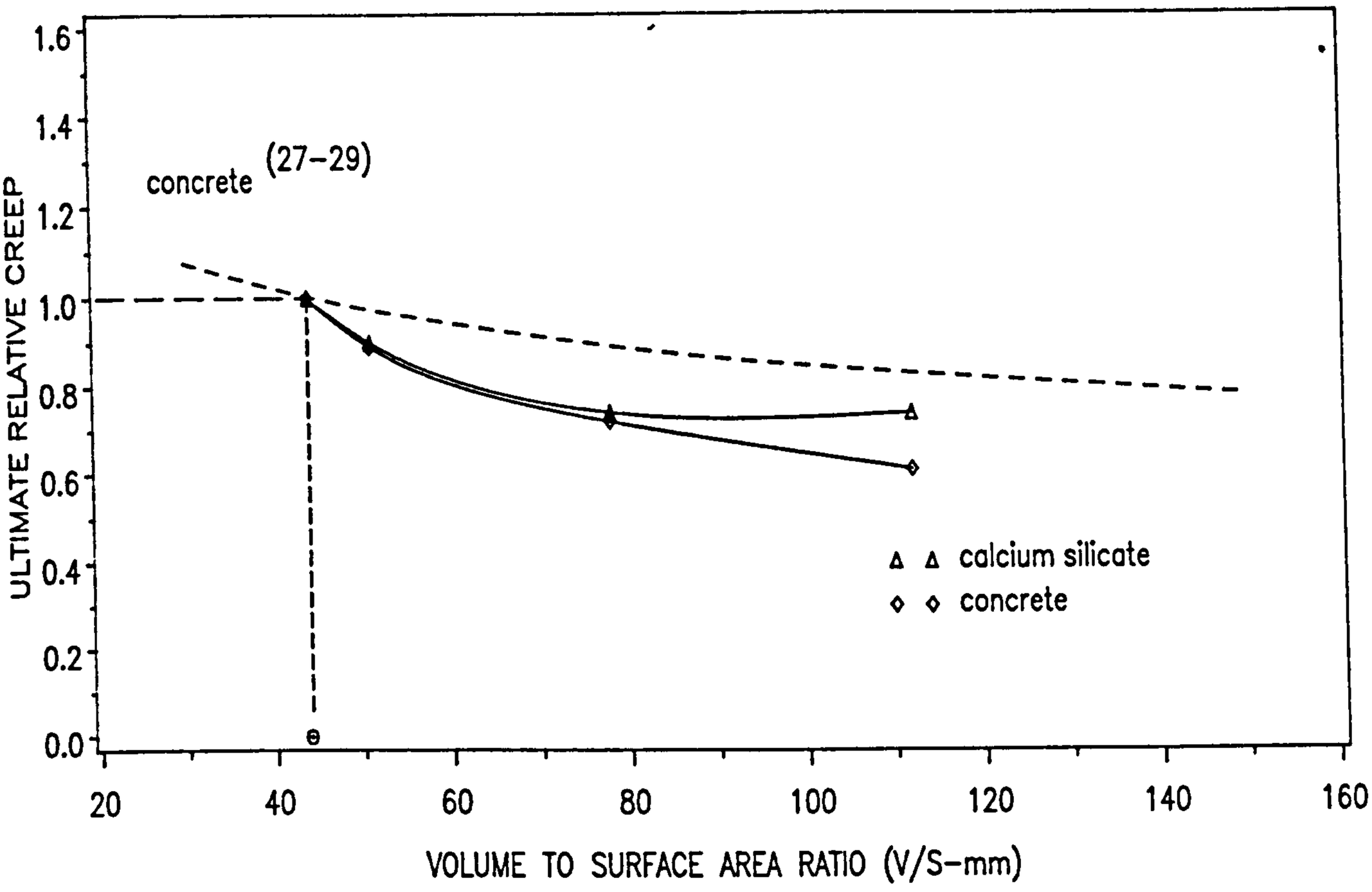

FIG. 7.10 – Ultimate Creep of Unit Relative to That Having a V/S Ratio of 44 mm for Present Investigation and Previous Data

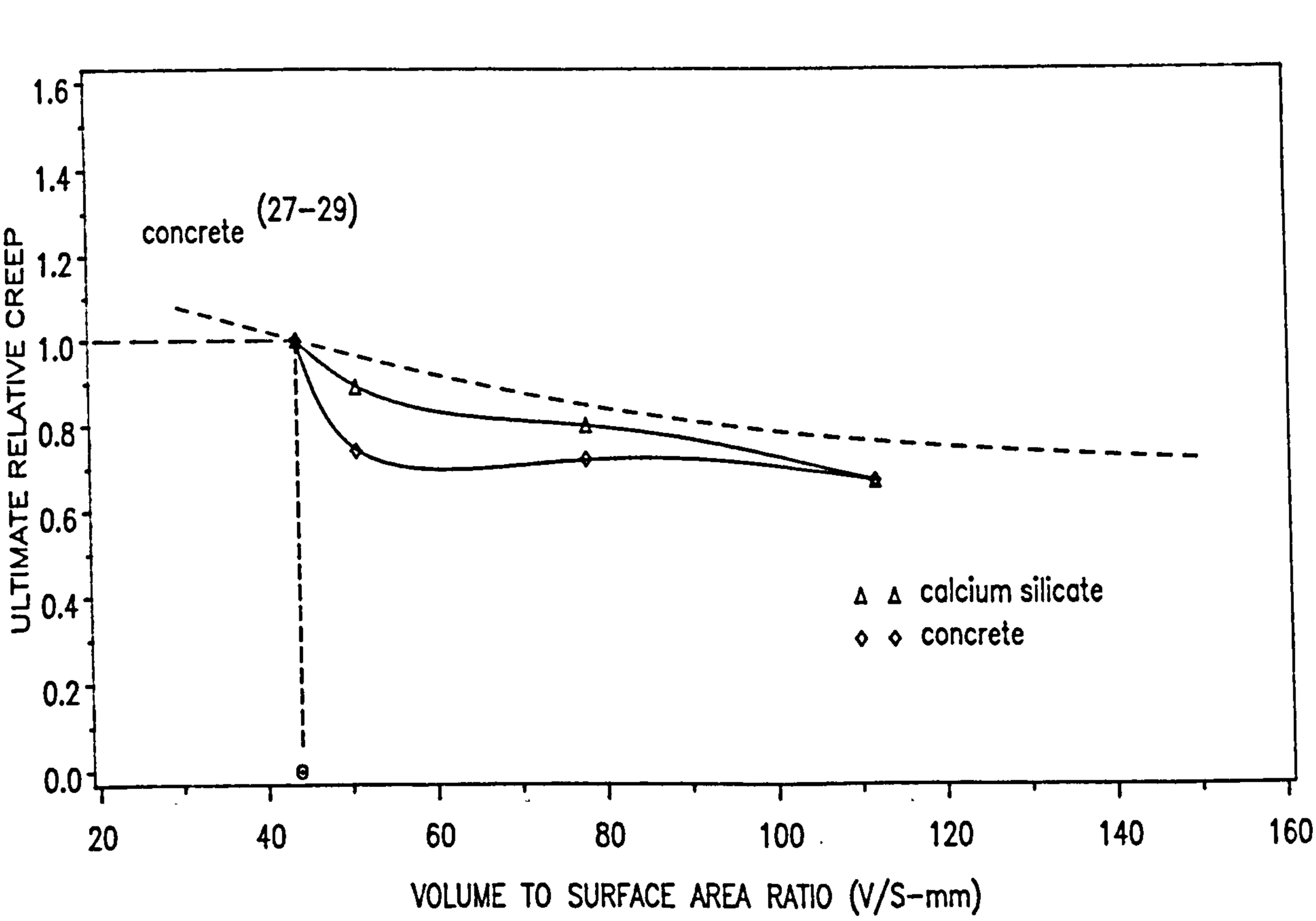

FIG. 7.11 – Ultimate Moisture Strain of Unit Relative to That Having a V/S Ratio of 44 mm for Present Investigation and Previous Data

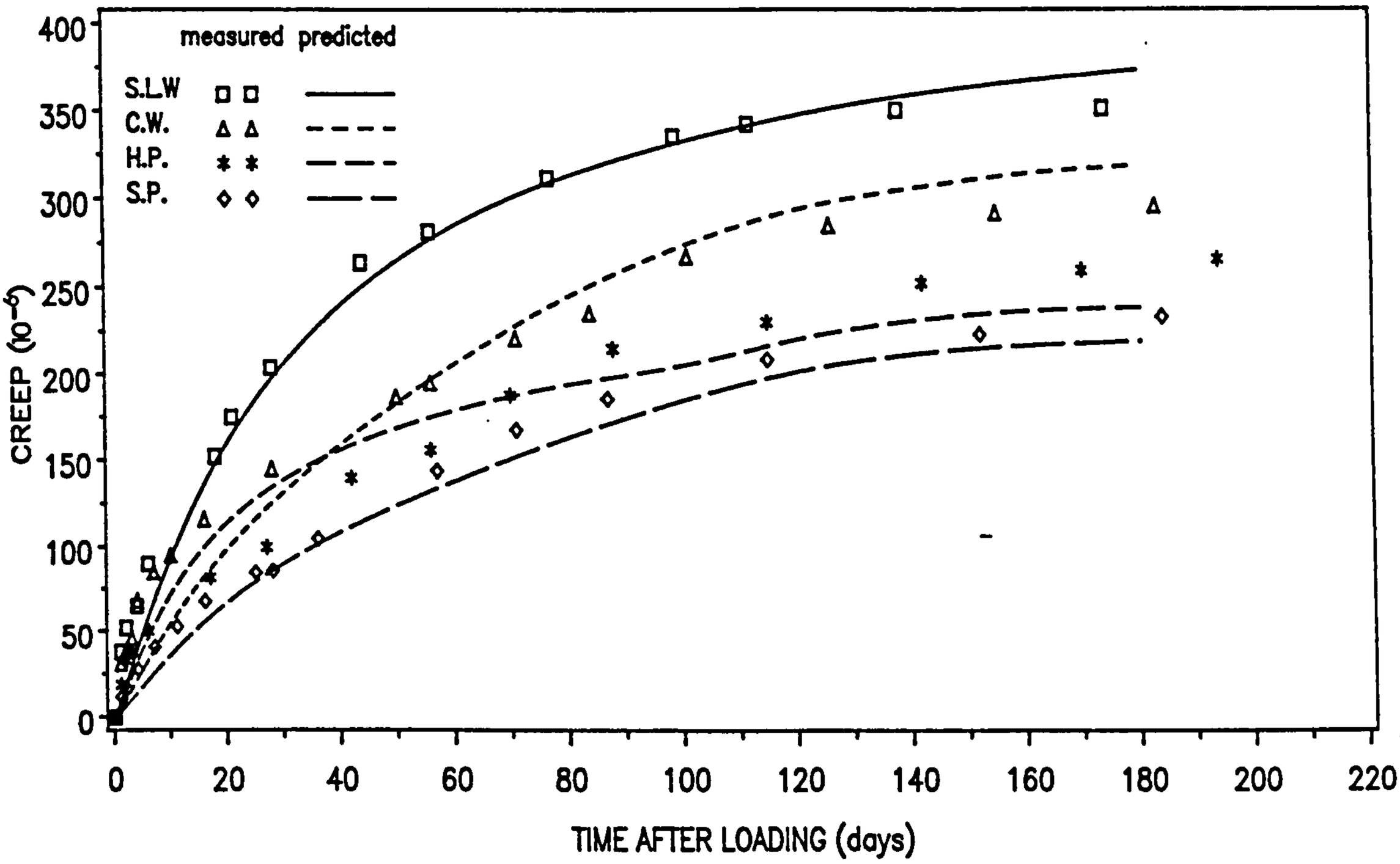

Fig. 7.12 – Composite Model Prediction for Creep (c_{wy}) of Clay Brickwork

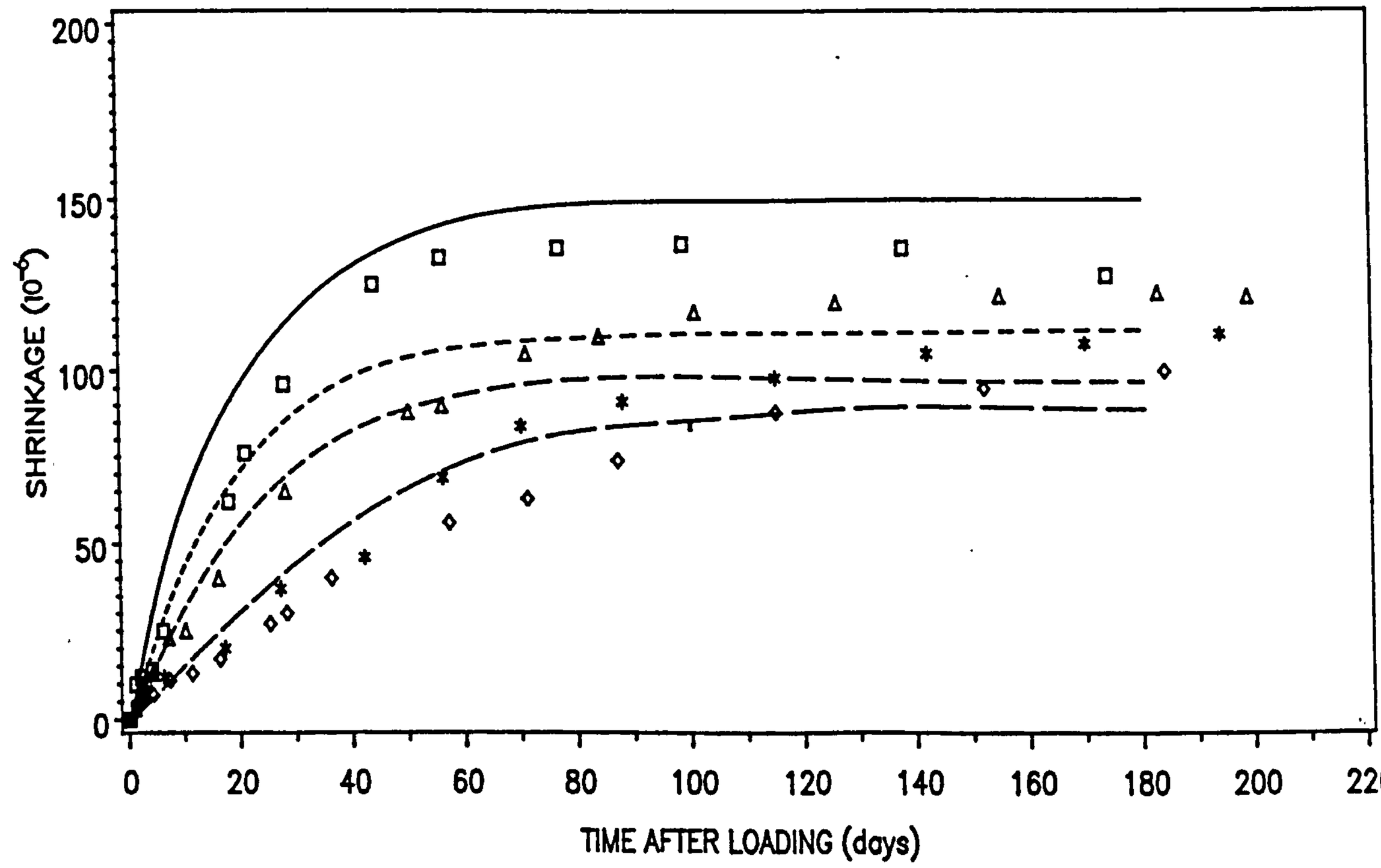

Fig. 7.13 – Composite Model Prediction for Shrinkage (s_{wy}) of Clay Brickwork

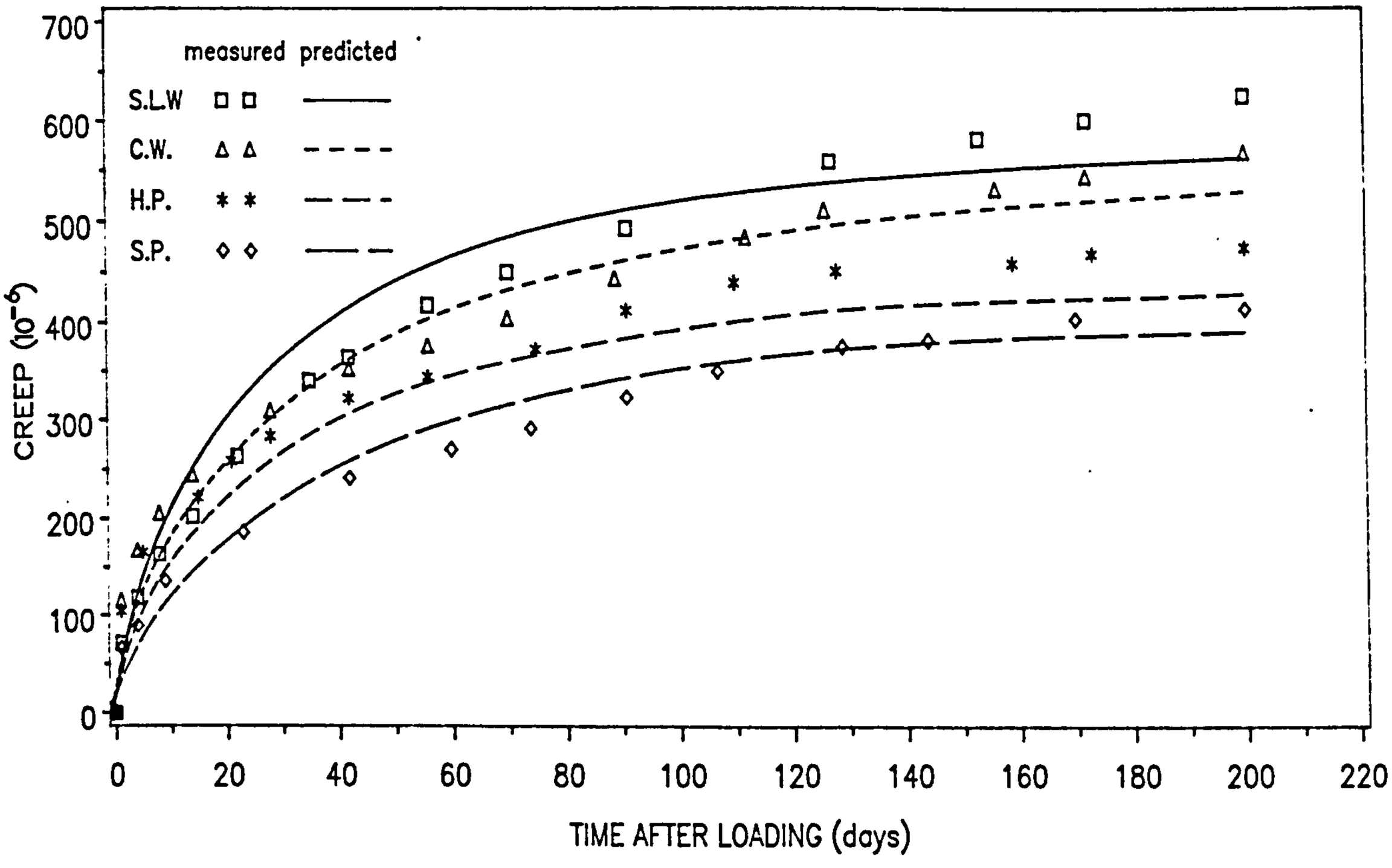

Fig. 7.14 – Composite Model Prediction for Creep (c_{wy}) of Calcium Silicate Brickwork

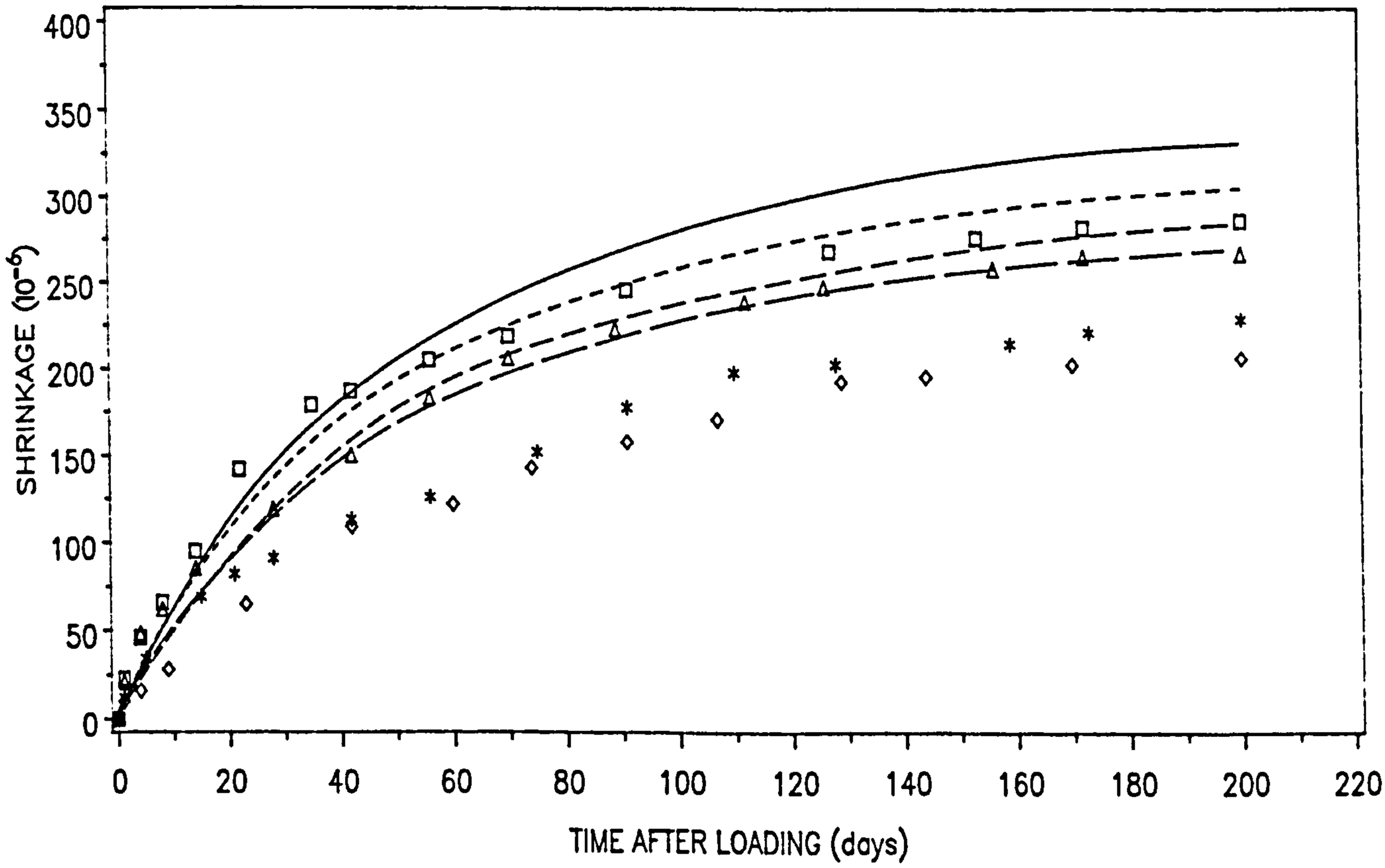

Fig. 7.15 – Composite Model Prediction for Shrinkage (s_{wy}) of Calcium Silicate Brickwork

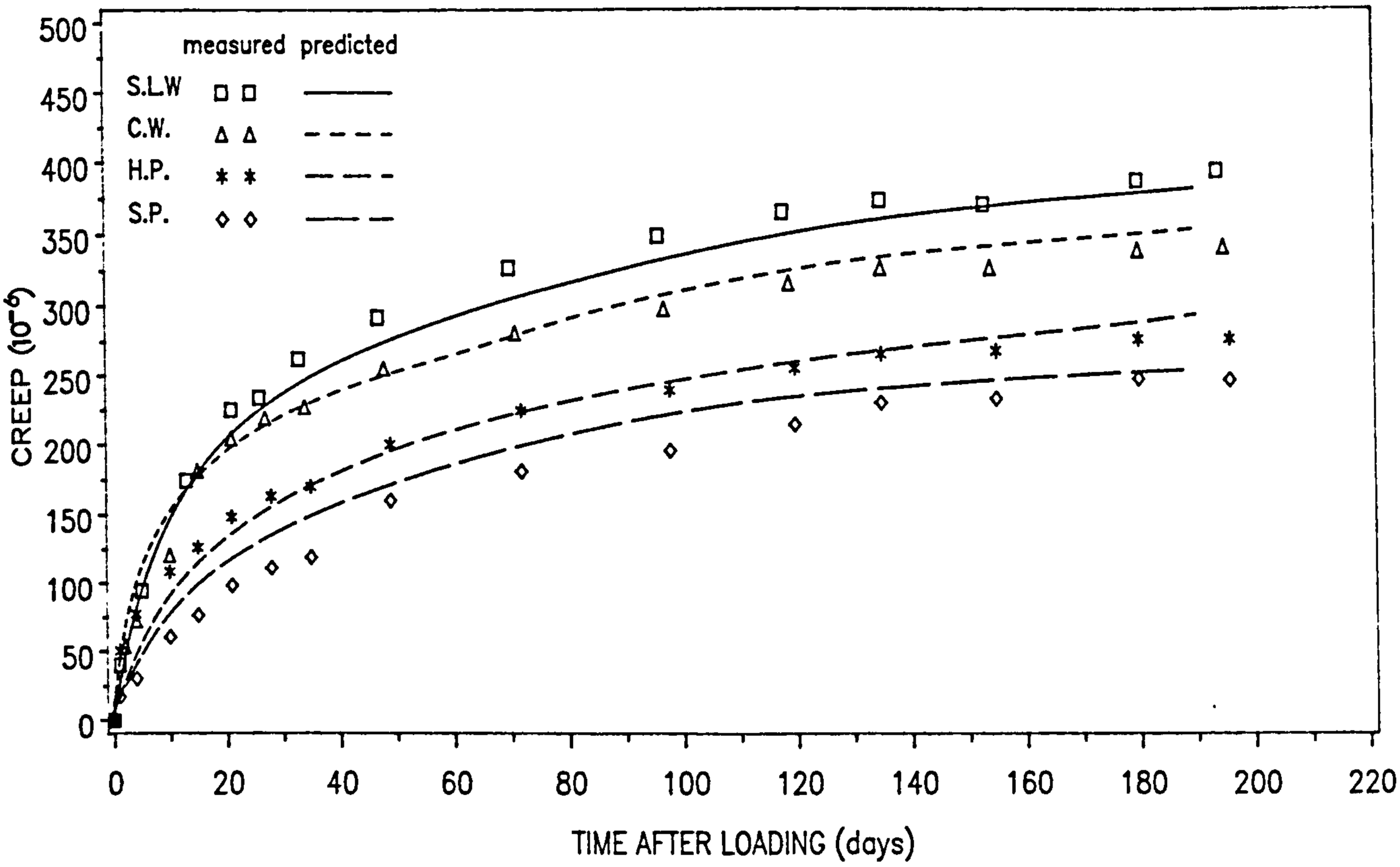

Fig. 7.16 – Composite Model Prediction for Creep (c_{wy}) of Concrete Blockwork

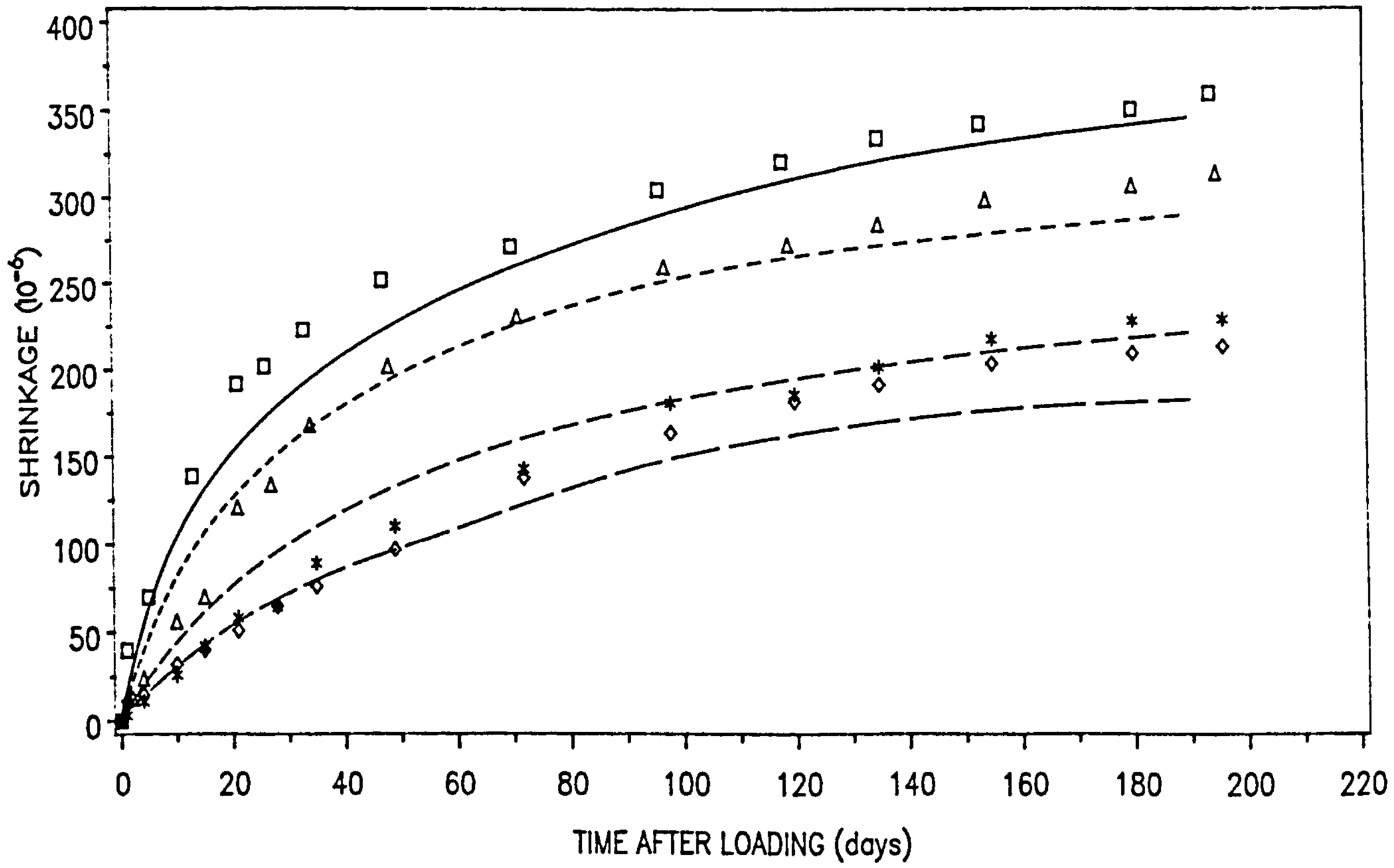

Fig. 7.17 – Composite Model Prediction for Shrinkage (s_{wy}) of Concrete Blockwork

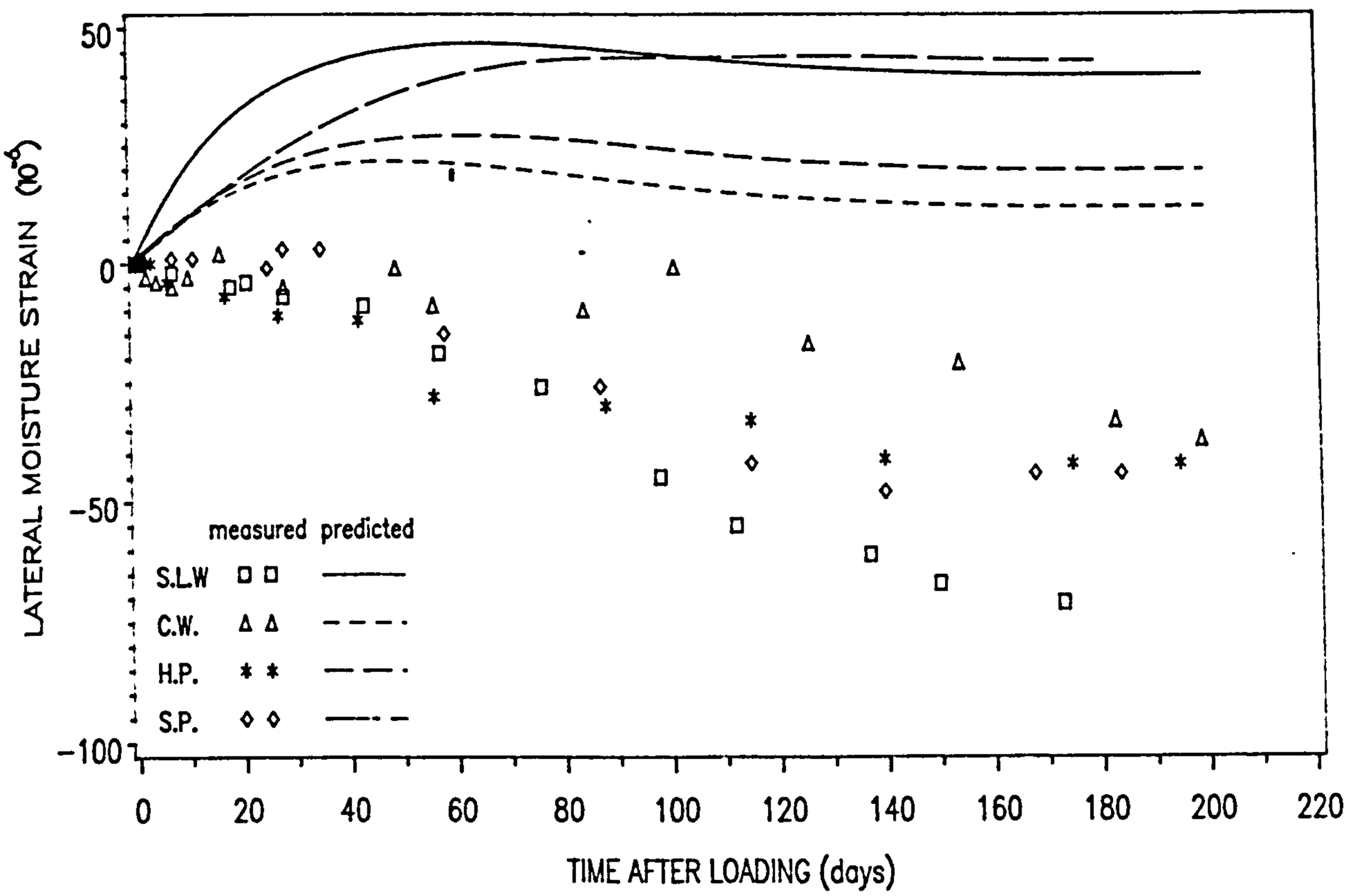

Fig. 7.18 – Composite Model Prediction for Lateral Moisture Strain (ε_{wx}) of Clay Brickwork

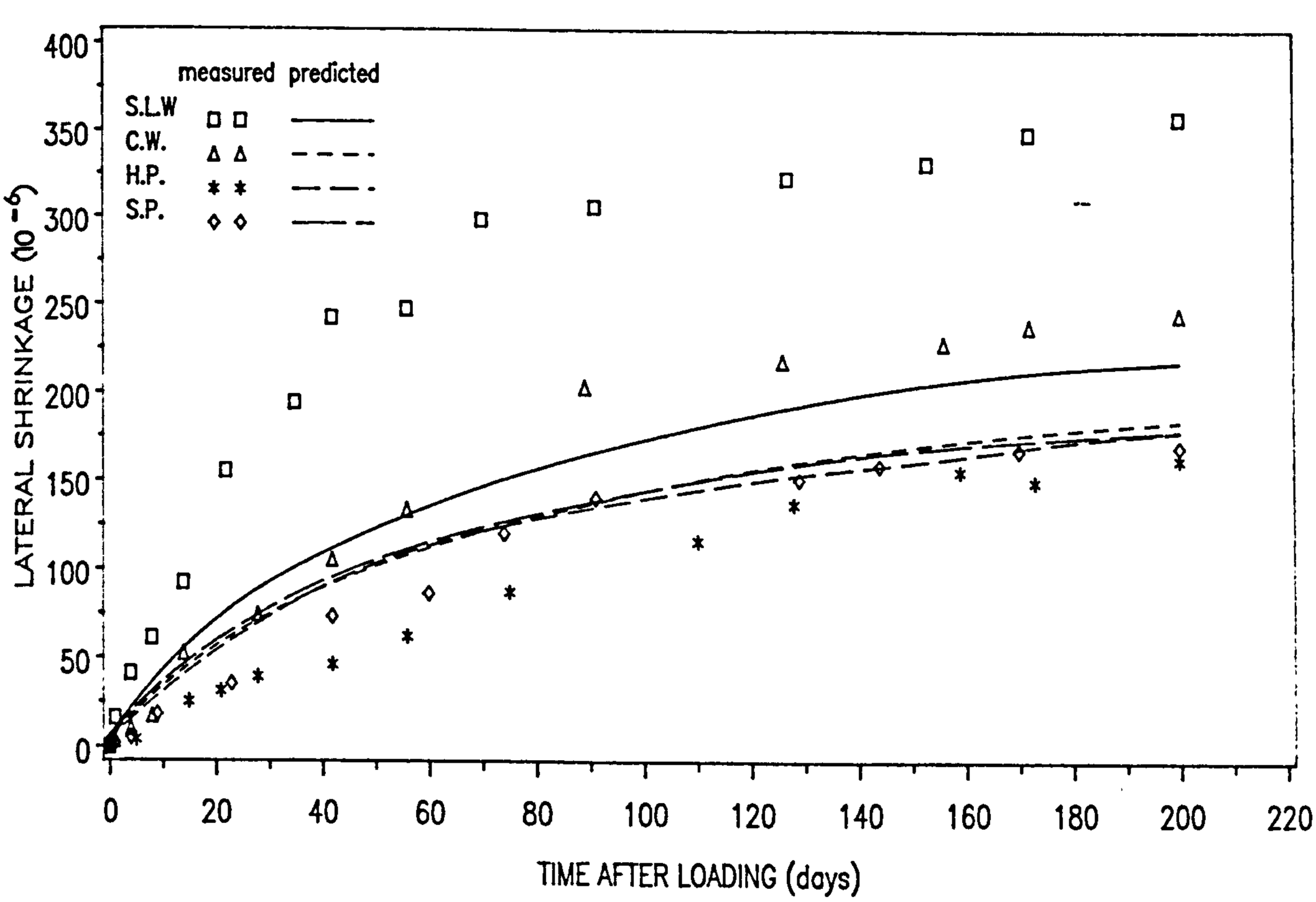

Fig. 7.19 – Composite Model Prediction for Lateral Shrinkage (s_{wx}) of Calcium Silicate Brickwork

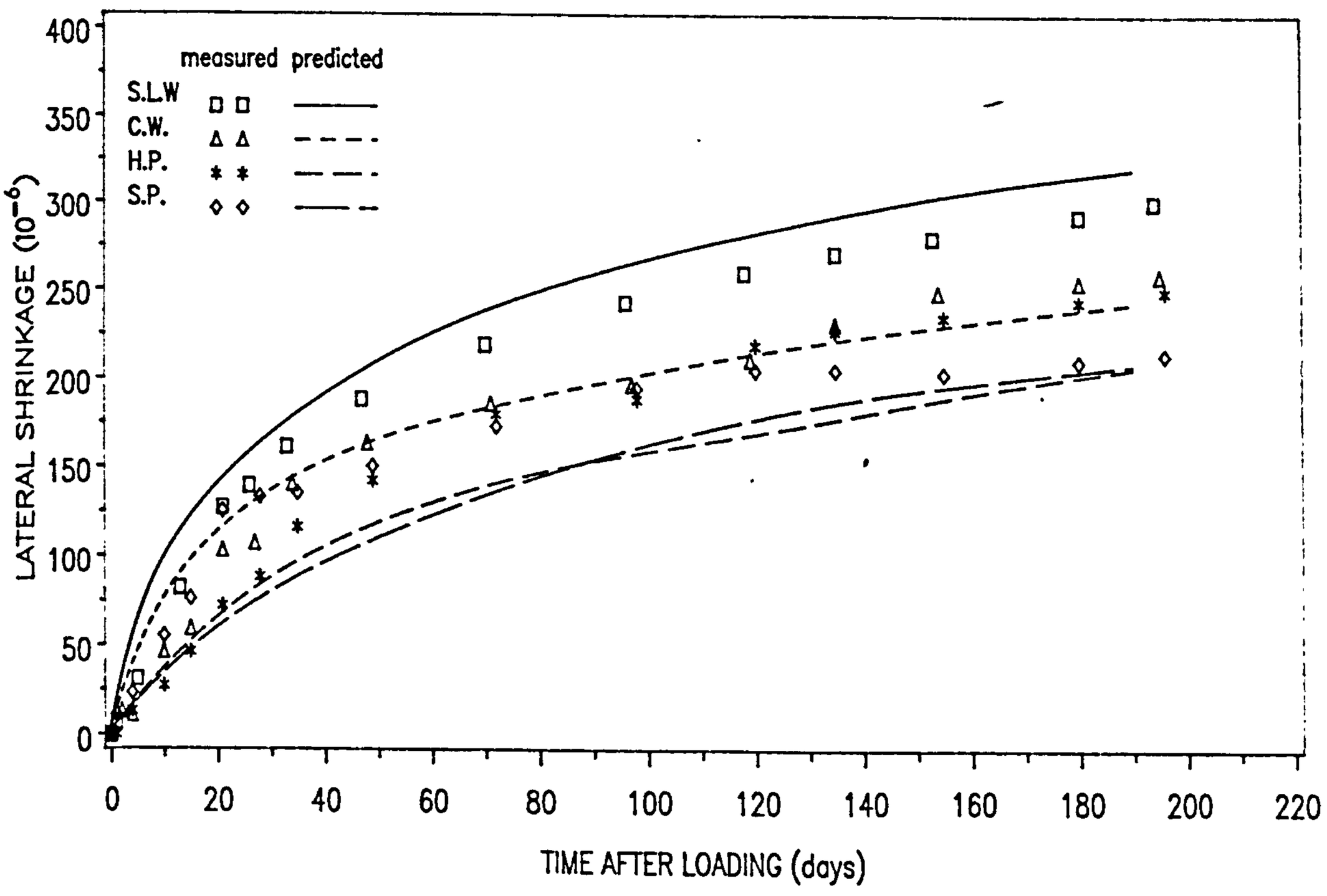

Fig. 7.20 – Composite Model Prediction for Lateral Shrinkage (s_{wx}) of Concrete Blockwork

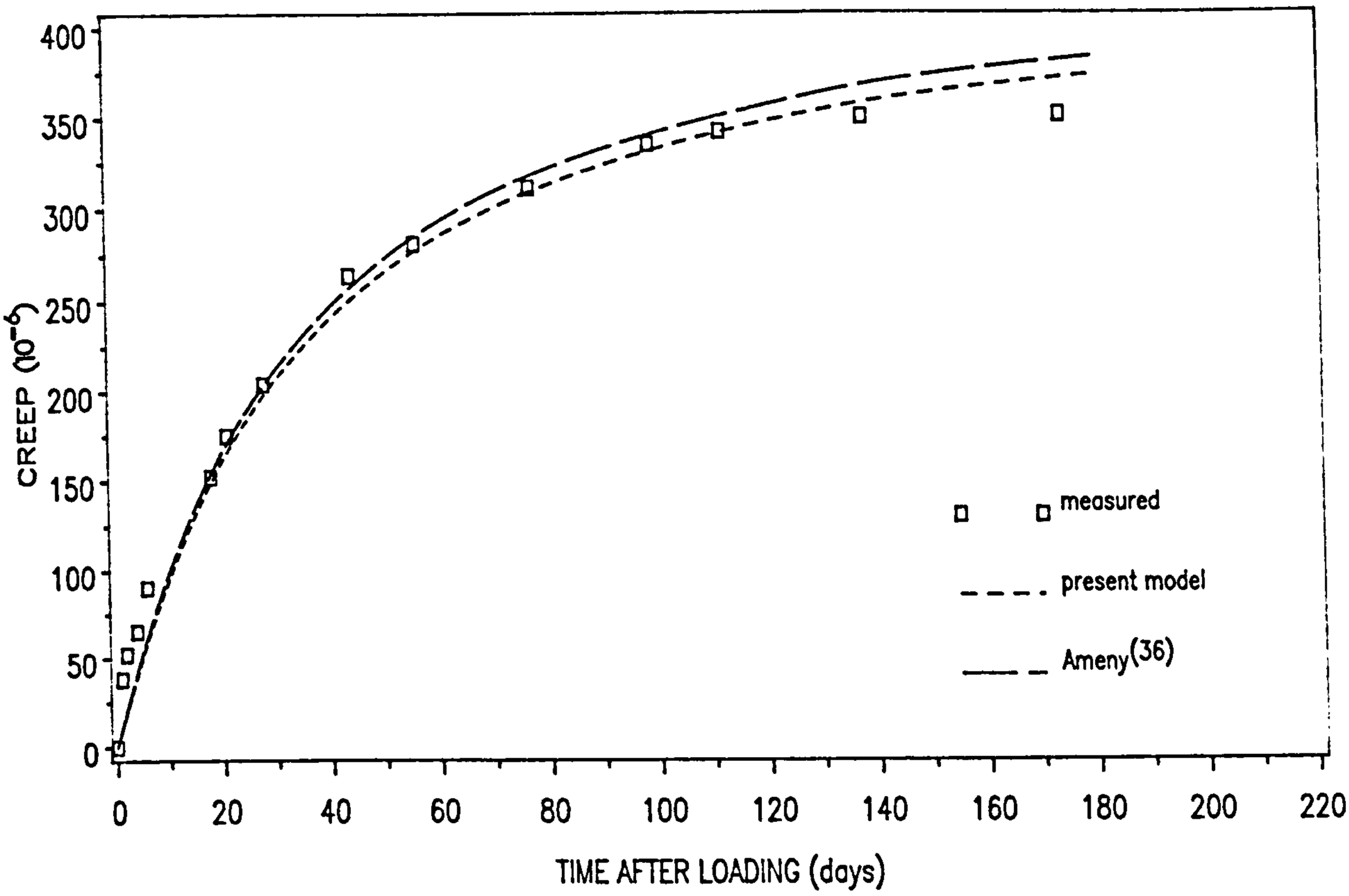

Fig. 7.21 – Comparison of Vertical Creep Prediction Using Composite Models for Clay Single–Leaf Wall

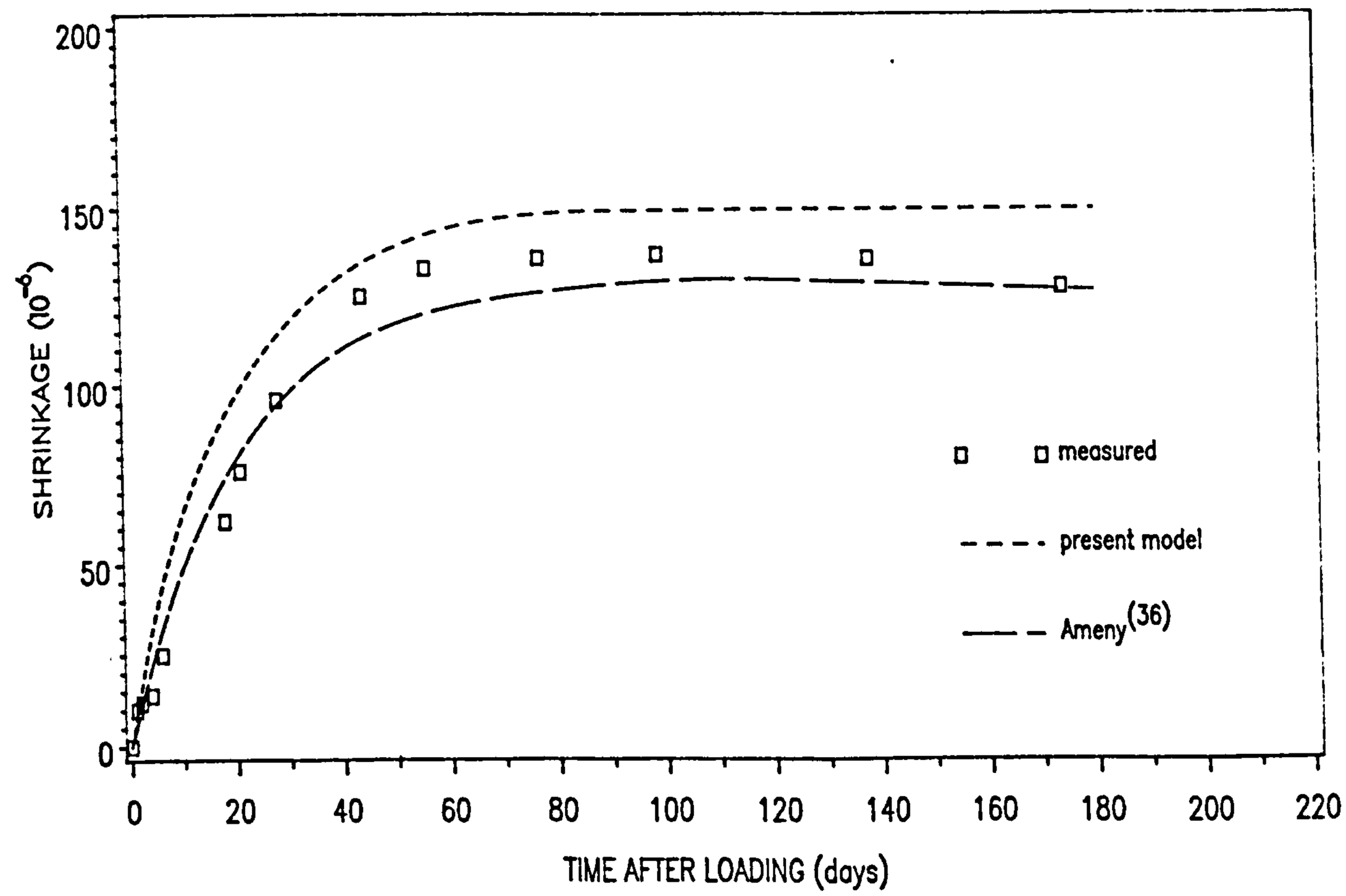

Fig. 7.22 – Comparison of Vertical Shrinkage Prediction Using Composite Models for Clay Single–Leaf Wall

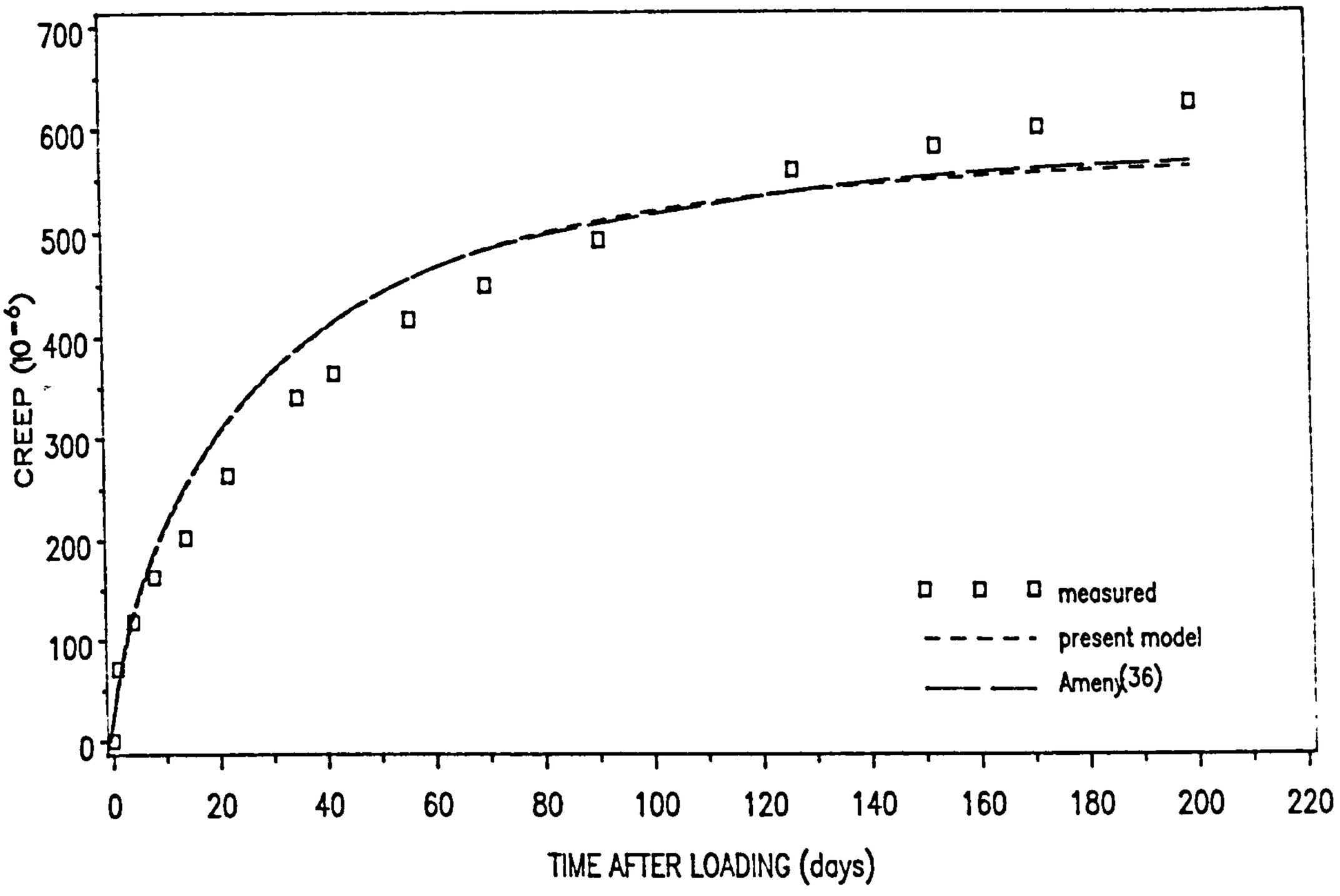

Fig. 7.23 – Comparison of Vertical Creep Prediction Using Composite Models for Calcium Silicate Single–Leaf Wall

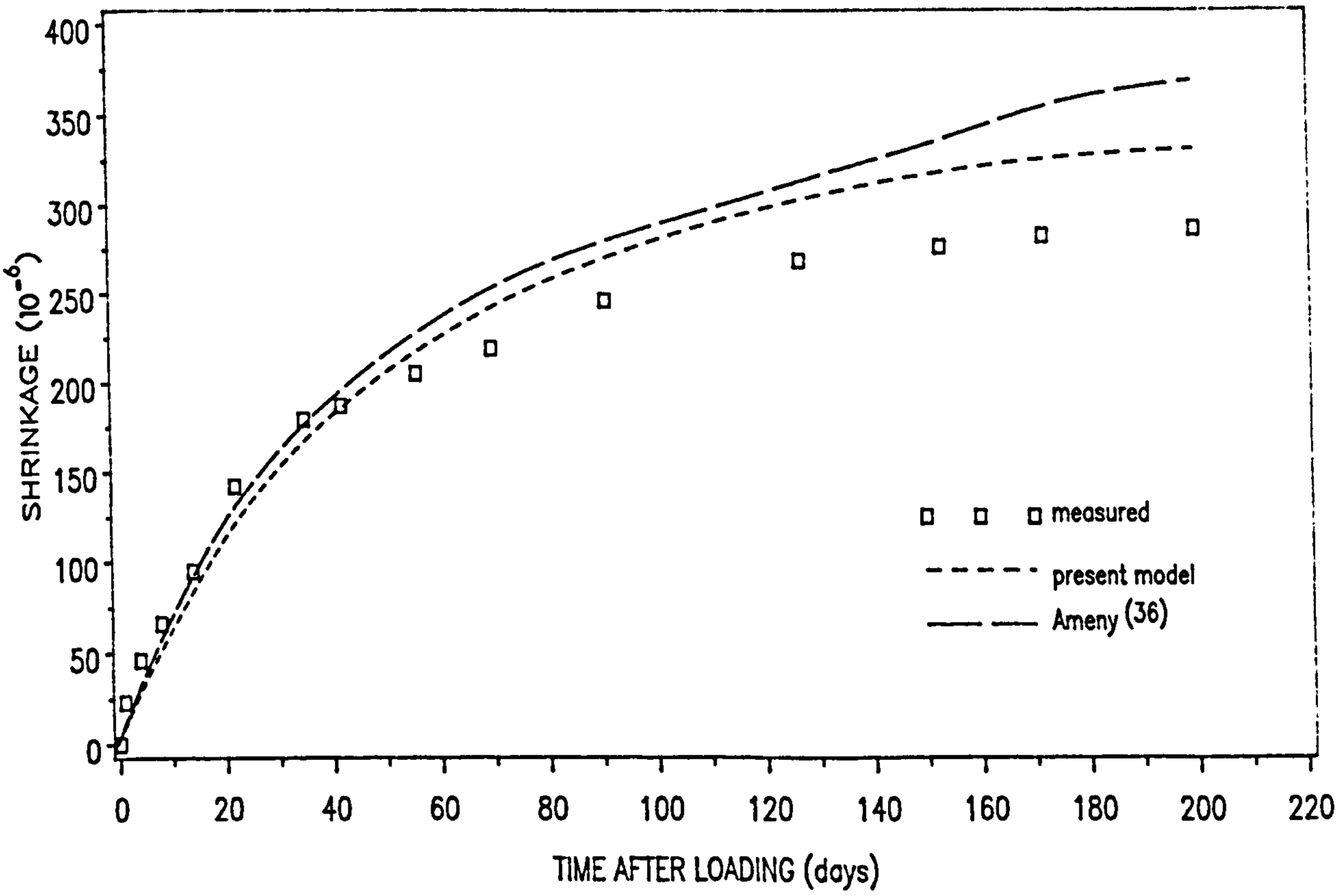

Fig 7.24 – Comparison of Vertical Shrinkage Prediction Using Composite Models for Calcium Silicate Single–Leaf Wall

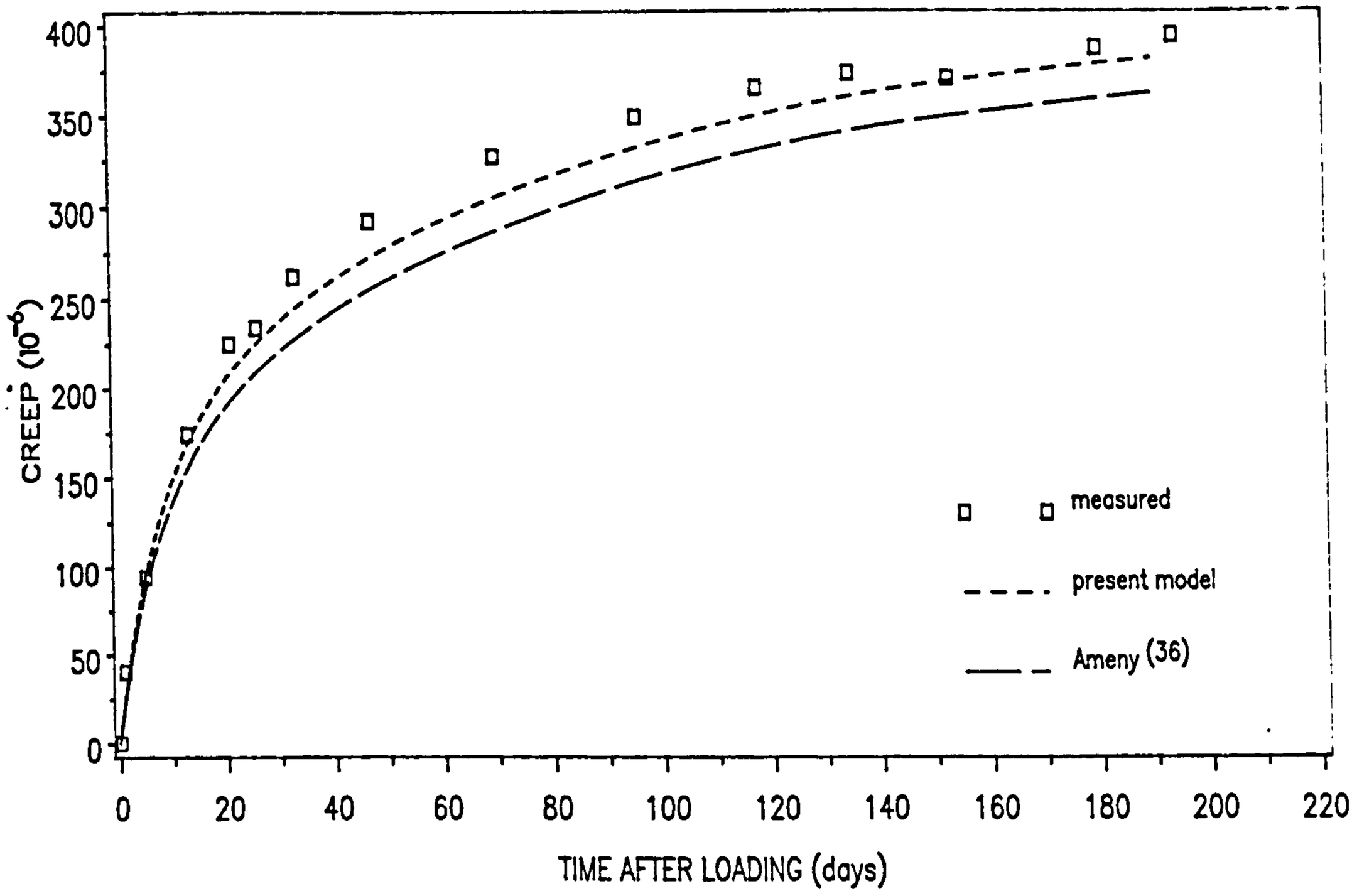

Fig. 7.25 – Comparison of Vertical Creep Prediction Using Composite Models for Concrete Single–Leaf Wall

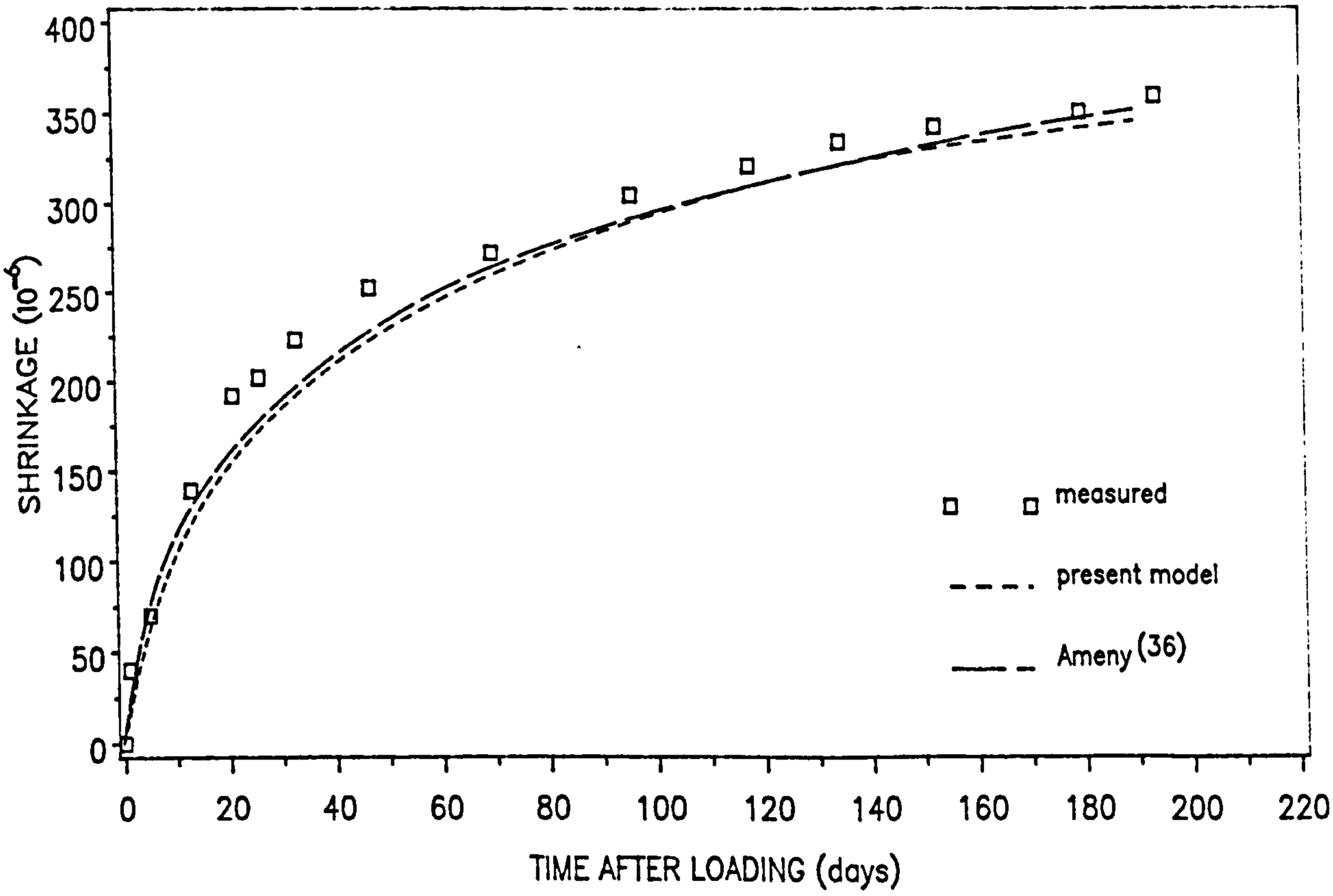

Fig. 7.26 – Comparison of Vertical Shrinkage Prediction Using Composite Models for Concrete Single–Leaf Wall

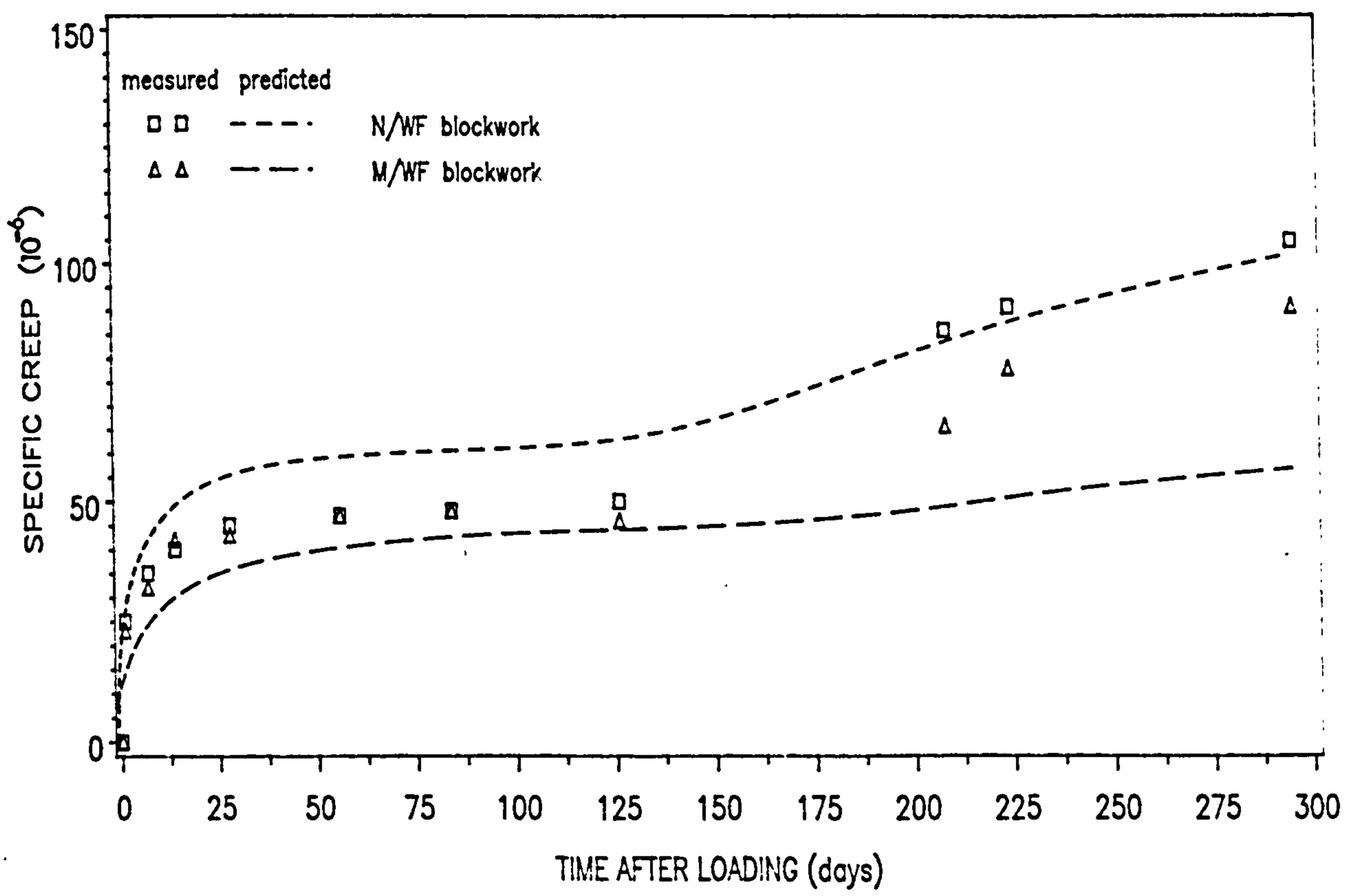

Fig. 7.27 – Composite Model Prediction for Vertical Creep (Eq.(4.24)) on Data of Ameny et al[38]

CHAPTER 8

DISTRIBUTION OF STRAIN

8.1 Introduction

During the time-dependent tests, measurements were made for the 13-course masonry units to record the distribution of strain over the height of the masonry and to record the strain in centrally embedded brick or block. This chapter discusses those measurements.

8.2 Vertical strain

Vertical strain measurements were made using 150mm and 200mm Demec gauges for clay/calcium silicate brickwork and concrete blockwork, respectively. These measurements also served to confirm the measurements made by 750mm and 400mm Demec for the overall strains described in previous chapters. Generally, the difference of measurement between the shorter and the longer gauges was found to be less than 5%.

8.2.1 Load strain

Figures 8.1, 8.2 and 8.3 show the variation of load strain (elastic plus creep strain) over the height of clay, calcium silicate and concrete masonry, respectively, for four periods. It is apparent that there exist significant differences in the strain profile between the different types of masonry and also between the different geometries of each masonry, and generally the profiles of load strain do not show any consistent pattern.

For clay brickwork, except for cavity wall, the upper and lower section of the masonry showed opposite trends, i.e. while the upper section of single-leaf wall exhibited higher strain than the lower section, the hollow and solid piers showed the opposite effect. Except for the single-leaf wall, the maximum strain (being about 30%

higher than the overall strain) occurred at the lower section near to the base of the brickwork. Also, strains at the central section of masonry are generally higher than the average strain, the exception being the cavity wall.

For calcium silicate brickwork, the profile of single-leaf wall and hollow pier exhibited an approximate S-shape with maximum strain over the top section, and the minimum strain occurring at the bottom section of the brickwork. The profile of the cavity wall and solid pier exhibited an opposite trend with an approximate Z-shape. The strains at the mid-height of single-leaf and cavity walls were up to 35% higher than the average strain whereas the mid-height strains of hollow and solid piers were slightly lower.

In contrast to the clay and calcium silicate single-leaf walls, the concrete single-leaf wall showed the minimum strain at the top section of the wall. The strain profiles of the cavity wall and hollow pier showed an approximate C-shape with the minimum strain at the central section of the masonry, while, the solid pier showed an approximate Z-shaped strain profile with the minimum strain at the base of the masonry. The maximum strains were generally 25% higher than the average strain.

Overall, the profiles of load strain for calcium silicate brickwork and concrete blockwork were nearly similar for different periods under load, the process of creep did not significantly change the distribution of strain for the two types of masonry units. On the other hand, the profiles of load strain are less stable for clay brickwork. It should be noted that, however, the change in profiles of load strain depended on the profiles of the moisture strain as it was assumed that the moisture strain occurring at any section of the unloaded masonry was the same as that in the loaded masonry over the same section, which may not be correct.

Generally, there existed only small variations of the elastic strain (time of loading = 0) over the height of the wall with the position at the mid-height showing

a good compliance with the overall elastic strain. However, for the single-leaf walls, for most cases, the minimum strains occurred at the middle-third height of the walls; a similar trend was observed by Bradshaw and Hendry[121].

8.2.2 Moisture strain

The profiles of moisture strain over the height of clay, calcium silicate and concrete masonry are illustrated in Figs. 8.4, 8.5 and 8.6, respectively. More consistent results on the profiles of moisture strain were obtained than for load-strain of clay brickwork, since, for all geometry the maximum moisture strain occurred over the top section of the brickwork. However, for the clay single leaf wall, the central section gradually expands with time after undergoing an initial shrinkage at earlier periods. This effect can also be detected in the moisture strain-time curve as illustrated in Fig. 6.2, which consequently also affected the value of extrapolated ultimate shrinkage of the single-leaf wall. The reason for this cannot be readily explained, but during the tests, some horizontal cracks were noticed at the mortar bed joints over the section at the mid-height of the wall, which may have been caused by the high strain gradient. The lower strain at the base could somehow be connected to the external restraint although this should only affect the horizontal moisture strain rather than the vertical moisture strain; this subject is discussed in Section 8.4. Except for the clay single-leaf wall, the strain at the mid-height of masonry provided a good representation of the average strain. However, the maximum strain occurring can be about 40% higher than the overall strain.

Again, for calcium silicate brick, it can be seen that the single leaf wall behaved differently compared to the other brickwork geometry where the former brickwork showed minimum strain at its mid-height. In contrast to clay brickwork, for all geometries of calcium silicate brickwork, the strain levels at the top and bottom

sections of the brickwork were more or less the same with the maximum strain occurring generally at the central section, having a value of up to approximately 15% higher than the overall strain.

The different trend of the single leaf wall compared to other sizes of masonry was also observed for concrete blocks. Whereas the central section of single-leaf and cavity walls have higher than the average strains, the hollow and solid piers have lower strain. Different trends can also be seen between the top and bottom section of masonry than that of either clay or calcium silicate brickwork. Except for the single-leaf wall, the bottom section exhibited more shrinkage than the top section, being approximately up to 20% higher than the overall strain.

In general, calcium silicate and concrete masonry showed a more stable profiles with time than clay brickwork which, as described earlier, exhibited expansion as well as shrinkage. No consistent trend of the moisture strain profile can be deduced from the above observations.

8.3 Horizontal strain

The horizontal strains were measured using the 400mm Demec gauge for all masonry units, except for single-leaf concrete block walls where 750mm Demec gauge was used instead. The related figures of this section show the profile of horizontal strain taken at various sections over the height of masonry (as shown in Figs. 5.14 and 5.15) and are compared with the average values of these measurements.

8.3.1 Load strain

The profiles of lateral load strains for clay, calcium silicate and concrete masonry are shown in Figs. 8.7, 8.8 and 8.9, respectively. The lateral load strains in clay brickwork showed inconsistent trends over the height, since some sections exhibited expansion, while others contracted. For the single leaf wall, for example, there was a high strain gradient between the top and bottom sections of the wall. Also,

in some cases, there was a change from lateral contraction to an extension or vice versa. A common feature of both the vertical and horizontal strain of the clay single-leaf wall is that, as the time after loading increases, the strain gradient between each section also increases. However, generally, the level of horizontal extension or contraction is small.

It was apparent that for the cavity, hollow and solid calcium silicate brickwork the sections near the base contracted on the application of load and thereafter began to extend slowly with time as do the other sections. In most cases, the central sections (points 3 and 4) gave reasonable measurement of the average strain. In can also be seen that the top sections of the brickwork were quite unstable and do not show a uniform progression of strain with time.

As for calcium silicate brickwork, the bottom sections of concrete blockwork initially contracted after the application of load, and with time extended slowly. The maximum extension was 100% higher than the average strain and occurred at the top section, but despite this the central section behaved quite consistently in that the average strain showed a fairly uniform development with time.

8.3.2 Moisture strain

The variation of lateral moisture strains over the height of clay, calcium silicate and concrete masonry is given in Figs. 8.10, 8.11 and 8.12, respectively.

At earlier periods, overall, the clay brickwork exhibited small shrinkage before starting to expand, the maximum (up to approximately 30% higher than the average strain) occurring at different sections for different geometries of brickwork, and the minimum occurring at the base for all cases. Surprisingly, for the single-leaf wall, the variation of vertical expansion over the centre of the wall did not seem to reflect any influence on the horizontal expansion at the same section.

All the profiles of the calcium silicate brickwork exhibited lateral shrinkage, with the minimum strain occurring at the base of the brickwork and the maximum strains occurring near the central part which were generally slightly higher than the average strain. As for vertical shrinkage, the profile of lateral shrinkage of calcium silicate brickwork have nearly similar shapes over the period of testing.

Similar uniform profiles to those for calcium silicate brickwork can be seen for concrete blockwork. The difference in lateral shrinkage between the top and bottom sections are less marked except for single-leaf wall. For the solid pier, where more half-size units were used, there was a larger variation of strain, although the maxima were only 15% higher than the average strains. For most masonry, lateral shrinkage of the central section was representative of the average lateral shrinkage, the exception being one or two cases for clay brickwork.

8.4 Effect of external restraint

The external restraint to movement was thought to influence the strain behaviour of the loaded and the control masonry units in different ways.

8.4.1 Loaded masonry

Theoretically it would be expected that the profile of load strain to be symmetrical over the mid-height of the masonry but in most cases this was not so. As was reported in the previous sections there was a considerable variation of the axial load strain. Except for the single leaf walls where, the maximum strain occurred in the upper half of the walls, the maximum strain in other cases occurred in the lower half of the masonry and could be much greater than the overall average strain. The latter pattern was also reported by Brooks[41] for single leaf brickwalls which means that the present observations for single-leaf walls showed an opposite trend to that of Brooks'. Initially, the difference in pattern was thought to be due to a different loading systems. In Brooks' case, the load was transmitted to the top of the wall by spreader

beams through four rollers positioned on an embedded steel platen to provide a uniform distribution of stress across the wall. In this investigation, the load was applied at the ends (at corners for other geometries of masonry) such that if any bending of the steel platens occurred there would be higher stress concentrations at the ends of the wall and the loading would not be purely uniaxial. However, the measurement of axial strains did not show any significant differences between the end positions and the centre position.

The difference in behaviour between the single-leaf walls and the rest of the masonry may have been related to the 2-bar loading system which might have initially induced an eccentric load not only between the two faces of the wall but also between the narrow sides of the wall; the bars were tensioned alternately in small load increments, but each time when one bar was tensioned it also altered (usually increasing) the stress in the other bar quite significantly resulting in a 'surge' of stress. This resulted in non-uniform load distribution during the loading process although, finally, equal forces on each bar were attained. This was not a problem when the 4-bar system was used for the concrete single-leaf wall.

For the cavity walls, the profile of axial load strain of calcium silicate brickwork behaved differently from clay brickwork and concrete blockwork. All the hollow piers do not show any similarity in behaviour while for the solid piers, concrete blockwork behaved differently from the brickwork. The comparison of axial load strain profiles between the different geometries of the same material, or between the same geometry of different material, seem to indicate that other factors might have influenced the strain profile, for example, thickness and strength of the mortar bed joints which may have varied slightly from one course to another.

The platen effect can also be a possible cause of the 'two-stage' creep as reported by various investigators[16,38] in the case of brickwork undergoing moisture expansion. The early resultant moisture movement in brickwork is a shrinkage which

is dominated by the shrinkage of mortar but, in time, the shrinkage is opposed by the expansion of the brick units, which may result in an overall moisture expansion. In the loaded masonry unit, this expansion (upward movement in the case of vertical movement) would be restrained by the platen which would induce an additional compressive stress particularly in the mortar bed joint. Consequently, there could be an acceleration of creep rate. As the moisture expansion of clay bricks is highly variable, the foregoing effect would be localised and therefore could explain the large and inconsistent strain gradients in clay brickwork.

In the horizontal direction, a high stress concentration at the top of the single leaf walls occurred due to the relatively higher extensional strain. The lower extensions near the bottom section were undoubtedly due to the base restraint. It should be pointed out that the top steel platen was not 'bonded' with the mortar capping layer as that with the case of steel base plate; the top steel plates were lifted prior to loading (to remove the polythene sheet) and were re-positioned again, thus, possibly, providing much less restraint to horizontal movement. All the other geometries for all the types of masonry showed the effect of restraint at the bottom section near to the base even though the strain profiles were generally unstable over the time period.

8.4.2 Control masonry

It has been reported[124] that in concrete walls built on a fixed foundation undergoing thermal cooling (contraction), an induced axial tensile stress as well as induced lateral tensile stress occur in the bottom half of a restrained wall, the level of induced stress increasing as the height/width ratio decreases. The axial tensile stresses arises from the need to prevent warping of the wall due to induced lateral tensile stress caused by restraint of the foundation. The pattern of induced stress is complex such that the resulting strain at any position in any one direction is the nett strain resulting from stress plus Poisson's lateral strain. Thus, in general, the maximum induced axial strain occurs not at the bottom but somewhere in the bottom half of the wall[124]. The

resulting 'measured' strain or restrained strain is then the nett result of the induced strain plus free unrestrained strain. The same explanation can be applied for concrete undergoing shrinkage. In the design of concrete walls, the foregoing temperature effects are allowed for by restraint factors.

As reported by Brooks[41], a similar pattern is envisaged when moisture movement occurs in brickwork walls although the situation in the present investigation can be more complex with the cavity walls and piers. With shrinkage, the induced system of stress is tensile. Similarly, for loaded masonry with a compressive external load, restraint of the lateral extension of the wall will induce compressive stresses in the bottom part of the wall. In the former case, the induced tensile stress is thought to be responsible for the lower axial in the lower part of masonry. While in the latter case, the induced compressive stresses are then thought to be responsible for a greater axial strain in the lower part of the masonry (as observed for concrete single-leaf wall, all types of cavity walls, hollow and solid piers except for concrete solid piers; the clay and calcium silicate single leaf walls do not behave so because of the reasons explained earlier). It was obvious that the influence of restraint for the control masonry units is not symmetrical from top to bottom because the top had no external restraint. This may also account for the discrepancy in computing the load strain over the top half of masonry where the effect of restraint between the loaded and the control specimens are not the same.

The effect of restraint on the horizontal moisture movement is to reduce expansion at the base in the case of clay brickwork, and to reduce shrinkage in the case of calcium silicate brickwork and concrete blockwork. The variation of strain above the base is basically caused by the differential restraint due to the variation in the properties of material.

8.4.3 General remarks

The effect of restraint on the strain distribution in masonry is complex and depends on various factors such as the properties of mortar and brick or block units[41], the size and shape of the wall as well as the manner in which the load is distributed over the structure. Since, in practice, masonry of various size and shape is used with different loading patterns, it is important to know the effects of restraint since actual strain can be much greater (up to 40% and 100% for axial and lateral strains, respectively) than the overall average strain. Large local strains and, hence stresses need to be avoided or taken into account to avoid cracking due to time-dependent effects. It seems that the variation of axial strain may normally be less important than the overall strain, but it is important to take into account the variation lateral strain since this may result in local vertical cracking if the induced tensile stresses exceed the bond strength of mortar vertical joints.

8.5 Deformation of embedded brick/block

The axial deformations of a centrally embedded clay brick, calcium silicate brick and concrete block unit were measured using 50 mm Demec gauges, 51 mm acoustic vibrating wire gauges and 150 mm Demec gauges, respectively, while 150 mm and 200 mm Demec gauges were used to measure the horizontal strains for clay and calcium silicate bricks, and concrete block, respectively. Results of these measurements are based on an average of two readings except for the concrete single-leaf walls where the average is based on four readings taken from two whole blocks situated near the mid- height of the walls because there were no actual centrally embedded blocks. It should be noted that the pair of measurements made were not from the same brick or block but rather from two different units situated at similar position on opposites faces of the masonry, except in the case of the single-leaf walls.

8.5.1 Axial strain

8.5.1.1 Load strain

The axial load strains for centrally embedded units for clay, calcium silicate and concrete masonry are given in Figs. 8.13, 8.15 and 8.17, respectively. As in the part-sealed individual units, there was no clear influence with geometry of brickwork, and the load strain of embedded clay brick was approximately 10% to 25% of the overall load strain of masonry.

On the application of load, the calcium silicate brick carried about 55% the overall masonry strain, but thereafter the strain appeared to decrease before showing a slow increase with time so that, at 180 days, the brick carried about 40% of the overall strain. To a certain degree, there was an influence of geometry on the deformation, although there was no appreciable difference between the larger hollow and solid masonry. The higher strain in the single-leaf wall appears to correspond with the strain distribution over the wall, i.e. the central part showed a higher strain than the overall strain of the wall as illustrated in Fig. 8.2.

The influence of geometry on the embedded concrete block (Fig. 8.15) followed a similar trend as observed in Figs. 8.3(a)-(d) for strain distribution. The single-leaf wall exhibited a lower strain than cavity wall, a trend which can be related to the strain distribution (Figs. 8.3(a) and (b)). It can also be notice that the irregularity of strain curve (Fig. 8.15) for the single leaf wall corresponded to the strain profiles at 50 and 100 days, as shown in Fig. 8.3(a). At loading the brick strain was between 50% and 85%, and gradually changed to between 60% to 70% of the overall strain at 180 days; the lower range was for the bigger units which generally had a lower strain at the central part of the masonry.

8.5.1.2 Moisture strain

The axial moisture strain as measured on the embedded units are shown in Figs. 8.14, 8.16 and 8.18 for the clay brickwork, calcium silicate brickwork and concrete blockwork, respectively. The scatter of points in Fig. 8.14 indicated that clay bricks exhibited both shrinkage and moisture expansion although the levels are very small. The results also demonstrated similar behaviour of embedded bricks with partially sealed individual bricks, which suggested an insignificant influence of moisture absorption of brick from mortar joint. However, the extension over the mid-height of the single leaf wall, as shown in Fig. 8.4(a), appears to have not affected the behaviour of the embedded brick which infers that the mortar joints were responsible.

Shrinkage of the embedded brick in single-leaf wall was higher than that for the other geometries of calcium silicate brickwork, the effect of geometry being apparent only at later periods. The embedded bricks showed a more consistent behaviour when compared with the overall shrinkage of the brickwork, such that, at 180 days shrinkage of the brick was approximately 60% of the overall shrinkage for all the geometries of calcium silicate brickwork.

Although there was an influence of size of blockwork on shrinkage of embedded blocks, the influence was not as apparent as that for the partly sealed units, because the level of shrinkage of the embedded blocks was marginally lower than the partly-sealed units. At 180 days, the levels of shrinkage were about 75% of the overall shrinkage of blockwork for all geometries.

8.5.2 Lateral strain

8.5.2.1 Load strain

The progression of lateral strain under vertical loading for embedded clay, calcium silicate and concrete units is shown in Figs. 8.19, 8.21 and 8.23, respectively.

As for axial strain, there was a large scatter in the lateral direction for clay brick, although the magnitude of either extension or contraction was very small.

The contraction of calcium silicate brick embedded in the single leaf wall corresponded with the strain profile over the central section of the wall as illustrated in Fig. 8.8(a), probably due to the nature of loading as described in Section 8.4.1, otherwise the other bricks showed an extension but without any particular trend with geometry of brickwork, and had a magnitude as high as 80×10^{-6}.

All the embedded blocks exhibited extensions with time, corresponding very well to the strain profiles of the blockwork; the magnitude of the extension was as high as 100×10^{-6}.

8.5.2.2 Moisture strain

The development of moisture strain with time of the embedded units are shown in Figs. 8.18, 8.22 and 8.24 for clay, calcium silicate and concrete masonry, respectively. Again, there was a high scatter for the clay bricks with a tendency to expand with a very small magnitude, and there were no appreciable differences when compared to the part-sealed brick units.

The levels of lateral shrinkage of calcium silicate bricks are generally the same as that for axial shrinkage and the part-sealed units, but there was no definite trend with geometry of brickwork. Shrinkage at 180 days was about 50% of the overall shrinkage for all bricks except that the embedded in the cavity wall which was about 90% of the overall shrinkage.

The trend of lateral shrinkage of the embedded block corresponded to the trend with geometry of blockwork as that in vertical direction, the levels being approximately the same, although there was some variation at early periods. Also, the shrinkage was similar to that of the part-sealed blocks except for some cases at early periods.

8.5.3 General remarks

From the above observations it can be concluded that, for calcium silicate and concrete bricks, the strains in the embedded units show less influence with the geometry of masonry than the part-sealed units. Although the levels of strain are similar the possible reasons for this are as follows: Firstly, the exposed area to drying of the embedded units is not the same as for the part-sealed units. The overall average V/S ratios of the units in the single-leaf walls, cavity walls, hollow pier and solid piers were 44, 51, 78 and 112 mm, respectively. On the other hand, the centrally embedded bricks in single leaf and cavity walls had a V/S ratio of 51mm, while the unit centrally embedded in hollow and solid piers had a ratio of 103mm. Thus, the pattern of moisture diffusion would be different. Secondly, the embedded units are restrained as that described earlier in this chapter.

Initially, it was thought that the accuracy of prediction of strains in clay brickwork (in particular, the moisture movement) using composite models (Chapter 7) was affected mainly by the embedded bricks behaving differently from the part-sealed units. However, this was not so, since it has been stated above that there was no significant different in the strain behaviour between the two units possibly due to the low moisture absorption properties of the clay brick. Hence the variability of the bricks appear to be the possible reason for inaccuracy of prediction as readings were made from an average of only two bricks, although the general level of load strain in embedded units were not significantly different from that in the part-sealed units. However, the bricks in other parts of the brickwork could have had different properties. In this connection, observations by Ameny et al[38] are of interest; they reported similar levels of strain between embedded and individual WF bricks, but for BF blocks there was a higher creep in embedded blocks than in the individual specimen by about 6 times at early periods and by about 2 times at 300 days .

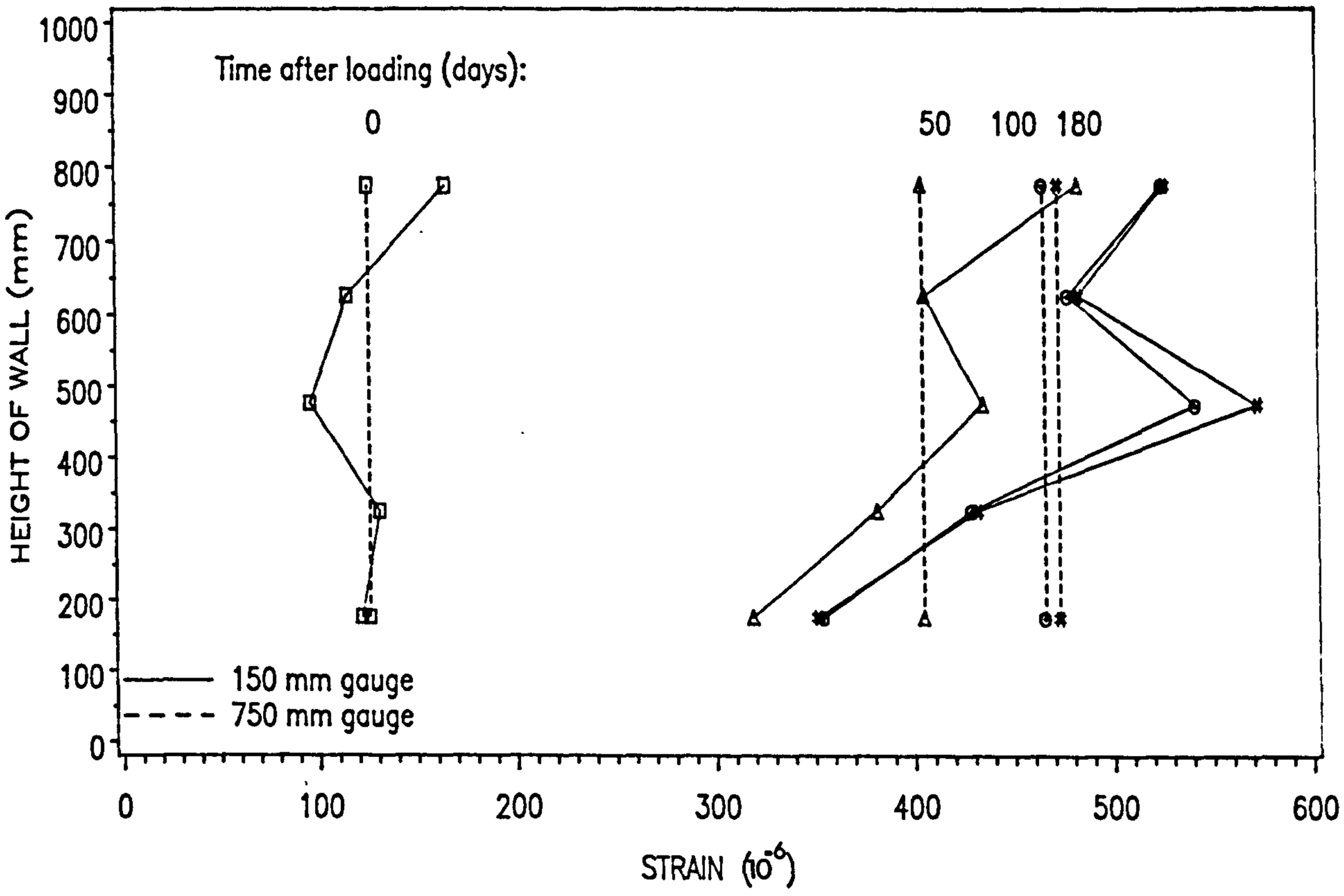

Fig. 8.1(a) – Variation of Vertical Load Strain with Height of Clay Single–Leaf Wall

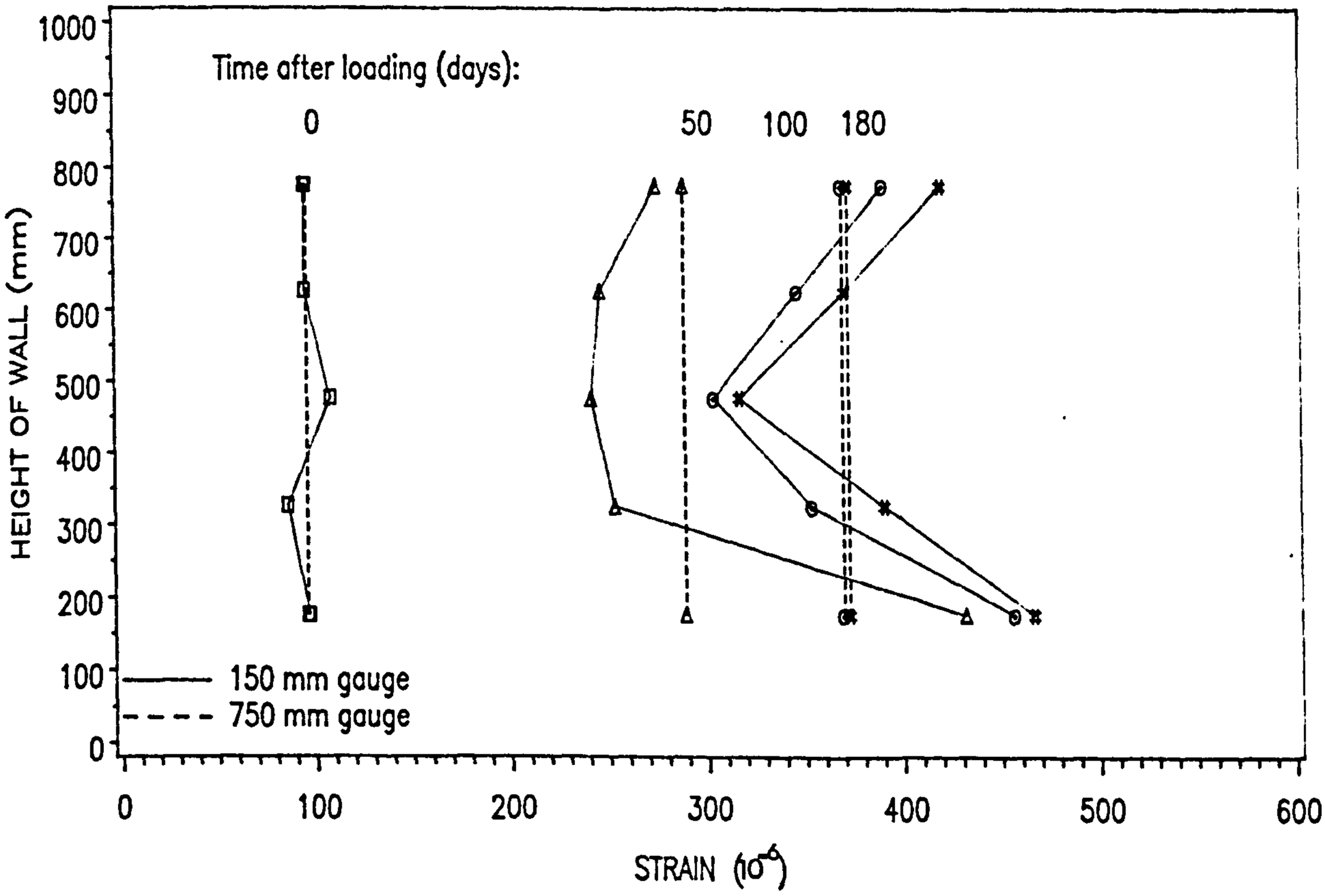

Fig. 8.1(b) – Variation of Vertical Load Strain with Height of Clay Cavity Wall

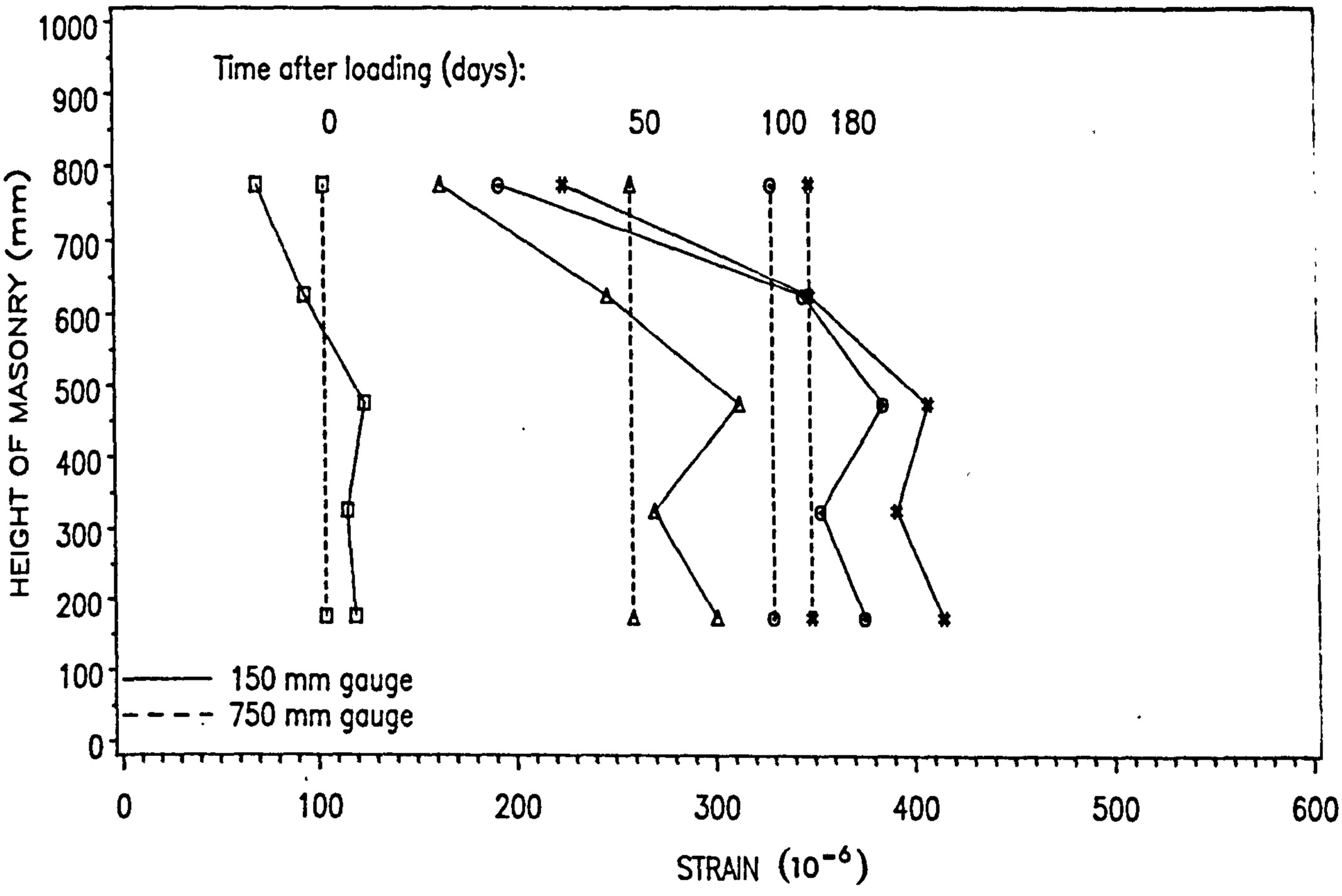

Fig. 8.1(c) – Variation of Vertical Load Strain with Height of Clay Hollow Pier

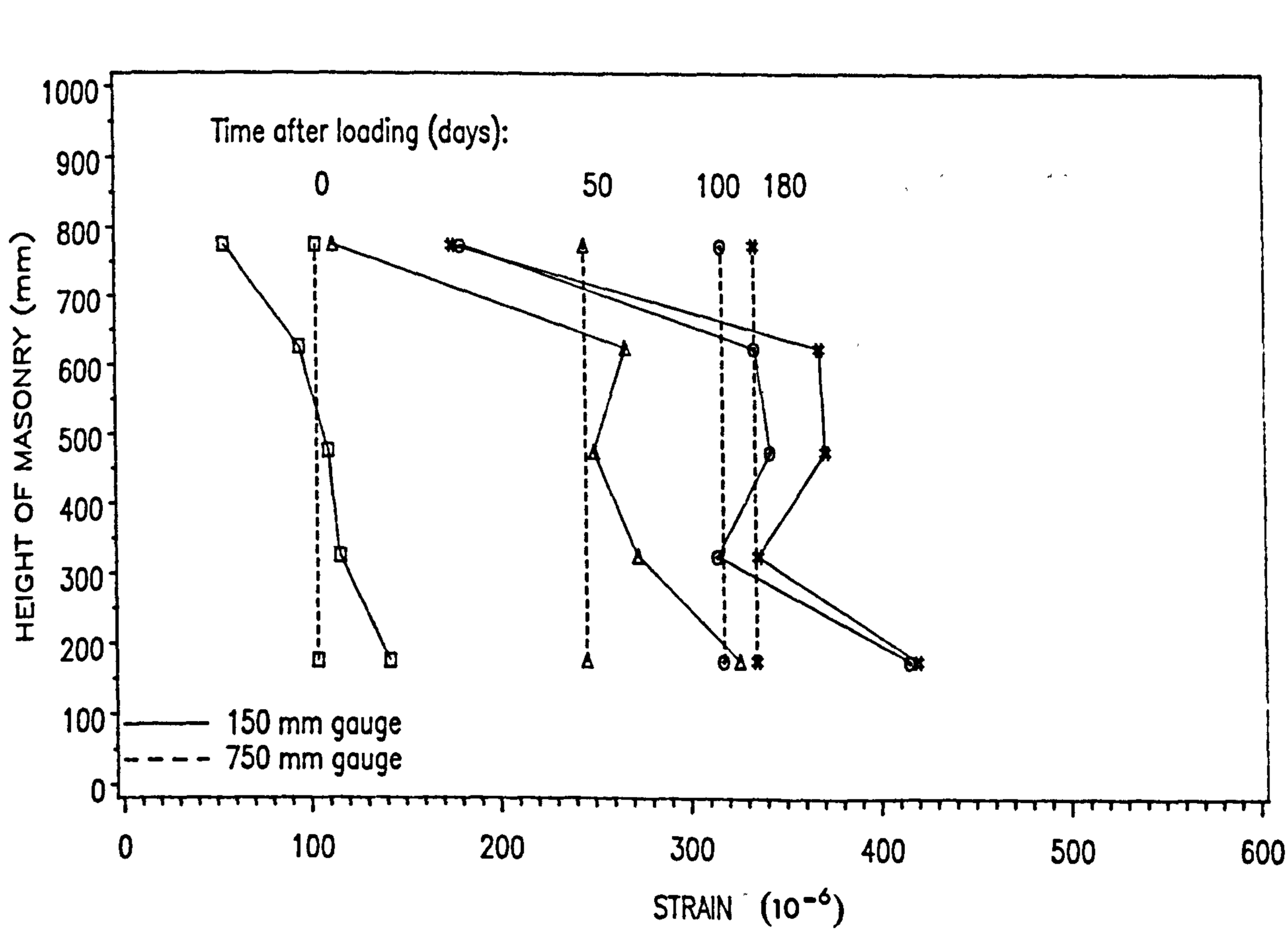

Fig. 8.1(d) Variation of Vertical Load Strain with Height of Clay Solid Pier

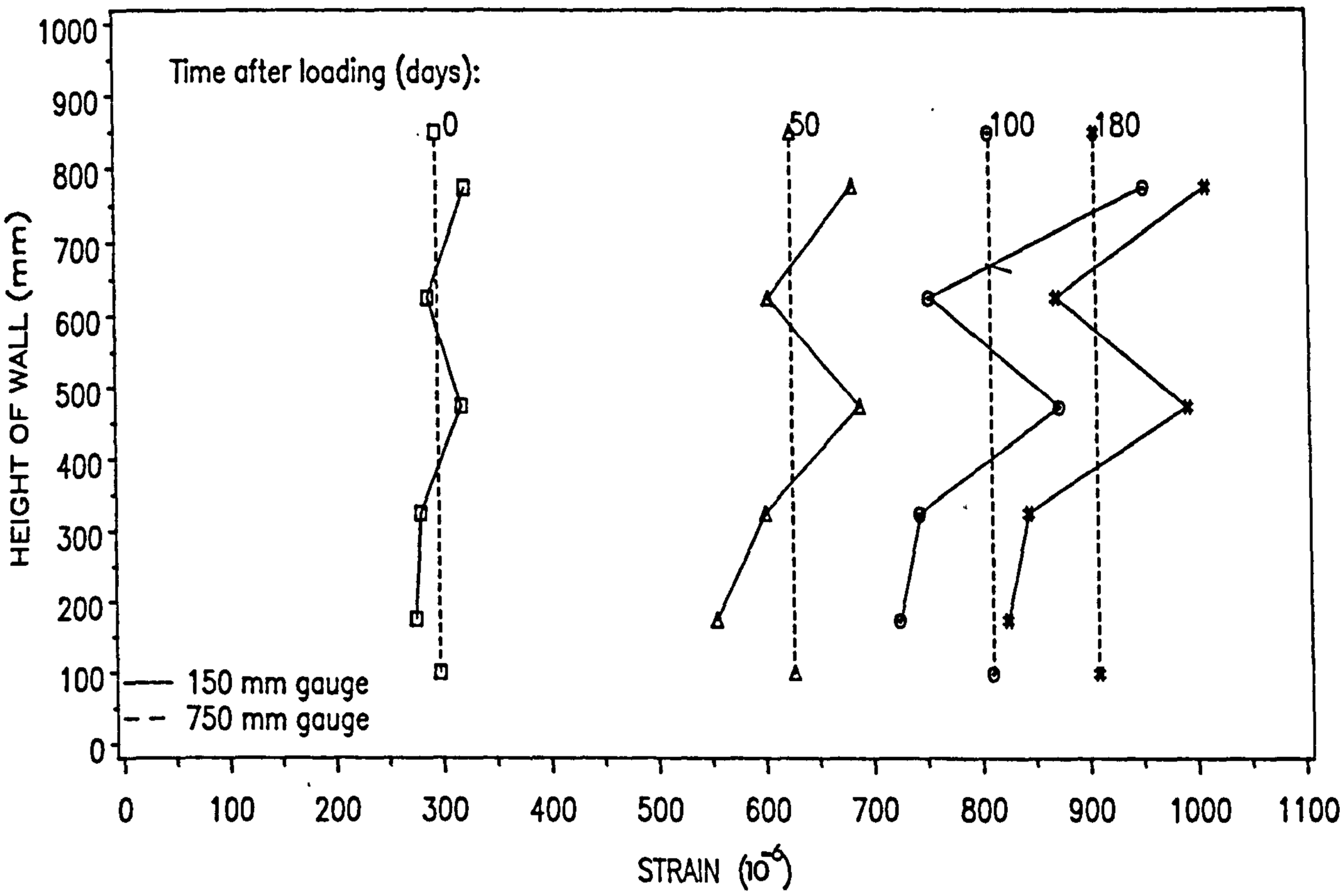

Fig. 8.2(a) – Variation of Vertical Load Strain with Height of Calcium Silicate Single-Leaf Wall

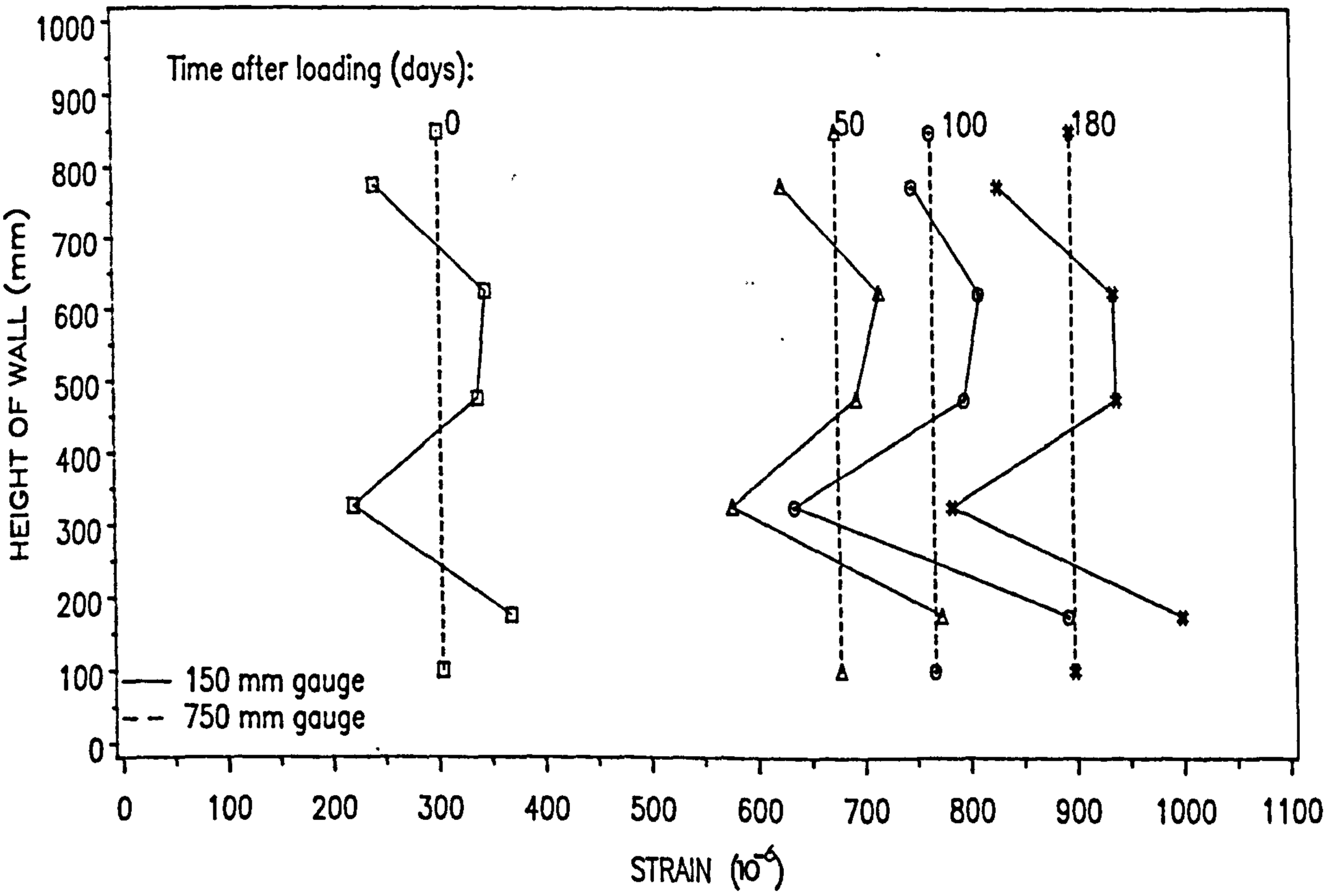

Fig. 8.2(b) – Variation of Vertical Load Strain with Height of Calcium Silicate Cavity Wall

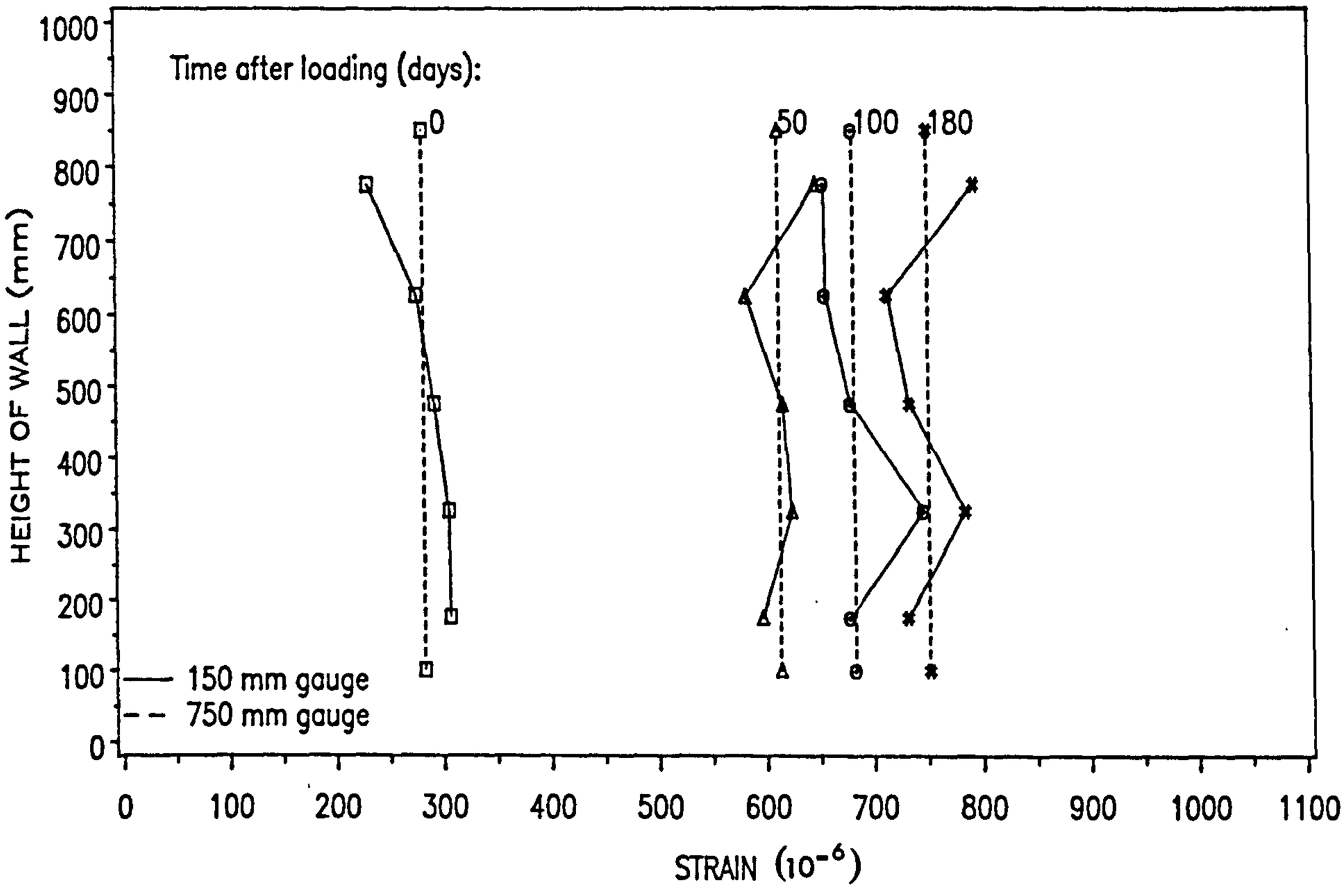

Fig. 8.2(c) – Variation of Vertical Load Strain with Height of Calcium Silicate Hollow Pier

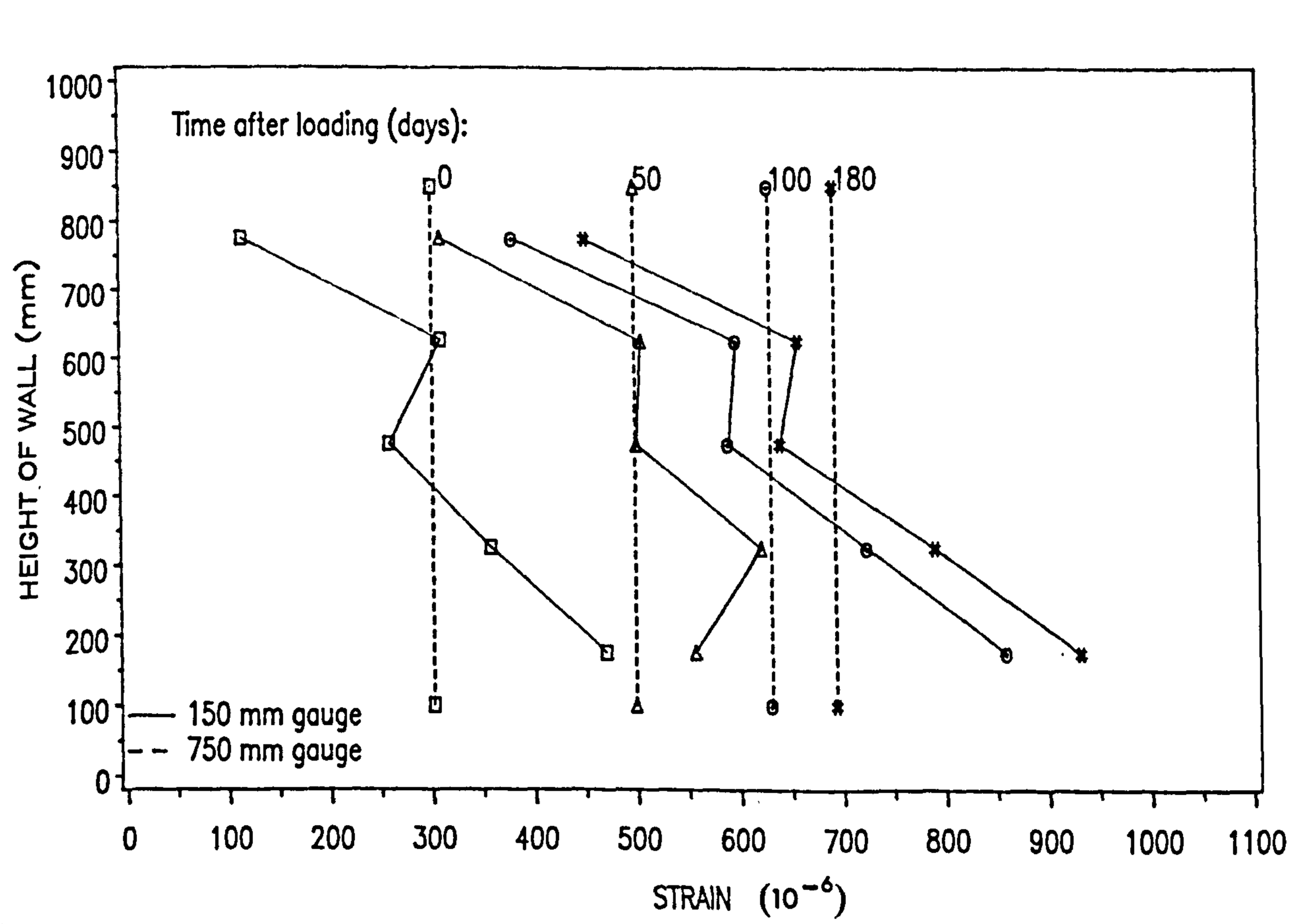

Fig. 8.2(d) – Variation of Vertical Load Strain with Height of Calcium Silicate Solid Pier

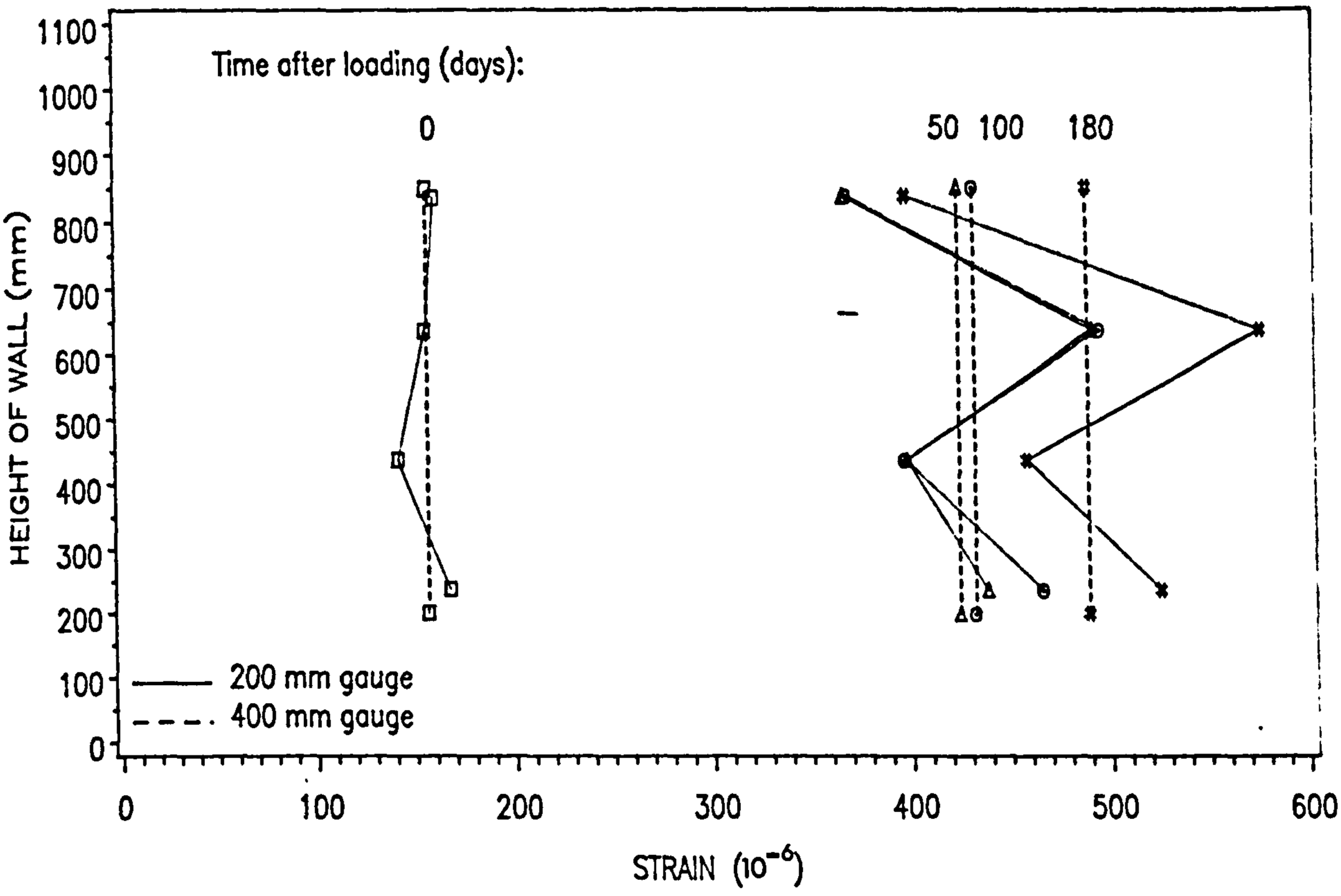

Fig. 8.3(a) – Variation of Vertical Load Strain with Height of Concrete Single-Leaf Wall

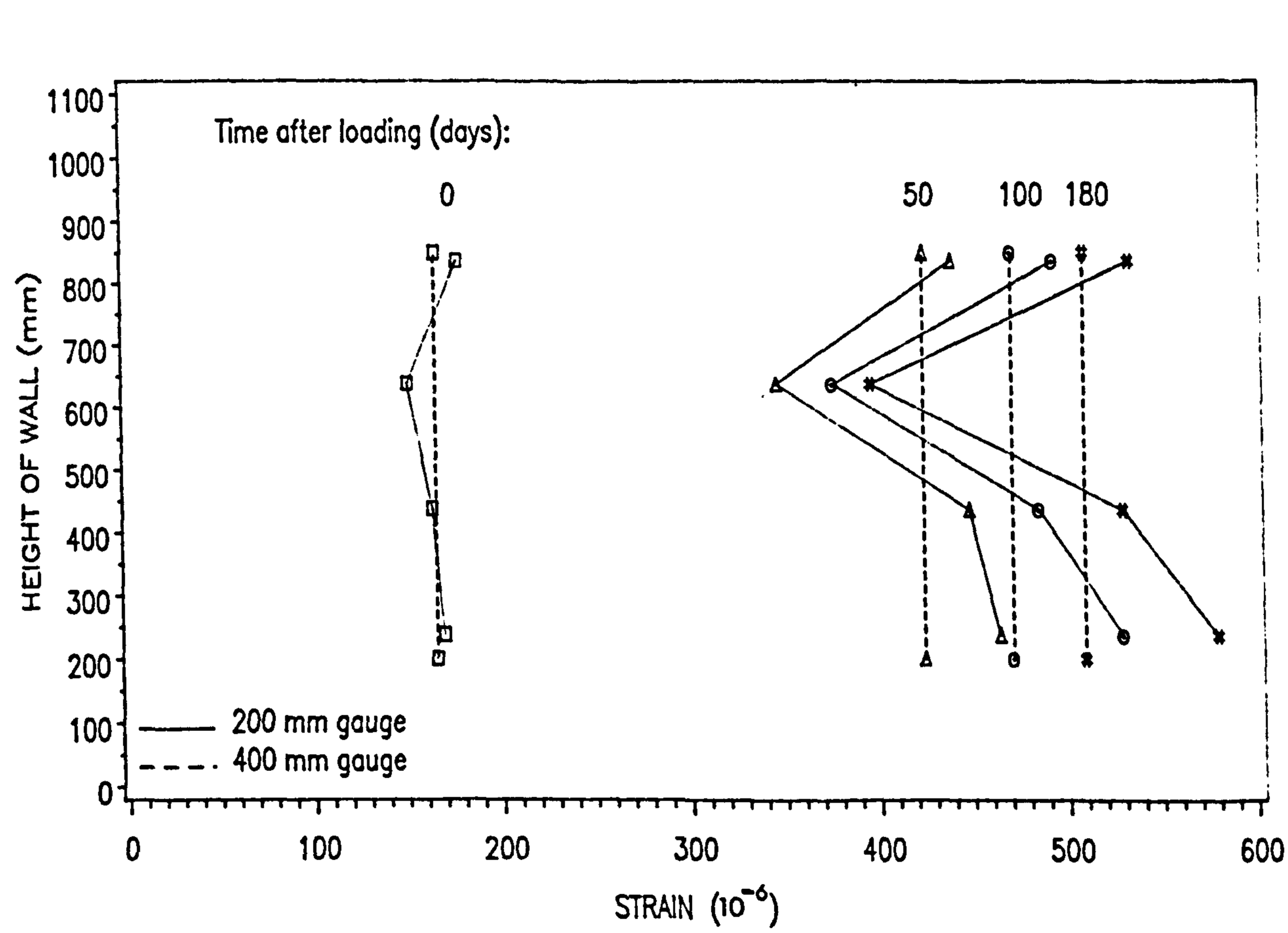

Fig. 8.3(b) – Variation of Vertical Load Strain with Height of Concrete Cavity Wall

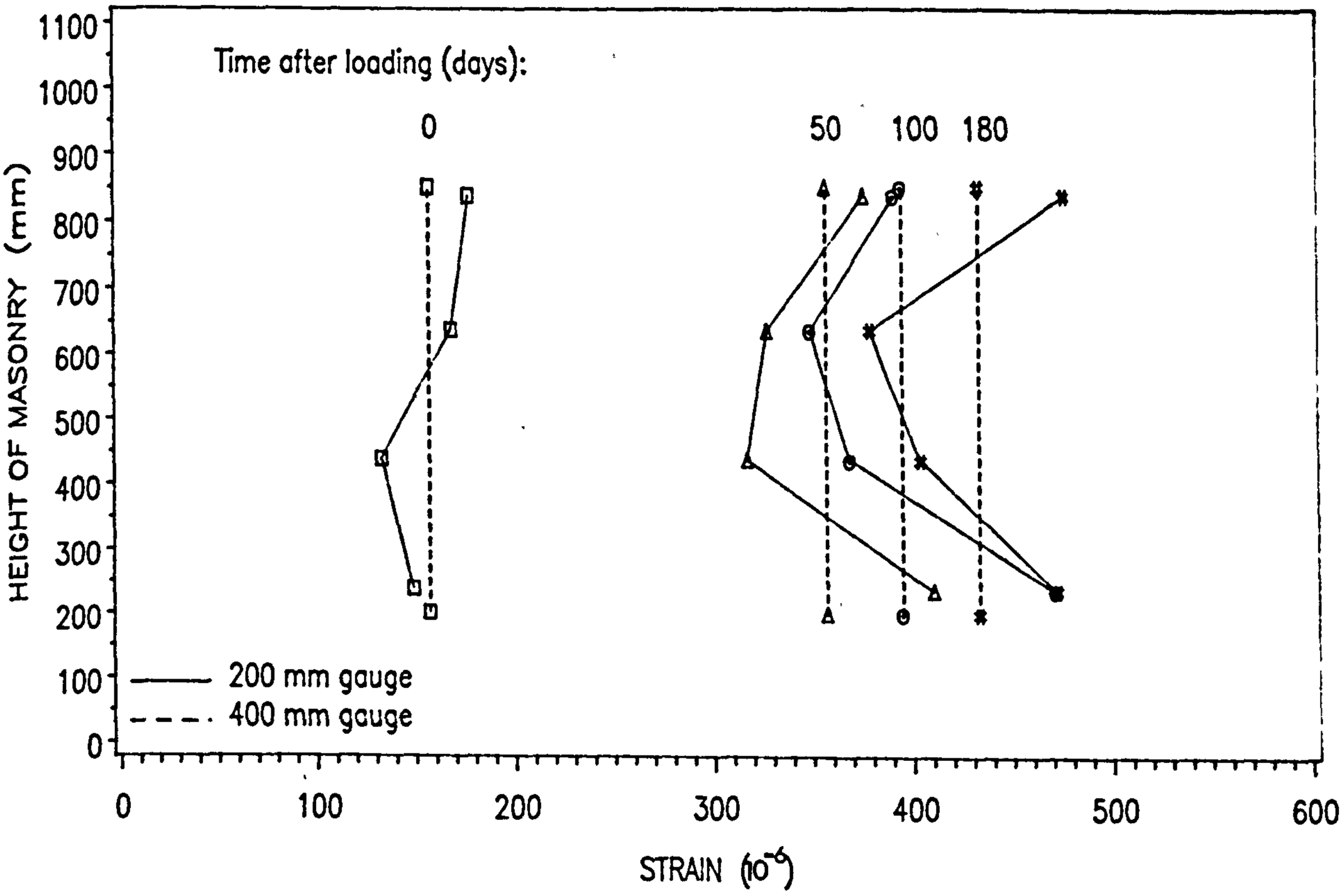

Fig. 8.3(c) – Variation of Vertical Load Strain with Height of Concrete Hollow Pier

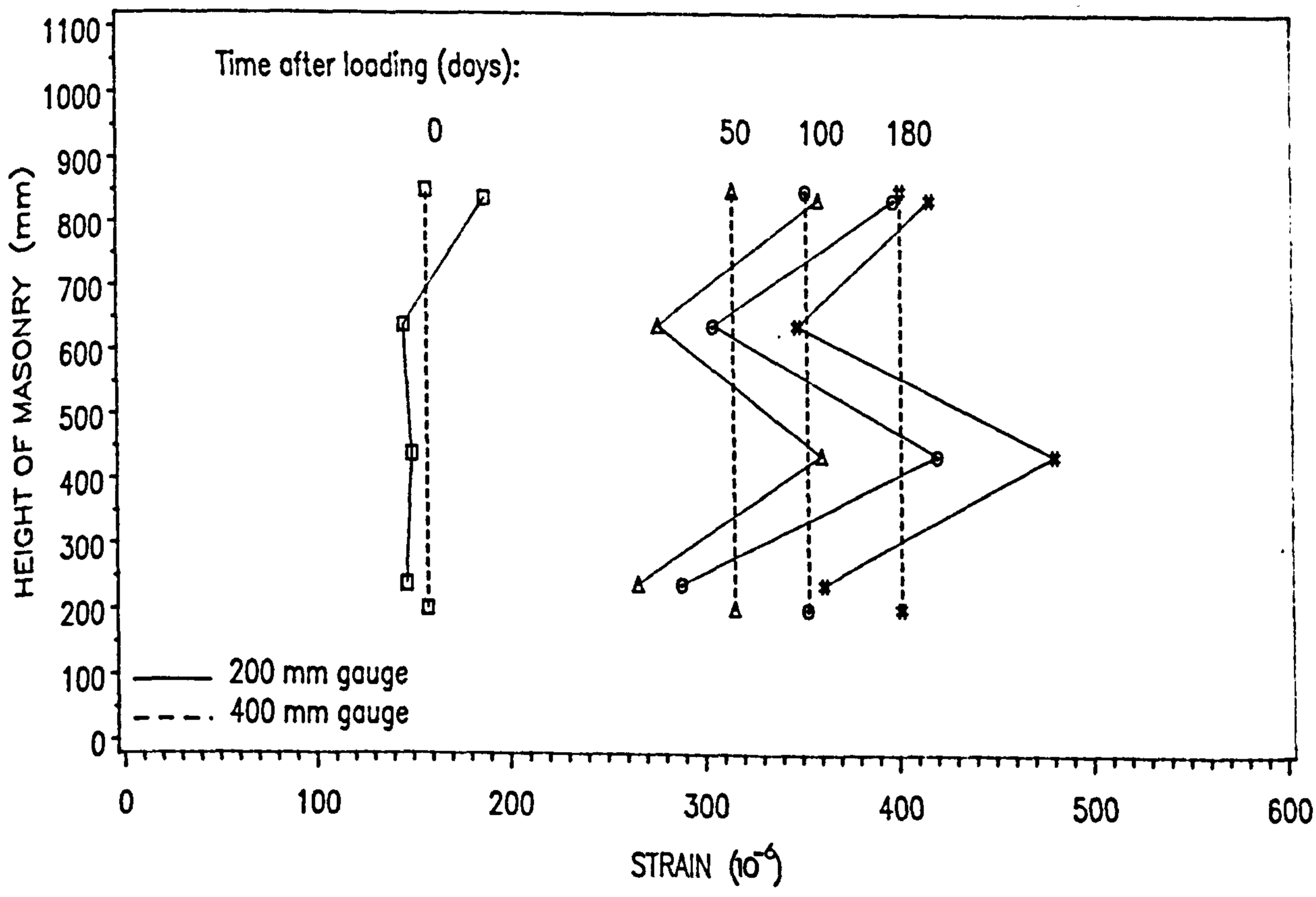

Fig. 8.3(d) – Variation of Vertical Load Strain with Height of Concrete Solid Pier

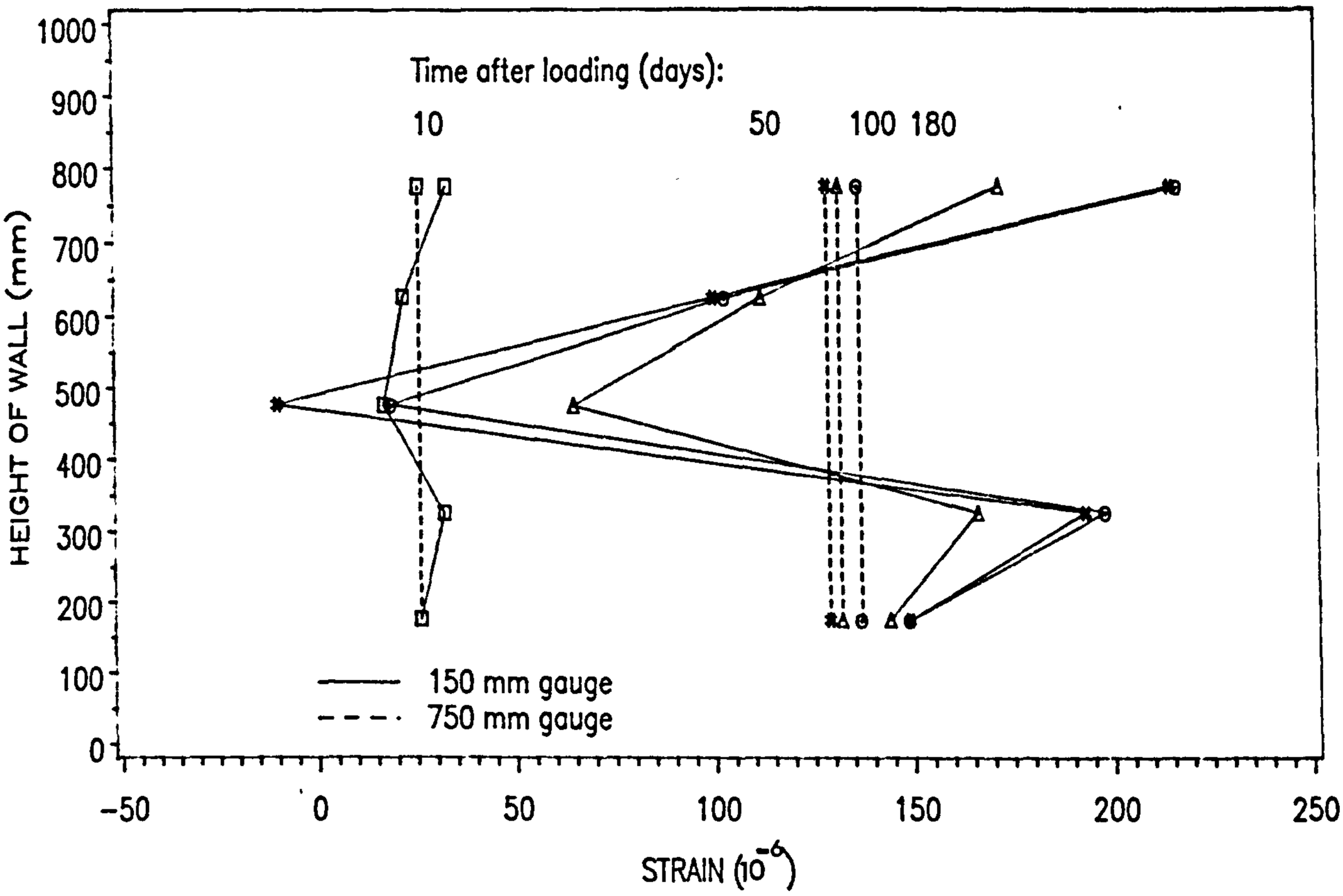

Fig. 8.4(a) – Variation of Vertical Moisture Strain with Height of Clay Single–Leaf Wall

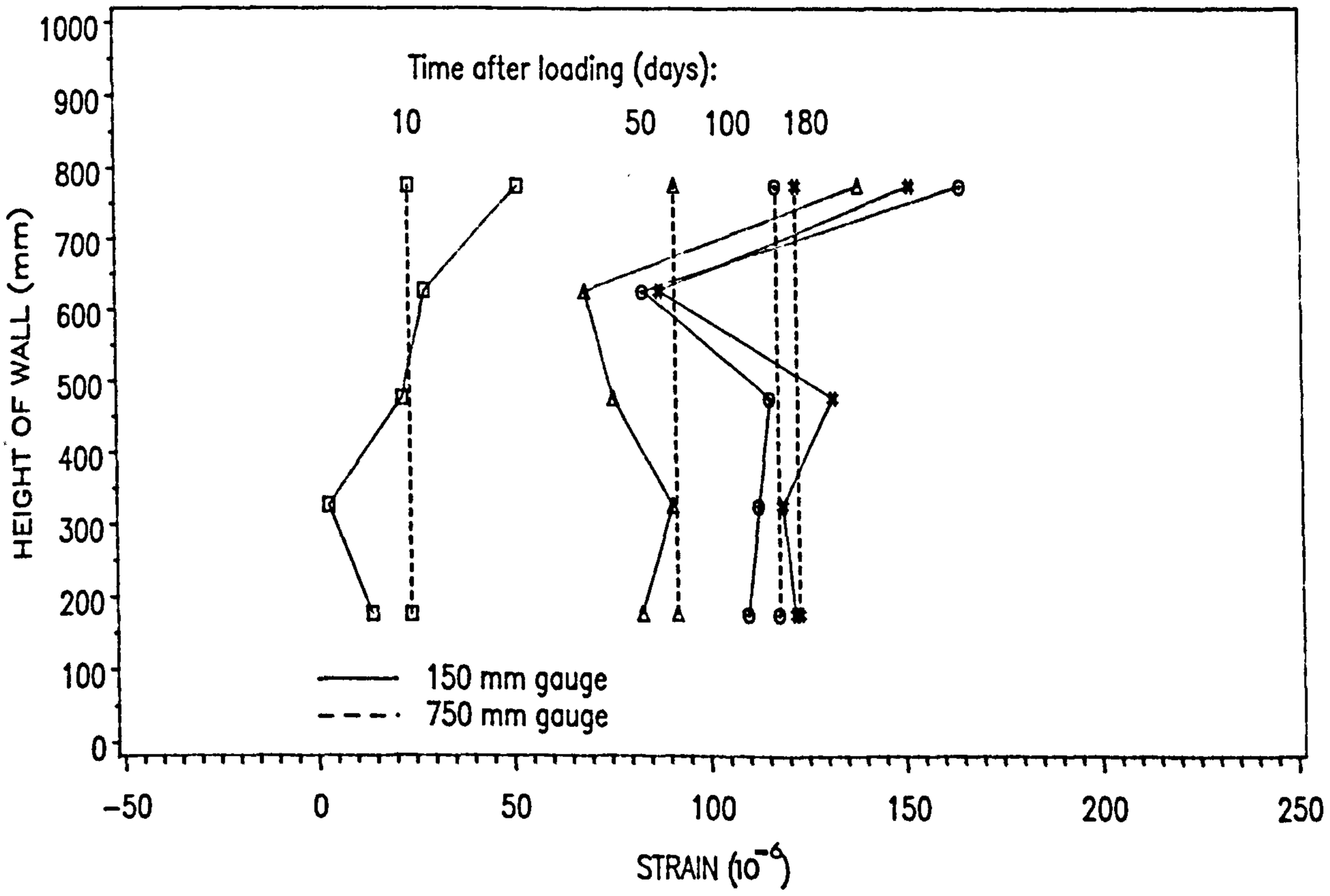

Fig. 8.4(b) Variation of Vertical Moisture Strain with Height of Clay Cavity Wall

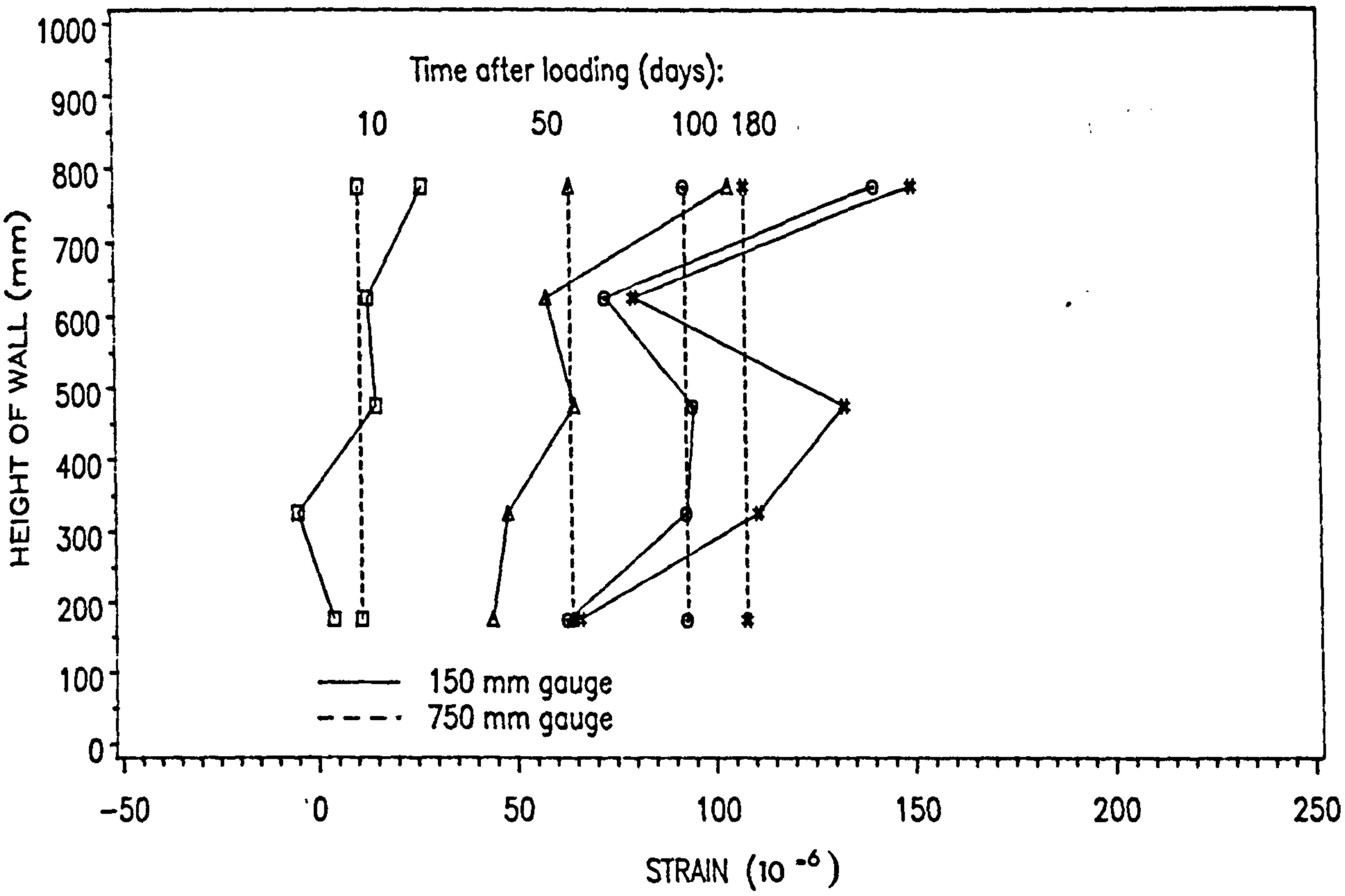

Fig. 8.4(c) – Variation of Vertical Moisture Strain with Height of Clay Hollow Pier

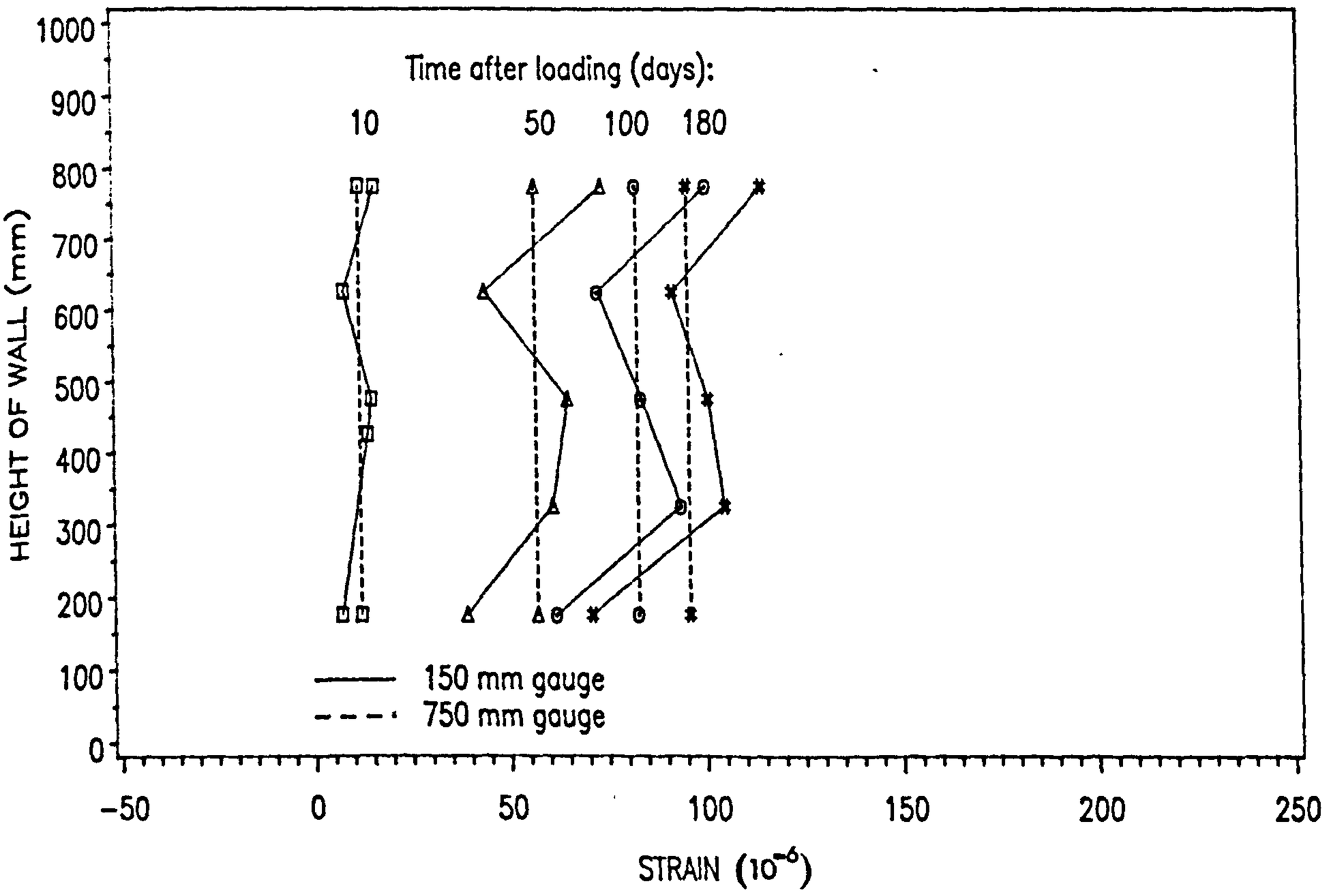

Fig. 8.4(d) Variation of Vertical Moisture Strain with Height of Clay Solid Pier

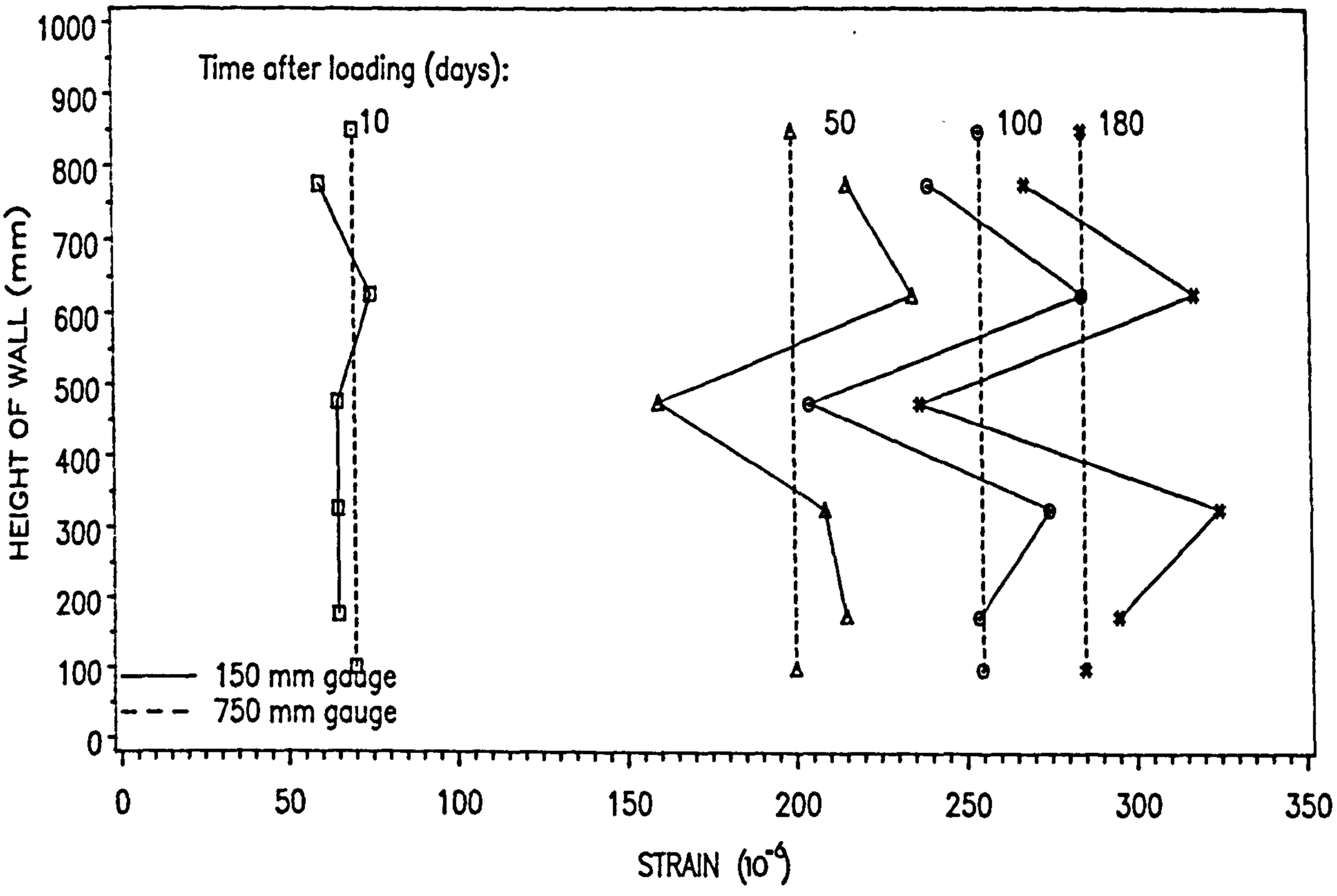

Fig. 8.5(a) – Variation of Vertical Moisture Strain with Height of Calcium Silicate Single–Leaf Wall

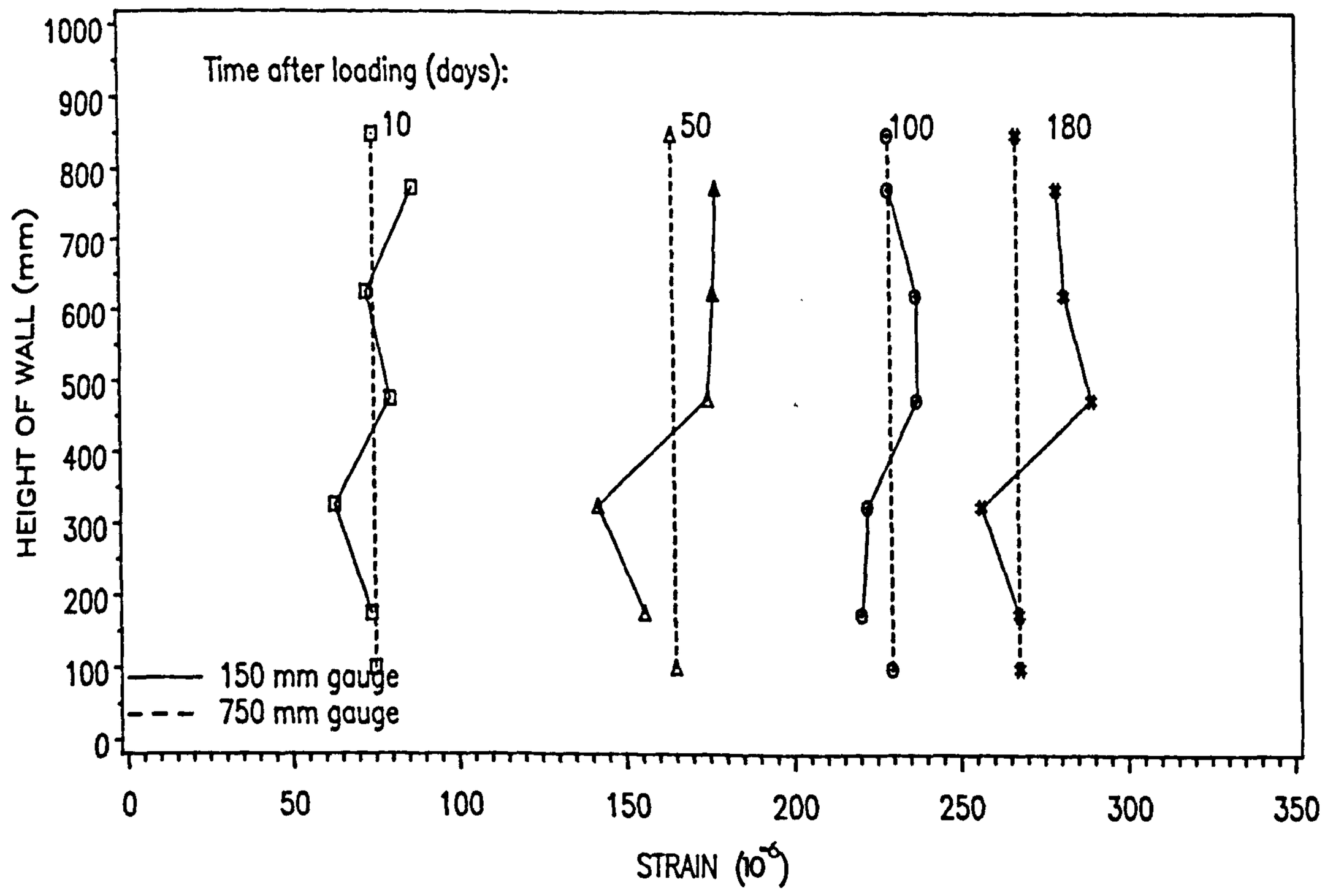

Fig. 8.5(b) – Variation of Vertical Moisture Strain with Height of Calcium Silicate Cavity Wall

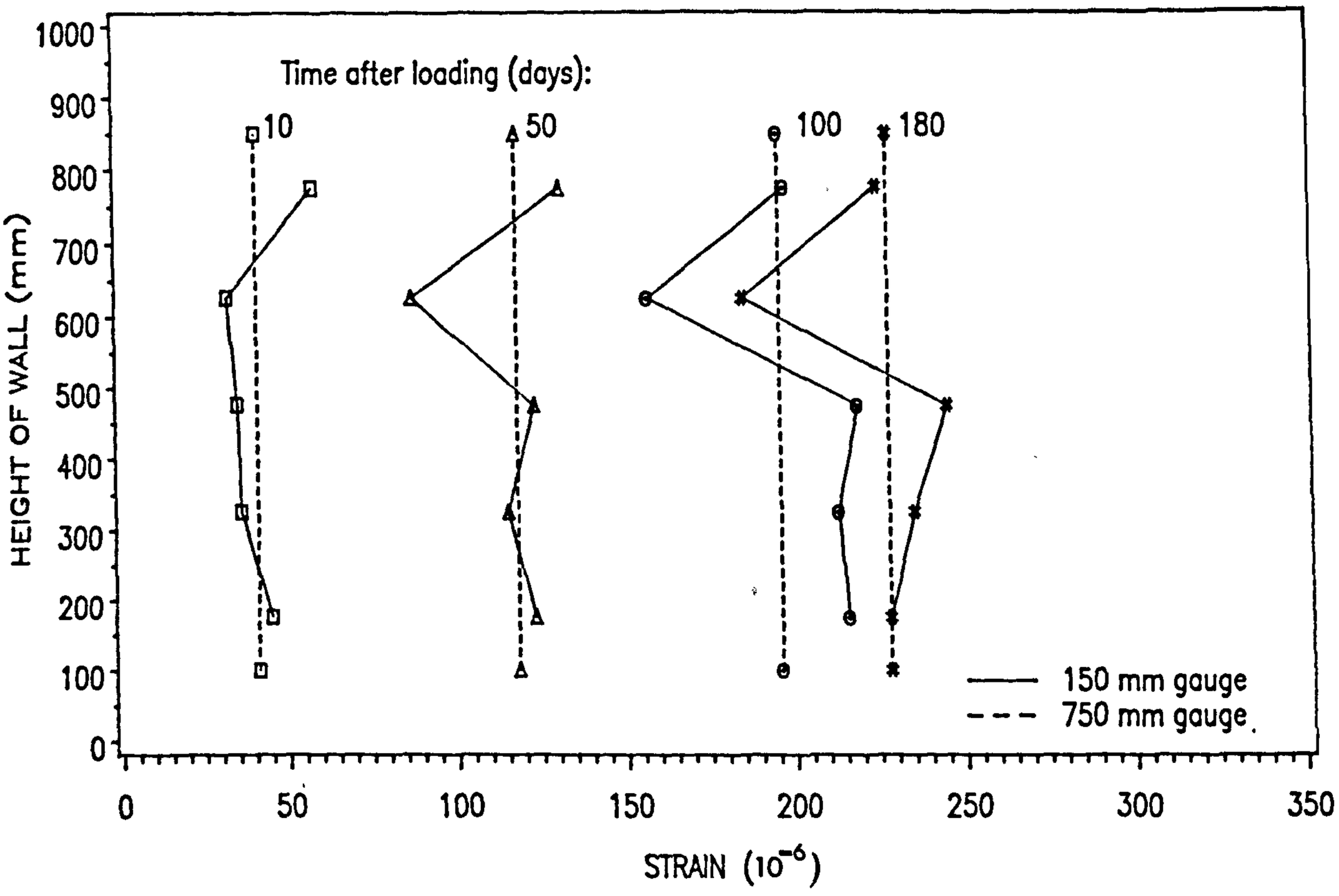

Fig. 8.5(c) – Variation of Vertical Moisture Strain with Height of Calcium Silicate Hollow Pier

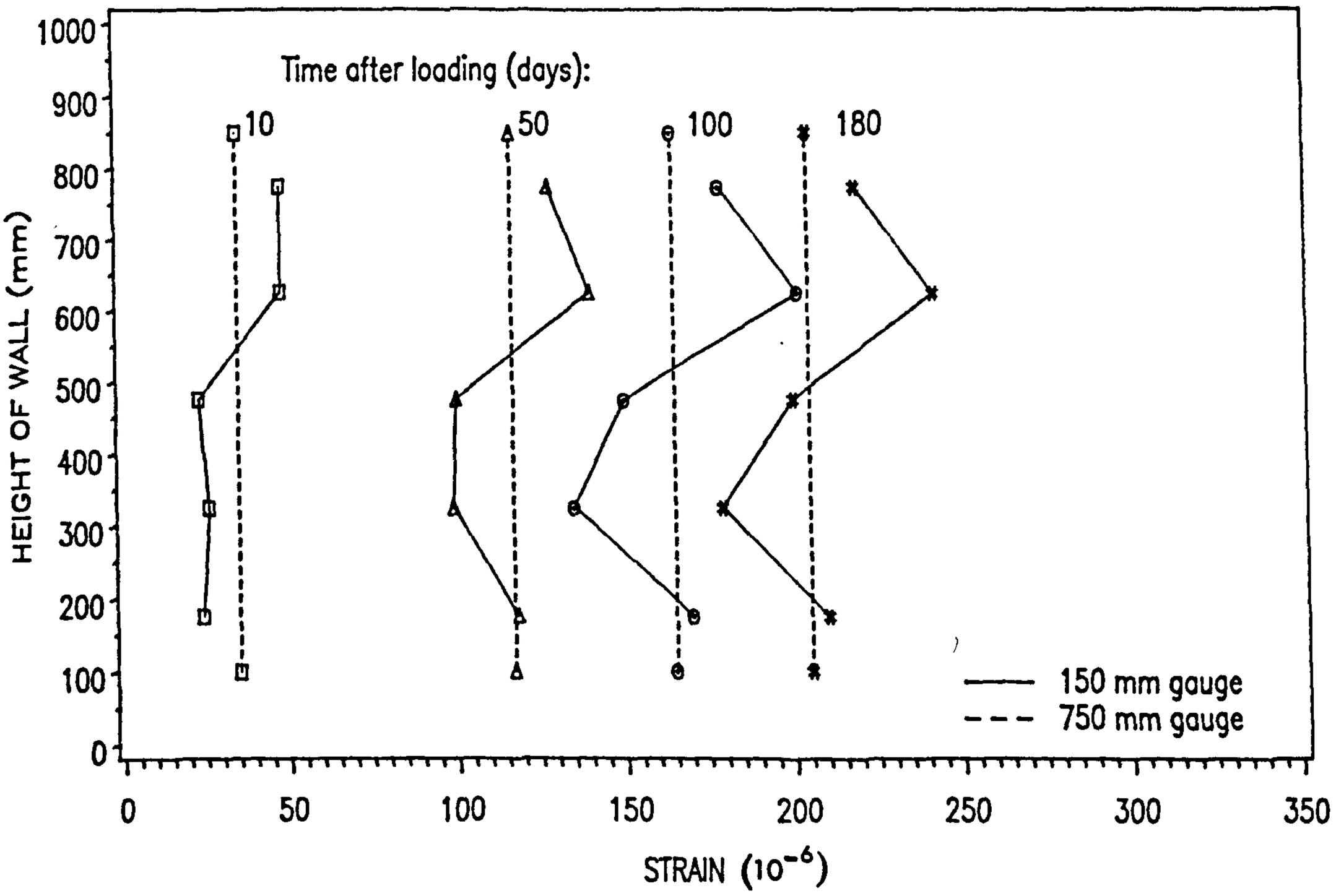

Fig. 8.5(d) – Variation of Vertical Moisture Strain with Height of Calcium Silicate Solid Pier

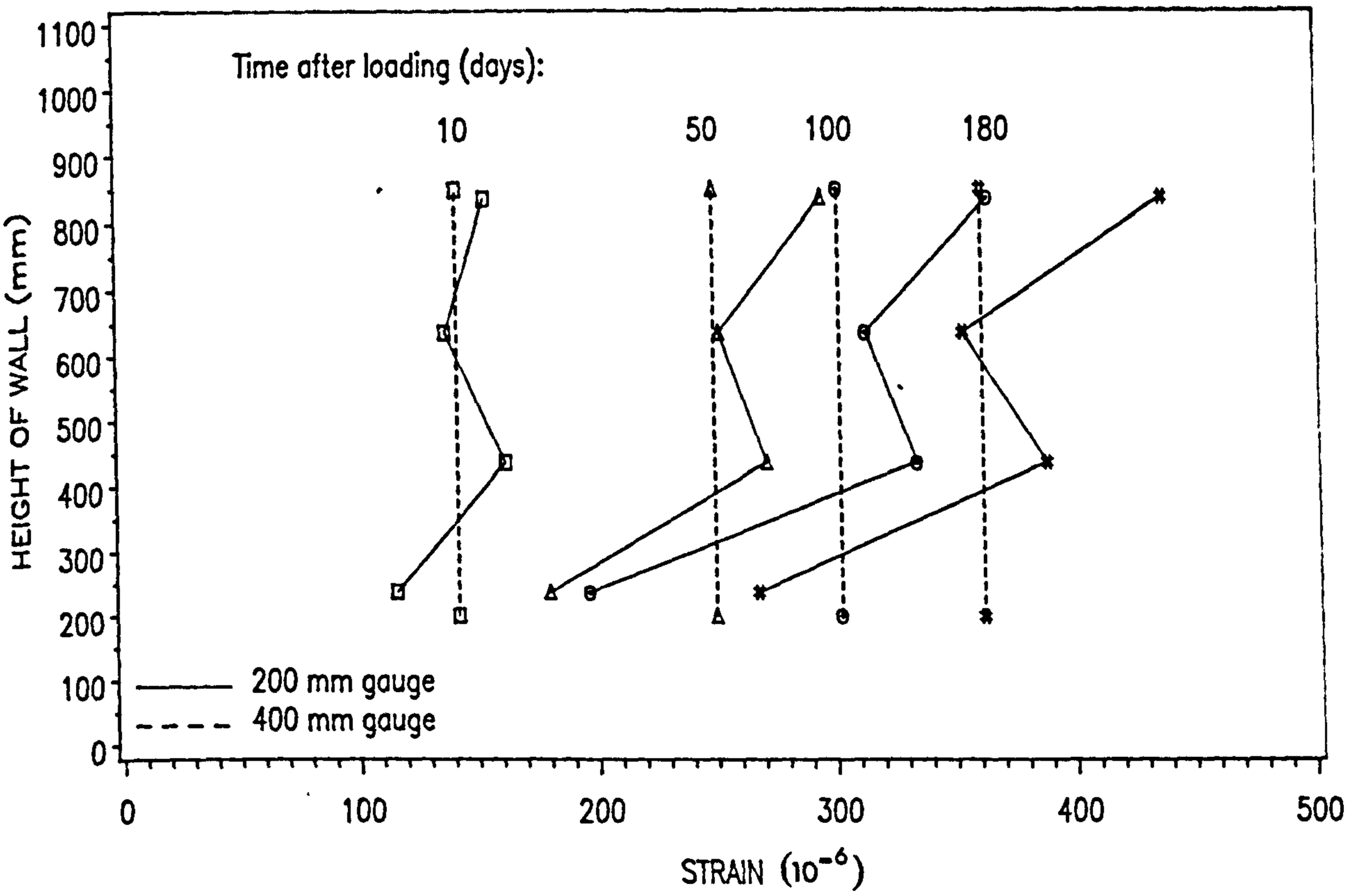

Fig. 8.6(a) – Variation of Vertical Moisture Strain with Height of Concrete Single–Leaf Wall

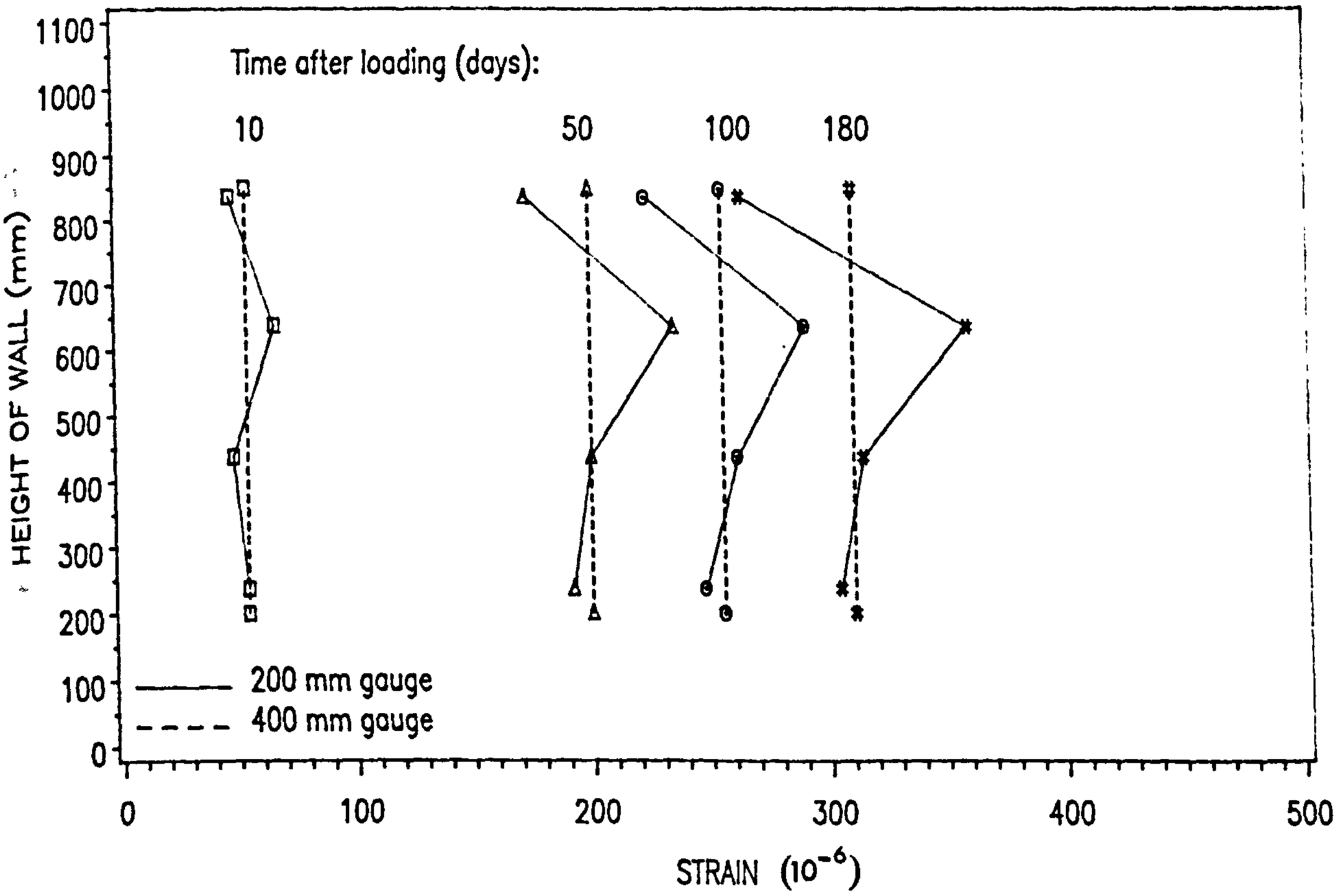

Fig. 8.6(b) – Variation of Vertical Moisture Strain with Height of Concrete Cavity Wall

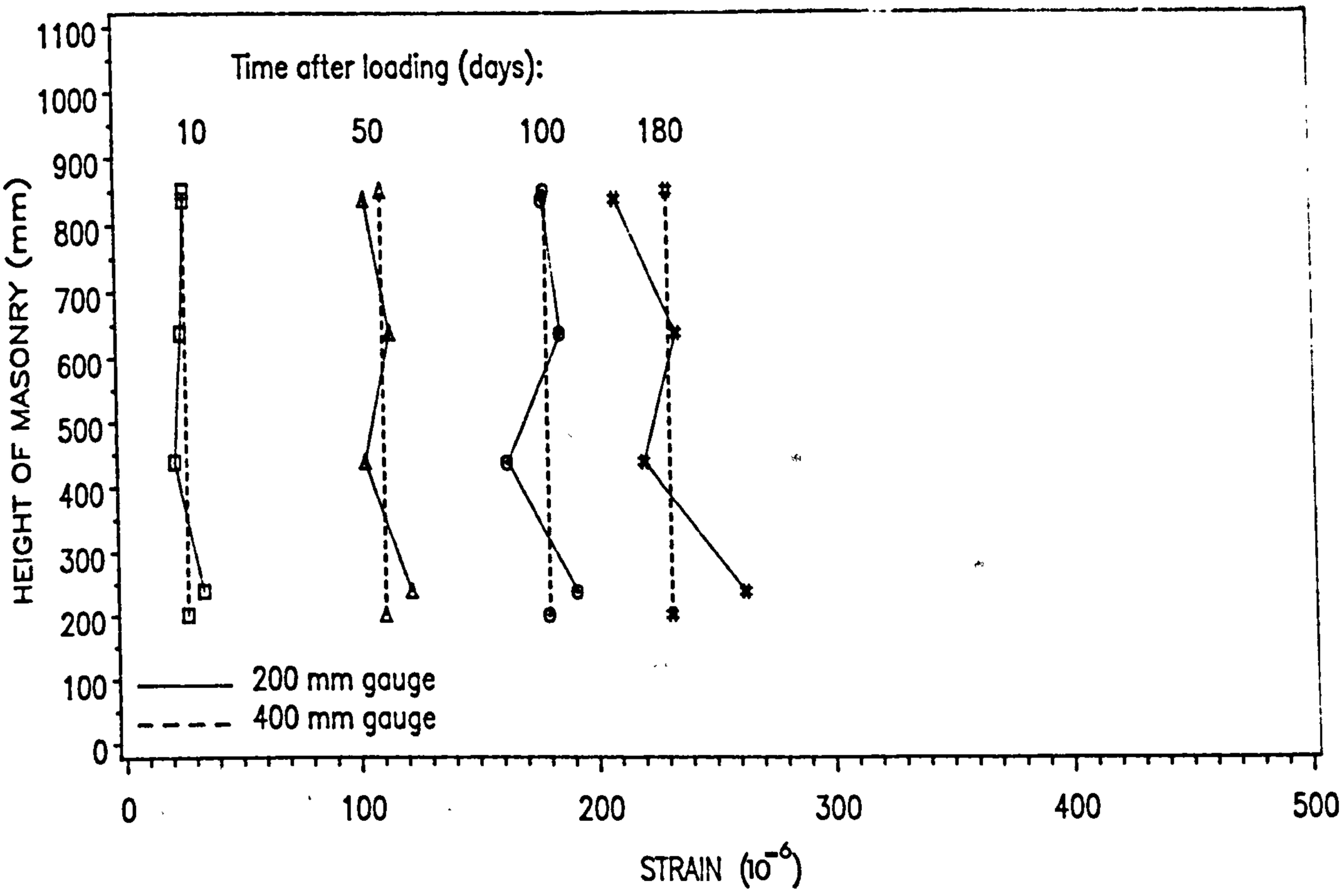

Fig. 8.6(c) – Variation of Vertical Moisture Strain with Height of Concrete Hollow Pier

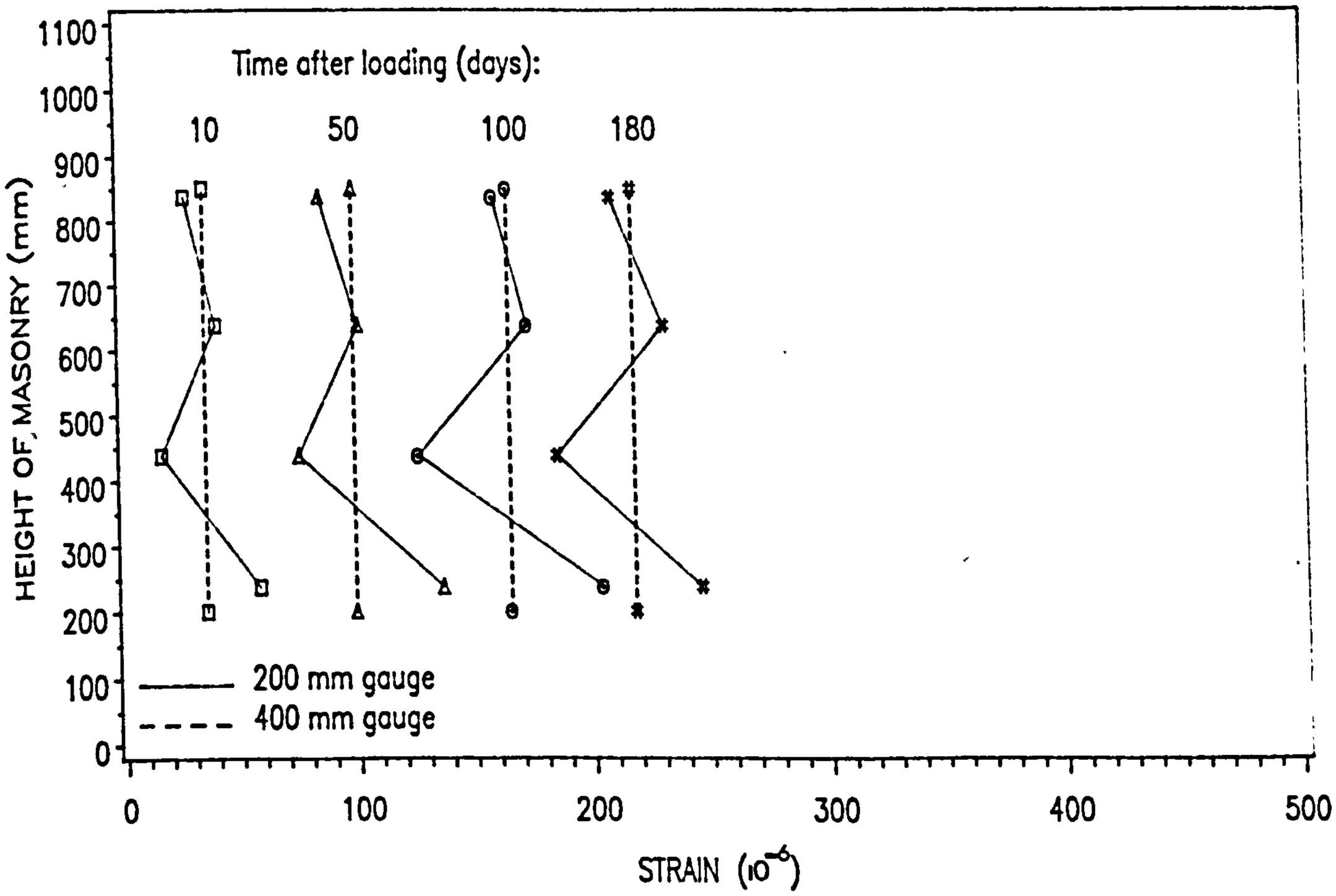

Fig. 8.6(d) – Variation of Vertical Moisture Strain with Height of Concrete Solid Pier

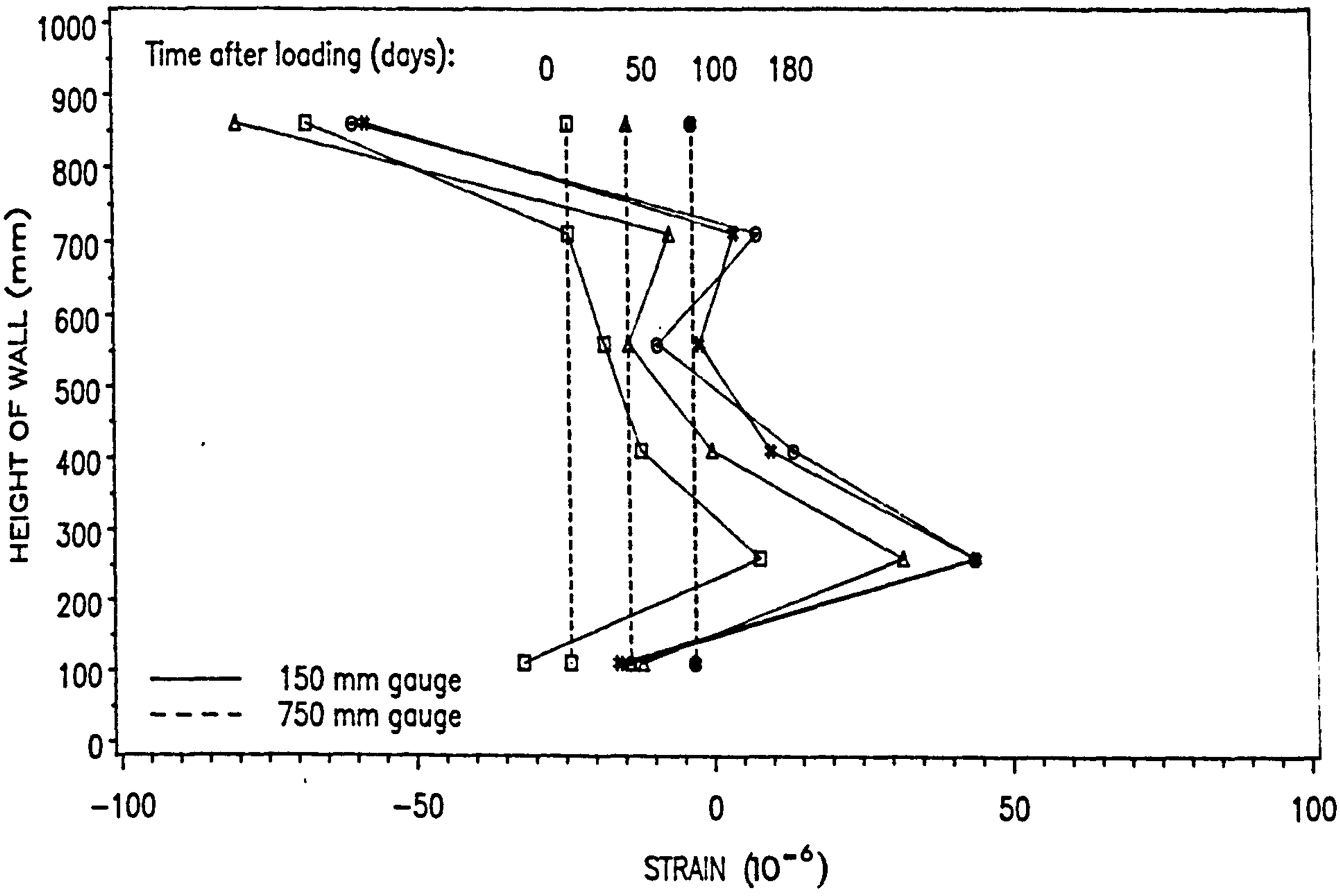

Fig. 8.7(a) – Variation of Lateral Load Strain with Height of Clay Single-Leaf Wall

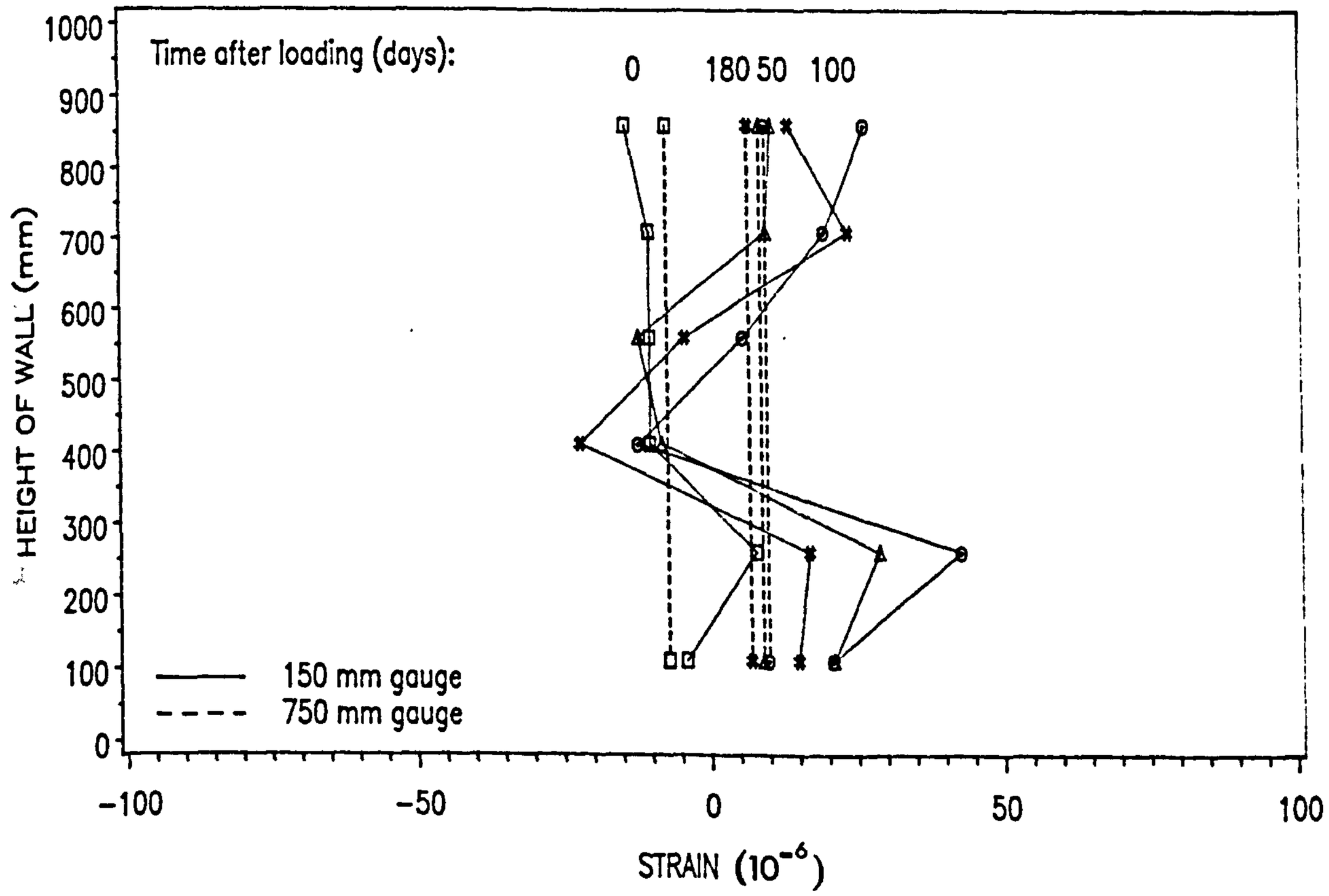

Fig. 8.7(b) – Variation of Lateral Load Strain with Height of Clay Cavity Wall

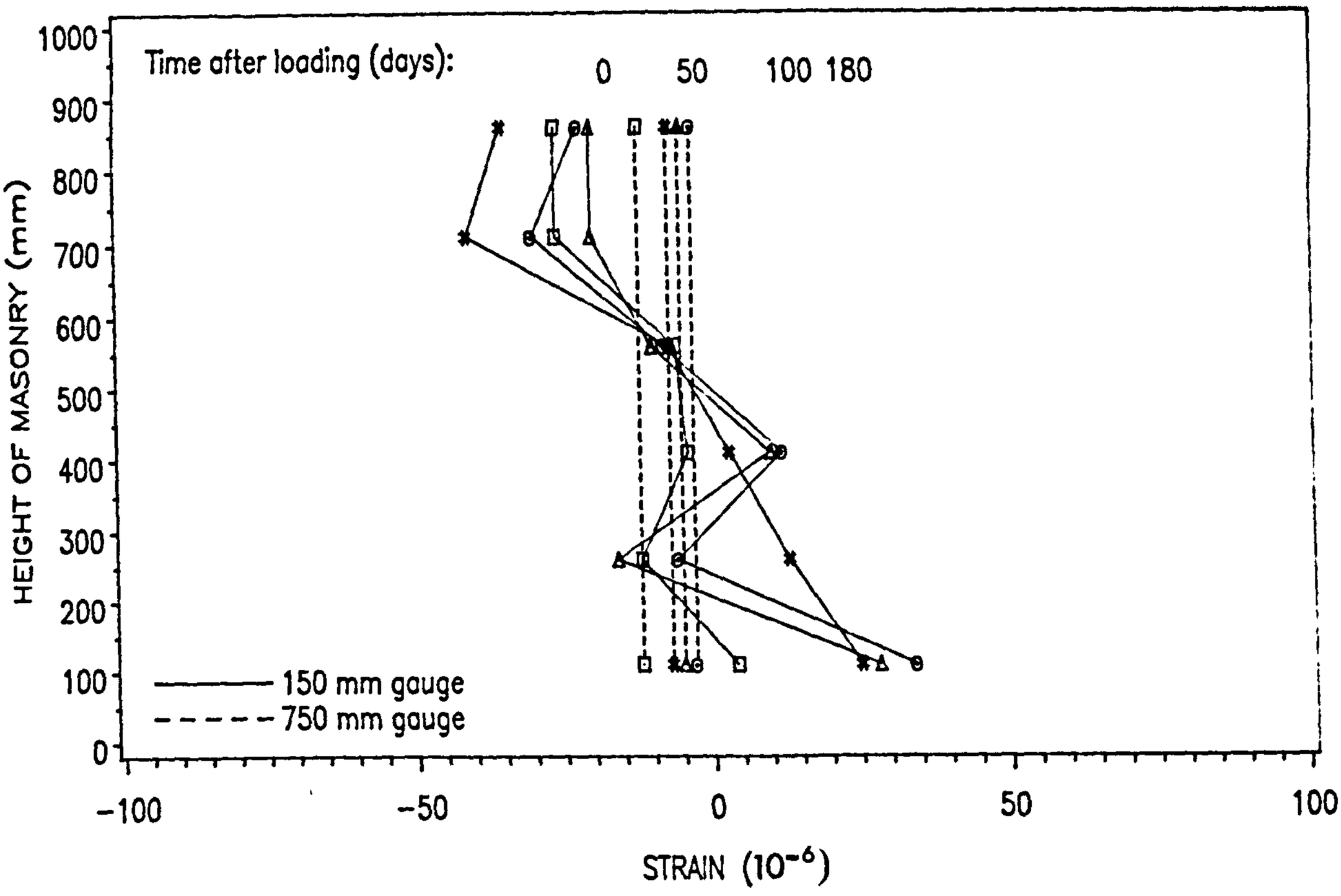

Fig. 8.7(c) – Variation of Lateral Load Strain with Height of Clay Hollow Pier

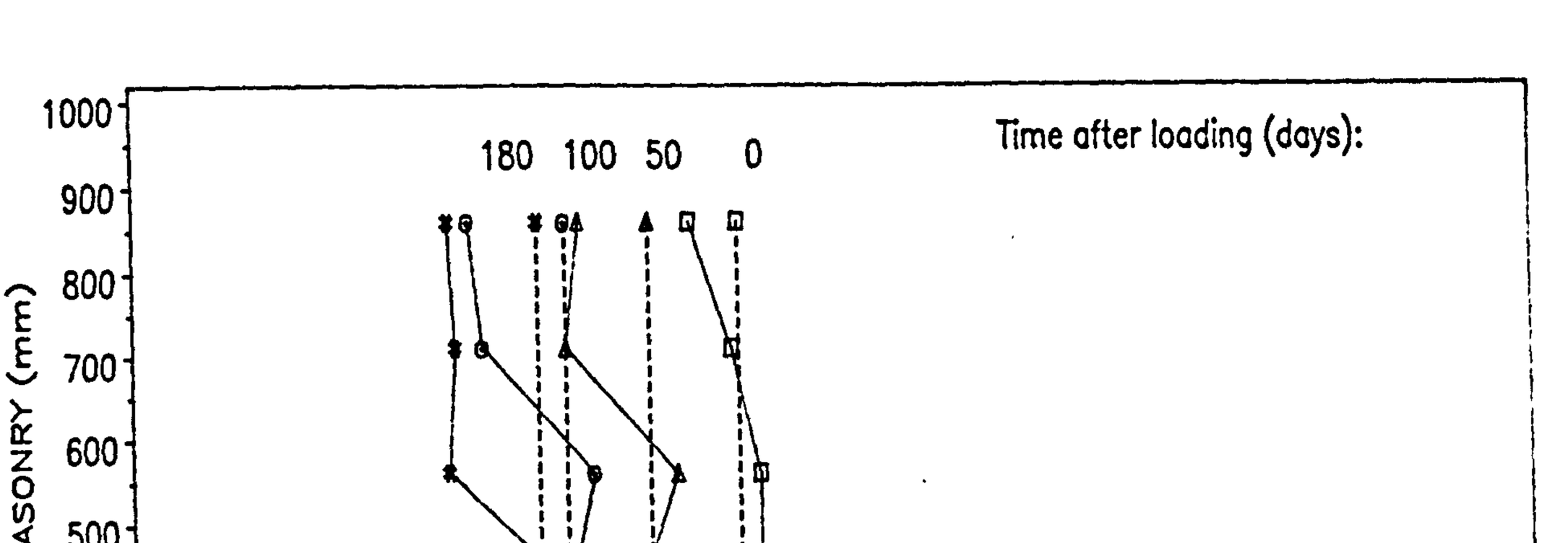

Fig. 8.7(d) – Variation of Lateral Load Strain with Height of Clay Solid Pier

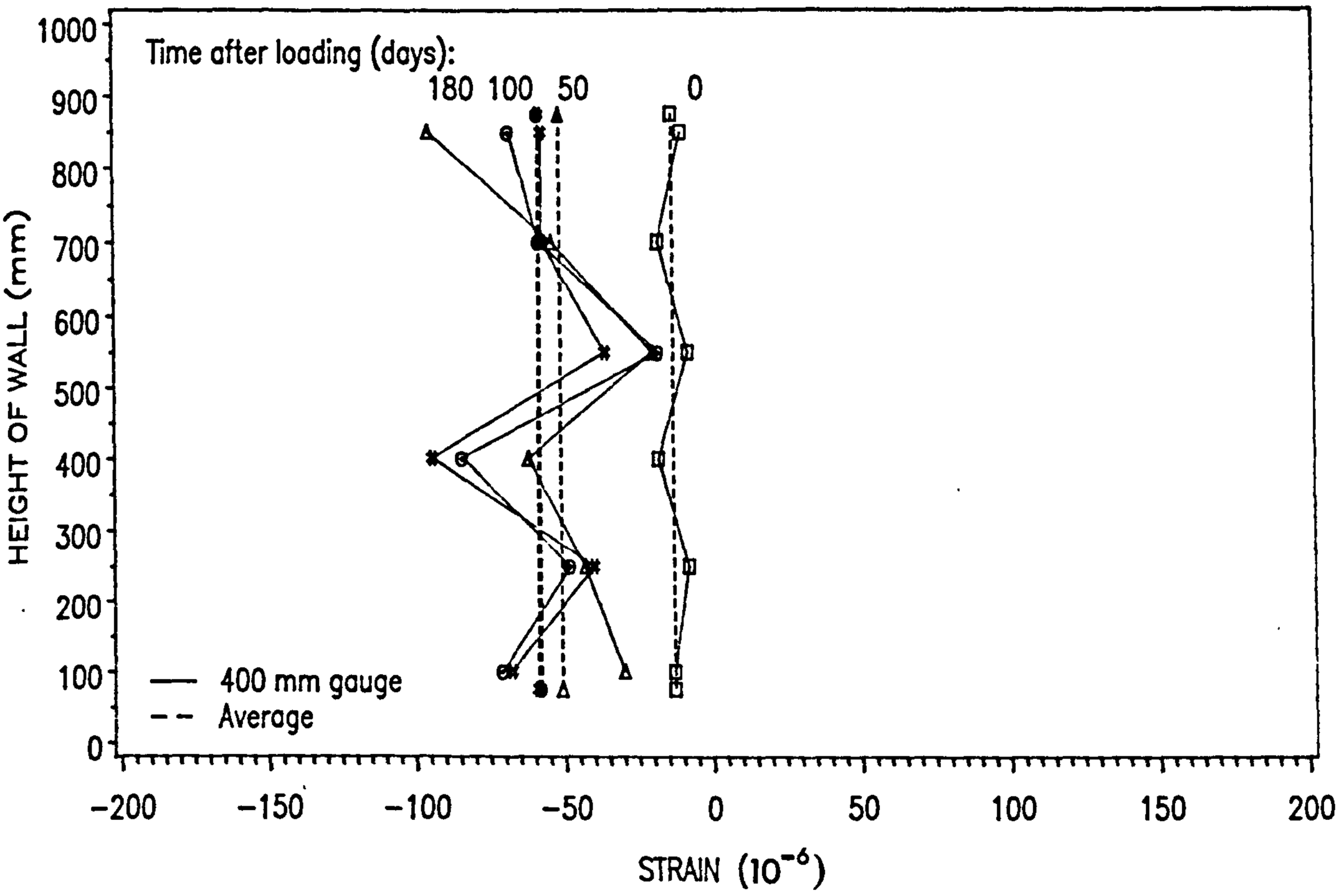

Fig. 8.8(a) – Variation of Lateral Load Strain with Height of Calcium Silicate Single–Leaf Wall

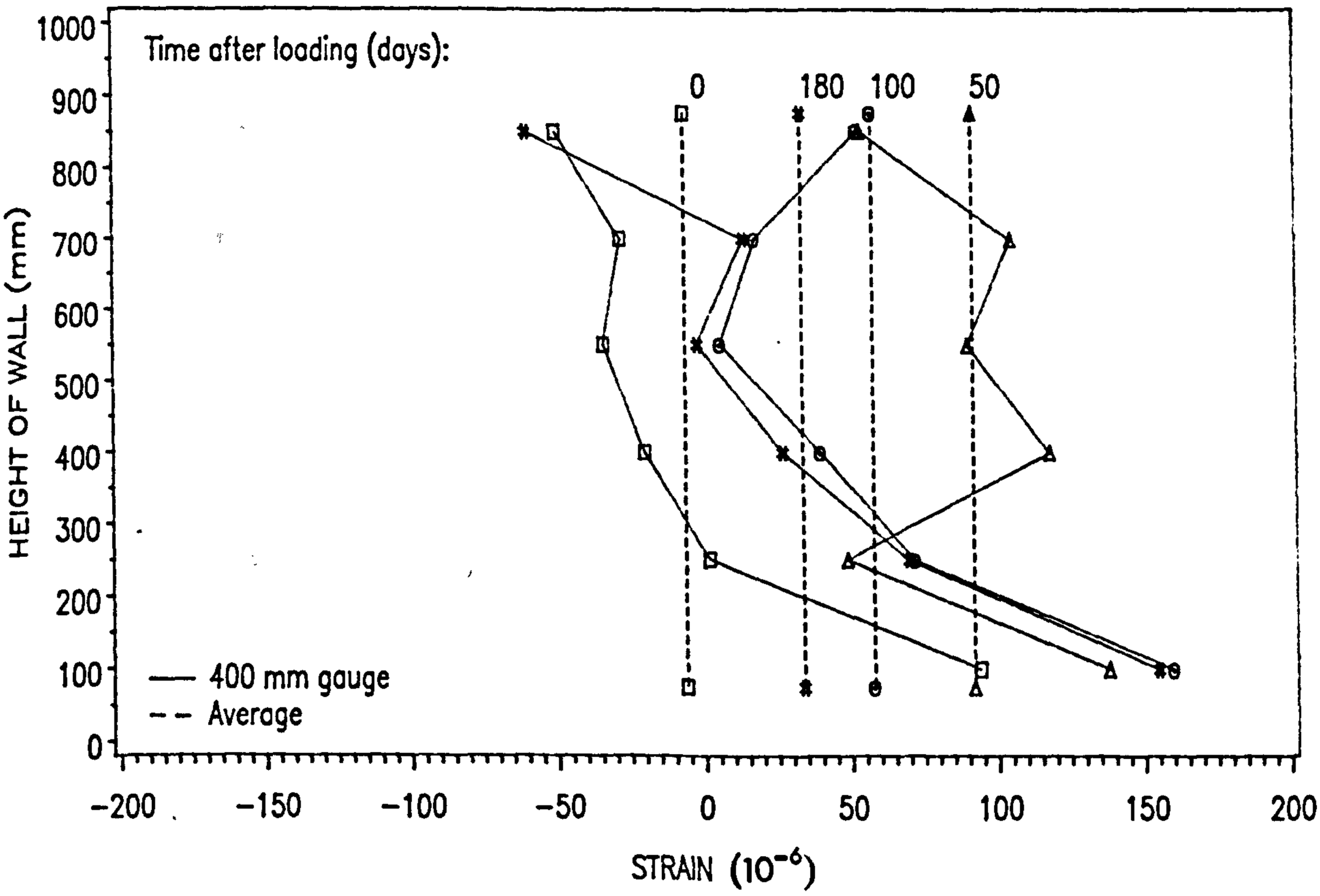

Fig. 8.8(b) – Variation of Lateral Load Strain with Height of Calcium Silicate Cavity Wall

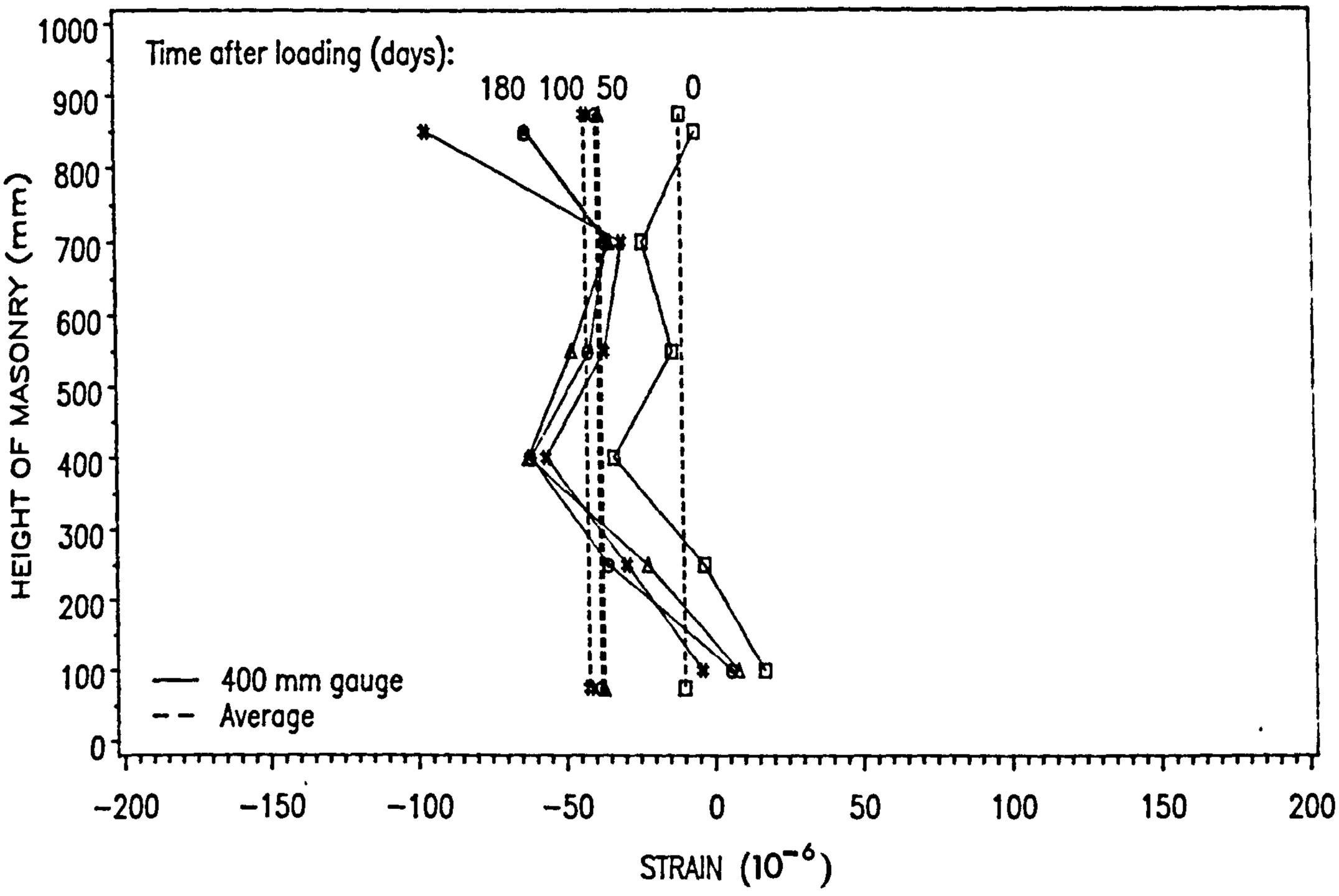

FIG. 8.8(c) – Variation of Lateral Load Strain with Height of Calcium Silicate Hollow Pier

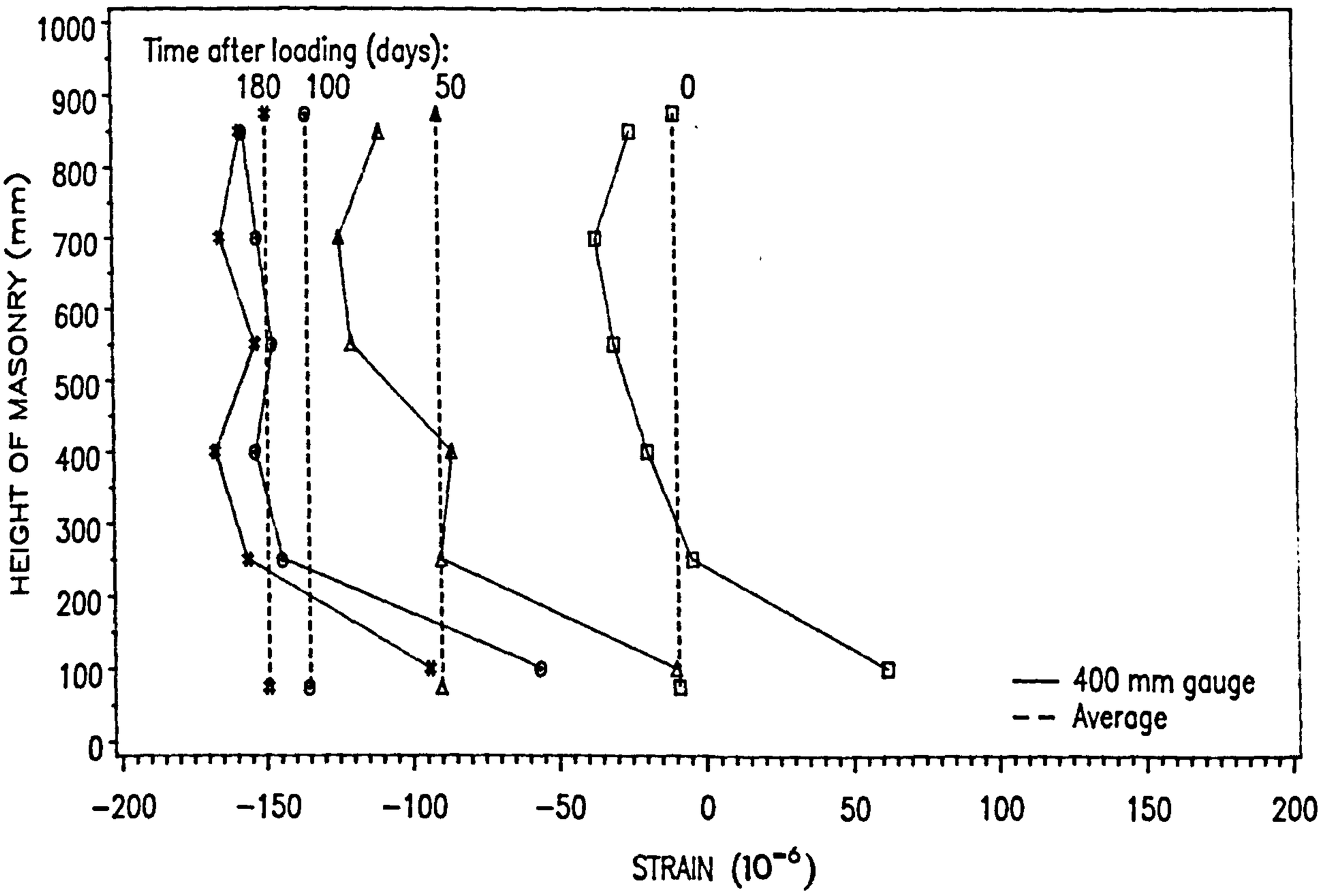

FIG. 8.8(d) – Variation of Lateral Load Strain with Height of Calcium Silicate Solid Pier

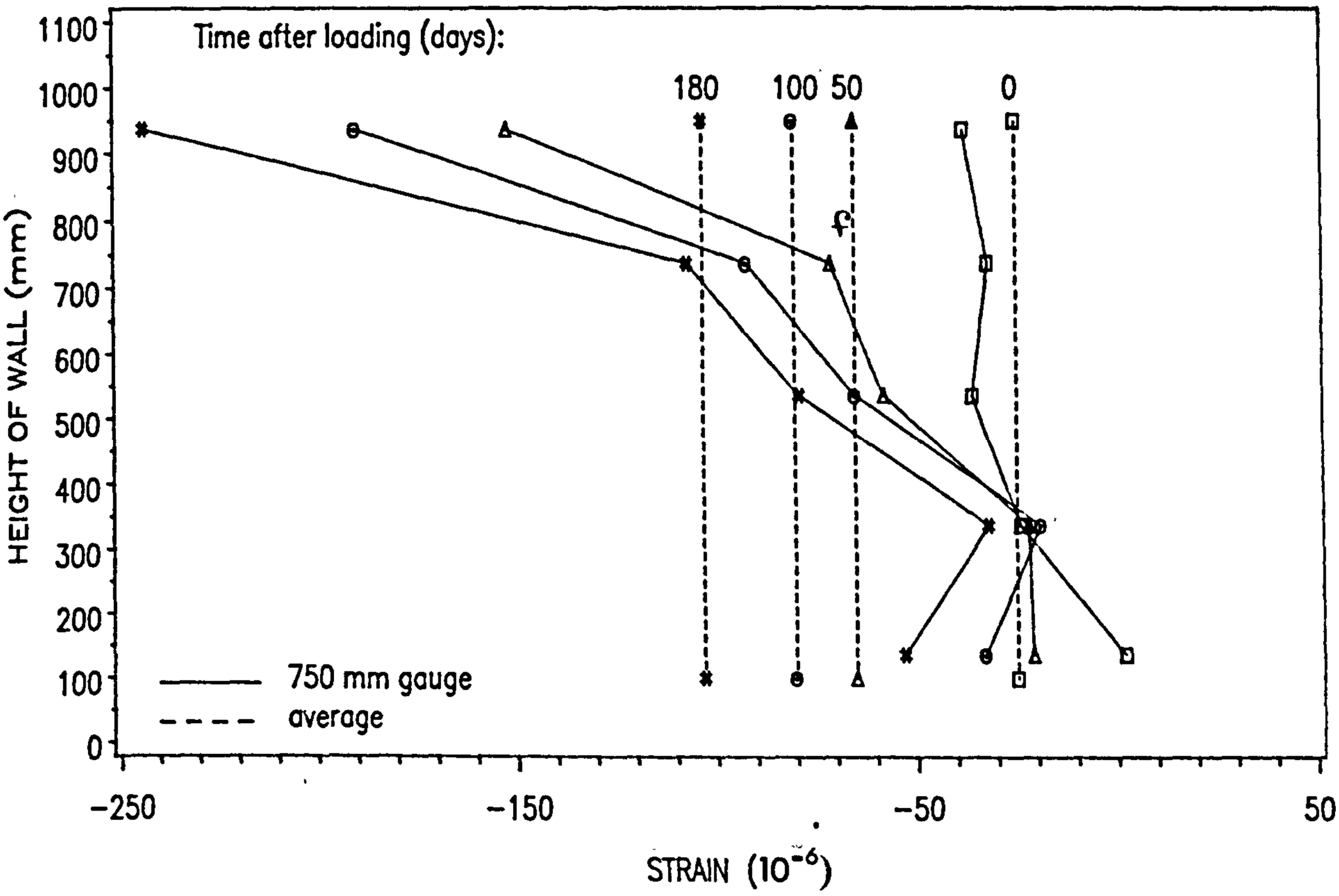

Fig. 8.9(a) – Variation of Lateral Load Strain with Height of Concrete Single–Leaf Wall

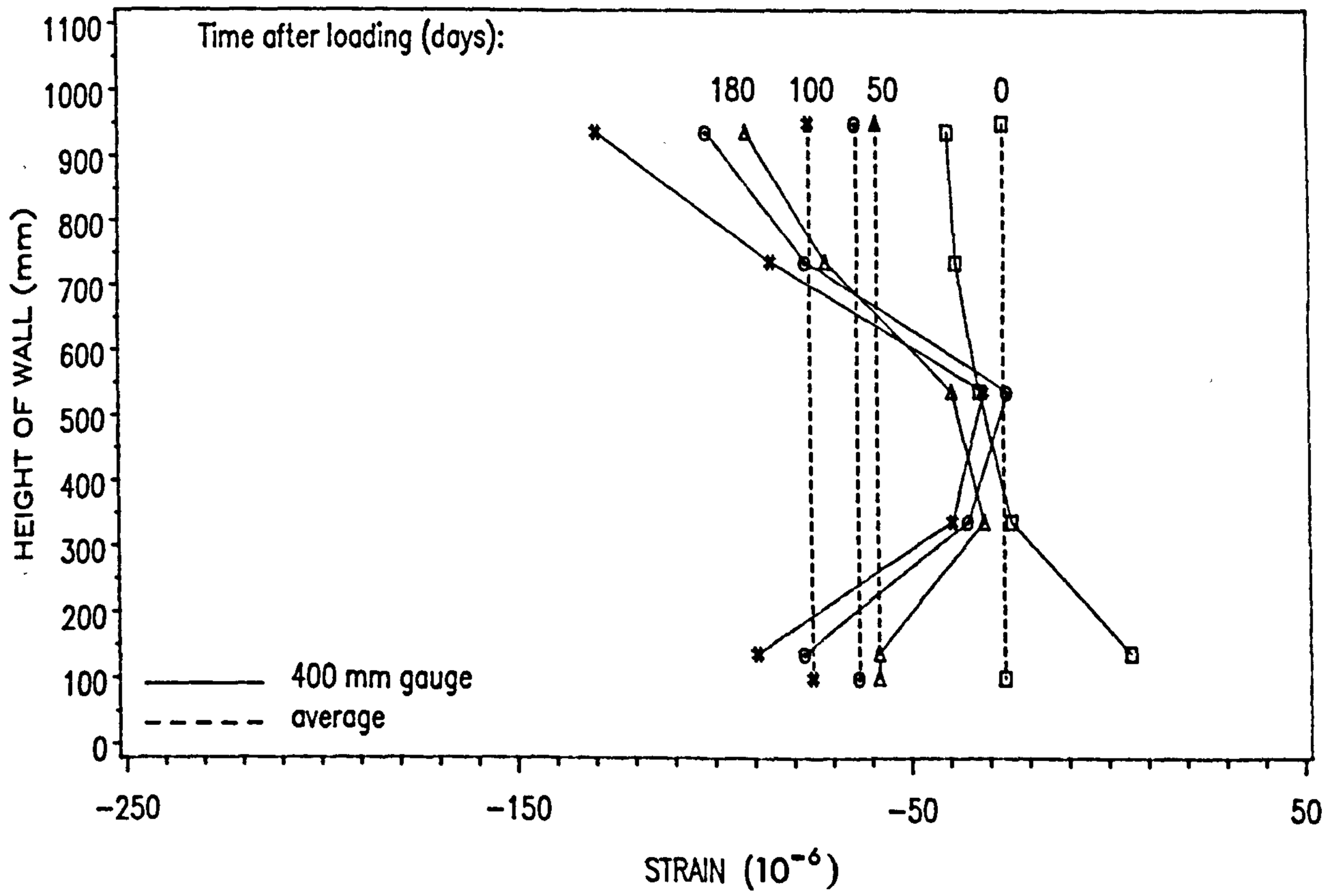

Fig. 8.9(b) – Variation of Lateral Load Strain with Height of Concrete Cavity Wall

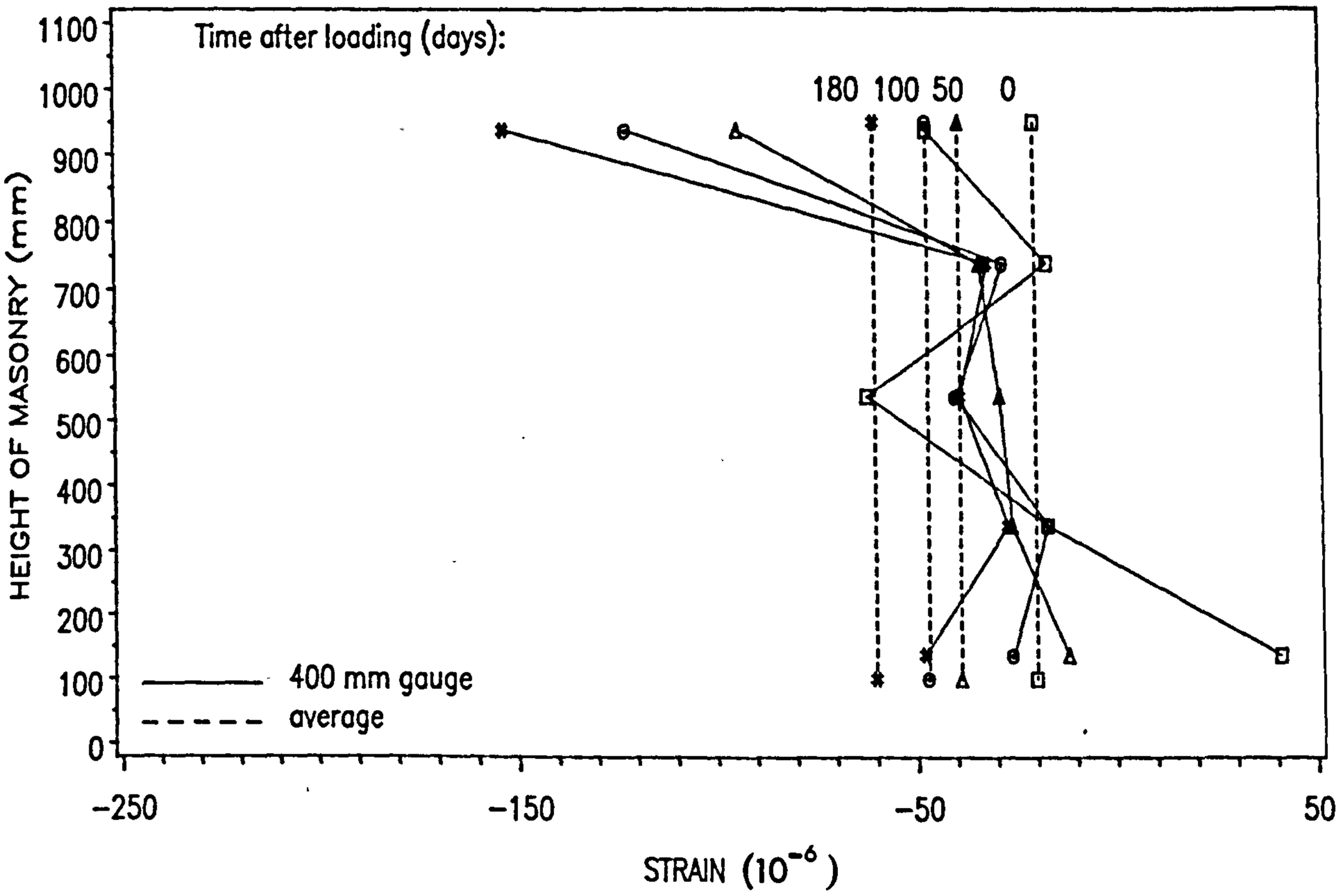

Fig. 8.9(c) – Variation of Lateral Load Strain with Height of Concrete Hollow Pier

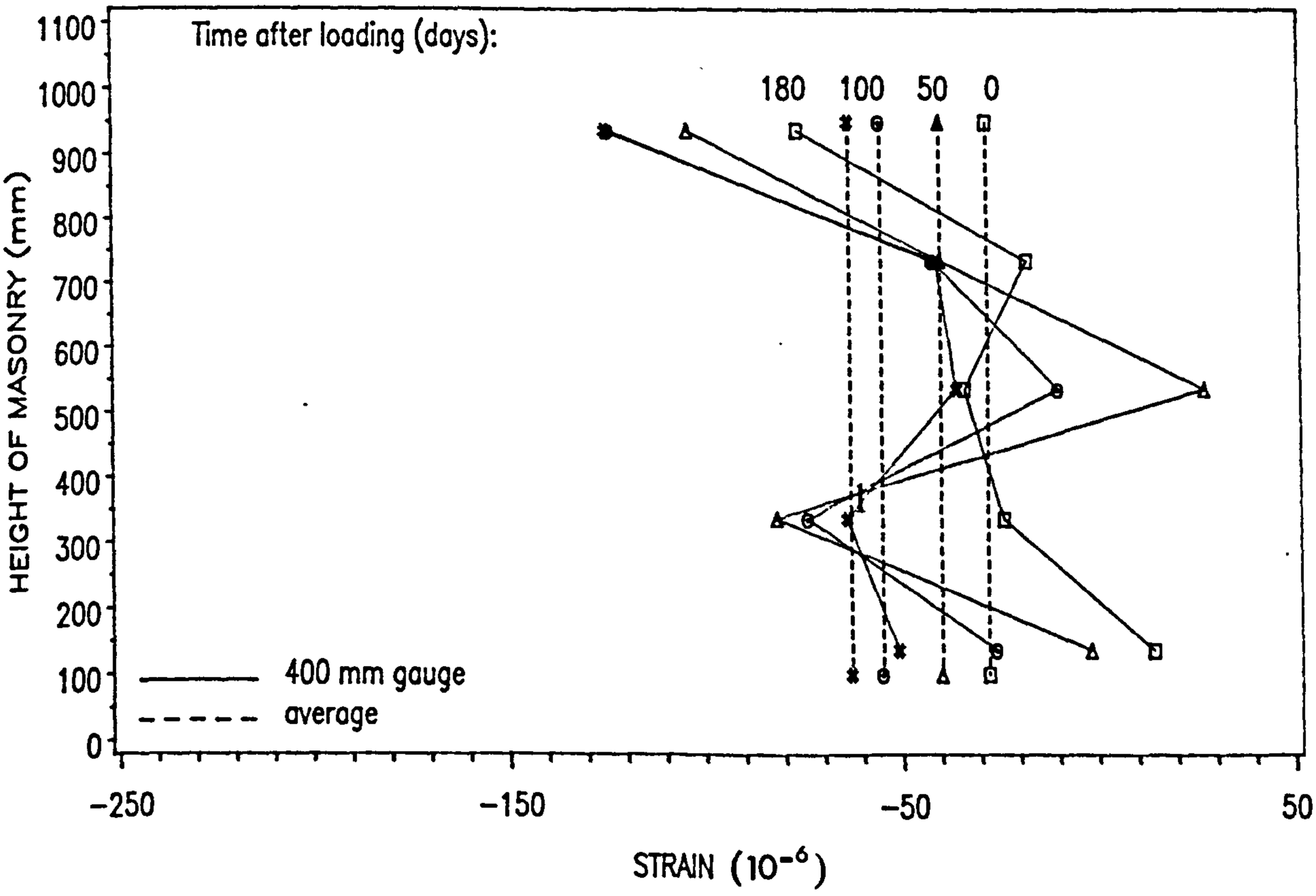

Fig. 8.9 (d) – Variation of Lateral Load Strain with Height of Concrete Solid Pier

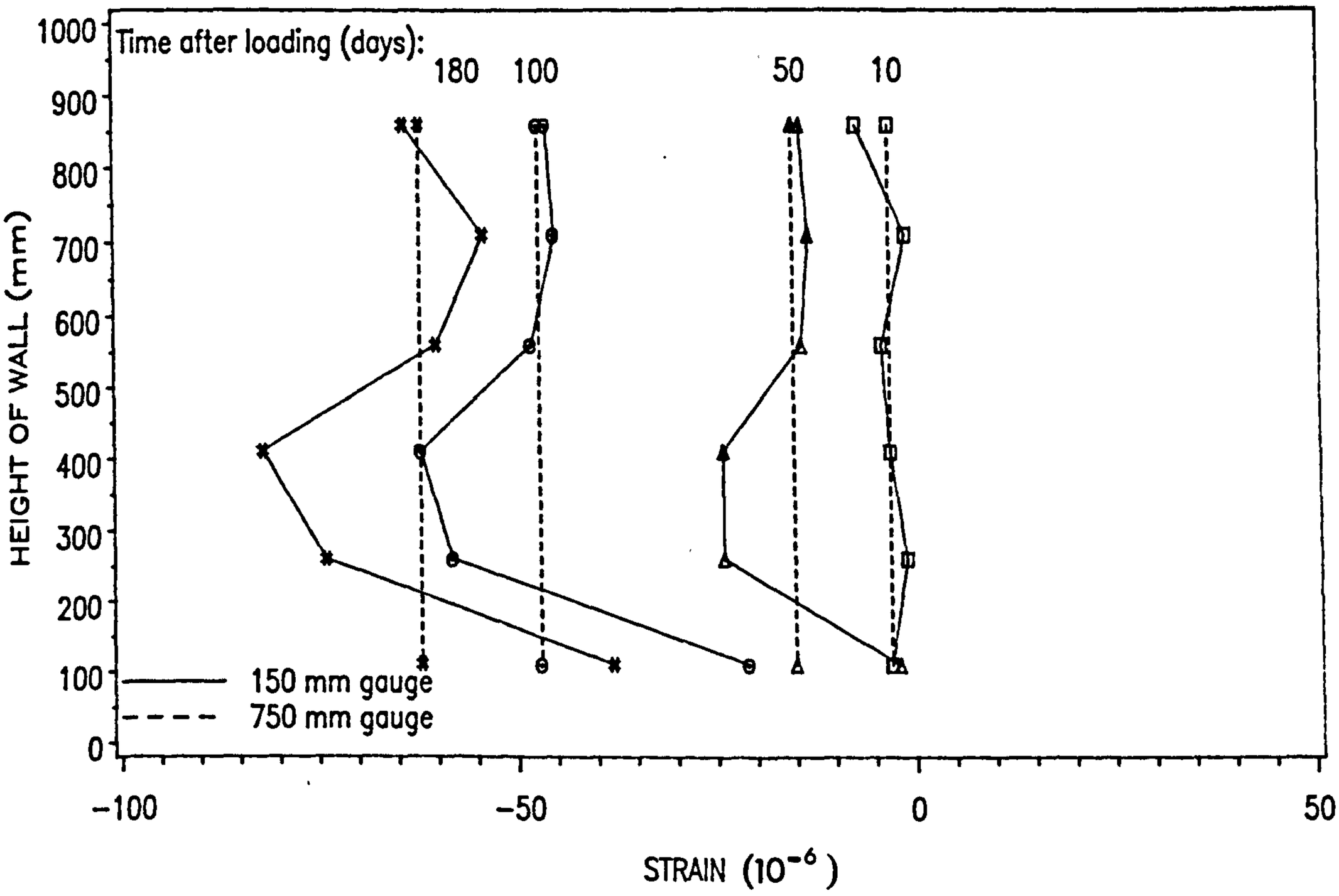

Fig. 8.10(a) – Variation of Lateral Moisture Strain with Height of Clay Single-Leaf Wall

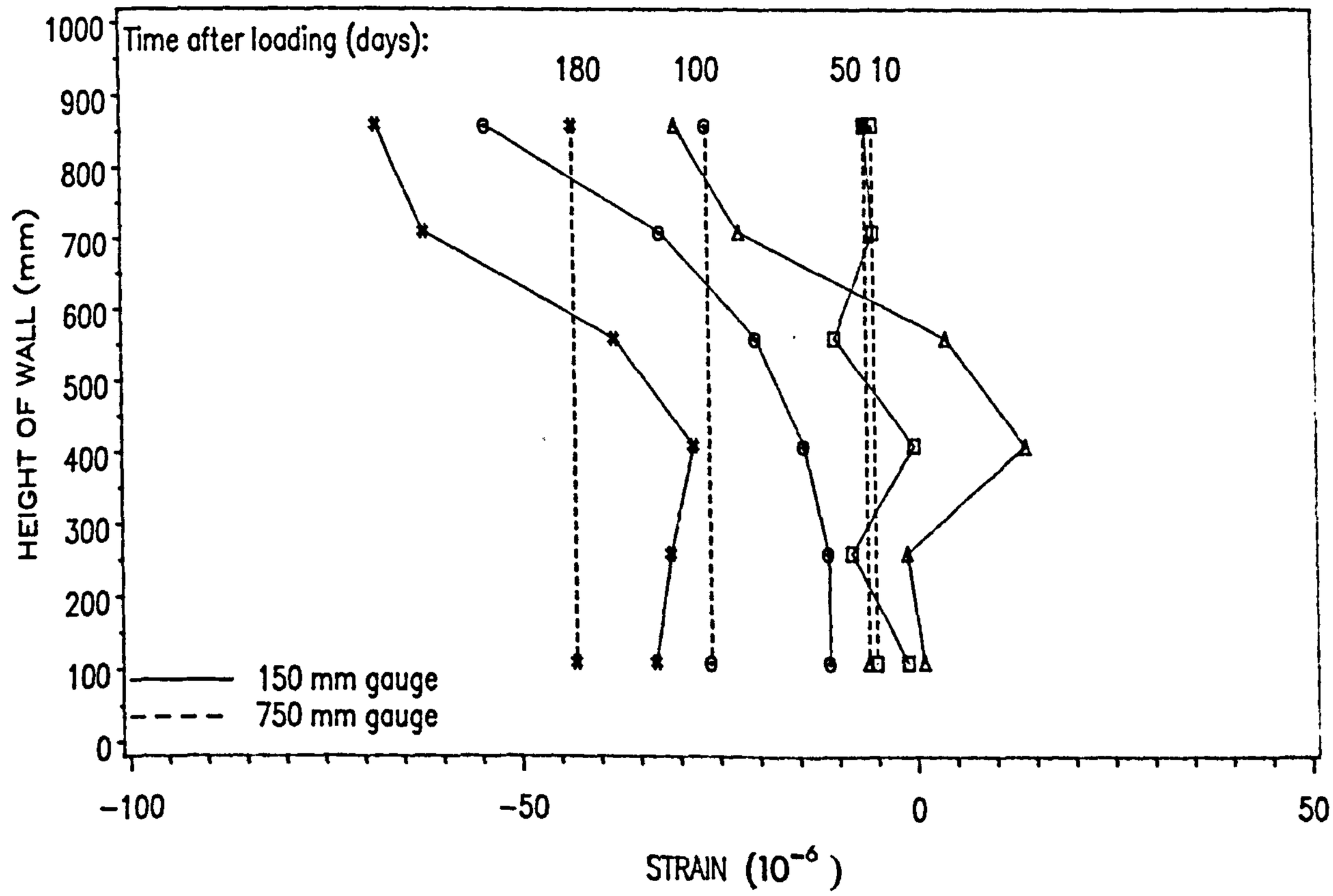

Fig. 8.10(b) – Variation of Lateral Moisture Strain with Height of Clay Cavity Wall

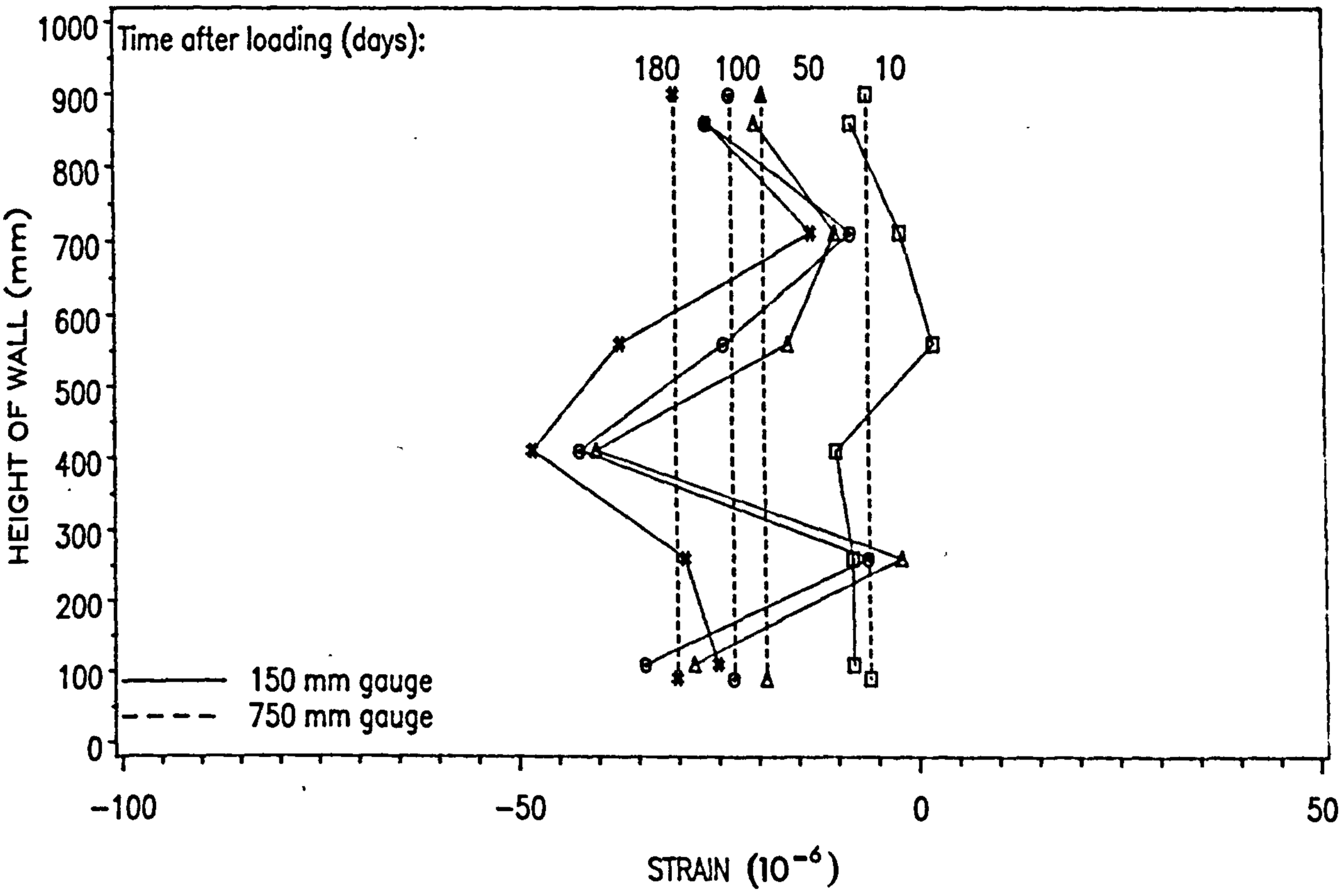

Fig. 8.10(c) – Variation of Lateral Moisture Strain with Height of Clay Hollow Pier

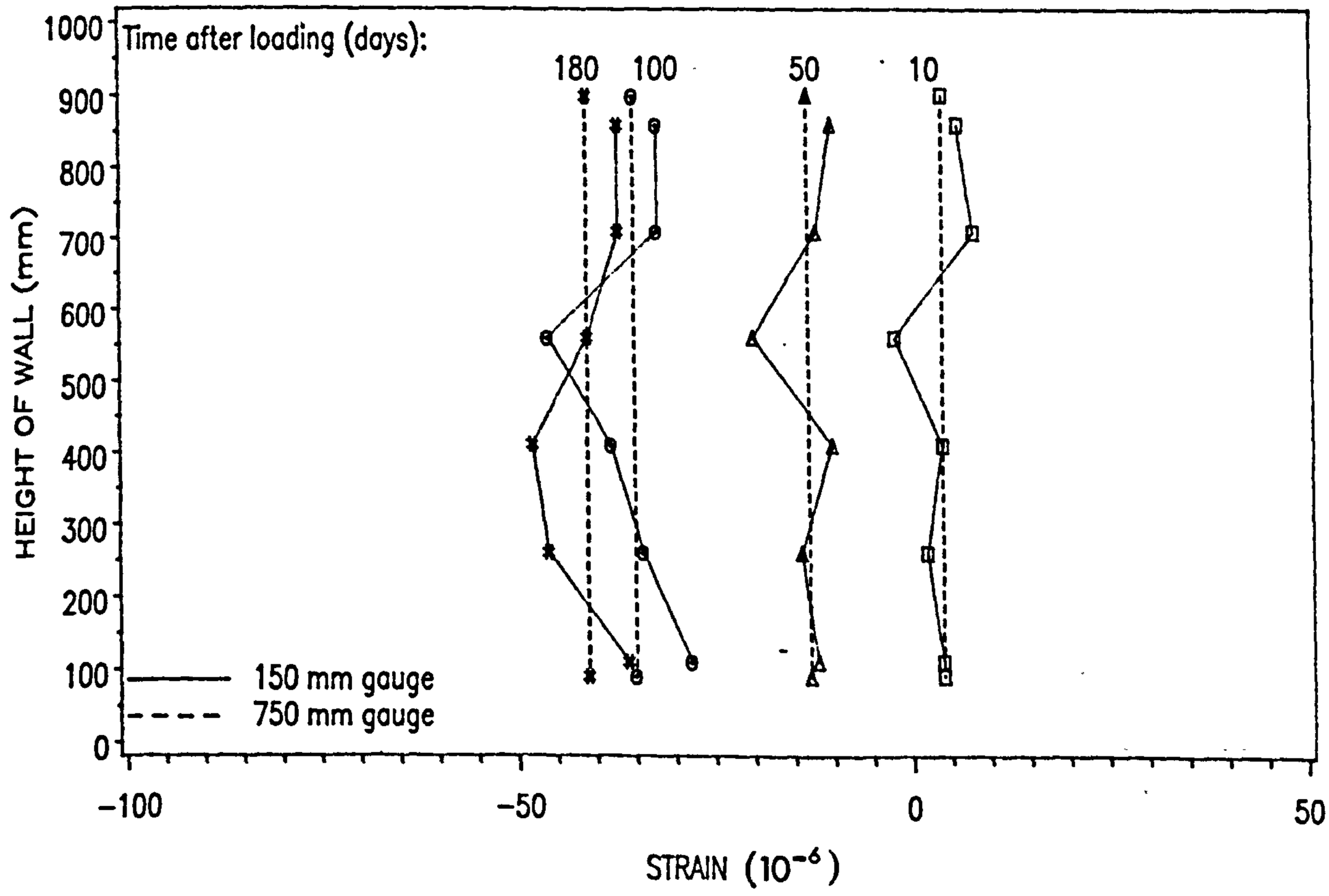

Fig. 8.10(d) – Variation of Lateral Moisture Strain with Height of Clay Solid Pier

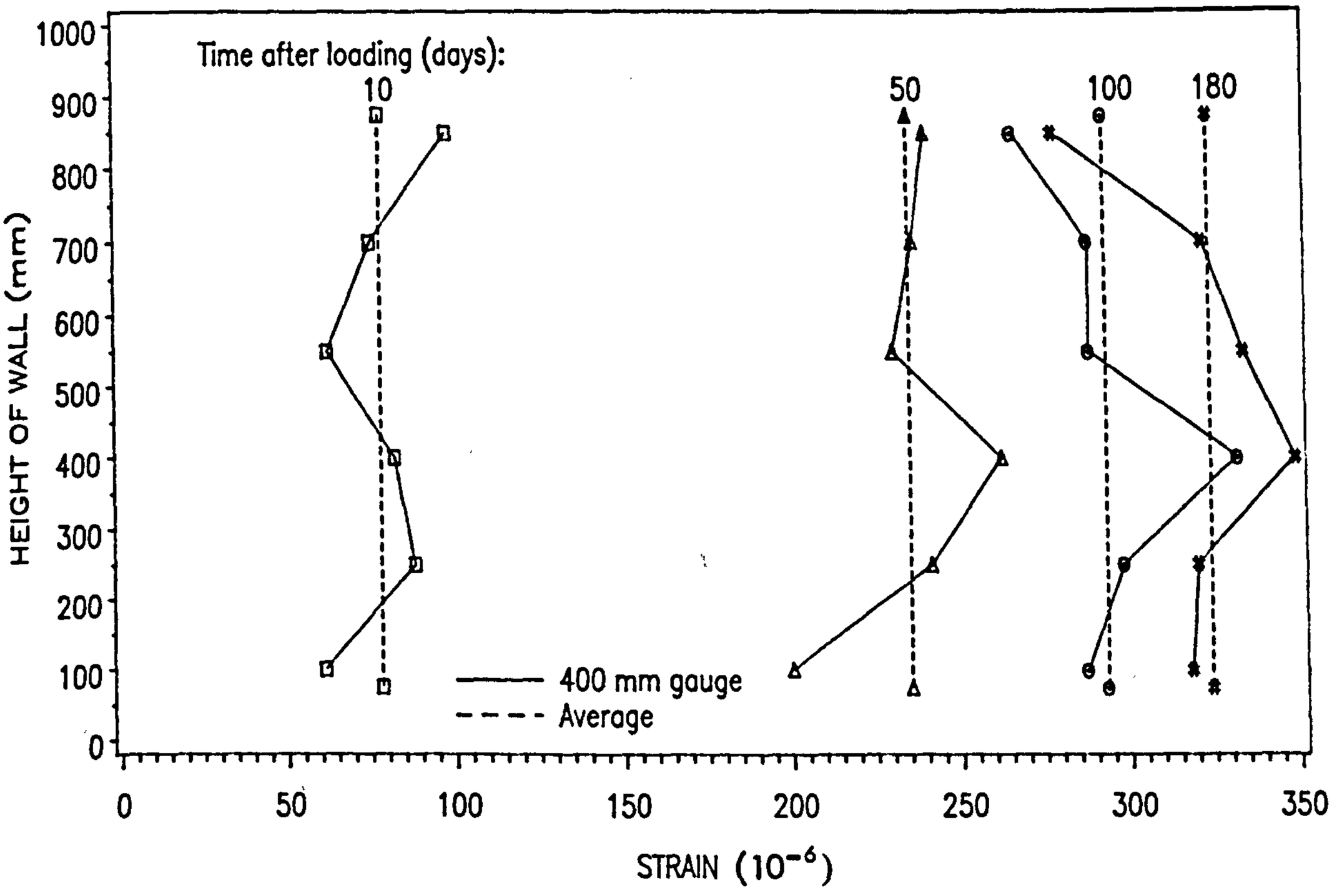

Fig. 8.11(a) – Variation of Lateral Moisture Strain with Height of Calcium Silicate Single-Leaf Wall

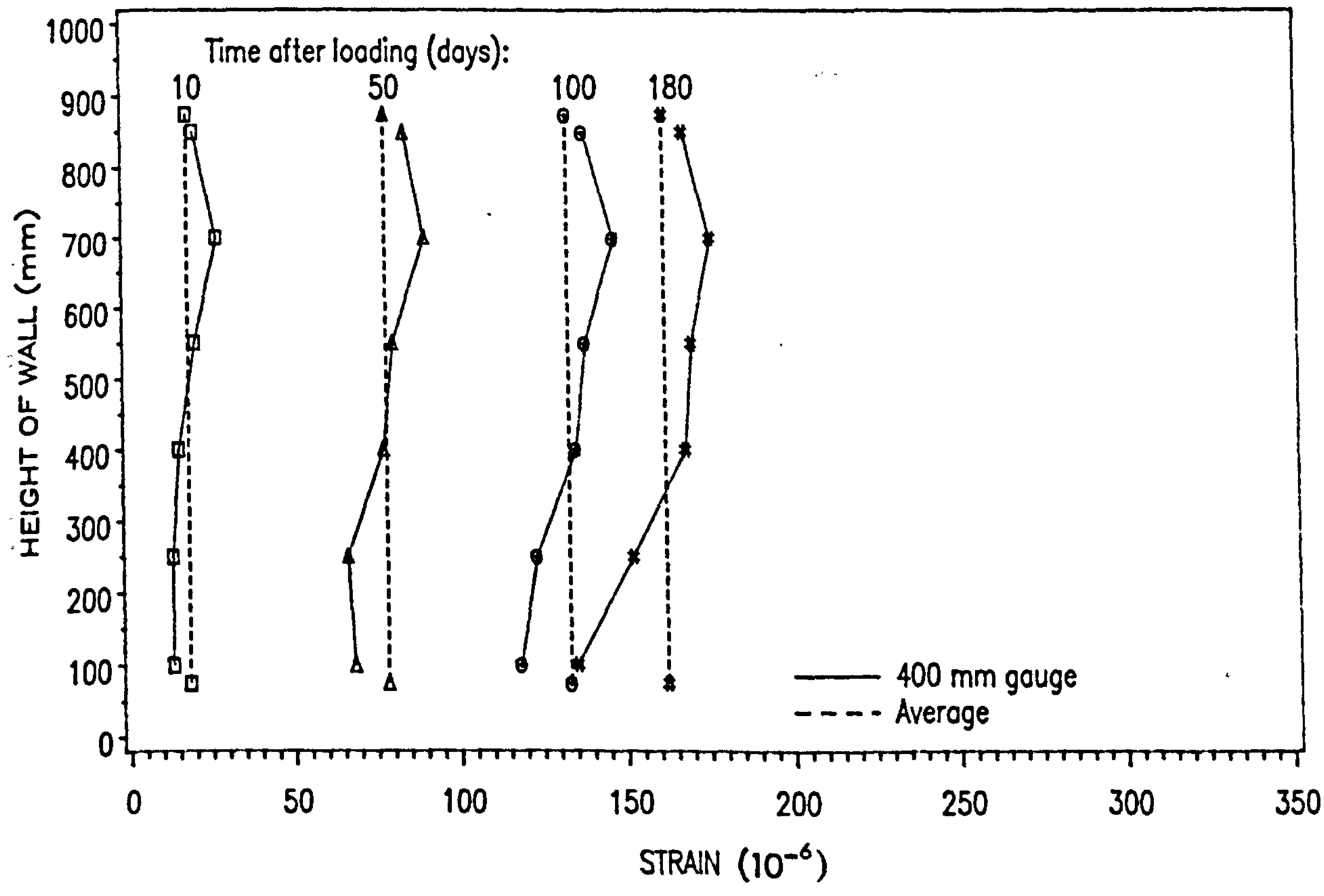

Fig. 8.11(b) – Variation of Lateral Moisture Strain with Height of Calcium Silicate Cavity Wall

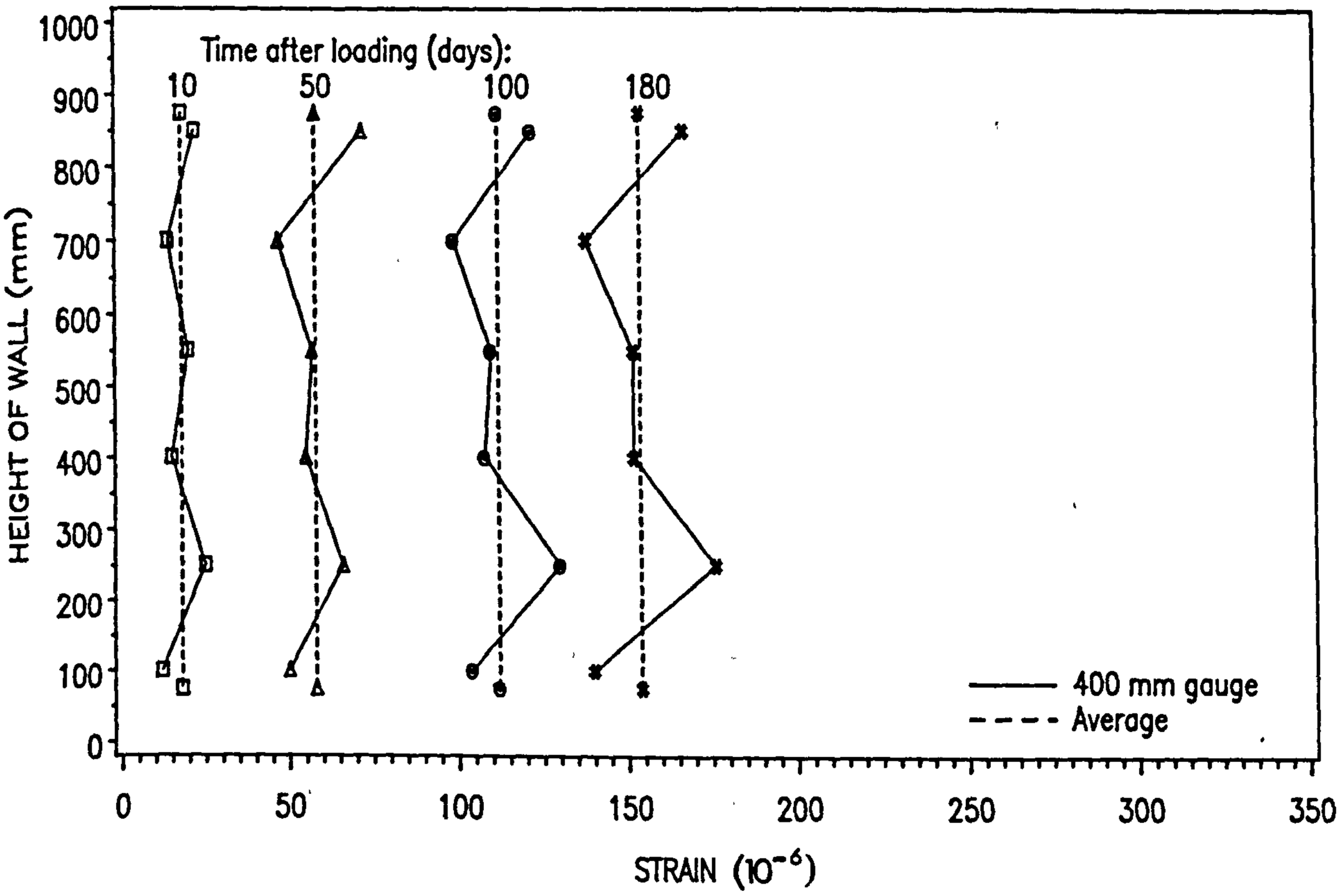

Fig. 8.11(c) – Variation of Lateral Moisture Strain with Height of Calcium Silicate Hollow Pier

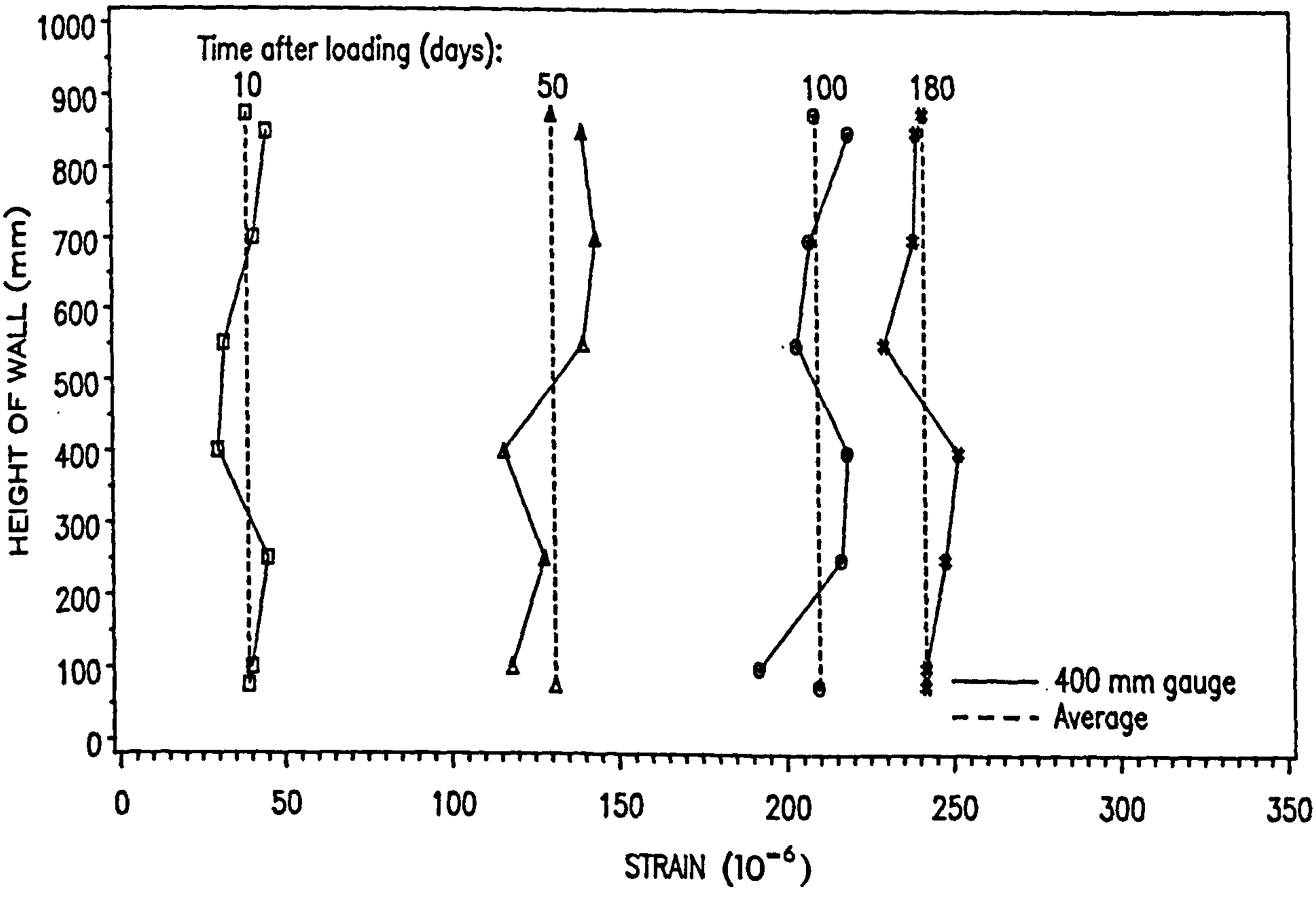

Fig. 8.11(d) – Variation of Lateral Moisture Strain with Height of Calcium Silicate Solid Pier

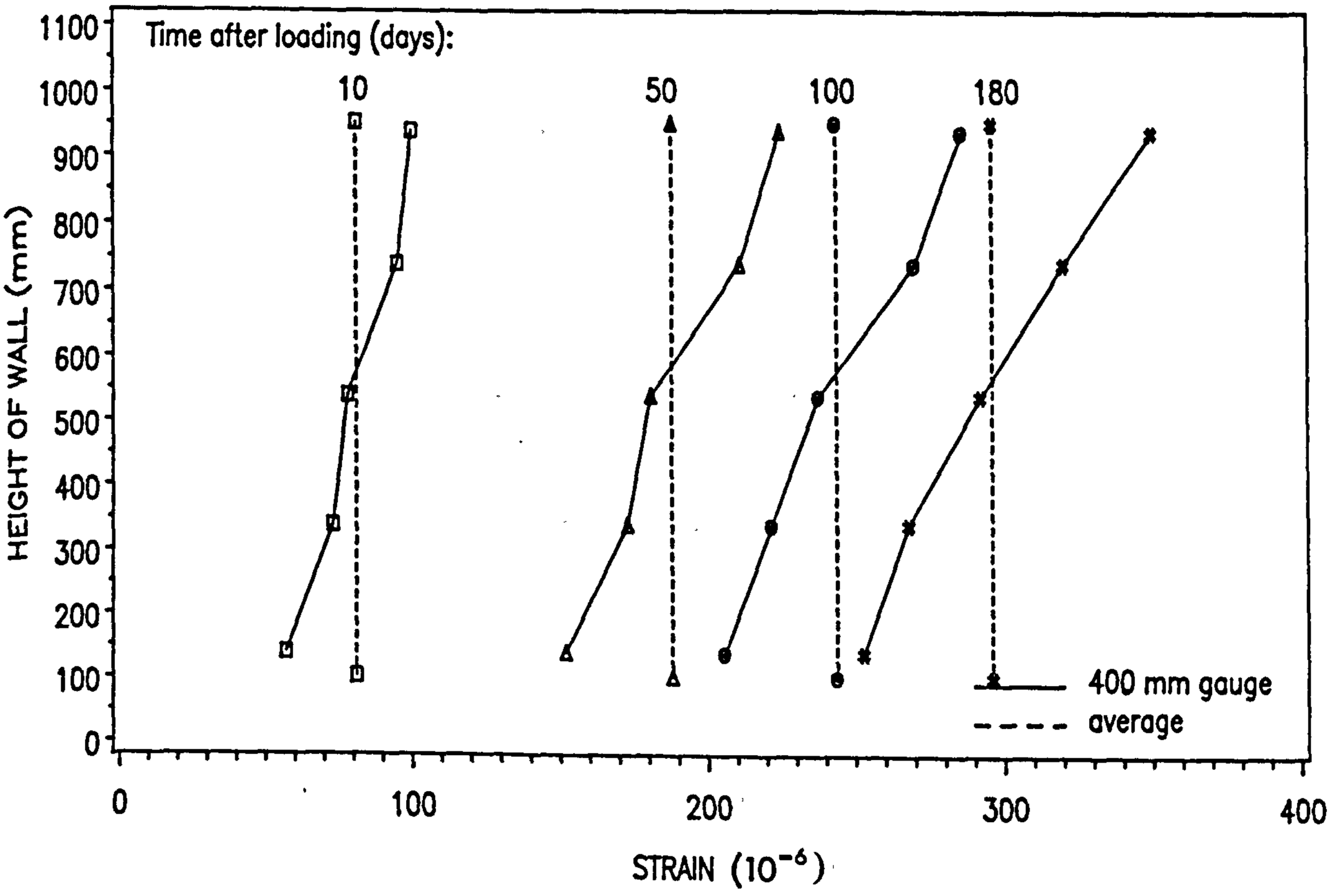

Fig. 8.12(a) – Variation of Lateral Moisture Strain with Height of Concrete Single-Leaf Wall

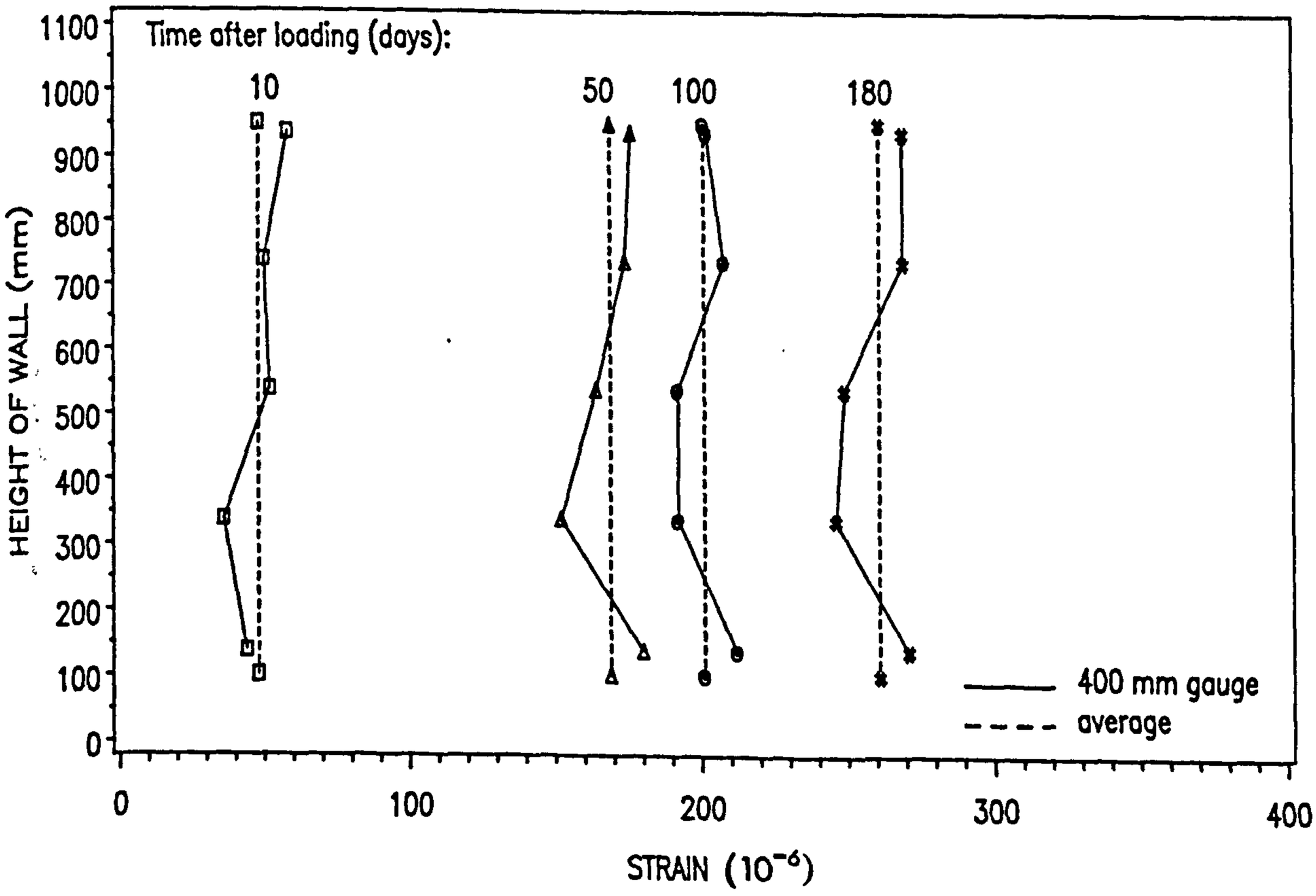

Fig. 8.12(b) – Variation of Lateral Moisture Strain with Height of Concrete Cavity Wall

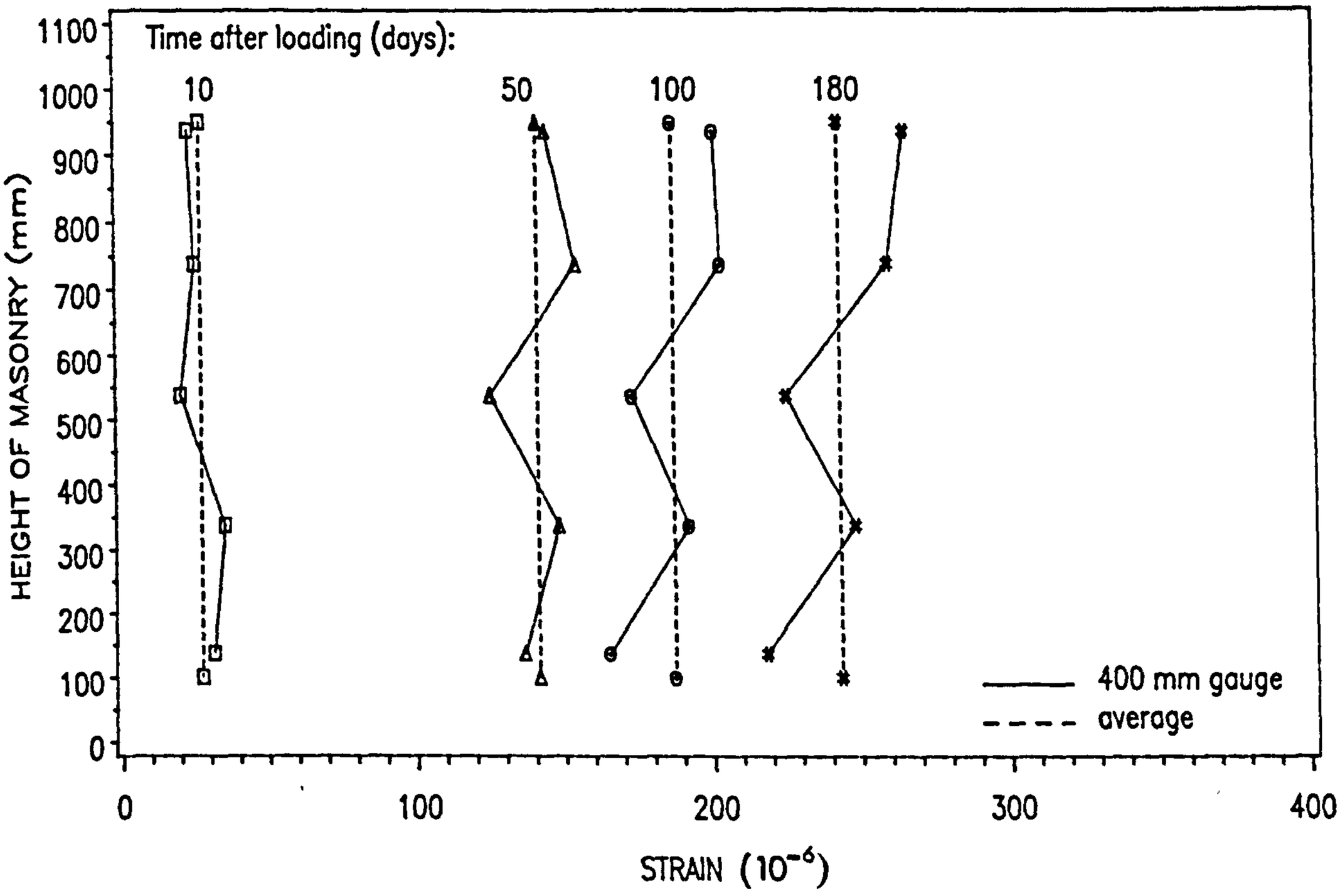

Fig. 8.12(c) – Variation of Lateral Moisture Strain with Height of Concrete Hollow Pier

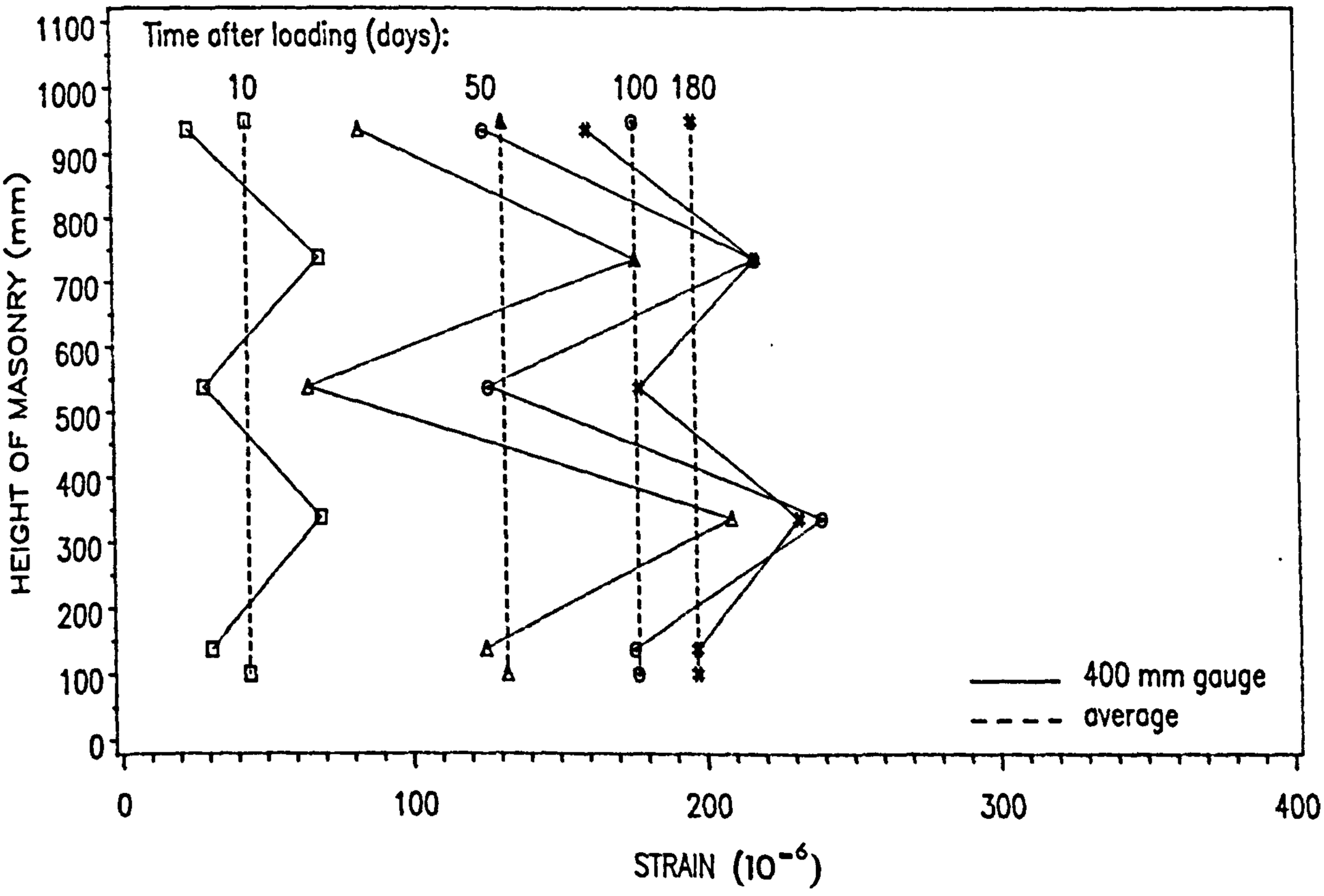

Fig. 8.12(d) – Variation of Lateral Moisture Strain with Height of Concrete Solid Pier

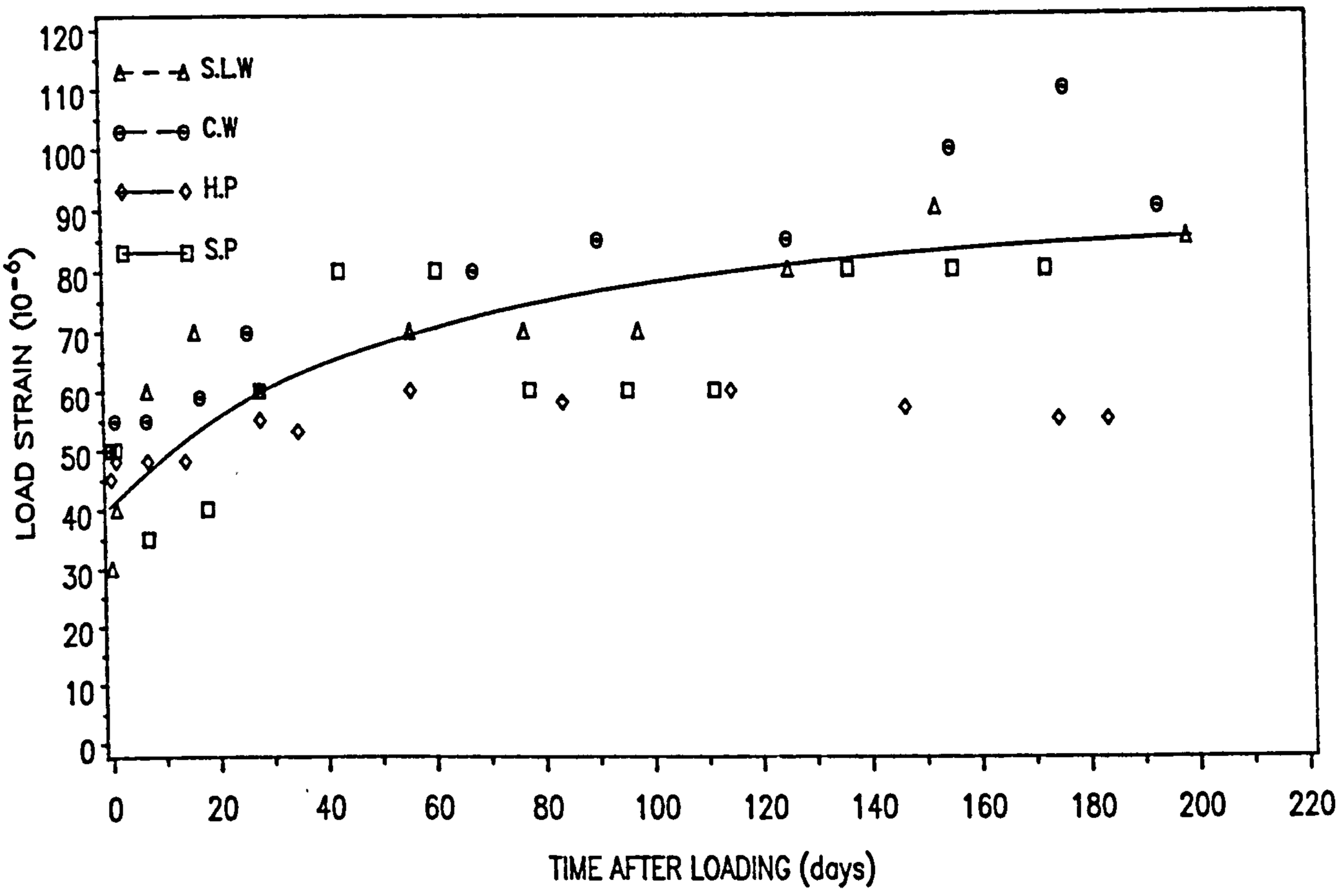

Fig. 8.13 – Axial Load–Strain Curves for Centrally embedded brick in Clay Brickwork

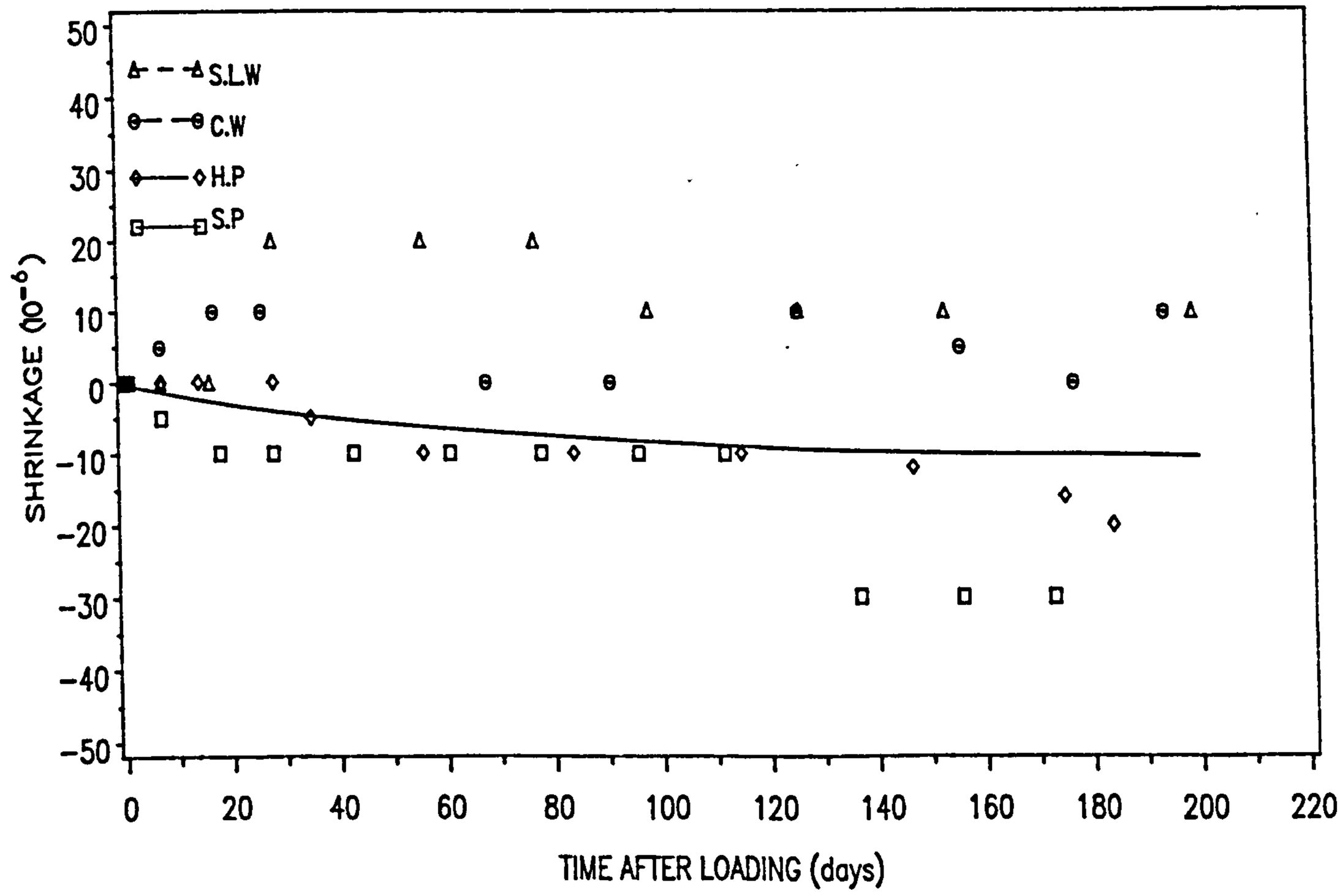

Fig. 8.14 – Axial Moisture Strain Curves for Centrally Embedded Brick in Clay Brickwork

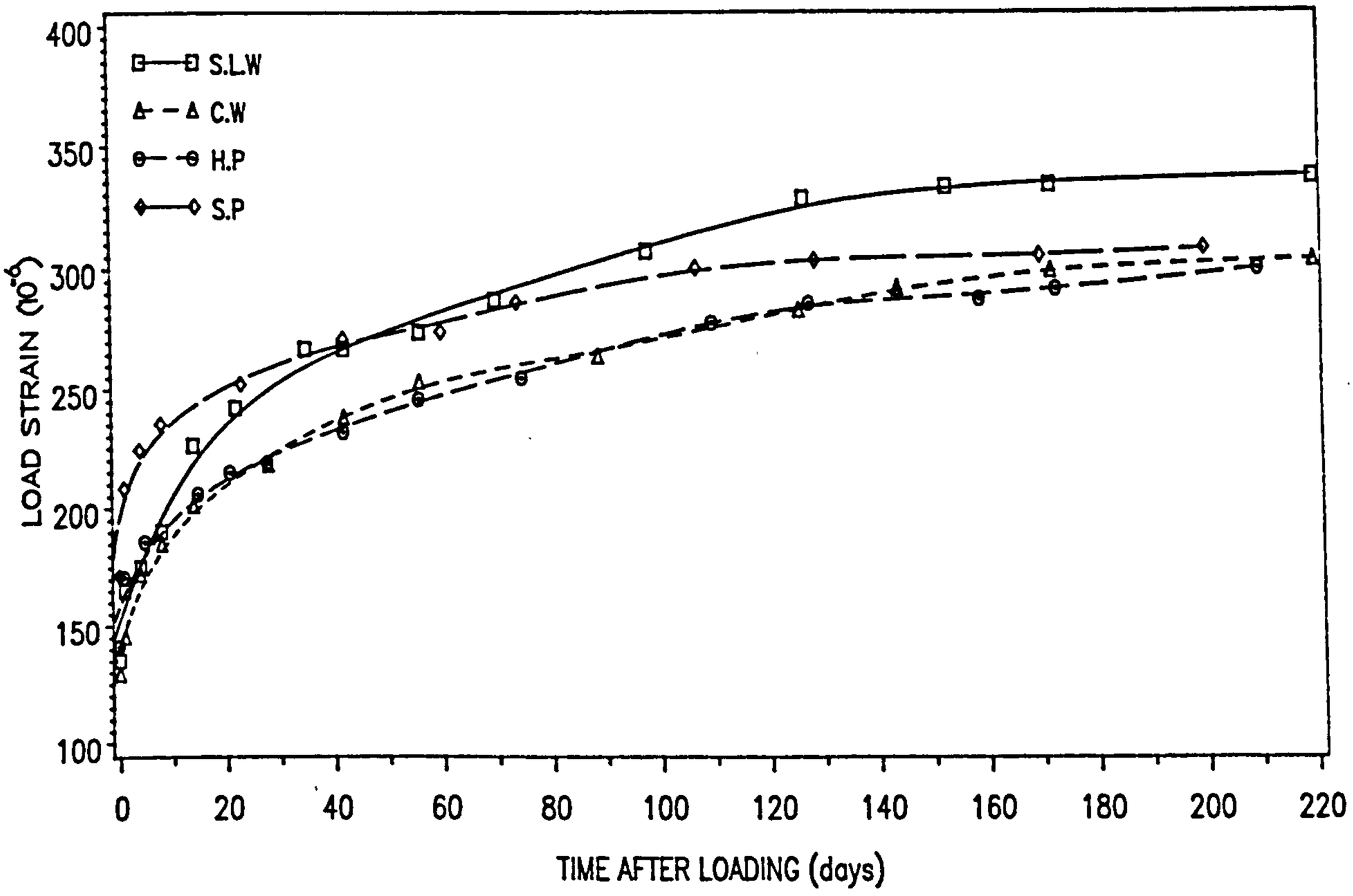

Fig. 8.15 – Axial Load Strain Curves for Centrally Embedded Brick in Calcium Silicate Brickwork

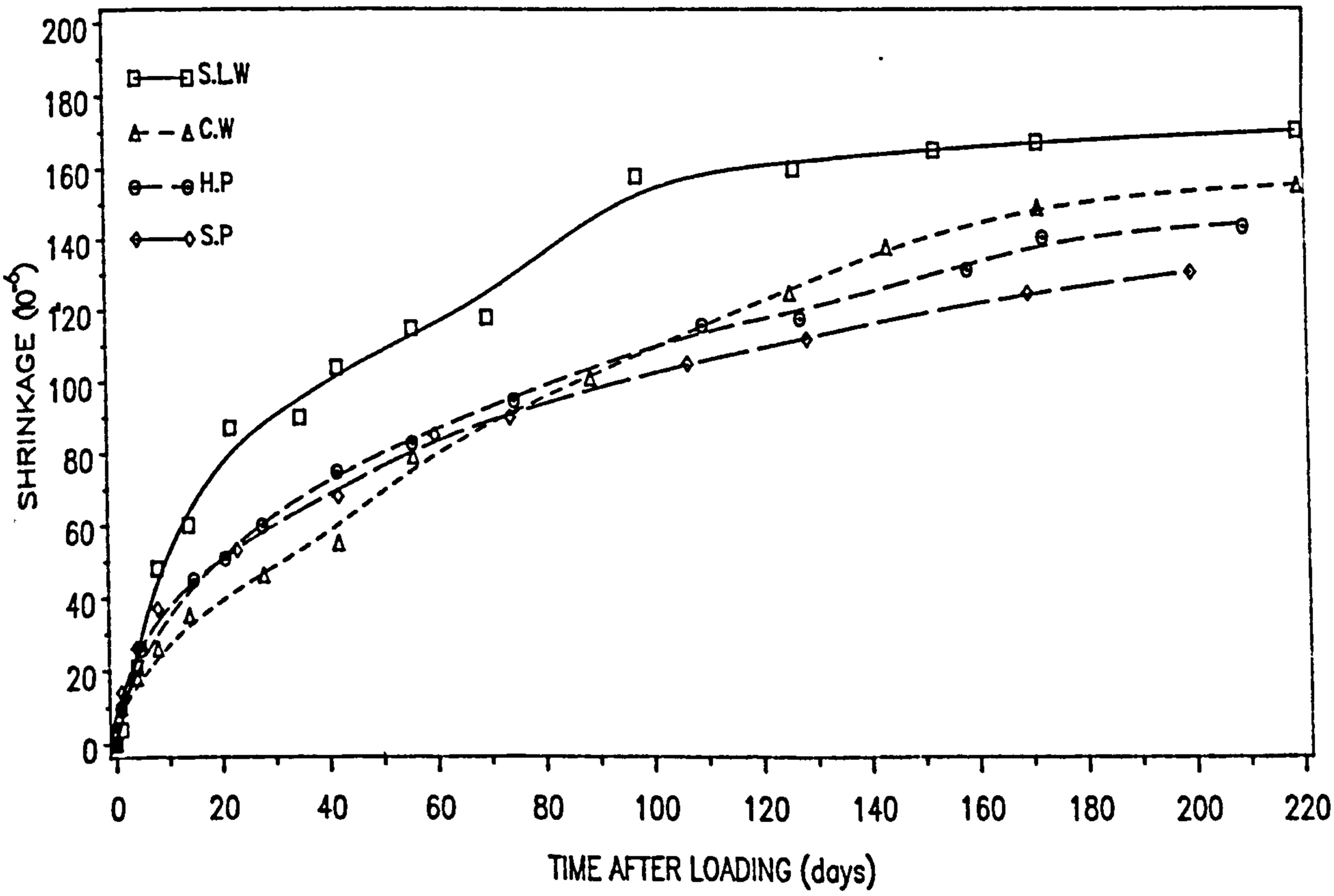

Fig. 8.16 – Axial Shrinkage–time Curves for Centrally Embedded Brick in Calcium Silicate Brickwork

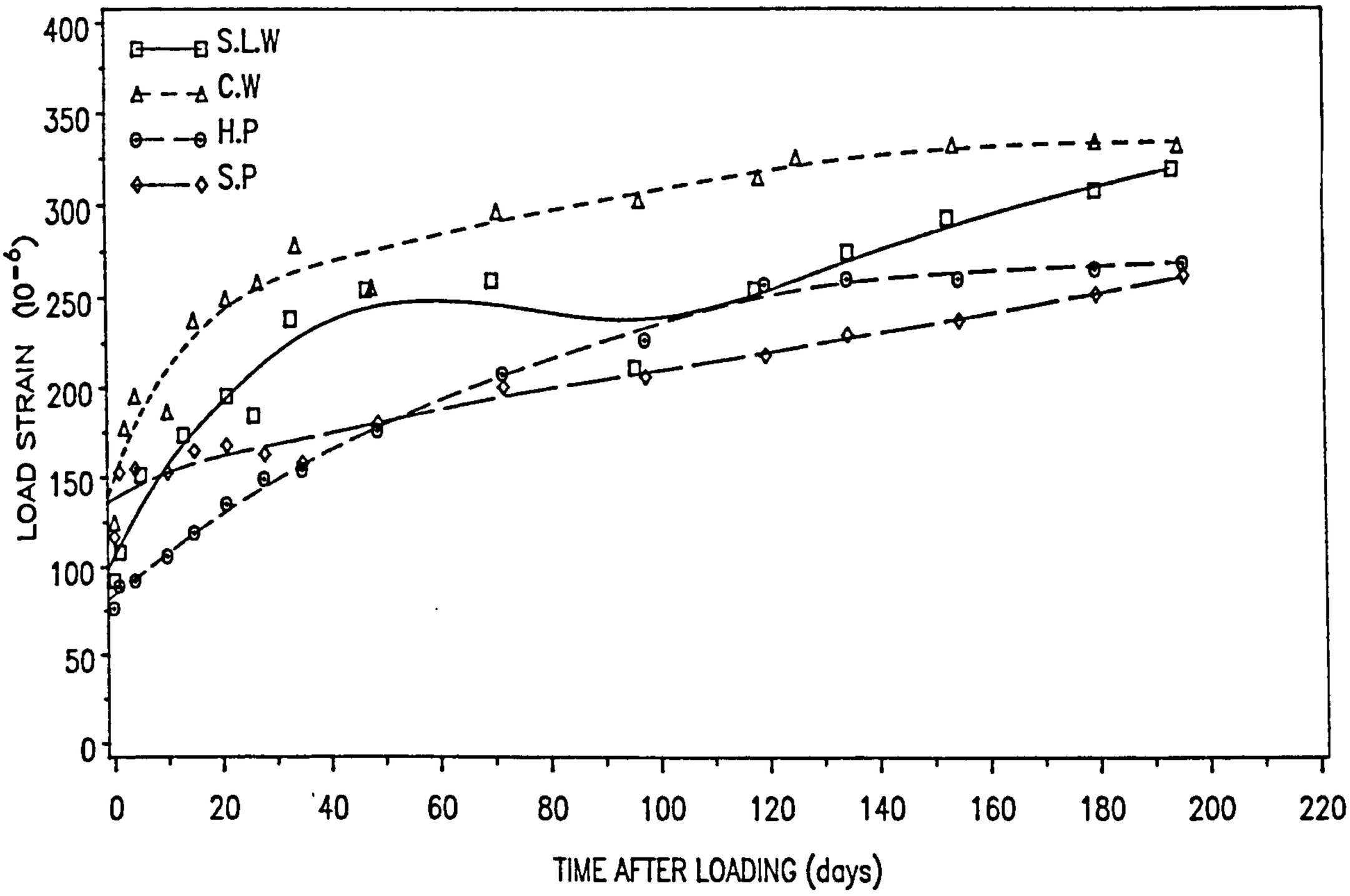

FIG. 8.17 – Axial Load Strain Curves for Centrally Embedded Unit in Concrete Blockwork

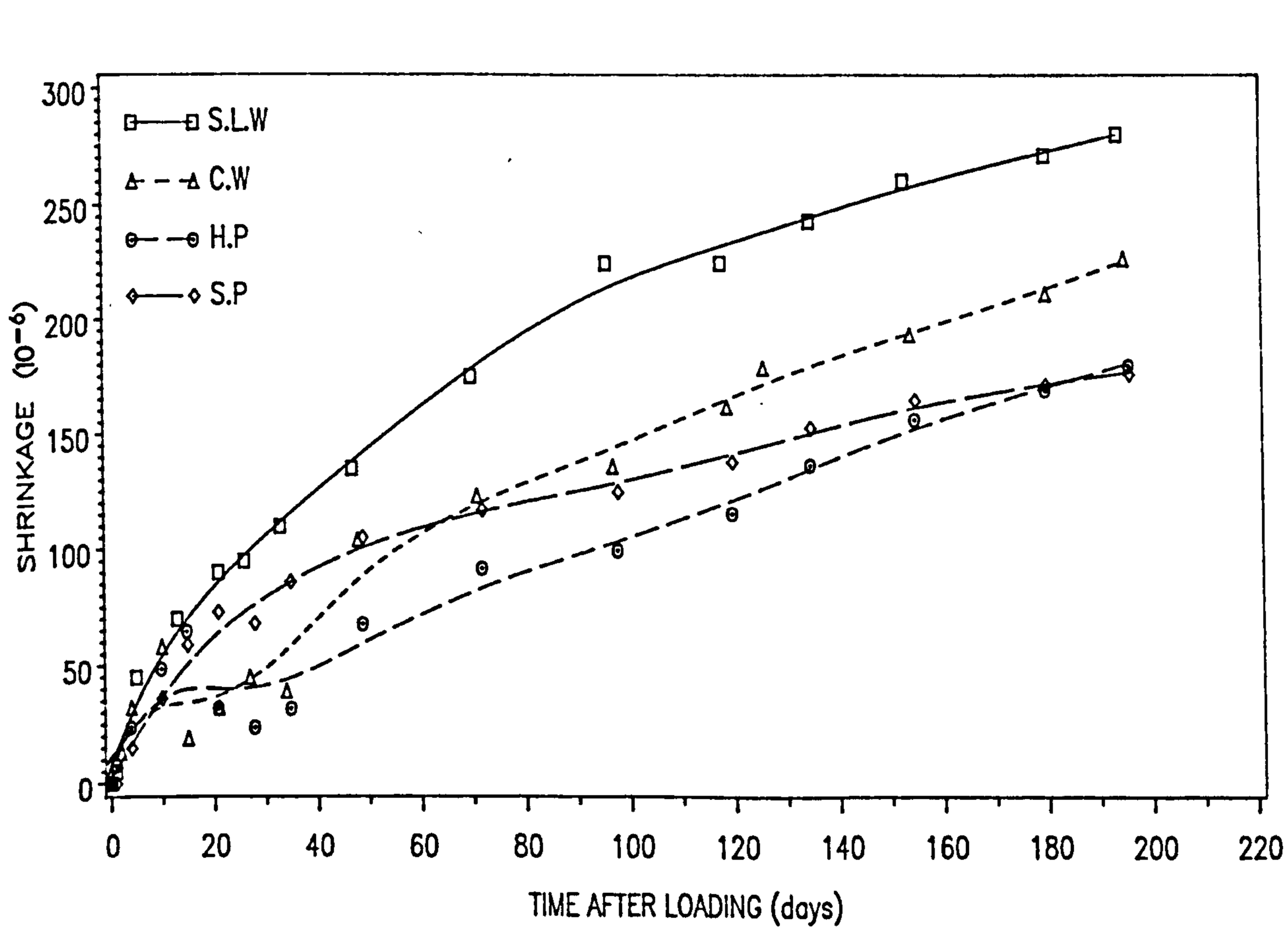

FIG. 8.18 – Axial Shrinkage–time Curves for Centrally Embedded Unit in Concrete Blockwork

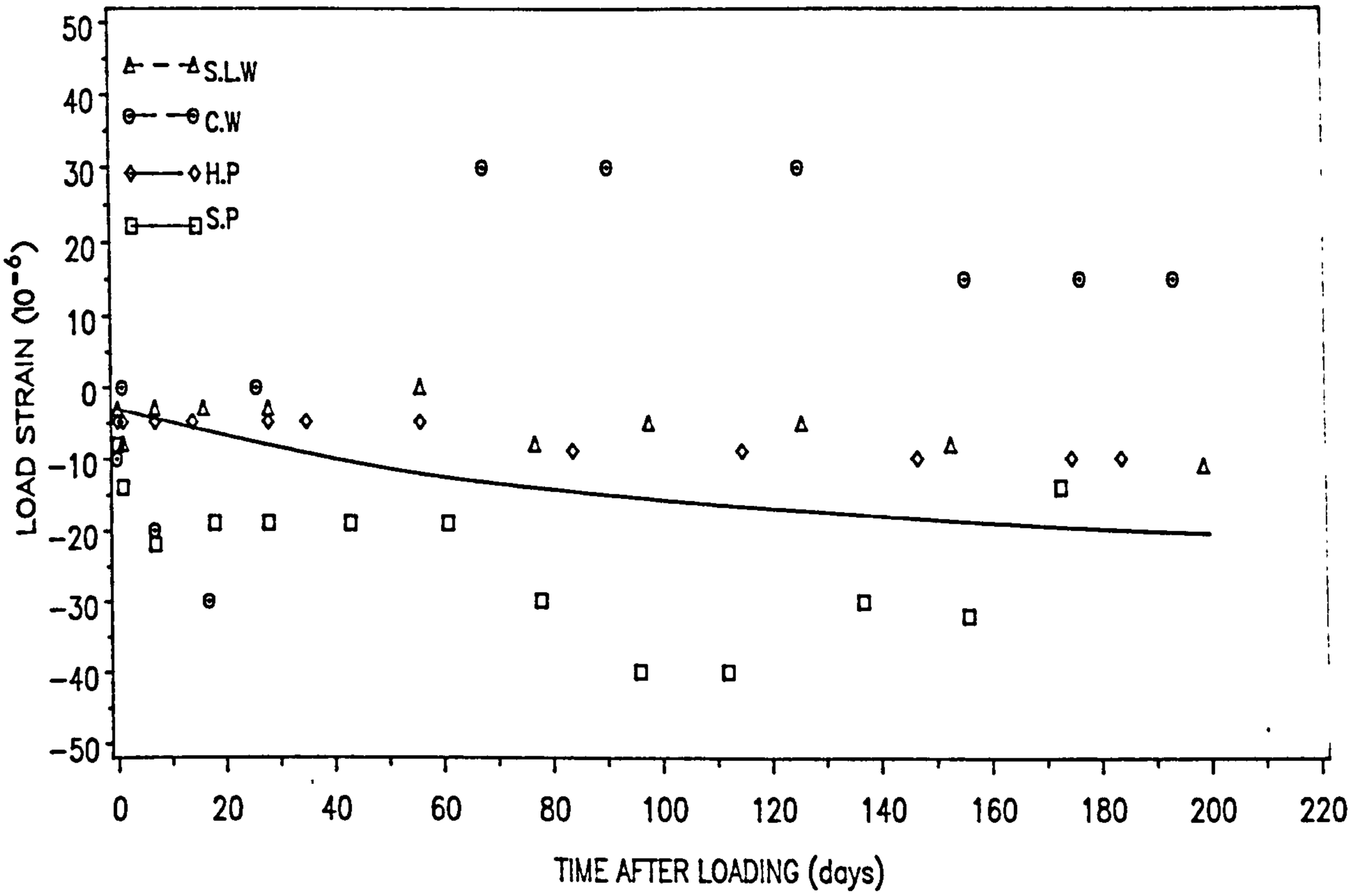

Fig. 8.19 – Lateral Load–Strain Curves for Centrally Embedded Brick in Clay Brickwork

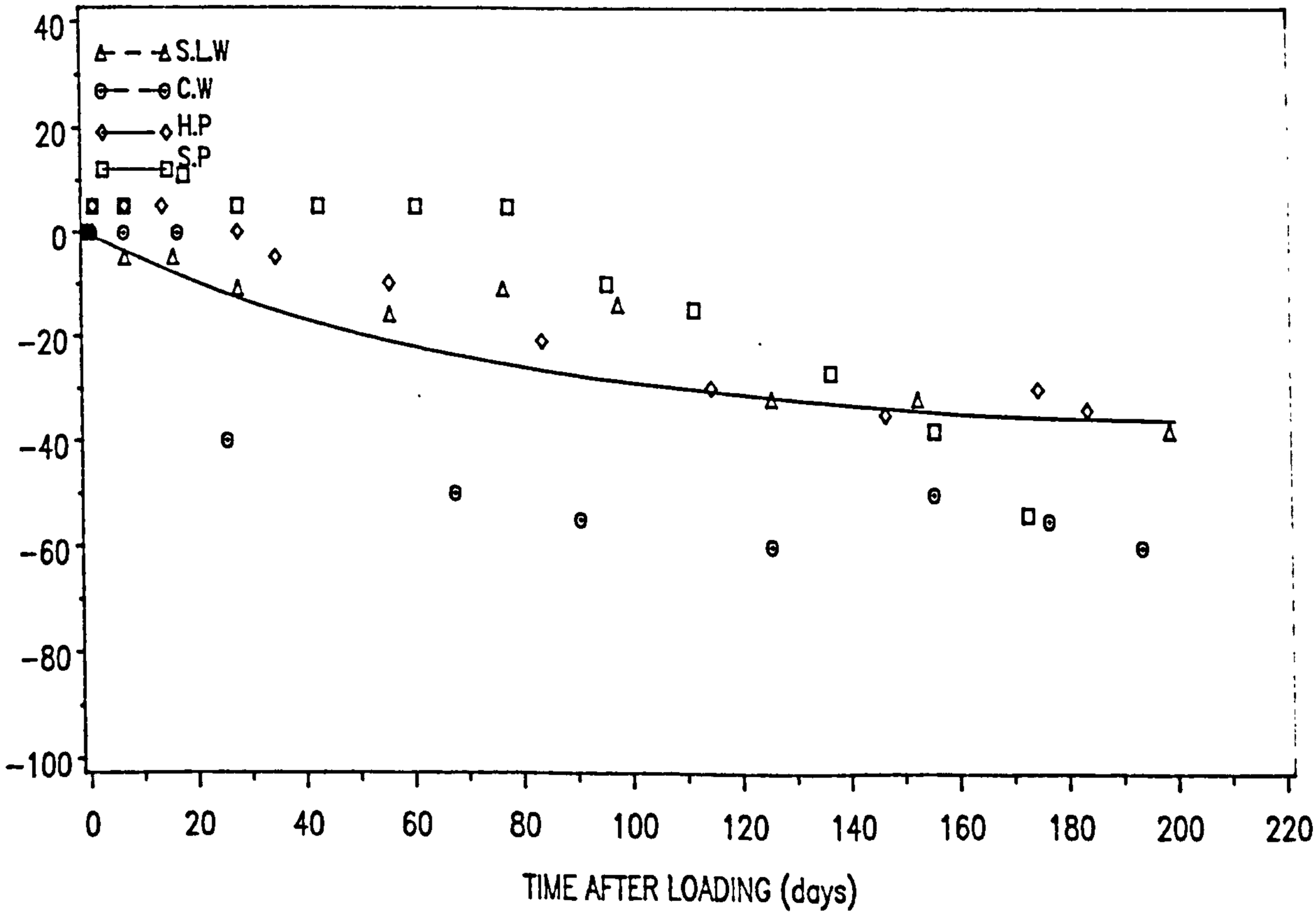

Fig. 8.20 – Lateral Moisture Strain Curves for Centrally Embedded Brick in Clay Brickwork

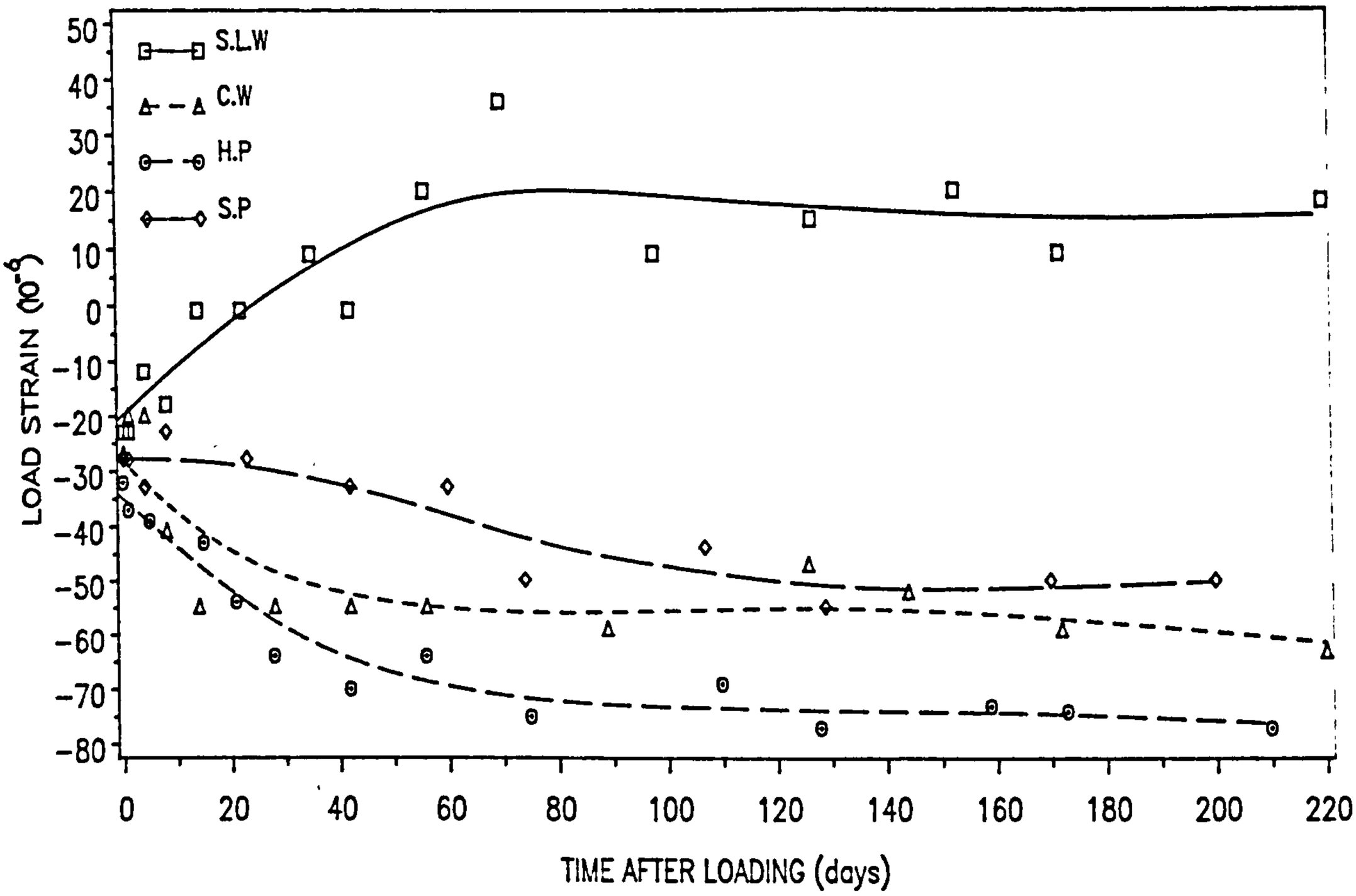

Fig. 8.21 – Lateral Load–Strain Curves for Centrally Embedded Brick in Calcium Silicate Brickwork

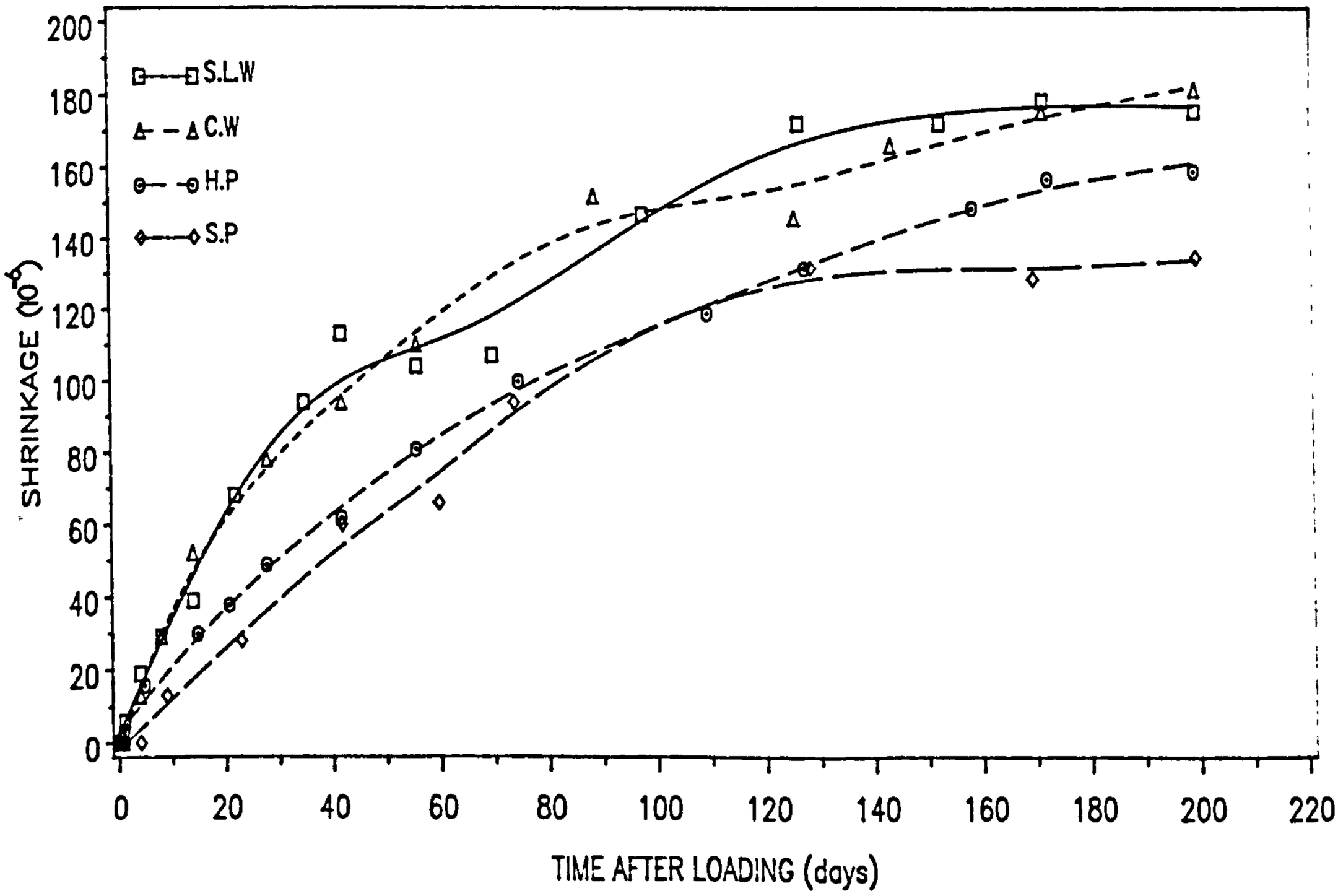

Fig. 8.22 – Lateral Shrinkage–time Curves for Centrally Embedded Brick in Calcium Silicate Brickwork

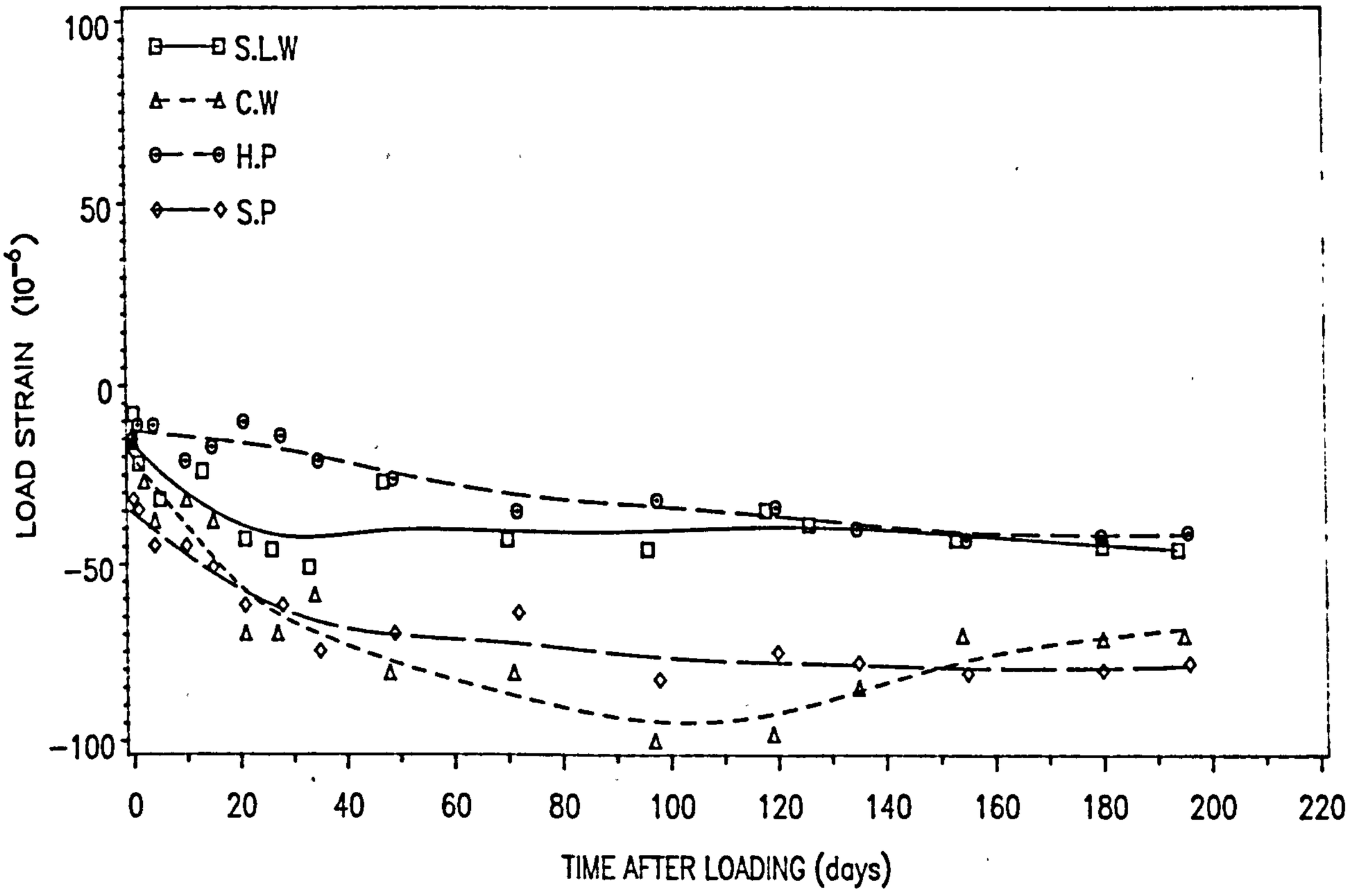

Fig. 8.23 – Lateral Load Strain Curves for Centrally Embedded Unit in Concrete Blockwork

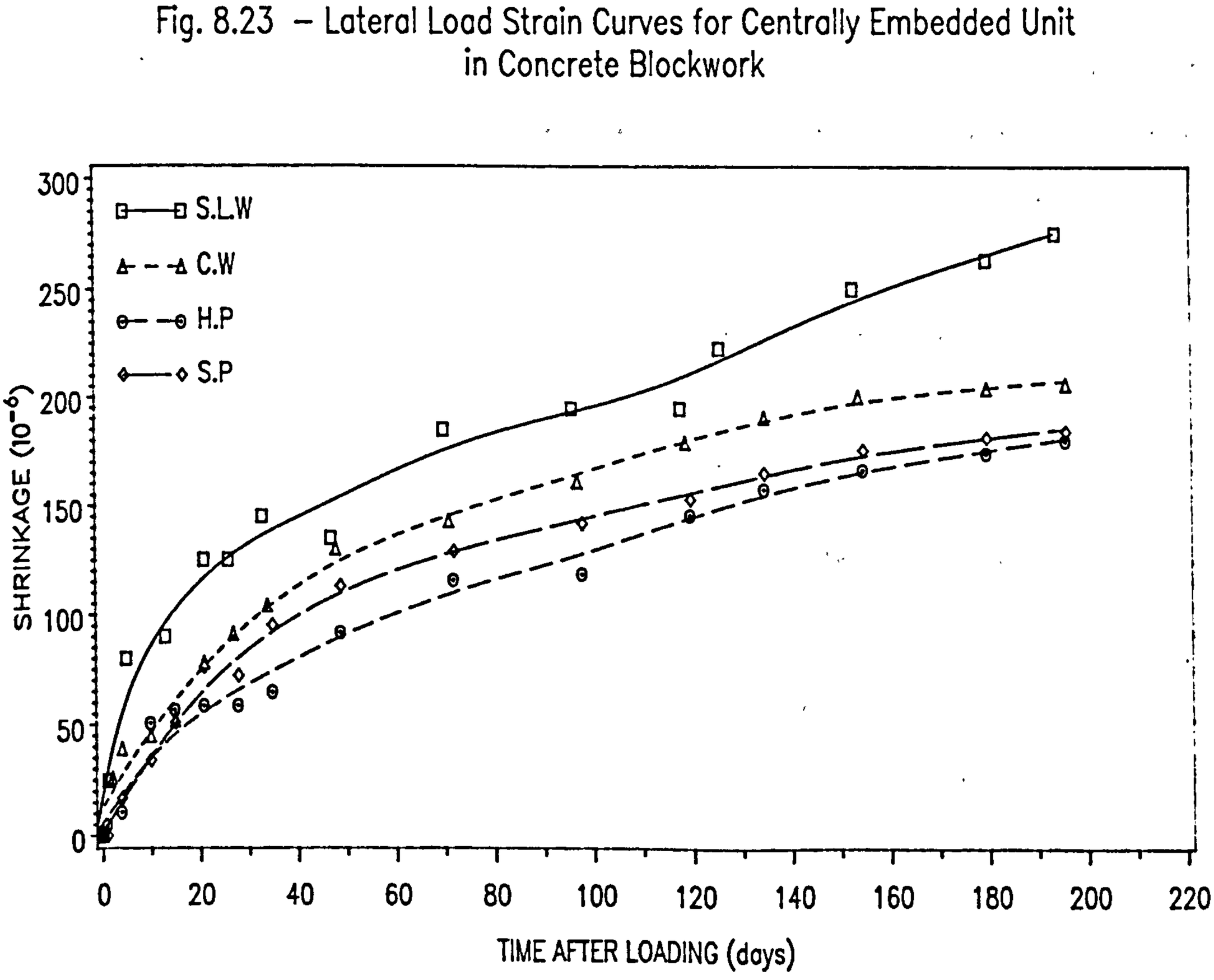

Fig. 8.24 – Lateral Shrinkage–time Curves for Centrally Embedded Unit in Concrete Blockwork

CHAPTER 9

CONCLUSIONS AND RECOMMENDATIONS FOR FURTHER RESEARCH

9.1 Conclusions

Six month experimental results on clay, calcium silicate and concrete masonry of various geometries reveal the following conclusions:

(1) The modulus of elasticity is independent of masonry geometry, which is in agreement with the findings of Lenczner[16].

(2) There is a clear influence of geometry on the ultimate creep of clay, calcium silicate and concrete masonry. The creep depends on the rate of moisture diffusion expressed in terms of V/S ratio, so that creep decreases as the V/S ratio increases. This trend explains Lenczner's observation[16] that creep in single-leaf walls is greater than creep of piers for clay brickwork. It is also found that the effect of V/S ratio on creep is more pronounced in the order: concrete blockwork > calcium silicate brickwork > clay brickwork. Generally, there is greater influence of V/S ratio on masonry members than in concrete members. However, the pier/wall creep ratio is much greater than that reported by Lenczner[16] for clay brickwork stored at a lower relative humidity.

(3) Lateral creep for all types of masonry is small compared with vertical creep. The elastic and creep Poisson's ratio can be assumed to be equal with values of 0.10 for clay and calcium silicate brickwork, and 0.20 for concrete blockwork.

(4) Ultimate vertical and horizontal shrinkage of calcium silicate brickwork and concrete blockwork also tend to decrease as V/S ratio increases but the relationship is influenced, possibly, by storage condition and pre-drying before measurements are taken. Ultimate vertical shrinkage of the clay brickwork is

less than calcium silicate shrinkage and appears to increase with an increase on V/S ratio. In the horizontal direction, the clay brickwork exhibited a small moisture expansion was independent of V/S ratio.

(5) A convenient parameter to quantify the geometry effect on creep and shrinkage of masonry is the V/S ratio.

(6) The levels of modulus of elasticity, creep and moisture movement of model walls are generally similar to that of the larger brickwork units. This finding is encouraging since model walls can be used with reasonable accuracy to predict the long-term deformation of brickwork so long as the behaviour of moisture diffusion of the component materials in the model wall is simulated. The high creep of model walls compared to the larger brickwork as reported by Lenczner[4] can be explained by a lack of proper simulation of moisture diffusion although other factors may be involved. For horizontal strains, the correlation between the model walls and the larger brickwork was not as good as for vertical strains, which was generally due to the inherent variability of the brick.

(7) The estimated creep and moisture movement of clay and calcium silicate brickwork were generally higher than that given by the various standard design guides, but for concrete blockwork the estimates generally agree with the range of values given by the standards; the standard guides do not include a provision for the influence of geometry.

(8) The prediction equation given in BS 5628 gives good estimates of modulus of elasticity of masonry.

(9) Creep in part-sealed mortar prisms is high; the creep coefficient ranges from 5.2 to 6.8 for the various V/S ratios.This consequently resulted in a high creep coefficient measured in the brickwork.

(10) Creep and moisture expansion in clay bricks are small and not affected by V/S ratio. On the other hand, for calcium silicate brick and concrete block, these movements are significant and are clearly affected by the V/S ratio.

(12) The application of the composite model to the deformation of masonry shows satisfactory agreement with the measured values, the exception being the modulus of calcium silicate brickwork laid 'frog-down' where higher predictions were obtained possibly because of the closing of air cavity formed during laying.

(13) When the models are used to predict the geometry effect on deformation of masonry there are satisfactory agreements for vertical creep and shrinkage for all masonry. For horizontal strain less satisfactory agreements were obtained particularly for clay brickwork, where shrinkage is predicted instead of moisture expansion. It should be remembered that the prediction of horizontal moisture strain is more complex, because of the influence of creep and, possibly, of external restraint to movement at the base. The main reason for the discrepancy of prediction is probably associated with the variability of brick properties; only two bricks were used which may not have been representative of the larger numbers in the masonry.

(14) When using composite models, by simulating the volume/surface ratio of embedded bricks or blocks and mortar, experimental data from unembedded specimens can be used successfully to predict creep and shrinkage of masonry.

(15) Composite modelling of deformations of masonry is a practical proposition provided the rate of moisture diffusion is taken into account for long term deformations, particularly in the horizontal mortar bed joints. The present model yields expressions for both the short-term and long-term deformations in any direction, for any configuration of masonry and has been verified to be applicable

to a wider range of masonry types. A representative sample of mortar and bricks should be tested in order to assess the range of properties and to assess the degree of anisotropy.

(17) Both the vertical and horizontal strains vary considerably over the height of the wall. There is no definite trend of the strain profile between the different masonry geometry. The variability of brick properties and the effect of restraint causes the actual strain to be very much higher than the overall average strain. This phenomenon should be considered by the designer so as to avoid local cracking resulting from induced stress because of restraint, particularly in the horizontal direction.

(18) The development of new design and construction techniques for masonry necessitate for more research in the deformation behaviour of masonry particularly the long-term deformation. There havebeen less than 50 publications on creep in masonry compared to more than 2500 publications on the similar topic for concrete, a fact which indicates the limitation of knowledge.

9.2 Recommendations for further research

Although this investigation has contributed significant data in the study of creep in masonry further research on the related topics should be enhanced.

(1) Future tests on creep in masonry should be prolonged to a much longer period, since in this investigation, for most cases movement was still continuing when the tests were terminated so that a better estimate of the ultimate strains could be obtained.

(2) The disadvantage of previous tests on creep is that only one specimen is normally used and therefore more tests are required in order to established the repeatability

of the results. For the effect of V/S ratio more data are required so that an equation can be established as for concrete technology. Similar tests should also be carried out on other types of masonry.

(3) Model wall tests can be improved by using scaled down model bricks as that used by Lenczner[4] but by proper simulation of moisture diffusion. This can reduce the effect variability of brick properties so that equal numbers of bricks and mortar are used in the model walls with that of the larger units.

(4) More data on creep and shrinkage of the partly sealed bricks and mortar specimens are necessary such that the variability of the brick properties could be statistically quantified in order to enable better predictions.

(5) Tests are required for the verification of composite models (Eq.(4.37)) for the deformation of masonry when subjected to lateral loading.

(6) The results of strain distribution measurements of this investigation could be used for theoretical modelling using finite element techniques.

(7) The ratio of ultimate horizontal shrinkage to ultimate vertical shrinkage of calcium silicate brickwork of this investigation was found to contradict that found by Brooks and Bingel[23]. The reason for this is not known but possibly was due to the different layout of the brick units used, (frogged in this investigation and solid by Brooks and Bingel) and may be due to the different degree of shrinkage anisotropy. These aspects require further investigation.

(8) From the literature review contradicting results have been reported on the effect of mortar type on creep of masonry. These results may have been influenced by the pre-drying condition of the masonry before loading. It is therefore necessary to investigate this effect in detail so that the use of the curves in Fig. 2.5 can be fully justified.

(9) The influence of pre-drying and other factors (age at loading, relative humidity, mortar bed reinforcement, temperature, etc.) require further investigation with the application of the composite model. Eventually, the accumulation of sufficient data will permit the development of a comprehensive design method for estimating masonry movement.

REFERENCES

1. Nylander H and Ericsson E.
Effect of wall perforations on floor slab loads and floor slab deformations in multi-storey houses. Nordisk Betong, 1957, Vol. 1, Part 4, pp. 269-292.

2. Poljakov S V.
Some problems on creep in ordinary and reinforced masonry members. Int. Council for Building Research, Studies and Documentation, Paris, 1962.

3. Lenczner D.
Design of creep machines for brickwork. Proc. British Ceram. Society, No. 4 , July 1965, pp. 1-8.

4. Lenczner D.
Creep on model brickwork. Designing engineering and constructing with masonry products. Gulf Publication, Houston Texas, 1969, pp. 58-67.

5. Lenczner D.
Creep in brickwork. Proc. 2nd. Inter. Brick Masonry Conference, Stoke-on-Trent, Brit. Ceram. Soc. 1970, pp. 44-49.

6. Lenczner D.
Creep in brickwork with and without damp proof course. Proc. 4th Inter. Sym. on loadbearing brickwork. Brit. Ceram. Soc., 1971, pp. 97-101.

7. Lenczner D.
Creep in concrete blockwork piers. Structural Engineers, Vol 52, No.3, March 1974, pp. 97-101.

8. Lenczner D, Salahuddin J, Wyatt K.
Effect of stress on creep in brickwork piers. Proc. British Ceram. Soc., Load-bearing brickwork (5), No 24, Sep 1975, pp. 1-9.

9. Wyatt K, Lenczner D, Salahuddin J.
The analysis of creep data for brickwork. Proc. British Ceram. Soc. Loadbearing brickwork (5), No 24, Sep. 1975, pp. 11-19.

10. Lenczner D.
Creep and Moisture Movements in Brickwork and Blockwork. Proc. Int. Conference on Performance of Building Structures, Glasgow, No.1, 1976, pp. 369-383.

11. Lenczner D and Salahuddin J.
Creep and moisture movements in brickwork wall. Proc. 4th Int. Brick Masonry Conf. Bruges. Section 2, 1976, pp. 2.A.4.0-2.A.4.5.

12. Lenczner D and Salahuddin J.
Creep and Moisture Movements in masonry piers and walls. First Canadian Masonry Symposium, Calgary, 1976, pp. 72-86.

13. Lenczner D.
The effect of strength and geometry on the elastic and creep properties of masonry members. Proc. of the North American Masonry Conf. University of Colorado at Boulder, 1978, pp. 23.1-15.

14. Lenczner D.
Creep in brickwork and blockwork in cavity walls and piers. Proc. British Ceram Soc. Loadbearing brickwork (6), No.27, Dec. 1978, pp. 53-66.

15. Lenczner D and Warren D.
Measurement of the creep strain distribution in axially loaded brickwork wall. T.M.S Journal, June 1983, pp. 27-36.

16. Lenczner D.
Brickwork: Guide to Creep. SCP 17, Structural Clay Product Ltd, 1980, 26 pp.

17. Lenczner D.
The loss of prestress in post-tensional brick masonry members. Masonry International, Vol.5, 1985, pp. 9-12.

18. Lenczner D.
In-situ measurement of creep movement in a brick masonry tower block. Masonry International, Vol.8, 1986, pp. 17-20.

19. Lenczner D.
Creep and prestress losses in brick masonry. The Structural Eng. Vol.64b, No.3, Sept. 1986, pp. 57-62.

20. Lenczner D.
Creep in brickwork walls at high and low stresses/strength ratio. Proc. 8th IBMAC, Dublin, 1988, pp. 324-333.

21. Wyatt K J and Morgan J W.
The role of creep in brickwork. Architectural Science Review, Vol. 17, Part 2, pp. 22-27.

22. Warren D, Lenczner D.
A creep-time function for single brickwork walls. Int. J. Masonry Const. Vol 2, Part 1, 1981, pp. 13-20.

23. Brooks J J.
Time-Dependant Behaviour of Calcium Silicate and Fletton Clay Brickwork Walls. Masonry(1), Proc. of Brit. Mas. Soc., No.1, 1986, pp. 17-19.

24. Othick G I.
Effect of temperature and relative humidity on creep in brickwork. PhD Thesis, University of Wales, 1982.

25. Johnson G D.
Creep and shrinkage in stressed clay brickwork. PhD thesis, University of Wales Institute of Science and Technology, Wales, 1984.

26. Schubert P.
Deformation of masonry due to shrinkage and creep. 5th Int. Brick Masonry Conference, 1978, pp. 132-138.

27. ACI 209R-82.
Prediction of creep, shrinkage and temperature effects in concrete structures, Part 1: Materials and general properties of concrete. ACI Manual of Concrete Practice, reapproved 1986.

28. CEB-FIP.
International recommendations for the design and construction of concrete structures - Principles and recommendations, Comite Europeen du Beton - Federation Internationale de la Precontrainte, FIP Sixth Congress, Prague, June 1970; published by Cement and Concrete Association: London, 1970, 80 pp.

29. CEB-FIP.
Model code for concrete structures, Comite Europeen du Beton - Federation Internationale de la Precontrainte, Paris, 1978, 348 pp.

30. Ross A D.
Concrete creep data, The Structural Engineer, 15, No.8, 1937, pp. 314-26.

31. Jessop E L, Shrive N G, England G L.
Elastic and creep properties of masonry. Proc. the North American Masonry Conference, Boulder, Colarado. 1978, pp. 12.1-16.

32. Brooks J J, Bingel P R.
Influence of Size on Moisture Movements in Unrestrained Masonry. Masonry International, No.4, March 1985, pp. 36-44.

33. Shrive N G, Jessop E L and Khalil M R.
Stress-strain behaviour of masonry walls. Proc. 5th. Int. Masonry Conference, 1979, pp. 453-458.

34. Ameny P, Loov R E and Jessop E L.
Strength, elastic and creep properties of concrete masonry. Int. Journal of Masonry Construction, Vol 1, Part 1, 1980, pp. 33-39.

35. Ameny P, Loov R E and Shrive N G.
Prediction of elastic behaviour of masonry. The Int. J. Masonry Construction, Vol.3, No.1, 1983, pp. 1-9.

36. Ameny P.
Modelling the deformations of masonry. PhD Thesis, The University of Calgary, 1982.

37. Shrive N G and England G L.
Elastic, creep and shrinkage behaviour of masonry. Int. Journal of Masonry Construction, Vol 1, Part 3, 1981, pp. 103-109.

38. Ameny P, Loov R E and Shrive N G.
Models for long term deformation of brickwork. Masonry International, Vol 1, 1984, pp. 27-28.

39. Brooks J J.
Composite Models for Predicting Elastic and Long Term Movements in Brickwork Walls. Masonry (1), Proc. of Brit. Mas. Soc., No.1, Nov. 1986, pp. 20-23.

40. Brooks J J and Bingel P R.
A composite model for masonry shrinkage. Proc. of Brit. Mas. Soc., No.2, April 1988, pp. 12-14.

41. Brooks J J.
Composite modelling of elasticity and creep of masonry. Report Dept. of Civil Engineering, University of Leeds, Jan. 1987, 24 pp.

42. Brooks J J.
Composite modelling of moisture movement and thermal movement of masonry. Report Dept. of Civil Engineering, University of Leeds, Jan. 1987, 21 pp.

43. Harris H G and Becica I J.
Behaviour of concrete masonry structures. Proc. North America Masonry Constr. University of Colorado, Boulder USA, 1978, paper 10, 18 pages.

44. Francis A J, Horman C B and Jerrem L E.
The effect of joint thickness and other factors on compressive strength of brickwork, Proc. 2nd. Int. Brick Masonry Coference. British Ceram. Res. Ass., 1971, pp. 31-37.

45. Richard O H, Litvin A and Hanson J A.
Influence of mortar and block properties on shrinkage cracking of masonry. Journal PCA research. Vol.10, No.1, 1968, pp. 34-51.

46. British Standard Institution, BS 5628:Part 2:1985.
Use of masonry:Part 2: Structural use of reinforced and prestresses masonry, BSI, London, 1985.

47. Sahlin S.
Structural Masonry. Prentice-Hall Inc., 290 pages.

48. Hilsdorf H K.
Investigation into failure mechanism of brick masonry under axial compression, Proc. 1st. Int. Masonry Conference, 1963, pp. 34-41.

49. ACI Committee 318-83.
Building Code requirements for reinforced concrete, Part 3: Use of concrete in building - Design, specifications, and related topics, ACI Manual of concrete practice, 1984.

50. Lenczner D.
Strength and Elastic Properties of the 9-in Brickwork Cube. Trans. British Ceram Society, No. 65, 1966, pp. 363-382.

51. Base G D and Baker L R.
Fundamental properties of structural brickwork. J. Australian Ceram. Soc., Vol.9, 1973, pp. 1-6.

52. Binda L, Fontana A and Frigerio G.
Mechanical behaviour of brick masonries derived from unit and mortar characteristics. Proc. 8th Int. Brick/Block Masonry Conference, Dublin, 1988, pp. 205-216.

53. Page A W.
A model for the in-plane deformations and failure of brickwork. Engineering Bulletin CE8, Department of Civil Engineering, University of New Castle, Australia, March 1978.

54. Brooks J J and Amjad M A.
Elasticity and strength of clay brickwork test units. Proc. 8th Int. Brick/Block Masonry Conference, Dublin, 1988, pp. 342-349.

55. Richart F E, Moorman R R and Woodworth P M.
Strength and stability of concrete masonry walls. Engineeering Experimental Station Bulletin, No.251, University of Illinois, July, 1932.

56. Read J B and Clements S W.
The strength of concrete block walls, Phase II: Under Axial loading. Cement and Concrete Association, 1972. 17 pp.

57. British Standard Institution, BS 1881: Part 116:1983.
Method of determining of compressive strength of concrete cubes. BSI London, 1983.

58. Allen D E.
Limit states design - a probabilistic study. Canadian Journal of Civil Engineering, Vol.2, 1975, pp. 36-49.

59. Rao R N S.
Experimental investigation on structural performance of brick masonry prisms. Proc. 1st. IBMAC, Texas, pp. 74-79.

60. Yokel F Y and Dikkers K D.
Strength of load bearing masonry walls. Proc. ASCE, Structural Division, May 1971, pp. 1593-1609.

61. Edgell G J.
Stress-strain relationships for brickwork. Their application in the theory of unreinforced slender members. British Ceram. Research Assoc., Technical Note No. 313, Oct. 1980.

62. Hegemier G A, Krishnamoorthy G, Nunn R O and Moothy T V.
Prism tests for compressive strength of concrete masonry. Proc. of North American Conf., 1978, pp. 18.1-18.17.

63. Hamid A A, Drysdale R G and Heidebrecht A C.
Effect of grouting on the strength characteristics of concrete block masonry. Proc. North American Masonry Conference, The Masonry Society, August 1978, pp. 11.1-11.17.

64. Hatzinikolas M, Longworth J and Warwaruk J.
Failure modes for eccentrically loaded concrete block masonry walls. ACI Journal, Vol.77. Aug. 1980, pp. 258-263.

65. Plowman J M.
Modulus of elasticity of brickwork. Trans. British Ceram Society, No.4, 1965, pp. 37-64.

66. Sinha B P and Hendry A W.
The effect of brickwork bond on the load-bearing capacity of model brickwalls, Proc. British Ceram. Soc. ,No.11, 1968, pp. 55-67.

67. Grimm C T.
Strength related properties of brick masonry. Proceedings of the American Society of Civil Engineers, Structural Division, Vol.101, No.STI, January 1975, pp. 217-232.

68. Brooks J J and Amjad M A.
Strength and elasticity of calcium silicate and concrete masonry. Paper to be presented at the Second Int. Masonry Conference, The Brit. Mas. Soc., London, Oct. 1989.

69. Baker L R, Jessop E L.
Moisture movement in concrete masonry : a review. Int. Jour. of Masonry Const, Vol. 2, part 2, 1982, pp. 75-80.

70. Baker L R, Jessop E L.
Moisture movement in clay brickwork : a review. Int. Jour. of Masonry Const, Vol. 2, part 2, 1982, pp. 103-109.

71. Kalousek G L.
Fundamental factors in drying shrinkage of concrete block. Journal ACI, No.26, Part 3, 1954, Title No. 51-10.

72. Washa G W.
High pressure steam curing: Modern practice, and properties of autoclave products. Report by ACI Committee 516, Journal ACI, 1965, Title 62-53,8.

73. Allan W D M.
Shrinkage measurement of concrete block masonry, final report. Journal ACI, Proceedings 26, 1930, pp. 177.

74. Kinniburgh W.
Comparison of drying shrinkage of autoclaved and air-cured concrete at different humidities. RILEM Symposium on Steam-Cured Lightweight Concrete, 1960, Goteburg.

75. Hedstrom R O.
Influence of mortar and block properties on shrinkage cracking of masonry walls. Portland Cement Association, Research and Development Laboratories, Vol.10, Part 1, 1968, pp. 34-51.

76. West H W H.
Moisture movement of bricks and brickwork. Trans. British Ceramic Society, 66(4), 167, pp. 137-160.

77. Smith R G.
Moisture expansion of structural ceramics: Expansion of unrestrained Fletton brickwork, Trans. Brit. Ceram. Soc., 73(6), pp. 191-198.

78. Hosking J S, Hueber H V, Waters E H and Lewis R E.
The permanent moisture expansion of clay products. I Bricks, Division of Building Research Technical Paper No.6, Commonwealth Scientific and Industrial Research Organisation, Australia, 1959, 71 pp.

79. Lomax J and Ford R W.
Investigations into a method for assessing the long term moisture expansion in clay bricks. Trans. British Ceramic Society, Vol.82, No.3, May-June 1983, pp. 79-82.

80. Beard R, Dinnie A and Sharpes A B.
Movement of brickwork - A review of 21 years experience. Trans. British Ceramic Society, Vol.83, No.3, May-June 1983, pp. 82-86.

81. Beard R, Dinnie A and Richards R.
Movement of brickwork. Trans. British Ceram Society, Vol.68, No.73, 1969, pp. 73-90.

82. De Vekey R C.
Moisture expansion in clay masonry. Trans. British Ceramic Society, Vol.82, No.2, March-April 1983, pp. 55-57.

83. Foster D and Johnson G D.
Design for movement in clay brickwork in the UK. Proc. British Ceram. Soc., Load-bearing brickwork (7), No. 30, Sep 1982.

84. Lomax J and Ford R W.
A method for assessing the long term moisture expansion characteristic of clay bricks. Proc. 8th IBMAC, Dublin, 1988, pp. 92-10r.

85. British Standard Institution. CP 121: Part 1, 1973.
Walling - Brick and block masonry. BSI London 1973.

86. Building Research Station.
Digest, Second series, 165, 2, 1965.

87. Bryant A H and Vadhanavikit C.
Creep, shrinkage - Size and age at loading effects. ACI Material Journal, March-April 1987, pp. 117-123.

88. Carlson R W.
Drying shrinkage of large members. J. ACI, Vol.33, Jan.-Feb. 1937, pp. 327-336.

89. Becker N K and Macinnis C.
A theoretical method for predicting the shrinkage of concrete. J. ACI, Sep. 1977, pp. 652-657.

90. Bazant Z P, Osman E and Thonguthua W.
Practical formulation of shrinkage and creep of concrete. Materials and Structures (RILEM, Paris), Vol.5, 1972, pp. 3-11.

91. Bazant Z P and Najjar L J.
Non-linear water diffusion in non-saturated concrete. Materials and Structures (RILEM, Paris), Vol.5, 1972, pp. 3-11.

92. Ross A D.
Shape, size and shrinkage. Concrete and Constructional Eng.(London), August 1944, pp. 193-199.

93. Keeton J R.
Study of creep in concrete. Technical Report No. R333-1,2, U.S. Naval Civil Engineering Laboratory, Port Hueneme California, 1965, Phase 1 - 5.

94. Kesler C E, Wallo E M and Yuan R L.
Free shrinkage of concrete mortar. T and A.M Report No. 664, Department of Theoretical and Applied Mechanics, University of Illinois, Urbana, Illinois, July 1966.

95. L'Hermite R G and MaMillan.
Further results of shrinkage and creep tests. Proc. of Int. Con. on the structure of concrete and its behaviour under load, London, September, 1965. Cement and Concrete Association, 1968, pp. 423-433.

96. Hansen T C and Mattock A H.
Influence of Size and Shape of Member on the Shrinkage of Concrete. ACI Journal,63,1966, pp. 267-290.

97. Hobbs D W.
Influence of specimen geometry upon weight change and shrinkage of air-dried concrete specimens. Magazine of Concrete Research, Vol.29, No.99, June 1977, pp. 70-80.

98. Parrott L J.
Moisture profiles in drying concrete. Advances in Cement Research, Vol.1, No.3, July 1988, pp. 164-170.

99. Terill J M, Richardson M and Selby A R.
Non-linear moisture profiles and shrinkage in concrete members. Magazine of Concrete Research, Vol.38, No.137, Dec. 1986, pp. 220-225.

100. Bazant Z P and Panula L.
Simplified prediction of concrete creep from strength and mix. Structural Engineering Report 78-10/6405, Civil Engineering, North Western University, Illinois, 1978, 24 pp.

101. Weil G.
Influence des dimensions et des tensions sur le retrait et le fluage du beton, RILEM Buletin, Paris, No.3, July 1959, pp. 4-14.

102. Ulistkii I I.
A method of computing creep and shrinkage deformation of concrete for practical purposes, Beton i Zhelezobeton, N0.4, 1962, pp. 174-180; Translation No.6030, Commonwealth Scientific and Industrial Research Organisation, Melbourne, Australia.

103. Neville A M, Dilger W H and Brooks J J.
Creep of Plain and Structural Concrete. Construction Press, 1983.

104. England G L.
Steady-state stresses in concrete structures subjected to sustained temperatures and loads. Nuclear Engineering and Design, Vol.3, 1966, pp. 54-65.

105. Trost H.
Auswirkungen des superposions prinzips auf kriechund - Probleme vei beton und spannbeton. Beton und Stahlbetronban, Vol.62, 1967, pp. 230-238, 261-269.

106. Hansen T C.
Creep for concrete. Bulletin No.33, Swedish cement and Concrete research Institute, Stockholm, 1958, 45 pp.

107. Hansen T C and Nielson K E C.
Influence of aggregate properties on concrete shrinkage. ACI Journal, 62, 1965, pp. 783-794.

108. Hirsch T J.
Modulus of elasticity of concrete as affected by elastic moduli of cement paste matrix and aggregate. ACI Journal, 59, 1962, pp. 427-451.

109. Kameswara Rao C V S, Swamy R N and Mangat P S.
Mechanical behaviour of concrete as a composite material. Materials and Construction, Vol.7, No.40, pp. 265-270.

110. Hobbs D W.
The dependence of bulk modulus, Young's modulus, creep, shrinkage and thermal expansion of concrete upon aggregate volume and concentration. Materials and Construction, Vol.7, No.40, pp. 265-270.

111. Counto U J.
The effect of the elastic modulus of the aggregate on the elastic modulus, creep and creep recovery of concrete. Magazine of Concrete Research, Vol.16, No.48, Sept. 1964, pp. 129-138.

112. Tatsa E, Yishai O and Levy M.
Loss of steel stresses in prestressed concrete blockwork walls. Structural Engineer, No.5, Vol.51, May 1973, pp. 177-182.

113. Deutsches Institut Fur Normung, DIN 1053: Part 2, 1984.
Masonry : Masonry design on the basis of suitably tests. Design and Construction. Berlin.

114. International Standard Organisation.
Masonry, Working documents for TC179, revised 1987.

115. BS 3921: 1974.
The Specification for Clay Bricks. BSI London 1974.

116. British Standard Institution, BS 187: 1978.
Specification for calcium silicate bricks., BSI London, 1974.

117. British Standard Institution, BS 6073: Part 1: 1981.
Specificaton for precast concrete masonry units, BSI London 1981.

118. British Standard Institution, BS 4551: 1980.
Method of testing mortars, screeds and plasters. BSI, London 1980.

119. Alexander S J and Lawson R M.
Design for movement in buildings. CIRIA Technical Note 107, 1981, 54pp.

120. Bingel P R.
Moisture movements in brickwork and blockwork. MSc. Thesis, Department of Civil Engineering, Leeds University, 1984.

121. Bradshaw R E and Hendry A W.
Further crushing tests on storey-height walls 4.5 inch thick. Proc. Brit. Ceram. Soc., No.11, July 1968, pp. 25-53.

122. Hansen T C.
Theories of multiphase materials applied to concrete, cement mortar and cement paste. Proceedings of the International Conference on the Structure of Concrete, Cement and Concrete Association, London 1968, pp. 16-23.

123. Paul B.
Prediction of elastic constants of multiphase materials. Transaction of the Metallic Society, American Institute of Mechanical Engineers, Vol.219, February 1960, pp. 36-41.

124. Harrison T A.
Early-age thermal crack control in concrete. CIRIA Report No.91, Construction Industry Research and Information Association, London, 1981, 48 pp.

125. Haseltine B A.
A design guide for reinforced and prestressed brickwork. Proc. the North American Masonry Conference, The Masonry Society, August 1978, University of Colarado.

126. Hendry A W.
Structural Brickwork. The Macmillan Press Ltd., 209 pages.

127. Hobbs D W and Mears A R.
The influence of specimen geometry upon weight change and shrinkage of air-dried mortar specimens. Magazine of Concrete Research, Vol 23, No 75-76, June-September 1971.

128.Jackson N.
Civil Engineering Materials. The MacMillan Press Ltd., 3rd Edition, 412 pp.

129. Lenczner D.
Movements in Buildings. Pergamon Press, 2nd edition, 109 pages.

130. Lenczner D.
Elements of load-bearing Brickwork. Pergamon Press, 113 pages.

131. Neville A M.
Properties of Concrete, Pitman Publishing, 1975.

132. British Standard Institution, BS1200: 1976.
Building sands from natural sources, BSI London, 1976.

133. Powell B and Hodgkinson H R.
Determination of stress-strain relationship of brickwork. British Ceramic Research Assoc., Technical Report 249, January 1976.

134. Hendry A W and Murthy C K.
Compressive tests on 1/3 and 1/6 scale model brickwork piers and walls. Proc. Brit. Ceram. Soc., No.64, 1965.

135. Rao C V S R, Swammy R N and Mangat P S.
Mechanical behaviour of concrete as a composite material. RILEM, Vol.7, No.40, pp. 365-271, 9174.

136. Shrive N G.
Effects of time dependent movement in composite and post-tensioned masonry. Masonry International, Vol.2, No.1, 1988, pp. 25-29.

137. Shrive N G and Jessop E L.
Anisotropy in extruded clay units and its effect on masonry behaviour. Proc. 8th IBMAC, Dublin, 1988, pp. 39-50.

138. Structural Clay Products Institute (SCPI)
Recommended practice for engineered brick masonry, McLean, Virginia,1969.

139. Brooks J J and Abdullah C S.
Composite model prediction of the geometry effect on creep and shrinkage of clay brickwork. Proc. 8th. Int. Masonry Conference, Dublin, 1988, pp. 342-349.

140. Brooks J J and Abdullah C S.
Geometry effect on creep and moisture movements of brickwork. Publication for Masonry International.

141. Brooks J J.
Composite modelling of masonry deformation. Paper to be published in Materials and Construction, RILEM, Paris, 1990.

142. Rad P F.
Inherent compressive and tensile strengths of structural bricks. Proc. of North American Masonry conf., 1978, pp. 9.1-9.9.

143. Brooks J J and Abdullah C S.
Composite modelling of the geometry influence on creep and shrinkage of calcium silicate brickwork. Paper for the Second Int. Masonry Conference, London, Oct. 1989.

144. Brooks J J and Abdullah C S.
Creep and drying shrinkage of concrete blockwork. Paper for Magazine of Concrete Research.

APPENDIX A

Table A1 : Results of 5-hour boiling tests

(a) Clay brick

Specimen	Weight (Kg)		Absorption $\frac{(a-b)}{b}\times 100$ (%)
	Wet (a)	Dry (b)	
1	2879	2705	6.4
2	2757	2697	2.2
3	2767	2695	2.7
4	2808	2705	3.8
5	2834	2738	3.5
6	2839	2695	5.3
7	2872	2700	6.4
8	2840	2692	5.5
9	2864	2686	6.6
10	2881	2693	6.9
Average			4.9
Standard Deviation			

(b) Calcium silicate brick

Specimen	Weight (Kg)		Absorption $\frac{(a-b)}{b}\times 100$ (%)
	Wet (a)	Dry (b)	
1	2834	2603	8.9
2	2871	2640	8.7
3	2806	2563	9.5
4	2793	2525	10.6
5	2868	2604	10.1
6	2775	2510	10.6
7	2789	2522	10.6
8	2878	2631	9.3
9	2797	2561	9.2
10	2820	2566	9.9
Average			9.7
Standard Deviation			0.67

Table A2 - Weight Losses of Unsealed, Part-sealed and Fully sealed Mortar Prisms

Drying time (days)	Unsealed	Part-sealed	Fully Sealed
3	3.8	2.1	0.2
21	4.2	2.3	0.2
49	4.4	2.4	0.2
98	4.5	2.6	0.1
175	4.6	2.8	0.2

Table A3 - Calculations for the Determination of Load

Ultimate load = $1.4g_k + 1.6q_k$ ---> $1.5q_k$
Fig. 1, Table 2, BS 5628, part 2
class B (48.5 MPa) ---> $f_k = 12.0$
class 4 (27.5 MPa) ---> $f_k = 7.9$ -- mortar designation (ii)
Table 4,
f_m = 2.8 to 3.5 say 3.5
If class 4,
working stress = 8/(1.5 x 3.5)
= 1.52 MPa
Table 7, slenderness effect,
working stress = $\frac{2}{3}$ x 1.52 ~ 1.0 MPa.
If class B,
working stress = 12/(1.5 x 3.5)
= 2.30 MPa
Table 7, slenderness effect,
working stress = $\frac{2}{3}$ x 2.3 ~ 1.5 MPa.

$\therefore$ Apply a load of 1.5 MPa

Table A4 - Moisture Movement of Brick Specimens Covered with Mortar on Bed Faces (Average of 6 Specimens)

Time (days)	Moisture Strain (10^{-6})	
	Clay Brick	Calcium Silicate Brick
0	0	0
20	-10	51
40	7	67
60	-10	85
100	-19	113
140	-10	139
180	-15	157

APPENDIX B

TYPICAL VERTICAL STRAINS OF MASONRY AS MEASURED AT VARIOUS POSITIONS

Table B1 - Clay Brickwork

(a) Single-leaf Wall

time after loading (days)	Overall Strain (10^{-6})									Moisture Strain (10^{-6})								
	A1	A2	A3	A4	B1	B2	B3	B4	ave.	A1	A2	A3	A4	B1	B2	B3	B4	ave.
0	208	185	171		66	55	77		127	0	0	0		0	0	0		0
6	353	311	287		180	134	139		234	24	26	24		19	25	31		25
56	586	564	521	-	518	463	447	-	517	119	119	122	-	124	152	162	-	146
112	625	604	559		583	540	512		574	117	117	111		120	165	175		153
174	637	623	576		555	549	518		577	116	114	97		107	165	172		148

(b) Cavity Wall

time after loading (days)	Overall Strain (10^{-6})									Moisture Strain (10^{-6})								
	A1	A2	A3	A4	B1	B2	B3	B4	ave.	A1	A2	A3	A4	B1	B2	B3	B4	ave.
0	89	80	84		117	97	103		95	0	0	0		0	0	0		0
7	177	164	192		247	217	213		202	34	14	17		14	33	25		23
56	33	350	352	-	406	413	416	-	379	71	64	81	-	118	120	87	-	90
101	436	404	395		481	502	501		453	100	100	107		132	145	118		117
199	518	511	505		502	522	521		513	112	118	118		132	145	120		123

(c) Hollow Pier

time after loading (days)	Overall Strain (10^{-6})									Moisture Strain (10^{-6})								
	A1	A2	A3	A4	B1	B2	B3	B4	ave.	A1	A2	A3	A4	B1	B2	B3	B4	ave.
0	104	98	127		87	116	75		101	0	0	0		0	0	0		0
6	147	162	172		149	193	153		163	10	10	10		10	16	16		12
56	315	333	331	-	269	369	344	-	327	87	77	72	-	65	58	54	-	69
115	451	467	464		362	421	408		429	113	108	105		90	86	84		98
194	502	501	513		415	475	453		477	119	115	111		110	106	103		111

(d) Solid Pier

time after loading (days)	Overall Strain (10^{-6})									Moisture Strain (10^{-6})								
	A1	A2	A3	A4	B1	B2	B3	B4	ave.	A1	A2	A3	A4	B1	B2	B3	B4	ave.
0	75	121	121	114	109	80	87	92	100	0	0	0	0	0	0	0	0	0
7	128	171	162	174	157	139	139	140	151	10	13	4	8	8	8	18	16	11
57	275	333	331	329	297	266	284	283	300	33	66	49	77	57	53	60	50	56
115	353	447	455	453	389	348	365	367	397	53	90	81	104	98	92	101	86	88
184	381	457	465	473	442	396	431	425	434	82	105	101	105	106	106	101	97	100

Table B2 - Calcium Silicate Brickwork

(a) Single-leaf Wall

time after loading (days)	Overall Strain (10^{-6})									Moisture Strain (10^{-6})								
	A1	A2	A3	A4	B1	B2	B3	B4	ave.	A1	A2	A3	A4	B1	B2	B3	B4	ave.
0	297	297	313		280	319	298		301	0	0	0		0	0	0		0
8	529	513	547		518	539	532		530	68	70	80		53	60	73		66
56	912	886	952	-	916	933	933	-	922	233	206	197	-	186	198	212	-	205
111	1019	1002	1079		1052	1049	1037		1040	254	234	224		208	234	237		235
200	1153	1156	1254		1276	1253	1183		1213	302	291	286		268	284	293		287

(b) Cavity Wall

time after loading (days)	Overall Strain (10^{-6})									Moisture Strain (10^{-6})								
	A1	A2	A3	A4	B1	B2	B3	B4	ave.	A1	A2	A3	A4	B1	B2	B3	B4	ave.
0	321	266	308	349	283	393	245	207	297	0	0	0	0	0	0	0	0	0
8	524	462	510	559	659	560	640	601	564	64	62	62	60	62	65	68	57	62
56	803	748	803	863	969	829	937	892	856	192	190	171	198	172	174	186	178	183
112	967	902	969	1036	1143	986	1101	1047	1019	251	247	226	238	228	237	249	233	239
200	1088	1019	1116	1175	1250	1076	1193	1143	1133	274	274	257	271	258	265	279	265	268

(c) Hollow Pier

time after loading (days)	Overall Strain (10^{-6})									Moisture Strain (10^{-6})								
	A1	A2	A3	A4	B1	B2	B3	B4	ave.	A1	A2	A3	A4	B1	B2	B3	B4	ave.
0	286	280	349	301	341	236	204	198	275	0	0	0	0	0	0	0	0	0
5	508	464	499	457	510	444	450	452	473	23	32	34	27	44	43	33	32	34
56	783	712	738	724	782	721	753	744	745	96	117	128	128	152	149	123	112	126
110	942	882	907	897	953	883	921	916	913	171	182	195	197	225	223	197	190	198
200	1017	937	985	980	1027	959	996	986	986	224	216	234	237	251	263	236	230	237

(d) Solid Pier

time after loading (days)	Overall Strain (10^{-6})									Moisture Strain (10^{-6})								
	A1	A2	A3	A4	B1	B2	B3	B4	ave.	A1	A2	A3	A4	B1	B2	B3	B4	ave.
0	286	277	279	308	303	312	320	303	298	0	0	0	0	0	0	0	0	0
9	456	425	430	473	471	477	493	471	462	33	27	20	31	26	25	28	34	28
60	680	683	685	735	674	671	705	694	691	122	124	118	133	120	117	117	126	122
107	766	762	778	858	860	862	856	816	820	160	165	154	169	184	178	178	180	171
198	860	850	870	948	972	970	956	918	918	191	204	194	204	216	209	217	217	207

Table B3 - Concrete Blockwork

(a) Single-leaf Wall

time after loading (days)	Overall Strain (10^{-6})									Moisture Strain (10^{-6})								
	A1	A2	A3	A4	B1	B2	B3	B4	ave.	A1	A2	A3	A4	B1	B2	B3	B4	ave.
0	148	120	136		180	181	140		151	0	0	0		0	0	0		0
5	330	225	308		344	363	320		316	96	52	83		71	64	56		70
47	650	619	667	-	742	799	689	-	695	288	232	267	-	207	240	276	-	252
96	775	733	807		837	898	778		805	346	297	315		245	300	327		305
194	879	852	897		918	1006	873		904	396	351	393		310	352	352		359

(b) Cavity Wall

time after loading (days)	Overall Strain (10^{-6})									Moisture Strain (10^{-6})								
	A1	A2	A3	A4	B1	B2	B3	B4	ave.	A1	A2	A3	A4	B1	B2	B3	B4	ave.
0	186	176	182	200	130	134	152	152	164	0	0	0	0	0	0	0	0	0
10	370	340	395	368	343	291	297	312	340	47	53	47	55	67	55	61	61	61
48	642	624	672	647	644	577	567	591	621	190	190	172	193	239	207	210	216	218
97	727	698	783	767	735	680	681	703	721	252	246	221	249	299	268	274	271	278
195	835	792	884	862	817	789	774	786	818	303	297	282	294	350	320	332	329	333

(c) Hollow Pier

time after loading (days)	Overall Strain (10^{-6})									Moisture Strain (10^{-6})								
	A1	A2	A3	A4	B1	B2	B3	B4	ave.	A1	A2	A3	A4	B1	B2	B3	B4	ave.
0	164	144	172	144	149	139	158	166	155	0	0	0	0	0	0	0	0	0
10	281	264	283	248	314	302	292	325	289	24	27	38	27	21	27	27	21	26
49	471	455	487	454	478	463	487	518	477	112	124	145	112	98	95	98	98	110
98	577	561	609	561	561	560	580	599	576	194	204	233	181	162	156	152	166	181
196	659	653	706	646	637	632	655	698	661	247	264	287	232	202	205	193	208	230

(d) Solid Pier

time after loading (days)	Overall Strain (10^{-6})									Moisture Strain (10^{-6})								
	A1	A2	A3	A4	B1	B2	B3	B4	ave.	A1	A2	A3	A4	B1	B2	B3	B4	ave.
0	115	122	148	166	202	173	169	155	156	0	0	0	0	0	0	0	0	0
10	193	189	212	227	303	300	298	263	248	28	28	28	28	31	28	37	44	32
49	390	371	410	430	444	434	428	397	413	106	111	125	106	67	55	108	94	97
98	504	491	535	548	525	528	512	491	516	175	190	224	170	129	115	157	152	164
196	604	610	658	645	628	619	594	573	617	231	253	277	222	195	174	180	177	214

Table B4 - Clay Model Wall

(a) Model Wall (V/S = 44)

time after loading (days)	Overall Strain (10^{-6})			Moisture Strain (10^{-6})		
	side A	side B	Ave.	side A	side B	Ave.
0	129	100	115	0	0	0
7	233	241	237	27	30	29
48	498	450	474	126	131	128
98	537	504	520	134	137	135
170	575	521	548	127	143	135

(b) Model Wall (V/S = 51)

time after loading (days)	Overall Strain (10^{-6})			Moisture Strain (10^{-6})		
	side A	side B	Ave.	side A	side B	Ave.
0	128	109	119	0	0	0
7	232	223	228	33	25	29
48	435	394	415	107	116	111
98	519	442	481	1120	136	128
170	554	462	508	124	140	132

(c) Model Wall (V/S = 78)

time after loading (days)	Overall Strain (10^{-6})			Moisture Strain (10^{-6})		
	side A	side B	Ave.	side A	side B	Ave.
0	108	81	94	0	0	0
7	162	166	164	31	18	24
48	336	330	333	108	75	91
98	433	424	429	136	107	121
170	463	463	463	135	120	127

(d) Model Wall (V/S = 112)

time after loading (days)	Overall Strain (10^{-6})			Moisture Strain (10^{-6})		
	side A	side B	Ave.	side A	side B	Ave.
0	121	95	108	0	0	0
7	145	161	153	18	9	13
48	284	295	290	81	72	76
98	384	416	400	107	99	103
170	424	469	447	125	104	115

Table B5 - Calcium Silicate Model wall

(a) Model Wall (V/S = 44)

time after loading (days)	Overall Strain (10^{-6})			Moisture Strain (10^{-6})		
	side A	side B	Ave.	side A	side B	Ave.
0	285	290	287	0	0	0
8	486	614	550	77	77	77
42	840	950	895	240	177	209
91	1029	1167	1098	312	240	276
200	1162	1339	1250	345	266	306

(b) Model Wall (V/S = 51)

time after loading (days)	Overall Strain (10^{-6})			Moisture Strain (10^{-6})		
	side A	side B	Ave.	side A	side B	Ave.
0	258	359	308	0	0	0
14	584	686	635	78	110	94
56	793	885	839	136	197	167
112	953	1032	992	194	223	209
200	1087	1185	1136	238	262	250

(c) Model Wall (V/S = 78)

time after loading (days)	Overall Strain (10^{-6})			Moisture Strain (10^{-6})		
	side A	side B	Ave.	side A	side B	Ave.
0	271	308	289	0	0	0
15	517	607	562	59	40	50
42	645	733	689	99	73	86
112	840	897	868	180	141	160
200	936	1009	972	231	209	220

(d) Model Wall (V/S = 112)

time after loading (days)	Overall Strain (10^{-6})			Moisture Strain (10^{-6})		
	side A	side B	Ave.	side A	side B	Ave.
0	313	327	320	0	0	0
8	461	514	487	65	22	43
42	618	677	647	104	65	84
106	821	861	841	164	138	151
197	904	970	937	216	173	194

APPENDIX C

EXAMPLES OF COMPOSITE MODELS CALCULATIONS

Table C1 - Dimensions of Bricks, Block and Mortar Joints (mm)

Dimension	Clay Brick	Calcium Silicate Brick	Concrete Block
length width heigth	216 102.5 65	216 102.5 65 (61)	440 100 215
Mortar joint	11	11 (15)	11

( ) - *Effective height or thickness due to frog*

Table C2 - Data for Predictions of Vertical Strains (Refer to Figs. 4.5 - 4.8)

(a) Clay Brickwork

Parameters	Single-leaf Wall (V/S = 44)	Cavity Wall (V/S = 51)	Hollow Pier (V/S = 78)	Solid Pier (V/S = 112)
A_b (mm^2)	44280	111240	133488	177984
A_m (mm^2)	2791	7004	9476	24516
A_w (mm^2)	47071	118244	142964	202500
E_{by} (GPa)	34.2	34.2	34.2	34.2
E_m (GPa)	3.15	3.15	3.15	3.15
C	13	13	13	13
H (mm)	998	998	998	998
b_y (mm)	65	65	65	65
b_x (mm)	428	385	365	422
b_z (mm)	102.5	289	365	422
m_y (mm)	11	11	11	11
m_x (mm)	8	4.5	6.5	14.5
m_z (mm)	0	6.0	6.5	14.5
W_x (mm)	444	394	378	451
W_z (mm)	102.5	301	368	451

(b) Calcium Silicate Brickwork

Parameters	Single-leaf Wall (V/S = 44)	Cavity Wall (V/S = 51)	Hollow Pier (V/S = 78)	Solid Pier (V/S = 112)
A_b (mm^2)	44280	110700	133488	177984
A_m (mm^2)	1845	7544	9476	24516
A_w (mm^2)	46125	118244	142964	202500
E_{by} (GPa)	11.76	11.76	11.76	11.76
E_m (GPa)	4.95	4.95	4.95	4.95
C	13	13	13	13
H (mm)	998	998	998	998
b_y (mm)	61	61	61	61
b_x (mm)	428	386	364	422
b_z (mm)	102.5	288	364	422
m_y (mm)	15	15	15	15
m_x (mm)	8	6	5.1	14
m_z (mm)	0	4.5	5.1	14
W_x (mm)	444	398	375	450
W_z (mm)	102.5	297	375	450

(c) Concrete Blockwork

Parameters	Single-leaf Wall (V/S = 44)	Cavity Wall (V/S = 51)	Hollow Pier (V/S = 78)	Solid Pier (V/S = 112)
A_b (mm^2)	87750	132000	176000	132000
A_m (mm^2)	1650	4800	4400	14520
A_w (mm^2)	89400	136800	180400	146520
E_{by} (GPa)	12.00	12.00	12.00	12.00
E_m (GPa)	3.17	3.17	3.17	3.17
C	5	5	5	5
H (mm)	1142	1142	1142	1142
b_y (mm)	215	215	215	215
b_x (mm)	877	470	420	420
b_z (mm)	100	280	420	420
m_y (mm)	10	11	11	11
m_x (mm)	8.5	2.5	2.6	10.1
m_z (mm)	0	4	2.6	10.1
W_x (mm)	894	477	425	440
W_z (mm)	100	285	425	440

Table C3 - Calculation Examples

(a) Prediction of Modulus of Elasticity and Creep of Clay Single-leaf Wall (Eqs. (4.24), (4.38a) and (4.40a))

Replacing E with E' in Eq.(4.24),

$$\frac{1}{E'_{wy}} = \frac{b_y \cdot C}{H} \cdot \frac{1}{E'_{by}} \left[\frac{A_w}{A_b + \frac{E'_m}{E'_{by}} \cdot A_m} \right] + \frac{m_y \cdot (C+1)}{H} \cdot \frac{1}{E'_m} \qquad (4.24a)$$

From Eqs. (4.38a) and (4.48a)

$$E'_{m_y} = \frac{1}{\left(C_{m_y} + \frac{1}{E_{m_y}} \right)} \text{and} E'_{by} = \frac{1}{\left(C_{by} + \frac{1}{E_{by}} \right)}$$

Considering the 13-course single-leaf wall (see Table C2(a)), Eq.(4.24a) becomes

$$\frac{1}{E'_{wy}} = \frac{0.9}{1 + 0.063 \left(\frac{E'_m}{E'_{by}} \right)} + \frac{0.154}{E'_m}$$

time (days)	C_{my}	E'_m	C_{bx}	C_{by} $(0.52 C_{bx})$	E'_{by}	E'_{wy}	C_{wy}	C_{wy} $(1.5 \times C_{wy})$
0	0	3.15	0	0	34.2	13.31	0	0
20	663	1.02	9.3	4.9	29.3	5.49	107	160
40	992	0.76	14	7.3	27.3	4.26	160	240
60	1178	0.67	16.7	8.7	26.3	3.77	190	285
80	1289	0.62	18.7	9.7	25.6	3.53	208	312
100	1320	0.59	20.7	10.8	24.9	3.37	221	332
120	1432	0.57	21.3	11.1	24.7	3.26	231	347
140	1482	0.56	22.0	11.4	24.5	3.18	239	359
160	1513	0.55	22.7	11.8	24.2	3.13	244	367
180	1537	0.54	23.0	12.0	24.1	3.09	248	373
ultimate	1733	0.49	24.0	18.7	23.8	2.82	279	419

(b) Prediction of Vertical Moisture Strain (S_{wy}) on Calcium Silicate Cavity Wall(Eq.(4.48))

Considering the 13-course cavity wall (Table C2(b)), Eq.4.48 becomes

$$S_{wy} = 0.795 \cdot S_{by} + 0.210 \cdot S_m + 0.795 \cdot \frac{(S_m - S_{by})}{\left[1 + 14.67 \frac{E'_{by}}{E'_m}\right]}$$

Time (days)	E'_{by}/E'_m *	S_m	S_{by} ($= S_{bm}$)	S_{wy}	S_{wy} #
0	2.38	0	0	0	0
1	3.00	27	6	11	11
4	3.69	73	12	26	27
8	4.17	148	18	47	49
23	5.66	305	30	89	96
41	6.64	507	41	139	152
62	7.12	623	51	171	188
84	7.21	692	61	194	212
112	7.20	762	72	217	237
140	7.19	794	83	232	253
156	7.23	807	87	238	259
170	7.24	816	90	242	264
200	7.24	823	96	249	270
ultimate	7.58	1039	114	307	335

(c) Prediction of Horizontal Moisture Strain (S_{wx}) on Concrete Solid Pier (Eqs.(4.61) - (4.64))

Considering the 5-course solid pier, Eqs.(4.62), (4.63) and (4.64), respectively become

$$K_{wx} = 1.003 + 1.27\left[\frac{1}{1+20.8\frac{E'_{by}}{E_m}}\right]$$

$$K_{bx} = 0.955 - 0.955\left[\frac{1}{1+20.8\frac{E'_{by}}{E'_m}}\right]$$

$$K_{mx} = 0.0487 + 2.245\left[\frac{1}{1+20.8\frac{E'_{by}}{E'_m}}\right]$$

$$S_{wx} = \frac{K_{bx}\cdot S_{bx} + K_{mx}\cdot S_{mx}}{K_{wx}}$$

Time (days)	E'_b/E'_m *	S_m	S_{bx}	K_{wx}	K_{bx}	K_{mx}	S_{wx}	S_{wx} #
0	3.79	0	0	1.0188	0.9426	0.0767	0	0
10	4.91	80	33	1.0152	0.9453	0.0704	36	37
20	5.59	180	54	1.0137	0.9464	0.0678	62	64
40	6.15	360	78	1.0127	0.9471	0.0660	96	99
60	6.53	500	97	1.0122	0.9476	0.0650	123	127
80	6.79	605	114	1.0118	0.9478	0.0644	145	151
100	6.92	690	128	1.0116	0.9480	0.0641	164	170
120	7.09	750	140	1.0114	0.9481	0.0638	179	186
140	7.18	790	150	1.0113	0.9482	0.0636	190	198
160	7.18	820	156	1.0113	0.9482	0.0636	198	206
180	7.20	820	164	1.0113	0.9482	0.0635	205	213
190	7.22	826	167	1.0113	0.9482	0.0635	208	217
ultimate	7.81	1287	253	1.0106	0.9487	0.0624	317	331

** obtained from vertical creep calculations as in Table C3(a)*
\# neglecting the effect of creep i.e. using E_{by} and E_m.